Deciphering The Role Of The Gut Microbiome In Autoimmune Thyroid Disease

Thesis submitted in fulfillment of the requirements for the degree of Doctor of Philosophy (PhD), School of Medicine.

Giulia Masetti

2019

Author's Declarations

Declaration

I hereby declare that this work has not been submitted in substance for any other degree or award at this or any other University or place of learning, nor is being submitted in candidature for any other award.

Signed……..(candidate) Date……

Statement 1

This thesis is being submitted in partial fulfilment of the requirements for the degree of Doctor of Philosophy (PhD).

Signed……..(candidate) Date……

Statement 2

This thesis is the result of my own independent work/investigation, except where otherwise stated, and the thesis has not been edited by a third party beyond what is permitted by Cardiff University's Policy on the Use of Third Party Editors by Research Degree Students. Other sources are acknowledged by explicit references. The views expressed are my own.

Signed……..(candidate) Date……

Statement 3

I hereby give my consent for my thesis, if accepted, to be available for photocopying and for inter-library loans, and for the title and summary to be made available to outside organisations.

Signed……..(candidate) Date……

Statement 4: Previously approved Bar on Access

I hereby give my consent for this thesis, if accepted, to be available for photocopying and inter-library loans **after the expiration of a bar on access, previously approved by the Academic Standard & Quality Committee.**

Signed……..(candidate) Date……

Ai miei genitori

Acknowledgments

This work was supported by the Marie-Sklodowska Curie Industry-Academia Pathways and Partnerships (IAPP) action, GA number 612116 project INDIGO (Investigation of Novel biomarkers and Definition of the role of the microbiome In Graves Orbitopathy, http://www.indigo-iapp.eu/). My role in the project as an “early-stage” researcher was to perform the microbiome analyses on both patients and mouse model samples, which were recruited/generated in other work packages of this project.

I thank my former PTP Science Director Dr. John Williams, for giving me the opportunity to participate in such a dynamic and interesting project. I wish to thank all the INDIGO colleagues for these four years of work together. The specific contribution of each colleague to the work I performed and presented in this thesis is acknowledge at the beginning of each chapter.

I’m also thankful for patients and healthy controls all over Europe who voluntarily and kindly donated their time and their samples, without whom this work couldn’t have been performed.

I couldn’t get very far without the amazing support provided by my supervisors. I wish to thank Prof. Marian Ludgate for always being supportive and for always providing the right direction, even when the statistics was getting “exotic”. She is truly an inspirational role model both as a researcher and as a woman, wife, mother and grandmother. Thank you to my second supervisor Prof. Julian Marchesi for his presence, his constant support and for believing in me and my skills. I also wish to thank Dr. Filippo Biscarini, my former PTP supervisor, for the outstanding mentorship and support he provided on statistics and bioinformatics and during the completion of this thesis.

I wish to thank my former Science Director Dr. Alessandra Stella and my colleagues and friends at PTP Science Park (Lodi, Italy). Even if we are not working together anymore and we are spread all over the world, I really value the time we spent together.

Moreover, this work couldn’t have been finished without the amazing support of Dr. Sue Plummer and my colleagues at Cultech Ltd (UK).

During these four years I’ve met amazing friends (Evi, Andreas, Debbie, Ally and Duaa). Thank you for your presence and constant support. A special thanks to my friend and colleague Dr. Ilaria Muller for the huge support and the help both at work and outside.

To my Italians lifelong friends: thank you for your amazing support even if I was not always physically present. I’m really lucky to have you in my life.

At last but not least: thank you to my wonderful parents. All of this couldn’t have even existed without you. I like to think that this work reflects both of you: medics from mum and informatics from dad! A massive thanks to my “bear”-in-life and in-crime Fabrizio, I honestly don’t know what I would have done without you.

Grazie di cuore,

Thank you,

Diolch i chi.

Summary

The aetiology of hyperthyroid Graves' disease (GD) is incompletely understood. I hypothesized that the gut microbiome affects tolerance to the thyrotropin receptor (TSHR) leading to GD and associated Graves' orbitopathy (GO). My work comprises two observational studies and two interventional trials, applied to a GD/GO mouse model and GD/GO patients.

I applied metataxonomics (16S rRNA gene sequencing) to samples from TSHR-immunised mice from two independent laboratories and observed significant differences in alpha-diversity, beta-diversity and taxonomic profiles. I also compared TSHR-treated and control mice in one centre and identified disease-associated taxonomies (i.e. reduced *Bacteroidetes* and enriched *Firmicutes*), correlating with orbital-adipogenesis in diseased but not controls.

Changes in gut microbiota taxonomy (e.g. reduced *Bacteroides*/increased *Roseburia* spp. and increased *Firmicutes:Bacteroidetes* ratio) were also observed in GD (n=59) and GO (n=46) patients compared with controls (n=41), and associated with hyperthyroidism or GO severity. Moreover, GD/GO patients-predicted metagenomic pathways included increased "Bacterial epithelial invasion" and "glycosaminoglycan synthesis".

The role of the gut-microbiota in TSHR-induced GD/GO was confirmed by manipulating it in early life using antibiotics which enriched *Bacteroides* spp. and reduced/ablated disease symptoms. The faecal material transplant from GO patients, despite showing similarities with the GO patients gut microbiota, did not exacerbate murine GO, which also remained unaffected by probiotics. In contrast, in a randomised trial, GD/GO patients receiving probiotics (in addition to anti-thyroid therapy) displayed a more stable gut microbiota composition and sustained improvement in thyroid hormone levels compared with placebo.

My results illustrate significant perturbation in the gut microbiota in TSHR-induced murine GD/GO and patients with spontaneous disease. Furthermore, the similarities in differential abundance and disease-associated taxonomies noted in both species support their relevance to disease. Future studies are needed to dissect the mechanistic role of the gut microbiome in activating the immune system and determining the onset of GD/GO.

List of publications

Masetti G, Moshkelgosha S, Kohling H-L, Covelli D, Banga JP, Berchner-Pfannschmidt U, Horstmann M, Diaz-Cano S, Goertz G-E, Plummer S, Eckstein A, Ludgate M, Biscarini F, Marchesi JR and the INDIGO *consortium* (2018). Gut microbiota in experimental murine model of Graves' orbitopathy established in different environments may modulate clinical presentation of disease. *Microbiome* 6:97. Doi:97.10.1186/s40168-018-0478-4.

Moshkelgosha S, **Masetti G**, Berchner-Pfannschmidt U, Verhasselt H-L, Horstmann M, Diaz-Cano S, Noble A, Edelman B, Covelli D, Plummer S, Marchesi JR, Ludgate M, Biscarini F, Eckstein A, Banga P (2018). Gut microbiome in BALB/c and C57BL/6J mice undergoing experimental thyroid autoimmunity associate with differences in immunological responses and thyroid function. *Hormone and Metabolic Research.* Doi:10.1055/a-0653-3766.

Zhang L, **Masetti G**, Colucci G, Salvi M, Covelli D, Eckstein A, Kaiser U, Draman MS, Muller I, Ludgate M, Lucini L, Biscarini F (2018). Combining micro-RNA and protein sequencing to detect robust biomarkers for Graves' disease and orbitopathy. *Scientific Reports* 8:8386, Doi:8386.10.1038/s41598-018-26700-1.

Manuscripts in preparation:

Moshkelgosha S, Verhasselt H-L, **Masetti G**, et al. (proposed title) Gut microbiota modification in a TSHR-induced murine model of Graves' orbitopathy confirms its role in modulating the autoimmune response*. In preparation*.

Biscarini F, **Masetti G** et al. (proposed title) The role of the gut microbiome in an European cohort of Graves' disease and orbitopathy. *In preparation*.

Covelli D, **Masetti G**, Colucci G, et al. Immune reaction to food antigens in Graves' disease (GD) patients: role of gliadin and other food antigens. *In preparation*.

Poster and oral presentations

Masetti G. and the INDIGO *Consortium*. “Investigation of Novel biomarkers and Definition of role of microbiome in Graves’ Orbitopathy (GO) (INDIGO): Microbiota analysis of patients at recruitment”. Flash presentation and poster presentation at MicrobiotaMI, University of Milano-Bicocca (5th-7th November 2018, Milano, Italy).

Masetti G. “Contribution of the gut microbiota to heterogeneity of induced GO in mice“. Invited speaker at the 48th Cambridge Ophthalmological Symposium (September 2018, St. John’s College, Cambridge, UK).

Masetti G. “Contribution of the gut microbiota to the in-vivo model and correlation with induced disease“. Oral presentation at the British Thyroid Association Conference (15th May 2018, Birmingham, UK).

Masetti G, Biscarini F, Marchesi JR, Moshkelgosha S, Ludgate M. and the INDIGO *Consortium*. ”Unravelling the functional role of the gut microbiota in a murine model of Graves’ orbitopathy”. Poster presentation at the Cardiff Institute of Infection & Immunity Annual Meeting (November 2017, Cardiff UK).

Masetti G. “Deciphering the role of the gut microbiota in Graves’ orbitopathy”. Oral presentation at the Infection & Immunity Seminar Series (25th September 2017, Cardiff, UK).

Masetti G. “Microbiome comparison in autoimmune thyroid/eye disease and healthy controls“. Oral presentation at the “Deciphering the role of the microbiome in Autoimmune Thyroid and Ocular disease Symposium (21st and 22nd April 2016, Cardiff, UK).

Masetti G, Biscarini F, Koehling HL, Covelli D, Ludgate M. "Do bacterial antigens play a role in Autoimmune Graves' disease?". Poster presentation at Cardiff University Institute of Infection & Immunity Annual Meeting (November 2015, Cardiff UK).

Masetti G, Biscarini F, Ludgate M, Marchesi JR and the INDIGO *Consortium*. "Interaction between the microbiota and immune response in the context of Autoimmune Thyroid Diseases: a Graves' disease and Graves' orbitopathy study". Poster presentation at the Gut microbiome in health and diseases congress (25-26 June 2015 Milano).

Abbreviations list

^{131}I, radioiodine
16S, subunit 16 Svedberg of the ribosomal RNA
18S, subunit 18 Svedberg of the ribosomal RNA
50S, subunit 50 Svedberg of the ribosomal RNA
A, adenine
aa, amino-acid
ABC, ATP-binding cassette
ACE, abundance-based estimator
AD, autoimmune disease
AGE, advanced glycosylation end products
AICD, activation-induced cell death
AIRE, autoimmune regulator
AITD, autoimmune thyroid disease
ALPS, autoimmune lymphoproliferative syndrome
ANA, anti-nucleus antibody
ANOVA, Analysis of Variance
APC, antigen-presenting cells
APECED, autoimmune polyendocrinopathy-candidiasis–ectodermal dystrophy/dysplasia
APS-1, autoimmune polyendocrine syndrome type 1
ARG, antibiotic-resistance genes
ATD, antithyroid drug
ATP, adenosine triphosphate
B cells, B lymphocytes
B10, regulatory B-cells expressing IL-10
BALB/c, albino mouse
BAT, brown adipose tissue
BCR, B-cell receptor
BH, Benjamini Hochberg
BL, baseline
C-, C-terminus (-COOH)
C, citosine
C, degree *Celsius*
C/EBP, CCAAT-enhancer-binding proteins
C57BL/6, black-6 mouse
$Ca2^{+}$, Calcium ion
cAMP, cyclic adenosine monophosphate
CAS, clinical activity score
CBZ, carbimazole
CCL, chemokine (C-C motif) ligand
CD, cluster differentiation
CD, Crohn's disease
cDNA, complementary DNA
CFA, Complete Freund's Adjuvant
cfu, colony-forming unit
CHO, Chinese hamster ovary cells

CNS, central nervous system
CpG, -C-phosphate-G-
CSS, cumulative sum-scaling
Ct, thermal cycle
CTLA-4, Cytotoxic T-Lymphocyte Antigen 4
CV, cross validation
db/db, obese and diabetic mice
DC, dendritic cells
DE, differential expression
DIABIMMUNE, Pathogenesis of Type 1 Diabetes - Testing the Hygiene Hypothesis
DNA, Deoxyribonucleic acid
DSS, dextran-sodium sulphate
e.g., *exempli gratia*
E.U., European Union
EAE, experimental autoimmune encephalitis
EC, *Escherichia coli*
ECM, extracellular matrix
EFU, end of follow-up
ELISA, Enzyme-Linked Immunosorbent Assay
EOM, extra-ocular muscles
ERK, extracellular signal–regulated kinases
EU, euthyroid
EUGOGO, European Group on Graves' Orbitopathy
F, female
F:B, *Firmicutes* to *Bacteroidetes* ratio
FADD, Fas-associated protein with death domain
FAO, Food and Agriculture Organisation
Fas-l, Fas ligand
FDA, Food and Drug Administration
FOS, fructo-oligosaccharides
FoxO, Forkhead box O
FoxP3, forkhead box P3
FSHR, Follicle Stimulating Hormone Receptor
fT4, free thyroxine
Fw, forward
G-CSF, Granulocyte-colony stimulating factor
g, grams
g, gravity force
G, guanine
GALT, gut-associated lymph nodes
GBS, Guillain-Barre syndrome
GC, germinal centre
GD, Graves’ disease
gDNA, genomic Deoxyribonucleic acid
GF, germ-free
GI, gastrointestinal tract
GO, Graves’ orbitopathy
GPCR, G-protein coupled receptor

GSS, global severity score
H_2O_2, hydrogen peroxide
HA, hyaluronic acid
HAS2, hyaluronic acid synthase 2
HAT, histone acetyltransferase
HC, healthy controls
HCl, hydrochloric acid
HDA, histone deacetylase
HFD, high fat diet
hFMT, humanized faecal material transplant
HLA, human leucocyte antigen
HMP, Human Microbiome Project
HSD, Honest Significant Difference
HT, Hashimoto's thyroiditis
hTSHR, human TSHR
i.e., *id est*
I.S., intestine scraping
IAP, intestinal alkaline phosphatase
IBD, inflammatory bowel disease
IBS, inflammatory bowel syndrome
IEC, intestinal epithelial cells
Ig, immunoglobulin
IGF1R, insulin growth factor receptor 1
iHMP, integrative Human Microbiome Project
IL, interleukin
INDIGO, Investigation of the role of the gut microbiome and biomarkers in GO
INFy, interferone-gamma
IQR, interquartile ranges
ITT, intention-to-treat
K, thousands
kDa, kilo-Dalton
KEGG, Kyoto Encyclopedia of Genes and Genomes
KO, KEGG orthologs
KO, knockout
L, litre
LAB, lactic-acids producing bacteria
Lab4, commercial probiotic
LDA, linear discriminant analysis
LEfSe, linear discriminant analysis effect size
LHR, luteinizing hormone receptor
LP, lamina propria
LPS, lipopolisaccaride
LRRs, leucine-rich repeats
LTA, lipoteichoic acid
M cells, microfold cells
M, male
mAb, monoclonal antibody
ManR, mannose receptor

MetaHIT, METAgenomics of the Human Intestinal Tract
MHC, major histocompatibility complex
miRNA, micro RNA
mL, millilitre
MLN, mesentheric lymph nodes
MRI, magnetic resonance imaging
mRNA, messenger Ribonucleic acid
MRSA, Methicillin-resistant *Staphylococcus aureus*
MS, multiple sclerosis
MSE, mean squared error
mTOR, target of rapamycin
mTORC, mammalian target of rapamycin complex 1
MTZ, methimazole
mU, milli Unit
MUC, mucin producing gene
N-, N-terminus (-NH2)
NAFLD, non-alcoholic fatty liver disease
NB, negative binomial
NEC, necrotizing enterocolitis
NF-kB, Nuclear Factor kappa-light-chain-enhancer of activated B cells
NIH, National Institutes of Health
NK cells, natural-killer cells
NMDS, non-metric dimensional scaling
NOD, non-obese diabetic
ntree, number of trees
nTregs, naturally induced regulatory T cells
OH, hydroxide
OOB, out-of-bag
OS, obese strain
OTU, Operational Taxonomic Unit
P, probability value
PAMP, Pathogen Associated Molecular Patterns
par., paragraph
PBMC, peripheral blood mononuclear cell
PCA, principal component analysis
PCR, polymerase chain reaction
PD-1, Programmed cell death protein 1
PDAM, pathogen-driven autoimmunity mimicry
PERMANOVA, permutational analysis of variance
pH, potential of hydrogen
PI3K, phosphatidylinositol 3-kinase
PICRUSt, Phylogenetic Investigation of Communities by Reconstruction of Unobserved States
PIP2, Phosphatidylinositol (4,5)-bisphosphate(2)
PLZF, promyelocytic leukaemia zinc finger protein
PMA, propidium monoazide
pmol, pico mole
PPAR-γ, peroxisome proliferator-activated receptor gamma
PPI, proton-pump inhibitors

PRR, Pattern Recognition Receptors
PSA, polysaccharide A
PTPN22, Protein tyrosine phosphatase, non-receptor type 22
PTS, phosphotransferase system
PTU, propyl-tiouracile
Q1, 25%-tile
Q3, 75%-tile
QIIME, Quantitative Insights Into Microbial Ecology
qPCR, quantitative polymerase chain reaction
r, Pearson's correlation coefficient
RANTES, Regulated on Activation, Normal T Cell Expressed and Secreted
RDP, Ribosomal Database Project
RegIIIγt, Regenerating islet-derived protein 3 *gamma*
RF, Random Forests
Rho, Spearman's correlation coefficient
RIA, radioimmunoassay
RNA, Ribonucleic acid
RNAi, RNA interference
ROR-c, Retineic-acid-receptor-related orphan nuclear receptor C
ROR-γt, Retineic-acid-receptor-related orphan nuclear receptor *gamma*
RR-MS, relapsing-remitting multiple sclerosis
rRNA, ribosomal RNA
rT3, reverse T3
Rv, reverse
RXR, retinoid X receptor
SCFA, short-chain fatty acid
SFB, segmented filamentous bacteria
SHM, somatic hypermutation
SLE, systemic lupus erythematosus
SNP, short-nucleotide polymorphism
SPF, specific pathogen free
spp, subspecies
ST, *Salmonella typhimurium*
STAMP, statistical analysis of taxonomic and functional profiles
STD, positive reference serum against YE
T cells, T lymphocytes
T, timine
T1D, Type-1 diabetes
T2D, Type-2 diabetes
T3, triiodothyronine
T3S, sulphated T3
T4, thyroxine
T4G, glucuronidated T4
TBII, thyrotropin-binding inhibitory immunoglobulin
TCR, T-cell receptor
Tg, thyroglobulin
TGF-β, transforming growth factor beta
Th, T helper cells

THR, Thyrotropin-releasing hormone
TLR, Toll-like receptor
Tn, training set
TNF-α, tumour necrosis factor-alpha
TPO, thyroid peroxidase
TR, thyroid hormone receptor
TRAB, thyrotropin receptor antibodies
TRAK, thyrotropin receptor antibodies
TRE, T3 response element
Tregs, regulatory T cells
TSAb, thyroid-stimulating antibodies
TSBAb, thyroid-stimulating blocking antibodies
TSH, thyroid-stimulating hormone or thyrotropin
TSHR-A, thyroid-stimulating hormone receptor or thyrotropin receptor A-subunit
TSHR, thyroid-stimulating hormone receptor or thyrotropin receptor
TSI, thyroid-stimulating immunoglobulins
UC, ulcerative colitis
UDP, uridine diphosphate
UGT, Uridine 5'-diphospho-glucuronosyltransferase
UI/L, International Units Per Litre
UK, United Kingdom
USA, United States of America
V, variable regions
vs., *versus*
VSL#3, commercial probiotic
WHO, World Health Organisation
WMS, whole-genome sequencing
YE, *Yersinia enterocolitica*
βgal, beta-galactosidase
µg, microgram
µm, micrometer
µM, microMole

List of Figures

List of Tables

Table of Contents

1. Chapter 1

General introduction

1.1. AUTOIMMUNE THYROID DISEASES

Mention of autoimmune diseases (AD) first appeared in the medical and scientific literature in 1950 [1], and initially constituted a puzzling medical problem, because the possibility that the immune system could react against self-molecules had not been previously recognised. Initially, the majority of the scientific literature and reviews considered autoimmunity as the result of the malfunctioning of the immune system, which fails to recognize self-antigens, but directing the immune-response against the host; and most of the theories related to the mechanisms underlying the outcome of an AD referred to this concept. However, later investigations recognised the importance of self-recognition in the correct functioning of the immune system. What is illustrated by the need for endogenous and exogenous antigens to be associated with self MHC-I and MHC-II molecules respectively to illicit an immune response. More recently it has been suggested that the presence of self-reactive immune system cells (both T and B cells) might be physiological for the process of regeneration and clearance of the damaged-self (e.g. damaged cells undergoing death and cellular debris after apoptosis) [2]. At the basis of an auto-immune response leading to an autoimmune disease there is overproduction of self-reactive T and B cells and auto-antibodies against self-antigens. Synergism between these, pro-inflammatory mediators (e.g. TNF-α, IL-1βb, IL-1) and other types of immune cells (e.g. Antigen-Presenting-Cells, APC, such as dendritic cells or macrophages), cause the damage, dysfunction or the over-stimulation of the one or more targeted tissue and organ leading to disease.

When self-antigens are localized into a specific tissue, organ or region, we speak of organ-specific autoimmunity. Examples of organ-specific ADs include autoimmune thyroid diseases like Graves' disease (GD) or Hashimoto's thyroiditis, Crohn's disease (CD, chronic inflammation of the intestine) and type 1 diabetes (T1D). When, on the other hand, self-antigens are scattered throughout the body, they are described as systemic ADs, such as Systemic Lupus Erythematosus (SLE), in which the autoantigen is the DNA itself, more specifically the ribonucleoprotein complexes of the spliceosome [3].

Until now, there are more than eighty recognized autoimmune conditions, twenty-four of them have been well characterized in epidemiological studies (data according to NIH statistics on autoimmunity[1]). Autoimmune diseases, both systemic and organ-specific, are therefore a growing public health concern, compounded by the discovery of

[1] NIH, National Institute of Environmental Health Sciences. "Autoimmune Diseases" available at https://www.niehs.nih.gov/health/materials/autoimmune_diseases_508.pdf

autoimmune features in pre-existing diseases (i.e. Parkinson's disease [4]) and to the increasing number of affected patients [5].

1.1.1. The thyroid function in health

The thyroid gland, with its prototypical "butterfly" shape is located close to the larynx, and is essential in regulating growth and the metabolic processes (e.g. brain and nerves development and function, intestinal and heart functions) through the production of two main thyroid hormones, triiodothyronine (T3) and thyroxine (T4), which are released into the circulation and transported to virtually all cells in the body. Synthesis of thyroid hormones from the thyroid follicular cells is regulated by the thyroid stimulating hormone (TSH) secreted by the pituitary gland when the levels of T3 and T4 are low, to increase their production. The TSH production in the pituitary gland is itself regulated by the hypothalamic-produced TSH releasing hormone (TRH); secretion of TRH is also regulated by T3 and T4 in a negative feedback loop (Figure 1.1).

Thyroid hormones T3 and T4 are synthetized from iodide (I^-) and the amino acid tyrosine by the thyroid peroxidase (TPO) enzyme, an integral membrane protein in the apical plasma membrane of the thyroid epithelial cells. Iodide, usually derived from food, is sequestered from the blood via the sodium iodide symporter (NIS) located on the outer plasma membrane of the thyroid epithelial cells and transported to the follicular lumen in conjunction with thyroglobulin (Tg), a large soluble glycoprotein (330 kDa) produced by the thyroid epithelial cells and secreted into the thyroid follicular lumen, which contains approx. 134 tyrosine residues undergoing iodination operated by TPO. Such a post-translational modification is necessary for the production of thyroid hormones from two iodinated tyrosine. Thyroid hormones are stored in epithelial cells and released into the blood. TSH regulates the T3 and T4 release process: the higher the TSH levels, the faster the production and the rates of endocytosis and release into the circulation, and *vice versa* in the presence of low TSH amounts. The hypothalamus-pituitary-thyroid axis regulates also the gene expression and the production of NIS, TPO and Tg themselves *via* the binding of TSH to the TSH receptor (TSHR), as will be explained in further details later in this section.

In humans, only 20% of the thyroid hormones are secreted in the active T3 form, while 80% are released as T4 [6], termed a "prohormone", since deiodination by deiodinase enzymes in the outer ring of the T4 can reverse the less-active T4 isoform to its more active counterpart T3. However, deiodination occurring in the inner ring leads to an inactive form of T3 called reverse T3 (rT3) [7]. Deiodinases enzymes have mainly three different isoforms (D1, D2 and D3) that reside in different tissues and while the D1 and

D3 are more likely to produce the inactive rT3, the D2 isoform (expressed in the brain, placenta and adipose tissue) is more involved in the outer ring T4 deiodination, as reviewed in [8]. Other modifications in the thyroid hormones structure may occur in the 4'-OH of the phenolic group by either sulphation or glucuronidation, which result in the inactivation of the thyroid hormones. Phenol sulfotransferases promote the sulphation of both T3 and T4, which facilitate the D1 deiodination into the inactive form rT3S. UDP-glucuronyl transferase (UGTs), instead, promote the attachment of glucuronic acid which may occur more frequently on T4. Both sulphation and glucuronidation increase the water-solubility of thyroid hormones facilitating their secretion through the serum, bile, urine and also in the intestine [9]. It is interesting to note that, as reviewed in [10], sulphatase and beta-glucuronidase enzymes from tissues, but also from the gut microbiota, may convert the inactive form of T3S or T4G into T3 and T4 respectively, acting as a reservoir for thyroid hormones.

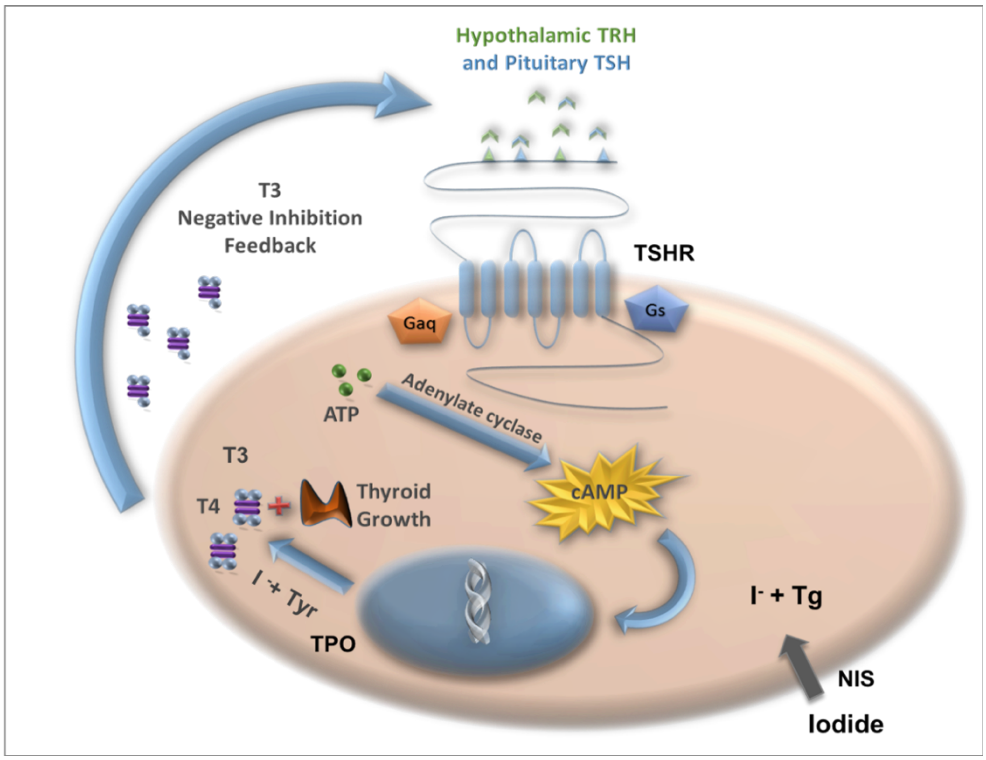

Figure 1.1. Production of thyroid hormones in health.
Thyroid-stimulating hormone (TSH) secreted by the pituitary activates the production of thyroid hormones (T3, triiodothyronine and T4, thyroxine), in the thyroid follicular cells. T4 is produced from Iodide (I^-) and the amino acid Tyrosine (Tyr) by the thyroid peroxidase enzyme (TPO). Iodide is obtained from food, captured from the blood by the sodium iodide symporter (NIS) and internalized in the thyroid follicles with thyroglobulin (Tg). The prohormone T4 undergoes deiodination to produce the active form T3. Once T4 and T3 are released in the bloodstream, they are transported to virtually all cells in the body. The production of TSH by the hypothalamic-produced TSH releasing hormone (TRH) is regulated through a negative feedback loop by high levels of T3/T4. (Modified from http://www.indigo-iapp.eu). Description of the pathological status in Figure 1.4.

To exert their physiological role in regulating neurodevelopment, growth and metabolic processes, thyroid hormones bind to the thyroid hormone receptors (TRs) to initiate the expression of target genes, inducing a conformational change of the receptor structure. TRs are part of the nuclear receptors family encoded by two genes *Thra* and *Thrb*, which express for TR-alpha and TR-beta, although four alternative splice variants are described according to tissue and developmental stages (e.g. TR-B1 mainly expressed in brain, heart, kidneys, liver and thyroid; TR-B2 exclusive in hypothalamus, anterior pituitary and developing ear and TR-beta generally over-expressed after birth) [11]. TRs themselves bind via zinc-fingers to short-repeated "AGGTCA" hexamers called T3 response elements (TREs), which can be arranged in a direct, palindromic or inverted manner. Moreover, TRs can bind TREs as a monomer (either alpha or beta), homodimer (e.g. alpha/alpha, alpha/beta, beta/beta) or heterodimer in conjunction with the retinoid X receptor (alpha/RXR or beta/RXR), which also has the highest binding affinity. TR-TRE binding to DNA would occur independently of the T3-TR binding, which would then determine the activation or the repression of the gene expression. In a T3-free state, in fact, the TR bound to the chromatin forms a co-repressor complex with histone deacetylase (HDA), repressing the gene expression [12], while in presence of T3, a conformational change of the receptor activates the expression of target genes via histone transacetylase (HAT) [13], although a more dynamic mechanisms has been recently proposed [14].

Healthy individuals with a normal thyroid function are considered as euthyroid, while disease conditions are usually diagnosed when TSH and "free" T4 levels are out of ranges. Hyperthyroidism is diagnosed in presence of a low or undetectable TSH and a high level of T3/T4, while the hypothyroidism is present with an above TSH and a below ranges free T4. Individuals with mutations in the TR-β gene, which is responsible for T3 binding, may develop a syndrome of thyroid hormone resistance, characterized by signs of hypothyroidism. Also due to the role of thyroid hormones in neurological and brain development, imbalances in the maternal thyroid hormones levels or in the T3-TR-TRE might lead to developmental defects and neurocognitive disorders [15].

1.1.2. Graves' disease

Graves' disease (GD) is an organ-specific antibody-mediated autoimmune disease, characterized by the presence of thyroid-stimulating antibodies (TRAB) that mimic the TSH in activating the TSHR, which results in an overproduction of thyroid hormones (both T3 and T4), hyperthyroidism, goitre and thyrotoxicosis (i.e. elevated thyroid hormone levels); but also a range of extrathyroidal manifestations, of which Graves' orbitopathy (GO) is the most common - as I will later describe. GD constitutes the majority

of cases of the thyrotoxicosis [16] afflicting about 2% of the UK population, with a 8:2 female predominance. Clinical symptoms are mostly related to hyperthyroidism including: loss of weight, tachycardia, heat intolerance and tremor, but also bowel discomfort, exophthalmos and pretibial myxedema (Figure 1.2). Diagnosis of GD is usually made on patients who already have some of the clinical symptoms described, with a biochemical signature of low or undetectable TSH, high T3 and free-T4 and presence of TRAB and other thyroid autoantigens such as TPO.

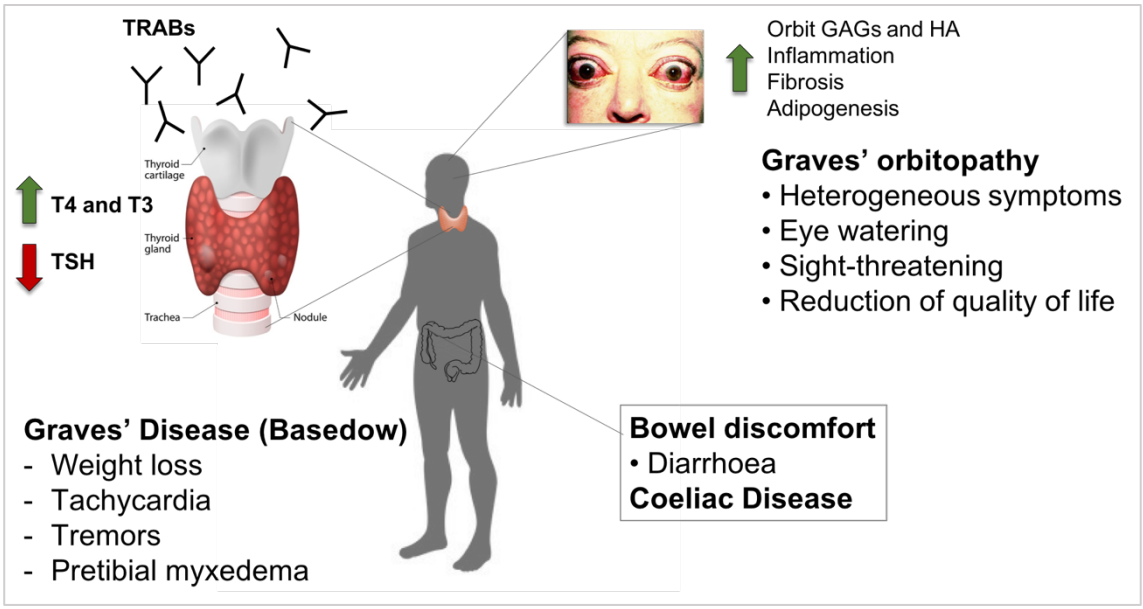

Figure 1.2. Summary of Graves' disease and Graves' orbitopathy characteristics. Graves' disease (GD; also called Basedow disease in Italy and France) is caused by the presence of antibodies (TRAB) directed against the thyroid-stimulating hormone receptor (TSHR), which activate the TSHR in over-producing T3 and T4 hormones, at the expenses of the TSH. Hyperthyroid is manifested through weight loss, tachycardia, tremors and some extra-extrathyroidal manifestations (i.e. pretibial myxedema). Also, bowel discomfort is usually reported with an increased intestinal mobility and diarrhoeal episodes. The concomitant presence of Coeliac Disease has been reported [17, 18]. Around 50% of GD patients may experience some sign of eye disease called Graves' orbitopathy (GO), while 5% of them develop a severe form, which involves inflammation and remodelling of the orbital tissues leading to proptosis, corneal exposure, and diplopia. Symptoms are heterogenous ranging from eye irritation, watering, discomfort to dry eyes, grittiness and photophobia. Most severe cases GO may result in blindness. GO patients experience a reduction of their quality of life, and develop psychological distress due to the disfiguring phenotype of the disease (i.e. protrusion of the eyeball, eyelid retraction).

The main GD autoantigen is TSHR, whose gene is located on chr. 14q31 and is composed of ten exons [19]. It is expressed at high level on the plasma membrane of the follicular epithelial cells in the thyroid, but also in other sites such as adipose tissues, fibroblasts and - most important for further descriptions - the human retro-orbital tissue [20, 21]. The TSHR belongs to the G-protein-coupled receptor (GPCR) family, sharing structural similarities with the follicle-stimulating hormone receptor (FSHR) and the lutropin receptor (LHR), however retaining unique characteristics. The large extracellular domain (Subunit A) of the TSHR contains several leucine-rich repeats (LRRs), with a cysteine-rich N and C-terminus including some polypeptides that differentiate the TSHR amongst LHR, while the second domain (B subunit) is 'rhodopsin-like' having the seven transmembrane spanning helices characteristic of the GPCR (Figure 1.3). The TSHR structure at the thyrocyte surface is the result of several post-translational modifications including glycosylation, intracellular cleavage, and disulphide-bond formation. During the intracellular cleavage, probably operated by a metalloproteinase [22], a 50aa peptide (C peptide) originally located at the N-terminus of the B subunit (aa 317-366, Figure 1.3) is removed. The two subunits are linked together via a disulphide bridge. For some TSHRs, cell-surface enzymes could reduce the disulphide bond, releasing the A-subunit by so-called "receptor shedding". The TSHR is highly glycosylated, approximately 40% of the A-subunit [23], due to six N-linked glycosylation sites located on the ectodomain, at least four of which are necessary for the location of the TSHR at the cell surface.

Physiological TSH binding occurs in multiple sites of the A-subunit of the TSHR, specifically between residue 280-400, potentially favoured by the concave shape of the A-subunit. The binding itself leads to a conformational change of the receptor which assumes an agonist state and activates the signal transduction via the cyclic AMP (cAMP), PI3K-Akt and PIP2/$Ca2^{+}$/arachidonate signalling pathways, as extensively described in [24], resulting ultimately in the regulation of gene expression, regulation of the iodide efflux, Tg degradation, production of thyroid hormone and thyrocyte growth. Whilst these signalling pathways increase the gene expression of Tg, TPO and NIS, expression of the TSHR is down-regulated, as well as the expression of Human Leukocyte Antigen (HLA) -class I genes.

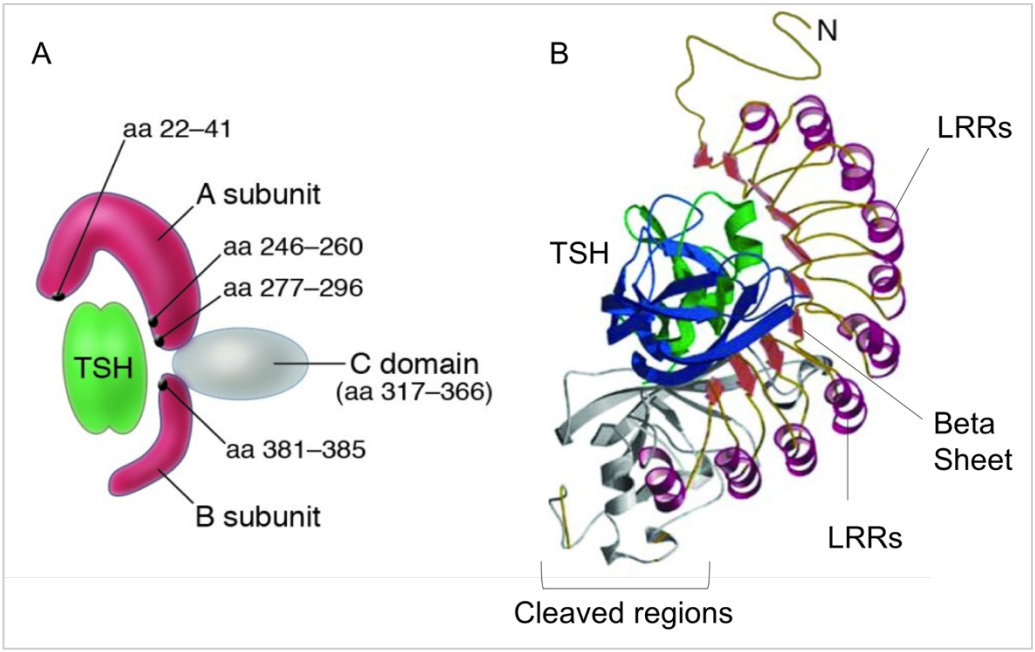

Figure 1.3. Molecular structure of the thyroid-stimulating hormone receptor.
(**A**) The TSHR is a G-protein-coupled receptor constituted of a large extracellular domain (Subunit A) and of a B-subunit. The TSHR expressed at the thyrocyte surface is the result of several post-translational modifications such as glycosylation, intracellular cleavage, and disulphide-bond formation. The intracellular cleavage removes a peptide of 50aa (C-peptide). A-subunit and B-subunit are bond through a disulphide bridge, which, if reduced, it may result in a "receptor shedding". (**B**) A-subunit of the TSHR contains several leucine-rich repeats (LRRs), with a cysteine-rich N and C-terminus, characterized. The B-subunit is constituted of a 'rhodopsin-like' seven transmembrane spanning helices, characteristic of the GPCR. Physiological TSH binding occurs in multiple sites of the A-subunit of the TSHR, specifically between residue 280-400, potentially favoured by the concave shape of the A-subunit. (Modified from [25]).

In GD, TRABs compete with the TSH for binding the TSHR. Due to the high levels of T3 and T4, the TSH expression is repressed and the TRAB signalling predominate, along with the overexpression of the genes and the overproduction of thyroid hormones (Figure 1.4). As the result of the failure of immunological mechanisms that will be further described, self-specific B cells secrete auto-antibodies against the TSHR (TRABs), and the type of auto-antibodies binding to the TSHR would decide the fate of this activation. Besides the thyroid-stimulating antibodies (TSAb), in fact, TSHR blocking and neutral antibodies have been described. TSHR stimulating antibodies are a class of IgG1 antibodies that, by mimicking the TSH, are able to bind the receptor when in a natural conformation, inducing the cAMP pathway and inhibiting any binding of naturally-occurring TSH itself [24]. Blocking antibodies (TSBAb) also prevent TSH binding to the receptor, but also block any other thyroid functions, possibly resulting in hypothyroidism, although there is the report of signal cascade activation via preferred pathways in some

of the TSBAb [24], which would act like a weak agonist. The binding sites of both TSAb and TSBAb might be different from that of the natural TSH and from each other's. In fact, the TSH requires the complete structure of the TSHR; while the TSAbs display high affinity for epitopes located along the ectodomain LRRs in its natural concave conformation [26] or the shed A-subunit itself [27, 28], the TSBAb are conformationally dependent [29]. Moreover, the glycosylation patterns of the TSHR are necessary for the binding of both TSAb and TSBAb [30]. Neutral antibodies do not activate or block the TSH and they do not induce the signalling through the cAMP; although two neutral TSHR antibodies, when tested on rat thyroid cell, were capable of suppressing the signalling activity or stimulating some signalling cascades independent from cAMP, respectively [31].

The TBII (thyrotropin-binding inhibitory immunoglobulin) and the TSAB or thyroid-stimulating immunoglobulins (TSI) are methods used to measure levels of TRABs in the sera of patients. The TBII measures both stimulating and blocking antibodies since it quantifies the titre of Igs that inhibit the binding of the TSH to the TSHR. On the other hand, TSAB measure the levels of stimulating or blocking antibodies through the quantification of the cAMP production in a cell line (CHO) stably transfected to express the TSHR [32]. In recent years M22, a human monoclonal TSAB derived from a patient with severe hyperthyroidism [33], and whose structure has also been characterized in depth [26, 33-35] has been invaluable in providing insight into the TSAB/TSHR interaction.

Most GD patients also produce autoantibodies against the other two autoantigens involved in the AITD: Tg and TPO, showing a possible overlap in the mechanisms of loss of immune-tolerance to one or more thyroid autoantigens [36].

Treatment options for GD includes anti-thyroid drug administration, radioiodine and thyroid surgery, depending on the severity of the disease itself and the presence of co-occurrent eye disease or other conditions. Hyperthyroid GD patients are usually treated with thionamide anti-thyroid drugs such as methimazole (30 mg/day) or carbimazole (CBZ, 40 mg/day), according to the country of residency (e.g. CBZ is used in UK, while methimazole is prescribed in Italy and the USA) for 4 to 8 weeks to achieve the euthyroid status [37]. Such a compound becomes preferentially iodinated by TPO, avoiding the iodotyrosine formation by Tg and gradual disruption of iodine storage in the thyroid, since the iodinated thionamide residues are metabolized peripherally [38]. Once the euthyroidism is reached, CBZ can be administered in a "dose titration" regimen starting at 20 mg/day dosage and gradually reduced to 5-10 mg/day, according to the thyroid functions (i.e. TSH and fT4 levels), which have to be tested every one or two months.

The lowest effective dosage is usually administered for 12-18 months, to ensure the optimal remission (i.e. recovery from the disease) of the disease, and stopped. In GD patients with already a concomitant eye disease (which will be extensively discussed in the following paragraph), a “block and replace” regimen is usually preferred (e.g. CBZ at a fixed dose of 40 mg/day plus levothyroxine 100 µg/day to maintain the euthyroid status) to quickly control the thyroid function and avoid the hyper-hypothyroid fluctuations, known to worsen the eye condition. In case of recurrent GD relapses after thionamides withdrawal, radioiodine (^{131}I) or thyroidectomy followed by a lifelong replacement with levothyroxine might be considered. Relapsing GD patients with eye disease may also undergo thyroidectomy instead of radioiodine treatment. Since some GD patients may experience side effects with CBZ (e.g. erythema, agranulocytosis), the propylthiouracil (PTU) might be used instead, although it can have higher risk of developing neutropoenia (i.e. abnormally low concentration of neutrophils in the blood) and liver toxicity than CBZ. PTU is only preferred in the first trimester of pregnancy, since it has been shown to lower the incidence of foetus malformations compared to CBZ, which is then used from the second trimester onwards.

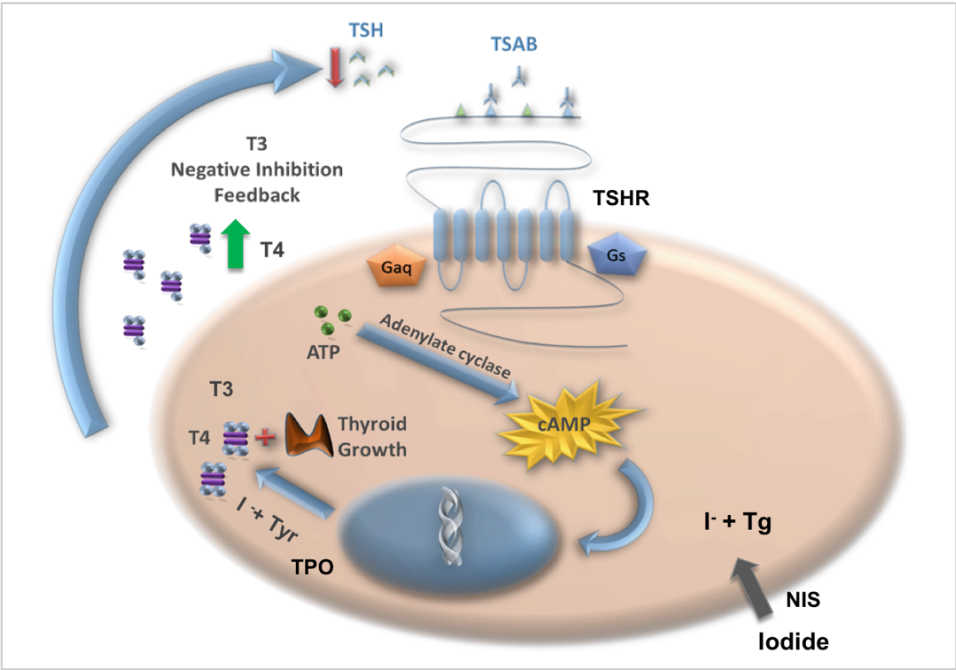

Figure 1.4. Activation of the TSHR in Graves’ disease.
TSHR autoantibodies (TRABs) compete with the TSH for binding the TSHR. The high levels of T3 and T4, repress the TSH expression and the TRAB signalling predominate, along with the overexpression of the genes and the overproduction of thyroid hormones. (Modified from http://www.indigo-iapp.eu).

1.1.3. Graves' orbitopathy

About 30-50% of GD patients may experience some sign of eye disease called Graves' orbitopathy (GO), while 5% of them develop a severe form, which involves inflammation and remodelling of the orbital tissues leading to proptosis, corneal exposure, and diplopia. Symptoms range from eye irritation, watering, discomfort to dry eyes, grittiness and photophobia; in severe cases GO (3-5% cases) may result in blindness (Figure 1.2). For these reasons, GO patients may experience a reduction of their quality of life, and develop psychological distress due to the disfiguring phenotype of the disease (i.e. protrusion of the eyeball, eyelid retraction). GO is still considered a rare disease, with 10-16 per million per year incidence and 2-4/10,000 prevalence [39].

The excess of adipogenesis (i.e. differentiation of pre-adipocyte into mature adipose tissue) and the over-production of extracellular matrix (ECM) have been shown to drive the orbital tissue remodelling and the increase in volume of the adipose/connective tissues that lead to proptosis, as extensively reviewed in [40, 41]. The adipogenic cascade is responsible for the orbital fibroblast expansion (ranging from a 30μm diameter of a pre-adipocyte to 150μm in mature adipocyte) and involves the activation of different key transcription factors for adipocyte differentiation, namely the CAAT/enhancer-binding proteins alpha (C/EBPa) and the peroxisome proliferator activated receptor-gamma (PPAR-γ). Oedema and proptosis are instead consequences of the overproduction of ECM including glycosaminoglycans (GAGs) and collagens. The hyaluronate (HA) is the major representative amongst GAGs in the orbital tissues and is mainly produced by the HA synthetase 2 (HAS2) [42], followed by the chondroitin sulphate. The two mechanisms of adipogenesis and HA production in the orbit are not acting independently one to another; but perhaps they are linked to each other through the regulation of the HAS2 expression itself in a depot-specific manner [43].

Are TRABs and pathways involved in GD also responsible for GO pathogenesis? In the majority of the cases, GO arises after the first episode of hyperthyroidism, suggesting a temporal association between the two diseases and patients with higher titres of TSAB are more likely to develop signs of GO [44]. Moreover, the more relapsing episodes of GD (i.e. uncontrolled hyperthyroidism), the higher the risk of developing GO. We have recently confirmed a higher TRAB levels in a group of GO patients used to identify disease biomarkers using proteomics and genomics, when compared to the cohort of patients with GD but free of GO [45]. The second evidence is supported by the fact that the TSHR is expressed in the orbital fibroblasts. Zhang and collaborators reported the activation of the TSHR signalling via the cAMP pathway in human orbital fibroblast leading to the initiation of adipogenesis [46], and to the HA production in human pre-

adipocytes/fibroblasts cell line [42]. The monoclonal antibody M22, instead, was able to induce the differentiation of the human orbital fibroblast into adipocytes through the PI3K pathway, at least in part [47]. It has been reported later that the mechanistic target of rapamycin complex 1 (mTORC1) is necessary for adipogenesis, while the PI3K signalling regulates the HA production via HAS2 in the orbit [48]. Such pathways have been further investigated to possibly develop non-immunosuppressive therapy for GO, such as inhibitors of the transcription factor Forkhead box O (FoxO) activated in the PI3K pathway [49]. It is interesting to note that in our recent study on proteins and miRNAs as circulating biomarkers for GD and GO, PI3K-Akt signalling and ECM-receptor interaction pathways but also mTOR, FoxO and PPAR were identified [45].

Also, orbital fibroblasts express the insulin like growth factor receptor-1 (IGF1R) [50], considered as a possible second autoantigen in GO. However, whether autoantibodies against the IGF1R are present in GO patients, remains controversial [51]. Studies from Zhang and collaborators demonstrated the involvement of the IGF1R signalling via PI3K-mTORC in activating the production of HA in the orbit alone [43] or in combination with the TSHR, specifically triggering the HAS2 isoform [48]. The latest data sustained a previous hypothesis that both autoantigens (TSHR and IGF1R) are involved in GO pathogenesis [52].

Pharmacological and surgical treatments for GO are usually based on the clinical activity score (CAS), which consists of ten items assigned on four signs of inflammation (e.g. pain, redness, swelling and impaired functions). CAS was initially developed to predict the efficacy of immunosuppressive treatments in GO [53] and still used nowadays [54]. Intravenous steroid bolus (as immunosuppressive regimen) and/or local radiotherapy are mostly performed in the active phase of disease (i.e. inflammation signs and CAS > 4), while during the inactive or fibrotic phase, in case of persistent exophthalmos or diplopia, a surgical orbital decompression might be recommended. Supplementation with selenium has also shown beneficial effects, since it improved the quality of life of GO patients accompanied by a slowed progression of the eye disease and less eye involvement compared to placebo in a 6-months trial [55], possibly due to its antioxidant function.

1.1.4. Immunological basis of GD/GO

The immune system plays a major role in GD and GO pathogenesis. On one hand, the autoimmune response to thyroid autoantigens requires a first break-down of the immune-tolerance, resulting in the production of IgG1 subclass autoantibodies [56]. On the other hand, pro-inflammatory and innate immune system cells are usually present in high

number in both the thyroid and the orbital fibroblasts during GD/GO pathogenesis. GD patients serum was enriched by a number of circulating proinflammatory cytokines such as tumour necrosis factor-alpha (TNF-α), IL-2, IL-6, IL-8 and IL-17 [57-59], while IL-1 and TNF-α were produced by intrathyroidal infiltrated lymphocytes [60]. Such an inflammatory status is also sustained by thyroid-cells-secreted proinflammatory cytokines such as TNF-α, interferon-gamma (IFN-γ) and IL-1. Interestingly, increased serum and PBMCs levels of IL-37, known to suppress inflammatory response, were reported in a Chinese GD cohort compared to healthy control, possibly representing an attempt of the immune system to suppress the concomitant inflammation in GD [61].

Antigen-specific T cells have been reported in the thyroid, in which the Th1 immune response may sustain a more destructive outcome in the thyroid cells via apoptosis, and the Th2-mediated response, in turn, may sustain the production of stimulating antibodies by B cells and enhance the autoimmune response [62]. RNA sequencing performed on thyroid tissue of GD patients revealed the high expression of immune system genes (in particular B cells genes in the top 100 genes), followed by signalling cascades and metabolic processing genes compared to normal thyroid tissues [63]. In particular, six human leukocyte antigen (HLA) genes were in the top-15 most upregulated genes, followed by four between chemokines and cytokines gene or regulators, plus growth and synthesis-related genes and one uncharacterized protein compared to that of healthy controls. HLAs, the human counterpart of the MHC genes, play a key role in the immune system through the presentation of the processed antigens to the T cells in a specialized manner. Class I HLA in fact, interacts with the CD8 lymphocytes activating a cytotoxic immune response, while Class II HLA presents the antigen to CD4 which are involved in the regulation of specific immune response. Antigen presentation pathways were the most abundant from those related to the immune system, followed by T-helper signalling and B cell development, suggesting considerable involvement of immune system activation in GD compared to normal thyroid, from both the innate and the adaptive sides.

Within the orbit, infiltration of macrophages, B and T cells (Th1 and Th2) and natural killer (NK) cells have been reported. Cytokines such as IL-6 and RANTES participate in the recruitment of T cells in the orbital fibroblasts, while TGF-β, IFN-γ and TNF-α possibly counteract the adipogenesis mechanism, as reported in [62].

Mechanisms preventing or driving the autoimmune response are described in the next paragraphs, more in general and with specific examples for GD/GO, since they tend to be quite common amongst autoimmune conditions. It is also possible that patients with a particular autoimmune disease would develop a second different autoimmune condition later.

1.2. MECHANISMS PREVENTING AUTOIMMUNITY

A singular characteristic of adaptive immunity is the sufficiently large repertoire of receptors, expressed by both T cells (TCR) and B cells (BCR). The activation of these cells usually requires a two-signal process: the antigen-specific stimulatory signal and the non-antigen stimulatory signal (or co-stimulation) often provided by the interaction with other molecules produced by the innate immune response actors. Generally, the activation of a B cell requires a first signal of activation provided by the interaction between the B-Cell Receptor (BCR) and the antigenic epitope and the co-stimulation provided by T cells (T-helper cells). Once the appropriate lymphocyte recognizes and binds selectively to the antigen, the resulting activation is serially replicated and production of a clone of lymphocytes all expressing the same antigen-specific receptor. The efficacy of the adaptive immune system relies on the total range of receptors on the lymphocyte populations which are able to recognize virtually any foreign epitopes they would have previously encountered [64]. The immune tolerance to self-antigens, instead, is generally well preserved by both T cells and B cells in the central immune system and in peripheral tissues.

1.2.1. Central immune tolerance

During their development, lymphocytes undergo a mechanism of “clonal selection” through which the early exposure (i.e. during the generation of the lymphocyte) of the cognate antigen of a lymphocyte receptor leads to the death of that lymphocyte rather than its proliferation [65]. This should avoid the presence of circulating clones that react to self-antigens defined as auto-reactive cells. The selection process is different for T cells in the thymus and B cell clones in the bone marrow. T cells usually undergo a two-step selection process. Their T-Cell Receptors (TCR) have a unique ability to transmit both weak and strong signals depending on the number and the specificity of the antigenic peptides bound, in other words, depending on their affinity and avidity for that antigen. In the “positive selection”, weak signals derived from the interaction between TCR and the antigen processed and presented by the major histocompatibility complex (MHC) generally allows the survival and the differentiation of a T cell clone, otherwise strong signals would eliminate that clone via apoptosis. On the other hand, during the “negative selection” process all clones that react with self-antigens would usually be removed from the thymus, promoting the immune tolerance at a central level [66]. The process of thymus education is sustained by the self-antigen presentation that arises in the thymic medulla. Central immune tolerance to thyroid antigens such as the TSHR is sustained by the intrathymic expression of the TSHR mRNA. One proposed

mechanisms, in fact, involved the exposure of thyroid antigens to T cells in the thymus, promoting a state of anergy (i.e. non-responsiveness to specific antigens) against them [67, 68]. A lower intrathymic expression of the TSHR mRNA either due to genetic variants, epigenetic, environmental contributions or a combination of those (which will be described later in in this chapter), might be responsible for the loss of immune-tolerance to this antigen leading to self-reactive T-cells survival, as also demonstrated in a recent study in an animal model of GD [69]. Also, evidence supporting this proposed mechanism come from the autoimmune polyendocrinopathy-candidiasis-ectodermal-dystrophy (APECED) in mice [70] or the polyendocrine syndrome type 1 (APS-1) in humans [71], caused by defects in the autoimmune regulator (AIRE) protein leading to the production of autoantibodies to multiple organs. The AIRE gene, primarily expressed in the thymus, but also on peripheral tissues on dendritic cells, encodes for a transcription factor which regulates the expression of numerous self-proteins in the thymic medulla such as for example insulin [72]. Accordingly to its function, mutations in this gene impairs the presentation of the self-antigens and leads to autoimmune response.

Positive and negative selection processes, however, are likely to be influenced by the absence of the secondary co-stimulation signal but also by the modality of antigen presentation itself [73]. Unlike T cells, B cells diversify their antigen receptors (BCR) binding specificity at two different stage of diversification. After the initial variable (V) region gene rearrangements, B cells undergo the negative selection in the bone marrow. The encounter of the B cell with an antigen in the absence of the non-antigenic specific signal may lead the cell to enter a state of anergy. However, this state of non-responsiveness may be reversed if the secondary stimulatory signals are provided later in life from other sources as, for example, an infection. On the other hand, auto-reactive BCRs can avoid deletion undergoing a secondary receptor re-arrangement mechanism or receptor editing [74]: the rearranged Ig V-region gene with specificity for an auto-antigen can be “edited” and replaced with different antibody gene arrangements. After receptor differentiation, the unique challenge to maintain the B-cell self-tolerance is the second run of BCR diversification in which B cells are recruited into the germinal centres (GCs) in a T-cell-dependent immune response fashion [75]. In GCs, somatic hypermutation (SHM, i.e. accumulation of mutations in the variable V-regions of the immunoglobulins) naturally occurs in order to generate high-affinity antigen binding sites [76]. However, the random nature of mutations in V-regions via SHM may lead to the generation of self-reactive B cells in the GCs that have the potential to trigger production of antibodies directed against self-antigens (auto-antibodies).

According to the general view provided by the large amount of literature over the past sixty years, the elimination processes of self-reactive lymphocytes, both T cells and B

cells, are naturally imperfect and the survival of lymphocytes capable of auto-immune response is quite common [77], also for the clearance of self-damaged cells. The presence of autoantibodies specially, is remarkable since it was observed that much of the total immunoglobulin content of the human serum includes naturally-occurring autoantibodies [78], while cross-reactive autoantibodies have been characterized in a number of autoimmune diseases, often preceded by infections, such as rheumatic arthritis [79], Chagas disease, Guillain-Barrè syndrome [80] and, as already described, GD [56]. Moreover, the presence of SHM features on most pathogenic autoantibodies suggests a failure in self-tolerance mechanism in GCs [75]. Patterns of somatic hypermutation in both light and heavy chains were described in two mAbs derived from a mouse model of GD immunised with TSHR [81]. Whether the immune tolerance is broken at either T cell or B cell level is still debated.

1.2.2. Peripheral tolerance

The process of elimination of self-reactive B or T lymphocytes in the thymus might be incomplete, leading to the escape of self-reactive clones into the circulation. Since many antigens may not be presented at a sufficient level of expression in the thymus, antigen presentation is sustained also at the draining lymph nodes and/or in organs, such as the thyroid gland. Evidence suggested that the presentation of the thyroid autoantigens such as the thyroglobulin and the shed TSHR A-subunit, either in the thyroid gland or in the peripheral draining lymph nodes, is mediated by the mannose receptor (ManR) expressed at the cell surface of dendritic cells. Whether such an auto-antigen presentation leads to immune response or tolerance has to be further investigated as proposed in [82]. The immune tolerance is also promoted peripherally (peripheral immune tolerance) through a different mechanisms [83].

Anergy of T lymphocytes prevents auto-immune response also in peripherally sites. As mentioned before, proliferation and differentiation of naïve T cells require i) the signal provided by the TCR and the processed peptide-MHC and ii) co-stimulation via APCs (CD80 and CD86). While CD28 constitutively expressed on T cells sustains their survival, CTLA-4 (CD152) promotes T lymphocytes anergy, along with the inhibition of IL-2 expression. Moreover, CTLA-4 blocks the $CD4^+$ lineage with higher influence compared to the $CD8^+$.

Apoptotic death of T cells leads to the removal of pro-inflammatory lymphocytes at the end of the immune response to foreign antigens, but also of T cells with high avidity for a self-antigen. Repeatedly antigen-stimulated lymphocytes are usually removed through the activation-induced cell death (AICD) pathway, which promotes apoptosis mediated

by Fas, Fas-ligand (Fas-l) and caspase 8. Inhibition of AICD is performed by both protein blocking the death receptor (e.g. FADD-like IL-1B converting enzyme protein) and IL-2. Mutations in the *Fas* gene in lpr mouse model inhibits the regulation of the peripheral tolerance and leads to lymphadenopathy (i.e. enlarged secondary lymphoid tissues) along with autoimmunity and production of auto-antibodies similarly to SLE [84]. Similarly, the autoimmune lymphoproliferative syndrome (ALPS) is caused by mutations in either Fas or Fas-l genes [85].

A particular case of peripheral tolerance is represented by the self-antigen sequestration by barriers or its expression into a privilege site (e.g. brain, eye and testis), where the self-antigen is not physiologically and immunologically available to lymphocytes or processed via APCs. In privilege sites, in fact, self-antigens or pro-inflammatory antigens are removed via apoptosis or suppressed via cytokines (IL-10/ TGF-β) as a general suppressive mechanisms without any distinctions on the type of antigens.

Tregs are T-helper lymphocytes characterized by the expression of CD4 (T helper), CD25 (IL-2 receptor a chain) and the transcription factor Foxp3, as extensively reviewed in [9, 36, 86] (Figure 1.5). Naturally-occurring Tregs (nTregs) are produced in the thymus during the normal T cells maturation process and enter the blood circulation to exert their function in protecting against self-reactive lymphocytes. While they already express Foxp3, IL-2 and TGF-β are essential for their generation, expansion and their survival outside the thymic environment, respectively [87]. Induced Tregs (iTregs), instead, are generated directly in the peripheral lymph nodes as the result of the antigen presentation to the naïve $CD4^+$ T cells. Foxp3 expression driven by IL-2 and TGF-β is essential for their differentiation. By secreting TGF-β and anti-inflammatory IL-10, Tregs are involved in the clearance of self-reactive T cells in the periphery, usually operated by a subset of cells expressing the $CD8^+$ and $CD122^+$ (IL-2 receptor β-chain) [88]. Moreover, Tregs negatively regulates the immune response against foreign antigens (e.g. through the expression of the CTLA-4), avoiding a prolonged inflammation which may turn into a chronic disease. The role of gut-mucosa associated Tregs is described in section 1.6 below.

An important concept in the outcome of autoimmune diseases is the disruption of the balance between Tregs and Th17 cells. Beside the Th1 and the Th2 immune response, driven respectively by IL-18/IL-12 and IL-2/IL-4, the Th17 immune response is characterized by the IL-17-secreting T-helper 17 (Th17) cells involved in the protection of mucosa such as skin, gut and lung against fungal (e.g. *Candida albicans*) or bacterial infections [86, 89]. Pathways and molecules differentiating naive T cells into Th17 cells are very similar to those differentiating into Tregs (Figure 1.5). TGF-β plays a critical role

in determining the activation of one immune response at the expenses of the other, since the expression of Foxp3 (Tregs) and RORγt (Th17) transcription factors is regulated by the same cytokines but in a mutually exclusive manner [90]. TGF-β alone provided to naïve T cells, without any other inflammatory stimulations, promoted the Tregs differentiation inducing the Foxp3 expression *in vitro*, which inhibited the RORγt expression [91]. However, the TGF-β induce the retinoid-related orphan receptor (RORγt in mice and ROR-c in humans) and the signal transducer and activator of transcription 3 (STAT3) in differentiating into Th17 in presence of IL-6, IL-21 and IL-23 [9, 90, 91]. In murine Th17-cell differentiation, TGF-β and IL-6 cytokines are sufficient for inducing the IL-17 expression in naïve T cells through the expression of RORγt; while IL-21 and IL-23 are necessary for their subsequent amplification, expansion and phenotype stabilization, respectively [86]. In humans, both TGF-β and IL-21 are able to induce the differentiation in Th17, while amplification of ROR-c-expressing cells is sustained by IL-1β and IL-6 and ultimately, IL-23 is responsible for their expansion and stabilisation. Interestingly, the IL-23 receptor (IL-23R) expression is likely to be promoted by TGF-β/IL-6/IL-21 [92]. Once differentiated, Th17 cells secrete not only IL-17 but also IL-21 and IL-22 and their effects are reviewed in [89, 93], including the activation of proinflammatory chemokines and cytokines in non-hematopoietic and mesenchymal cells or in myeloid cells (IL-6 and G-CSF). Interestingly, IL-17, as well as the NF-kB, may activate the CAAT/enhancer-binding proteins (C/EBP) transcription factors [94], which I've previously described involved into the orbital adipogenesis cascade.

The imbalance between Tregs and Th17 leading to autoimmune conditions can be promoted by the presence of elevated Th17 cell numbers or by self-reactive Th17 cells on one hand, and by the reduction in the number of the Tregs milieu or of a reduced efficacy on the other hand. Multiple sclerosis, psoriasis and IBD, amongst others, showed an impairment of the Tregs/Th17, as reviewed in [86, 89, 93]. In GD patients not treated with antithyroid medications, Mao and colleagues showed a reduced $CD4^+$ $CD25^+$ $Foxp3^+$ natural Tregs milieu, possibly due to the polarization of the dendritic cells which induced their apoptosis. Moreover, hyperthyroidism worsened such condition [95].

B-cell tolerance is also exerted peripherally, since B cells leaving the bone marrow can be considered relatively immature. B cells outer the T cell area are usually short-lived (1-3 days) and only in the follicles can survive longer (1-4 weeks) re-circulating. In presence of self-reactive B cells, mechanisms of anergy, preventing migration into B cells follicles and cell death are promoted. Although self-reactive clones may be left circulating to enhance the immune response to a wider range of foreign antigens. In absence of infection and co-stimulation, B cells enter anergy and apoptotic pathways rapidly. Also

secondary B cells, thus generated from memory B cells, are highly susceptible to tolerance and would be eliminated as soon they acquire self-reactivity. Similarly to Tregs, B cells with suppressor functions (Bregs or B10) have been described, as extensively reviewed in [96]. Heterogeneous subsets of Bregs have been described and they are more likely to be derived from B cells to suppress local inflammation under certain stimuli, since there is no particular transcription factor at the moment capable of driving their differentiation as for the Tregs. By producing IL-10, TGF-β and IL-35, Bregs directly promote a T cells differentiation into Tregs both in humans and mice [97, 98]. Moreover, they indirectly suppress the Th1 and Th17 differentiating lymphocytes suppressing the driving pro-inflammatory cytokines production by DCs [99]. Zha et al. [100] isolated and stimulated *ex vivo* B10 cells from GD patients (without any antithyroid drug) and healthy controls PBMCs and quantified the amount of IL-10 produced. Newly diagnosed GD patients showed a lower proportion of B10 cells, which belonged to the $CD19^{+}CD24^{high}CD27^{+}$ B-cell subset, compared to healthy controls. Interestingly, GD patients in disease remission shared similar frequency of B10 cells with that of healthy controls, but a lower proportion of them in the total PBMCs. Such a subset of Bregs was shown to negatively regulate $CD4^{+}$ T cells proliferation through both IL-10-dependent and independent pathways, at least *in vitro*, and this function was impaired in GD patients. Patients with other autoimmune disorders such as rheumatoid arthritis, multiple sclerosis and SLE reported a higher B10 proportion compared to healthy controls [101].

1.2.3. Role of the innate immune system cells

For years the innate immune response was not considered to be important in the outcome of ADs and most of the theories proposed, in fact, did not take into account the role played by innate immunity cells, receptors and pro-inflammatory molecules as possible inducers of an autoimmune response. As the first line of immune defense, the innate immune system acts to recognise conserved microbial features, known as pathogen-associated molecular patterns (PAMPs), through a group of germline-encoded pattern recognition receptor (PRRs). Toll-Like receptors (TLRs) are able to recognize PAMPs, such as bacterial lipopolysaccharide (LPS) and flagellin and initiate an effective immune response that may involve the activation of the adaptive immune system. As well as the adaptive immune response, several pathways of the innate immune response may lead to an autoimmune outcome, as reviewed in [102]. Variants in innate immunity-related and autophagy genes that confer susceptibility to the host have been described [103]. In particular, single-nucleotide polymorphisms (SNP) in the TLR4 and TLR5 able to selectively recognize and bind the bacterial LPS and the bacterial flagellin, respectively, have been associated with different autoimmune conditions such as

rheumatoid arthritis, Crohn's disease and SLE, as recently reviewed in [104, 105]. More recently, the polymorphism rs5744174 of the TLR5 gene was associated with GD in females but not in males in a Chinese cohort. In particular, the AC haplotype in TLR5 (rs2072493–rs5744174) and the C of rs5744174 were associated with reduced susceptibility, while the TC and TC/CC genotypes were shown to be protective for the disease [106]. Instead, no significant association of TLR4 polymorphisms were found in the Chinese cohort [106] or in a Taiwan Chinese population [107].

Figure 1.5. Schematic representation of the $CD4^+$ and $CD8^+$ T-cell lineages and their differentiation into regulatory T cells.
(next page). $CD4^+$, $CD8^+$ T cells and $CD4^+$ $CD25^+$ $Foxp3^+$ natural Tregs (nTrges) originate in the thymus and colonise secondary lymphoid tissues, after surviving clonal selection process. In periphery, Naïve T cells undergo Th1/Th2/Th17 differentiation according to the type of interleukins they are expose to, or become cytotoxic $CD8^+$ T cells. Th17 cells differentiate under exposure of IL-6 and TGF-β (in humans under IL-21 and TGF-β) and necessitate of IL-1β and IL-6 for amplification and IL-23 for clonal expansion and stabilisation. nTregs need IL-2 and TGF-β for expansion and stabilisation in the peripheral sites. Inducible Tregs (iTregs) originate instead from either $CD4^+$ or $CD8^+$ T cells after the antigen (or self-antigen) presentation *via* APCs. iTregs in presence of IL-2, TGF-β and retinoic acid (RA) differentiate into $CD4^+$ $CD25^+$ $Foxp3^+$ iTregs, while in presence of IL-10 differentiate into Tr1 $CD4^+$ $CD25^{low}$ $Foxp3^+$ iTregs. Suppression of APCs activity is mediated by iTregs *via* the downregulation of co-stimulatory signals or upregulation of CTLA4 or by nTregs *via* DCs inhibition. Suppression of the Th1/Th2/Th17 responses is mediated by both nTregs and CD4+ and CD8+ iTregs, through cell-to-cell contacts, the upregulation of CTLA4 and production of IL-10, TGF-β and possibly IL-35. (Modified from [108]).

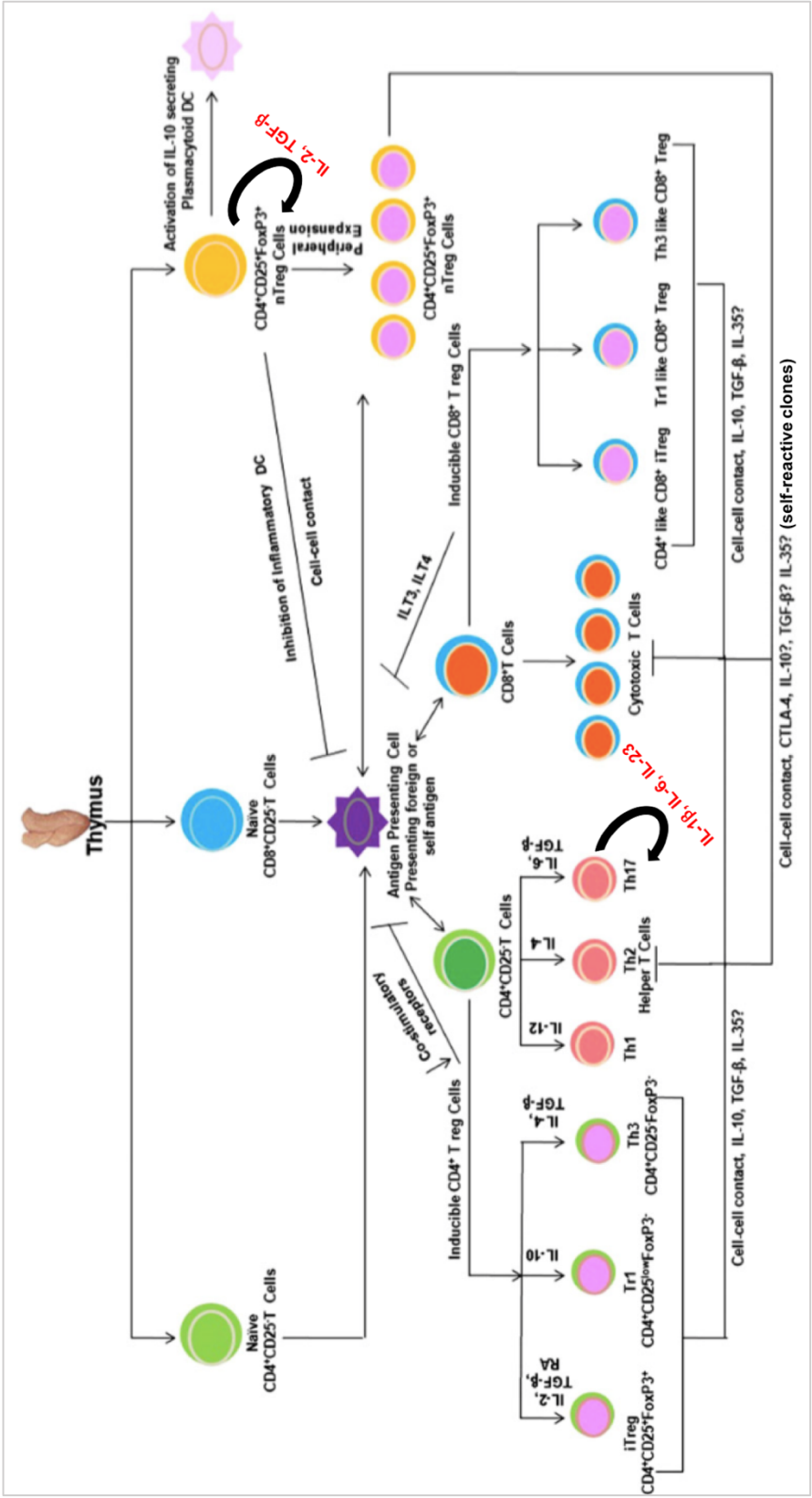
Thymus
Naive CD4+CD25-T Cells
Naive CD8+CD25-T Cells
Activation of IL-10 secreting Plasmacytoid DC
CD4+CD25+FoxP3+ nTreg Cells
IL-2, TGF-β
Peripheral Expansion
CD4+CD25+FoxP3+ nTreg Cells
Inhibition of Inflammatory DC
Cell-cell contact
Antigen Presenting Cell Presenting foreign or self antigen
Co-stimulatory receptors
ILT3, ILT4
Inducible CD4+ T reg Cells
Inducible CD8+ T reg Cells
CD8+T Cells
Cytotoxic T Cells
IL-1β, IL-6, IL-23
CD4+CD25-T Cells
IL-12
IL-4
IL-6, TGF-β
Th1
Th2
Th17
Helper T Cells
IL-2, TGF-β, RA
IL-10
IL-4, TGF-β
iTreg CD4+CD25+FoxP3+
Tr1 CD4+CD25low FoxP3-
Th3 CD4+CD25-FoxP3-
CD4+ like CD8+ iTreg
Tr1 like CD8+ Treg
Th3 like CD8+ Treg
Cell-cell contact, IL-10, TGF-β, IL-35?
Cell-cell contact, IL-10, TGF-β, IL-35?
Cell-cell contact, CTLA-4, IL-10?, TGF-β? IL-35? (self-reactive clones)

1.3. MECHANISMS TRIGGERING THE AUTOIMMUNE OUTCOME

"*Even if some form of B cell and T cell natural autoimmunity is universal, autoimmune diseases are not a frequent event* [64]". So what may determine the breakout of an autoimmune condition seems to be a combination of the auto-immune stimulus, possibly given by the environment and the polygenetic predisposition of the host. Those factors have been investigated for years and molecular mechanisms whereby tolerance can be broken have been proposed. To better represent their contribution in the breakdown of immunological tolerance, they could be divided into two classes, the "intrinsic and extrinsic mechanisms".

1.3.1. "Intrinsic mechanisms" leading to autoimmune diseases

"Intrinsic mechanisms" include molecular mechanisms distinct to the host by which immune tolerance can be broken down, such as the genetic background, mechanisms of antigen presentation, education processes of lymphocytes, B cells and T cells regulatory pathways, some of which have already been described in previous paragraphs. It is not fully understood how they start to get compromised.

The genetic background of ADs was investigated both in humans and animal models (as reviewed in [36, 64, 109]) and the general assumption is that genes confer most susceptibility to the host, determining the risk of developing an autoimmune disorder, rather than directly causing the disease. There are very few autoimmune conditions that are connected to rare single-gene mutations, such as the mutations in the Autoimmune Regulator (AIRE) gene responsible for the development of APECED, previously mentioned. However it has been generally recognized that the most common autoimmune diseases are non-Mendelian polygenic diseases. The main source of genetic susceptibility is the Human Leukocyte antigen (HLA), also known as Major Histocompatibility Complex (MHC) in mice, whose contribution was discovered initially in experimental thyroiditis and then attributed to virtually any autoimmune diseases, both in murine models and humans [110, 111].

In the past years, HLA loci were associated to either conferring susceptibility or protection from the development of GD to the host, as reviewed in [112]. In Class II HLA, the variant HLA-DRB1*03 with an Arginine in position 74 seemed to confer susceptibility to GD [113], although it was not always confirmed; while the HLA-DRB1*07 with Gln-74 was associated with a decreased frequency among GD compared to controls. For Class I HLA, the HLA-C*07 was associated with GD, while C*03 and C*16 had a more protective effect [113]. However, even if common variants or genetic loci remain to be identified, HLA remain the strongest amongst the genetic factors for predisposition of

GD. Other genes found to confer susceptibility in most autoimmune conditions belong to the cluster of genes that usually regulates immune responses such as the cytotoxic T lymphocyte-associated protein 4 (CTLA4), CD40, protein tyrosine phosphatase-22 (PTPN22), programmed death 1 (PD1) and IL-23 receptor (IL-23R), which are commonly shared amongst different autoimmune conditions. Of interest, two polymorphisms of IL-23 (rs10889677 and rs2201841), despite conferring susceptibility for Crohn's and rheumatoid arthritis, were associated to GO rather than to GD [114], suggesting a possible cross-talk of the Th17 immune response in the GO pathogenesis.

Genetic susceptibility is also often attributed to gene variants expressed in the target organ such as the TSHR in GD, Tg in Hashimoto's thyroiditis and Insulin in T1D. Gene variants that occur at the promoter site of those genes, especially, seem to affect the expression of the autoantigens in the thymus: the lower the intrathymic expression of these genes, the higher the risk of developing autoimmunity. In individuals with particular genetic variant for the insulin gene, a decreased intrathymic expression of insulin was associated with a decreased central tolerance to insulin that can lead to an autoimmune response to insulin and to type 1 diabetes [115]. Similarly, several Single Nucleotide Polymorphisms (SNPs) have been described in the TSHR gene conferring genetic susceptibility to GD [116-118]. In particular, two of them mapping to the TSHR promoter region [112, 119], were recently associated with a decreased expression of the TSHR in the thymus and, in turn, a higher risk of developing autoimmunity to TSHR, as previously introduced [67, 68]. However, loci conferring genetic susceptibility to AD (and GD in particular) failed to be completely generalized since they reflected the genetic variability of the ethnic groups in which they have been investigated [112].

Another component of genetic susceptibility of interest is sex, especially for autoimmune thyroid diseases (AITDs) such as GD, where the female predominance is remarkable. Establishing the reasons why women are more likely to develop ADs is difficult. Female hormones seem to play an important role in the outcome of these pathologies, as shown by the influence of oestrogens in the B cell repertoire [120]. Hormone levels themselves might be regulated by the presence of certain types of gut bacteria, regulating the risk of developing an AD [121]. In AITD, the connection between sex differences and leptin has been proposed [122]. Also, the role of foetal microchimerism in pregnant women has been connected either to the initiation or the exacerbation of AITD and GD, but also to cancer development [123, 124]. The presence of foetal cells in the maternal body during pregnancy, in fact, may lead to the breakdown of immune tolerance, especially after the delivery when the mother's immune suppression mechanisms are lost. However, these theories are not applicable for other autoimmune conditions such as rheumatoid arthritis

and multiple sclerosis that are quite balanced between sexes, or for myocarditis which occurs more in males.

In parallel to the genetic variation of the host, an emerging compromising mechanism seems to involve epigenetics that, instead of genetics, refers to molecules and pathways that control expression of individual genes in a manner that goes beyond the sequence of DNA. The structural composition of the chromatin, in fact, influences whether a gene is expressed and at which level and, on the structural chromatin composition itself is regulated by epigenetic modifications. These include post-translational modification of a single residue, e.g. methylation of DNA cysteines, or important post-translational modification at a nucleosome level (e.g. ubiquitination, acetylation and methylation), but also chromatin remodeling or gene silencing by RNA interference (RNAi) and non-coding RNAs. All together, these modifications can either activate or inactivate gene expression, depending on their amount and localization [125]. Several lines of evidence connect epigenetics to autoimmune outcomes. The case of the AIRE gene, encoding for a transcription factor that regulates the expression of several important self-proteins in the thymus (e.g. insulin) [72], represents the contribution of the epigenetics in the APECED's outcome. In GD, the reduction of the intratymic TSHR mRNA expression resulting in the loss of immune-tolerance might be triggered by epigenetics. As described in elegant work by Tomer and collaborators, thyroid cells exposed to INF-alpha (triggered for example by a viral infection) display an enriched methylation pattern in the intron 1 of the TSHR spanning two SNPs previously associated with GD. One of those, rs12101261, serves as a binding motif for the transcriptional repressor promyelocytic leukaemia zinc finger protein (PLZF). These results can also be transposed to the central immune system, since the intrathymic down-regulation of the TSHR mRNA was observed in patients homologous for the rs12101261 SNP which negatively correlated with levels of PLZF in the thymus [67].

MicroRNA (miRNA) are small non-coding RNA sequences (about 22 nucleotides) that can regulate the expression of protein-coding genes even *in trans* since they can be found circulating in the blood. Their role in repressing gene expression was found in cancer and in autoimmune diseases [126], such as multiple sclerosis, type 1 diabetes and systemic lupus erythematosus. In GD, two (hsa-miR-30c-2* and hsa-let-7b*) out of 16 miRNAs differentially expressed were upregulated in the peripheral blood mononuclear cells (PMBC, i.e. lymphocytes and monocytes) of patients compared to controls. Three miRNA were associated with the newly diagnosed patients, since they were normally regulated in remission [127]. Other upregulated miRNA (miR-636 and miR-30a-5p) suppressed genes involved in the retinoic acid pathway in the Tregs of GD patients [128]. Recently, we identified five novel circulating miRNA as biomarkers for

distinguishing GD or GO patients, such as Novel:19_15038 miRNA and Novel:hsa-miR-182-5p both up-regulated in GO, from controls from a robust analysis combining both differential expression (DE) analysis and Lasso-penalized prediction models. miRNAs with a known functions were identified from the DE analysis only [45].

Given that genetic/epigenetic susceptibility is necessary but not sufficient for the development of autoimmunity, immune tolerance is at the very basis of an autoimmune outcome and environmental factors, in combination with the genetic predisposition, account for its breakdown.

1.3.2. "Extrinsic mechanisms" underlying autoimmune diseases

1.3.2.1. The hygiene hypothesis

Epidemiological observations are reporting an increase in type I hypersensitivity (allergy) and autoimmune diseases incidence (such as IBD, ulcerative colitis, and MS…) in developed countries, as reviewed in [129, 130], whereas the exposure to potentially harmful microbes is reduced by a number of preventing measures such as vaccinations, personal hygiene, antibiotic usage and water treatments. Although allowing a higher survival rate and an improved quality of life, such measures may lead to a dysregulation of the immune system for not being exposed to a sufficiently wide repertoire of environmental and microbial epitopes. In the so-called "hygiene hypothesis" [131], a correct exposure to micro-organisms and parasites is of a particular importance in the early-stage of life, when the immune system is trained to discriminate between self and non-self. Children growing up in a farm environment seem to be more protected from asthma and allergies reactions than children in urban environment, possibly due to proper modulation of both innate and adaptive immune systems by microbial and environmental exposure before or soon after birth [132]. Also differences in farming practises may also have an impact. USA Amish children, exposed to a traditional farming environment shown a lower incidence of asthma and allergic reactions along with an increased levels of endotoxins compared to the USA Hutterite children, living in a more industrialized farming environment. The exposure to the dust extracts of the Amish, but not to the Hutterite's homes, prevented the development of allergic features in an experimental allergic asthma mouse model [133]. Hygienic measures may also influence the composition of the gut microbiota, which in turn (as it will be later discussed) has an effect in training a proper immune response, possibly increasing the incidence of autoimmune responses. Vatanen and collaborators from the DIABIMMUNE project reported the higher presence of *E. coli*-derived lipopolysaccharide (LPS) in the gut microbiota of Russian children along with a decreased incidence of developing type 1

diabetes (TD1) compared to that of infants from Estonia and Finland, whose microbiota was increased in *Bacteorides dorei* LPS and with an higher incidence of TD1. Moreover, administration of *B. dorei*-LPS did not prevent the development of diabetes in non-obese diabetic (NOD) mice [134].

1.3.2.2. Mechanisms involving bacterial antigens

Since the majority of lymphocyte receptors recognise non-self antigens from microbial and viral epitopes it is logical to consider infection as the activator of autoimmunity. This is reflected in the literature of the past 10 years, which highlights the role of infections in human autoimmune disease [135-140] and in induced animal models. Moreover, the role of the infectious agent in the induction of autoimmune disease in animal models has been established [141]. Theories such as hidden/cryptic antigens, epitope spreading, anti-idiotypes, molecular mimicry, antigenic complementarity and bystander effects have been largely proposed as mechanisms by which immune tolerance can be compromised, largely reviewed in [135].

The most popular theory is molecular mimicry, first proposed in 1964 by Damian [142] as a definition of the molecular mechanism by which microorganisms should become "invisible" to the host immune system, escaping the control of the immune response. The role of the molecular mimicry as a mechanism to drive autoimmunity [142, 143]: a susceptible host acquires an infection with an agent that has antigens with immunological similarity to the host antigens but they differ sufficiently to induce an immune response when presented to T cells. As a result, the tolerance to auto-antigens breaks down, and the pathogen-specific immune response cross-reacts with the host structure to cause tissue auto-damage or auto-stimulation. The theory was further defined as molecular-epitope mimicry [64] since T cells and B cells are tailored to recognize particular short amino acid sequences or peptides processed upon presentation by APCs. Several lines of evidence have connected the role of epitope mimicry to the induction of autoimmune conditions [144]. Auto-antibodies against the serum glycolipids constitute the hallmark feature of the Guillain-Barre syndrome (GBS), causing a paralysis of the peripheral nervous system by targeting neural tissues. They are potentially derived from a cross-reaction with *Campylobacter jejuni* antigens, whose infection may occur days or weeks before the GBS onset [80]. Other examples include *Streptococcus pyogenes* in rheumatic fever and in rheumatic heart disease [145] and of *Borrelia burgodoferi* in Lyme disease [146].

In GD, the molecular mimicry between *Yersinia enterocolitica* (YE) antigens and thyroid auto-antigens has been proposed [147] and recently extensively reviewed in [148], as it will be further discussed in Chapter 4. Ultimately, the contribution of viral infection was

described as well, indicating the Coxsakie B and the Hepatitis C viruses as an increased risk factor for the development of autoimmune thyroiditis [149, 150].

The second theory which has to be considered is the epitope spreading mechanism. This introduces the possibility that the resulting autoantigenic epitope may be different from the early stage of the disease pathogenesis [151], since the spreading of the epitope would be the result of the normal activation of the immune response. At the first encounter of the pathogen's epitope, the immune system produces T cells and B cells with high affinity against it. At the second re-encounter of the same pathogen, the immune system would produce a response to a second epitope of the pathogen to assure the enhancement of the immune response in future events. In line with this theory, it seems that multiple infections result in multiple auto-autoantibodies, some of which are capable of driving an autoimmune disease, and temporally that the autoimmune disease must be preceded by infections and epitope spreading and not simultaneously [135].

These two theories assume that the initiating event in the development of ADs is the infection driven by a single pathogen. Along with some of the theories mentioned above, two other theories have been recently proposed [152], namely molecular modification pathway and hyper immune-inflammatory response pathway also defined as "pathogen-driven autoimmunity mimicry" (PDAIM). The first implies that the infecting mechanisms of the pathogen might enzymatically modify proteins or targets of the host, thus inducing the normal host's immune response acting against that, causing an autoimmune-disease-like condition. The second implies that an individual with one or more genetic disorders in the immune-inflammatory molecular signaling pathways is more likely to have a prolonged immune-inflammatory response against infection, which may lead to the development of an autoimmune condition. Although these two new mechanisms are not prone to compromise self-tolerance and the contextual auto-reactive cell reactivation, some evidence seems to support them for AD's outcome, as reviewed in [152], moreover there are no described examples for the thyroid autoimmune diseases.

In contrast to the theories above, another popular theory called the "adjuvant effect or bystander effect" is more referred to general infections rather than to a specific pathogen triggering the AD outcome. It is well known that infections stimulate the activation of the innate immune response leading to the release of cytokines and other pro-inflammatory molecules, preventing the outcome of infectious disease. On the other hand, these molecules might activate some auto-reactive T or B cells which escaped deletion processes, to drive or exacerbate autoimmunity [135]. As previously described, lymphocytes need two signals to initiate the immune response. In the context of the induction of AD, the second non-antigen-specific signals necessary to activate the

response could be given by the bystander or the adjuvant effect. The most striking examples of this theory and the role of microorganisms to induce the overcoming of self-tolerance come from the induction of experimental autoimmune disease in animal models using complete or incomplete adjuvants that seem to mimic microbial infections, which are described in the next paragraph. In particular, adjuvants such as inorganic salts (e.g. alum and magnesium) but also bacterial or viral product, such as LPS or the complete Freund's adjuvant (CFA, i.e. heat-killed *Mycobacterium tuberculosis* in emulsion oils) can act concentrating the antigen in a specific site where it would be exposed to the immune system ("depot effect") or induce the cytokines production enhancing the immune response and the subsequent antibodies production. Different types of adjuvants may induce a different response: alum may cause the "depot effect" but also activate the inflammasome, as well as LPS via TLR4 signaling; while CFA triggers a Th17/Th1 immune response [153] and the incomplete Freund's adjuvant, by lacking the *Mycobacterium* contribution, may enhance a Th2 response. Nevertheless, autoimmunity was induced without adjuvants when non-autologous antigens are used to immunize the animal model [154].

1.3.2.3. Other environmental factors

Apart from the genetic and microbial contribution in predisposing an autoimmune response, other common environmental factors may play an additional role in predisposing GD and its progression to GO.

Cigarette smoking has been directly associated to other conditions such as lung carcinoma and vascular diseases and may increase the susceptibility for an individual to develop an autoimmune disease [155]. In autoimmune thyroid diseases, smoking is considered a strong risk factor for GO development rather than GD, as reviewed in [155, 156]. While there were no differences in the TRAB serum levels between smokers and non-smokers GD patients, smokers group experienced a slower reduction of TRAB levels during anti-thyroid drug treatments [156] and an increased risk of GO after radioiodine treatment [157]. Moreover, smoking increases the chances of relapsing GD [158], which is in turn a strong predisposing factor for GO (as previously described in par. 1.1.3). Currently smokers GD patients are more likely to develop signs of GO rather than non-smokers or ex-smokers [159] accompanied by a less effective GO treatments with steroids or irradiation [58], and to develop a more severe GO condition in a dose-dependent manner [160]. Smoking induces pro-inflammatory cytokines expression, activating the both the innate and the adaptive immune systems. Human orbital fibroblasts when exposed to cigarette smoke extract *in vitro* showed an increase of

prototypical pathways described in GO in the previous par. 1.1.3, such as adipogenesis and hyaluronan overproduction [161].

1.4. PRECLINICAL AND INDUCED GD/GO DISEASE MODELS

Diagnosis of AD is usually made on patients who already present some or all the clinical symptoms. For this reason, mechanisms underlying the loss of immune-tolerance may have to be investigated in depth using pre-clinical models, which can resemble the characteristic of the disease in question.

1.4.1. Animal models of GD/GO

Spontaneous thyroiditis was reported in obese strain (OS) chickens, dogs, marmosets and in Bio-breeding rats, non-obese diabetic (NOD) mice and NOD.H2h4 mice, as reviewed in [36, 162]. Specifically the thyroid autoimmune response in chickens and rats is directed against Tg, while the NOD mice have an anti-TPO response. On the contrary, spontaneous form of GD and TSHR auto-antibodies production are rarely found in non-human species, including great apes [163]. Few possible explanations of this lack of spontaneous GD/GO in animal models, according to [164], are that: i) the TSHR has the lowest expression amongst thyroid autoantigens, while Tg is the most expressed, and ii) the murine TSHR A-subunit lacks one N-glycan pattern compared to the human and they only share less than 90% sequence identity. Therefore, models for the hyperthyroid GD and GO have to be induced and different methods were developed so far, leading to heterogeneous responses as reviewed in [36, 162, 165].

One of the main limitation initially faced by researchers was the production of an adequate amount of TSHR from protein recombination techniques [166], with a correct and functional N-glycosylation patterns and folding [167]. The first successful method for inducing a GD model was reported in 1996 and consisted in the injection of a fibroblast cell line expressing the MHC-II and the full-length and functional human TSHR (hTSHR) [168]. The majority of female AKR/N mice injected with the murine RT4.I5HP fibroblasts - co-expressing the full-length hTSHR and MHC-II - shown the induction of TBII and 20% of them developed higher T4 and TSAb activity. Control mice injected with either MHC-II or hTSHR alone fibroblast did not developed any sign of disease. The aberrant expression of MHC-II itself, and not the regulation via non-MHC genes, served for the presentation of the hTSHR to helper T cells in thyrocytes, acting as APCs, and leading to the induction of the auto-immune response and TSABs production [169]. When the same protocol was replicated providing alum as a Th2-adjuvant, an earlier onset of the disease with higher T4 levels and goitre were reported in some of the animals, while in

presence of complete Freund's Th1-adjuvant, a slower onset of the disease was observed but high T4 levels were retained for a longer period of time (14 weeks) [170].

The *in vivo* expression of the hTSHR cDNA in eukaryotic plasmids, or genetic immunization, initially led to TBII-TSBAb development and some signs of thyroiditis with only one inbred BALB/c mouse positive for TSAb [171] and inconsistency in model replication [172, 173]. However, when performed in outbred mice, hyperthyroidism was induced in some female mice and some signs of eye involvement were reported [171]. Increased incidence (i.e. hyperthyroidism in 50% of BALB/c immunised mice) and reproducibility of the model were obtained by employing adenoviral plasmids for *in vivo* hTSHR expression [174]. Moreover, the highest incidence of hyperthyroidism in immunised mice (60-80%) was achieved using the shed A-subunit of the hTSHR, indicating not only the auto-antigenic nature of the ectodomain but also its immunogenic role in inducing autoimmunity in murine models [175]. Even if the adenoviral delivery of hTSHR A-subunit became one of the most common method for inducing GD in murine models [175], the duration of the anti-TSHR response and the strength of the antigenic stimulus were not enough adequate to induce the eye disease [165].

Different approaches were reported to induce changes in the orbital histology typical of GO. Based on their previous observation regarding the TSHR expression in orbital tissues [162, 176], Ludgate and colleagues specifically investigated orbital tissues from BALB/c and NOD female mice receiving either unfractionated or CD4+-enriched *in vitro* primed T cells generated from an *in vivo* primed mice with either GI or by recombinant hTSHR-ectodomain fusion protein [177]. While NOD group developed a disruptive thyroiditis but no changes in orbital tissues, BALB/c mice shown a more heterogenous response in terms of T4 levels between 4 and 18 weeks after transfer, and changes in orbital histology such as adipogenesis accumulation, oedema and immune-cells infiltration were reported in 17 out of 25 T-cells primed mice. Banga and colleagues, instead, optimized the electroporation procedure in the biceps femoris for the injection of hTSHR plasmid previously described [178] and reported signs of orbital fibrosis [179]. Interestingly, their work described an interaction between the anti-TSHR and anti-IGF1R immune responses possibly implicated in GO, which was also previously described in par. 1.1.3. Subsequently, the protocol was replicated including *in vivo* magnetic resonance imaging (MRI) for the evaluation of the orbital muscles and an in-depth analysis of the orbital pathology. Despite mice were mostly hypothyroid with TSBABs levels, retrobulbar inflammation, adipogenesis and chemosis (i.e. swelling of the conjunctiva) were reported [180].

The heterogeneous response to the induction of GD and GO in animal model somehow recapitulates the heterogeneous manifestation of the disease in humans, caused by a combination of genes and environmental factors. In fact, some MHC-mediated genetic background seemed resistant to GD development, such as the C57/BL6 strain [167, 169]. Resistance in developing GD/GO is also imputable to the use of human TSHR (either full length or the A-subunit), whose induced TSAbs has to cross-react with the murine TSHR in order to breaks the immune tolerance in mice [36]. Strains such as the BALB/c and C3H/He, but not the C57/BL6 demonstrated cross-reactivity of TSAbs when measured in CHO cells expressing the murine TSHR [181]. Using the murine TSHR led to a variety of outcomes. BALB/c mice treated with baculovirus-expressed murine TSHR recombinant protein, in presence of alum and pertussis toxin as adjuvant, shown presence of TBII/TSBAb and reduced T3, with consequently increased TSH, but no signs of thyroiditis [182]. TSHR knockout (KO) conferred susceptibility to BALB/c female mice immunised with the mouse TSHR A-subunit in producing TSAb levels with activity against the murine TSHR, but poorly cross-reacting with the human TSHR. Instead, TSHR-KO mice immunised with hTSHR A-subunit adenovirus generated high levels of TSAb cross-reacting well with the murine TSHR *in vitro*. However, no thyroiditis was reported [183]. A transient hyperthyroidism (TSAb levels and low-incidence high T4) followed by a persistent hypothyroidism (TSBAb abd high TSH) were obtained when transferring splenocytes from TSH-KO mice immunised with mouse TSHR A-subunit into wild-type athymic nude BALB/c mice (i.e. lacking mature lymphocytes). Interestingly, only 2 out of 9 athymic mice Tregs-depleted after adoptive transfer shown signs of immune cells infiltration in the orbits [184]. Only recently, Banga and Eckstein group reported the induction of GO through the injection via electroporation of the mouse TSHR-A subunit in female BALB/c mice. TSAb levels shown activity against the mouse TSHR but low cross-reactivity with the human TSHR. Despite T4 and thyroiditis were not induced, immunised mice shown adipogenesis and increased inflammation accompanied by immune infiltrates in the orbit [185].

One can argue that only limited mechanisms of loss of immune tolerance can be drawn from these experiments on the moment that the majority of the studies used female mice, being a disease with a female prevalence. Only recently, GO was induced in both male and female BALB/c mice [185]. Also, studies present in literature so far involved mice being immunised when at no more than 8 weeks old; disease mechanisms in an older cohort might be different and it would be of interest to observe specially because the average age of disease onset in GD/GO patients is between 30 and 50 years old, even if it can arise at any age [186].

Other environmental factors such as the use of adjuvants but also the housing of the mice (specific pathogens free, more sterile, *vs.* conventional caging) may interfere with the auto-immune response and determine slightly different disease phenotypes [187] or cause the failure when replicating the animal model [172, 188]. Also, the role of the microbial environment and the gut microbiota composition were suggested to be implicated in the heterogeneity of the disease outcomes [64, 187, 188].

1.4.2. Induced GD after Alemtuzumab treatment

Immunosuppressive treatment with alemtuzumab (Campath-1H) is usually required in presence of relapsing-remitting multiple sclerosis (RR-MS), characterized by of new or increasing symptoms followed by disease remission episodes [189], but also in cases of rheumatoid arthritis and after some organ transplants. Alemtuzumab is a humanized mAb directed against CD52, expressed on the surface of lymphocytes, monocytes and some DCs. It causes the fast and long-lasting depletion of lymphocytes (both B and T cells), namely lymphocytopenia, followed by the so-called “immune reconstitution” phase which can last few months to years, as recently reviewed in [190]. B cells are the first to recover, usually after 3 months from depletion, and are generally characterized by mature naïve lymphocytes. T cell-reconstitution appear to be delayed, within 35 months for $CD4^+$ and 20 months for $CD8^+$-T cells, and usually derived from circulating memory T-cell clones [191]. In this context, during the period in-between B and T cells reconstitution, B cells are left without the proper co-stimulatory signals which may enhance auto-immune responses post-Alemtuzumab [192]. Also the T cells reconstitution itself may lead to autoimmunity, since the newly formed T cell-clones mostly derive from circulating memory T cells, more prone to react against self-antigens. Interestingly, no involvement of the innate immune system has been observed.

About 40% RR-MS patients develop GD in five years-time after alemtuzumab administration (40.7% in a recent Belgium assessment [193]), with a higher risk of developing the disease in the first year up to three years after lymphocytes depletion, with a lower risk after four years. GD symptoms and disease progression seem to be more manageable with anti-thyroid drugs than normal GD [193], and shift from hyperthyroidism to hyperthyroidism spontaneously occurs [194], suggesting the involvement of both TSAb and TSBAb. Low incidence of GO was also reported, i.e. 1.7% in [194] and 7/62 with two severe GO cases reported in [195]. Interestingly, post-alemtuzumab GD patients had a higher level of IL-21 compared to patients without autoimmunity after alemtuzumab [196]. IL-21, as already described in par. 1.2.2, is involved in IL-17 proliferation/Tregs suppression and a consequently antibodies

production, and therefore higher IL-21 levels before immune reconstitution may constitute a risk factor for developing GD after alemtuzumab.

GD post Alemtuzumab-induced immune reconstitution can be considered as an induced human model of GD, which can help providing new insights on the loss of immune-tolerance mechanisms, as recently proposed [197].

1.5. INTRODUCTION TO THE GUT MICROBIOME

1.5.1. The gastrointestinal tract

The digestive or gastrointestinal tract (GI) tract is formed by oral cavity, oesophagus, small and large intestines and the anus (Figure 1.6). Salivary glands, liver and pancreas constitute the associated glands of the GI. GI functions include: i) digestion of nutrients and macro-molecules, which are ingested and pre-processed via mastication, ii) absorption of water and electrolytes, iii) energy production, iv) synthesis of vitamins (e.g. Vitamin B12) , v) hormones release and vi) elimination of indigestible food source.

The oral cavity, or mouth, is responsible for the pre-processing of food via the mechanical action of teeth and the enzymatic digestion of complex carbohydrates via ptyalin, mucin and amylase enzymes secreted in the saliva. The oesophagus, a 25-26 cm-long muscular tube, transports the food bolus after swallowing through involuntary peristalsis from the pharynx to the stomach, which is located in the abdominal cavity, under the diaphragm. The stomach content of an adult varies from 1L at pH 2 during fasting to doubled its volume at pH 3-4 after a meal intake, depending on the status of the ingested meal (solid *vs*. liquid; as reviewed in [198]). Besides the digestion of the complex carbohydrates already initiated by amylase, secreted gastric enzymes including lipases and pepsin initiate the digestion of triglycerides and proteins, respectively, in presence of a highly acidic environment sustained by the secretion of hydrochloric acid (HCl), which can last on average 3 hours (depending on the caloric values of the meal), accompanied by low peristaltic movement. The small intestine is about 5 meters-long and is divided into duodenum, jejunum and ileum. The leading function of the small intestine is the absorption of the nutrients, which is enhanced by its microscopic structure. The wall of the small intestine, in fact, presents circular creases (*plicae circulares,* especially situated in the jejunum) and its mucosa is characterized by finger-like protrusions into the lumen, called *villi*, which contain lamina propria tissue connecting microcirculation and lymphatic system (lacteals). *Villi* are finely covered by columnar enterocytes and some goblet cells, and the apical section of each enterocyte is itself characterized by microvilli, increasing the absorption of degraded nutrients (Figure 1.6C).

While di- or mono-saccharides and amino acids are absorbed by enterocytes and released in the microcirculation, lipids and fats are further processed by the liver-secreted bile and the pancreas-secreted pancreatin enzyme, in a basic environment (pH 6.5-7.5). Glycerol, short and medium-chain fatty acids are introduced into the blood circulation, while triglycerides covered by lipoproteins (chylomicrons) enter the lacteal[2] (Figure 1.6). Transit time through the small intestine takes on average 3 hours. The large intestine is about 1.8 meters-long and is composed in cecum (with ileocecal vales and appendix), colon (ascending, transverse, descending and sigmoid, respectively) and rectum, comprising the distal end or the anal canal. Mucus layer is produced by goblet cells, especially in the colon and the rectum. Water and electrolytes absorption is mediated by an increased number of columnar colonocytes with irregular microvilli through the large intestine, which terminates at the distal end of the rectum, where non-absorbed and indigested food (e.g. high-fibre vegetables) are stored before being expelled as faeces.

Studies on the involvement of the gut in human diseases (as they will be further implemented in this work) often rely on the use of mouse models, also due to the similarity in terms of anatomical and physiological structures of the gut between the two mammalian species (Figure 1.6A and B). However, as a result of the adaptation to different diets, energy requirements and metabolisms, important differences can be identified; i.e. larger cecum, taller intestinal *villi*, smooth and single colon tract with a thin mucosa, amongst others, as reviewed in [199] and Figure 1.6.

[2] Digestive Tract. In: Mescher AL. eds. *Junqueira's Basic Histology, 14e* New York, NY: McGraw-Hill

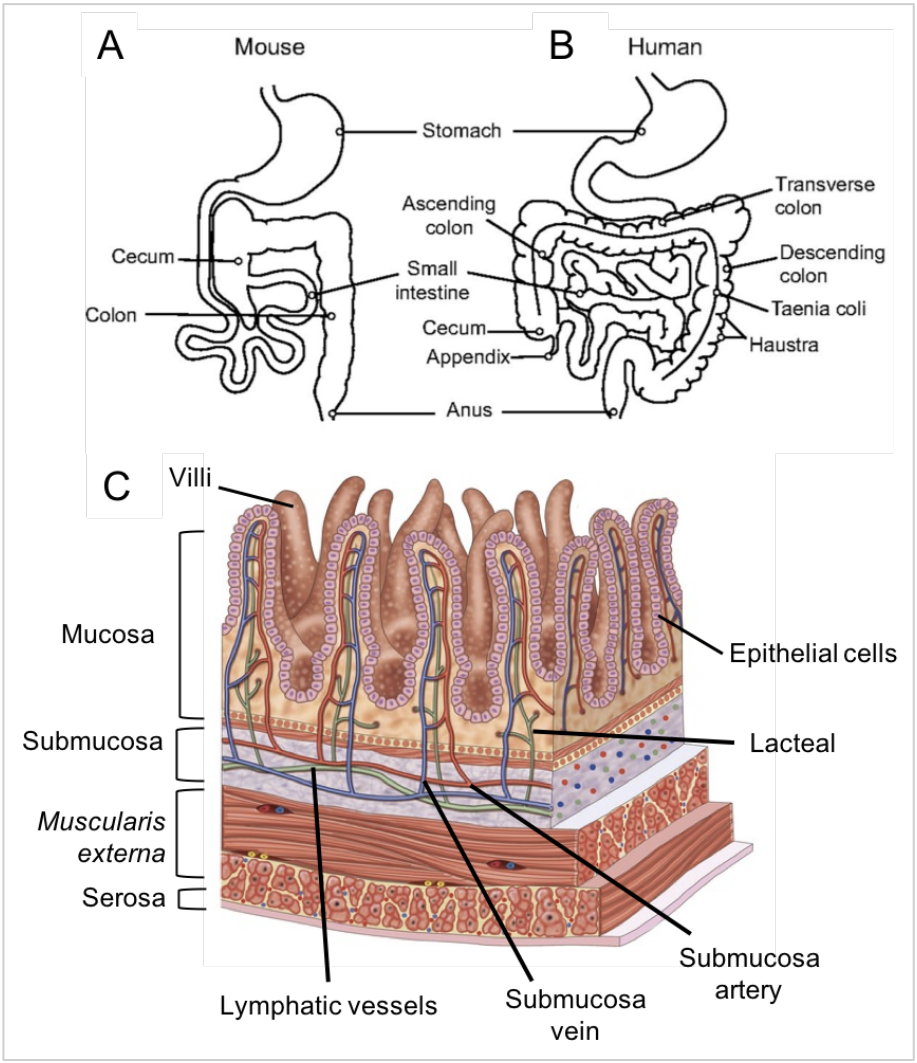

Figure 1.6. Anatomy of the gastrointestinal tract.
The gastrointestinal tract (GI) is constituted of stomach, small and large intestines, in both (**A**) mice and (**B**) humans, with some differences (e.g. larger cecum, taller intestinal *villi*, smooth, single colon tract with a thin mucosa, lack of *taenia coli* and haustra in the colon tract of mice). (Modified from [199]). (**C**) The leading function of the small intestine is the absorption of the nutrients, which is enhanced by its microscopic structure. The wall of the small intestine in humans, characterized by finger-like protrusions into the lumen, called *villi*, which contain lamina propria tissue connecting microcirculation and lymphatic system (lacteals). *Villi* are finely covered by columnar enterocytes (intestinal epithelial cells) and some goblet cells, and the apical section of each enterocyte is itself characterized by microvilli, increasing the absorption of degraded nutrients. (Modified from https://bio.libretexts.org).

1.5.2. The microbiota-microbiome concept

A microbiota is a collection of microorganisms such as bacteria but also fungi, *Archaea*, viruses and protozoa residing in a specific ecological area, whose term was first introduced by Lederberg and McCray [200], referring to microorganisms associated with human health or to a disease status. As proposed by Marchesi and Ravel [201], such a terminology should be used to indicate the results of a microbial survey (identity and relative or absolute quantification) based on a genetic marker. Beside the standard microbiology methods, which can suffer of some limitations due to the stringent culture conditions required by most of anaerobic bacteria, molecular techniques were developed to study the microbiota in its overall composition based on the variable regions of the 16S rRNA gene for bacteria or the 18S rRNA gene for fungi [202], or based on real-time quantitative PCR [203, 204], to overcome the impossibility of culturing most of the bacteria due to their unique growth conditions.

Metataxonomics is a culture-independent approach based on the high-throughput sequencing of variable regions of the bacterial 16S rRNA gene to obtain information about the taxonomic diversity, such as the identity and the relative quantification usually involving complex microbiomes, such as the gut microbiome [205]. Polymerase Chain Reaction (PCR) primers used for the amplicon-sequencing are often based on the highly conserved regions of the 16S rRNA gene to target variable regions (e.g. V1-V2 or V3-V4), which belong to a determined bacterial species and may act as a marker for phylogenetic analyses [206]. As the results of the high-throughput sequencing, e.g. Illumina platform (Illumina, San Diego, USA), reads are processed via bioinformatics pipelines (e.g. Mothur [207] or QIIME [208]) to filter poor quality bases and chimeric reads (i.e. generated when two markers are joint together during amplification, leading to an apparent novel taxon [205]) out and to align the passing-filter reads to one of the 16S gene reference databases now available (e.g. SILVA [209], the Ribosomal Database Project [210] or GreenGenes [211]), which were created from previous studies and collections of different ranges of cultured and environmental bacterial isolates. Aligned tags which cluster together at a certain cut-off (usually 97%) are considered as identical and referred to as Operational Taxonomic Unit (OTU), often representative of bacterial species. OTUs can be binned into phylogenetic levels from phylum to genus or species. A pivot table called OTU table with OTU or taxonomic abundances in rows and each sample in columns is used for subsequent analysis, which would be described extensively in the subsequent chapters. The term “microbiome”, instead, should be used when referring to the interplay between microorganisms, the surrounding environment and their genomes [209]. Since such a term includes also the functions of

microorganisms, a metagenomics or metatranscriptomics approach should be used. Metagenomics or whole-metagenome shotgun (WMS) involves the sequencing of the whole microbial genome (e.g. bacterial, but also *Archaea* and fungal).

One of the advantages in using such methodologies relies on their high-throughput, enabling processing of several samples in a run and being suitable for large trials and longitudinal studies, benefitting also from the decreasing cost for sequencing and the increased speed in sequencing the DNA. Some major projects contributed to the establishment of the bacterial genomic reference catalogues used nowadays when processing and analysing microbiome data. The Human Microbiome Project (HMP) was a direct consequence of the Human Genome Project, aiming to characterise the microbiome and factors that influence the presence of such microorganisms, to better understand the variability in human genetic and physiology diversity [212]. Initially funded by the NIH and with the collaboration of other international *consortia*, the first phase of the project (2008-2012) obtained the genomes from 900 strains sequenced by the HMP Jumpstart Centres [213], 100 genomes from the E.U.-funded Metagenomics of Human Intestinal Tract (Meta-HIT) project from 124 healthy individuals [214], plus additional genomes sequenced by other international centres, along with the generation of technologies and bioinformatic tools for analysis and data repositories. The healthy microbiome of 18 body sites from 242 individuals has been extensively characterized in terms of taxonomy and functions [215], which was further extended to a second wave of analysis including 1,631 new metagenomes from different body sites and multiple timepoints from 263 individuals [216]. In the second phase of the project (2014-2017), in fact, the Integrative Human Microbiome Project (iHMP) aimed at the complete characterization of the human microbiome, in longitudinal studies with a focus on the relationship of the microbiota in healthy and specific-diseases cohorts, such as preterm babies, type 2 diabetes and inflammatory bowel diseases [217].

1.5.3. Colonisation and development of the human microbiota

The human body is colonized by 3.8×10^{13} bacterial cells in males and 4.4×10^{13} in females [218]. Due to the differences in compositions and functions, microbiota can be distinguished in skin, ocular, oral cavity (including both the dental plaque and the oral mucosa), lungs and upper respiratory tract, gastro-intestinal (GI) and vaginal. Of those, the gut is the most colonized organ accounting for a 10^{11} bacterial cells/mL of the colon content as revised in [218].

The metabolic functions of the GI tract are exerted in different GI-specialised areas. As they are characterized by a different gradient of pH (from acid to neutral from the stomach

to the colon), along with a different mucus production, digestive enzymes and acid or bile secretions, they are colonized in a specialised manner. Due to the variable peristalsis, high level of acids (e.g. HCl) and a consequently low pH (1-3), the stomach and the upper small intestine (duodenum) have a reduced bacterial composition, which is dominated by facultative anaerobes capable of growing through adhesion to the epithelial-mucus layer and in a transient manner. Bacterial genera such as *Prevotella*, *Streptococcus*, *Veillonella*, *Rothia* and *Haemophilus sp*. were described to reside in the gastric environment of healthy individuals, as reviewed in [219]. Long-term infection with the Gram-negative *Helicobacter pylori* has been shown to alter a normal gastric mucosal microbiota and promote the development of gastric cancer [218]. Members of the *Lactobacillaceae* family, in which the genus *Lactobacillus* is included, were identified in both murine and human small intestines. The ileum, characterized by a physiological pH (7-9), is more favourable for bacterial growth which is increased compared to that of the duodenum. The large intestine is highly colonized by strictly anaerobic bacteria capable of digesting complex carbohydrates through fermentations. *Firmicutes* and *Bacteroidetes* are the predominant phyla residing in the colon [220-222], and their ratio (*Firmicutes:Bacteroidetes*) has been associated to disease conditions such as obesity [223], although it has also shown variability amongst healthy individuals. Prevalence of genera *Bacteroides, Prevotella* and *Ruminococcus* were associated to a healthy gut microbiota [224], along with a reduced presence of *Proteobacteria* and other pathogenic species. When combined the NIH-HMP and E.U.-funded Meta-HIT dataset, Arumugam and collaborators described the presence of enterotypes of the gut microbiota, which were identifiable by the prevalence of one of these genera: *Bacteroides* (enterotype 1), *Prevotella* (enterotype 2) or *Firmicutes*-prevalence of *Ruminococcus* (enterotype 3) [225]. The presence of one of these led to a preferred microbial composition in the gut, which was not associated to age, gender, BMI or country of origin (Denmark, Spain and US). Most of the studies on the human gut microbiota is based on faecal samples, due to its non-invasive collection method; however differences between faecal and luminal or colonic mucosa gut composition were observed, e.g. higher *Bacteroidetes* counts in faecal/luminal contents compared to the mucosa samples, while *Clostridium* cluster XIVa higher in mucus layer compared to the lumen [226].

How is the human body colonized by bacterial species? It was believed for years that the foetal environment was mostly sterile until birth, however it has been recently shown the presence of bacterial DNA in the womb and a possible placenta colonisation with *Proteobacterium* spp. [227]. The delivery methods, whether natural or through C-section, determine a colonisation of the new-born through the maternal bacteria transmission. The gut microbiota of newborns in their first day after natural birth was more similar to

the maternal vaginal microbiota, while that of babies from a C-section delivery was more similar to the maternal skin microbiota [227, 228]. The breastfeeding or the administration of an artificial formula can shape the gut microbiota composition and the immune system of the newborn in the following months after birth. The human breast milk is highly populated by bacterial species which share similarity with other maternal microbiotas (e.g. gut, saliva and skin), but also being a result of the retrograde transmission from the baby, although precise mechanisms of transmission are not fully understood [229-231]. Faecal samples of breastfed babies showed a higher concentration of *Actinobacteria* phylum, in which the genus *Bifidobacterium* spp. is included, compared to samples from babies fed on formula milk [232].

From childhood and adolescence through adulthood, the composition of the gut microbiota is generally stable, unless perturbed by external factors (i.e. diet, surgery or medications) which will be described in the next paragraph. A change of the gut microbiota composition can be observed at the age 63/65. Elderly individuals (63-76 years old) showed a more similar gut microbiota to that of younger individuals (aged 25-40), rather than that of centenarians (99-104 years old) [233]. The latter showed, in fact, reduction of the Clostridium XIVa group. Interestingly, in an Italian cohort of semi-supercentenarians (105-109 years old), the gut microbiota was enriched of genera previously associated to health status (i.e. *Akkermansia* and *Bifidobacterium* spp.) [234].

Older people may attend day hospital or residential care (either short or long-stay) and are also at risk of recurrent hospitalizations. Claesson and colleagues showed differences in the gut microbiota of elderly (mean age 78 years old) attending the long-stay residential care compared to that of community-dwelling or younger subjects [235]. In particular, long-stay residents showed increased Bacteroidetes compared to an enriched *Roseburia* and *Coprococcus* spp. in community-dwelling individuals. Moreover, changes in the gut microbiota from community-dwellers to long-stay residents correlated with indices of frailty.

1.5.4. External factors modulating the gut microbiota composition

As mentioned before, from adolescence to senescence, the microbiota composition of a healthy individual is considered generally stable. Dethlefsen and Relman analysed the gut microbiota variations in people over 18 years old on a daily basis for ten months. In an unperturbed status, daily shifts of the gut microbiota composition were observed, but they were based on an average community structure which was stable for months [236]. Lloyd-Price and colleagues reported a higher similarity of the stool microbiota in the within-subjects compared to the between-subjects, although a slight reduction in the

similarity index was observed within-individuals across time [216]. However, environmental factors such as lifestyle and diet, medications intake, but also the genetic background and the immune system might trigger some modifications.

1.5.4.1. The effect of the diet on the gut microbiota

Bacteria residing in the gut, especially those in the colon, are capable of producing unique metabolites from host-undigested molecules, usually derived from food intake. The effects of those metabolites on the host is related to the type of substrate available to bacteria. In excess of carbohydrate, the saccharolytic fermentation process would preferably lead to health-related molecules, such as short-chain fatty acids (SCFAs), while carbohydrate-deprivation may cause the production of potential harmful products. SCFAs, including acetate, propionate and butyrate (Appendix 25), play an important role in the host homeostasis not only by providing energy sources to intestinal epithelial cells but also through the interaction with the immune cells, as reviewed in [237] and as discussed later in the present study. Other products of the gut microbiota metabolism include gas, proteins and vitamins (i.e. vitamin A, B12 and B6), as reviewed in [238]

The diet has been considered one of the factors modulating the gut microbiota composition, since the early days of life. As previously described, in fact, breastfeeding or formula have the first impact on the colonisation of the gut microbiota of the newborn, possibly conferring a long-term health status and cognitive development[3]. Dietary habits can be very different in relationship to the country of residence and the lifestyle. A most striking example of this interplay is represented by the work of De Filippo and colleagues [239]. By comparing the gut microbiota of African children to that of children in Western countries, they reported different *Firmicutes* and *Bacteroidetes* phylum counts, accompanied by an increased production of SCFAs in the African children [239]. Children from a rural African village in Burkina Faso were on a prevalent rural vegetarian diet rich in fibres, plant polysaccharides and starch, which favours the fermentative activity (as previously described). Western diet, on the other hand, is high in processed food, animal proteins, fat, sugars and starch (i.e. high fat and high sugars diet), but low in fibres.

Another example on the relationship between the gut microbiota composition and the diet/lifestyle is represented by the study of the Hadza hunter-gatherers, a Tanzanian rural population whose diet is based on hunted and foraged products [240]. Their gut microbiome was characterised of an increased levels of *Firmicutes*, *Bacteroidetes*

---

[3] Horta BL and Victora CG, 2013. "Long-term effect of breastfeeding. A systematic review. WHO Library Cataloguing-in-Publication Data. ISBN 978 92 4 150530 7.

phyla, but also in *Proteobacteria* compared to that of the a Westernized population (i.e. Italian group). In terms of SCFAs production, the Hadza showed increased levels of propionate, while Italians were enriched in butyrate. The diet of the Hadza population is high in meat, tubers, honey and baobab, while Italians are on a Mediterranean diet which includes fruits and vegetables, dairy products, meat (i.e. poultry and read meat), processed foods and especially carbohydrates (i.e. pasta), which may have increased the amount of butyrate-producers bacteria in the gut microbiota. To this extent, the Hadza gut microbiota lacked of the *Bifidobacterium* spp., which might be due to the lack of any dairy products intake. Moreover, the availability of food from hunt and gather is influenced by seasons, also the gut microbiome of the Hadza population showed seasonal modifications, which was absent in industrialized population [241].

One may argue that the lack of adaptability of the human gut microbiome upon diet, and a consequent loss of certain bacterial species, can thus be a contributing factor to the increased numbers of autoimmune and chronic diseases. The latter has been considered to be as a risk factor for developing Western-prevalent disorders, such as cardiovascular [242-244] and metabolic diseases, but also cancer [245]. High-fat diet (HFD) which is rich in fat but low in fibres and proteins (the prototypical fast-food diet), has been associated to obesity [246]. Changes in the gut microbiome following HFD included a reduced diversity of the bacterial community and an increased *Firmicutes* [247]. Interestingly, HFD can also be used to induce disease phenotype in animal models. HFD-induced obesity was shown to increase the neuronal cell death and cognitive impairment in the triple transgenic mouse model of Alzheimer's disease (3xTg-AD) [248]. On the other hand, a protective effect conferred by HFD was observed in the mouse model of the human's chronic recurrent multifocal osteomyelitis (CRO), an inflammatory disease afflicting bones especially in children and adolescence [249]. The CRO mouse model, established through a mutation in the *Pombe* Cdc15 homology family protein PSTPIP2, showed a significant less severe induced phenotype, accompanied by a reduction of the genus *Prevotellae* and reduced production of pro-IL-1β in neutrophils following HFD administration [250].

In contrast to the previous examples, a less extreme dietary intervention may lead to none or moderate changes in the gut microbiota or "*may take several generations to evolve*" [251]. As described in the work of Wu et al. [251], the composition of the gut microbiome following a vegan diet was less perturbed than expected. Moreover, the increased amount of fibres and substrates for saccharolytic fermentation did not increase the amount of faecal SCFAs compared to that produced in omnivores. The modification of long-stay residential care individuals occurred one year after the initiation of the

residential care diet [235], supporting the hypothesis of a more resilient microbiome upon moderate dietary changes.

1.5.4.2. The effect of medications intake on the gut microbiota

Medical therapies may also have considerable impact on the gut microbiota composition, since the majority of the active compounds would be processed and absorbed in the gut when orally administered, and in turn, the gut microbiota composition can alter their absorption, efficacy and toxicity [252].

Antibiotics, first introduced in 1940s, are among the antimicrobial drugs able to block the growth of certain pathogenic bacterial species, through a different inhibition mechanisms provided by the type of each active compound. Considered broad-spectrum antibiotics (e.g. fluoroquinolones and β-lactams) are usually able to target both Gram-positive and Gram-negative bacteria, while other types of antibiotics might more specific for certain strains. β-lactams antibiotics, including penicillin and cephalosporin, block the synthesis of the bacterial cell wall of both Gram-positive and negative bacteria, through the interactions between their β-lactam ring and the transpeptidase enzyme involved in the construction of the bacterial cell wall. Although they are able to target both Gram-negative and Gram-positive bacteria, their effects depend on the susceptibility of those bacteria to the antibiotic itself and they are widely used in medical practice [253]. Fluoroquinolones, in which ciprofloxacin and levofloxacin are included, inhibit the bacterial growth targeting the DNA-gyrase (Topoisomerase II) for Gram-negative and the Topoisomerase IV in Gram-positive bacteria [254, 255]. Although fluoroquinolones have been considered a broad-spectrum antibiotic, they were shown to be less effective on anaerobic bacteria, and mostly used against *Haemophilus influenzae*, *Legionella pneumoniae* and *Mycoplasma pneumoniae*. Also efficacy against GI pathogens such as *Salmonella*, *Shigella*, *Yersinia enterocolitica* and *Campylobacter jejuni* was observed [255]. Vancomycin, instead, is a non-absorbing glycopeptide able to block the second-stage of the cell wall synthesis, more specific for both aerobic and anaerobic Gram-positive bacteria, including methicillin-resistant *Staphylococcus aureus* (MRSA), clostridia and also *Lactobacillus* sp. [256]. Another class of antibiotics - macrolides - in which clarithromycin and azithromycin are included, are known to have a most broad-spectrum bacteriostatic mechanisms since they inhibit the bacterial protein synthesis through the irreversible binding of the 50S ribosomal subunit. Such a class of antibiotic can also target fungi and may also have immunomodulatory effects in the host, as reviewed in [257].

Apart from their efficacy against most pathogenic bacterial isolates, antibiotics show anti-commensal effects, often resulting in a reduction of the richness and the diversity of the

bacterial communities in the gut microbiota. A 7-day intake of either the β-lactams amoxicillin-clavulanic acid or the fluoroquinolone levofloxacin decreased the diversity metrics of the microbiota composition, accompanied by an increase of the *Bacteroidetes:Firmicutes* ratio in hospitalized patients with non-digestive diseases [258]. The restoration of the gut microbiota composition after antibiotics exposure has been investigated and, in the majority of the cases, it resulted incomplete when compared to its pre-antibiotic status. In healthy individuals, ciprofloxacin intake resulted in a dramatic shift in the microbiota composition within 3-4 days from the first dose; the shift started to resolve and restore pre-antibiotic status soon after the antibiotic interruption. A second course with the same antibiotic after six months had a less dramatic effect on the gut microbiota compared to the first. However, at the end of the second antibiotic intake, the microbial composition in each subject differed from the pre-antibiotic composition, but of the newly acquired microbiota was stable for the following two months, with some inter-individuals differences observed [259]. The long-term impact of a one-week clarithromycin intake was reported by Jakobsson and colleagues' study [260], in which they observed a partial recovery of the gut microbiota after one and four years from the antibiotic intake, without any other antibiotic intake in the meantime.

When describing the restorative process of the gut microbiota after an antibiotic exposure, several studies reported an important inter-individual variability component, which has been possible attributed to each individual composition of the gut microbiota before the antibiotic intake [259, 260]. Raymond and collaborators performed a metagenomic study (i.e. shotgun sequencing) on faecal samples of eighteen young, healthy and carefully selected volunteers before and after 7-days cefprozil (cephalosporin) intake. Despite such strict enrolment criteria, the gut microbiota displayed inter-individual differences at the beginning of the study, while the antibiotic intake produced a similar effect in almost all the participants, with the decrease of several bacterial families and the increase of a number of specific genera. After 90 days, the gut microbiota of 16 out of 18 individuals was comparable to that of the controls [261].

In many cases, an incomplete restorative process of the gut microbiome was accompanied by an increased abundances of certain bacterial species and, on the other hand, of antibiotic-resistance genes, as was proposed and observed in the some of the previously cited works. The human microbiota can serve as a reservoir for antibiotic resistance genes (ARGs) [262] and an antibiotic intake, in fact, even for a short-time period, may select the resistance genes which are expressed at a low or undetectable levels before the treatments, such as the beta-lactamases [261].

Also, non-antibiotic drugs can have an impact on the gut bacterial communities. That might be the case of the proton pump inhibitors (PPIs) which act to increase the stomach pH via the inhibition of the hydrogen-potassium pumps releasing hydrochloric acid, usually prescribed to treat or prevent oesophagitis, gastric ulcers and reflux. Use of such medications lowered the diversity and the abundance of the gut microbial populations, with an increase of *Streptococcaceae* counts in PPI users. Increased abundance of bacteria were also likely to be from the pharyngeal microbiota, due to a change of pH between the upper GI and lower gut [263].

Maier and colleagues recently tested *in-vitro* the Prestwick Chemical Library, a collection of 1,079 FDA-approved drug compounds, against 40 bacterial isolates from healthy human gut microbiota [264]. Apart from the proven anti-commensal activity of most antibiotics (sulfonamides and aminoglycosides were the exception), 27% of non-antibiotics drugs showed activity on at least one isolate tested, including anti-fungal and antivirals, while 24% were anti-human drugs including hormones, immunosuppressive azathioprine, antidepressant and anti-inflammatory agents, also confirming previous reports [265, 266]. Authors also reported a positive correlation between the anti-commensal activity and the abundance of the bacterial species: those with higher relative abundance were, in fact, significantly more susceptible to anti-human drugs. Interestingly, anti-thyroid drugs (i.e. those described in the paragraph 1.1.12 as a treatment for GD/GO) are included in the Prestwick Chemical Library. They were tested at a final concentration of 20μM on the gut microbiota *in vitro*: carbimazole had no anti-commensal effect, methimazole seemed to have an effect against *Bacteroides caccae*, although not reaching the significance threshold after multiple corrections. Similarly, propylthiouracil (PTU) significantly interfered with *Ruminococcus bromii* growth although only before correction. Levothyroxine, instead, exhibited anti-commensal effects on three bacterial species also after adjustment for multiple corrections such as: *Clostridium saccharolytimun*, *Eubacterium eligens* and *Lactobacillus paracasei*.

1.6. INTERPLAY BETWEEN GUT MICROBIOME AND IMMUNE SYSTEM

Relationships between the microbiota and the host varies from mutualistic (i.e. both members benefit from the symbiosis) to commensal (i.e. beneficial association of bacteria, with unknown effects on the host), to ammenalistic (i.e. when one species is negatively affected by an event but the other stays unaffected), to pathogen. Pathogenicity potential of the gut bacteria is considered highly contextual, since the same bacteria can shift from being commensal to parasitic according to their localization, possible co-infections and/or the activation of host immune response. In a steady-state,

commensals can control the growth of pathobionts (i.e. potential pathogen bacteria within the microbiota) with the “colonization resistance“ [267, 268] through nutrients/metabolites competitions [269], downregulation of virulence factors, and antimicrobial peptides production [270]. However, on the other hand, they can also promote pro-inflammation and autoimmune responses.

In the past years, a great effort has been made in unravelling the complex relationship between the gut microbiome and the immune system, as showed by an increasing number of studies and reviews on this topic [267, 271-274]. Here are summarized the most important concepts on how the gut microbiota is tolerated by the immune system and, in turn, how it shapes the immune system. Association of the gut microbiota and autoimmune diseases, both in humans and mouse models, will be addressed in the course of the following chapters.

1.6.1. Gut-associated lymphoid tissues (GALT)

The GI tract is exposed daily to millions of foreign antigens derived from food intake (dietary proteins or haptens), but also to the dense population of residing microbes, possibly explaining the high amount of immune resident cells. Nevertheless, an immunological irresponsiveness or anergy has to be maintained because of the beneficial effects they exert within the host; however, the translocations of pathogenic bacteria through the mucosal barrier, which could result in systemic infections, has to be avoided. Intestinal epithelial cells (IECs) express a range of pattern recognition receptors (PRRs), such as Toll-like receptors (TLRs), capable of selectively recognizing and binding bacterial endotoxins such as lipopolysaccharide (LPS), peptidoglycans, flagellin and CpG DNA motifs. As a result, the innate immune response is activated with the production of proinflammatory molecules, such as chemokines (e.g. IL-8) and antimicrobial peptides via the NF-kB and MAPK pathways.

Both innate and adaptive immune systems of the GI tract reside in both lamina propria (LP) and epithelium (called the “effector sites” as reviewed in [275]), which are enriched in lymphocytes (both $CD4^+$ and $CD8^+$ T cells and antibody-secreting plasma cells), dendritic cells (DCs) and macrophages, and in gut-associated lymphoid tissue (GALT), rather considered the “inductive sites” [275]. GALT can be sparsely isolated or aggregated in Peyer’s patches (PP), especially situated in the small intestine and characterized by B and T cells follicles, and in gut-draining mesenteric lymph nodes (MLNs). Microfold (M) cells are situated in the epithelium above the PP/isolated follicles and mediate both the uptake and the transport of antigens (even from the microbiota) from the gut lumen to the GALT lymphoid area [276]. Dendritic cells (DCs) are situated

at the basolateral side of the M cells, while recruitment of more DCs can be performed through the secretion of CCL20, to collect the M-cells-internalized antigens [277]. Other soluble or exosome-containing antigens (i.e. those derived from class II MHC enterocytes) can be directly sequestered in the gut lumen by DCs [275]. At the "effector sites", LP-residing $CD103^+$ DCs can sequestrate soluble antigens passing through the tight-junction of *villi* or throughout other transcellular routes (i.e. transcytosis at the apical sites of enterocytes). Also, LP-residing $CX3CR1^{high}$ macrophages can sequestrate antigens in the epithelium, which are further presented to $CD103^+$ DCs [275].

1.6.2. Immunological tolerance (ignorance) to commensal bacteria

How the intestinal immune system discriminate between pathogenic and non-harmful antigens; in other words, how it does not activate against dietary antigens or the commensal microbiota? Dietary or orally-administered soluble antigens are tolerated through the so-called "oral tolerance" mechanism [278]. GALT and effector sites-associated DCs are actively involved in promoting the oral tolerance to dietary antigens by up-regulating the production of nTregs and iTregs, under an IL-10-rich environment, TGF-β and retinoic acid [279, 280]. Such anergy can last several months after only a single encounter with the antigen, although maintenance mechanisms are necessary, as reviewed in [278]. Oral tolerance is characterized by a systemic effect, since food-related antigens can be detected into the blood, possibly enhanced also by tolerance mechanisms mediated in the liver. Food-sensitive enteropathies, such as the coeliac disease, are a result of the breakdown of the oral tolerance to dietary antigens [281].

Tolerance to the gut microbiota is better addressed to as "mucosally-induced tolerance" [278] or "immune ignorance" [271], since it implies the physical separation of the commensal bacteria in the gut lumen from the mucosa. The mucus layer (i.e. mucin glycoproteins) produced by goblet cells prevents the bacterial adhesion to the mucosa; moreover, goblet cells produce a range of antimicrobial peptides such as α-defensins, lipocalin 1 and the C-type lectin RegIII-γ, that kill bacteria by targeting the bacterial cell wall, amongst other mechanisms. Intestinal alkaline phosphatase (IAP) is a brush-border enzyme secreted by enterocytes, and mainly present at high concentrations in luminal vesicles, released in both the circulatory and luminal sides of the gut epithelium. IAP has several identified functions within the gut environment [282]; its role in protecting the gut barrier is achieved through the ability of detoxifying endotoxins and limiting bacterial translocations through the mucosal barrier into the lymph nodes [283]. Bacterial LPS is dephosphorylated by the cleavage of acyl-chains from the lipid A moiety, which is responsible for the endotoxic activity [284]. Bacterial adhesion to the epithelium is further prevented by Immunoglobin A (IgA), which can be commensal bacteria-specific [285].

“Mucosally-induced tolerance” to microbiota antigens has no systemic effects, compared to the oral tolerance, but it can be extended to virtually all the gut mucosa *via* circulation of B and T cells through lymphatics and microvasculature [278]. The continuous sampling of the microbial lumen content via DCs is necessary to maintain the adequate tolerance at the mucosa.

In the event of a commensal bacterial translocation through the mucosa, the MLNs act as a “mucosal firewall”, as defined in the review [273] (Figure 1.7). The first response mechanism to bacterial translocation involves the rapid clearance or sequestration of the bacterial antigen: macrophages, in fact, rapidly clear through phagocytosis translocating bacteria/antigens and DCs prevent further penetration beyond the LP by sequestering the antigen in MLNs. T cells-residing in the intestinal mucosa play a double role in promoting the tolerance through natural and induced Tregs with the production of anti-inflammatory cytokines (TGF-β and IL-10) on one hand, and the maintenance of the adequate firewall against bacterial translocation, on the other hand. A proportion of iTregs in colon showed antigen-specificity against commensal bacteria [286]. A constitutive activation of the Th17/Th1 responses is therefore needed for the intestinal barrier integrity maintenance, other than for the pro-inflammatory response itself, since it sustains the production of mucus and antimicrobial peptides *via* IL-17 and IL-22 secretion [287] and the activation of macrophages via INFγ.

Breakdown of the mucosal tolerance to commensal microbiota causes autoimmune diseases, such as Crohn’s disease (CD), which will be further described later in this work, and the necrotizing enterocolitis (NEC) in premature babies [288].

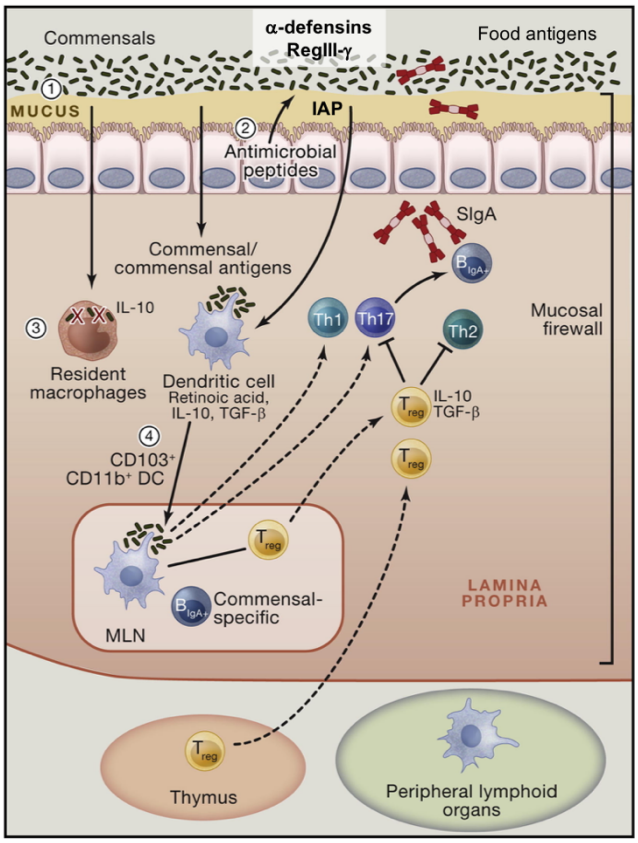

Figure 1.7. The "mucosa firewall". (**1**) The first line of defense from translocating bacteria is the mucus layer produced by goblet cells to prevent the bacterial adhesion to the mucosa. (**2**) Goblet cells produce a range of antimicrobial peptides such as α-defensins, lipocalin 1 and the C-type lectin RegIII-γ, that kill bacteria by targeting the bacterial cell wall, amongst other mechanisms. Intestinal alkaline phosphatase (IAP) detoxifies endotoxins and limits the bacterial translocation. (**3**) Bacterial antigens translocated through the mucosa are rapidly sequestered and cleared by macrophages through phagocytosis, while dendritic cells prevent further penetration beyond the lamina propria by sequestering the antigen in MLNs (**4**). T cells-residing in the intestinal mucosa play a double role in promoting the tolerance through natural and induced Tregs with the production of anti-inflammatory cytokines (TGF-β and IL-10) on one hand, and the maintenance of the adequate firewall against bacterial translocation, on the other hand. (Modified from [273]).

1.6.3. Gut microbiota and immune homeostasis

Germ free (GF) animals show reduced expression of innate immunity molecules such as TLR and MHC II [289, 290], smaller PPs and lowered number of $CD4^+$ T cells and IgA-secretory plasma cells in the LP [291-293]. Besides, GF mice are more susceptible to infections, for the concept of colonisation resistance previously introduced. Therefore, the gut microbiota is needed for defining the correct development of secondary lymphoid tissues and promoting the tolerance, which, in turn, has no reasons for being induced in their absence. At birth, the absence of a mature immune system, whereas regulatory response is preferred, prevents any inflammatory activation against colonising bacteria. Bacterial translocation from mother to foetus during pregnancy and components of the breast milk (oligosaccharides, IgAs, DCs and bacteria) may promote the colonisation of defined beneficial bacteria, such as the *Bifidobacterium* genus. Lactic acid-producing bacteria (LAB), such as *Lactobacillus* and *Bifidobacterium* genera, inhibited the adhesion and the growth of intestinal pathogens by either lowering the lumen pH or producing antimicrobial peptides (e.g. bacteriocins), as reviewed in [294]. *Bifidobacterium infantis*

[295], as well as *Faecalibacterium prausnitzii* [296], induced the production of Foxp3$^+$ CD4$^+$ Tregs and iTregs in the intestinal mucosa. The role and mechanisms of action of probiotic bacteria will be describe more in details in Chapter 5.

In fact, the gut microbiota can directly produce immune-modulation effects on the host. The polysaccharide A (PSA), uniquely produced by *Bacteroides fragilis*, protected the development of an intestinal inflammation in the induced colitis mouse model, possibly mediated by IL-10 from a subset of Tregs [297] (Figure 1.8). On the other hand, the segmented filamentous bacteria (SFB) were associated with increased Th17 response [298] (Figure 1.8). One of the most striking example is the experimental autoimmune encephalitis (EAE) mouse model of multiple sclerosis, whose disease phenotype was exacerbated by the presence of SFB in the small intestine in a Th17-mediated manner [299]. To note, SFB were only described in mice, rats and chickens, while their human counterpart seems to cluster within a *Clostridiaceae* clade [300]. Interestingly, *Clostridium* species from the cluster IV and XIVa, normally present within the gut microbiota, increased the number of Foxp3$^+$ Tregs, under TGF-β environment in the murine colonic mucosa [301]. Early-life inoculation of those clostridia in conventional mice prevented the induced colitis and the immune-modulatory effects were also extended to the adult life. Seventeen clostridial strains belonging to the IV, XIVa and XVIII clusters were isolated from human healthy microbiota based on the capacity of expansion and differentiation of Tregs under TGF-β production. When transferred into adult mouse models of allergic diarrhoea, the colitis symptoms were attenuated [302].

Tolerogenic immune-modulation can also be exerted by commensal-derived metabolites and peptides, rather than from a determined species or bacterial cluster. Butyrate, acetate and propionate SCFA (Appendix 25), synthesized by commensals bacteria through fermentation, induced a potent stimulation of Tregs specifically in the colon [303]. As elegantly presented in the review [304], SCFAs, in particular butyrate, exert immune-regulation by i) enhancing the generation of Tregs, including those pre-existing, via epigenetic mechanisms [303]; ii) inducing the differentiation of naïve CD4$^+$ T cells into Tregs via the epigenetic-mediated upregulation of Foxp3 [305, 306] and iii) inducing the differentiation of Tregs via DCs stimulation under genetic and epigenetic mechanisms [307]. Butyrate, in fact, acts as histone deacetylase (HDA) inhibitor, thus leading to acetylation of histone-H3 and allowing gene expression [308]. Specifically, butyrate inhibits class-II HDAs, which naturally suppress Tregs expansions [309], allowing the transcription of Tregs-induction genes via histone acetylation [306].

As previously introduced, the unbalance between regulatory (Tregs) and inflammatory (Th17) responses may lead to inflammation and autoimmune responses. Similarly for

commensal-specific Tregs, also intestinal Th17 cells with commensal-antigens specificity were described [89], which may trigger autoimmunity. Promoting and/or restoring tolerogenic response in the gut may assume a therapeutic importance. *In vitro* supplementation of six butyrate-producing bacteria, plus *Faecalibacterium prausnitzii* or *Butyricicoccus pullicaecorum*, to Crohn's disease-derived samples increased the butyrate production and improved the intestinal barrier integrity [310]. Probiotics bacteria, including lactic-acid-producing bacteria (LAB) such as *Lactobacillus* and *Bifidobacterium* spp., deliver – by definition[4] - beneficial effects to the host health. One of them consists in the induction of Tregs in the gut, through different mechanisms (not necessarily mediated by butyrate, i.e. immunomodulins secreted by *Lactobacillus plantarum* [311]). The role of probiotics in autoimmune diseases will be further discussed in the next chapters.

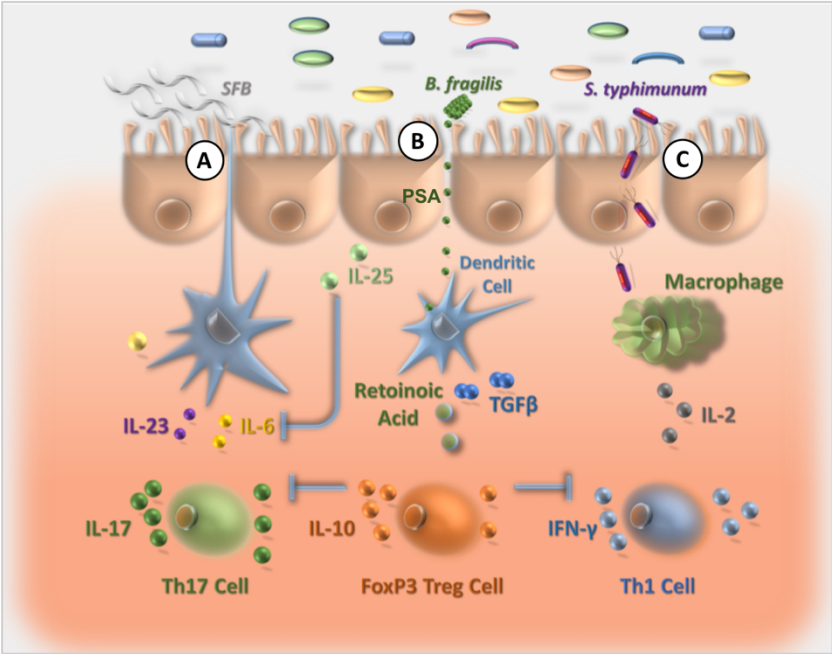

Figure 1.8. Immunomodulatory effects of the gut microbiota.
(**A**) Segmented filamentous bacteria (SFB) induced a Th17 immune response in the small intestine, which exacerbated the experimental autoimmune encephalitis (EAE) mouse model of multiple sclerosis [299]. (**B**) Polysaccharide A (PSA), specifically produced by *Bacteroides fragilis*, induced the expansion of IL-10-producing-Tregs and protected the development of an intestinal inflammation in the induced colitis mouse model mediated [297]. (**C**) Bacterial translocation rapidly activates macrophages and

[4] FAO/WHO. Probiotics in food: health and nutritional properties and guidelines for evaluation: report of a Joint FAO/WHO Expert Consultation on Evaluation of Health and Nutritional Properties of Probiotics in Food, including powder milk with live lactic acid bacteria: Cordoba, Argentina, 1–4 October 2001: report of a Joint FAO/WHO Working Group on Drafting Guidelines for the Evaluation of Probiotics in Food (Food and Agriculture Organization of the United Nations, 2006).

pro-inflammatory Th1 response for the clearance of translocated antigens. (Modified from http://www.indigo-iapp.eu).

1.7. HYPOTHESIS AND AIMS OF THE PRESENT THESIS

Given the emerging role of the gut microbiota as a triggering factor in various diseases and the possible role of bacterial antigens in the breakdown of the immune-tolerance in autoimmune diseases, I hypothesized that the gut microbiota composition and functions can be considered as an environmental risk factor for the outcome and/or the progression of GD and GO. Therefore, I aimed at describing:

i) the composition of the gut microbiota during the induction of GO in a mouse model, its correlation with disease features and how it influences the replicability of animal models in different laboratories;

ii) the adjuvant role of the gut microbiota in inducing GO through the manipulation of its composition in early-stage of life;

iii) the gut microbiota composition of GD and GO patients in a multi-centre observational study compared to matching healthy controls, and its correlation with immunological (TRAB) and endocrinological (TSH, T4) features;

iv) the gut microbiota of GD/GO patients administered either a *consortium* of probiotics or placebo, along with the anti-thyroid drugs, in a pilot double-blind randomized trial, to possibly observe beneficial effects of a probiotics intake in the disease progression.

2. Chapter 2

Gut microbiota composition in an experimental murine model of Graves' orbitopathy, established in different environments, may modulate clinical presentation of disease.

Acknowledgments:

Dr. Sajad Moshkelgosha (SM), Dr. Utta Berchner-Pfannschmidt (UBP), Prof. Anja Eckstein (AE) and Prof. Paul Banga (PB) and their collaborators of the Department of Ophthalmology, University Hospital Essen/University of Duisburg-Essen and the King's College London, for having established the GO animal models and provided gut, faecal samples and clinical observations used in this chapter.

Dr. Hedda-Luise Köhling (HLK) and Dr. Danila Covelli (DC), during their secondment at Cultech Ltd. (UK), for extracting the genomic DNA from faecal samples and performing in parallel the traditional microbiological cultures.

2.1. INTRODUCTION

The poor reproducibility of murine models of human diseases has become a puzzling phenomenon in recent decades. Apart from the genetic background of the strains used, the type of animal housing, diet and even the vendor can influence disease phenotype [312, 313].

Several mouse models have been developed using different immunization protocols, however with no signs of concomitant eye disease, as previously discussed in Chapter 1 par. 1.4.1. Ludgate and colleagues established a TSHR-induced GO model by genetic immunization; i.e. injecting an expression plasmid carrying the human TSHR full-length cDNA [177]. Female BALB/c mice developed thyroiditis plus some aspects of GO and the disease could be transferred to naïve recipients using the TSHR-primed T cells from the genetically immunised mice. However, the model could not be reproduced in a different animal unit (neither was specific-pathogen free (SPF)) and the TSHR-induced disease was quite distinct from that previously described, which the authors postulated might be due to microorganisms [188]. It has also been reported that TSHR-immunised mice from a conventional environment had higher and more persistent TSAb levels than mice in SPF units (Bhattacharyya et al., Poster presentation 2005[3]).

Recently, Berchner-Pfannschmidt and colleagues reported the induction of GO-like disease in two independent SPF units [187]. The immunization protocol utilized the genetic delivery of human TSHR A-subunit plasmid by close field electroporation, which leads to features of GD accompanied by symptoms of eye disease, such as adipogenesis and inflammatory infiltrates in the orbit [165, 180]. Controls received a plasmid encoding the β-galactosidase (βgal) gene delivered by the same procedure. Most aspects of the model were reproduced successfully, however, there was heterogeneity in induced disease and differences in thyroid function in the animals undergoing experimental GO in the two locations [187].

Over the years, the gut microbiota not only has been associated with several diseases, as it will be extensively discussed in Chapter 4, but its confounding role in establishing or reproducing disease phenotype in murine models has also been proposed [314].

The murine model of multiple sclerosis, experimental autoimmune encephalomyelitis (EAE), proved to be highly influenced by the gut microbiota. Oral antibiotic immunization and consequent depletion of the gut bacteria, before disease induction, resulted in

---

[3] Poster presentation: Bhattacharyya KK, Coenen MJ, Bahn RS. Effect of environmental pathogens on the TSHR-directed immune response in an animal model of Graves' disease. *Thyroid* 2005; 15:422-426.

protection from disease development, along with reduction in pro-inflammatory mediators such as IL-17 and an increased Th2-immune response [315]. On the contrary, the intestinal monocolonization of germ free mice (sterile) with segmented filamentous bacteria (SFB) restored the disease phenotype, along with an increased number of Th17 cells in the central nervous system (CNS), suggesting a direct interplay of the gut microbiota and the immune response in EAE development [316].

2.2. AIMS OF THE CHAPTER

Based on these observations, I hypothesized that the gut microbiota itself might play a major role not only in the establishment, but also in the reproducibility of the GO animal model described above. The aim of the present chapter is therefore the characterization of the gut microbiota of the GD/GO models, recently replicated in two different centres [187], using the 16S rRNA gene sequencing (metataxonomics).

For this study the gut microbiota of TSHR immunised mice from the two centres was compared, to understand whether variation in gut microbiota composition could explain differences in the disease induced. Within one centre, the gut microbiota between different immunizations (TSHR and βgal) was characterized and compared with untreated mice, to determine whether the gut microbiota can influence the outcome and correlate with disease features.

2.3. MATERIALS AND METHODS

2.3.1. GO preclinical mouse model samples

Mouse samples used in the present work were collected by UBP and SM in a recent work [187], conducted in parallel in two independent animal housing units, under comparable SPF conditions. The study was approved by the North Rhine Westphalian State Agency for Nature, Environment and Consumer Protection, Germany and by the Ethics Committee of King's College London, United Kingdom (UK).

Samples from the animal unit of King's College London (UK) will be referred to as the "Centre 1" and included a total of 5 TSHR-immunised mice (TSHR). Samples from the University of Duisburg-Essen (Germany) will be referred to as the "Centre 2", including 10 TSHR-immunised (TSHR), 8 βgal plasmid controls (βgal) and 6 untreated mice (included as a background control), as shown in Table 2.1.

The GO immunization protocol has been previously described [180]. Briefly, 6-8 weeks old BALB/cOlaHsd female mice were immunised via intramuscular injection into each biceps femoris muscle [179] and electroporation of either the eukaryotic expression

plasmid carrying the human TSHR-A subunit gene (pTriEx1.1Neo-hTSHR or hTSHR289) (TSHR group) or the control plasmid pTriEx1.1Neo-β-gal (plasmid-control, βgal group). All animals, whether TSHR or βgal controls, received a total of four plasmid injections at three week-intervals of the experiment (0, 3, 6, 9 weeks). Mice in Centre 1 were maintained conventionally in open cages in one room and co-housed at a maximum of 3 animals per cage. In Centre 2, the mice were co-housed according to their immunizations, 2-4 animals per individually ventilated cage in one room. All mice were provided by different outlets of the same supplier (Harlan Ltd. or Harlan laboratories BV). All immunised and control mice in both locations were sacrificed nine weeks after the last immunization (18 weeks) to permit the development of the chronic phase of the disease in the TSHR group (Figure 2.1).

After sacrifice, murine intestines were snap-frozen, stored in sterile containers at −80°C and shipped in dry ice to Cultech Ltd. (UK). The microbial content of each animal was immediately obtained by HLK and DC via the scraping of the large intestine from oral to aboral end and prepared for subsequent analysis. Within the Centre 2 only, faecal pellets of βgal and TSHR immunised mice were also collected in sterile tubes before each injection (week 0, 3, 6, 9), immediately stored at -80°C and shipped to Cultech Ltd. in dry ice. Total DNA was extracted from faecal pellets as described below.

Clinical and histological assessment was conducted by UBP, SM, AE and PB and already described in Berchner-Pfannschmidt et al. Supplementary Methods [187]. Briefly, i) thyroid hormone thyroxine blood levels (fT4) and TRAB (both stimulating TSAb and blocking TSBAb) antibodies were quantified in a single experiment in Centre 2. Serum thyroid hormone T4 was determined by RIA (RD Ratio Diagnostics, Germany). The TSH binding inhibitory immunoglobulin activity (TBII) measured using human TRAK assay kit, following manufacturer instructions (ThermoFisher, BRAHMS, Germany), while the TSAb and TSBAb subtypes were determined using an hTSHR stably transfected CHO cells, as described in Zhao et al. [179]; ii) the measurement of the expansion of fat cells (adipogenesis) was assessed in orbital sections of extraorbital nasal and inferior muscle with ImageJ, as described previously [180], with a normalization of the adipose tissue area to the area of the optic nerve, and iii) muscular atrophy in the orbit has been quantified by diameter (<50μm) and round shape of muscle fibers. A full description of the mice involved, and samples collected in the present study is represented in Table 2.1.

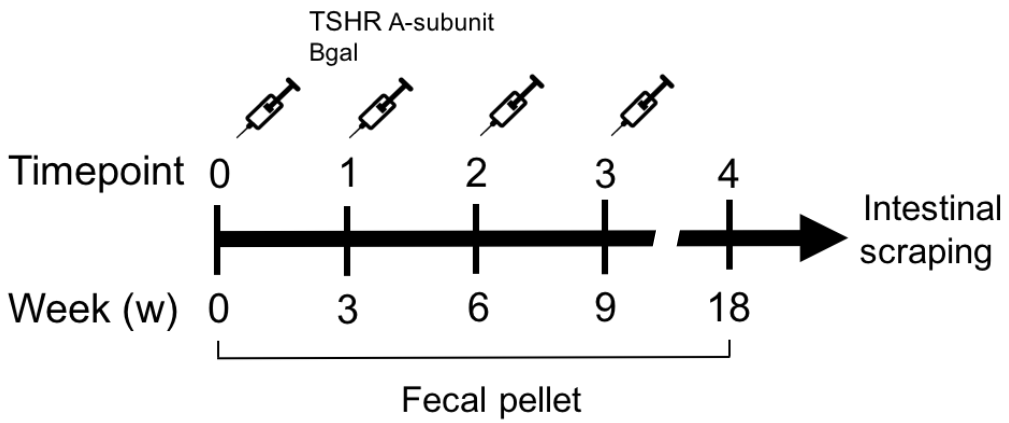

Figure 2.1. Schematic representation of the GO immunization protocol and sample collection.
Female BALB/cOlaHsd, 6-8 weeks old mice were immunised via the intramuscular injection and electroporation of either the eukaryotic expression plasmid pTriEx1.1Neo-hTSHR (hTSHR289) to develop signs of GO (TSHR A-subunit) or the control plasmid pTriEx1.1Neo-β-gal, as a plasmid-control group (βgal). Each animal received a total of four plasmid injections at three week-intervals. All immunised and control mice were sacrificed 9 weeks after the last immunization to permit the development of the chronic phase of the disease in the TSHR immunised group. Faecal pellets have been collected during the time course of the immunization trial from the baseline (T0) and before any other injection until the end of the procedure (T4). After euthanasia, the microbial content residing on the colonic mucosa has been collected through scraping.

Table 2.1. Description of the mouse groups involved in this study

No. of animals	Immunization	Centre [a]	Source [b]	Timepoint
5	TSHR	1	Intestinal scraping	T4
10	TSHR	2	I.S./Faces	T0-T4[§]
8	βgal	2	I.S./Faces	T0-T4[§]
6	Untreated	2	I.S./Faces	T4°

A total of 23 female BALB/cOlaHsd, 6-8 weeks old mice were challenged either with the pTriEx1.1Neo-hTSHR to induce disease (TSHR group) or with pTriEx1.1Neo-β-gal as a plasmid control group (βgal group). An untreated group of 6 mice has been included as a background control. [a] Independent SPF animal units were based in London (Centre 1) and Essen (Centre 2). [b] Samples collection comprised of intestine scraping (I.S.) from Centre 1 and both faecal pellets and I.S. within the Centre 2. [§]Faecal pellets of βgal and TSHR immunised mice have been collected before any immunization (T0) and during the time course of the immunization protocol until the sacrifice (T4), as represented in Figure 2.1. °Untreated mice were sampled at T4 before (faecal) and after the sacrifice (intestinal scraping).

2.3.2. Extraction of total DNA from gut contents and faeces and 16S rRNA gene sequencing

The extraction of total DNA was performed by HLK and DC. A total of 29 scraped intestinal samples and 95 faecal pellets were individually placed in 2mL microcentrifuge tubes prefilled with 0.1 mm silica and zirconia bead mix (Benchmark Scientific, Edison, USA), dissolved in 1 mL InhibitEX buffer (Qiagen Ltd, West Sussex, UK) and vortexed until homogenized. A bead-beating step (Beadbug microcentrifuge homogenizer, Benchmark Scientific, USA) was applied for 3 x 60 sec at 5 m/s with 5 min rest in-between. The DNA extraction has been performed with QiAmp Fast DNA Stool Mini kit (Qiagen Ltd, UK), following the manufacturer's instruction. Total genomic DNA was eluted in sterile microcentrifuge tubes and quantified by Qubit Fluorimetric Quantitation (ThermoFisher Scientific Ltd, UK), following manufacturer's instructions. DNA aliquots were kept at -20°C until used. Sequencing of the variable regions of the 16S rRNA gene was performed at Research and Testing Laboratory LLC. (Lubbock, Texas, USA). Primers such as the 28F and 388R were used to amplify the V1-V2 regions of 16S rRNA gene (Table 2.2), while 28F-combo and 388R primers were used to amplify the V1-V2 regions including the bifidobacteria-specific regions. Sequencing was performed using an Illumina Miseq (Illumina, San Diego, USA), with 10K paired-end sequencing protocol.

2.3.3. Quantification of the total bacterial load via 16S rRNA quantitative real-time PCR

E. coli Nissle 1917 (from Marchesi lab collection) was grown in Nutrient Broth (Sigma Aldrich, Germany, Appendix 1) at 37°C and viable cells (expressed as Colony Forming Unit, cfu) were counted through serial dilutions on Nutrient Agar (Sigma Aldrich, Germany, Appendix 1), incubated for 48 hours at 37°C. Half of a confluent plate ($7.75x10^8$ CFU/mL) was harvested, resuspended in 1mL broth and centrifuged for 10 min at 5,000 x g. Supernatant was discarded and pellet was resuspended in 1mL InhibitEX buffer (Qiagen Ltd., UK) for DNA extraction, following the procedure described in the previous paragraph, including the bead-beating step. Genomic DNA was quantified with Qubit© (ThermoFisher Scientific Ltd., UK), following manufacturer's instructions. The effective *E. coli* 16S rRNA gene copy number was calculated from the gDNA concentration and a standard curve was run in every experiment using $8.9x10^7$ to $8.9x10^1$ *E. coli* 16S gene copy number.

The total bacterial load or 16S rRNA copy number of faecal and gut gDNA was tested according to the BactQuant protocol [203], with some modifications. Briefly, 2.5µl of template DNA were added to 5µl of Platinum® Quantitative Polymerase Chain Reaction (PCR) SuperMix-UDG with ROX (Invitrogen), in presence of 1.8 µM of each BactQuant

forward and reverse primer (Invitrogen), 225 nM of the TaqMan® probe (Applied Biosystem, Warrington, UK) and molecular-grade water to reach 10 µl final volume.

Probe and primers sequences are listed in Table 2.2 below. Real-time PCR cycles and fluorescence signal acquisition were performed on Chromo4™ Real-Time PCR Detection (Bio-Rad, USA), with the following thermal cycles: 50°C for 3 mins, 95°C for 10 mins, 95°C for 15 sec and 60°C for 1 min repeated 40 cycles. Each sample's reaction, including the standard curve, was tested in duplicates. Data were analysed with Opticon Monitor software (Bio-Rad, USA) with a manual Cycle Threshold value (Ct) of 0.05 and blank-reduction was applied. Copy numbers were log-transformed for statistical analysis.

Table 2.2. Primers set used to detect the V1-V2 regions of the 16S rRNA gene, including bifidobacteria-specific regions (28F-combo) and for quantitative 16S rRNA gene load qPCR.

Primer ID	Sequence (5' to 3')
28Fw	GAGTTTGATCNTGGCTCAG
28F-YM[a]	GAGTTTGATYMTGGCTCAG
28F-Borrelia[a]	GAGTTTGATCCTGGCTTAG
28F-Chloroflex[a]	GAATTTGATCTTGGTTCAG
28F-Bifido[a]	GGGTTCGATTCTGGCTCAG
388Rv	TGCTGCCTCCCGTAGGAGT
BactQuant Fw[b]	CCTACGGGDGGCWGCA
BactQuant Rv[b]	GGACTACHVGGGTMTCTAATC
BactQuant probe[b]	6FAM-CAGCAGCCGCGGTA-MGBNFQ

[a] These primers are mixed at a 4:1:1:1 ratio (28F-YM is at 4 parts) and referred to as a 28-combo. [b] From the BactQuant protocol [203].

2.3.4. Processing of metataxonomic sequences

Processing of the sequences was performed using Mothur v1.36, to reduce possible PCR effects and to cluster sequences into Operational Taxonomic Units (OTUs) at the 97% identity cut-off and provide the taxonomic annotations [207] (see Appendix 2 for detailed explanation of the pipeline). Paired-end reads (R1 and R2) were joined for each sample using the Mothur function "make.contigs" and trimmed at the 2.5%-tile and 97.5%-tile on the distribution lengths of the amplicons. Sequences with any ambiguities (i.e. Ns) were removed by setting parameter N=0. Filtered sequences were aligned against the SILVA 16S rRNA gene reference database (http://www.arb-silva.de) [209]. Removal of chimera sequences was done with the Uchime tool [317]; singleton and non-

bacterial sequences (e.g. *Archaea*, Eukaryotic, Chloroplast and Mitochondria) have been removed from the analysis. The taxonomic assignment from phylum to genus level of the processed sequences was done using the Ribosomal Database Project (RDP) Naïve Bayesian Classifier, using Trainset 14 with a cut-off of 80% [210]. FastTree (version 2.1.7) has been used to build a phylogenetic tree, using an approximated maximum likelihood solved by Jukes-Cantor evolutionary model [318]. To reduce the effect of possible different sampling methods and to obtain comparable sequencing libraries, each sample library has been subsampled based on the smallest library size. OTUs with less than 10 counts have been excluded from the dataset and grouped as "OTU_low", and the analysis has been performed collapsing OTUs at the phylum-genus levels.

2.3.5. Statistical methods for analysis of metataxonomic data

Statistical analysis was performed in R version 3.2.2 and STAMP tool for metataxonomic data analysis [319]. Statistical tests with $P \leq 0.05$ were considered as significant.

2.3.5.1. Diversity indices

Rarefaction curves were calculated to check whether sequencing depth and sample size were adequate to characterize the composition of the gut and faecal microbiota. The sequence-based rarefaction curves were calculated in Mothur through the function "rarefaction.single".

Alpha diversity indices, whose mathematical formula are included in Appendix 3, were calculated from Mothur function "summary.single" and tested for association with covariates (e.g. locations or immunizations) using a linear model, followed by Tukey's Honest Significant Difference (HSD) post-hoc analysis.

Beta-diversity was calculated according to the weighted UniFrac [320] (Appendix 3) and the between-samples distances were represented in a Non-Metric Dimensional Scaling (NMDS) plot. The non-parametric permutational multivariate analysis of variance (PERMANOVA) was calculated through the Adonis function [200] in R Vegan package (using 999 permutations) and was used to test the association between the microbiota composition and the covariates (e.g. location of the laboratories or immunizations).

2.3.5.2. Testing differential abundant taxonomy

The hierarchical clustering of genera was performed using the Spearman distance and the Ward agglomeration method. Annotated heatmap of the top-30 most abundant genera amongst samples was created using the heatmap function of the NMF R package

with scaled genus abundances to column Z-scores after clustering (e.g. center and standardize each column separately to column Z-scores).

Differences in the taxonomic abundances (e.g. phylum to genus level) between locations were assessed using the analysis of variance (ANOVA) with Tukey's HSD post-hoc analysis and 95% confidence interval (c.i.). Differences between immunizations groups were assessed using a Welch's T-test assuming unequal variance with Welch's inverted 95% c.i. as implemented in STAMP.

2.3.5.3. Longitudinal analysis of faecal microbiota

Over multiple timepoints, the effects of time, immunizations and their interactions, have been estimated on the faecal microbiota composition, all by means of the following linear model (**Equation 1**):

$$y_{ijk} = \mu + Time_i + Immunization_j + (Time * Immunization)_{ij} + e_{ijk}$$

where y_{ijk} is the vector of either the log-transformed 16S rRNA gene copy number, alpha-diversity Chao or Shannon indices, or of the *Firmicutes/Bacteroidetes* ratio calculated from the relative abundances in each sample at each timepoint; μ is the overall mean; time is the effect of timepoint in classes (T0, T1…T4); immunization is the type of immunization (either the TSHR or βgal). The factorial interaction between immunization and time has also been included in the model; e_{ijk} is the vector of residual effects. Comparison between βgal and TSHR immunizations at each timepoint was made using the pairwise t-test in R.

To test differences in genera counts between immunizations over timepoints, the design model represented in Equation 1 was used to calculate the dispersion and fitting the negative binomial (NB) generalized linear model (GLM) with the glmFit function in EdgeR package [321]. The output of such function was passed to the EdgeR glmLRT function to compute contrasts between coefficients from the design model (i.e. immunisation over timepoints) through the likelihood ratio test. The baseline timepoint (T0) was used as a reference. Pairwise comparisons of genera counts between immunizations in each timepoint, including the T0, have been assessed with Fisher's Exact Test in EdgeR package with the dispersion calculated from the same design model of Equation 1.

2.3.5.4. Stability of the faecal microbiota over time

The function Adonis [200] implemented in the Vegan package was used to test the variations between-samples of the microbial communities (calculated using the weighted Unifrac distance) over timepoints and among cages, via a permutational analysis of

variance or non-parametric MANOVA. The linear predictors and response matrix were as described in **Equation 2:**

$$y_{ijkl} = \mu + T_i + I_j + (T * I)_{ij} + C_k + (C * T)_{ki} + (C * I)_{kj} + e_{ijkl}$$

whereas: y_{ijk} is the weighted Unifrac matrix for treatment *i*, time *j* and cage *k*, *μ* is the overall mean; T_i is the effect of the *i*th time which was set as a class (T0, T1…T4); I_j is the type of *j*th immunization which is represented by either TSHR or βgal; C_k is the effect of *k*th cage which is expressed as a class (C1, C2…C5); $(TI)_{ij}$, $(CT)_{ki}$ and $(CI)_{kj}$ represent factorial interactions between time, immunizations and cage; e_{ijkl} is the vector of the residual effects. A pairwise interaction within immunizations, cages and timepoints has been assessed using a built-in pairwise PERMANOVA script in R.

2.3.5.5. Correlations between gut microbiota and disease features

Correlations of either the taxonomy counts (phylum and genus relative abundances) and disease features, such as anti-TSHR antibodies and thyroid hormone thyroxine levels (fT4), orbital adipogenesis or muscular atrophy values, were estimated using the Spearman correlation coefficient (Rho) and represented in a correlation plot, using the R Corrplot package.

2.4. RESULTS

2.4.1. Summary of the GO clinical outcomes

Clinical differences of GO models replicated in the two centres were already described by UB-P, SM1 and colleagues [187]. From the original set of experiments, I was able to obtain the gut of 5 (out of 11) TSHR-immunised mice from Centre 1 and 10 out of 10 TSHR-immunised from Centre 2. We assume that the mice from Centre 1 were randomly selected and therefore there was no selection bias. A summary of the disease characteristics of this reduced cohort of mice collected by UBP, SM and colleagues is shown in Table 2.3 below. TRAB were induced successfully in all mice being immunised with TSHR-plasmid in both laboratories, while levels of TSAb were detected in 40% of the animals analyzed in both locations. Mice in Centre 2 showed a higher level of TSBAb (90% animals) and were more euthyroid compared to those of the Centre 1.

Table 2.3. Summary of disease characteristics induced in mice in Centre 1 and Centre 2 using the TSHR expression plasmid illustrating the heterogeneity of response.

Disease Feature	Centre 1 (n=5)	Centre 2 (n=10)
TRAB (%)	5/5 positive	10/10 positive
TSAb (pmol/mL)	2/5 positive	4/10 positive
TSBAb (%)	3/5 positive	9/10 positive
Thyroxine fT4 (mg/dL)	2/5 hyperthyroid	10/10 euthyroid
Orbital adipogenesis	N.A.°	4/8 increased
Orbital muscle atrophy	N.A.°	3/8 significantly increased
Thyroid Histology	2/5 thyroid focal infiltration	10/10 normal histology

° N.A. not available.

2.4.2. Total bacterial load and metataxonomics metrics

The total bacterial load of each sample was obtained from the real-time qPCR Ct value by interpolating the *E. coli* 16S rRNA gene copy number standard curve. Data were generated from reactions presenting a standard curve with a slope near -0.3 and R-squared (R^2) near 0.99 with an efficiency of 90-100%, otherwise the experiment was repeated. An average of 9.74e+06 copy number, ranging from 2.29e+05 min to 4.40e+07 max, were observed in total. A difference in the copy number was observed between the total of gut (mean 3.77e+06 copy number) and faecal samples (mean 1.57e+07 copy number) used in this chapter ($P<0.001$).

From the 16S rRNA gene sequencing (V1-V2 regions), a total of 5,333,798 reads were obtained which reduced to 4,047,186 reads after a first quality filtering. Following alignment on SILVA reference database, an average of 20,534 reads was obtained per sample, ranging from 3,502 to 134,901. The complete summary of the number of reads and 16S rRNA gene copy number in each category is described in Table 2.4.

Subsampling per library size resulted in a 96% average coverage per OTU definition at 3,052 reads per sample. The averaged coverage and subsampling was sufficient to describe gut bacterial communities according to sequence-based rarefaction curves (Figure 2.2).

A total of 4,281 OTUs were identified: 1,037 OTUs had more than 10 counts across samples and were grouped in taxonomic levels, which resulted in a total of 7 phyla, 16 classes, 27 orders, 49 families and 129 genera identified amongst samples.

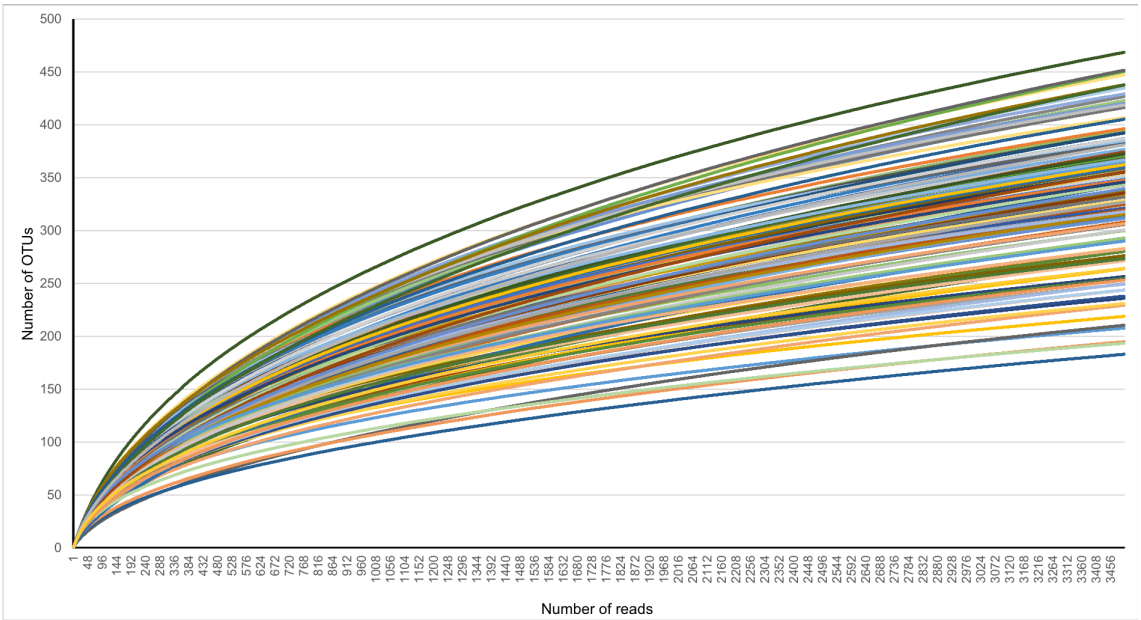

Figure 2.2. Murine microbiota rarefaction curves.
Sequence-based rarefaction are represented to as the number of detected OTUs in function of the reads sequenced. Library sub-sample was performed according to the smallest library size (i.e. 3,502 reads/sample). Each curve, in a different colour, represents a unique sample. Curves tended towards a plateau: increasing the sequencing depth would therefore not increase the number of OTUs described.

Table 2.4. Summary of the sequencing metrics (mean number of reads before subsampling) and the 16S gene copy number (bacterial load) according to different metadata categories.

	Mean number of reads	Mean 16S copy Number[#]
Microbiota source[a]		
Faecal samples (n=95)	22,071.21	1.57e+07[§]
Gut samples (n=29)	17,943.14	3.77e+06[§§]
P value		<0.001
Locations[b]		
Centre 1 (n=5)	13,910.4	3.55e+06
Centre 2 (n=10)	21,140.3	3.61e+06[§]
P value		0.96
Immunizations[c]		
TSHR (n=10)	21,140.3	3.61e+06[§]
βgal (n=8)	12,512	3.24e+06[§]
Untreated (n=6)	23,216.66	4.82e+06
P value		0.04
Timepoint[d]		
T0 (n=18)	23,314.5	2.23e+07
T1 (n=17)	17,128.58	1.77e+07
T2 (n=18)	25,207.22	1.14e+07
T3 (n=18)	21,464.38	1.04e+07
T4 (n=24)	22,742.87	1.62e+07
P value		0.009

[a]Faecal and gut samples are comprising of all the timepoints, immunizations and locations. [b]Differences in locations for TSHR-immunised mice gut samples. [c]Differences in immunizations comprising only Centre 2 gut samples. [d]Timepoint from faecal samples collected in Centre 2, including both TSHR and βgal immunizations. [#]Statistical test computed on log-transformed data. [§]Number of sample failed on 16S qPCR.

2.4.3. Comparative analysis of the gut microbiota of GO preclinical mouse models in different centres

To assess whether the microbiota has an impact on the GO mouse model in different laboratories, I compared the gut microbial contents of 5 TSHR mice from Centre 1 and 10 TSHR immunised BALB/c female mice from Centre 2, after sacrifice (T4).

The bacterial load (16S copy number) was very similar in both centres (Table 2.4). Comparison of the alpha diversity indices shown a significant reduction in the richness (P=0.01), but not in the diversity of the Centre 2 microbial community (P>0.05, Figure 2.3A). The gut microbiota composition from the two centres showed a good separation according to the Spearman distance and Ward hierarchical clustering (Figure 2.3B), and

a PERMANOVA test on the weighted UniFrac distances revealed a spatial difference between bacterial communities (P=0.005 with 999 permutations, data not shown).

At a phylum level, *Bacteroidetes* and *Firmicutes* were the most represented of the 7 phyla identified, with no differences between them in the two centres (P=0.99). *Lactobacillaceae*, *Ruminococcaceae* and *Porphyromonadaceae* families were more abundant in Centre 2 than in Centre 1 TSHR mice (P<0.01, Figure 2.3C). Significant differences were observed in the abundance of eighteen genera between the two centres, as detailed in Table 2.5.

The results obtained using metataxonomics largely confirmed results obtained via the traditional microbial culture approach performed by HLK and DC at Cultech Ltd. [322]. However, a few differences have been highlighted. Microbial cultures revealed significantly higher yeast counts (P=0.0318) in Centre 2 TSHR-immunised mice - which obviously could not be seen via the bacterial metataxonomics - and a nearly significant difference in the *Actinobacteria* genus *Bifidobacterium* (P=0.057), which was not detected in our metataxonomics data. Primers based on the V1-V2 regions of the 16S rRNA gene did not detect *Bifidobacterium* OTUs. Consequently, a new set of primers (28F-combo) capable of targeting the V1-V2 with bifidobacteria-specific regions (Table 2.2) was selected, with which a significant enrichment of bifidobacteria counts was reported in the Centre 1 (Table 2.5 and Appendix 4), in agreement with the microbial culture results.

Table 2.5. Genera differentially abundant between Centre 1 (n=5) and Centre 2 (n=10) TSHR-immunised mice intestinal scraped samples from the analysis of variance with Tukey's HSD post-hoc analysis (95% confidence interval), generated with STAMP.

Genera[a]	Centre 1: mean freq. (%)[b]	Centre 1: std. dev (%)[c]	Centre 2: mean freq. (%)[b]	Centre 1: std. dev (%)[c]	P values
Allobaculum	1.001	1.306	0.003	0.009	0.042
Alloprevotella	6.135	4.462	0.432	0.717	0.003
Bacteroides	9.370	8.401	1.525	0.855	0.017
Bifidobacterium°	0.668	0.505	0.006	0.012	0.003
Clostridium XI	0.840	0.733	0.000	0.000	0.005
Coprobacter	1.835	0.976	4.226	1.973	0.033
Fusicatenibacter	0.989	0.429	3.295	1.983	0.032
Guggenheimella	0.006	0.011	0.169	0.114	0.011
Helicobacter	0.200	0.231	0.000	0.000	0.024
Intestinimonas	0.097	0.034	0.861	0.339	0.000
Lactobacillus	2.304	1.436	18.632	13.893	0.030
Lactonifactor	0.023	0.021	0.401	0.309	0.025
Meniscus	1.149	0.671	0.000	0.000	0.000
Oscillibacter	0.640	0.501	1.748	0.698	0.011
Parabacteroides	0.292	0.265	0.031	0.045	0.015
Pseudoflavonifractor	0.154	0.106	0.466	0.252	0.028
Rikenella	3.921	1.693	1.216	1.097	0.004
Turicibacter	3.629	2.673	0.000	0.000	0.002

[a] Genera were entered in alphabetical order. [b] Mean freq: mean frequency (%) normalized through a cumulative sum-scaling (CSS) implemented in STAMP. [c] std. dev: standard deviation. °Generated from 28-combo primers detecting V1-V2 regions and bifidobacteria sequences.

2.4.4. Gut microbiota differences in immunised and control mice within the Centre 2

To observe the possible contribution of the gut microbiota in the disease, I compared the gut microbiota composition between immunization groups in mice within the Centre 2. No significant differences were observed in alpha diversity indices among immunizations, apart from the Abundance-based Coverage Estimator (ACE) index between untreated and TSHR groups (Figure 2.4A, P=0.01), which relies on the presence of rare OTUs[5]. A higher bacterial load was also observed in the untreated group compared to the plasmid-immunised mice (P=0.04, Table 2.4). The βgal group

[5] Chao A. 2005. Species estimation and applications. In *Encyclopedia of Statistical Sciences*, ed. N Balakrishnan, CB Read, B Vidakovic, 12:7907–16. New York: Wiley.

showed a slightly skewed distribution of the Shannon index when compared to the others; however, the *post-hoc* comparison was not significant.

The non-metric dimensional scaling (NMDS) of the weighted UniFrac distances matrix showed a separation of the three immunization groups, confirmed by a significant permutation test ($P<0.01$, 999 permutations; Figure 2.4B). βgal bacterial communities were closer to those of the untreated mice, while a spatial shift of the TSHR immunised bacterial communities was observed.

OTUs from *Bacteroidetes* and *Firmicutes* phyla were the most abundant among the phyla identified (Figure 2.4C) and showed a different distribution pattern among immunised groups. In particular, *Firmicutes* counts were higher in TSHR immunised mice ($P=0.05$) and *Bacteroidetes* were found to be higher in the untreated group ($P=0.012$). Differential taxonomic abundances analysis was performed pairwise between groups and described in the Table 2.6. At the genus level, eight genera were differentially abundant between TSHR and βgal groups; three genera between TSHR and the untreated group and four genera between βgal and the untreated group. I reported an enrichment of OTUs in the *Acetitomaculum* genus in the βgal group compared to both TSHR ($P=0.004$) and the untreated group ($P=0.003$); an enrichment of *Lactobacillus* OTUs in the TSHR compared to the untreated group ($P=0.018$) and a reduction of *Bacteroides* OTUs in TSHR when compared to the βgal group ($P=0.047$).

In the scraped intestinal samples, no cage effect on the composition of the large intestine microbiota was observed (PERMANOVA $P>0.05$; Figure 2.4D).

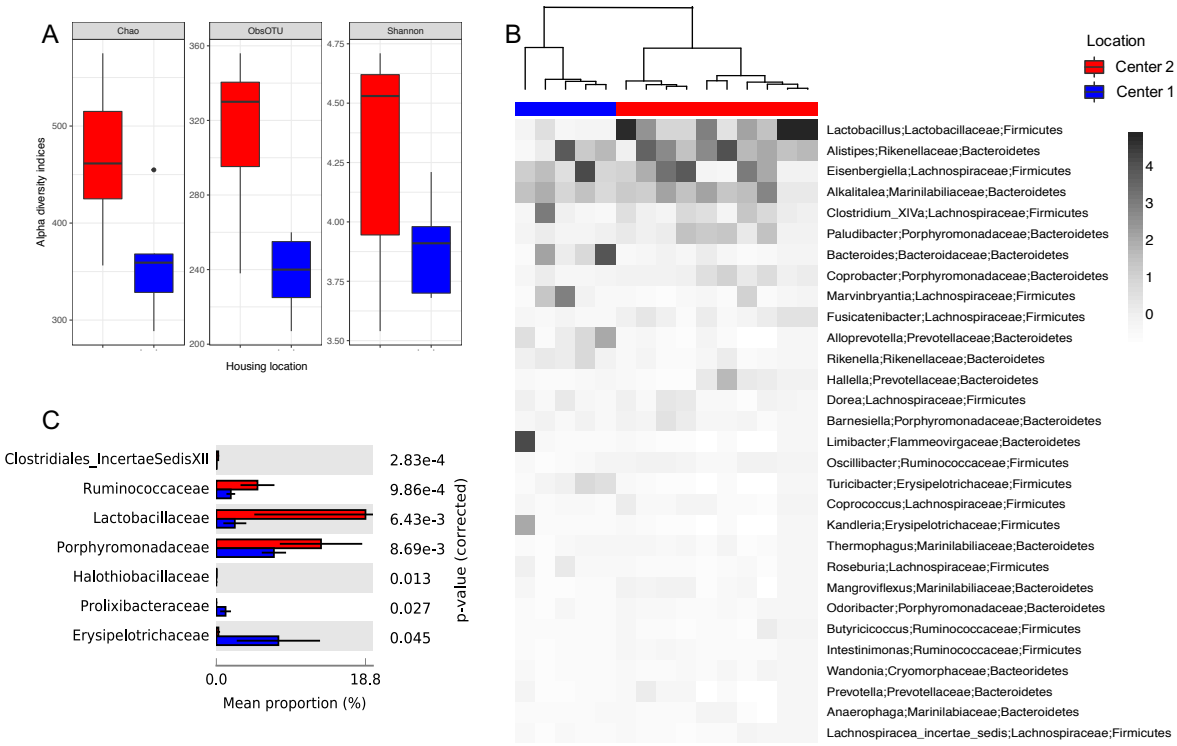

Figure 2.3. Comparative analysis of the gut microbiota in independent animal units.

(**A**) Box and whisker plot of the alpha diversity indices for richness (Chao1 and observed OTUs indices) and evenness (Shannon index) of the bacterial communities in TSHR immunised mice housed in Centre 1 (blue) and Centre 2 (red), respectively. Tukey's HSD post-hoc: Chao1, P=0.01; Observed OTUs, P<0.001; Shannon, P=0.08. (**B**) Annotated heatmap based on Spearman distance and Ward hierarchical clustering of the top-30 genera shows how well the two locations cluster together. Taxonomy explanation includes genera, family and phylum, which are entered in order of abundance. Genus abundances were centered and standardized according to each column Z-scores and described by the change in the intensity of the grey colour, as annotated. (**C**) Differentially abundant family from a pairwise comparison with Welch's t-test with 95% confidence intervals (STAMP).

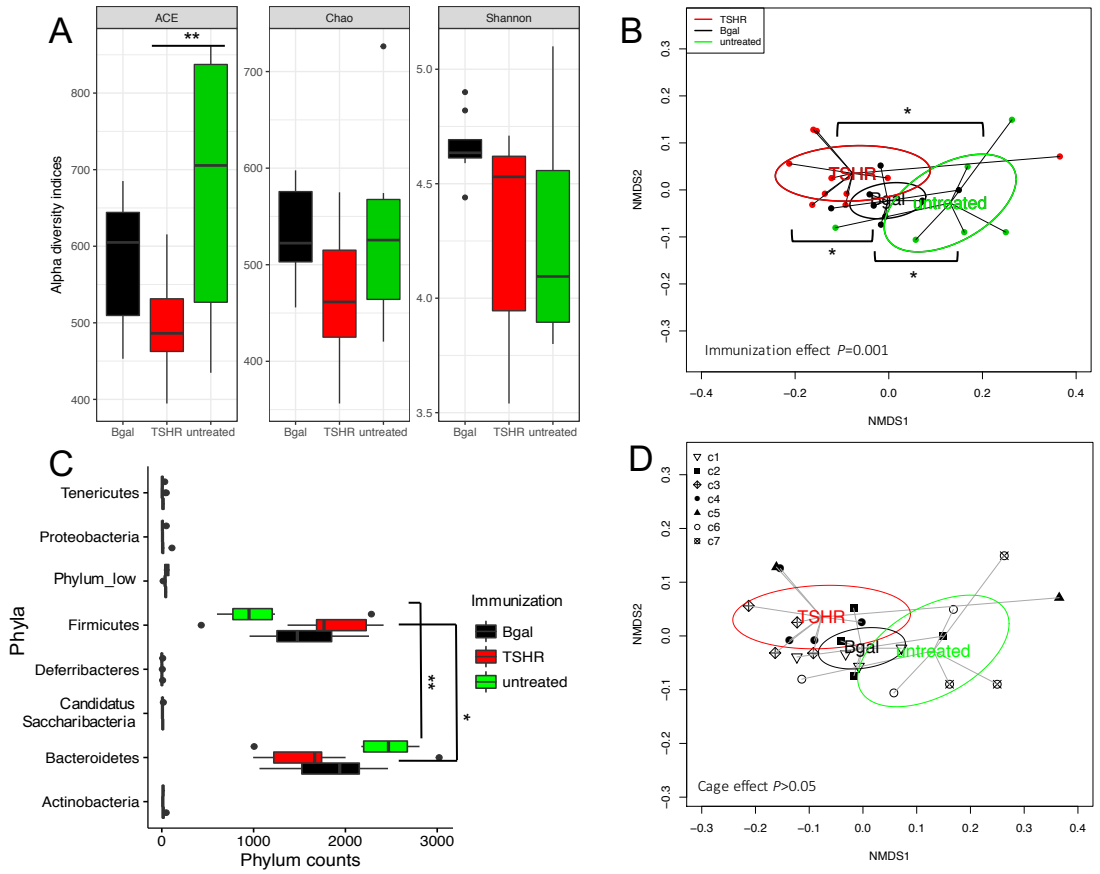

Figure 2.4. Gut microbiota composition in TSHR immunised mice and control mice in Centre 2 at final timepoint.

(**A)** Box and whisker plot describing the measurement of alpha diversity (Chao, ACE and Shannon indices). Tukey's HSD post-hoc analysis Chao and Shannon P>0.05, ACE index between TSHR and untreated groups, P=0.01. (**B)** Non-metric dimensional scaling (NMDS) plot of weighted Unifrac distances showed a spatial separation of microbial communities according to the immunizations. PERMANOVA based on 999 permutations P=0.001. Pairwise PERMANOVA TSHR-βgal P=0.024; TSHR-untreated P=0.026; βgal-untreated=0.024. (**C)** Boxplot of the phylum counts according to immunizations. ANOVA on phylum counts P<0.0001 and pairwise T-test between *Bacteroidetes-Firmicutes* counts adjusted P=0.0003. Pairwise t-test comparing *Bacteroides-Firmicutes* counts in immunizations: TSHR P=0.05, βgal *P*=0.2 and untreated P=0.012. (**D)** Non-Metric Dimensional Scaling (NMDS) plot based on weighted Unifrac distances shows spatial separation of the microbial community according to the immunization groups within the Centre 2 (black ellipses). PERMANOVA based on 999 permutation P=0.0005. Pairwise PERMANOVA Benjamini-Hochberg (BH) adjustment TSHR-βgal P=0.024, TSHR-untreated P=0.026, βgal-untreated P=0.024. Superimposed lines with different colours represent distances of the bacterial community according to the cages as described in the legend. Mice were co-housed according to their immunization at a maximum of 4 animals. No significant difference in cage effect is observed. PERMANOVA based on cage effect (999 permutations) for all comparisons P=0.12.

Table 2.6. Differential abundant taxonomic analysis between TSHR (n=10), βgal (n=8) and untreated (n=6), within Centre 2. Welch's T-test with 95% confidence interval using STAMP.

Comparison	Genus	mean freq. (%)[a]	std. dev. (%)[b]	mean freq. (%)	std. dev. (%)	difference between means	P value
TSHR *vs.* βgal	Acetitomaculum	0.086	0.068	0.285	0.129	-0.200	0.004
	Bacteroides	1.520	0.853	3.430	2.055	-1.909	0.047
	Fusibacter	0.040	0.039	0.007	0.012	0.033	0.035
	Genus_low	1.075	0.249	1.372	0.263	-0.297	0.037
	Lachnobacterium	0.317	0.238	0.620	0.304	-0.304	0.049
	Parabacteroides	0.031	0.045	0.078	0.034	-0.047	0.030
	Parasporobacterium	0.331	0.158	0.139	0.138	0.192	0.020
	Peptococcus	0.086	0.075	0.367	0.301	-0.282	0.043
TSHR *vs.* untreated	Flavonifractor	0.128	0.067	0.043	0.048	0.086	0.016
	Lactobacillus	18.591	13.883	5.048	3.732	13.543	0.019
	Thiofaba	0.034	0.033	0.005	0.011	0.029	0.031
βgal *vs.* untreated	Acetitomaculum	0.285	0.129	0.071	0.056	0.214	0.003
	Alloprevotella	0.157	0.288	1.344	0.873	-1.187	0.027
	Caminicella	0.053	0.052	0.000	0.000	0.053	0.030
	Flavonifractor	0.160	0.082	0.043	0.048	0.118	0.009

[a]Mean frequency, normalized through a cumulative sum-scaling (CSS) method, as implemented in STAMP. [b]Standard deviation, std. dev.

2.4.5. Dynamics and stability of faecal microbiota during the immunization protocol

To assess whether the immunization plasmids and the duration of the protocol could have influenced the gut microbiota composition, I calculated the total bacterial load and sequenced the bacterial 16S rRNA gene from the faecal pellets of the βgal and TSHR group from the baseline (T0) for 18 weeks afterwards, until the end of the experiment (T4).

From Equation 2, I observed a significant association of the 16S copy number with time (P=0.016, Table 2.7); however, no significant differences between immunisations were observed in each timepoint, a part in the latest timepoint.

A significant increase of the richness (Chao index, figure 2.5A; P=0.02) and the diversity (Shannon index, figure 2.5B) were observed over time, which were less apparent in the TSHR immunised group. Significant differences regarding richness between TSHR and βgal have been observed at T4 (P=0.027, Table 2.7). The Shannon index of diversity was significantly different between TSHR and βgal immunization at T1 (P=0.023, Table 2.7).

The murine faecal microbiota comprised *Bacteroidetes* and *Firmicutes* phyla predominantly (Figure 2.5C); followed by *Tenericutes*, *Proteobacteria, Deferribacteres* and Candidatus Saccharibacteria phyla. The *Firmicutes*/*Bacteroidetes* ratio has been used to describe the shift in the gut microbiota associated with ageing [323] and also in disease conditions such as obesity [223]. The ratio showed differences amongst the timepoints of the experimental procedure (P<0.01) and between TSHR and the βgal group after three weeks from the first injection (T1, P=0.011; Figure 2.5C).

Table 2.7. Summary of the statistical test (P values) from the time-course analysis of the faecal microbiota during the immunization protocol (T0-T4) and between immunizations (βgal and TSHR).

Index	Linear regression model[a]			TSHR *vs*. βgal group[b]				
	Immunization	Time	Time x Immun	T0	T1	T2	T3	T4
16S[#]	0.129	0.016	0.81	0.74	0.49	0.56	0.56	0.08
Chao	0.006	0.02	0.8	0.75	0.066	0.28	0.33	0.03
Shannon	0.054	0.28	0.47	0.44	0.023	0.35	0.35	0.29
F:B°	0.406	0.0003	0.16	0.39	0.028	0.46	0.2	0.26

[#]Log-transformed 16S gene copy number. °F:B, *Firmicutes*/*Bacteroidetes* ratio. [a]ANOVA model as described in equation 1. [b]Pairwise comparison between βgal and TSHR in each time point.

I fitted a generalized linear model (GLM) to compare the taxonomic counts at different timepoints within each group independently (either TSHR or βgal). Thirty-four genera have been identified as differentially abundant amongst all timepoints in reference to the baseline (T0) in the TSHR immunised group (Appendix 5), while 25 were found in the βgal group (Appendix 6). Differences in the taxonomic profile between TSHR and βgal groups were observed at each timepoint using an exact test (EdgeR). Once again T1 was identified as the timepoint with the highest number of genera differentially abundant, as illustrated by the diversity indices. Such genera were more abundant in the TSHR group, in particular, the genus *Prevotella* was nearly 9-fold more abundant in TSHR than in the βgal group (P=0.0163) (Table 2.8).

In contrast to data obtained from the gut microbiota (Figure 2.3D), a cage effect was observed in the faecal microbiota, in particular, in interaction with time (P=0.001) and immunization (P=0.002; Figure 2.6). The latter is probably due to the mice being caged according to the type of plasmid injection they received, but I also observed a significant difference within the same immunization group (e.g. TSHR in cage 4 and cage 5, P=0.01).

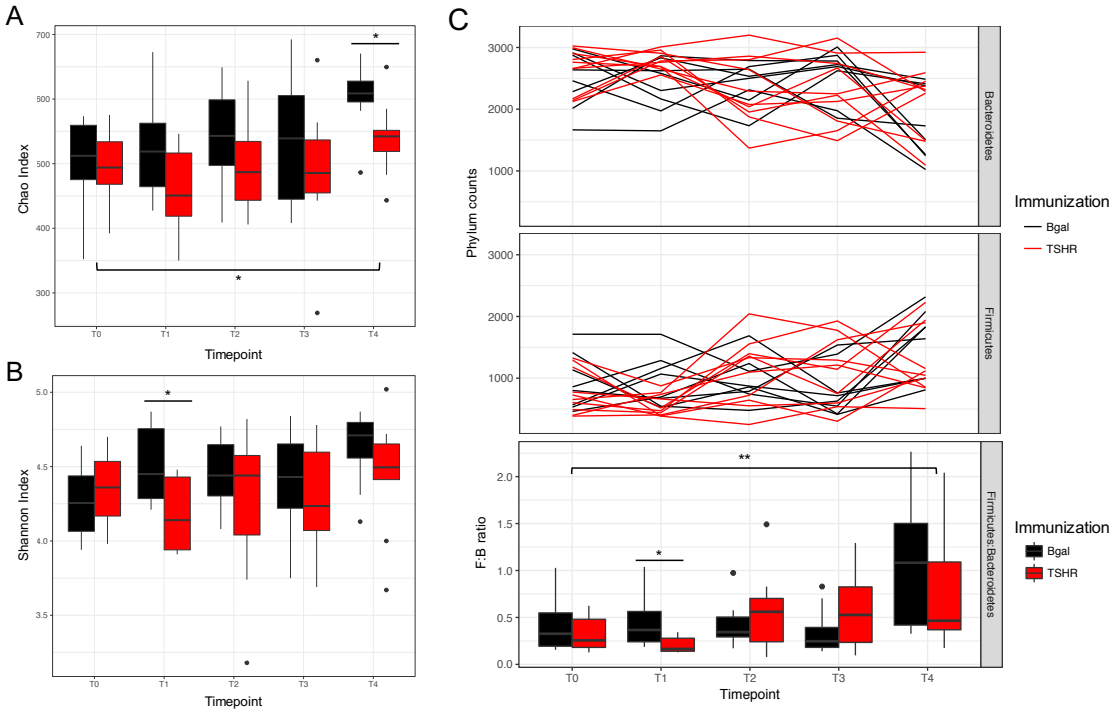

Figure 2.5. Time-course analysis of GO preclinical faecal microbiota during the immunization protocol.
Box and whisker plot of alpha diversity such as Chao, **(A)**, and Shannon, **(B)**, indices showed differences over time. Differences in richness (Chao) over time (ANOVA, P=0.02) in particular between the baseline and the last timepoint (post-hoc test, P=0.04) and between immunizations (P=0.006). A slightly significant difference in the Shannon diversity index was observed between immunizations (P=0.054). **(C)** Phylum dynamics over time and between immunizations. *Firmicutes* and *Bacteroidetes* were the most abundant phyla, showing differences with time and immunizations. Significant differences among timepoints have been observed at the *Firmicutes/Bacteroidetes* ratio (P<0.001), in particular between the baseline T0 and the last timepoint T4 (*post-hoc*, P=0.0013), but not related to immunization. A significant difference in the ratio was observed after three weeks from the first injection (T1) between βgal and TSHR (pairwise T-test, P=0.011).

Figure 2.6. Temporal stability of faecal microbiota and cage effect of the immunizations.

(Next page) Weighted Unifrac distances of mice faecal microbial communities represented over the time course of the experiment according to the immunization (**A**) or the cage (**B**). PERMANOVA of weighted Unifrac distances according to timepoint, immunizations, caging and their interactions (time x cage; time x immunization; immunization x cage) as described in Equation *2.* The time had a significant effect on the stability of the faecal microbiota (P=0.001), in particular between the baseline (T0) and the latest timepoint (T4, P=0.003); and between the T1 and T4 (P=0.009). The interaction between time and immunization was significant (P=0.007). Cage was also significant, in particular the interaction cage x timepoint (P=0.001) and cage x immunization (P=0.002). Significant differences within the same immunization group cage has been observed (TSHR group in C4 and C5, P=0.01).

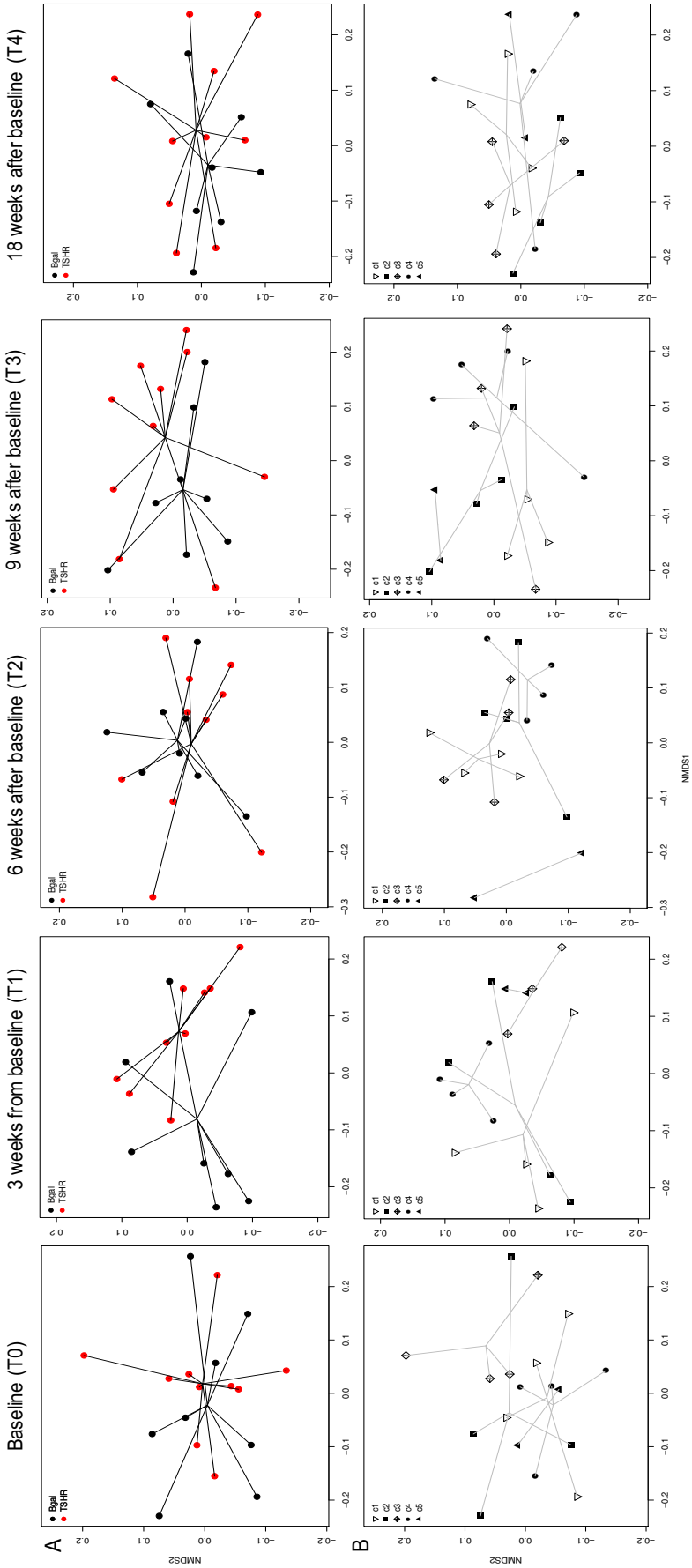
Baseline (T0)
3 weeks from baseline (T1)
6 weeks after baseline (T2)
9 weeks after baseline (T3)
18 weeks after baseline (T4)
A
B
Bgal
TSHR
c1
c2
c3
c4
c5
NMDS1
NMDS2

Table 2.8. Pairwise comparison of TSHR and βgal mice using Fisher's Exact Test in EdgeR at each timepoint (T0 to T4).

Timepoint	Genera	logFC[§] (βgal vs. TSHR)	*P* value
T0	Guggenheimella	-1.5934	0.0030
	Peptococcus	-2.6142	0.0195
	Lactobacillus	1.3432	0.0246
T1	Robinsoniella	-3.0655	0.0012
	Clostridium_IV	-2.7232	0.0036
	Butyrivibrio	-2.2934	0.0066
	Mucispirillum	-2.7743	0.0134
	Prevotella	-8.9035	0.0163
	Acetitomaculum	-2.1154	0.0179
	Anaerovorax	-1.7909	0.0179
	Lachnospiracea incertae sedis	-1.5169	0.0236
	Faecalibacterium	-3.0879	0.0265
	Intestinimonas	-1.2177	0.0403
	Lachnobacterium	-1.3480	0.0449
T2	Parasporobacterium	2.6409	0.0075
	Parabacteroides	-1.4670	0.0156
	Lactobacillus	1.2957	0.0292
	Galenea	-3.5744	0.0459
	Barnesiella	-0.9705	0.0492
T3	Papillibacter	-2.4871	0.0006
	Butyrivibrio	2.6026	0.0029
	Marvinbryantia	1.8713	0.0049
	Butyricimonas	-1.4919	0.0226
	Ruminococcus	-2.2425	0.0307
T4	Lachnobacterium	-1.7259	0.0067
	Acetitomaculum	-1.8684	0.0202
	Parasporobacterium	2.2330	0.0221
	Coprobacter	0.7723	0.0224
	Clostridium IV	-1.5336	0.0327

[§] LogFC, Log2 fold change of βgal compared to TSHR at each timepoint.

2.4.6. Correlating the gut microbiota composition with clinical features and differences in GO development

I then investigated possible correlations between disease features, such as anti-TSHR antibodies, thyroxine levels (fT4), orbital adipogenesis and muscular atrophy, and the gut microbiota composition to determine whether it contributes to the heterogeneity of induced responses, previously summarized in Table 2.3.

Within the Centre 1 TSHR-immunised group, OTUs from *Firmicutes* and *Bacteroidetes* negatively correlated to each other (Rho=-1, P<0.0001). Moreover, a positive correlation between levels of TSAb and *Deferribacteres* phylum, which include one-genus *Mucispirillum*, was found (Rho=0.92, P=0.028; Figure 2.7A).

From those genera differentially abundant between TSHR-immunised mice from Centre 1 and Centre 2 (Table 2.5), identified via metataxonomics, a strong negative correlation of the *Firmicutes* genus *Intestinimonas* spp. and the levels of TSBAb was observed in the Centre 1 (Rho=-0.89, P<0.05), but not in the Centre 2 counterpart (Figure 2.7B). No significant correlation was observed between OTUs from the genus *Intestinimonas* spp. and levels of TSAb or levels of free thyroxine hormone (fT4; data not shown).

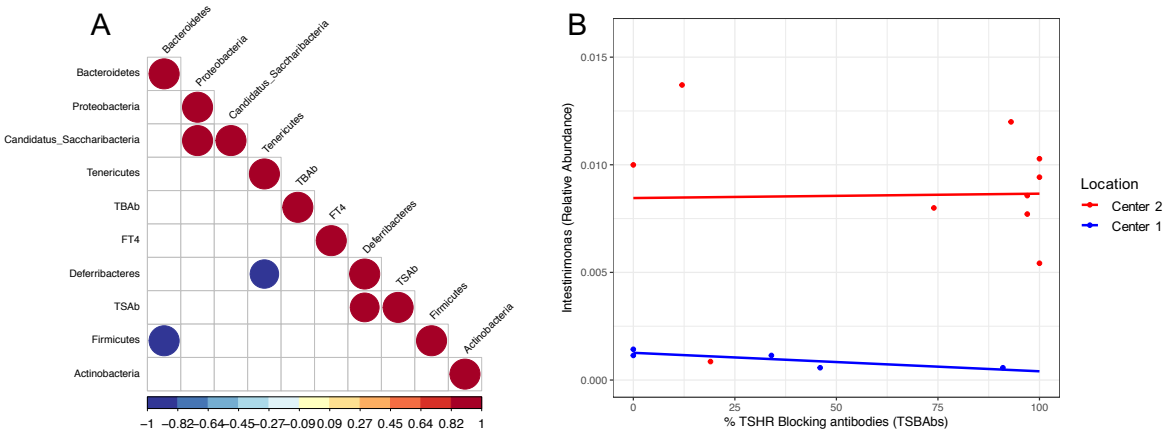

Figure 2.7. Correlating the gut microbiota and disease features in Centre 2 TSHR group.
(A) Spearman correlation coefficient strength (Rho) of phylum counts from TSHR mice in Centre 2. *Firmicutes* and *Bacteroidetes* showed a strong negative correlation between each other. A positive correlation between the one-genus phylum *Deferribacteres* and the level of thyroid-stimulating antibodies (TSAb) has been observed. Correlations with *P*<0.05 are shown and strength of the Rho coefficient is represented by the change in the colour intensity. fT4, free thyroid hormone thyroxine levels; TSAb, thyroid stimulating antibodies; TSBAb, thyroid-stimulating blocking antibodies (as a percentage values). **(B)** Enriched *Firmicutes* genus *Intestinimonas* between Centre 1 (blue) and Centre 2 (red) showed a strong negative correlation with the percentage of thyroid-stimulating blocking antibodies (TSBAbs) at 95% confidence interval in Centre 1 (Rho=-0.8, P=0.04), but not in Centre 2.

Within the Centre 2, *Bacteroidetes* and *Firmicutes* negatively correlated to each other (Rho=-0.99, P<0.0001). I also found a significant positive correlation (Rho=0.6, P=0.009) between the OTUs from the *Firmicutes* and the orbital adipogenesis value and a negative correlation of this value with the phylum *Bacteroidetes* (Rho= -0.57, P=0.014; Figure 2.8A). These correlations were specific to the TSHR immunised mice, moreover, the correlation pattern previously reported (*Firmicutes* positively correlated, *Bacteroidetes* negatively correlated) was also recapitulated at the genus level. Among the genera of the *Firmicutes*, three, within the Clostridia family (*Butyricicoccus*, *Parvimonas* and *Fusibacter*) and the genus *Lactobacillus* were correlated positively with adipogenesis; while three *Bacteroidetes* genera (*Anaerophaga*, *Paraprevotella* and *Tannerella*) correlated negatively with the orbital adipogenesis values (Figure 2.8B).

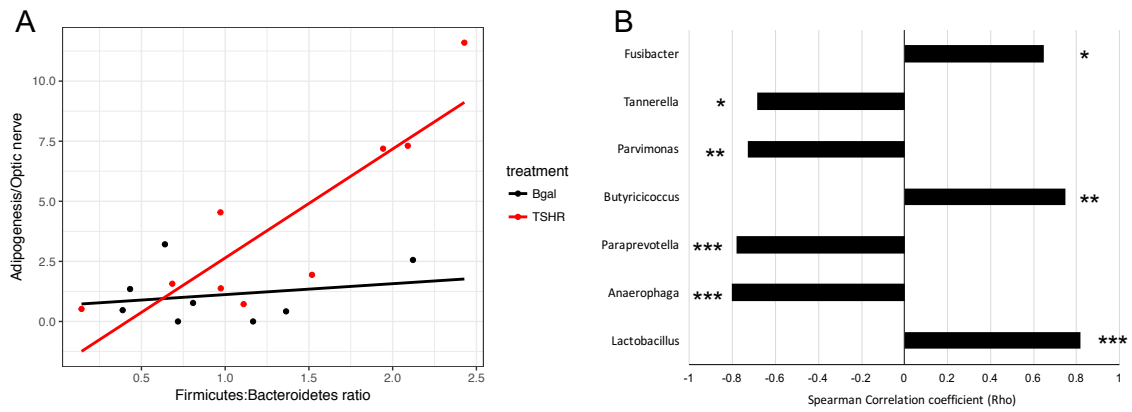

Figure 2.8. Correlation of the gut microbiota composition with clinical features and differences in Centre 2 mice.
(A) Positive strong correlation of the *Firmicutes/Bacteroidetes* ratio with the adipogenesis value (calculated in the orbit) resulted significant in TSHR immunised group (Rho=0.8, P=0.013) but not in the βgal group (Rho=0.08, P=0.98). **(B)** Spearman correlation coefficient (Rho) of genera among phyla *Bacteroidetes* and *Firmicutes* and the orbital adipogenesis values. The strength of the correlation coefficient is represented on x-axis: bars on the left represent a negative correlation coefficient, while bars on the right represent a positive correlation coefficient. Correlations with P<0.05 are shown; order of entrance depends on their P values: * P<0.05; ** P<0.01; *** P<0.005.

2.5. DISCUSSION

Animal models have been invaluable in dissecting the mechanisms causing loss of immune tolerance leading to autoimmune conditions such as GD. Thus, the hypothesis to be tested was "*that the gut microbiota may affect both outcome and reproducibility of induced autoimmune disease*", such as reported in the recent research article of UB-P and co-workers [187].

2.5.1. Animal conditions and effect of the conventionalized housing

Animals were maintained in similar conditions. We are confident that there were no infections ongoing at the moment of sampling, since animals in both centres were routinely tested for the presence of viruses, mycoplasma and parasites; moreover, housing facilities had comparable SPF conditions. Animals were from the same supplier but in different countries (Harlan Ltd. for Centre 1 and Harlan Lab. BV for Centre 2) and had been fed similar commercial diets, with the exception that food pellets provided in Centre 2 contained twice the amount of iodide compared to Centre 1 food. Although iodide excess can be associated with abnormal thyroid function, this dietary variation is not enough to explain the results (i.e. elevated thyroxine levels were apparent in the Centre 1, but not Centre 2 mice).

The importance of SPF conditions is indicated by a previous study which failed to reproduce a GO animal model, despite using mice from the same supplier and identical bedding, water and chow [188]. However even SPF may be inadequate since differences were found in the gut microbiota of C57BL/6 colonies bred in two different rooms of the same SPF facility [324], fortunately mice in our study were all housed in the same room.

Cage effects were apparent in the faecal microbiota results, which highlight the importance of studying the gut microbiota instead when comparing autoantigen (TSHR)-immunised and control mice, which is in the close proximity of the intestinal mucosa and the immune system, enabling us to explore its relationship with disease features. The total bacterial load was significantly different between the gut and the faecal microbiota. Also, faeces and intestinal scrapings of the same animals before and after euthanasia showed a heterogeneous composition of the microbiota in terms of richness and diversity of the bacterial communities and spatial organization of the beta-diversity (Appendix 7). Moreover, paired faecal and intestinal samples showed a highly variable strength of correlations (Spearman coefficient) ranging from weak (Rho = 0.50) to strong (Rho > 0.80) correlation depending on the sample, which is possibly attributed to the collection method of the faecal materials from the cage or the coprophagy habits of the mice.

2.5.2. Correlations between gut microbiota and disease features

Several disease-associated taxonomies were described; the abundance of the newly described butyrate-producing genus *Intestinimonas* [325] was reduced in the Centre 1 group compared to Centre 2 and correlated negatively with TSBAb. The *Intestinimonas* species *butyroproducens* has a unique ability to produce butyrate from lysine and is involved in the detoxification of Advanced Glycosylation End (AGE) products such as fructoselysin, which have been linked to type-1 diabetes [326]. Administration of short-chain fatty acids (SCFA), including the butyrate, ameliorated the severity of the EAE model by increasing the Tregs, but increased the severity of the antibody-induced arthritis model [327]. At the present, we are unaware of any link between butyrate-producing bacteria and thyroid autoimmunity.

The TSHR-immunised group developed some signs of GO and their gut microbiota had increased OTUs of the phylum *Firmicutes* but decreased *Bacteroidetes* compared with controls. This difference mirrors preliminary data in human disease, where we observed a dramatic reduction in the *Bacteroides* genus in GD patients when they develop GO, which will be further described in Chapter 4 of this thesis.

A positive correlation between several *Firmicutes* counts, such as clostridia and bacilli, with orbital adipogenesis in TSHR-immunised mice was also reported. Million and co-workers have previously reported a positive correlation between OTUs from the *Firmicutes* and weight-gain/obesity in both animal models and humans [328]. Interestingly, the role of the genus *Lactobacillus* and its products in either triggering or protecting from adipogenesis has been debated and seems to be species-specific. In the present work, we could exclude a possible gain-of-weight relationship with the adipogenesis value calculated in the orbit since no changes in mouse weights have been observed during the development of the chronic phase of the disease (data not shown). Furthermore, molecular mechanisms driving obesity and orbital adipogenesis may well be different, since the latter is derived from the neural crest and the gut microbiota may have varying effects on different fat depots [329].

2.5.3. Longitudinal analysis for faecal microbiota dynamics and stability

Time series or longitudinal analysis of the microbial communities can be useful to investigate the dynamics and the stability of those microbiota over time in the presence or absence of certain stimuli. Different methodologies are now available to be applied to ecological data as reviewed by Faust et al. [330]. The approach adopted in this chapter was to consider the time as a factor and test its interaction with other covariates in a model, using alpha, beta diversity indices or genus profiles as response variables.

Amongst observed covariates, our longitudinal analysis revealed that time had a dramatic role in shaping the faecal microbiota of the female mice which were 6-8 weeks-old at the outset and 24-26 weeks at the end of the experiment, confirming previously published works [331, 332]. The richness and diversity of βgal control mice increased with age, but this was less apparent in the TSHR immunised animals. Significant differences in microbiota composition between control and TSHR immunizations were most apparent three weeks after the first immunization, at the initiation of the induced immune response.

2.5.4. Use of the βgal expression plasmid as plasmid-control animals

The control group comprised mice immunised with the βgal expression plasmid in which I observed a reduced bacterial load and a slight skew in the microbiota richness and diversity which may be caused by the systemic overexpression of the β-galactosidase enzyme, whose natural role is in glycan metabolism, e.g. the hydrolysis of the lactose to galactose and glucose [333]. Kaneda and collaborators reported a βgal overexpression peak in the muscle fibres following electroporation from five days to 2 weeks after the injection [178]. This effect merits further investigation, but we are confident that the βgal vector plasmid provides the optimum control group since its microbial communities were more closely related to that of the naïve non-immunised group than to TSHR immunised mice.

2.6. CHAPTER CONCLUSIONS

In conclusion, results presented in this chapter indicate a role for the gut microbiota in modulating the heterogeneity apparent in the TSHR-induced model of GD and GO. Whether the correlations observed also correspond to causation has to be further proved. For example, the transfer of the gut microbiota of TSHR-immunised mice from one location to those in the other would determine whether the gut microbiota composition is directly responsible for the differences in the clinical outcomes observed in the two centres. Similarly, the faecal material from severe GO patients can be transplanted into murine recipients to observe the potential of the gut microbiota in transferring signs of GO.

In the next chapter the presence, absence or amounts of certain bacteria and their ability to directly influence the outcome of the GO model will be investigated, via the manipulation of the gut microbiota with the administration of either antibiotics, probiotics or the faecal material transplant from GO patients.

3. Chapter 3

Functional role of the gut microbiome in GO mouse models undergoing manipulations of the gut bacterial composition

Acknowledgments:

Dr. Utta Berchner-Pfannschmidt (UB-P), Dr. Sajad Moshkelgosha (SM), Prof. Anja Eckstein (AE), Prof. Paul Banga (PB), Dr. Hedda-Luise Köhling (now HLK) and their collaborators at the University Hospital of Duisburg-Essen for the manipulation study along with the immunisations of the GO mouse model and for having provided the DNA samples for sequencing

HLK, Dr. Sue Plummer and colleagues at Cultech Ltd. (Port Talbot, UK) for the production of the freeze-dried faecal material used as faecal transplant and for the production of Lab4 probiotic.

3.1. INTRODUCTION

In the previous chapter, a possible role for the gut microbiota was observed in the establishment of the mouse model of Graves' orbitopathy (GO) and its replication in a different laboratory. Moreover, some of the taxonomies differentially present in the disease model compared to controls showed a positive correlation with disease features, such as the orbital adipogenesis in the hTSHR-immunised mice. Such an association or correlation itself, however, is not sufficient to explain the causative role of these bacteria in triggering the disease status. For that reason, experimental manipulations of the gut microbiota would be necessary to allow functional and mechanistic description of the host-microbe interactions, and possibly assess a direct causality in disease-associated alterations in gut microbiota composition [199].

The type of diet, age, hormones and medications may naturally modulate the gut microbiota composition in humans and mouse models, as previously described in the general introduction. However, several and more specific gut microbiota manipulation strategies are now available and have been used in the past years to study the interplay between the immune response and the gut microbiota in autoimmune disease mouse models.

As previously described (chapter 1, par.. 1.5.5), apart from pathogenic bacteria, the gut microbiota composition can be affected by the use of antibiotics, showing a reduction of the richness and diversity of bacterial communities and, on the other hand, the growth of certain resilient or resistant bacterial species, depending on the type of antibiotic, dose and the duration of the treatment. When studying the functional role of the gut microbiota in a disease model, it might be of interest to observe changes in the disease phenotype due to the absence of certain or all bacterial species [334], which can be obtained using antibiotics or germ-free (GF, sterile) mice. Systemic lupus erythematosus (SLE), a systemic autoimmune conditions characterized by the presence of anti-nuclear antibodies (ANA), can be reproduced spontaneously in the MLR/lpr mice (i.e. homozygous for the lymphoproliferation spontaneous mutation Fas^{lpr}) [335]. The administration of either vancomycin alone or a mixture of broad-spectrum antibiotics to female SLE-prone MLR/lpr mice after the onset of the disease, attenuates the symptoms, with decreased serum levels of pro-inflammatory IL-6 and increased IL-10 levels – a known protective cytokine for SLE. The gut microbiota composition of these mice is significantly enriched in *Lactobacillus* spp. [336]. A delayed and less severe disease was also observed in the spontaneous model of autoimmune uveitis in R161H mice (transgenic for the expression of the TCR against the retinal protein IRBP) after treatment with a broad-spectrum antibiotics or in GF conditions [337]. While the absence of the gut

bacteria seemed to be protective for the development of some autoimmune conditions, in non-obese diabetic (NOD) mice – which spontaneously developed type-1 diabetes (T1D) with similar features as humans - treated with broad-spectrum antibiotics from conception to the end of the experimental procedure, showed a significantly increased incidence of type-1 diabetes (T1D), along with an accelerated onset compared to controls [338]. A similar situation was observed in GF MyD88-deficient NOD mice (i.e. lacking the innate immunity signal adaptor for bacterial stimuli) [339].

Another method of microbiota manipulation includes the transfer or the transplant of faecal material (FMT), which can be performed between murine strains (faecal material transfer) or from human to mice (humanized mice), depending on the purpose of the experiment. Such a transfer is usually performed through a gavage using either freshly-passed or frozen faecal samples, usually preceded by an antibiotic treatment or using GF animals, to reconstitute the entire microbiota. Faecal transfer from different murine strains might confer resistance or susceptibility to a certain disease from the donor to recipients; in fact, the microbiota from the diabetes-resistant MyD88-deficient NOD mice significantly delayed the onset of the disease when transferred into the diabetes-prone NOD mice [340]. In the case of humanized mice, the FMT is performed from humans to murine models usually to recapitulate the human microbiota possibly associated to a disease status [341]. In recent developments, faecal microbiota transplantation from a healthy donor, has been used as an efficient treatment to clear infections with the antibiotic-resistant *Clostridium difficile* in humans, which may arise after hospitalization and recurrent usage of antibiotics and might have a fatal outcome. Several strategies have been implemented to avoid the use of conventional faecal slurry transfer through colonoscopy in humans [342], aiming to retain the efficacy of the transplant such as the production of freeze-dried faecal microbial products [343] or the transfer of faecal filtrate [344].

Ultimately, modification of the intestinal bacterial composition can be also be driven by the administration of probiotics or “live organisms which when administered in adequate amounts confer a health benefit on the host”, according to FAO and WHO guidelines and the probiotic consensus statement [345]. Probiotics, as a dietary supplementation, can be administered as a single-strain or in *consortium*, most of them include the lactic-acid producing bacteria (LAB) *Lactobacillus* and *Bifidobacterium* spp. As will be further discussed in Chapter 5, one of the beneficial effects of probiotic intake is related to their ability to induce an anti-inflammatory immune response. A prevention of the TD1 onset was observed in NOD mice receiving multiple strains of *Lactobacillus* and *Bifidobacterium* spp. and of *Streptococcus salivarius* subsp. *thermophilus* which was associated with an increased production of IL-10 [346].

As a summary of the various manipulation strategies available, the experimental autoimmune encephalomyelitis (EAE) mouse model for multiple sclerosis has been extensively characterized in the past years, employing several of the manipulation methods described above, to dissect the functional role of the gut microbiota in the disease phenotype. The administration of antibiotics seemed to prevent the onset of the disease, due to a reduction of IL-17 levels and the increase of the Th2 immune response [315]. On the other hand, the mono-colonization with the segmented filamentous bacteria (SFB) of GF EAE mice increased the disease phenotype, associated to an increase of the IL-17 levels and a Th17 cells in the central nervous system [316]. The administration of a single-strain *Lactobacillus paracasei* or in combination of a three-strains probiotic reduced the pro-inflammatory response and reversed the induced phenotype with the up-regulation of Tregs via the production of IL-10 [347]. Similarly, oral administration of the LAB *Pediococcus acidilactici* R037 before the immunisation until the end of the study ameliorates the EAE onset in both C57BL/6 and SJL/L mice and contributed to a milder disease phenotype perpetuated as a therapeutic effect [348]. Recently, the transfer of faecal material derived from MS patients increased the frequency of a spontaneous development of relapsing-remitting EAE SJL/J mice (i.e. transgenic for the TCR-specific against the myelin oligodendrocyte glycoprotein [349]), along with the reduction of IL-10 and the decreased abundance of the genus *Sutterella* compared to mice receiving samples from healthy donors [350].

3.2. AIMS OF THE CHAPTER

The aim of the present chapter was to understand the complex host-microbiome interplay that underpins the TSHR-induced GD/GO model via the modification of the gut microbiota at the early-stage of life with either antibiotics, probiotics or FMT from sight-threatening GO patients compared to controls (water), along with the hTSHR-A subunit immunisation protocol described in the previous chapter. Specific goals from the microbiome analysis would cover: i) differences in the gut microbiota during the course and at the end of the study amongst treatments and immunisations groups and their correlations with the disease features, ii) the accuracy in the prediction for treatments and immunisations based on the gut microbiota composition through a Random Forest classification algorithm, iii) quantification of the extent of the hFMT from donors to recipients (engraftment) expressed as a percentage of similarity and calculated through an iterative Bayesian model (SourceTracker), iv) the prediction of the metagenomic functional profile and their differential variances amongst treatments and immunisations.

3.3. MATERIALS AND METHODS

3.3.1. Patient recruitment

Six Graves' orbitopathy (GO) patients with sight-threatening disease were recruited at the Ophthalmic Clinic of the University Hospital of Duisburg-Essen (Germany) by AE in the framework of the E.U.-FP7 Indigo project (http://www.indigo-iapp.eu/). The study was approved by the local research ethical commission (Ethik-Kommission reference 14-5965-BO) and written informed consent was obtained from each patient at the time of the enrollment. Eye disease activity and severity were assessed based on the EUGOGO guidelines [351]. All six patients were treated with steroid bolus and selenium before orbital decompression surgery (performed between 2014-2015). One patient (4011) had the decompression of both eyes, and two patients (4011 and 4015) continued steroid treatment after surgery. Faecal samples were collected at the time of the enrolment, when all patients were euthyroid, following procedures further described in Chapter 4 par. 4.3.1, stored at -80°C and shipped frozen to Cultech Ltd. (Port Talbot, UK). Samples were processed to generate the product to be used in faecal material transplant (hFMT) and DNA was extracted for metataxonomics by HLK, DC and GM. Thyroid function tests (TSH and FT4) and levels of the thyroid stimulating antibodies (TRAB) were measured according to the University Hospital of Duisburg-Essen local bioassays. A complete description of the patient characteristics used for hFMT production is described in Table 3.1.

Table 3.1. Characteristic of patients with sight-threatening GO recruited at the University Hospital Duisburg-Essen providing samples for hFMT production**.**

Patient ID	Age	Gender	Smoking	TSH[1]	FT4[2]	TRAB[3]
4008	43	female	current	2.72	13.2	1.45
4009	59	male	never	0.01	10.7	3.89
4010	60	female	current	5.76	14.2	14.75
4011	50	male	current	0.02	25.1	n.a.
4015	74	female	current	1.52	20.6	16.83
4020	51	female	current	5.2	16.1	n.a.

[1]TSH is expressed as mU/L; [2]FT4 is expressed as pmol/L and [3]TRAB is expressed as UI/L. n.a. not available.

3.3.2. Production of freeze-dried faecal material for transplant (hFMT)

Faecal samples from sight-threatening GO patients were processed by HLK at Cultech Ltd. (Port Talbot, Wales, UK) for the production of a freeze-dried faecal material to be administered to mice (hFMT). Faeces were pooled together and prepared for a sequential culture method in maximum recovery diluent broth (MRD). Initially, 0.1g of the pooled sample was added to 50 mL pre-reduced MRD broth and incubated overnight at

37°C under aerobic or anaerobic conditions. The mixture was further inoculated into 500mL pre-reduced MRD, followed by an overnight incubation at 37°C under aerobic or anaerobic conditions. As a control, pooled faecal samples from each inoculum were plated on non-selective agars (horse blood agar and anaerobic blood agar) and incubated overnight at 37°C under aerobic or anaerobic conditions in order to count viable cells. After a centrifugation step at 3,000 x g for 30 min, the resulting supernatant was discarded and the pellet was weighed and transferred into petri dishes, where they were supplemented with 10% w/v skimmed milk powder as a cryoprotectant agent, and placed at -80°C until completely frozen. The freeze-dried process was performed in a freeze-dryer machine from overnight to several days. 50µl from a stock of 0.5g powder in 4.5 mL MRD were used to count viable cells on non-selective agars (as previously described), MRS agar for lactobacilli and MRSx agar for bifidobacteria and incubated overnight at 37°C under aerobic or anaerobic conditions. The resulting powder was aliquoted into small vials to 0.125g final content and shipped to SM at the University Hospital of Duisburg-Essen (Germany) to be provided via a gavage to mice.

3.3.3. GO animal model and treatments

Female BALB/c mice used in this study were bred at the University Hospital of Duisburg-Essen (Germany) facility, in order to administer the treatments from an early-stage of life, and manipulation studies were performed by SM, UB-P and colleagues. The study was approved by the North Rhine Westphalian State Agency for Nature, Environment and Consumer Protection, Germany.

The antibiotic vancomycin was provided in the drinking water at a starting dose of 0.2 g/L to both dams first and pups later from their first day of life for the entire course of the experiment.

The probiotic Lab4® (Cultech Ltd., Port Talbot, UK) is a *consortium* of lactic acid-producing bacteria (LAB) comprising two strains of *Lactobacillus acidophilus* CUL60 (NCIMB 30157) and CUL21 (NCIMB 30156), *Bifidobacterium lactis* CUL34 (NCIMB 30172) and *Bifidobacterium bifidum* CUL20 (NCIMB 30153) and was administered at a total of $1x10^{10}$ CFU/50µl autoclaved water in each gavage. The hFMT powder was dissolved in sterile water and provided at a final concentration of $1x10^{10}$ CFU/gavage. A group of mice receiving autoclaved water was included as a control. Administration of both interventions and control was performed through a gavage (50µl) on pups for a total of four times from the first day after birth, at weaning, before and in the middle of the immunisation procedure, as described in figure 3.1. After receiving three gavages, at 6-7 weeks old, mice from each treatment or control group were divided in two more groups

for being immunised with either the immunisation with the human TSHR-A subunit (TSHR) or the β-galactosidase (βgal) control for immunisation, following the same protocol previously described in chapter 2 par. 2.3.1.

Faecal pellets were collected from mouse cages after three treatment-gavages, but before any immunizations with hTSHR or βgal (baseline), and after four gavages, but before the 3rd immunization (mid timepoint). At the end of the experimental procedure (6 weeks after the last immunization and almost 9 weeks after the last gavage), after the sacrifice of the mice, the contents of small, colon or entire intestines were collected for analysis by metataxonomics (endpoint), as described in Table 3.2.

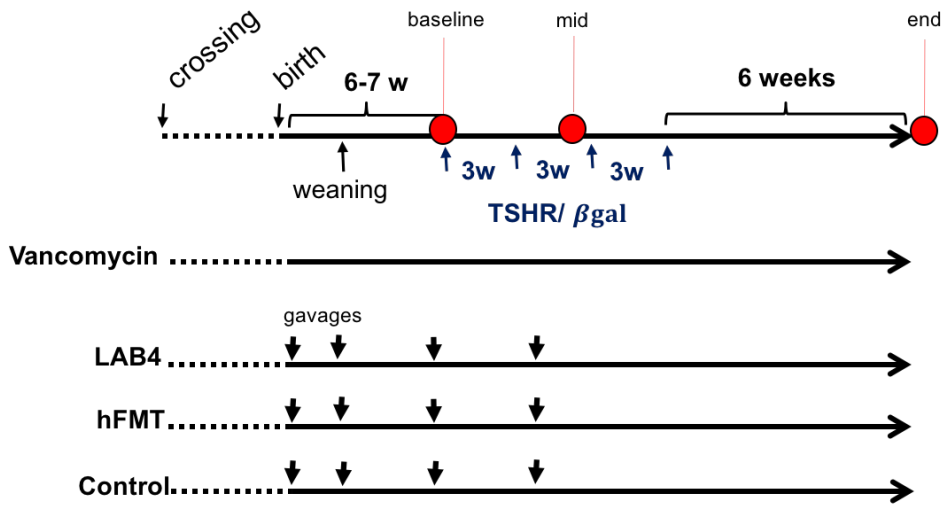

Figure 3.1. Experimental design of the gut microbiota manipulation.
Female BALB/c mice were immunised either with TSHR or the βgal expression plasmids alone (control) or in combination with a *consortium* of probiotics (Lab4) or faecal material transplant from severe GO patients (hFMT), or long-term treatment with vancomycin. Vancomycin was provided in the drinking water to dams before and pups from birth for the entire duration of the study; other treatments (hFMT and Lab4) and water (control) were provided through a gavage after birth, at weaning, before the first immunisation and before the third immunisation. Immunisation protocol (in blue) was the same as described in Chapter 2. Samples for microbiome analysis (red dots) were collected after three gavages but before the first immunisation (baseline), after four gavages but before the third immunisation (mid) and at the end of the experiment, after the sacrifice of the mice (end).

3.3.4. DNA extraction and 16S rRNA gene sequencing

A total of 297 mouse samples from either faecal pellets or intestinal contents (small, colon or entire sections) were extracted using the QiAmp Fast DNA Stool Mini kit (Qiagen, Germany), as previously described in Chapter 2 par. 2.3.2, by SM, UB-P and colleagues at the University Hospital Duisburg-Essen. Faecal samples from six GO donors for hFMT were processed for DNA extraction before the freeze-drying at Cultech

Ltd. (UK) using the same protocol as above. Metataxonomic sequencing (16S rRNA gene sequencing) was performed at Research & Testing RTL Genomics (Lubbock, Texas, USA), using primers detecting the V1-V2 regions of the 16S rRNA gene plus bifidobacteria regions (28F-combo, Chapter 2 Table 2.2) to generate 10,000 paired-ends reads on a Illumina MiSeq (Illumina, San Diego, USA).

3.3.5. Processing of metataxonomic reads

A first quality check on raw demultiplexed paired-end sequences (R1 and R2) was done using FastQC. All of the below steps were performed with the QIIME 1.9 open-source bioinformatics pipeline for microbiome analysis [208], which were configured and run using PipEngine (https://github.com/fstrozzi/bioruby-pipengine), as represented in Appendix 8. The complete QIIME command-line is available in Appendix X. Joining of paired-end sequences was done using the function “multiple_join_paired_end.py”, using the SeqPrep method (https://github.com/jstjohn/SeqPrep), which were quality-filtered according to the Phred quality score (Q), or the probability of a base-calling error (P), which is defined by the following equation: $Q = -\log_{10} P$. In particular, the following filtering parameters have been selected, as we have previously described [352]: i) maximum of three consecutive low-quality base calls (Phred < 19) allowed; ii) fraction of consecutive high-quality base calls (Phred > 19) in a read over total read length >= 0.75; iii) no “N”-labeled bases (missing/uncalled) allowed. A Phred > 19 would allow 1 error in 100 base-calling, resulting in 99% accuracy (to note that the default QIIME parameter is Phred = 3). Reads not matching all the above criteria were filtered out. Passing-filter reads were combined into a single FASTA file and were aligned against the SILVA 123 reference database using the “pick_closed_reference_otus.py” approach. A pre-defined taxonomy file of reference sequences to taxonomies is used for taxonomic assignment with a 97% cluster identity [353]. The OTU-table was created by counting the abundance of each OTU in each sample, and OTUs with total counts lower than 15 in fewer than 2 samples were filtered out. To correct potential biases in library size due to sampling procedures or sequencing depth, OTUs were normalized in each library through the cumulative sum scaling (CSS), where OTU counts were divided by the cumulative sum of counts up to a percentile determined using a data-driven approach [354] implemented in the “normalized_table.py” function. Filtered and normalized OTUs were collapsed into each phylogenetic level (from phylum to genus) using the function “taxa_summary.py”.

3.3.6. Statistical analysis

Statistical analysis, figures and tables were produced within the R environment (v3.4.1), unless specifically stated. In particular, the R packages ggplot2 and ggpubr were used.

The annotated heatmap including taxonomic data was produced with the NMF R package, scaling the values to each library size.

3.3.6.1. Alpha and beta diversity indices

To check whether sequencing depth was adequate, sequence-based rarefaction curves were generated from the unfiltered OTU table using the “alpha_rarefaction.py” function in QIIME 1.9, using the median sequence counts per sample as a “max_rare_depth” parameter. Within-sample alpha diversity indices of richness and diversity (Appendix 2) were estimated from the filtered OTU-table using the QIIME function “alpha_diversity.py”. Association of indices with variables (e.g. immunisations, treatments or microbiota sources) was done using the non-parametric Kruskall-Wallis analysis of variance, followed by a non-parametric pairwise Wilcox-test with Benjamini-Hochberg (BH) adjustment for multiple corrections [355]. Between-sample beta diversity matrix was calculated with the Qiime function “beta_diversity.py” with “SILVA123_QIIME/trees/97/97_otus.tre” as the phylogenetic tree. In particular, the Bray-Curtis matrix [356] was calculated from the filtered and normalized OTU table, according to the equation listed in Appendix 2. Dissimilarities amongst and pairwise variables were evaluated non-parametrically using the permutational analysis of variance approach (PERMANOVA) with 999 permutations [200], as implemented in the R Vegan package. When necessary, a stratification of the permutations was applied to correct for the different microbiota sources sampled (e.g. small, entire and colon samples).

3.3.6.2. Analysis of differential abundant taxonomies

Within each immunisation group (TSHR or βgal), differences in the microbial counts amongst treatments were tested using a linear regression model, correcting for the source of the anatomical site sampled (e.g. colon and entire). Pairwise differences between treatments were tested using a pairwise t-test with Benjamini-Hochberg (BH) adjustment for multiple corrections. Within each treatment (either control, Lab4, hFMT or vancomycin), differences between the two immunisations were assessed using a Welch’s t-test for unequal variance, with BH adjustment.

3.3.6.3. Random Forest

Random Forest (RF) is a statistical learning method [357, 358], based on the construction of a forest of “decision trees” for classification and regression purposes. A single decision tree is composed of i) internal nodes or splits, ii) branches that connect nodes and iii) terminal nodes or leaves carrying the label/value of prediction. RF usually grows a very large number of trees and each tree provides the classification/value of the

input vector. The RF training set is selected from a bootstrapped sample of *N* records (with the same size, but different composition due to sampling with replacement) and a subset of *M* variables (e.g. sqrt(M)). Every decision tree is different from any other, since they originate from randomly bootstrapped copies of the original dataset (bagging) and randomly sampled subsets of the variables [359]. Usually, 1/3 of *N* records are left out of the training set and can be used to test the model and they are called "out-of-bag examples" (T*n*). When the input values pass through each tree, they return an output (one per tree) and the final prediction is given by the majority of the vote (classification), or the average (regression). The out-of-bag (OOB) classifier would count the vote specifically over T*n*. In such a way, OOB is estimating the general classification error based on the OOB error rate of the training set, which has been proved to be unbiased, since both bagging and RF mainly reduce the variance component of the error (i.e. variance of the prediction) [359]. Variables that played the major role in the prediction accuracy can be derived [357] e.g. based on the mean decrease Gini Index for "node impurity" (classification) or on the mean squared error (MSE). A high decrease in the Gini index, for instance, defines important prediction variables that most likely played the major role in the classification algorithm. In this chapter, RF was employed to classify samples either amongst treatments (control, hFMT, Lab4 or vancomycin) or between immunizations (βgal or TSHR) based on their microbiota composition (classification), and to identify genera driving the classification (variable importance). Relative abundance counts with non-zero values in at least 20% samples were retained, scaled and centred. To estimate the accuracy of prediction, a repeated cross-validation (repeatedcv) method with number=10 and repeats=3 was used. The tuning hyperparameter *mtry*, calculated around the square root of the number of variables of the dataset, was tuned testing from 10 to 50 and 5,000 or 10,000 number of trees (ntree) using the R package Caret. RF was next run using the identified parameter values providing the highest prediction accuracy during the cross-validation step using the R package RandomForest. The mean decrease Gini was used for the variable importance selection.

3.3.6.4. Correlation analysis between gut microbiota and disease features

Disease features were grouped into specific categories such as: Lymph node T cells ($CD25^+$, $CD4^+$ and memory/effector T cells), orbital pathology (muscular atrophy, brown fat and total fat), thyroid function and auto-antibodies (fT4, TRAK and mTSAB) and orbital T cells ($CD4^+$ and $CD8^+$, but only available for some mice). Finite values (missing data were excluded) were correlated to the abundance of microbial biomarkers from the large intestine (obtained from the RF analysis) in each treatment and per immunisation through the Spearman correlation coefficient (Rho), using the Corrplot R package.

3.3.6.5. Prediction of metagenomic functions (Tax4Fun)

The functional profile of the metagenome can be imputed or predicted from the taxonomic composition obtained in a 16S rRNA gene sequencing in a cost-effective manner, using a database of pre-computed reference genomic profiles, as we previously employed [352]. However, the main limitation of this approach derives from the prediction of a whole set of metagenomic functions from the variable regions of the 16S rRNA gene and thus should need the validation through a whole-genome sequencing (metagenomic) approach. The Tax4Fun R package [360] employs the nearest neighbor identification with a minimum sequence similarity to link the representative 16S rRNA gene sequences to functional annotations of prokaryotic genomes [361], with the SILVA123 release reference sequence collection. Gene ontologies and associated metabolic pathways of the predicted metagenomes were obtained from the Kyoto Encyclopedia of Genes and Genomes (KEGG) reference database of genome annotations [362].

3.3.6.6. Longitudinal analysis

The combined effects of treatment, immunisation and time in shaping the gut microbiota of the GO model were estimated and considered to as fixed effects in the following linear model (**Equation 3**):

$$y_{ijkl} = \mu + Treat_i + Immun_j + Time_k + (Treat * Immun)_{ij} + (Treat * Time)_{ik} + (Immun * Time)_{jk} + e_{ijkl}$$

where y_{ijkl} is one of the alpha-diversity indices, Bray-Curtis matrix (assessed using the Adonis function in the Vegan package) or the *Firmicutes/Bacteroidetes* ratio calculated from the *Firmicutes* and *Bacteroidetes* normalized relative abundances in each sample; μ is the overall mean; Treat is the type of manipulation treatment (i.e. control, hFMT, Lab4 or vancomycin administration), Time is the effect of timepoint (either baseline or mid); Immun, is the type of immunisation (either the TSHR or βgal). The factorial interactions between immunisation and time, immunisation and treatment and time per treatment were also included in the model; e_{ijkl} is the vector of residual effects. Comparison between βgal and TSHR immunizations at each timepoint was made using the pairwise t-test with BH correction.

3.3.6.7. SourceTracker Bayesian model

The SourceTracker R package [363] was used to determine the possible transfer of taxonomies from donors to recipients – or engraftment [342] - as a result of the hFMT in mice. Originally created to test the contamination level of a microbiota sample, the

software implements an iterative Bayesian model which calculates the probability that recipient microbiota samples (sink) come from one donor sample (source), through the calculation of the posterior probability *via* Gibbs sampling in the donor samples.

An extensive description of the methodology is presented in the original paper [363]. Given each sink sample (**x)** a set of *n* taxonomic sequences, each of those can be assigned to any of the source environments $v \in 1 \ldots V\}$, including also unknown sources. Implementing the collapsed Gibbs sampling for topic model, each sink-taxon is assigned to a random source environment**,** termed "hidden variable" $\boldsymbol{z}_{i=1\ldots n} \in 1 \ldots V\}$. Assuming that these assignments are correct - although random – the proportions of source environments in the sink samples are tallied. Subsequently, one taxon is removed from the tallies, and the assignment of the source environment is repeated. Thus, the probability of selecting each source environment is proportional to the probability of observing that sink-taxon in that source, times to the probability of observing the source in the sink sample. Once re-assigned, the tally is updated for the selected taxon and the operation is repeated on another randomly chosen taxon. At the end of all the possible assignment iteratively performed, each obtained set is the representative distribution of the possible taxon/sources assignment. Repeating such operation *n* times, it provides the estimation of the conditional distribution. The original equation is as follow (**Equation 4**):

$$P\left(z_i = v \middle| \boldsymbol{z}^{\neg i}, x\right) \propto P(\boldsymbol{x}_i|v) \times P\left(v \middle| \boldsymbol{x}^{\neg i}\right) = \left(\frac{m_{x_i v} + \alpha}{m_{tv} + \alpha m_{tv}}\right) \times \left(\frac{n_v{}^{\neg i} + \beta}{n - 1 + \beta V}\right)$$

Whereas: m_{tv} is the number of training sequences from taxon *t* in environment v; n_v is the number of sink sequences assigned to environment *v*, while $\neg i$ represents the exclusion of the ith sequence. The first fraction is the posterior distribution calculated on sink taxa in the source environment, while the second provides the posterior distribution calculated over source environments in the sink sample. Such Bayesian model uses Dirichlet continuous distribution: α and β are the Dirichlet parameters to smooth the distribution for low-coverage source and sink samples. Moreover, they allow the assignment to the unknown source, when the sink sample is not like to any sources.

The GO patients and the control mice microbiota were used as "source" while the hFMT microbiota was used as "sink" (later defined as a test). To test the specificity of the hFMT engraftment, I used the hFMT and human microbiota communities as "source" and the murine control microbiota as "sink" (later defined as a control). The SourceTracker was run on the filtered OTU table, using either OTU, genus or family taxonomic levels (as integers) and default parameters (10 restart Gibbs sampling, 100 burn-in iterations for Gibbs sampling and 1,000 rarefaction depth). Counts that could not be assigned to a

source at a certain significant threshold (α=0.001) were defined as “unknown”. The command-line for the SourceTracker activation and run is listed in Appendix 8.

SourceTracker returns a list of possible “invaders”. I selected the most abundant taxonomies and the extent of the invasion for each taxa specifically occurring in the hFMT-receiving mice (sink) was quantified. For each taxa, in fact, I subtracted the mean value of the control group (murine source) from that of the hFMT group (**Equation 5**):

$$dFMT_x = \mu x_{hFMT} - \mu x_{control}$$

Where x is the each taxonomy and μ is the mean of that taxonomy in the group, either hFMT or controls. For each taxonomy, I next calculated the mean percentage change of the dFMT from the GO patients (human source) as in **Equation 6**:

$$ddFMT_x = \frac{\mu x_{dFMT} - \mu x_{GO}}{\mu x_{GO}} \times 100$$

Where x is the each taxonomy and μ is the mean of that taxonomy in the group, either the dFMT previously calculated or GO patients.

Table 3.2. Summary of the total murine sample processed according to timepoint and variables such as treatments, immunisations and microbiota samples.

	Baseline	Mid	Final
Treatment & Immunisation°			
Control	16 (6/10)	20 (9/11)	33 (14/19)
hFMT	15 (6/9)	24 (9/15)	39 (16/23)
Lab4	14 (5/9)	22 (11/11)	20 (10/10)
Vancomycin	20 (8/12)	28 (14/14)	37 (18/19)
Immunisation#			
βgal	25	43	58
TSHR	40	51	71
Microbiota Sources^			
Faecal samples	65 (16/15/14/20)	94 (20/24/22/28)	none
Small	none	none	51 (13/20/0/18)
Colon	none	none	48 (10/19/0/19)
Entire	none	none	30 (10/0/20/0)

° total amount of samples and per immunisation (βgal/TSHR); # total amount of samples; ^total amount of samples and per treatment: control/hFMT/Lab4/vancomycin. At the baseline and mid timepoints faecal samples were collected from each cage while at the end of the experimental procedure, after the euthanasia, microbiota samples were collected from the small intestine, the colon or from the entire intestine. °paired samples of small intestine and colon were obtained from the same mouse, but some paired samples (3/51) were lost during sequencing, although a few samples failed during sequencing; *entire intestines were collected from Lab4 treated and a small group of the control mice

3.4. RESULTS

3.4.1. Clinical outcomes of the GO model

Disease assessment was performed by SM, UB-P and AE. Briefly, antibodies against the human TSHR, measured by TSH binding-inhibition (TRAK assay) or their ability to alter thyroid function by stimulating cAMP production (TSAB), were induced in all TSHR-immunised mice, but not in the equivalent βgal controls (in all cases results between TSHR and βgal immunised mice were compared within the 4 treatment groups). An exception to this was observed in the vancomycin-treated mice in which no pathological TSAbs were detected. Hyperthyroidism, quantified as thyroxine levels (fT4), was significantly induced only in the Lab4 probiotics-treated TSHR-immunised mice. Orbital examination was assessed by quantifying adipose tissue volume, proportion of 'brown' adipose tissue ('BAT') and atrophy of the extra-ocular muscles (EOM). These evaluations revealed significantly more 'BAT' in TSHR-immunised compared to βgal, only in control and probiotic-treated mice. Significant expansion of orbital adipose tissue was not observed in any of the TSHR immunised mice although significant atrophy of the EOM was detected, but only in control TSHR immunised mice. In draining lymph

nodes, numbers of CD25$^+$ (Tregs) cells were significantly lowered in vancomycin-treated mice, while increased in the βgal-immune probiotic-treated mice.

3.4.2. Summary of the sequencing outcomes

Sequencing of the V1-V2 plus bifidobacteria regions of the 16S rRNA gene produced a total of 13,782,107 sequencing reads after the "join paired-end.py" function in QIIME 1.9, with an average of 2,297,017.83 (± 1,820,298.366). Filtering of reads with a Phred > 19, allowing about 1 error in 100 bases, retained a total of 12,884,785 sequences with an average of 2,147,464,17 (± 1,726,134.85), which resulted in 6.5% of sequences being removed. A summary of the per-group sequences is represented in Table 3.3. While the control, hFMT and the Lab4 treatment groups showed very similar numbers of reads, the vancomycin treatment group showed double the amount of reads. A smaller number of reads were obtained from the six GO patients (plus some replications) providing the samples for the hFMT production. A total of 3,623 OTUs were obtained from the "closed_OTUpicking.py" function, after filtering for less than 15 counts in at least two samples.

Imputation of metagenomic functions with Tax4Fun produced a total of 266 KEGG pathways, which were reduced to 38 when accounting for more than 0.001 of their relative abundances.

Table 3.3. Summary of the sequencing metrics before and after quality filtering.

Group	Input			Output		
	number of Seq	average	std^	number of Seq	average	std^
control	2,593,620.00	18,794.35	21,365.58	2,418,786.00	17,527.43	22,024.42
hFMT	2,972,296.00	19,053.18	22,141.82	2,757,051.00	17,673.40	22,825.32
Lab4	2,102,509.00	18,772.40	20,909.85	1,945,969.00	17,374.72	21,642.50
vancomycin	5,280,854.00	31,063.85	35,929.00	5,003,546.00	29,432.62	36,836.65
GO patients	483,510.00	24,175.50	17,947.64	428,852.00	21,442.60	20,137.71
unknown°	349,318.00	21,832.38	26,630.17	330,581.00	20,661.31	27,272.35
total	*13,782,107.00*	*2,297,017.83*	*1,820,298.36*	*12,884,785.00*	*2,147,464.1*	*1,726,134.85*

°unknown samples were mislabeled samples which were sequenced but not included in further analysis; ^ standard deviation.

3.4.3. Anatomical differences of the gut microbiome in GO mouse model

In the previous chapter, differences between the gut microbiota in controls (βgal) and TSHR immunised mice (not receiving any treatments) at the end of the experimental procedures were reported [322]. Here we replicated the same experiment, looking at

different anatomical sections of the intestine (i.e. small intestines and colon *vs*. entire), compared to the whole intestinal scraping as previously employed, of gavage-control mice either immunised with TSHR or βgal (immunisation control). As previously observed [364], the small intestine showed a reduced richness and diversity compared to large intestines ($P<0.05$, BH corrected, Figure 3.2A). There were no significant differences between the entire and the colon samples (as for Chao1 and observed-OTUs) after correction; while the diversity (Shannon) and the evenness indices were not significantly different also before corrections. Therefore, the combination the two intestinal sections will be referred to as "large intestine", where not specified which section was used.

As far as immunisations are concerned, TSHR-immune mice showed a reduced richness compared to βgal control in colonic samples, while entire intestines displayed a slight but not significant increase in richness. However, in the small intestine, immunisation with the TSHR-A plasmid seemed to increase the richness (although not significantly), the diversity ($P=0.05$) and the evenness ($P=0.03$) of the bacterial communities compared to the βgal (Figure 3.2B). A separation of the immunisations was also observed between-samples (beta-diversity) using the Bray-Curtis matrix in both large ($P=0.036$) and small intestines ($P=0.002$, using 999 permutations, figure 3.2C). Differential abundant taxonomies between immune groups were identified in each intestinal sites. At the phylum level, *Tenericutes* counts were reduced/absent in the colon samples in TSHR compared to βgal ($P=0.012$). A significant reduction in genera belonging to phylum *Bacteroidetes* were observed in TSHR-immunised colon and entire samples, while a prevalence of genera from *Firmicutes* were enriched in TSHR-immunised small intestines and entire samples, as summarized in Table 3.4. Also, an uncultured genus from *Bacteroidales* was decreased in TSHR immune mice compared to βgal in entire-gut samples.

Metagenomic functions were predicted from the filtered OTU table using the Tax4Fun tool [360] from the three anatomical sections of TSHR-immune and βgal mice. Metabolic pathways for nitrogen, starch and sucrose and methane metabolism, but also glycolysis and gluconeogenesis were prevalently described in the small intestine (Figure 3.3A), while those for the amino-sugar and nucleotide-sugar, fructose and mannose, galactose, glycine, serine and threonine, porphyrin and chlorophyll metabolism were present in colon and entire samples (Figure 3.3C and E), in line with the specialized functions of the gut microbiota. Moreover, RNA degradation was predicted in colon and entire samples, but not in the small intestinal microbiota. While most of the top-variant pathways were shared between colon and entire samples, the latter showed the unique presence of the oxidative phosphorylation pathway. Pathways such as the degradation

of other glycans, bacterial ATP-binding cassette (ABC) transporters and the two-component system, despite being in the top-10 most variant, were shared amongst intestinal sections. Differences between immunisations were observed in each intestinal section (Figure 3.3B, D and F). Although differences were not enormous, nitrogen metabolism and other glycan degradation had higher variance in the TSHR group compared to βgal in small intestine (Figure 3.3.B). In the colon samples, ABC transporters, the two-component system and the porphyrin and chlorophyll metabolisms were reduced in TSHR compared to βgal, while the other pathways were increased in TSHR (Figure 3.3.D). Amongst them, the fructose/mannose, galactose, glycine/serine/threonine metabolism and the degradation of other glycan were the most different. Interestingly, differences between the two immunisations in the entire samples seemed to be opposite to that in the colon samples, e.g. other glycans degradation reduced in TSHR (Figure 3.3F).

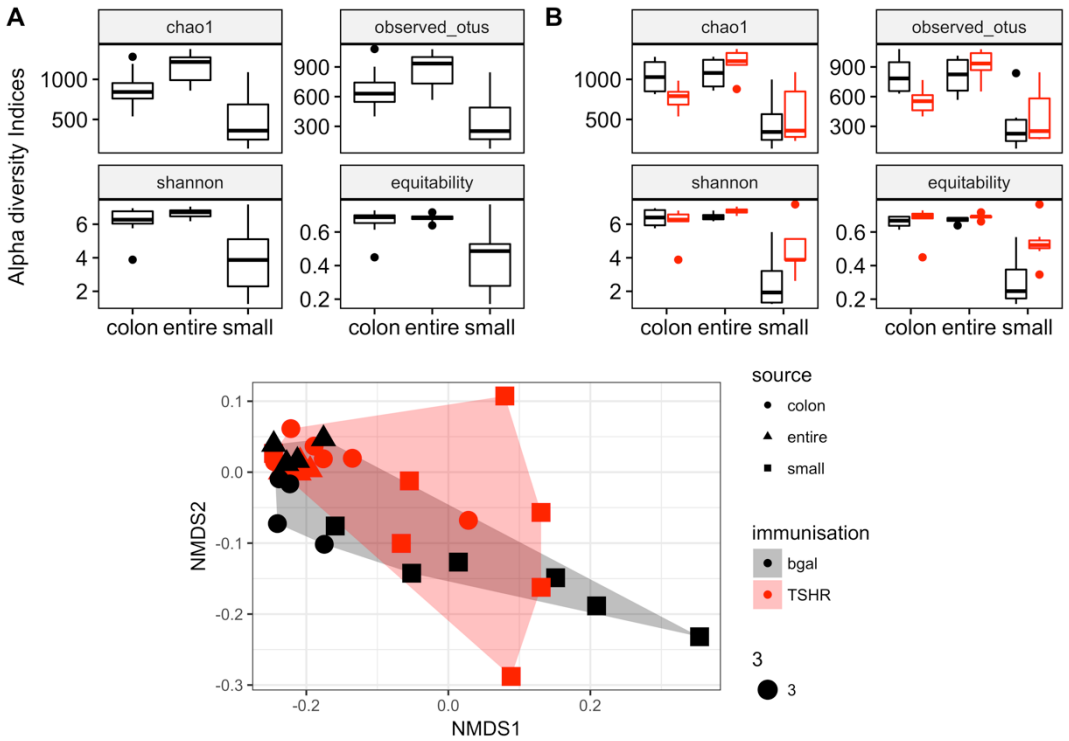

Figure 3.2. Microbiota composition of small intestine, entire intestine and colon in TSHR and βgal-immunised mice in control mice groups.
(**A**) Box-and-whiskers plot of alpha-diversity indices of richness (Chao1 and observed-OTUs), diversity (Shannon) and equitability (evenness) according to the source of the microbiota sampled (colon and small). (**B**) Alpha-diversity indices of richness, diversity and equitability between immunisations according to the source of the microbiota sampled (colon, entire and small). (**C**) Non-metric dimensional scaling (NMDS) based on Bray-Curtis distances according to immunisations and microbiota sources.

Table 3.4. Differentially abundant taxa between TSHR and βgal immunisation in different intestinal sections.

Differentially abundant taxonomy (phylum; genus)	Section	Diff. mean[a] (βgal - TSHR)	βgal (mean)	TSHR (mean)	P value[§]
Actinobacteria;Enterorhabdus	colon	19.110	32.898	13.789	0.036
Bacteroidetes;Parabacteroides	colon	6.930	12.705	5.776	0.032
Bacteroidetes;Paraprevotella	colon	3.142	4.355	1.212	0.005
Firmicutes;[Eubacterium] hallii group	colon	4.097	4.995	0.898	0.020
Firmicutes;[Eubacterium] nodatum group	colon	2.964	10.821	7.857	0.037
Firmicutes;[Eubacterium] oxidoreducens group	colon	6.990	10.638	3.647	0.015
Firmicutes;Anaerotruncus	colon	27.183	43.423	16.241	0.003
Firmicutes;Erysipelatoclostridium	colon	2.109	6.994	4.885	0.023
Firmicutes;Incertae Sedis	colon	18.706	23.135	4.429	0.034
Firmicutes;Intestinimonas	colon	4.625	11.013	6.388	0.015
Firmicutes;Lachnospiraceae FCS020 group	colon	3.670	5.788	2.117	0.006
Firmicutes;Peptococcus	colon	2.392	4.308	1.916	0.032
Firmicutes;Ruminiclostridium 5	colon	13.087	21.738	8.651	0.005
Firmicutes;Ruminiclostridium 9	colon	18.509	43.987	25.478	0.006
Firmicutes;Ruminococcaceae UCG-003	colon	4.985	8.098	3.112	0.005
Firmicutes;Ruminococcus 1	colon	17.752	26.337	8.585	0.000
Firmicutes;Ruminococcus 2	colon	1.379	1.701	0.323	0.039
Tenericutes;Anaeroplasma	colon	3.871	4.085	0.214	0.009
Tenericutes;Other	colon	5.422	5.422	0.000	0.019
Tenericutes	colon	9.293	9.507	0.214	0.012
Bacteroidetes;Prevotellaceae UCG-001	entire	1.850	17.892	16.042	0.029
Bacteroidetes;uncultured Bacteroidales bacterium	entire	5.227	13.309	8.081	0.001
Firmicutes;Blautia	entire	-8.571	10.914	19.486	0.024
Firmicutes;Family XIII AD3011 group	entire	-1.755	0.000	1.755	0.015
Firmicutes;Intestinimonas	entire	-5.168	8.249	13.417	0.019
Firmicutes;Lachnospiraceae FCS020 group	entire	-4.557	6.003	10.560	0.033
Firmicutes;unidentified	entire	-4.930	8.876	13.806	0.020
Proteobacteria;Bilophila	entire	-1.207	3.385	4.592	0.017
Proteobacteria;Escherichia-Shigella	entire	-2.754	2.054	4.808	0.044
Bacteroidetes;Alloprevotella	small	-1.826	0.358	2.185	0.046
Firmicutes;Allobaculum	small	7.000	14.626	7.626	0.036
Firmicutes;Blautia	small	-10.981	5.998	16.979	0.011
Firmicutes;Lachnospiraceae ND3007 group	small	-2.695	0.000	2.695	0.040
Firmicutes;Lachnospiraceae UCG-004	small	-16.709	3.927	20.636	0.000
Firmicutes;Ruminococcus 2	small	-2.335	0.287	2.621	0.030

[a] difference in means (βgal – TSHR); § only taxa with P value < 0.05 are shown.

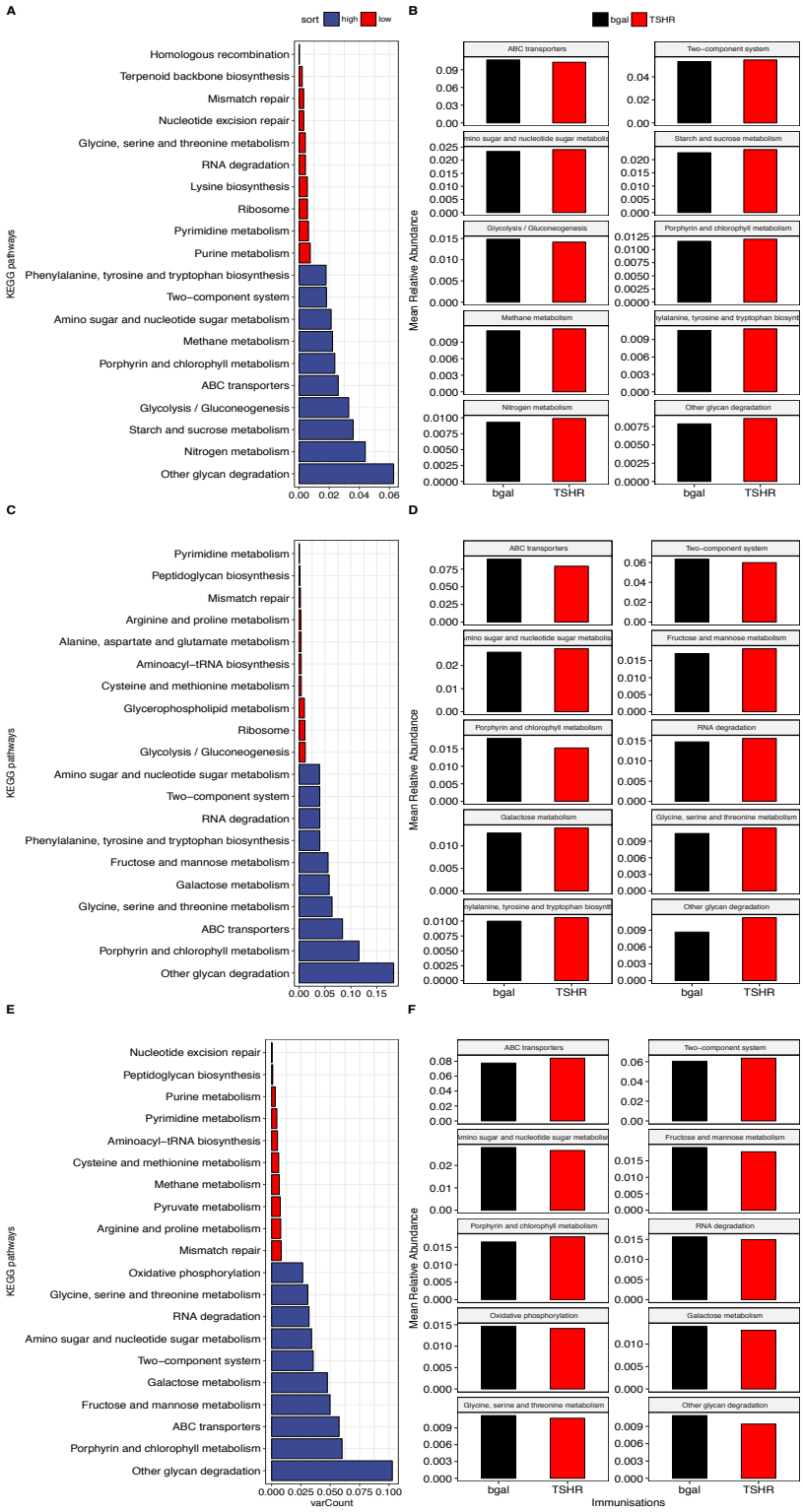

Figure 3.3. Metagenomic functions predicted in the control group between immunisation along the intestinal tract.

Top-10 and least-10 variant KEGG pathways according to anatomical sections of the gut: small (**A**), colon (**C**) and entire (**E**) and differences in the top-10 variant pathways between immunisations (TSHR or βgal) in each gut section (**B**, **D** and **F**). varCount, across-group coefficient of variation (standard deviation/mean pathway relative abundance) in percentage (%).

3.4.4. Treatment effect on endpoint βgal-microbiota composition

Differences amongst manipulation treatments in the βgal -control group were analysed. At the alpha diversity level, the entire and colon samples were analysed together as large intestine, since there was no differences between the two in terms of diversity and evenness (Figure 3.2A). The long-term vancomycin treatment depleted the microbiota composition in terms of richness and diversity (P<0.0002), while there were no significant differences between the other treatments and the control group (Figure 3.4A). On the contrary, the small intestines showed a less severe effect of the vancomycin treatment, with no significant reduction of the richness indices (Chao and observed OTUs). The hFMT treatment, on the other hand, increased the Shannon diversity (P=0.02) and the equitability indices (P=0.045) compared to vancomycin and to the controls, however, not reaching significance (Figure 3.4B). Between-group differences were observed using the Bray-Curtis matrix amongst treatments (P=0.001, 999 permutations), taking into consideration the different microbiota sources used. Pairwise differences were observed between all the treatments (P<0.05, with 999 permutations and BH adjustment), apart from the hFMT-control (P=0.42), whose centroids laid more closely to each other (Figure 3.4C).

Differential abundance analysis investigated the differences in taxonomic composition amongst treatment and in-pairwise. In large intestines, the abundance of eighty-three taxonomies (including phylum and genus levels) were significantly altered between treatments in the βgal group from a linear model (Appendix 9), correcting for different microbiota sections (e.g. colon and entire intestine). At the phylum level (Figure 3.5), *Actinobacteria* were enriched in the control group (37.39 ± 12) and drastically decreased in the vancomycin group (0.36 ± 1); *Bacteroidetes* were enriched in the Lab4 group (837.97 ± 131) and decreased in the vancomycin group (233.60 ± 42.59). *Firmicutes* was the most abundant phylum amongst all, whose counts were highest in the control group (1650.51 ± 374.94) and lowest in the vancomycin group (218.09 ± 65.59). The long-term vancomycin treatment increased the number of *Proteobacteria* (312.20 ± 129.71) and *Verrucomicrobia* (16.56 ± 1.6) compared to all the other treatments, while completely depleted the number of *Tenericutes*. At the genus level, while the majority of the genera were decreased or completely removed in the vancomycin treated mice (e.g. *Faecalibacterium*), the *Clostridium sensu-stricto* 1 was specifically enriched in the vancomycin group (1.98 ± 1.8 *vs*. 0 in other treatments), as well as the *Escherichia-Shigella* counts (84.27 ± 45.54 *vs*. average of 2 in other treatments), followed by *Enterobacter*, *Salmonella* and *Pseudomonas* sp.

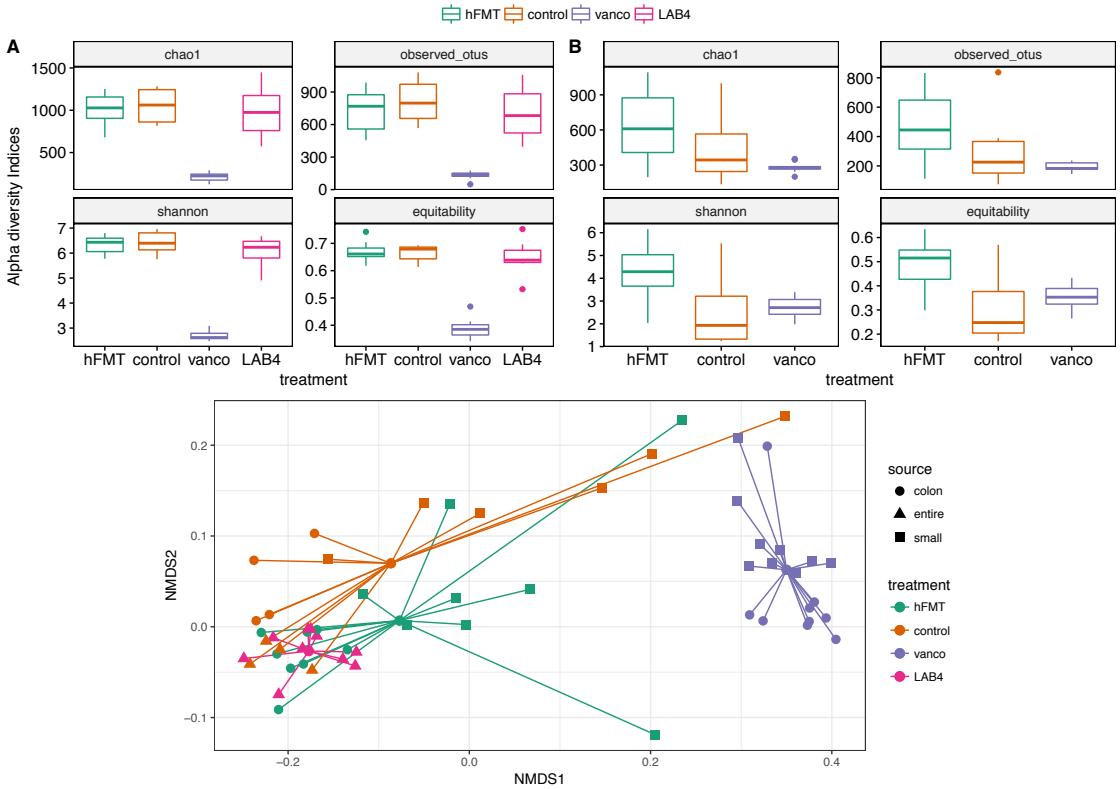

Figure 3.4. Alpha and beta diversity in βgal mice amongst treatments.
Box-and-whiskers plot of alpha diversity amongst treatment in (**A**) colon and entire, and (**B**) small intestines of βgal mice. Beta-diversity NMDS (**C**) based on Bray-Curtis amongst treatments (colors) and microbiota sources (shapes).

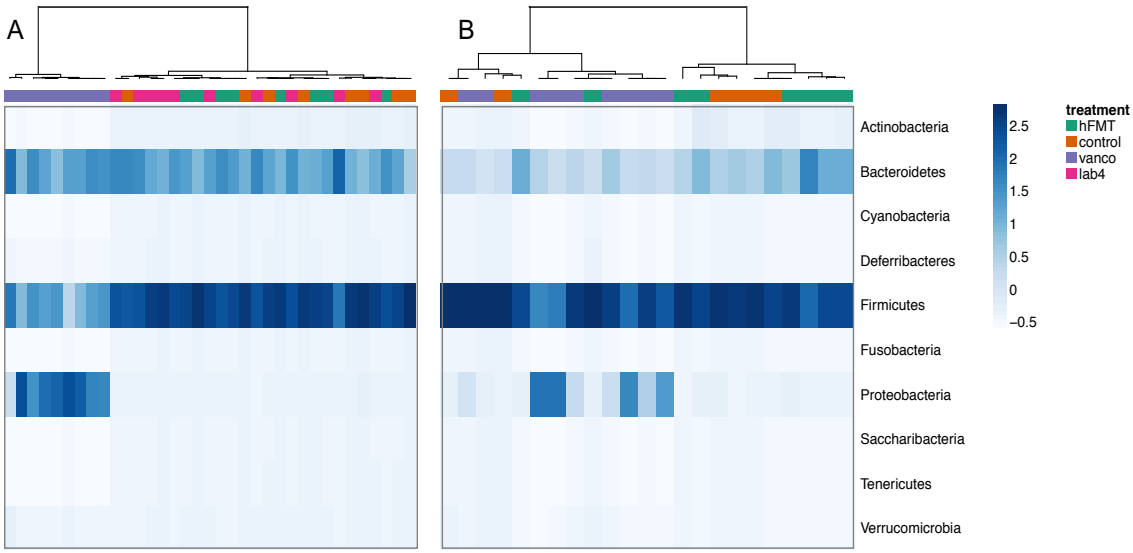

Figure 3.5. Heatmap of the phylum distribution in βgal-immunised mice amongst treatments.
(**A**) Large and (**B**) small intestines. Annotated heatmap based on Spearman distance and Ward hierarchical clustering. Phyla abundances were centered and standardized according to each column Z-scores and described by the change in the intensity of the blue colour, as annotated.

Differential abundance of genera was tested pairwise between treatments, taking into account the different intestinal sections (e.g. control and Lab4 only entire samples): the abundance of 72 genera were significantly different in the vancomycin group compared to controls (data not showed), while 71 genera between vancomycin and hFMT samples (data not showed). Twenty-four genera were differentially abundant between hFMT and controls samples, while 12 genera were differentially abundant between controls and Lab4 (using the entire samples only), as summarized in Table 3.5.

Similarly, what was observed in the large intestine was also found in the small intestines, for example, *Proteobacteria* enrichment and a decreased abundance of *Actinobacteria*, *Bacteroidetes* and *Firmicutes* in the vancomycin-treated mice (Figure 3.5B). On the contrary, a significantly different abundance of the genus *Bacteroides* was observed amongst groups, along with an increased count in the vancomycin treated mice (44.6 ± 12), and an increase of the genus *Lactobacillus* counts in both hFMT (433.66 ± 132.59) and vancomycin (441 ± 92.44) treated mice compared to controls (Appendix 10). Also, fewer *Ruminococcaceae* genera were differentially abundant in the small intestine compared to the large intestines. In the pairwise comparison, 28 genera were differentially abundant between mice in the vancomycin and the control groups (data not showed), 40 genera between vancomycin and hFMT (data not showed) and 7 genera between hFMT and controls (Table 3.5), all of them more prevalent in the hFMT such as the genus *Lactobacillus* (P=0.015).

Table 3.5. Pairwise differential abundant taxonomies between treatments in the βgal group.

Section	Differentially abundant genera	P value
hFMT *vs*. controls		
small	Bacteroidetes;Alloprevotella	0.0126
	Bacteroidetes;Odoribacter	0.0315
	Bacteroidetes;Rikenella	0.0165
	Firmicutes;Blautia	0.0012
	Firmicutes;Faecalibacterium	0.0260
	Firmicutes;Lachnospiraceae UCG-004	0.0009
	Firmicutes;Lactobacillus	0.0152
colon	Actinobacteria;Enterorhabdus	0.0020
	Bacteroidetes;Alistipes	0.0393
	Bacteroidetes;Other	0.0216
	Bacteroidetes;Paraprevotella	0.0323
	Bacteroidetes;Prevotellaceae UCG-001	0.0265
	Bacteroidetes;Rikenella	0.0122
	Firmicutes;[Eubacterium] brachy group	0.0009
	Firmicutes;[Eubacterium] nodatum group	0.0157
	Firmicutes;[Eubacterium] oxidoreducens group	0.0201
	Firmicutes;Coprococcus 1	0.0092
	Firmicutes;Erysipelatoclostridium	0.0481
	Firmicutes;Faecalibacterium	0.0016
	Firmicutes;Lachnospiraceae UCG-004	0.0443
	Firmicutes;Lachnospiraceae UCG-008	0.0002
	Firmicutes;Marvinbryantia	0.0259
	Firmicutes;Peptococcus	0.0305
	Firmicutes;Pseudobutyrivibrio	0.0060
	Firmicutes;Roseburia	0.0050
	Firmicutes;Ruminiclostridium 5	0.0000
	Firmicutes;Ruminococcaceae UCG-005	0.0001
	Firmicutes;Ruminococcus 1	0.0103
	Firmicutes;Turicibacter	0.0224
	Proteobacteria;Desulfovibrio	0.0098
	Tenericutes;Other	0.0000
Lab4 *vs*. controls		
entire	Actinobacteria;Coriobacteriaceae UCG-002	0.0349
	Bacteroidetes;Odoribacter	0.0286
	Bacteroidetes;Parabacteroides	0.0428
	Bacteroidetes;uncultured Bacteroidales bacterium	0.0036
	Firmicutes;Candidatus Arthromitus	0.0239
	Firmicutes;Coprococcus 1	0.0045
	Firmicutes;Lachnospiraceae NK4A136 group	0.0373
	Firmicutes;Oscillibacter	0.0464
	Firmicutes;Oscillospira	0.0268
	Firmicutes;Turicibacter	0.0136
	Firmicutes;Tyzzerella 3	0.0178
	Verrucomicrobia;Akkermansia	0.0153

Pairwise differences assessed using the Welch's t-test for unequal variance in control-Lab4 entire intestine; only tests with $P<0.05$, BH corrected are shown.

3.4.5. Treatment effect on endpoint TSHR-immunised microbiota composition

Similar to what was previously described for the βgal group, the vancomycin treatment determined the majority of the differences at the alpha diversity indices in the TSHR-immunised group large intestines as well (P<0.001, Figure 3.6A). Moreover, differences between the other manipulation treatments and controls were observed. The diversity of the hFMT (Shannon index) was reduced in comparison to the control group (P=0.019) and the equitability was lowered in the Lab4 compared to the controls (P=0.045). In the small intestines, the vancomycin treatment led to a significant reduction in richness (Chao1), diversity (Shannon) and equitability compared to both controls and hFMT (P<0.05), while it was significantly reduced compared to the hFMT only in terms of number of observed OTUs (P=0.0004). Vancomycin treatment also led to a unique spatial organisation of the between-group diversity (Beta-diversity) (P=0.001, 999 permutations and intestinal section as a stratification, Figure 3.6C).

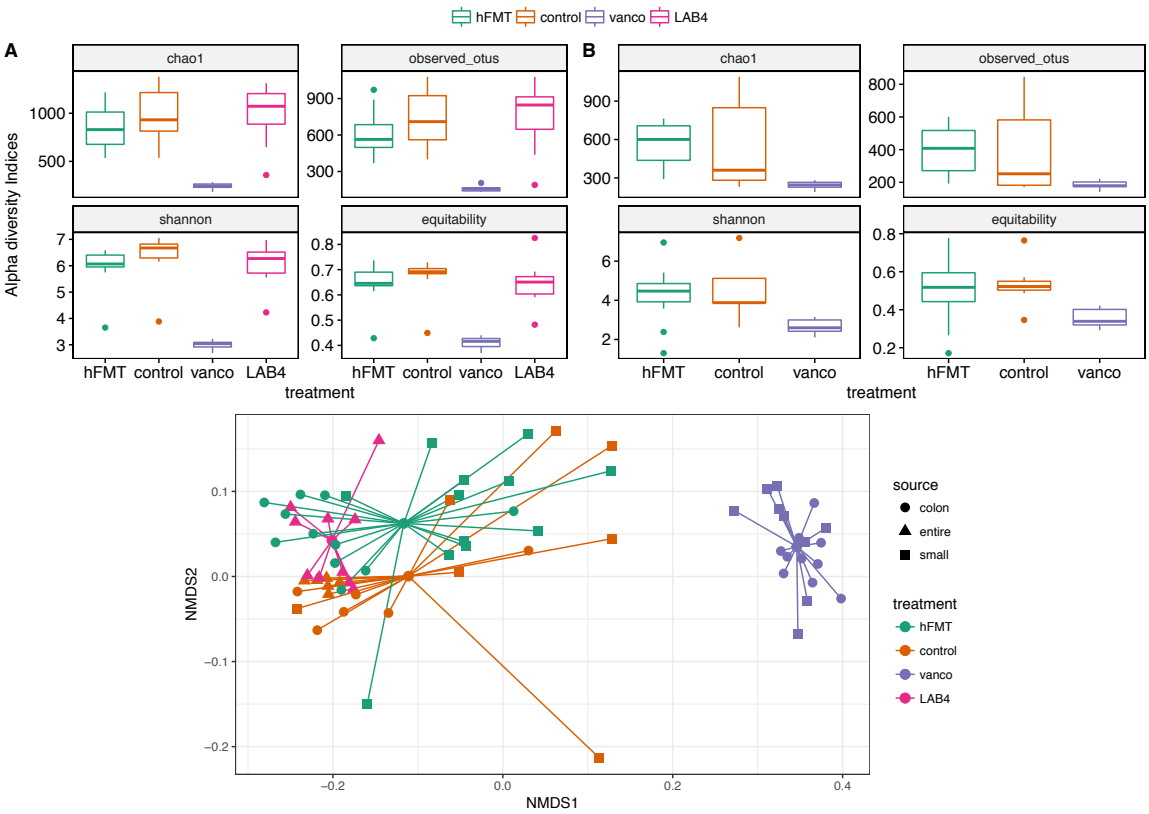

Figure 3.6. Alpha and beta diversity in TSHR-immunised mice amongst treatments. Box-and-whiskers plot of alpha diversity amongst treatment in colon and entire (**A**) and small (**B**) intestines of TSHR mice. Beta-diversity NMDS (**C**) based on Bray-Curtis amongst treatments (colors) and microbiota sources (shapes).

Significant differences in the taxonomic composition amongst treatment groups were reported, using a linear model adjusting for the different microbiota section (as for colon and entire samples, Appendix 11), followed by a pairwise comparison between groups. In the large intestines (colon and entire samples, Figure 3.7A), the phylum *Actinobacteria*, comprising the genus *Bifidobacterium*, showed higher counts in the Lab4 treated mice (32.77 ± 11.6) and was depleted by the vancomycin treatment (0.68 ± 1.45). A similar trend was shown by the phylum *Bacteroidetes*, increased in the Lab4 (815.75 ± 206.35) and decreased in the vancomycin group (220.90 ± 35.87), while the control and the hFMT showed a very similar abundance (685.39 ± 184.17 and 683.36 ± 219.56, respectively). Of interest, the genus *Bacteroides* was enriched in the vancomycin-treated mice (62.96 ± 12.87) compared to controls (54.77 ± 22.87), Lab4 (46.22 ± 37.51) and hFMT (23.28 ± 22.08), which showed the lowest counts (P=0.003). *Firmicutes* was the most abundant phylum amongst all and showed an enrichment in the Lab4 treatment (1550.55 ± 546.25), followed by controls and hFMT, while it was reduced by the vancomycin treatment (320.90 ± 113.11). Such a long-term antibiotic treatment had the most dramatic effects at the genus level, where it depleted a clade of the *Eubacterium* sp. (mean count 0), *Faecalibacterium* and clades of *Ruminiclostridium* and *Ruminoccocaceae sp*., while it specifically selected the growth of *Proteobacteria* genera *Citrobacter* and *Cronobacter* (9.95 ± 4.26 and 8.68 ± 2.57, respectively, *vs*. 0 in the other groups) and promoted an increased number of *Enterobacter*, *Escherichia-Shigella*, *Salmonella* and *Pseudomonas* species. Interestingly, a slight, but significant increase of the *Acetitomaculum* sp. (0.86 ± 1.48 *vs*. 0 in the other groups) was observed in the hFMT group and also a decrease of the *Faecalibacterium* counts compared to the controls and Lab4.

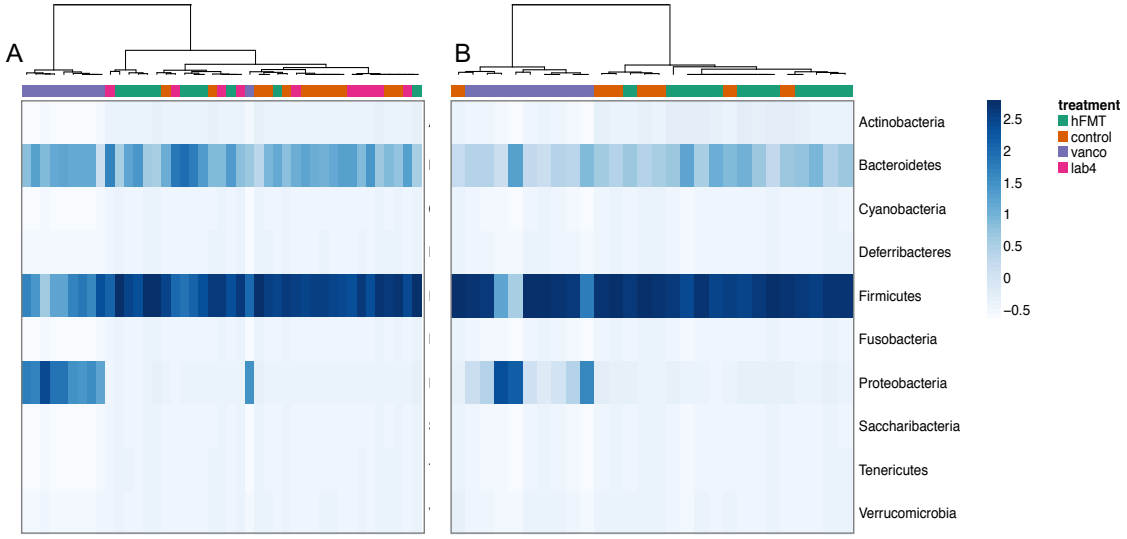

Figure 3.7. Heatmap of the phylum distribution in TSHR-immunised mice amongst treatments.
(**A**) Large and (**B**) small intestines. Annotated heatmap based on Spearman distance and Ward hierarchical clustering. Phyla abundances were centered and standardized according to each column Z-scores and described by the change in the intensity of the blue colour, as annotated.

From the pairwise comparisons, the abundance of 59, 66 and 15 genera were significantly different when comparing vancomycin with controls, hFMT with vancomycin (Data not showed), and hFMT with control, respectively (Table 3.6). In the entire samples, 12 genera were differentially abundant between Lab4 and control (Table 3.6).

In the small intestines (Figure 3.7B), the hFMT group had a higher amount of *Actinobacteria* (43.17 ± 26.89) and *Bacteroidetes* (400 ± 149.28) counts compared to controls and vancomycin groups, while the genus *Bacteroides* was enriched in the vancomycin-treated mice (49.97 ± 12.5). A higher abundance of *Firmicutes* was observed in the control mice (1077.7 ± 554.81), while higher prevalence of *Proteobacteria* was triggered in the vancomycin group, with a total of 53 phyla and genera differentially abundant amongst treatments (Appendix 12). Pairwise, 44 taxa (between phyla and genera) were differentially abundant between vancomycin and the controls, 45 between vancomycin and hFMT and 7 between hFMT and control, including also *Deferribacteres* and *Verrucomicrobia* phyla enriched in the control small intestines (Table 3.6).

Table 3.6. Pairwise differential abundant taxonomies between treatments in the TSHR group.

Section	Differentially abundant genera	P value
hFMT *vs*. control		
small	Deferribacteres;Mucispirillum	0.0288
	Firmicutes;Ruminiclostridium 6	0.0090
	Firmicutes;Tyzzerella	0.0105
	Firmicutes;Tyzzerella 3	0.0137
	Verrucomicrobia;Akkermansia	0.0230
colon	Actinobacteria;Enterorhabdus	0.0064
	Actinobacteria;Parvibacter	0.0049
	Actinobacteria;Slackia	0.0220
	Bacteroidetes;Alistipes	0.0384
	Bacteroidetes;Alloprevotella	0.0040
	Bacteroidetes;Odoribacter	0.0001
	Bacteroidetes;Paraprevotella	0.0336
	Bacteroidetes;Prevotellaceae UCG-001	0.0201
	Bacteroidetes;uncultured Bacteroidales bacterium	0.0173
	Firmicutes;[Eubacterium] ventriosum group	0.0311
	Firmicutes;Incertae Sedis	0.0212
	Firmicutes;Ruminiclostridium 6	0.0159
	Firmicutes;Tyzzerella 3	0.0001
	Tenericutes;Anaeroplasma	0.0096
	Tenericutes;Other	0.0002
Lab4 *vs*. control		
entire	Bacteroidetes;Other	0.0467
	Firmicutes;Acetatifactor	0.0112
	Firmicutes;Intestinimonas	0.0127
	Firmicutes;Lachnoclostridium	0.0397
	Firmicutes;Ruminiclostridium	0.0241
	Firmicutes;Ruminiclostridium 6	0.0306
	Firmicutes;Ruminococcaceae UCG-011	0.0082
	Firmicutes;Tyzzerella	0.0100
	Firmicutes;unidentified	0.0101
	Proteobacteria;Methylobacterium	0.0141
	Tenericutes;Anaeroplasma	0.0210
	Tenericutes;Other	0.0241

Pairwise differences assessed using the Welch's t-test for unequal variance in control-Lab4 entire intestine; only tests with $P<0.05$, BH corrected are shown.

3.4.6. Microbial biomarkers for manipulation treatments and immunizations classification

Random Forest (RF) analysis was used to classify the samples into treatments (control, Lab4, hFMT and vancomycin) or into immunisations (βgal or TSHR) based on their genus-level microbiota composition, using 10,000 decision trees. Three different models were tested for the treatment classification (for both small or large intestines samples), while two models were used for immunisation classifications (for either small or large intestines samples), and the best model fit was decided based on the smallest out-of-bag (OOB) error rate, as described in Table 3.7.

Table 3.7. Summary of the models used to run the RandomForest (RF) classification algorithm using either small or large intestine microbiota.

Source	Classification	predictive variables	CV mtry§	OOB error-rate (%)
Small	Treatments	treatment	43	66.67
		treatment + immunisation	34	64.71°
	Immunisations	immunisation	27	54.9
		immunisation + treatment	36	49.02°
Large (colon + entire)	Treatments	treatment	45	41.03
		treatment + source	23	26.92°
		treatment + source + immunisation	24	29.49
	Immunisations	immunisation	48	32.05
		immunisation + source	49	32.05
		immunisation + source + treatment	41	29.49°

§ derived from the repeated-cross validation (CV) step performed to tune the hyperparameters with the Caret R package; ° models used to obtain per-class OOB and variable importance.

Treatment classification using the large intestinal samples (including both TSHR and βgal immunisations) showed an initial OOB error-rate of 41.03%, which decreased to 26.92% when including the microbiota sources effect in the model and to 29.24% when including both immunisations and microbiota sources (Table 3.7). The OOB error rate was also obtained per-class, to observe a possible class-driving effect in the overall classification accuracy. In the “treatment+source” model, long-term vancomycin treatment showed a 0% per-class OOB error (19/19 correctly classified), having selected a unique microbiota. The Lab4 and hFMT treatments showed 30% and 26% class error with 14/20 and 14/19 samples correctly predicted in each group, respectively. The control

group, instead, showed a more overlapping composition of the gut microbiota with the other two treatments, with a per-class OOB of 50% with 10/20 samples correctly classified (Figure 3.8A). By growing decision trees, RF operates a variable importance selection, based on the Mean Decrease Gini index or the mean decrease in node impurity (not related to a mean decrease in accuracy). In the case of the treatment classification, the microbiota source was the most important effect, followed by the 9 most important genera (Figure 3.8B). In the small intestine, model for treatment classification originally showed an OOB error of 66.67%, meaning that the genus-level composition was highly shared amongst treatments, even when including the immunisation effect in the model (64.71% OOB). Differently to what was observed in the large intestine samples, the vancomycin treatment class error was 47%, while the hFMT and control class error rate resulted of 70% and 77%, respectively (Figure 3.9A).

For the immunisation classification, all the treatments were taken into account. The classification using the large intestine samples showed an initial OOB error-rate of 32.05% which was identical when including the source effect in the model. The OOB error-rate decreased to 29.49% when including both source and treatment effects. The βgal group showed a 37% per-class error rate (22/35 samples correctly classified), while 23% for the TSHR (33/43), as in figure 3.7C. The small intestine showed an overall 54.9% OOB error-rate, which decreased to 49.02% when including the treatment effect in the model. While the βgal showed a 65% per-class error (8/23 samples), the TSHR showed almost 36% per-class error with 18/28 samples correctly classified (Figure 3.8C). Variable importance was derived with the top-10 prediction variables in either the large intestine samples (Figure 3.8D) or in the small intestines (Figure 3.9D).

Genera with the highest mean decrease in Gini, from the prediction of treatments (Figure 3.8B) and immunisation (Figure 3.8D) in large intestines, were tested for differential abundance, in order to report robust bacterial biomarkers for either monitoring the success of the manipulation or differences between the two immunisations. Differentially abundant genera amongst treatments were mostly dominated by taxa depleted or enriched in the vancomycin group, apart from the *Lachnospiraceae* NK4A136 also differentially abundant in the hFMT compared to control ($P=0.038$, Table 3.8). Differences between the two immunisations in each treatment were identified (Table 3.9), with the genus *Bacteorides* reduced in TSHR compared to βgal in the hFMT group ($P<0.001$), resembling previous observations (Chapter 2, Table 2.6.).

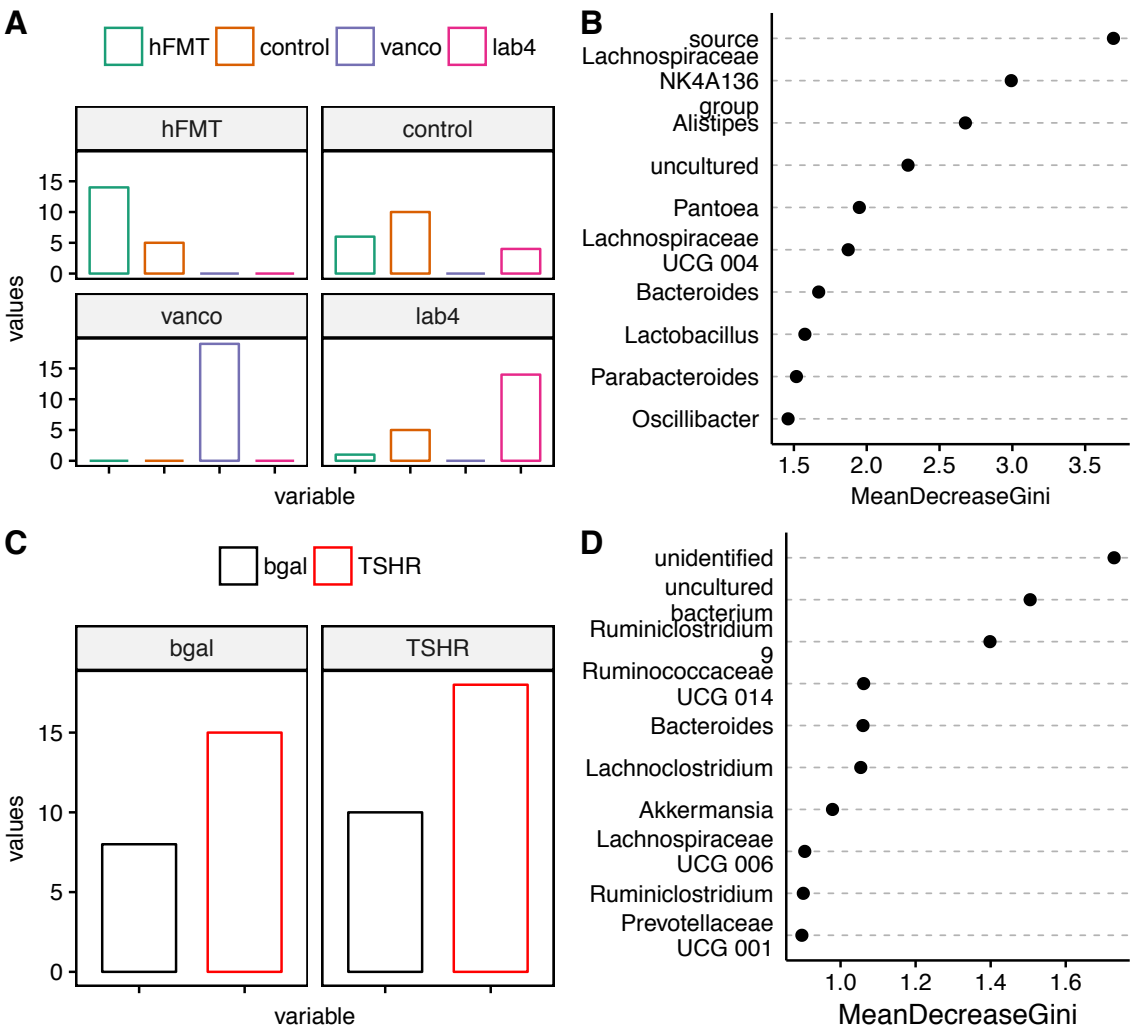

Figure 3.8. RF classification accuracy and variable importance amongst treatments and between immunisations in the large intestines (entire and colon samples).

(**A**) Confusion matrix with the per-class OOB and classification for treatments. Each box represents the true treatment while the bar-chart represents the number of samples being assigned to a treatment according to the model used. Vancomycin had the 100% accuracy in classification, followed by hFMT and Lab4, while the control group shared the microbiota composition with the other two treatments, excluding vancomycin. (**B**) Top-10 variable importance for treatment classification according to the Mean Decrease Gini. The model included the microbiota source as an effect which was identified as the most important variable. (**C**) Confusion matrix with the per-class OOB and classification for immunisations. Each box represents the true immunisation while the bar chart represents the number of samples being assigned to an immunisation according to the model used. The TSHR immunisation showed a higher accuracy in classification. (**D**) Top-10 variable importance for immunisation classification according to the Mean Decrease Gini.

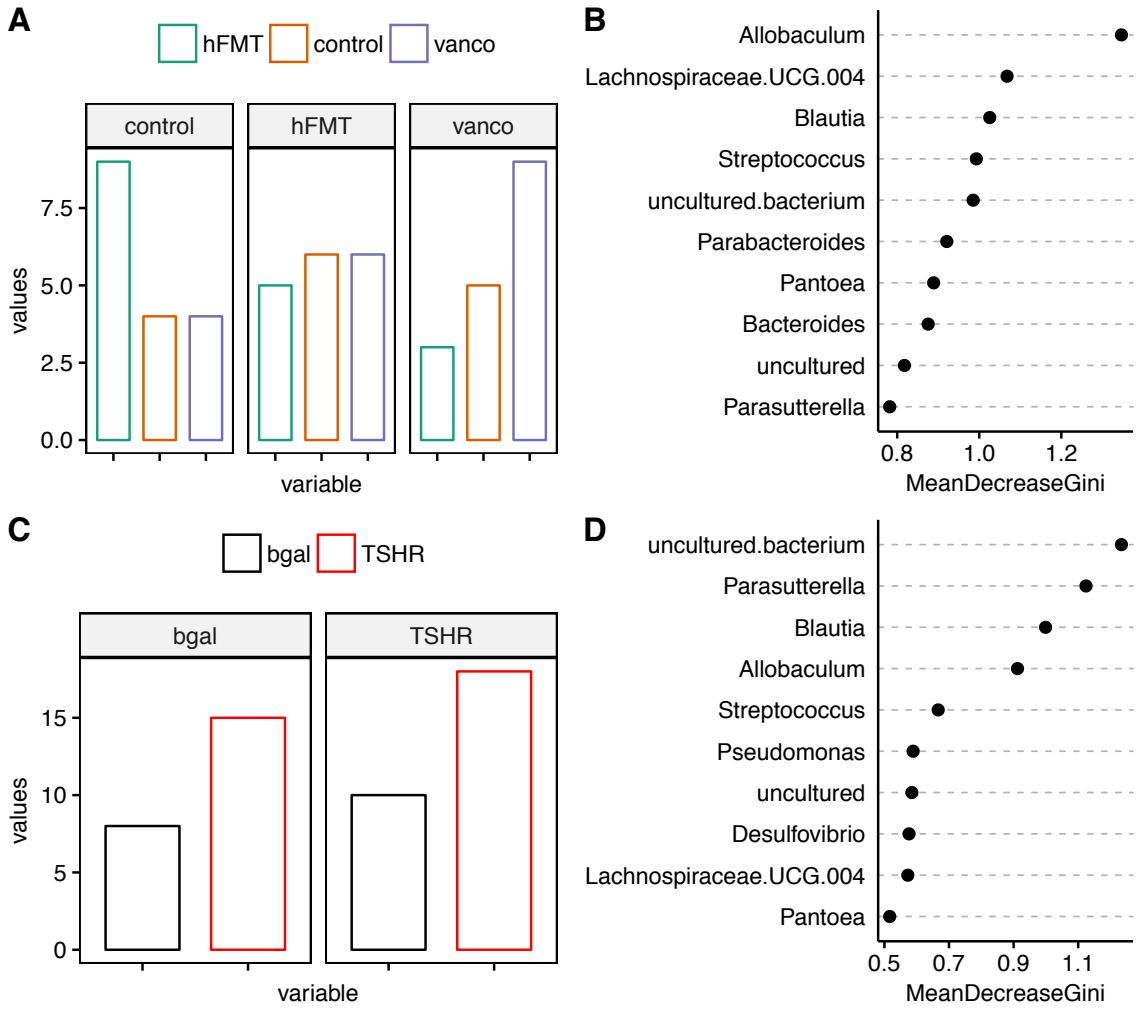

Figure 3.9. RF classification accuracy and variable importance amongst treatments and between immunisations in the small intestines.
Accuracy in prediction is lower than the one showed in the large intestines. (**A**) Confusion matrix with the per-class OOB and classification for treatments. Each box represents the true treatment while the bar-chart represents the number of samples being assigned to a treatment according to the model used. The majority of the hFMT and almost all of the vancomycin samples were predicted correctly. (**B**) Top-10 variable importance for treatment classification according to the Mean Decrease Gini. (**C**) Confusion matrix with the per-class OOB and classification for immunisations. (**D**) Top-10 variable importance for immunisation classification according to the Mean Decrease Gini.

Table 3.8. Differential abundance of genera derived from RF treatment model in large intestines.

Genus differentially abundant	group1	group2	P value°
Alistipes	vanco	control	3.10E-12
Alistipes	vanco	hFMT	6.46E-10
Alistipes	vanco	Lab4	1.79E-12
Lachnospiraceae NK4A136 group	hFMT	control	0.0388366
Lachnospiraceae NK4A136 group	vanco	control	6.20E-17
Lachnospiraceae NK4A136 group	vanco	hFMT	5.66E-13
Lachnospiraceae NK4A136 group	vanco	Lab4	1.03E-13
Oscillibacter	vanco	control	3.84E-13
Oscillibacter	vanco	hFMT	3.54E-11
Oscillibacter	vanco	Lab4	5.93E-10
Pantoea	vanco	control	9.46E-37
Pantoea	vanco	hFMT	1.92E-36
Pantoea	vanco	Lab4	9.46E-37
Parabacteroides	vanco	control	4.06E-33
Parabacteroides	vanco	hFMT	9.54E-33
Parabacteroides	vanco	Lab4	4.06E-33
uncultured	vanco	control	8.23E-06
uncultured	vanco	hFMT	6.74E-05
uncultured	vanco	Lab4	6.74E-05

° Welch t-test, BH corrected only P<0.05 are reported. Vanco, vancomycin. hFMT, humanized-faecal microbiota transplant. Lab4, probiotics.

Table 3.9. Differential abundance of genera derived from RF immunisation model in large intestines.

Genus	treatment	βgal (mean)	TSHR (mean)	P value°
Akkermansia	Lab4	6.744	8.583	0.04062332
Akkermansia	vanco	16.558	12.994	0.01134477
Bacteroides	hFMT	76.846	23.278	5.93E-05
unidentified	hFMT	12.183	7.685	0.02631315
unidentified	vanco	4.595	11.639	0.00134518

° Welch t-test, BH corrected only P<0.05 are reported. Vanco, vancomycin. hFMT, humanized-faecal microbiota transplant. Lab4, probiotics.

3.4.7. Correlation of the gut microbiota and the disease features amongst treatments and between immunisations

Disease features were correlated with the microbial biomarkers identified by the two RF models through the Spearman correlation coefficient. Irrespective of treatment, TRAK were induced in all TSHR-immune mice. A positive correlation was observed in the vancomycin-TSHR mice between the TRAK levels (calculated against the hTSHR, potentially including both stimulating and blocking antibodies) and counts of unidentified and uncultured genus of the phylum *Firmicutes*, respectively, and a negative correlation with the genus *Lactobacillus* (Figure 3.10C). A weak negative correlation (Rho< -0.5)

was observed in the hFMT-TSHR mice between TRAK levels and *Parabacteroides* genus counts (Figure 3.10G). Stimulating antibodies (TSAB) were induced in all TSHR-immune mice except for the vancomycin group. A negative correlation with TSAB was observed in the control-TSHR and the genus *Lactobacillus* (in colon samples, Figure 3.10A) and with two uncultured/unidentified *Firmicutes* genera and *Lachnoclostridium* counts in the hFMT-TSHR mice (Figure 3.10E). Thyroxine levels were not increased in the vancomycin treatment, and seemed to be increased in the TSHR mice of the control and the hFMT groups, although not reaching significance. A significant increase was however observed in the Lab4-TSHR group compared to βgal. A negative correlation was observed in the Lab4-TSHR mice between the fT4 and the genus *Ruminiclostridium* (Figure 3.10E), while a positive correlation was reported in the vancomycin-TSHR mice with *Lachnoclostridium* counts (Figure 3.10C). Serum thyroid functions (i.e. autoantibodies and thyroxine levels) did not correlate with any microbial biomarkers in the βgal-immune mice, apart from the positive correlation between an uncultured Firmicutes and fT4 levels in the entire control samples (Figure 3.10B).

The eye disease was calculated in the orbits in terms of total adipose tissue, muscular atrophy and the percentage of the brown fat out of the total adipose tissue. No significant differences were observed in the total adipose tissues between immunisations in each treatment, while the percentage of brown fat - out of the total adipose tissue – was increased in the TSHR-immunised control and Lab4 groups compared to βgal. Also, a significantly increased muscular atrophy was reported in the control-TSHR immune group compared to βgal. No significant correlations were reported in the control-TSHR mice and orbital pathogenesis. In the vancomycin-TSHR group, a strong negative correlation was observed between the total adipose value and the brown fat and the *Akkermansia* genus and the *Bacteroides* genus with the total adipose tissue, while a positive correlation was observed between *Lachnoclostridium* counts and the brown fat values (Figure 3.10C). The vancomycin- βgal group showed a negative correlation of the genera *Bacteroides* and *Parabacteroides* and the brown fat percentage, while two uncultured Firmicutes genera correlated negatively with the muscular atrophy. In Lab4-TSHR, atrophy correlated negatively with *Lachnoclostridium* and uncultured Bacteroidetes, while *Akkermansia* counts correlated negatively with the total adipose tissue (Figure 3.10E). In hFMT-TSHR, orbital muscular atrophy positively correlated with genus *Lactobacillus* counts, while uncultured *Firmicutes* positively correlated with brown fat (Figure 3.10G). The immune response at the draining lymph node was calculated in terms of $CD4^+$, CD25 positive fraction of the $CD4^+$ ($CD4^+CD25^+$) and the memory/effector T cells, while the response in the orbit was calculated in terms of $CD4^+$ and $CD8^+$ T cells.

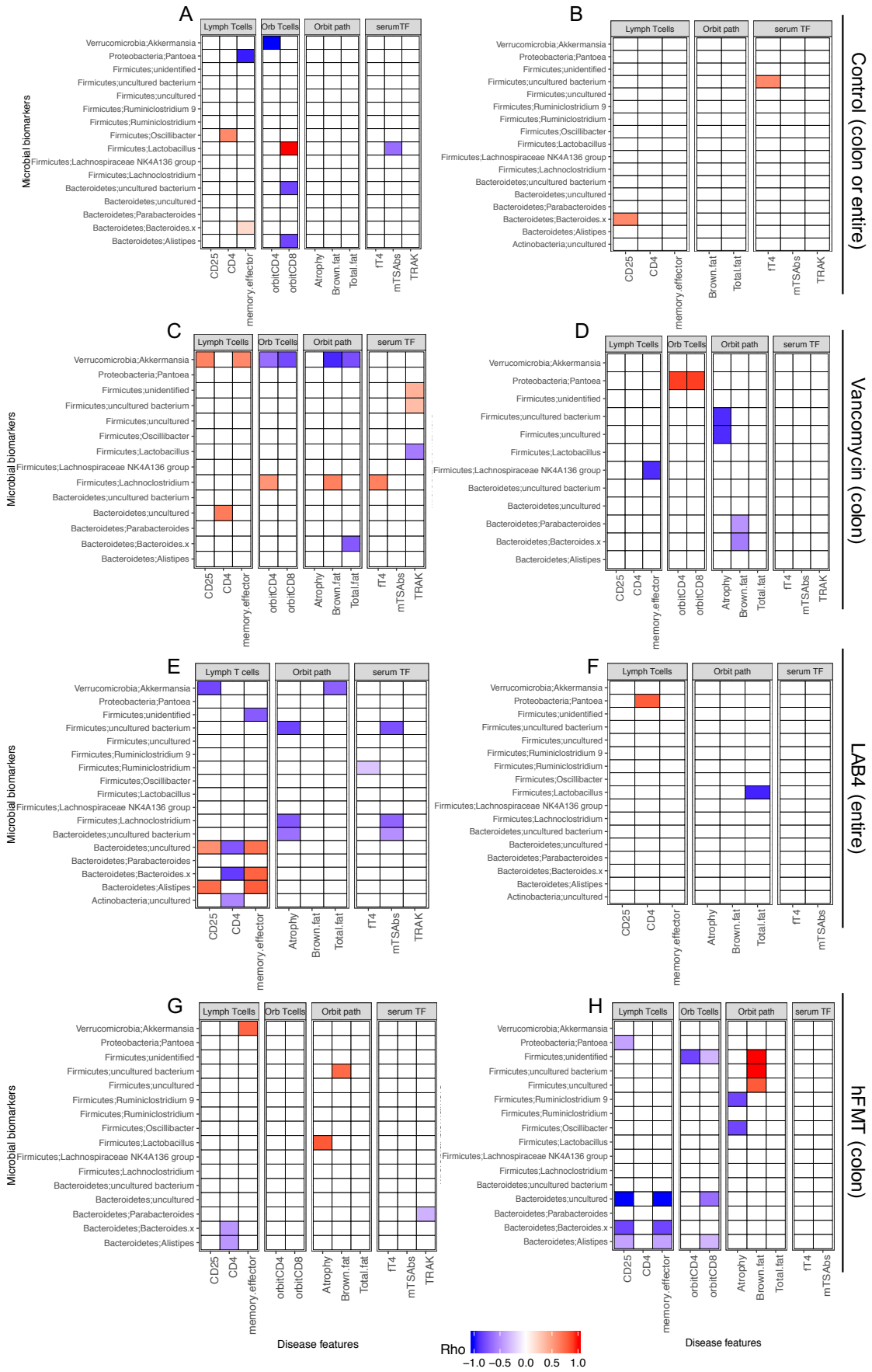

Figure 3.10. Correlations between microbial biomarkers and disease features in each treatment and per immunisation.

Correlations were calculated in colon and entire samples separately. TSHR-control mice in (**A**) colon and (**B**) entire samples, while control-βgal mice did not show any significant correlations. Vancomycin-TSHR mice (**C**) and βgal (**D**) using colon samples; Lab4-TSHR (**E**) and βgal (**F**) entire samples and hFMT-TSHR (**G**) and βgal mice (**H**) using colon samples. Only correlations with $P<0.05$ are shown and the strength of the Spearman correlation coefficient (Rho) is represented by the change in color from blue (negative) to red (positive correlation). Thyroid function calculated in the serum: %TRAK, fT4 (mg/dL). Lymph nodes: %CD4, %CD25 pos. of CD4 and %memory/effector T cells. Orbital T cells: %CD4 and %CD8.

No significant difference was observed in the percentage lymphocytes between immunisations. A positive correlation between $CD4^+$ and the genus *Oscillibacter* was observed in the control-TSHR colon samples, while the memory/effector T cells negatively correlated with *Pantoea* and weakly positively with *Bacteroides*. Orbital $CD4^+$ T cells negatively correlated with genus *Akkermansia* and $CD8^+$ T cells positively correlated with *Lactobacillus* counts and negatively with uncultured *Bacteoridetes* and *Alistipes* (Figure 3.10A). *Bacteroides* was positively correlated to $CD4^+CD25^+$ in the entire control-TSHR (Figure 3.10B). In the vancomycin-TSHR immune group, *Akkermansia* was positively correlated with both $CD4^+CD25^+$ and memory/effector T cells, while an uncultured *Bacteroidetes* was positively correlated with $CD4^+$ T cells (Figure 3.10C). Genus *Akkermansia* was also negatively correlated with both orbital $CD4^+$ and $CD8^+$ T cells, while genus *Lachnoclostridium* positively correlated to orbital $CD4^+$. On the contrary in the Lab4-TSHR, genus *Akkermansia* was negatively correlated to $CD4^+CD25^+$ (Figure 3.10E). In the same group, an uncultured *Bacteroidetes* correlated positively with CD25+ and memory/effector T cells, and negatively correlated to $CD4^+$; genus *Alistipes* negatively correlated to both $CD4^+CD25^+$ and memory/effector T cells, while genus *Bacteroides* positively correlated to memory/effector T cells and negatively correlated to CD4+. Uncultured *Actinobacteria* a weak negative correlation to $CD4^+$, while unidentified *Firmicutes* negatively correlated to memory/effector T cells. In hFMT-TSHR, genera *Bacteorides* and *Alistipes* negatively correlated to $CD4^+$ and genus *Akkermansia* positively correlated to memory/effector T cells (Figure 3.10G). In the hFMT-Bgal counterpart, uncultured *Bacteroidetes* genus, *Bacteroides* and in a weak manner also *Alistipes*, negatively correlated to $CD4^+$ and memory/effector, while *Pantoea* counts negatively correlated to $CD4^+CD25^+$ T cells (Figure 3.10H). In the same group, orbital CD8+ correlated negatively with uncultured *Bacteroidetes*, *Alistipes* and unidentified *Firmicutes* genera, which also strong negatively correlated (Rho> -0.5) with orbit $CD4^+$ (Figure 3.10H).

3.4.8. Imputed metagenomic functions across manipulation treatments and between immunisations

As previously described in different gut anatomical sections of the control GO mouse model, metagenomic functions were also predicted in the large intestine samples of GO mice, whose gut was manipulated either via hFMT, vancomycin or Lab4 administrations.

Across immunisations, high-variant metabolic pathways previously described in the control large intestines were also found in the hFMT microbiome, e.g. starch/sucrose, amino sugar/nucleotide sugar, glycine/serine/threonine and fructose/mannose metabolism, with the exception of the nitrogen metabolism, previously described in the control small intestine (Figure 3.11A). Also, the glycerophospholipid metabolism was described for the first time, possibly as a result of the hFMT itself. Of those top-10 most variant pathways, metabolic pathways including the nitrogen metabolism were increased in βgal, while the glycerophospholipid metabolism, ABC transporters and the glycolysis/gluconeogenesis were increased in the TSHR-immune mice (Figure 3.11B).

Across immunisations, long-term vancomycin treatment selected bacteria mostly involved in the ABC transporters (having the highest variance), bacterial secretion system, RNA degradation and nucleotide excision repair. Also, oxidative phosphorylation, two-component system and phenylalanine/tyrosine/tryptophan biosynthesis were described. Interestingly, metabolic pathways previously described being in the top-10 most variant pathways in the control group, such as the amino/nucleotide-sugar and starch/sucrose metabolisms, were now included in the least-10 variant group (Figure 3.11C). Between immunisations, ABC transporter, two-component system and the glycolysis/gluconeogenesis were increased in TSHR, while degradation of other glycans, RNA degradation, nucleotide excision repair and the bacterial secretion system were increased in βgal mice(Figure 3.11D).

Highest-variance pathways induced by Lab4 probiotic mostly included metabolic pathways, such as starch/sucrose, fructose/mannose, galactose, amino/nucleotide-sugar, glycine/serine/threonine and porphyrin/chlorophyll metabolisms, similarly to the control large intestine, and the nitrogen metabolism similar to the hFMT group. Also, bacterial secretion system, ABC transporter and other glycan metabolism pathways were described (Figure 3.11E). Interestingly, no major differences were found in the relative abundance of the top-10 most variant pathways between immunisations, with the degradation of other glycans increased in βgal and ABC transporter and porphyrin/chlorophyll metabolism slightly increased in the TSHR (Figure 3.11F).

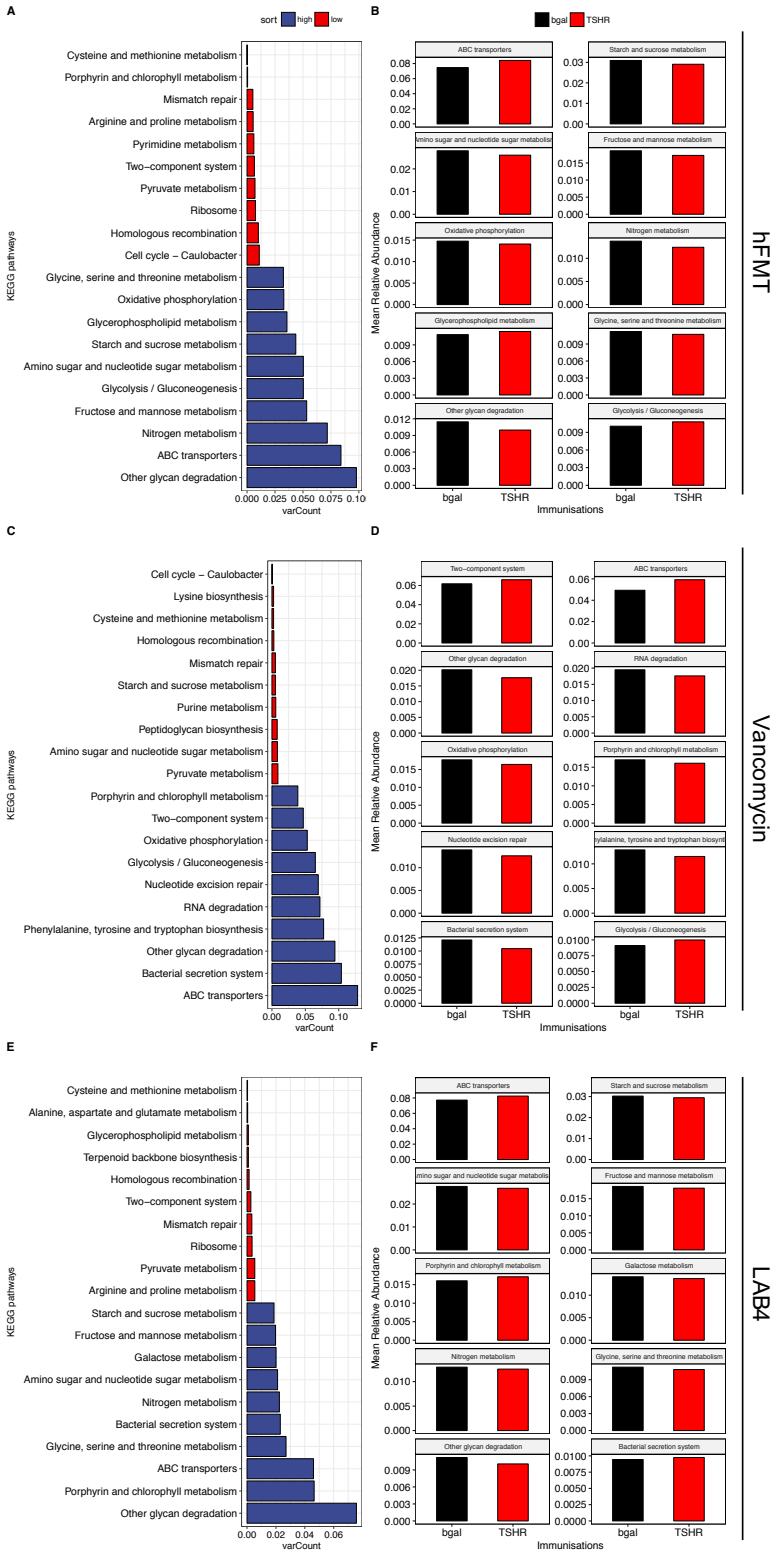

Figure 3.11. Metagenomic functions predicted in the control group between immunisation along the intestinal tract.

Top-10 and least-10 variant KEGG pathways according to anatomical sections of the gut: small (**A**), colon (**C**) and entire (**E**) and differences in the top-10 variant pathways between immunisations (TSHR or βgal) in each gut section (**B**, **D** and **F**). varCount, across-group coefficient of variation (standard deviation/mean pathway relative abundance) in percentage (%).

3.4.9. Combined effect of treatments, immunisations and time on the distal (faecal) microbiota composition of the GO mouse model

In the previous chapter, I demonstrated that time had a major effect in shaping the richness and the organization of the faecal microbiota in GO mouse model. To assess how the different gut-manipulation treatments interacted with immunisations over time, we collected and analysed the faecal microbiota after two gavages, but before any immunisations (baseline) and after four gavages and before the third immunisation (mid timepoint) and compared to that of respective controls. At baseline, differences in alpha diversity indices were uniquely associated to treatments ($P<0.001$). A slight increase in the richness (Chao1 and observed OTUs) appeared in the Lab4 treatment compared to that of the control, while the hFMT seemed to reduce the diversity (Shannon) and the evenness (equitability index) of the bacterial communities compared to controls, however, these did not reach significance. Significant differences were dominated by the antibiotic treatment ($P<0.001$), which drastically reduced the bacterial richness and diversity (Table 3.10). At this timepoint, prior to receive any immunisation, the two groups showed a similar composition of the gut microbiota, calculated through alpha diversity indices (Table 3.10).

At the mid timepoint, after two immunisations and four gavages, differences in the Shannon and in the equitability indices appeared significant between immune hFMT and controls ($P=0.002$), and in the richness between βgal-Lab4 and βgal-control ($P=0.021$, Table 3.11).

Table 3.10. Summary of the alpha diversity indices (mean values) and test statistics amongst treatments and between hTSHR and βgal immunisations within each treatment at baseline timepoint.

Index	immunization	control[a]	hFMT[a]	Lab4[a]	vancomycin	P value°
Chao1	βgal	785.64	868.81	1042.99	183.61	1.04E-07
	TSHR	876.29	781.37	816.43	179.69	3.51E-11
	P value[§]	0.361	0.464	0.108	0.8767	
Observed OTUs	βgal	575.33	661.33	774.00	120.88	9.02E-07
	TSHR	617.80	558.00	592.89	108.00	1.00E-09
	P value[§]	0.612	0.337	0.126	0.410	
Shannon	βgal	5.95	6.29	6.64	3.09	1.00E-10
	TSHR	6.59	5.95	6.24	2.93	6.27E-18
	P value[§]	0.095	0.267	0.307	0.129	
Equitability	βgal	0.65	0.68	0.70	0.45	8.00E-08
	TSHR	0.71	0.66	0.69	0.44	4.88E-12
	P value[§]	0.069	0.654	0.855	0.648	

[a] Mean values of each index per immunisation and treatment; ° Analysis of variance based on linear model; [§]Pairwise comparison between immunizations in each treatment.

Table 3.11. Summary of the alpha diversity indices (mean values) and test statistics amongst treatments and between hTSHR and βgal immunisations within each treatment at mid timepoint.

Index	Immunization	control[a]	hFMT[a]	Lab4[a]	vancomycin	P value°
Chao1	βgal	1095.04	930.77	915.15	176.12	1.04E-07
	TSHR	1054.38	968.09	893.78	216.71	3.51E-11
	P value[§]	0.723	0.622	0.833	0.097	
Observed OTUs	βgal	842.78	666.11	647.82	108.64	9.02E-07
	TSHR	812.18	731.53	638.91	128.21	1.00E-09
	P value[§]	0.763	0.312	0.919	0.140	
Shannon	βgal	6.69	6.66	6.46	2.77	1.00E-10
	TSHR	6.75	5.67	6.13	2.74	6.27E-18
	P value[§]	0.773	0.015*	0.056	0.801	
Equitability	βgal	0.69	0.71	0.70	0.41	8.00E-08
	TSHR	0.71	0.60	0.67	0.40	4.88E-12
	P value[§]	0.453	0.004*	0.072	0.447	

[a] Mean values of each index per immunisation and treatment; ° Analysis of variance based on linear model; [§]Pairwise comparison between immunizations in each treatment. * P<0.05.

As previously observed, time had a major effect in the richness (P=0.002 and P=0.003) and in the evenness (equitability, P=0.033), but not in the diversity of the bacterial communities. Factorial interactions of time with treatments and immunisations are represented in Table 3.12. A significant increase of the richness indices over time was observed in the hFMT-treated group (Chao1, P=0.0038) and in controls (Chao1 P=0.035; observed OTUs P=0.001), as represented in Appendix 13. In particular, the post-hoc analysis confirmed previous observations in the control groups (i.e. richness increase less apparent in the TSHR group) and showed a significant increase of the richness indices over time (Chao1, P=0.023; observed OTUs, P=0.019) in the TSHR-immune hFMT treated group (Table 3.13).

Table 3.12. Summary of the statistics from Equation 3 testing for treatments, immunisations, time and their factorial interactions in alpha, beta-diversity and in the *Firmicutes:Bacteroidetes* ratio.

Index	ANOVA model					
	Treatment	Immunisation	Timepoint	Treat x Immun	Treat x Time	Immun x Time
Chao1	<0.001	0.547	0.002	0.571	0.022	0.343
Observed OTUs	<0.001	0.501	0.003	0.77	0.004	0.174
Shannon	<0.001	0.012	0.709	0.001	0.064	0.205
Equitability	<0.001	0.056	0.033	0.001	0.226	0.036
Bray-Curtis	0.001	0.01	0.009	0.001	0.007	0.329
Firm:Bact[§]	0.0015	0.0001	0.718	0.003	0.117	0.290

[§]*Firmicutes:Bacteroidetes* ratio

Table 3.13. Summary of the alpha diversity indices (mean values) and test statistics between baseline and mid timepoint, for each treatment and for each immunisation.

Index	Treatment	Immunization	Baseline (mean)	Mid (mean)	P value
Chao1	control	βgal	785.644	1095.039	0.017*
		TSHR	876.288	1054.383	0.096°
	hFMT	βgal	868.806	930.774	0.592
		TSHR	781.373	968.093	0.023*
	Lab4	βgal	1042.988	915.151	0.229
		TSHR	816.426	893.776	0.524
	vancomycin	βgal	183.606	176.124	0.743
		TSHR	179.686	216.707	0.165
observed otus	control	βgal	575.333	842.778	0.021*
		TSHR	617.800	812.182	0.038*
	hFMT	βgal	661.333	666.111	0.961
		TSHR	558.000	731.533	0.019*
	Lab4	βgal	774.000	647.818	0.193
		TSHR	592.889	638.909	0.650
	vancomycin	βgal	120.875	108.643	0.337
		TSHR	108.000	128.214	0.188
Shannon	control	βgal	5.955	6.689	0.069
		TSHR	6.591	6.753	0.452
	hFMT	βgal	6.289	6.658	0.077°
		TSHR	5.948	5.671	0.494
	Lab4	βgal	6.645	6.465	0.149
		TSHR	6.244	6.131	0.705
	vancomycin	βgal	3.090	2.765	0.002*
		TSHR	2.932	2.740	0.088°
equitability	control	βgal	0.653	0.691	0.258
		TSHR	0.714	0.707	0.742
	hFMT	βgal	0.677	0.715	0.116
		TSHR	0.662	0.596	0.108
	Lab4	βgal	0.695	0.697	0.921
		TSHR	0.688	0.666	0.465
	vancomycin	βgal	0.452	0.411	0.025*
		TSHR	0.441	0.398	0.058°

Welch's t-test BH corrected between baseline and mid timepoint: * P <0.05, ° P<0.1

The between-sample bacterial community relationships were assessed using the Bray-Curtis dissimilarity matrix. At baseline, antibiotic, hFMT and Lab4-treated mice differed to each other ($P<0.05$), apart from hFMT and Lab4 mice, which became significant in the mid timepoint ($P=0.0015$). No significant differences were observed between immunisations at baseline, however, differences between the TSHR and the βgal immunisations were observed in the hFMT-treated mice ($P=0.008$) and retained at the mid timepoint ($P=0.016$, Figure 3.12B). Such a difference might be attributed to either the engraftment outcome itself or to a possible cage effect, which I showed to appear in the murine faecal microbiota in Chapter 2. Overall, the time had a significant effect on the stability of the faecal microbiota ($P=0.001$) between the two timepoints sampled, as it was its interaction with treatments ($P=0.007$), but not the interaction with immunisations, taking all the treatments together (Figure 3.12A). Differences in immunisations within each treatment were observed (Figure 3.12B), and centroids (sampling distribution of the mean) of each immunisation were close to each other similarly to what observed at T2 (9 weeks after second plasmid injection) in the previous chapter (Chapter 2, figure 2.6).

At the phylum level, the *Firmicutes*:*Bacteroidetes* ratio was significantly associated with treatments ($P=0.0015$) and immunisations ($P=0.0001$), overall, while the time seemed not to have any significant effect (Table 3.12). The factorial interaction between treatments and immunisations was significant ($P=0.003$), while there was no significant interaction between treatment and timepoint and immunisation and timepoint. In particular, a significant difference was observed between TSHR and βgal immunisation in the hFMT-receiving mice ($P=0.0006$). Although not significant, only the control group showed an increase in the *Firmicutes:Bacteroidetes* with time (Figure 3.12C).

The microbiota composition at baseline is the result of the various treatments without any influence from immunisations or aging. The vancomycin-receiving mice showed, as expected, a unique bacterial composition with increased *Proteobacteria* genera, *Akkermansia* and *Lactobacillus* spp. (Figure 3.12D and Appendix 15). hFMT and Lab4 groups showed quite a similar composition of the gut microbiota, with a reduced *Bacteroides* spp. compared to controls and vancomycin treatment. However, *Bacteroides* spp. counts significantly increased with time in Lab4 mice, in both immunisations (Appendix 14).

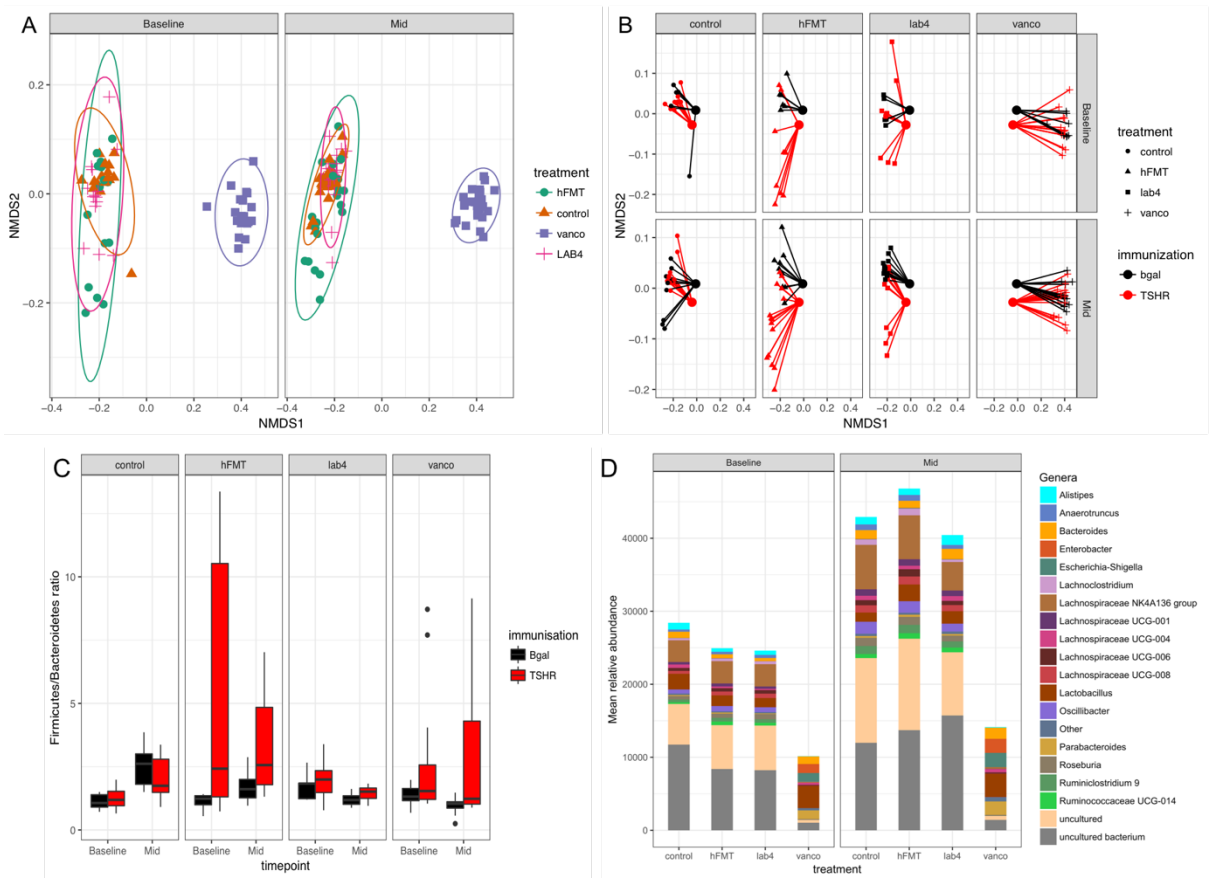

Figure 3.12. Stability and diversity of the gut microbiota between timepoints. (**A**) Differences amongst treatments between baseline and mid timepoint, (**B**) differences between immunisations in each timepoint and per treatment.
(**C**) *Firmicutes/Bacteroidetes* ratio between immunisations in each timepoint (either baseline or mid). (**D**) Distribution of the top-20 most abundant genera across treatments in each timepoint.

3.4.10. hFMT engraftment into GO mouse model gut microbiome

To test whether the resistance or the susceptibility to a certain disease is conferred by the composition of the gut microbiome, faecal material from human patients can be administered to murine models (either pretreated with antibiotics or GF), usually via gavage, leading to a humanized mouse model. The hFMT was performed three times before the start of the immunisation procedures (i.e. at birth, weaning and before the first immunisation) and once before the third immunisation, with 6-week interval from the third gavage. The NMDS based on Bray-Curtis matrix showed a clear separation between the human GO donors and the murine samples, both hFMT or control mice (PERMANOVA $P<0.001$, using 999 permutations). Within murine samples, a less clear separation between the hFMT-receiving and control mice was observed (Figure 3.13A)

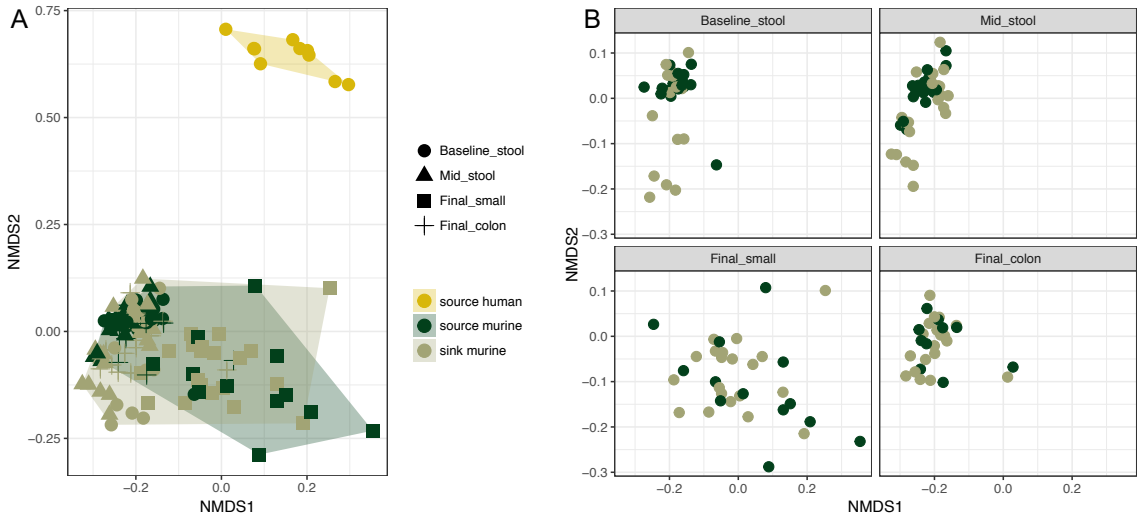

Figure 3.13. Between-sample relationship (beta-diversity) of the human donors, control and hFMT mice in the three timepoint and per intestinal sections.
NMDS based on the Bray-Curtis dissimilarity matrix showed a clear separation between human donors and murine samples, whether control or hFMT mice (**A**). Differences in the spatial organization between control and hFMT mice and (**B**) according to timepoint and anatomical section/sample used.

At baseline, there was a more pronounced spatial separation of some hFMT-receiving mice compared to controls, which became less evident in the mid-timepoint (Figure 3.13B). There were no differences between hFMT and control mice at the end of the experiment in the small intestine, whose groups were both spread along the two NMDS axis, while relying more closely in the colon samples.

Similarity of the gut microbiota composition at the family taxonomic level, between hFMT-receiving mice with that of the GO human donors, was calculated through the SourceTracker, with the rationale described in Figure 3.14A. At baseline (after three gavages), 4 out of 15 hFMT-receiving mice faecal samples (test) showed a >10% similarity with human source while none out of 16 control mice (control) shared any similarity with the human samples (Fisher's exact test with Yates' continuity correction, P<0.001, Figure 3.14B). At mid-timepoint (four gavages in total, after 6-week circa washout period between the third and the fourth gavage), half of the control mice (10/20) showed >10% similarity, while none of the hFMT-receiving mice (0/24) showed any similarity with the human donors (P<0.001, Figure 3.14C). Interestingly, at the end of the experiment (after 9 weeks after the fourth and last gavage), the same similarity to human donors samples was observed in both murine controls (26%) and hFMT-receiving colon samples (26%, P=1), while no similarity to human donors was observed in the small intestines (Figure 3.14D). Interestingly, when considering a >40% similarity with the

human donors, only the hFMT-receiving mice at baseline showed a significant observation (mean similarity 53% hFMT *vs*. 20% control). In particular, only the group that would have received the hTSHR immunisation showed a high similarity with the human donor pool, possibly due to a caging effect (P=0.001; Figure 3.15A and B). At mid timepoint (Figure 3.15C), the similarity to human donors was shared between both TSHR and βgal immune mice, while at the endpoint, the hFMT-receiving βgal-immune mice showed a higher similarity to human donors compared to the TSHR in the colon samples (P=0.001; Figure 3.15D). The engraftment however, was subjected to possible caging effect and individual variability.

The extent of the engraftment was also calculated at the taxonomic level. SourceTracker returned a list of possible bacterial invaders possibly derived from the human samples, and the top-14 most abundant invaders were analysed according to Equation 5 and Equation 6 (Appendix 16). At baseline and at the endpoint, *Peptococcaceae* abundance increased in the hFMT-receiving mice of nearly 623% and 30.5% compared to GO patients, respectively. Instead, *Lactobacillaceae* increased 30.5% at the mid timepoint in the hFMT-receiving mice compared to donor samples.

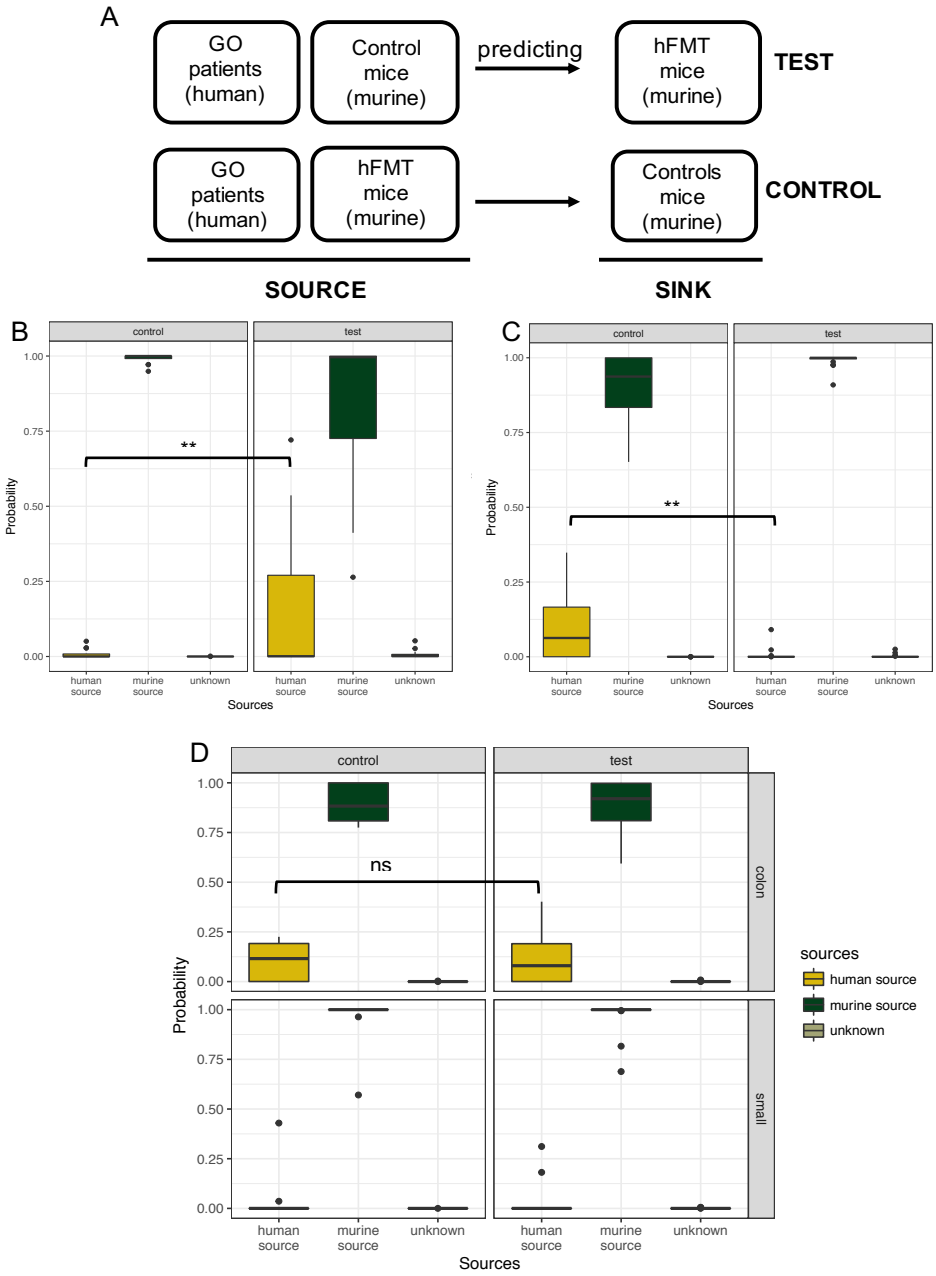

Figure 3.14. Engraftment analysis calculated using the SourceTracker.
(**A**) Rationale of the analysis: in the test analysis, both human donors and murine controls were used as sources to predict the similarity of the hFMT-receiving mice (sink). The control analysis used the human donors and the hFMT-mice as sources instead, to calculate the similarity of the control mice. Similarity was expressed as % probability using the control and the test analysis at baseline (**B**), mid timepoint faecal samples (**C**) and at the end of the experiment (**D**) in either small or colon samples. Unknown: observations not assigned to a specific source at the significant threshold (P=0.001). Fisher's exact test with Yates continuity correction: *** P<0.001; ns non-significant P value. The test statistic was calculated considering only the number of observations >10% similarity to human source between analysis (test and control) in each timepoint.

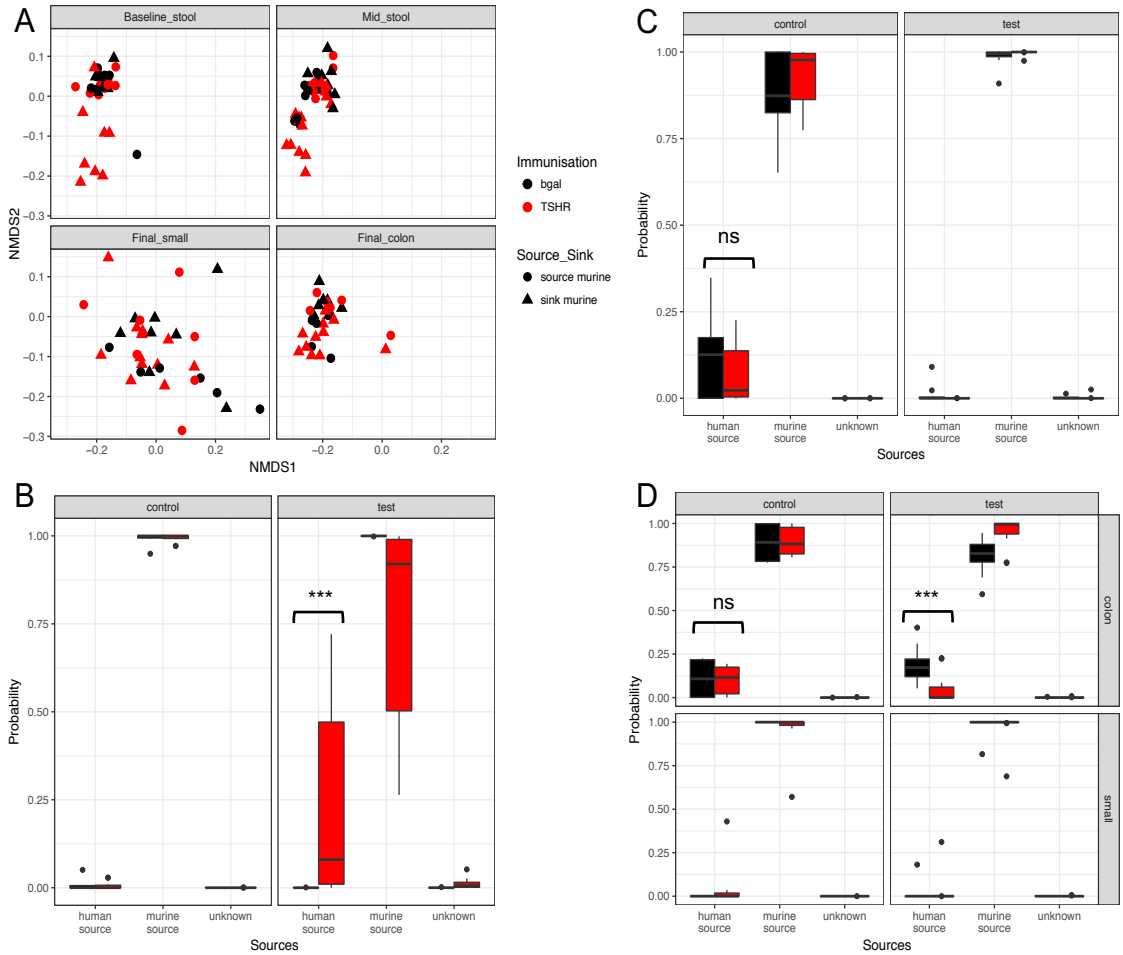

Figure 3.15. Engraftment differences between immunisations.
(**A**) NMDS based on the Bray-Curtis matrix for between-sample relationship in immunisations, according to timepoint and sources. (**B**) SourceTracker analysis for similarity to human or murine sources at baseline, (**C**) mid-timepoint faecal samples and (**D**) endpoint small and colon samples, based on immunisations. Fisher's exact test with Yates continuity correction: *** P<0.001; ns non-significant P value. The test statistic was calculated considering only the number of observations >10% similarity to human source between immunisations (TSHR and βgal) in each timepoint.

3.5. DISCUSSION

The aim of the present chapter was to investigate whether altered or absent composition of the gut microbiota through manipulation strategies in the early-stage of life may impact the outcome of the GO mouse model. In other words, whether the gut microbiota plays an important role in training the immune response, and whether certain bacterial species may have a protective/inducing role in the auto-immune response to TSHR in mouse model.

The GO mouse model developed by Banga and his group first [180], replicated at Eckstein laboratory later [187] and used in this thesis does not involve the use of conventional adjuvants to promote the breaking of the immune-tolerance against the human TSHR. As previously described (Chapter 1 par.. 1.3.2.2), adjuvants (e.g. complete or incomplete Freund's adjuvant, alum and pertussis extract…) can have a direct or an indirect effect on the immune system, creating a proper pro-inflammatory environment for the induction of the auto-immune response. Due to its close interplay with the immune system, the gut microbiota can itself act as a natural adjuvant, promoting (or not) the second immune stimulus needed for the activation of the (auto)immune response, as shown by [365]. We therefore manipulated the composition of the gut microbiota in the early-stage of life of mice (i.e. from birth) to expose their immune system to different environments before the immunisation procedures using either antibiotics, probiotics or faecal material transplant from GO patients.

3.5.1. Vancomycin treatment

The effects of a long-term vancomycin treatment on the large intestines were dramatic and resembled previous studies investigating chronic administration of antibiotics on the gut microbiota population [298]: the depletion of the richness and diversity indices was accompanied by a reduction of Gram positive bacteria (mainly represented by the *Firmicutes* phylum, e.g. *Faecalibacterium*, *Eubacterium* and *Ruminococcaceae*) and an increase in *Proteobacteria* species, including *Salmonella*, *Pseudomonas* and *E.coli*. Interestingly, the effects of the vancomycin were less evident in the small microbiota, at least in the βgal mice, remarking the concept that the gut microbiota has a different susceptibility to antibiotics depending on the gut anatomical site, as reviewed in [334].

The lack of induced disease in the vancomycin-treated TSHR-immune mice strongly suggests the need of the gut microbiota for the GO to be successfully induced, potentially training the immune system in the early-stage of life, although the precise mechanisms remain to be understood. We recently reported the induction of TSAb but a lack of hyperthyroidism and orbital pathology in C57BL/6 female mice undergoing the same

immunisation procedure, however no similarity with the gut microbiota of the vancomycin-treated mice was observed, suggesting that the lack of hyperthyroidism in C57BL/6 is more related to a genetic background-specific microbiota [366]. Ivanov and collaborators reported a decreased Th17-produced pro-inflammatory cytokines milieu in the small intestines of the EAE newborn pups treated with vancomycin, which may have contributed in the protection from the disease development [299]. Removal of the majority of Gram positive/*Firmicutes* bacteria have led to a general unbalance amongst bacterial species (also known as dysbiosis) rather than the removal of a particular species; thus, further investigations using a more targeted antibiotic may have to be performed as also suggested by [334]. Moreover, since also dams were treated during pregnancy, the maternal transmission of the microbiota has been compromised.

Such a long-term administration procedure, ideally to recapitulate the germ free (GF) status [367], have also led to the growth of resistant and compensating species, as also reported by [368], which may have been implicated in the disease outcome. Vancomycin treatment retained the highest counts of the *Bacteroidetes* genus *Bacteroides* (shown to be reduced in the TSHR-immune mice, Chapter 2) amongst other treatments in TSHR mice, which showed a negative correlation with the total fat in the orbit: the more the *Bacteroides* counts in the large intestine, the less the orbital fat. To a similar extent, the *Verrucomicrobia* genus *Akkermansia* was highly increased by vancomycin treatment in βgal compared to TSHR immunisations, and showed a significant negative correlation with both brown and total fat, CD4+ and CD8+ in the orbit and a positive correlation with the CD25+ (Tregs) and memory/effector cells in TSHR-immune mice, although there were no differences with those in the βgal. *Akkermansia muciniphila* constitutes a single-species of the genus *Akkermansia* [369], which is involved in the mucin degradation [370]. Interestingly, the postnatal vancomycin treatment of NOD mice reduced the incidence of T1D along with an increased proportion of *Akkermansia muciniphila* [371], despite the majority of the studies reporting exacerbation of T1D after antibiotics administration [338, 372]. According to the authors [371], a possible degradation of the mucus layer by *Akkermansia muciniphila* may have increased the accessibility of the remaining bacteria (e.g. Gram negative/*Proteobacteria*) to the gut immune cells and their receptors such as the TLR4, whose activation was previously shown to reduce diabetes incidence [373], even if debated [374]. However, the underlined mechanism has not yet been proved and there are no data available of the role of TLR4 in protecting from GO; on the contrary a more active TRL4 was associated to GD [375].

3.5.2. Humanized (GO) faecal microbial transplant

The faecal material transplant of sight-threatening GO patients' samples in female BALB/c mice aimed at creating a humanized mouse model which recapitulates the GO gut environment in the early-stage of life of the mice. To perform such engraftment, three gavages were performed prior the immunisation procedure (i.e. at the day after birth, at weaning and before the first immunisation) and before the third immunisation, with a washout period in-between. The resulting TSHR-humanized GO mice, at the end of the procedure, showed a significantly higher TRAB and TSAb titres compared to βgal; hyperthyroidism (T4 levels) and brown fat in the orbit were induced in some TSHR-immune mice, although not reaching the significance threshold. The gut microbiota of hFMT mice showed an increased richness between the baseline and the mid timepoint only in TSHR-immune mice. At the end of the experiment, the hFMT small intestines showed an increased diversity and evenness compared to the vancomycin-treated βgal-immune mice; while the TSHR-immune mice showed a reduced diversity compared to that of the control mice in large intestine samples. Such a reduction in bacterial diversity accompanied by an altered gut microbiota was often associated to Crohn's disease (CD) and IBD/colitis in both animal models and in humans [376]. Fourteen out of 19 mice were correctly predicted to the hFMT group based on their large intestine bacterial composition (74% class accuracy). In particular, *Bacteroides* spp. showed the lowest abundance amongst other treatments and it was significantly reduced compared to hFMT- βgal mice, possibly explaining the reduced microbiota diversity when compared to controls. Also, a negative correlation between *Bacteroides* spp. and $CD4^+$ lymphocytes at the draining lymph nodes was observed in TSHR-immune mice.

Given that the manipulation via FMT had some effect on the gut microbiota of the GO mouse model, I investigated the extent of the engraftment from the human donors to the murine recipients using the SourceTracker [363]. Such algorithms have been previously used to monitor the engraftment of faecal material transplant in the context of recurrent *Clostridium difficile* infections [342, 377] and in humanized mouse models [341, 378]. About 27% of hFMT-receiving mice showed more than 40% similarity (min 46%, max 72%) with the human donors' microbiota after three gavages but before any immunisations; thus, I can possibly speculate that at the start of the immunisation procedure at least some mice had a GO-like environment in their gut. At the mid timepoint (after 6 weeks washout), however, no similarity between hFMT and GO donors was observed, while at the end of the experiment, the large intestines of both controls and hFMT mice shared the same similarity with human samples. Such results may need some considerations: i) the SourceTracker was run using the OTU table at the family

level as in [341], because no similarity between murine (both hFMT and controls) and human samples (with a concomitant increased of unknown source assignment) was observed when using the genus and the OTU levels. Family level may be a less specific taxonomic description, since only OTUs/species and genera can discriminate between human and murine microbiota [199]. However, ii) we used a pooled, *in-vitro* cultured, freeze-dried faecal samples, which have been selected for certain viable anaerobic bacteria, possibly explaining the need of upper taxonomic description (e.g. family to phylum levels). Either freeze-dried or incapsulated freeze-dried faecal material transplants proved to be a safe and efficient treatment of diarrheal episodes in recurrent *C. difficile* infections, often accompanied by an increased/restoration microbiota diversity and a successful engraftment [379-381]. While there were no differences in the production of a humanized mouse model using either freeze-dried or freeze-dried plus *in-vitro* cultured samples [382]. The same group also tested various FMT strategies, from a single gavage only to repeated gavages (2 times a week for 4 weeks) after bowel cleansing. The engraftment of a single FMT lasted up to 4 weeks reaching a steady-state composition, while the repeated FMTs impacted negatively the stability of the gut microbiota, still showing individual or cage-related variability [382]. iii) Our strategy implied the manipulation at the very early-days of life, with three FMTs performed more closely to each other in a 6-8 week period of time, while the fourth gavage was performed after 6 weeks from the third. Such a washout period may have reduced the amount of transferred bacteria and also a possible cage effect might have been responsible for the heterogeneous engraftment, at least at baseline. Moreover, iv) the hFMT in GO mouse model was performed without any prior preparatory treatment (such as the bowel cleansing) or any antibiotic treatment to dams, thus the newborn mice, although being gavaged from the first day after birth, retained the maternal transmission of the gut microbiota, which can induce a colonization-resistance as discussed in [334].

3.5.3. Lab4 probiotic

Probiotics are considered to deliver beneficial effects to the host health, also involving the immune-modulation of the host [294]. Such an immune-modulation outcome was observed in our mice challenged with Lab4 probiotics prior to the immunisation procedure. In particular, $CD4^+CD25^+$ regulatory T cells were induced in the βgal but not in the TSHR-immune group, possibly suggesting a relevant connection with the disease mechanism. However, the gut microbiota of the TSHR-immune mice showed strong correlations with lymphocytes in the draining lymph nodes, e.g. *Bacteroidetes* uncultured genera, *Bacteroides* and *Alistipes* negatively correlated with $CD4^+$ and simultaneously positively with $CD4^+CD25^+$ and memory/effector T cells. We can possibly speculate that

the Lab4 administration promoted an anti-inflammatory response, increasing the $CD4^+CD25^+$ T cells in the βgal control mice, which was however prevented by the TSHR immunisation, despite gut microbiota-correlating features. Moreover, Lab4-treated TSHR-immune mice showed a significantly higher T4 levels and orbital brown fat compared to βgal. Varian and collaborators provided *Lactobacillus reuteri* daily in drinking water to one-year old (aging) outbred mice and reported an increased serum T4 levels, accompanied by a weight loss and increased activity levels in mice, compared to untreated group. Authors also observed an enlarged thyroid gland and induced activity dependent upon $CD4^+CD25^+$ Tregs [383]. Administration of *L. acidophilus* increased TSH and T3 levels but not T4 in weaning rats (30 days of life) for 32 days-treatment [384]. While providing a "*healthful aging*" in one-year old mice [383], it is possible that LAB supplementation worsens hyperthyroidism following TSHR immunisation. On the contrary, supplementation of *Bifidobacterium lactis* and *Lactobacillus rhamnosus* mitigated the outcome of the experimental autoimmune thyroiditis (EAT, i.e. similar to the Hashimoto's thyroiditis) [385].

Relationship between *Lactobacillus* and adipose tissue has been long debated, with evidence supporting the positive effect of the probiotics intake in ameliorating obesity [386, 387]. In the previous chapter, I identified a positive correlation between the genus *Lactobacillus* and the orbital adipogenesis in TSHR-immune mice. In the present work, no adipogenesis (in terms of total fat) and no correlation with the genus *Lactobacillus* was observed. Moreover, no correlation with brown adipose tissue (BAT) was reported. Since BAT was also induced in the control-TSHR mice, Lab4 did not prevent the BAT formation, which, however, has a different etiopathology compared to the white adipose tissue. Upon Lab4 treatment, TSHR-immunised mice showed an increase of *Akkermansia* spp. to the controls. Studies reported the increase of *Akkermansia* spp. upon probiotics intake [388] and potentially associated to a reduction in adipose tissue [389]. Interestingly, it correlated negatively with the total adipose tissue in Lab4-TSHR mice, although not significantly occurred as discussed previously.

3.5.4. Gut anatomical differences in GO model

TRAK and TSAb auto-antibodies titres were induced in the TSHR-immune control mice, however they were not hyperthyroid (T4 levels). This observation was consistent with the disease status observed in the centre 2 (Essen laboratory) in the previous chapter. Also orbital atrophy and BAT were induced; however, no adipogenesis (calculated as total fat) was here reported, which was instead induced in the TSHR group in the previous chapter. Interestingly, the genus *Lactobacillus* which correlated positively with orbital adipogenesis in chapter 2 (par.. 2.4.6), here, showed a positive correlation with orbital

$CD8^+$, One can argue that the apparent BAT production is a prelude to adipogenesis; thus a longer experiment might have resulted in increased orbital fat volume, as in mice reported in chapter 2.

The previous chapter analysed the gut microbiota from the scraping of the large intestines; however, no information are available on other anatomical sites of the gut in GO model, whose composition may be also involved in the pathogenesis. Notably, the Th17 lymphocytes involved in the pathogenesis of EAE mouse model specifically resided in the small intestine [299]. Compared to βgal, the TSHR-immune group showed a significantly increased Shannon diversity and evenness of the small intestines, despite the small intestine having a lowered richness and diversity compared to large/entire samples *per se*. Also, when predicting the immunisation groups with RandomForest, the TSHR-immune mice had a higher number of correct predictions. Correlations between small intestine microbiota and disease features are described in Appendix 17. Interestingly, significant positive correlation between the genus *Streptococcus* with both TSAb and atrophy were observed, which were both induced in TSHR-immune mice; while a negative correlation of *Streptococcus* and brown fat was observed in the βgal group. However, other manipulation treatments seemed to have minor impact on the composition of the small intestine.

For reasons that would be discussed in Chapter 6, a direct comparison of the results obtained in this chapter with those presented in Chapter 2 was not possible. Differences in the gut microbiota composition observed here may also be related to gavage-related stress, despite using sterile water, as proposed in [390].

3.5.5. Imputed metagenomic functions

The vancomycin-treated microbiome had an increased variation in ATP-binding components (ABC) transporters and bacterial secretion system pathways (reviewed in [391]), possibly related to the efflux systems for antibiotic resistance; while RNA degradation, nucleotide excision repair and oxidative phosphorylation are more likely to be related to apoptosis/bacterial death. However, for the concept of redundant metagenomics functions and/or the establishment of a compensating gut microbiota, functions described in more “physiological” conditions were as well retained, e.g. glycolysis and gluconeogenesis, porphyrin and chlorophyll metabolism and other glycan degradation, whose functions may act as a rescue mechanisms for homeostasis maintenance.

The hFMT predicted metagenome showed a proportion of metabolic pathways including those for glycine/serine/threonine, starch/sucrose, fructose/mannose, nitrogen and

glycerophospholipid metabolism, but also ABC transporters, other glycan degradation and the oxidative phosphorylation. While the oxidative phosphorylation was reported also in the vancomycin-treated metagenome, the glycerophospholipid metabolism has been uniquely predicted from the hFMT metagenome, and the combination of both pathways may suggest an increased oxidative stress in the large intestines. In particular, the glycerophospholipid metabolism has been previously related to intestinal mucosa inflammation in IBD [392] and a decreased *Bacteroides vulgatus* and *Bacteroides caccae*, along with an increase in glycerophospholipid metabolism was reported in Chron's disease [393]. Since no major differences between βgal and TSHR were described for those two pathways, it might be a more general effect of the engraftment *per se* rather than the interaction with the immunisation procedure. Interestingly, the glycerophospholipid metabolism was the least abundant by all means of pathways predicted from the donor GO patients, whose microbiome showed higher ABC transporters and two-component system, followed by metabolic and biosynthetic pathways (data not showed).

Lab4 probiotic treatment induced a range of metabolic pathways including the nitrogen metabolism. The bacterial secretion system pathway (which was also described in vancomycin metagenome) was reported as one of the top 10-most variant pathways. Interactions between probiotic bacteria and host mucosa may be promoted trough the secretion of extracellular proteins, as reviewed in [394].

Two predicted pathways may have biological relevance in the GD/GO pathogenesis: the other glycan degradation (K00511), involved in the N-glycan and ganglioside biosynthesis, and the phenylalanine, tyrosine and tryptophan biosynthesis (K00400). In particular, the first pathway was decreased in hFMT, vancomycin and Lab4-TSHR mice, while it was increased in small and large intestines in control-TSHR mice and it might be somehow related to the hTSHR A-subunit, used as immunisation antigen, which is highly glycosylated through N-glyc patterns. The second complex pathway involves tyrosine biosynthesis, which is a precursor of thyroid hormones T3 and T4, together with iodide (chapter 1, par. 1.1.1). A proportion of circulating thyroid hormones, specifically the T3, are secreted in the gut [395] or are stored in the gut as a reservoir [396]. The biosynthetic pathway was predicted from the gut microbiota of controls, whereas it was more abundant in TSHR small and large samples, and in vancomycin-treated mice, decreased in TSHR-immunisation.

3.6. CHAPTER CONCLUSIONS

The manipulation strategies adopted in the present chapter successfully modified the gut microbiota in the early-stage of life, with an impact on the induced GO phenotype. As potentially expected, the vancomycin treatment prevented the disease, while the hFMT from sight-threatening GO patients transferred, at least in part, some of the human disease characteristics. Unexpectedly, the Lab4, despite its immune-modulation effects on regulatory T cells, induced hyperthyroidism and did not protect from disease development. As previously mentioned and more extensively addressed in Chapter 6, future investigations would better dissect the mechanistic role of the gut microbiota in GO disease (i.e. treatment with different classes of antibiotics, use of GF mice and hFMT using different stage of human disease).

4. Chapter 4

Gut microbiome in European GD and GO patients at the time of recruitment: a multi-centre cross-sectional observational study

Acknowledgments:

All endocrine consultants across Europe for recruiting GD/GO patients in the present study and providing access to the clinical information

Dr. Hedda-Luise Verhasselt (previously HLK now HLV) and Dr. Danila Covelli (DC) for extracting the first batch of DNA from patients' faeces (2014-2015)

Utta Berchner-Pfannschmidt (UB-P) and Prof. Anja Eckstein (AE) for re-testing the TRAB titres

Dr. Filippo Biscarini (FB) for the in-house sample-based rarefaction script.

4.1. INTRODUCTION

As previously introduced, autoimmune diseases are caused by a combination of both genetic predisposition and environmental factors. Amongst the latter, viral, fungal or bacterial infections preceding the onset of autoimmunity may predispose, to some extent, the loss of the immune-tolerance to autoantigens *via* the molecular mimicry or the antigen-spreading mechanisms, as already described (Chapter 1 par.. 1.3.2.2**).** Evidence for the involvement of a molecular mimicry of *Y. enterocolitica* (YE) antigens in GD were based on: i) the relatively high prevalence of antibodies to YE in GD patients [397, 398], ii) the presence of binding sites for TSH on YE envelope [399, 400], and iii) that antibodies against thyroid membranes have been shown to bind YE [397]. Recent results from proteomics have identified cross-reactivity between TSAbs and the outer membrane protein F (OmpF) epitope of YE [401]. Additionally, a bioinformatic study of YE outer membrane proteins suggested that it contained epitopes which could stimulate an antibody response that cross-reacts with T cell epitopes [402]. However, it is likely that the cross-reactivity of YE proteins only explains the aetiology of GD in some patients. The contribution of other microorganisms in the pathogenesis of GD was investigated and homologies between the TSHR and the spirochete *Borrelia burgdorferi* was found [403, 404]; although such analysis was only performed *in silico*. However, the incidence of GD cases cannot only be explained by infections, including YE (whose mean annual incidence in Germany was 7.2/100,000 people between 2002-2008 [405]). On the other hand, a less specific but, still effective pro-inflammatory environment underlying the autoimmune response can be provided via “bystander activation”.

The gut microbiota plays an important role in the immune homeostasis of the host: bacterially-produced SCFAs exert beneficial effects by increasing a milieu favourable to regulatory T cells in the gut mucosa. Conversely, Gram’s negative LPS, and Gram’s positive-produced LTA and flagellin (i.e. those produced by a range of foodborne bacteria such as *Campylobacter jejuni*), but also commensal-derived metabolites themselves, can induce a Th1/Th17 pro-inflammatory response. We now know that such immune-modulation can be related to an imbalance amongst commensal bacteria, either due to the overgrowth or the under-representation of certain taxonomies (known until recently as “dysbiosis” [406]), rather than to a single-species pathogen. Given this fine relationship in health status, in the past ten years, the gut microbiome has been investigated in disease conditions and its association with inflammatory bowel diseases (IBD) was described. In Crohn’s disease (CD) and ulcerative colitis (UC), the auto-immune response is directly located in the gut. More specifically, CD is characterized by an abnormal presence of (auto)antibodies against intestinal microbiota antigens such as

the *Saccharomyces cerevisiae* oligomannan (ASCA), outer membrane porin (OmpC) and also against the bacterial flagellin (CBir1) [407]. Such auto-immune response is also sustained by predisposing polymorphisms in the host NOD2/CARD15 gene [408], coding for a protein expressed on macrophages and monocytes for LPS binding, which were associated to the auto-antibody reactivity, at least for CBir1 levels [409]. CD-associated gut microbiota showed an overall decreased diversity compared to that of healthy controls [410], along with increased abundance of *E.coli*, reduced counts of *Bacteroides* spp. [411, 412] and *Faecalibacterium prausnitzii* [296], a butyrate-producing *Clostridium* known to increase IL-10-mediated anti-inflammatory immune response.

The gut microbiome has also been associated with both systemic and organ-specific autoimmunity, not directly involving the gut. Rheumatoid arthritis (RA) is a chronic inflammation afflicting the joints and is characterized by a variety of auto-antibodies such as the rheumatoid factor, as reviewed in [413]. An increased amount of *Prevotella copri,* often accompanied by reduced *Bacteroides* genus, was associated with the new-onset untreated RA patients in the US [414] and in some Japanese patients [415]. A similar association was recapitulated in the RA animal model, in which *P. copri* induced a Th-17 response. However, geographical variability in the RA-associated taxonomies was observed (i.e. increased *Clostridium asparagiforme* and *Lactobacillus salivarius* instead of *Prevotella* in a Chinese RA cohort), as reviewed in [415]. To note, also the involvement of the oral microbiome in RA has been described [416], further sustained by a higher incidence of periodontal infections with *Porphyromonas gingivalis* in RA patients, which was associated with higher levels of anti-citrullinated auto-antibodies [417]. Insights on the role of the gut microbiota in inducing, as well as protecting from, the multiple sclerosis (MS)-like disease were obtained from the EAE mouse model, whose mechanistic contribution was extensively studied also through manipulation strategies, as described in the previous chapter. As well as the EAE induced in mice, MS in humans has long been considered a T cell-derived autoimmune disease afflicting the central nervous system (CNS); however there is a major involvement of B-cells, as reviewed in [418]. The relapsing-remitting MS patients gut microbiota showed a decrease in bacterial species belonging to the *Clostridia* clusters XIVa and IV, *Faecalibacterium*, *Prevotella* and *Alistipes* genera [419]. Another study reported increased abundance of *Methanobrevibacter* and *Akkermansia* spp., and a reduction in *Butyricimonas* spp. in a MS cohort, including both treated and untreated patients, which correlated with a set of immune-related differentially-expressed genes in patients' circulating mononuclear cells [420]. Interestingly, an increase in methane production quantified from breath was observed in MS patients, consistent with the increased *Methanobrevibacter* spp. abundance.

Type 1 diabetes (T1D) is an organ-specific autoimmune disease in which autoreactive T cells and inflammation are responsible for the destruction of the pancreatic insulin-producing β-cells. It has an incidence of 5-10% diabetes cases worldwide, with an onset in childhood and adolescence. In contrast, Type 2 diabetes (T2D) arises more often in adulthood and is characterised by insulin resistance and/or a failure in compensatory mechanisms for insulin secretion [421]. Although T1D is strongly sustained by predisposing genes, environmental factors, including infections, may still have a role in its onset, as shown by studies in monozygotic twins, in which only 40% concordance rate of the disease were reported [422]. The role of the gut microbiota in T1D was proposed [423] and disease-associated taxonomies and metagenomic functions were obtained from the NOD and the Biobreeding Diabetes-Prone mouse models for T1D [339, 340, 424, 425]. Children with T1D showed an increased *Bacteroides*, *Clostridium* and *Veilonella* genera, accompanied by a decrease in *Bifidobacterium*, *Lactobacillus* and *Prevotella* spp. in their faecal microbiome compared to healthy controls, suggesting a disruption of the intestinal barrier integrity. Such disease-associated taxa showed correlations with plasma glucose levels in T1D group [426]. A differential abundance of *Lactobacillus*, *Prevotella*, *Bacteroides* and *Staphylococcus* genera were associated to T1D susceptibility in children, i.e. autoantibodies-positive, seronegative first-degree relatives (FDRs) and new-onset T1D patients. Moreover, the gut microbiota of seropositive and seronegative FDRs, and that of new-onset patients and unrelated healthy controls, tended to cluster together but separately to each-other [427]. Increased *Bacteroides*, *Veilonella* and *Alistipes* spp. were reported in the faecal samples of a Finnish children T1D cohort, whose metagenomic functions were also described [428]. Interestingly, *Bacteroides dorei*-derived LPS, more prevalent in countries with high susceptibility to autoimmunity (i.e. Finland and Estonia in this study), may contribute to increased susceptibility to T1D in Finnish infants, *via* the inhibition of the immune-stimulation against endotoxins. On the other hand, Russian infants showed a higher prevalence of *E. coli*-LPS, which induced the immune response and was subsequently shown to confer resistance to T1D in NOD mice [134]. A possible but different role of the gut microbiota in T2D was also considered [429].

Gut microbiota metabolites not only cross-talk with the immune system, but also with a range of processes involved in the growth, reproduction, development and behaviour; and *vice versa* since its composition can be actively regulated by host-released hormones and metabolites. The gut microbiota itself, in fact, has been considered as the "neglected endocrine organ" [430], capable of synthetizing hormone-like molecules and to influence the endocrine system itself. Close interaction between bacterially-produced SCFAs and the neuro-endocrine system, more specifically the hypothalamic-pituitary-

adrenal (HPA) axis, has been described [431]. Also the interplay between sex-hormones and the gut microbiota was observed [432]. The gut microbiota itself can also be responsible for gender-prevalent autoimmune diseases: female NOD mice showed a decreased T1D incidence after receiving a microbiota transfer from male mice, possibly related to the high testosterone-levels [433]. A second study reported higher testosterone levels, along with higher counts of *Enterobacteriaceae* and SFB in GF, SPF and mono-colonized NOD male mice which protected them from developing T1D [434]. TD1 in humans has less gender prevalence; however, similar evidence of an interplay amongst hormones, gut microbiota and the immune system was also reported in the mouse model of SLE [304], which has a strong female bias in humans. Both steroid sex hormones (e.g. oestradiol, progesterone and testosterone) and thyroid hormones (thyroxine and T3) are metabolized in the liver and released with the bile. Gut-residing bacteria may play a direct role in metabolizing steroid hormones, as reviewed in [432]. Iodination, sulphation and glucuronidation of thyroid hormones, which are necessary for releasing the more active T3 hormone from reservoir, in certain conditions, may be performed by intestinal bacteria [435, 436] and SCFAs may promote such enzymatic reactions as reviewed in [432]. Moreover, SCFAs may also promote intestinal epithelial homeostasis by inducing a T3-mediated activation of the intestinal alkaline phosphatase (IAP) [437].

Bowel discomfort is often reported in thyroid autoimmune disease (AITD), varying from constipation in Hashimoto's thyroiditis (HT) (i.e. hypothyroidism) to diarrhoea in GD (reviewed in [16]). A recent study reported altered composition of the gut microbiota in HT patients compared to matched healthy controls: seven genera including *Blautia*, *Roseburia*, *Dorea* and *Fusicatenibacter* were increased in HT, while *Fecalibacterium*, *Bacteroides*, *Prevotella* and *Lachnoclostridium* were instead decreased in HT and such taxonomies correlated with disease features [438].

4.2. AIMS OF THE CHAPTER

At present, few studies described a possible role of the human gut microbiome in GD and it progression to GO [439, Shi, 2019 #2473]. The present chapter therefore aims to:-

i) describe the gut microbiota composition of GD and GO (mild and moderate-severe) patients compared to that of healthy controls in a multi-centre observational study;
ii) analyse the gut microbiota in hyperthyroid and euthyroid patients compared to euthyroid healthy controls irrespective of the diagnosis (whether GD or GO);
iii) predict the diagnosis (GD or GO compared to healthy controls) based on the gut microbiota composition using a classification algorithm;

iv) describe possible interactions between the gut microbiota and gender and smoking habits in GD/GO patients, since they are already implicated in the disease and not only as confounding variables; v) correlate the taxonomic differences between disease types to endocrine (TSH and T4 levels) and immunological (TRAB) observations and

vi) compare the imputed gut metagenomic functions between GD/GO and healthy controls and using the imputed KEGG orthologs to predict the patients' diagnosis.

4.3. MATERIALS AND METHODS

4.3.1. Patients recruitment and sample collection

Samples used in this chapter were collected between October 2014 and June 2016 within the framework of the E.U.-FP7 INDIGO project (http://www.indigo-iapp.eu/) from four European countries, in a total of eight centres: United Kingdom (University Hospital of Wales Cardiff, Merthyr, Newcastle and Moorfields), Italy (Policlinico ca' Granda Milano, Pisa), Belgium (Brussels) and Germany (University Hospital of Duisburg-Essen). An appropriate local research ethical approval was obtained from all recruitment centres (Essen: Ethik-Kommission reference 14-5965-BO; Cardiff: Wales Research Ethics reference 12/WA/0285; Milan: Comitato Etico Milano Area B, approval obtained on 11/11/2014; Brussels: 2015/05JAN/002 approval obtained by Comitè d'Ethique Hospitalo-Facultaire Saint-Luc-UCL). Written informed consent was obtained from each participant at the moment of the enrolment in the study. According to the INDIGO study, criteria for patient enrolment were: i) GD patients untreated or at maximum of six weeks from commencing the anti-thyroid treatment from a new diagnosis or disease relapse, ii) euthyroid GO patients, iii) newly diagnosed GD patients with overt GO, as previously described [440]. Moreover, patients must have not taken any antibiotics in the three months prior to enrolment in the study. According to the observational multi-centres study, samples (including blood and faeces) were obtained at enrolment (baseline, BL), when euthyroid (euthyroid, EU) and after 6 months from anti-thyroid treatment withdrawal or relapse (end of follow up, EFU) as represented in Figure 4.1.

Diagnosis was made by consultants in each recruiting centre. Patients were subdivided into GD patients with no sign of eye disease and GO with either mild, moderate-severe or sight-threatening signs of eye disease, based on the assessment of the EUGOGO guidelines [54]. Healthy donors from each recruitment centre, matched by age and gender, were all free of thyroid disease, with no signs of eye disease, euthyroid and negative for TRAB. Hyperthyroid patients were defined based on their suppressed or undetectable TSH, high T4 levels and positive TRAB titres. Euthyroid patients were

defined by the T4 thyroid hormone levels being in the normal range. Range values in each recruiting centre are represented in Table 4.1. Thyroid function tests and TRAB levels were measured in blood just before the enrolment in each recruiting centre. TRAB measurement in serum was also repeated by UB-P using the Immulite XPI (Siemens) for TSI (IU/L; positive result cut-off >0.1IU/L), the Cobas Roche for TRAK quantification (IU/L; cut-off >0.3IU/L) and an in-house bioassay for measuring the stimulating activity through cAMP production (pmol/mL; cut-off >1.67pmol/L), to obtain a more comparable results across recruiting centres.

Table 4.1. Reference values for the biochemical thyroid function tests in each recruiting centre.

Recruiting centre	TSH (mU/L)	fT4 (pmol/L)	TRAB (IU/L)
Brussels	0.3-4.2	12-22	>2.5 or >1.8°
Essen	0.3-3.0	11.5-22.7	>1.75
Cardiff	0.3-4.4	9-19.1	>1.6
Newcastle	0.3-4.7	9.5-21.5	>1.8
Milan	0.27-4.2	12-22	>2.5

° changes in the TRAB references after 2016.

A total of 211 patients and 46 healthy controls were initially enrolled in the INDIGO study; 171 patients and 42 controls provided at least one faecal sample, further reduced to 105 patients and 41 controls after removal of: i) patients with unclear diagnosis, ii) concomitant autoimmune conditions/with GD after immune reconstitution (i.e. MS patients treated with alemtuzumab) and iii) sight-threatening GO patients. The removal of those patients was dictated by the need of a more homogenous study cohort. At the time of the enrolment (baseline), characteristics per recruitment centre are summarized in Table 4.2 and Table 4.3. To facilitate the collection of the faecal sample at home, patients were provided with a packaged kit including the correct instructions for sampling, a sterile collection tube and a transport tube to be returned frozen to the clinic, where they were kept frozen at -20°C until shipped in dry ice to Cardiff University (UK) for processing.

Table 4.2. Characteristics of the patients enrolled in the INDIGO study at baseline (146 participants in total; 105 patients and 41 controls).

	Belgium	Germany	Italy	UK	Total
Age (mean)	44.15/54	44.46/48.6	45.4/31.2	48.1/47.9	46.4/46.3
Gender					
F	10/1	16/14	23/6	43/12	92/33
M	0/0	0/3	7/1	7/4	14/8
Ethnicity					
African	1/0	0/0	2/0	4/0	7/0
Asian	0/0	0/0	0/0	3/0	3/0
Caucasian	6/1	16/17	28/7	39/16	89/41
Other	3/0	0/0	0/0	4/0	7/0
Smoking					
current	3/1	6/3	5/2	11/1	25/7
ex	1/0	3/1	1/0	15/1	20/2
never	6/0	7/13	24/3	23/12	60/28
not stated	0/0	0/0	0/2	0/2	0/4

Values are expressed as case/control.

Table 4.3. Clinical characteristics of eligible patients providing samples at baseline and included in the microbiome analysis at recruitment.

Nation	Type	no.	Thyroid status[1]	Orbitopathy[2]	TSH[3]	fT4[4]	TRAB[5]
Belgium	control	1	1/0/0		0.86	19.10	0.20
	GD	6	1/5/0		0.09	17.72	16.67
	GO	4	0/4/0	4/0	0.01	41.10	20.10
Germany	control	17	17/0/0		1.59	12.86	0.02
	GD	6	0/6/0		0.01	31.88	10.84
	GO	10	1/9/0	7/3	0.04	24.17	16.44
Italy	control	7	7/0/0		NA	NA	NA
	GD	11	0/11/0		0.01	17.71	15.81
	GO	19	7/11/0	12/7	1.46	15.25	12.66
UK	control	16	17/0/0		1.22	13.39	0.30
	GD	35	2/32/1		0.56	34.55	9.92
	GO	14	3/11/0	13/1	0.68	22.71	11.46
Total	control	41	41/0/0		1.44	13.26	0.11
	GD	59	3/55/1		0.34	28.95	12.44
	GO	46	11/35/0	36/11	0.77	21.80	13.69

[1]Thyroid status expressed as eu/hyper/hypo (few patients were not assessed); [2]orbitopathy present only in GO patients and expressed to as mild/moderate-severe cases. [3]mean TSH values (mU/L); [4]mean free-T4 levels (pmol/L) and [5]mean TRAB levels (IU/L), obtained from each Hospital.

4.3.2. DNA extraction and 16S rRNA gene sequencing

DNA extraction was performed initially by HLV and DC (2014-2015) and by myself later. Faecal samples were kept frozen at -20°C for a maximum of two months prior to processing. Up to 180-220 mg of slowly-thawed faeces at room temperature were individually placed in 2mL FastPrep tubes prefilled with 0.1mm silica spheres (FastPrep lysing matrix B, MP Biomedicals, UK) and dissolved in 1 mL InhibitEX buffer (Qiagen Ltd, West Sussex, UK). Nucleic acid extraction procedure followed that described in Chapter 2, par. 2.2.2., including the bead-beating step. Aliquots of the extracted DNA were sent to Research and Testing RTL Genomics (Lubbock, Texas, USA) for 16S rRNA gene sequencing, using primers for V1-V2 regions of the 16S rRNA gene plus bifidobacteria regions (28F-combo, Table 2.2. Chapter 2) to generate 10,000 paired-ends reads per sample on an Illumina MiSeq (Illumina, San Diego, USA), for a total of two sequencing runs (obtained in October 2016 and September 2017). Processing of the metataxonomics reads was conducted following the procedure described in Chapter 3 par. 3.3.5 (Appendix 8) and in [352].

4.3.3. Software

Reads from 16S rRNA gene sequencing were processed with the QIIME pipeline [208], used also to estimate diversity indices (alpha and beta). The sample-base rarefaction was estimated using the in-house developed R (https://github.com/filippob/sampleBasedRarefaction) script. Assignment of the enterotypes of the gut microbiota in each sample was performed using the classification algorithm available at http://enterotypes.org, according to [225], which is based on the HMP and MetaHIT training datasets. The prediction of the functional profile of the gut microbiota from 16S rRNA sequences was carried out using the Tax4Fun R package [360]. Plots were generated using the ggplot2 and ggpubr R packages. Additional data handling was performed with the R environment for statistical computing (R Core Team, 2017).

4.3.4. Statistical analysis

4.3.4.1. Alpha and beta diversity indices

To calculate the differences in each alpha diversity index (i.e. observed OTUs, Chao1, Shannon and equitability) across nations of recruitment, a linear model with nation as a categorical fixed effect was used. When testing differences in alpha diversity indices amongst disease diagnosis (GD, GO and healthy controls), thyroid status (hyperthyroid, euthyroid and hypo) and the stratification of the eye-disease (no sign, GO mild and

moderate-severe), the linear model considered those as fixed effects (one per each model) and was designed to correct for nation, age, gender and smoking habits. Beta-diversity was calculated from the Bray-Curtis dissimilarity matrix and was represented using the non-metric dimensional scaling (NMDS) with the Vegan R package. Differences at the beta-diversity amongst and pairwise comparisons of the above fixed effects were assessed using the permutational analysis of variance (PERMANOVA) implemented in the Adonis function [200] with 999 permutations and the nation of provenance as a strata to block the permutations.

4.3.4.2. Differential abundance analysis

Similarly to the alpha diversity, differences in the taxonomic counts at phylum and genus levels were estimated using dedicated linear regression models. The disease diagnosis (GD, GO and healthy controls) or the severity of the eye-disease (no sign, GO mild and moderate-severe) were considered as fixed effects and were corrected for the thyroid status (hyperthyroid, euthyroid, euthyroid-control), nation of recruitment, age, gender and smoking habits. Post-hoc test was performed with the Bonferroni correction. When looking at the thyroid status as a fixed effect, correction was performed on the basis of nation of recruitment, age, gender and smoking habits. The hypothyroid patients were not included in the post-hoc analysis due the low number of samples.

4.3.4.3. RandomForest prediction analysis

A Random Forest (RF) model was trained to predict to which disease types (control, GD or GO) or GO status (no sign, GO mild, GO moderate-severe) each sample belonged, based on the microbiota composition at genus level. CSS-normalized and filtered CSS-normalised abundances with non-zero values in at least 20% samples were retained , scaled and centred. As described in Chapter 3 par. 3.3.6.3, the accuracy of the prediction was estimated through a repeated cross-validation (repeatedcv) method with tenfold and 3 repeats. The tuning hyperparameter *mtry*, approximated as the square root of the number of columns of the dataset, was tuned from 10 to 50 and 5,000 or 10,000 number of trees (ntree), with the R package Caret. RF was next run using the identified parameters providing the highest prediction accuracy during the cross-validation step using the R package RandomForest. The mean decrease accuracy was used for the variable importance selection (i.e. predictors driving the classification).

4.3.4.4. Correlation with disease features

Correlations between the gut microbiota biomarkers identified from the RandomForest variable importance and the diagnostic biochemical parameters (TSH and fT4 levels)

and the auto-antibodies titres (TRAB, TRAK, TSI), plus the cAMP levels, were assessed through the Pearson's product-moment correlation coefficient (*r*) in R, using the Corrplot and ggpubr packages. The Pearson's product-moment correlation calculates the best-fitting line between two variables, while the correlation coefficient describes how far the value relies from the calculated line. Compared to Spearman's rank correlation coefficient, Pearson's deals better with interval values.

4.3.4.5. Imputed metagenomic pathways and genes with Tax4Fun

Metagenomic functions such as orthologs and pathways were imputed against the KEGG database starting from the filtered and normalized OTU table with Tax4Fun R package [360] (see Chapter 3, par. 3.3.6.5). Similarly to the differential abundance analysis, a linear regression model was used to calculate differences in metagenomic functions amongst disease diagnosis (GD, GO and healthy controls) or the stratified eye-disease using either pathways or orthologs as dependent variables, and correcting for thyroid status (hyper, euthyroid), nation of recruitment, age, gender, smoking habits. Mean abundances of significant differentially abundant pathways in each group (whether GD,GO and controls or stratified by GO status) were represented in a heatmap using the "heatmap" function implemented in the gplot R package, with relative abundances scaled to row Z-score and the Euclidean function to compute dissimilarities between both rows and columns. Orthologs' relative abundances were auto-scaled and represented in a principal components analysis (PCA), using the PCA function of the FactoMineR package. Biplots were produced from the FactoMineR 'PCA' object and both variables and individuals were plotted using the FactoExtra R package. The top-10 variables with the highest Cos2 (i.e. value indicating the quality of the individuals on the map) were displayed.

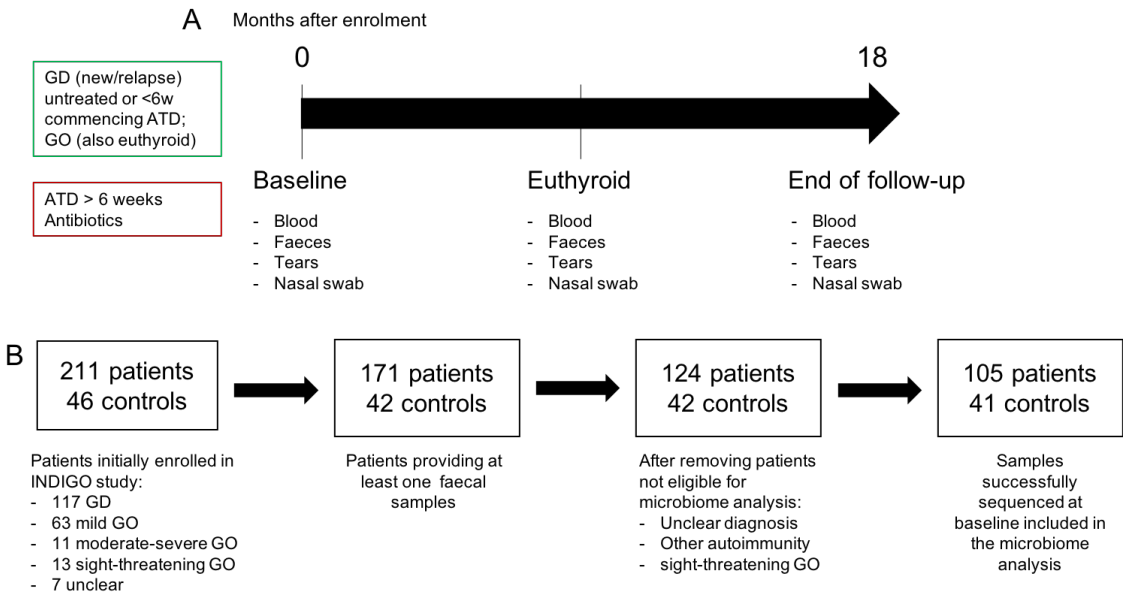

Figure 4.1. Design of the INDIGO study and patients/controls enrolled in the study. (**A**) GD patients (newly diagnosed/relapse untreated or within 6-weeks treatments with anti-thyroid drugs (ATD)) and GO patients (also euthyroid) enrolled in the study should have provided biological samples (blood, tears, nasal swab and faeces) at the time of recruitment (baseline), when being euthyroid (after ATD) and after 6 months of ATD withdrawal/relapse of the disease, ideally in 18-months' time. Exclusion criteria included ATD for more than 6 weeks and antibiotics intake in the past 3 months, at least. (**B**) Number of patients/controls initially enrolled in the study and those providing at least one faecal sample. Samples considered suitable for the microbiome analysis were those available at the baseline and from patients with clear diagnosis, non-sight threatening GO patients and without other concomitant autoimmune diseases (e.g. MS).

4.4. RESULTS

4.4.1. Sequencing metrics and replicability controls

Sequencing the V1-V2 regions plus bifidobacteria-specific primer of the bacterial 16S rRNA gene produced a total of 13,056,151 reads (after joined R1-R2 paired-end reads). After quality filtering, 23,436 sequences were removed, leaving 13,032,715 sequences for subsequent analyses (99.8% average retention rate: maximum 99.9%, minimum 95%). A complete summary is shown in Table 4.4. The closed-reference OTU picking step, which retains only those sequences that align to the reference database, almost halved the number of sequences, by removing chimeric, short and misaligned sequences, thus eliminating most spurious OTUs.

The initial number of OTUs identified was 10,426; after removing OTUs with less than 10 counts in at least 2 samples, 5,649 distinct OTUs were left. To check whether sequencing depth and sample size were adequate to characterize the composition of the gut microbiota, sequence-based and sample-based rarefaction curves were generated from the OTU table before pruning (10,426 OTUs). Sequence-based rarefaction curves were obtained from the QIIME pipeline [208]; the sample-based rarefaction curve was produced with *ad hoc* R functions (see: https://github.com/filippob/sampleBasedRarefaction). The observed number of OTUs detected was plotted as a function of the number of sequences (up to 25,000) in each sample (Figure 4.2A), and of the number of samples (Figure 4.2B). Both curves tend to plateau asymptotically towards a maximum, indicating that sequencing depth and the number of samples were adequate to characterize the gut microbiota in the present study. Deeper sequencing or the addition of any other samples would likely not increase significantly the number of new OTUs potentially discovered.

Between 2014 and 2017, two MiSeq full runs were performed in order to sequence all the samples obtained. Due to possible differences between sequencing batches, some samples were replicated to calculate the inter and intra-batch variability. No significant differences were observed amongst groups (Figure 4.2C) and between replicated samples (Figure 4.2D), suggesting a good replicability of the obtained results.

For the observational analysis of the microbiome at the time of recruitment, only samples matching the above-stated criteria were used (Table 4.4). A good sequencing depth was retained (data not shown), as well as the number of sample was sufficient to describe the microbiota composition.

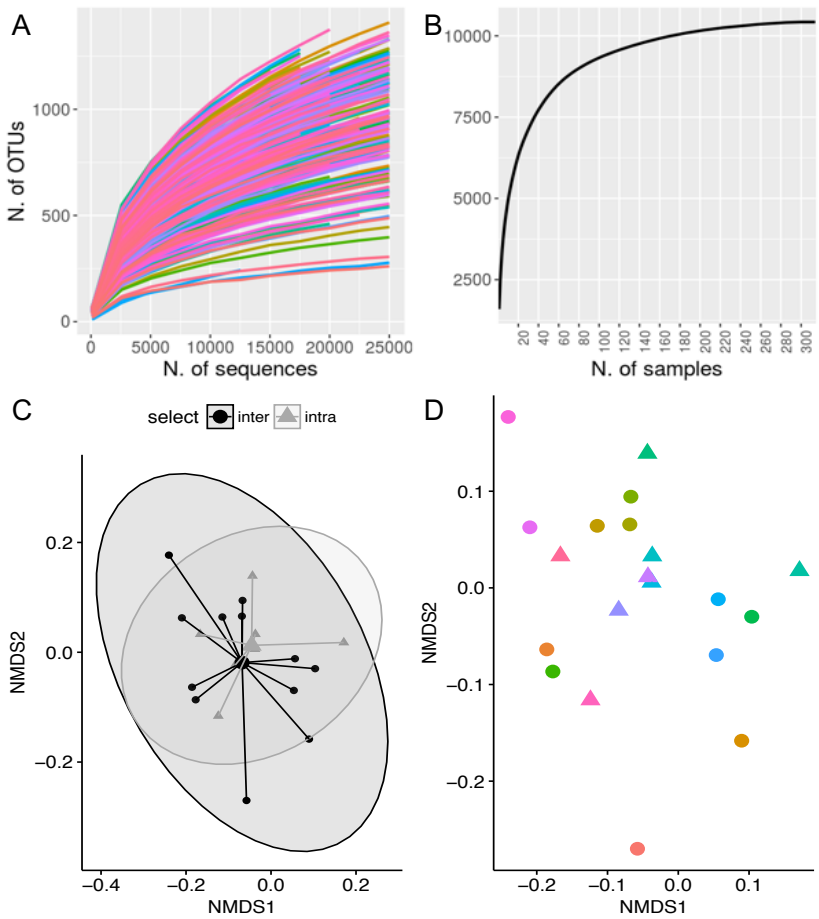

Figure 4.2. 16S rRNA sequencing depth and intra/inter batches replicability. OTU-based (**A**) and sample-based (**B**) rarefaction curves tended asymptotically to a plateau, meaning that the sequencing depth and the number of samples were sufficient to describe all the possible microbial species: increasing the sequencing depth or the number of sample would not increase the numbers of newly-discovered OTUs. NMDS representing the spatial organisation of (**C**) intra/inter batches variability (triangle and circle shapes) based on Bray-Curtis dissimilarity matrix and (**D**) between sample pairs (colours; both PERMANOVA P>0.05, 999 permutations).

Table 4.4. Quality filtering of reads through the main steps of the QIIME bioinformatics processing in terms of total number of sequence, percent reduction from the previous step and average number of reads per sample.

QIIME step	Total n. reads	Reduction	N.reads/sample
multiple_extract_barcodes	26,112,576	-	83,161
multiple_join_paired_ends	13,056,151	50.00%	41,580
multiple_split_library	13,032,715	0.18%	41,505
closed_otupicking	7,953,949	61.03%	25,331

4.4.2. Disease prevalence and gut microbiota differences across recruiting centres

GD and GO patients were enrolled in the INDIGO study from eight recruiting centres in four European countries (Germany, UK, Italy, Belgium). Median TSH values tended to zero in all centres in agreement with the GD diagnosis; in Italy and the UK, some outliers presented higher TSH levels, possibly due to the anti-thyroid drug intake. Thyroxine level (fT4) was all above the hyperthyroidism threshold, as per GD diagnosis, i.e. >19-22, according to each centre reference values. The Italian cohort was less hyperthyroid compared to the others. TRAB levels showed a more heterogenous distribution amongst centres, with a slightly higher level in Belgium, where the majority of patients were untreated and newly-diagnosed GD and a lower values in the UK cohort (Figure 4.3A).

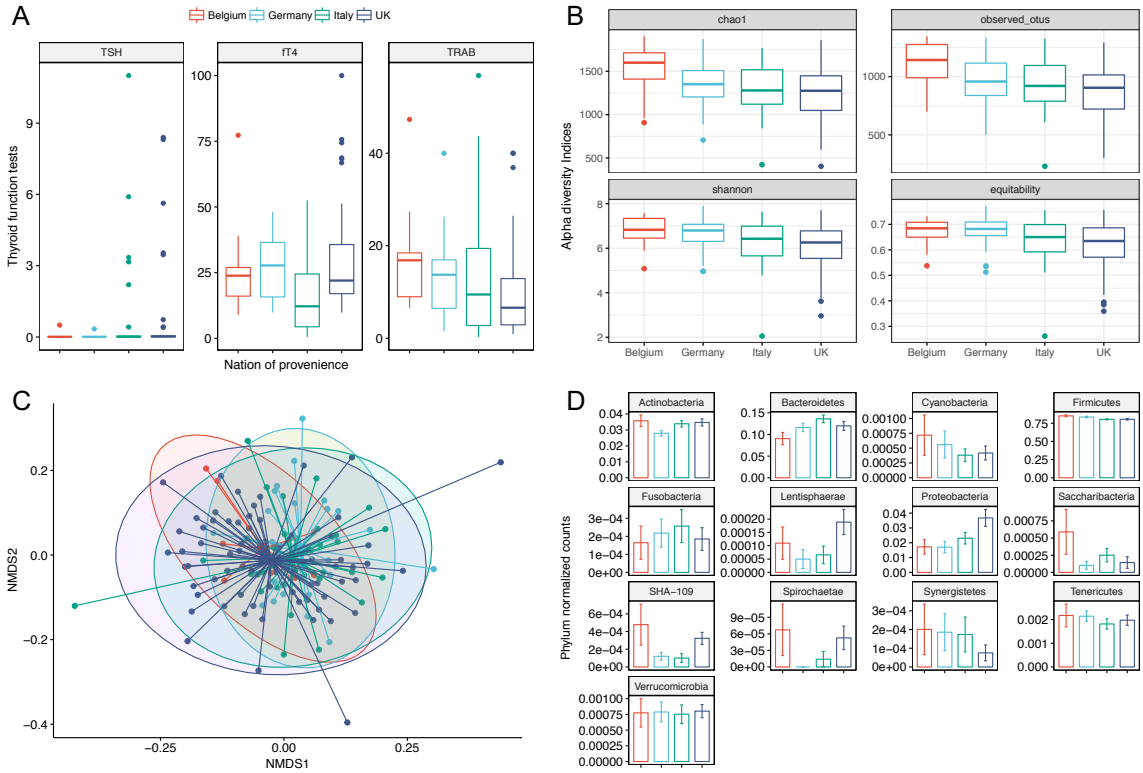

Figure 4.3. Geographical differences in thyroid functions and gut microbiota composition.
(**A**) Distributions of the thyroid function values in GD and GO patients across centres of recruitment. (**B**) Alpha diversity indices of richness (Chao1 and observed OTUs), diversity (Shannon) and equitability of both patients and controls gut microbiota across centres. (**C**) Non-metric dimensional scaling (NMDS) based on the Bray-Curtis dissimilarity matrix showed no spatial differences amongst nations. PERMANOVA P>0.05 with 999 permutations (**D**) Phylum distribution across nations of recruitment. Differences were observed in terms of Firmicutes and Proteobacteria counts.

Geographical variations of the gut microbiota were already reported, mostly associated to the type of diet and lifestyle (Chapter 1 par. 1.5.4.1). The analysis of alpha (Figure 4.3B) and beta diversity (Figure 4.3C) revealed no major differences in terms of overall gut microbiota composition (including both patients and healthy controls) across geographic origin, apart from differences in the Shannon diversity (P=0.007) and equitability (P=0.006) indices between Germany and the UK. At the phylum level (Figure 4.3D), significant differences amongst nations of provenance were reported in *Firmicutes* (P=0.045), *Proteobacteria* (P=0.031) and in the SHA-109 (P=0.01). More specifically, *Firmicutes* were enriched in the Belgium cohort compared to both Italy (P=0.024) and the UK samples (P=0.038). *Proteobacteria*, instead, were enriched in UK samples compared to Germany (P=0.03). The SHA-109 phylum was not significant after Bonferroni correction. At the deepest taxonomic level, 30 genera were differentially abundant amongst nations of provenience. Summary of the linear regression model and the post-hoc test statistic on genus level is presented in Table 4.5.

Table 4.5. Genera differentially abundant amongst nations of recruitment centres.

Genera differentially present	Belgium (n=11)	Germany (n=33)	Italy (n=37)	UK (n=65)	P value[1]	BH[2]
[Eubacterium]_nodatum_group	2.62E-04	8.29E-04	7.23E-04	3.51E-04	0.030	ns
Acidaminococcus	0.00E+00	2.44E-04	5.74E-04	1.87E-04	0.042	A
Christensenellaceae_R-7_group	1.67E-02	1.67E-02	1.51E-02	2.14E-02	0.024	B
Clostridium_sensu_stricto_1	8.77E-03	4.71E-03	5.75E-03	9.94E-03	0.001	B,C
Coprococcus_2	5.55E-03	2.66E-03	3.33E-03	4.62E-03	0.048	ns
Corynebacterium_1	1.53E-04	1.66E-05	0.00E+00	1.96E-05	0.010	ns
Cronobacter	2.99E-05	0.00E+00	1.20E-04	1.79E-05	0.010	ns
Enterobacter	1.61E-03	1.29E-03	3.44E-03	5.08E-03	0.020	C,D
Faecalibacterium	9.13E-02	1.04E-01	1.05E-01	7.95E-02	0.002	B,C
Family_XIII_AD3011_group	3.03E-03	2.20E-03	1.54E-03	2.60E-03	0.047	ns
Hafnia	1.49E-04	0.00E+00	4.00E-05	1.01E-05	0.015	ns
Intestinibacter	6.47E-03	3.03E-03	4.23E-03	5.31E-03	0.001	C,E
Klebsiella	0.00E+00	0.00E+00	3.11E-04	1.34E-04	0.028	ns
Lachnospiraceae_NC2004_group	1.15E-02	1.17E-02	1.21E-02	9.59E-03	0.007	B
Lachnospiraceae_NK4A136_group	7.51E-03	1.14E-02	7.13E-03	7.38E-03	0.000	C,D,F
Lactococcus	1.11E-03	1.14E-03	3.84E-04	5.03E-04	0.010	ns
Leuconostoc	5.84E-04	1.30E-05	7.01E-05	4.03E-05	0.000	ns
Pantoea	7.19E-04	5.10E-04	1.08E-03	1.47E-03	0.045	C
Paraprevotella	0.00E+00	6.98E-05	2.53E-04	3.68E-05	0.026	ns
Peptoclostridium	1.95E-02	9.65E-03	1.11E-02	2.06E-02	0.001	B,C
Peptococcus	4.70E-05	2.82E-04	4.19E-04	4.04E-05	0.043	ns
Romboutsia	2.60E-04	1.01E-04	4.21E-05	3.20E-04	0.010	B
Roseburia	3.53E-02	3.43E-02	3.60E-02	3.01E-02	0.034	ns
Ruminiclostridium	4.99E-03	4.56E-03	5.42E-03	3.96E-03	0.047	ns
Ruminiclostridium_5	9.27E-03	1.31E-02	1.04E-02	1.02E-02	0.003	C,E,F
Ruminococcaceae_V9D2013_group	3.74E-05	1.03E-04	1.19E-05	2.86E-05	0.044	ns
Saccharofermentans	8.52E-04	2.08E-04	8.91E-05	3.20E-04	0.001	ns
Sedimentibacter	6.66E-04	2.46E-04	2.66E-04	7.19E-04	0.019	B,C
Succiniclasticum	5.86E-04	0.00E+00	1.64E-04	0.00E+00	0.003	ns
Syntrophomonas	3.69E-04	1.07E-04	1.03E-04	4.21E-04	0.005	B,C

Mean values per nation of recruitment. Standard deviations are included in Appendix 18. [1] regression model; only P<0.05 are shown. [2] Post-hoc with Bonferroni correction. ns, not significant after correction; A: Italy *vs* Belgium; B: Italy *vs* UK; C: UK *vs* Germany; D: UK *vs* Belgium; E: Germany *vs* Belgium and F: Germany *vs* Italy.

4.4.3. Composition of the gut microbiota in GD/GO patients compared to healthy controls

A comparison amongst disease diagnosis (GD, GO) and GO status (no signs, mild and moderate-severe) compared to healthy controls was performed. The overall composition of the gut microbiota, in terms of richness, diversity and evenness (alpha diversity) of the microbial community was quite similar across disease types (Figure 4.4A) and GO groups (Figure 4.4B). None of the comparisons yielded a statistically significant difference. Between-sample distances measured as Bray-Curtis dissimilarities based on the gut microbiota composition (normalized abundances), did not show any clear clustering of the three groups, since controls, GD and GO patients overlapped substantially (Figure 4.4C), as it did for GO classes (Figure 4.4D). Beta-diversity organisation amongst disease types and eye-disease in each recruiting centre was also investigated, showing no significant clustering (Appendix 19).

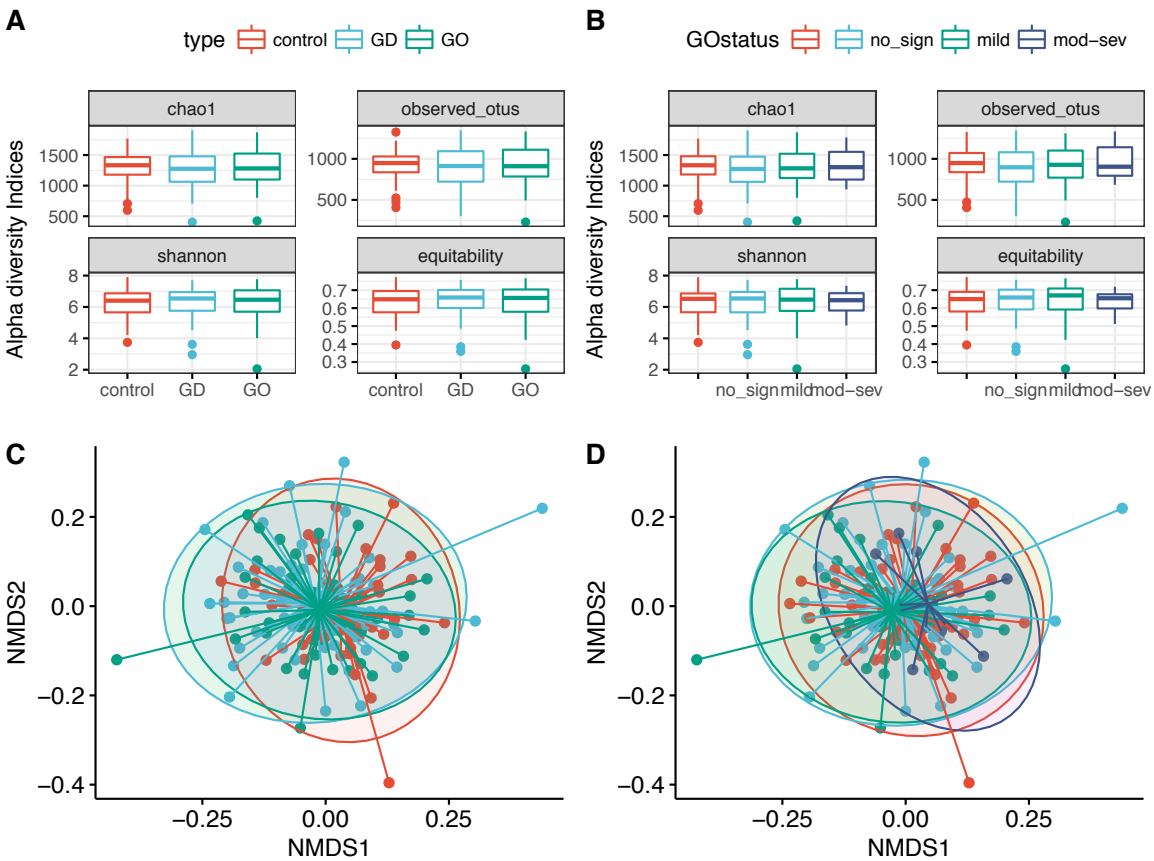

Figure 4.4. Diversity indices associated to disease types and severity of the eye disease.
Box-and-whiskers plots of the alpha diversity of richness, diversity and equitability amongst disease types (GD, GO) compared to healthy controls (**A**) and amongst GO groups (no sign, mild and moderate to severe GO) compared to controls (**B**). NMDS based on Bray-Curtis dissimilarity matrix amongst disease types (**C**) and GO groups (**D**). No significant associations were observed in either alpha or beta-diversity in both analysis.

Thirteen phyla were identified and quantified across samples, in which *Firmicutes* phylum dominated in terms of abundance followed by *Bacteroidetes* and *Actinobacteria*. Amongst disease types, phyla *Actinobacteria*, *Bacteroidetes* and *Proteobacteria* displayed significant differential abundance, with the increase in abundance of *Actinobacteria* in GD (P=0.0017) and GO (P=0.0001) compared to controls, a decrease in the abundance of *Bacteroidetes* in GD (P=0.019) and GO (P=0.019) compared to controls (Figure 4.5A). Counts of *Actinobacteria* phylum was significantly increased in GD patients (P=0.004) and GO with mild disease (P=0.0001) compared to controls; while *Bacteroidetes* reduced in GD (P=0.025) and mild GO (P=0.025) compared to controls. Interestingly, the *Firmicutes:Bacteroidetes* (F:B) ratio was significantly increased in cases *vs*. controls (Figure 4.5B), in particular in GD *vs*. controls (Figure 4.5C). At a deeper taxonomic level, 22 genera resulted differentially abundant displayed significant differential abundance amongst disease types, resembling what was previously observed at the phylum level. Amongst others, *Bacteroides* genus was significantly decreased in GD (P=0.018) and GO (P=0.009) compared to controls, while *Fusicatenibacter* counts were enriched in GD compared to controls (P=0.013), as well as in GO compared to controls (P=0.002, Table 4.6). As far as the eye disease is concerned, reduction of *Bacteroides* (P=0.014) and increased *Bifidobacterium* (P=0.001) and *Fusicatenibacter* counts (P=0.008) were significantly associated to mild-GO, but not to moderate-severe GO (Table 4.7). *Bifidobacterium* spp. moreover decreased in the moderate-severe GO compared to the mild-GO (P=0.032). On the other hand, *Roseburia* spp. counts were enriched in moderate-severe GO compared to both controls (P=0.018) and GD (P=0.033). *Luteimonas* was specifically enriched in moderate-severe GO compared to all the others, even if not significant, due to a very low abundance (Table 4.7).

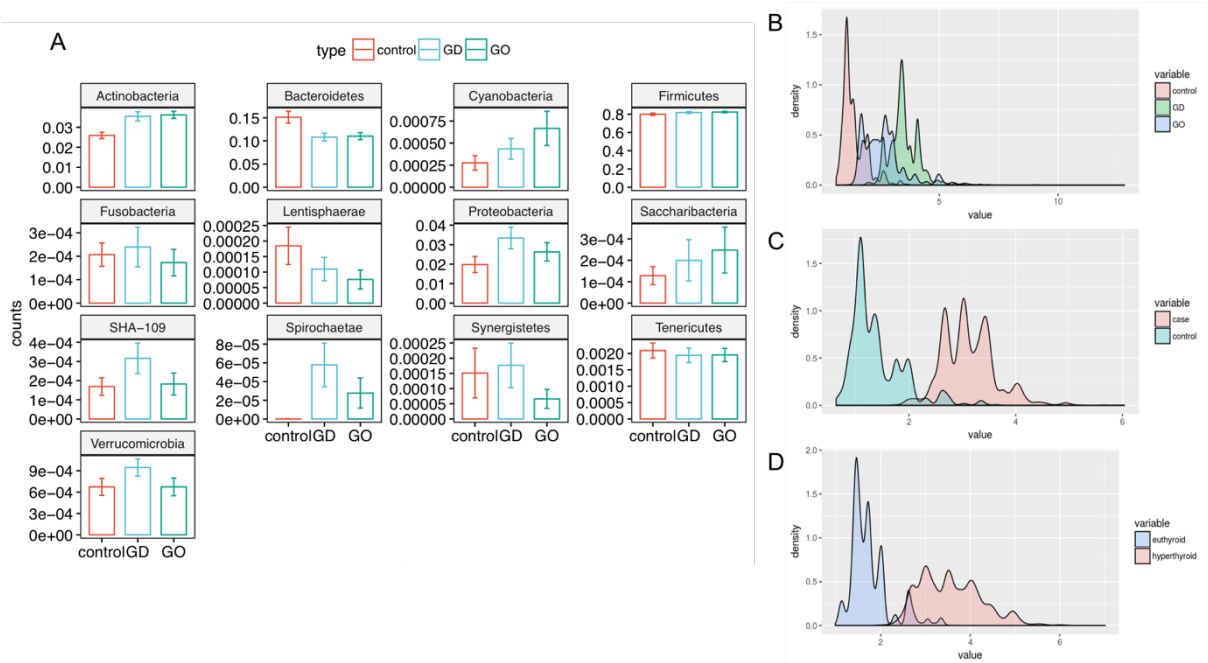

Figure 4.5. Phylum distribution and F:B ratio amongst types of disease. Differences amongst disease types (**A**). Only *Actinobacteria* and *Bacteroidetes* showed significant differences amongst groups, pairwise differences are explained in Table 4.6. Bootstrapped distribution of the F:B ratio over 500 datasets resampled according to disease type (**B**), cases vs. controls (**C**) or by thyroid status (**D**), as hyper *vs*. euthyroid.

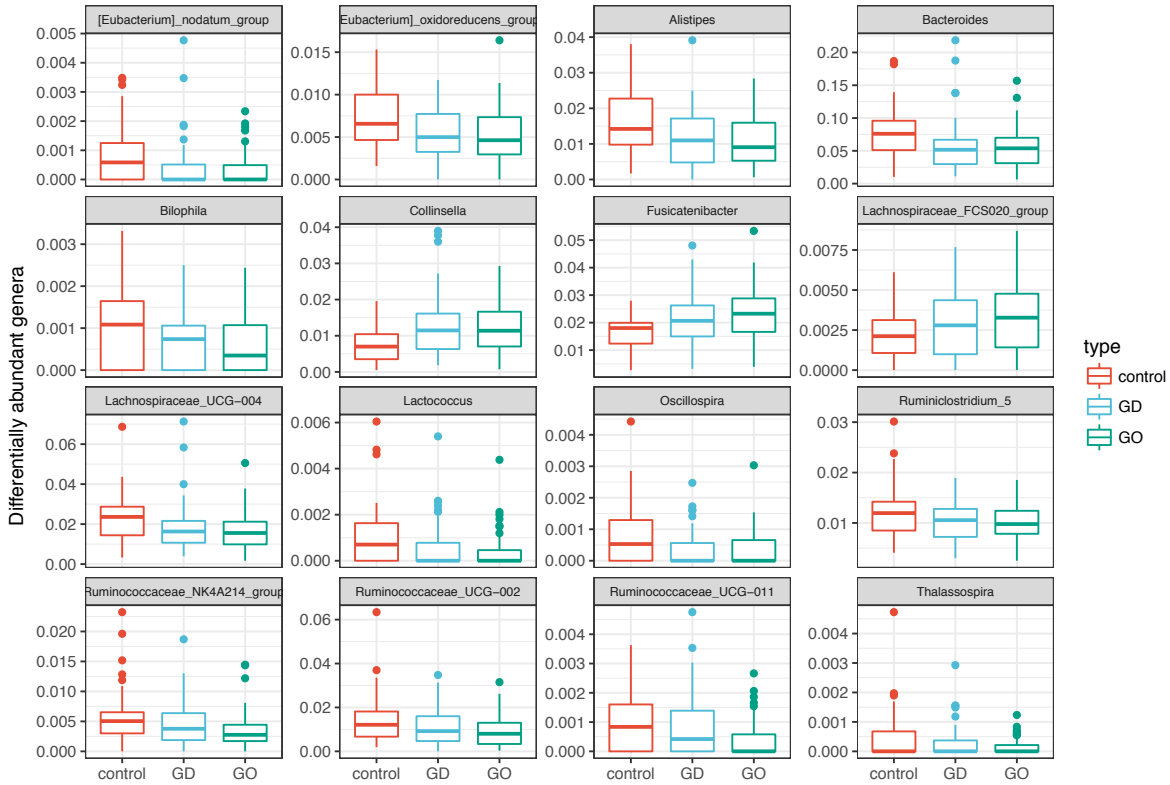

Figure 4.6. Differentially abundant genera in GD/GO compared to healthy controls. Only P<0.05 from the ANOVA model were shown. Pairwise differences are explained in Table 4.6.

Table 4.6. Pairwise differences between GD (n=59), GO (n=46) and healthy controls (n=41).

Differentially abundant taxa	group1	group2	P value
Actinobacteria (phylum)	GD	control	0.002
Actinobacteria (phylum)	GO	control	0.000
Bacteroidetes (phylum)	GD	control	0.019
Bacteroidetes (phylum)	GO	control	0.019
[Eubacterium]_nodatum_group	GD	control	0.033
[Eubacterium]_nodatum_group	GO	control	0.018
[Eubacterium]_oxidoreducens_group	GD	control	0.032
[Eubacterium]_oxidoreducens_group	GO	control	0.029
Alistipes	GD	control	0.038
Alistipes	GO	control	0.015
Bacteroides°	GD	control	0.018
Bacteroides°	GO	control	0.009
Bilophila	GO	control	0.032
Collinsella	GD	control	0.004
Collinsella	GO	control	0.004
Fusicatenibacter°	GD	control	0.013
Fusicatenibacter°	GO	control	0.002
Lachnospiraceae_FCS020_group	GD	control	0.049
Lachnospiraceae_FCS020_group	GO	control	0.020
Lachnospiraceae_UCG-004°	GO	control	0.018
Lactococcus	GO	control	0.022
Oscillospira	GD	control	0.009
Oscillospira	GO	control	0.019
Ruminococcaceae_NK4A214_group°	GO	control	0.036
Ruminococcaceae_UCG-011	GO	control	0.023

Pairwise t-test Bonferroni-corrected of ANOVA differentially abundant taxonomies in Figure 4.6, only $P<0.05$ are shown. °Bacterial biomarkers confirmed in the RandomForest prediction analysis below.

Table 4.7. Genus average abundance and test statistics (both ANOVA model and pairwise) amongst eye-disease status (no sign, GO mild and GO moderate-severe) compared to healthy controls.

Differentially abundant genera	control no sign (n=41)	GD no sign (n=58)	GO mild (n=36)	GO mod-sev (n=11)	P value[1]	PW[2]
[Eubacterium] nodatum group	**0.0009**	0.0004	0.0004	0.0003	0.0211	ns
[Eubacterium] oxidoreducens group	**0.0072**	0.0055	0.0055	0.0046	0.0483	ns
Alistipes	**0.0158**	0.0115	0.0104	0.0130	0.0314	B
Anaeroplasma	0.0002	0.0001	0.0000	**0.0005**	0.0110	ns
Bacteroides°	**0.0781**	0.0562	0.0529	0.0626	0.0151	A,B
Bifidobacterium°	0.0088	0.0117	**0.0135**	0.0088	0.0193	B
Clostridium sensu stricto 1	0.0062	**0.0092**	0.0080	0.0030	0.0231	C,D,E
Collinsella	0.0079	**0.0127**	0.0122	0.0100	0.0204	A,B
Fusicatenibacter°	0.0168	0.0214	**0.0234**	0.0213	0.0096	B
Intestinibacter°	0.0036	0.0050	**0.0056**	0.0030	0.0115	B
Lachnospiraceae FCS020 group	0.0021	0.0030	**0.0035**	0.0025	0.0353	B
Lactococcus°	0.0011	**0.0005**	0.0004	0.0004	0.0092	ns
Luteimonas	0.0000	0.0000	0.0000	**0.0003**	0.0092	ns
Oscillospira	**0.0008**	0.0003	0.0004	0.0004	0.0031	A
Peptoclostridium	0.0130	0.0177	**0.0182**	0.0062	0.0451	D,E,F
Rikenellaceae RC9 gut group°	0.0005	0.0005	**0.0022**	0.0001	0.0156	D
Roseburia	0.0310	0.0320	0.0339	**0.0418**	0.0228	C,E
Ruminococcaceae NK4A214 group	**0.0061**	0.0048	0.0042	0.0022	0.0247	C,E
Ruminococcaceae UCG-011	**0.0009**	0.0008	0.0005	0.0000	0.0158	C,D,E

In bold, genera with the highest average abundance across groups. Standard deviations are included in Appendix 20. [1]P values derived from the ANOVA model, only differentially abundant genera P<0.05 are shown. [2]Pairwise differences from the pairwise T-test Bonferroni-corrected: ns, not significant after correction; A, GD *vs*. controls; B, GO mild *vs*. controls; C, moderate-severe GO *vs*. GD; D, moderate-severe *vs*. GO mild; E, moderate-severe *vs*. controls and F, GO mild *vs*. GD. °Bacterial biomarkers confirmed in the RandomForest prediction analysis below.

4.4.4. Prediction of diagnosis based on gut microbiota composition

Random Forests (RF) classification analysis was used to predict the type of disease (whether GD, GO or healthy controls) and the stratification in eye disease (no sign, mild and moderate-severe GO compared to healthy controls), based on the gut microbiota composition at genus level, using 10,000 trees. Both models took into account the thyroid status, nations of provenance, age, gender and smoking habits within the predicting variables. Samples with missing values for one of the above variables were excluded from the analysis. Prediction of the diagnosis (or disease types) returned an overall out-of-bag (OOB) error rate of 40.14%, which accounted for 59.86% accuracy of the trained model. Within the healthy controls class, all but one sample (36/37) were correctly

predicted as controls (2.7% per-class OOB error rate); 42 out of 59 samples were correctly predicted as GD patients with 17 remaining GD samples predicted to as GO (28% per-class OOB error rate), and the majority of GO samples were erroneously predicted as GD (39/46) with only 7 samples correctly assigned to GO (84% per-class OOB, Figure 4.7A). When separating the GO class into mild and moderate-severe GO diagnosis, the accuracy of the model increased to 61.97% (overall OOB 38.03%). Forty-nine out of 58 samples were predicted as GD, with one sample as healthy control and 8 as GO mild (15.5% per-class OOB); 33/36 GO mild patients were predicted to as GD and just 3 to as GO mild (91.6% per-class OOB) and finally all of the eleven moderate-severe patients were predicted as GD with no signs of eye disease (100% per-class error-rate; Figure 4.7D). Variable importance features were obtained from the top-predicting variables, based on mean decrease accuracy parameter (Figure 4.7B and D). To note, *Bacteroides* spp. is present in both classification models and constitutes the first top-bacterial biomarker when predicting diagnosis with the eye disease stratification (Figure 4.7D). Bonferroni-corrected, pairwise differences amongst disease types and eye disease involvement are reported in Table 4.6 and 4.7.

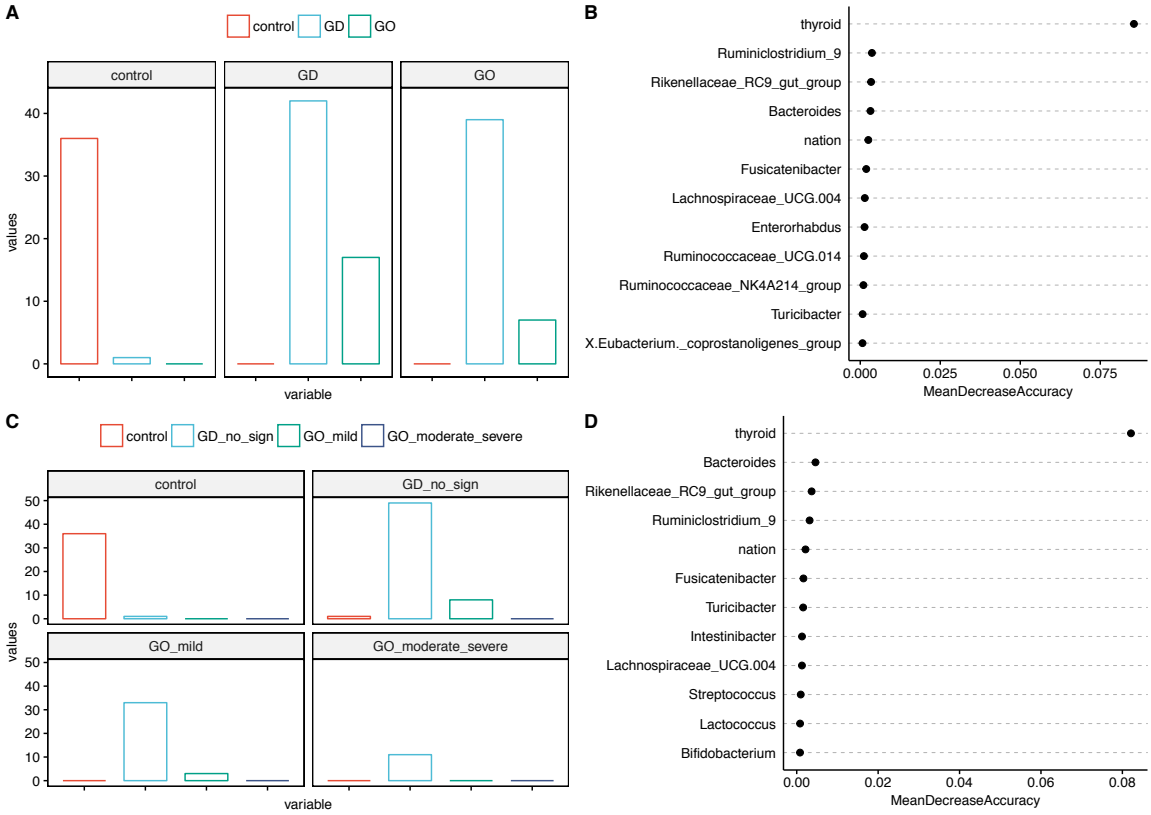

Figure 4.7. Random Forests classification accuracy and variable importance in predicting the disease diagnosis based on the gut microbiota composition at genus level.

(**A**) Confusion matrix with the per-class classification for disease type (GD, GO and healthy controls). Each box represents the true treatment while the bar chart represents the number of samples being assigned to a treatment according to the model used. (**B**) Top-10 variable importance for disease type classification according to the Mean Decrease Accuracy. The model included the thyroid status, nation of provenance, age, gender and smoking habits as predicting variables, of which thyroid status and nation of provenance were identified in the top-10 most important variables. (**C**) Confusion matrix with the per-class classification of the eye disease (no signs, mild, moderate-severe compared to healthy controls) and (**D**) Top-10 variable importance for eye-disease classification according to the Mean Decrease Accuracy.

4.4.5. Association of the gut microbiota with thyroid status

The RF model revealed a strong effect of the thyroid status (i.e. being hyperthyroid or euthyroid/control euthyroid) in predicting the disease types or the stratification of the eye disease based on the genus-level gut microbiota composition. Here I investigated the gut microbiota composition between the thyroid status, regardless of the initial diagnosis (GD or GO), and compared with that of the euthyroid controls. Only one patients was hypothyroid due to the ATD therapy and was excluded from the statistical analysis. Similarly for the disease type and GO severity, no significant differences were observed in the alpha diversity indices. The NMDS based on Bray-Curtis dissimilarity matrix showed a significant separation amongst groups overall (P=0.02, based on 999 permutations; Figure 4.8A), but not pairwise, even if a more clear separation was observed between hyperthyroid and euthyroid patients (Figure 4.8B), rather than euthyroid patients compared to euthyroid healthy controls (Figure 4.8C).

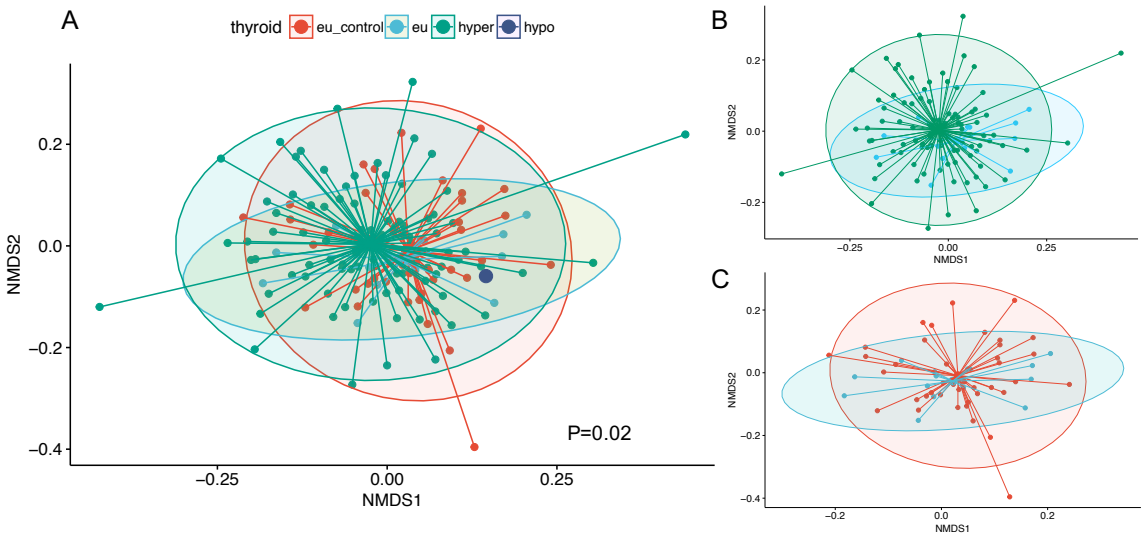

Figure 4.8. NMDS based on thyroid status.
(**A**) overall amongst thyroid status groups and (**B** and **C**) pairwise. P=0.02 overall, PERMANOVA based on 999 permutations. No significant differences were observed in pairwise comparisons after BH corrections, even if more separated groups were observed in (**B**) between hyper and euthyroid patients.

Firmicutes:Bacteroidetes ratio was higher in hyperthyroid compared to euthyroid patients (Figure 4.5E). At the genus level, 27 taxa were significantly different among groups (i.e. euthyroid-control, euthyroid and hyperthyroid). *Bacteroides* counts were significantly reduced in hyperthyroid patients compared to euthyroid controls (P=0.0003), while there were no significant differences between the two euthyroid groups, although the euthyroid patients showed a lower *Bacteroides* counts. On the other hand, *Fusicatenibacter* genus was significantly increased in hyperthyroid patients compared to euthyroid-controls

(P=0.0002), while higher counts were found in euthyroid patients compared to controls, although not significant (Table 4.8).

Table 4.8. Genus mean abundance and test statistics (both ANOVA model and pairwise) amongst thyroid status (hyperthyroid, euthyroid, hypothyroid) compared to euthyroid-healthy controls, regardless of the type of disease.

Differentially abundant genera	EU-HC (n=41)	Hyper (n=90)	EU (n=14)	Hypo (n=1)	P value[1]	PW[2]
[Eubacterium] hallii group	0.0336	**0.0346**	0.0224	0.0183	0.0333	A,B
[Eubacterium] nodatum group	**0.0009**	0.0004	0.0002	0.0000	0.0121	A,B,C
[Eubacterium]oxidoreducens group	**0.0072**	0.0056	0.0042	0.0032	0.0199	A,C
Alistipes	0.0158	0.0111	0.0116	**0.0231**	0.0169	C
Allisonella	**0.0001**	0.0000	**0.0001**	0.0000	0.0206	ns
Ambiguous taxa	0.0003	0.0002	0.0004	**0.0009**	0.0273	ns
Anaerostipes	0.0257	**0.0285**	0.0189	0.0091	0.0404	B
Bacteroides	0.0781	0.0538	0.0624	**0.1382**	0.0014	C
Bilophila	0.0010	0.0006	0.0006	**0.0015**	0.0356	C
Blautia	0.0846	**0.0998**	0.0895	0.0358	0.0208	C
Collinsella	0.0079	**0.0127**	0.0098	0.0026	0.0056	C
Comamonas	0.0000	0.0000	**0.0003**	0.0000	0.0225	ns
Filifactor	0.0000	0.0000	0.0000	**0.0006**	0.0000	ns
Fusicatenibacter	0.0168	**0.0225**	0.0196	0.0136	0.0062	C
Gordonibacter	0.0003	0.0005	0.0001	**0.0006**	0.0472	B,C
Lachnospira	0.0019	0.0016	0.0017	**0.0069**	0.0352	ns
Lachnospiraceae_FCS020_group	0.0021	0.0031	**0.0033**	0.0006	0.0497	ns
Lachnospiraceae_UCG-004	0.0236	0.0169	0.0195	**0.0400**	0.0102	C
Lachnospiraceae_UCG-006	0.0004	0.0003	**0.0007**	0.0000	0.0316	ns
Lactococcus	**0.0011**	0.0005	0.0005	0.0000	0.0103	C
Luteimonas	0.0000	0.0000	**0.0002**	0.0000	0.0336	ns
Oscillospira	**0.0008**	0.0003	0.0006	0.0000	0.0015	C
Prevotella_6	0.0000	0.0000	0.0000	**0.0006**	0.0000	ns
Ruminiclostridium_5	**0.0123**	0.0103	0.0101	0.0056	0.0333	ns
Ruminococcaceae_UCG-003	0.0032	0.0023	0.0037	**0.0076**	0.0080	ns
Sutterella	0.0029	0.0021	0.0031	**0.0165**	0.0000	ns
Thalassospira	0.0005	0.0002	0.0002	**0.0029**	0.0000	ns

In bold, most abundant average across groups. Standard deviations are included in Appendix 21. EU-HC, euthyroid-healthy controls; EU, euthyroid [1]P values derived from the linear regression model, only differentially abundant genera P<0.05 are shown. [2]Post hoc test Bonferroni-corrected, not taking into account the hypo status due to just one sample: ns, not significant after correction; A, EU-HC *vs*. EU; B, hyper *vs*. EU; C, hyper *vs*. EU-HC.

4.4.6. Correlation of the gut microbiota with thyroid function

Correlation between the gut microbiota features identified from the variable importance analysis represented in Fig. 4.7B and the levels of TSH and free-T4 (fT4) quantified in the blood was assessed using the Pearson's product-moment correlation coefficient (*r*). Out of the 10 genera selected, only counts of the genus *Bacteroides* showed a significant correlation with both TSH and fT4 levels in the GD group. Particularly, a positive correlation was reported with TSH, although the majority of the GD patients – as for definition of GD - had a low or undetectable TSH levels (r=0.51, P=0.0037; Figure 4.9A). On the other hand, *Bacteroides* spp. showed a weak negative correlation with fT4 levels (r= -0.37, P=0.046; Figure 4.9B). No significant correlation was observed in the GO patients group. In euthyroid patients, *Bacteroides* counts correlated negatively with TSH levels, although not significant (Figure 4.9C). Consistently, *Bacteroides* spp. showed a weak negative correlation with fT4 in hyperthyroid patients (r= -0.36, P=0.012), while showed a positive correlation in euthyroid patients, although not reaching the significant threshold (Figure 4.9D).

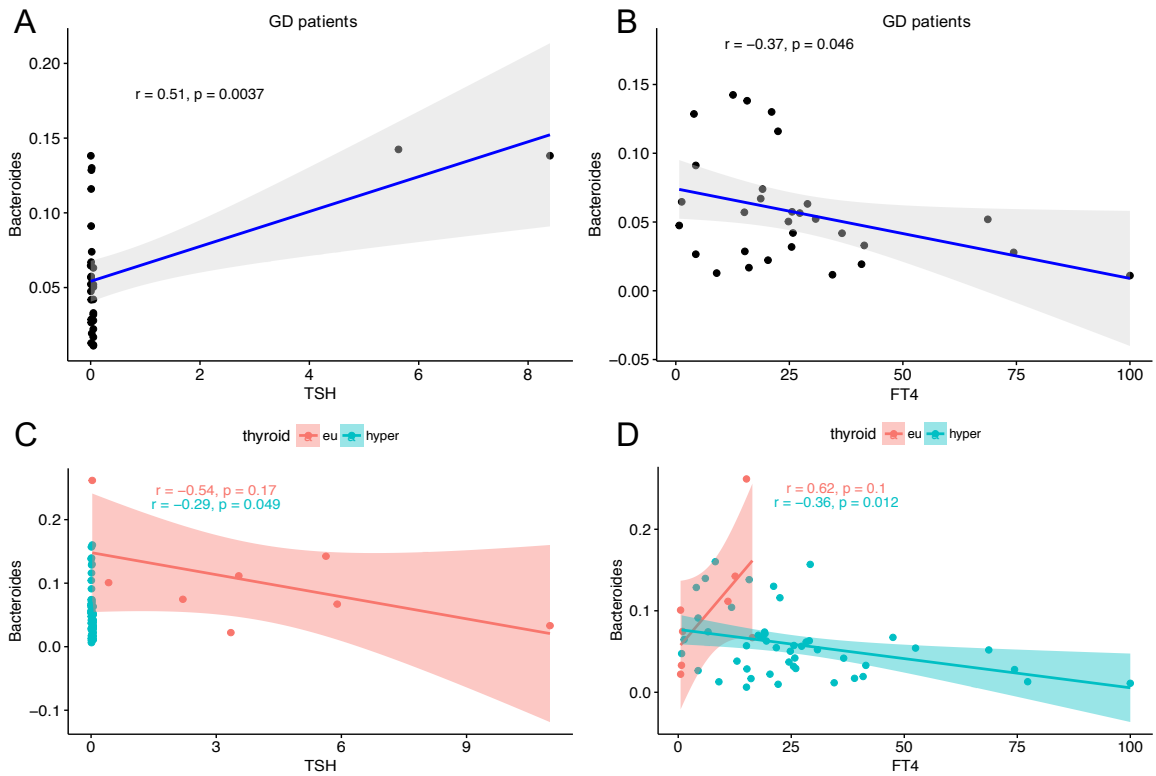

Figure 4.9. Pearson's correlation between *Bacteroides* counts and thyroid functions in GD patients hyperthyroid/euthyroid.
Weak-positive correlation between *Bacteroides* counts and (**A**) TSH, Thyroid-Stimulating Hormone (U/mL) and weak-negative correlation between *Bacteroides* counts and (**B**) free Thyroxine levels, FT4 (pmol/L) in GD patients. No significant correlations were observed in GO patients. *Bacteroides* correlation in hyperthyroid and euthyroid patients

(with GD and GO together) with TSH (**C**) and FT4 (**D**) levels. *r*, Pearson's product-moment correlation coefficient. Hyper, hyperthyroid patients. Eu, euthyroid patients.

4.4.7. Correlation of the gut microbiota with auto-antibodies titres

Correlation with the auto-antibodies titres (TRAB) and the GD/GO gut microbiota biomarkers was also assessed (Figure 4.10). In the GD cohort, counts of the *Firmicutes* genus *Turicibacter* showed a weak negative correlation with both TRAK/TRAB and cAMP levels, while two genera of the *Ruminococcaceae* (UCG-001 and NK4A214, respectively) showed a weak negative correlation with TRAK levels. GO patients showed the majority of positive correlations, potentially sustained by the fact that GO patients tend to have a higher TRAB titres. *Turicibacter* and *Ruminococcaceae* UCG-001 genera positively correlated with TRAK and TRAK and cAMP, respectively. Genera *Rikenellaceae* RC9 gut group and *Eubacterium coprostanoligenes* were both positively correlated with TRAB levels while *Bacteroides* spp. showed a weak negative correlation with the TRAB levels.

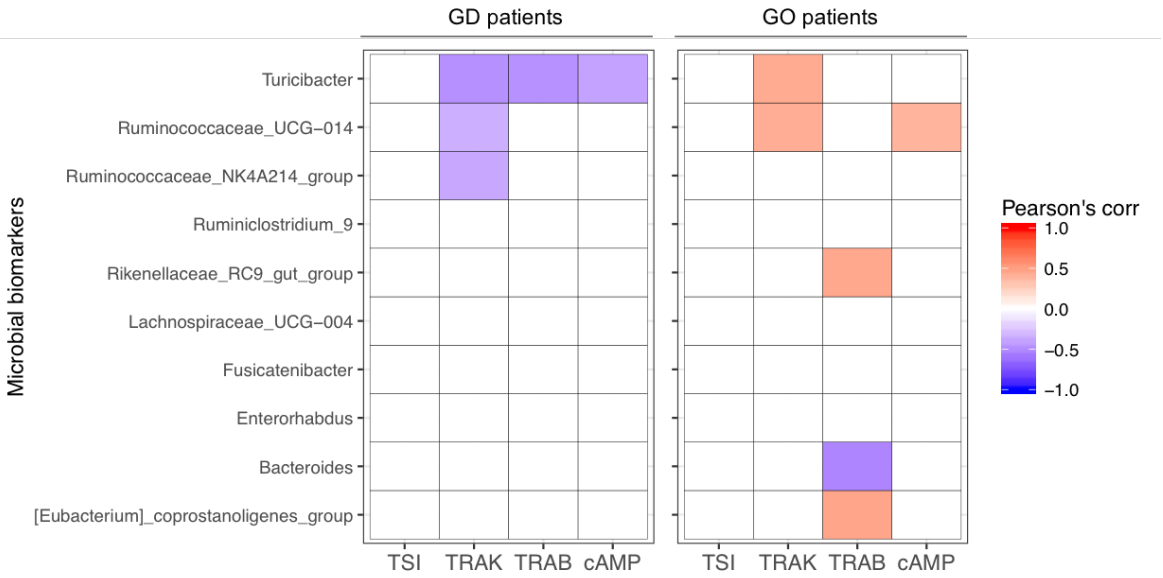

Figure 4.10. Correlation with auto-antibodies features quantified in GD and GO patients.
TSI, thyroid-stimulating immunoglobulin (IU/L). TRAK, thyrotropin receptor antibodies using the TRAK-assay (IU/L). TRAB, thyrotropin receptor antibodies (IU/L) measured in and cAMP (pmol/mL). Only correlation with P<0.05 are shown and the strength of the Pearson's correlation coefficient (*r*) is represented by the change of colour from red (positive) to blue (negative correlation).

4.4.8. Enterotypes of the gut microbiota and their association to GD/GO

As previously introduced, Arumugam and colleagues identified three enterotypes, or preferred composition of the gut microbiota, such as those dominated by *Bacteroides* (enterotype 1), *Prevotella* (enterotype 2) or *Firmicutes*-prevalent (enterotype 3) [225]. The classification algorithm based on HMP and MetaHIT training datasets assigned 11/157 samples to enterotype 1 (7%), 28/157 samples to enterotype 2 (17.83%) and the majority of samples (118/157; 75.15%) to enterotype 3. There was a significant separation of the three enterotypes overall (Figure 4.11A), which was consistent also across nations, apart from Belgium which had the lowest number of recruited patients (Figure 4.11B).

Redundancy analysis (RDA) showed an association of GD and hyperthyroid patients to the enterotype 3 (*Firmicutes*-prevalent), while GO lay in-between the enterotype 2 (*Prevotella*-prevalent) and enterotype 3 (Figure 4.11C). Mild-GO was associated in-between the enterotype 2, while the moderate-severe GO pointed towards a mixed group between enterotype 3 and enterotype 1 (*Bacteroides*-based) (Figure 4.11D).

4.4.9. Gender-differences of the gut microbiota in GD/GO patients

The model used in the previous analyses corrected for gender biases, since sex-related hormones may modulate the gut microbiota composition [432]. However, GD is more prevalent in females (92:14 in our cohort) and for that reason, differences in the gut microbiota between gender were also investigated in GD and GO groups, respectively. Twenty-two genera were differentially abundant between females and males in the GD group, while seventeen were differentially abundant in the GO group (Table 4.9). In GD, males' microbiota was significantly enriched in *Alloprevotella*, *Butyrivibrio*, *Clostridium sensu-stricto* 1, *Enterococcus* and *Prevotella* 2, amongst other genera, while females were enriched in *Eggerthella* spp. counts (P=0.036). GO microbiota in male patients, on the other hand, showed enrichment of *Acinetobacter*, *Comamonas* spp. and a clade of *Prevotellae* (1,2,6 and 9), while females GO patients showed increased *Lachnospiraceae* UCG-008 counts. Interestingly, none of these differentially abundant genera showed an association with either disease type or GO status, a part from *Rikenellaceae* RC9 gut-group, which was identified in the RF variable importance (Figure 4.7B), but not from the differential abundance linear regression model.

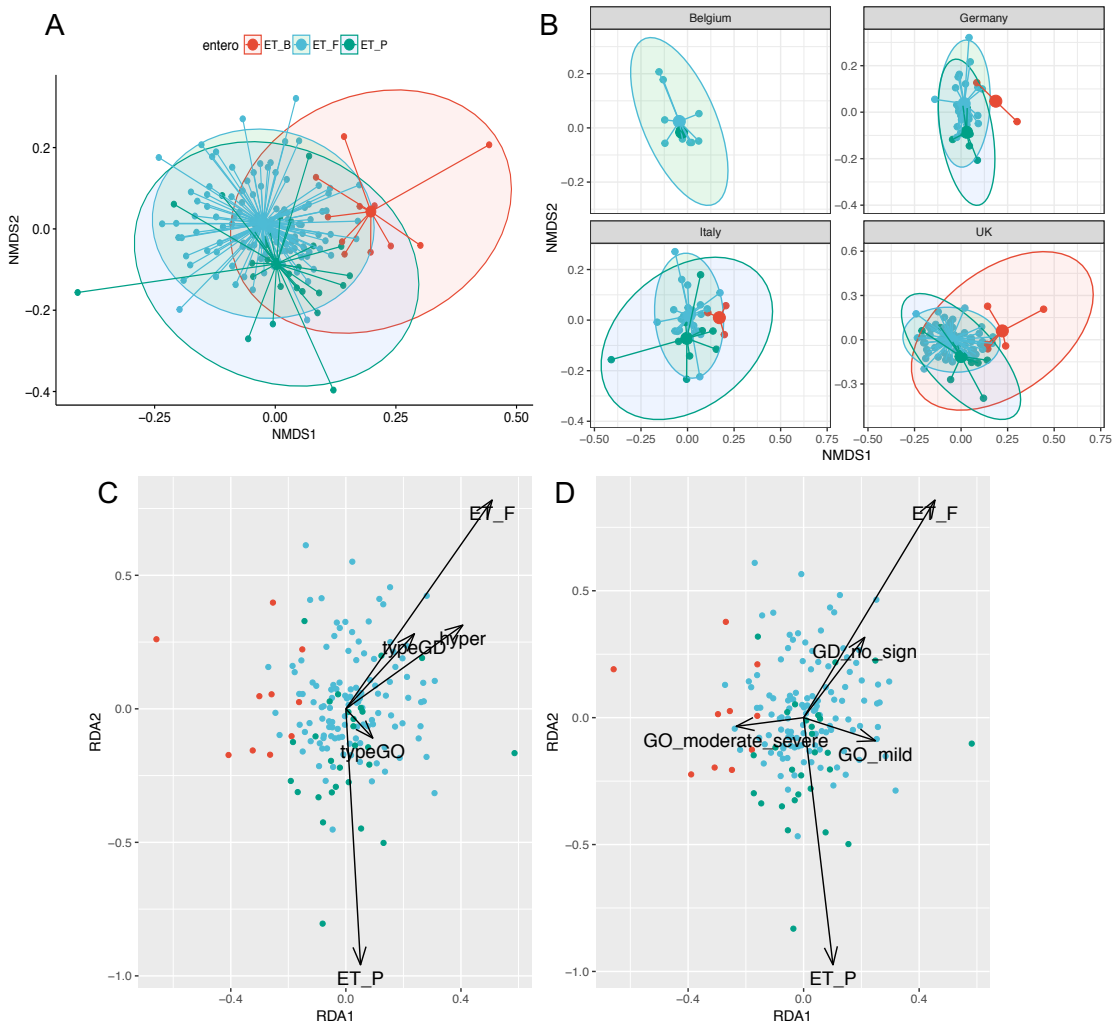

Figure 4.11. Enterotypes of the gut microbiota associated to disease, thyroid status and eye disease.

(**A**) NMDS based on the Bray-Curtis distribution of the three identified enterotypes: ET_B, enterotype 1 (*Bacteroides*-prevalent); ET_P, enterotype 2 (*Prevotella*- prevalent) and ET_F, enterotype 3 (*Firmicutes*-prevalent). (**B**) Redundancy analysis (RDA) was based on Bray-Curtis distances of the three enterotypes and superimposed arrows representing (**C**) both disease types (GD,GO and healthy controls) and thyroid status (hyper, eu, eu-control) or (**D**) signs of eye disease (GD no sign, GO mild and GO moderate-severe).

Table 4.9. Gender-related gut microbiota differences in GD (52 females and 7 males) and GO (40 females and 6 males) patients.

Genera differentially present in GD	Female (mean)	Female (st dev)	Male (mean)	Male (st dev)	P value[1]
Alloprevotella	1.48E-05	0.0001	0.0033469	0.0059	0.000
Butyrivibrio	0.00066173	0.0008	0.00184197	0.0018	0.006
Clostridium sensu stricto1	0.00833238	0.0078	0.01481178	0.0116	0.049
Desulfobulbus	2.28E-05	0.0002	0.00022419	0.0004	0.014
Eggerthella	0.00071418	0.0009	0	0.0051	0.036
Enterococcus	0.00043935	0.0001	0.00271936	0.0002	0.003
Fastidiosipila	1.71E-05	0.0003	0.00013241	0.0006	0.013
Halocella	8.16E-05	0.0003	0.0003992	0.0012	0.011
Lysinibacillus	5.08E-05	0.0142	0.00046353	0.0286	0.038
Peptoclostridium	0.01523107	0.0001	0.03427896	0.0020	0.002
Planomicrobium	2.18E-05	0.0011	0.0007482	0.0153	0.008
Prevotella_2	0.00064905	0.0006	0.00959271	0.0062	0.000
Rikenellaceae RC9 gut group	0.00026849	0.0004	0.00249368	0.0008	0.014
Romboutsia	0.00019373	0.0010	0.00073504	0.0025	0.004
Rummeliibacillus	3.33E-05	0.0009	0.00026846	0.0016	0.037
Sarcina	0.00110107	0.0000	0.00231618	0.0009	0.020
Sedimentibacter	0.0005297	0.0005	0.00144825	0.0009	0.018
Sporosarcina	0	0.0002	0.00045386	0.0004	0.000
Syntrophomonas	0.00029529	0.0011	0.0009008	0.0008	0.010
Terrisporobacter	4.32E-05	0.0000	0.0002342	0.0003	0.023
Victivallis	0	0.0001	0.00010796	0.0013	0.007
Weissella	8.09E-06	0.0001	0.00050067	0.0059	0.007
Genera differentially present in GO	**Female (mean)**	**Female (st dev)**	**Male (mean)**	**Male (st dev)**	**P value[1]**
[Eubacterium] ventriosum group	0.00364713	0.0029	0.00122805	0.0025	0.013
Acinetobacter	0.00019003	0.0001	0.00080923	0.0059	0.047
Alloprevotella	0.00021787	0.0002	0.00236527	0.0003	0.000
Anaerofilum	1.16E-05	0.0000	0.0002121	0.0000	0.002
Comamonas	0	0.0060	0.00066443	0.0066	0.010
Lachnospiraceae UCG-008	0.02705175	0.0019	0.02106659	0.0000	0.032
Megamonas	0.0003968	0.0007	0.00169057	0.0000	0.027
Oribacterium	8.84E-05	0.0006	0.00088919	0.0000	0.013
Pectobacterium	6.43E-05	0.0011	0.00067172	0.0153	0.048
Prevotella_1	0.00013616	0.0001	0.00070239	0.0000	0.010
Prevotella_2	0.00078099	0.0191	0.00842799	0.0176	0.000
Prevotella_6	0	0.0009	6.46E-05	0.0016	0.009
Prevotella_9	0.0104742	0.0035	0.03525487	0.0024	0.010
Ruminiclostridium_1	4.39E-05	0.0005	0.00020848	0.0009	0.034
Sedimentibacter	0.00033413	0.0000	0.00118022	0.0000	0.012
Syntrophomonas	0.00014302	0.0029	0.00068441	0.0025	0.006
vadinBC27_wastewater-sludge_group	0	0.0001	0.00023663	0.0059	0.009

[1] Post-hoc using Bonferroni corrected, only P<0.05 are shown

4.4.10. Association of the smoking habits with the gut microbiota in GD/GO patients compared to healthy controls

Smoking can alter the composition of the gut microbiota [441], therefore the previous model corrected for the smoking habits of both patients and healthy controls. However, cigarette smoking has long been considered a strong risk factor for GO, whose implications in the disease were explained in the introduction chapter (Chapter 1, par. 1.3.2.3). Therefore, association between smoking habits and gut microbiota composition was investigated in GD, GO and healthy controls individually. Amongst current, ex and non-smokers, 17 genera were differentially abundant in the healthy control group, 7 in GD and 21 in GO (Figure 4.12). None of the smoking-associated genera in GD patients showed similarities with those GD-associated genera, previously identified (Table 4.6). *Adlercreutzia*, *Faecalitealea*, *Gordonibacter* and *Prevotella* 7 genera showed an increased abundance in the ex-smoker group, with only the *Gordonibacter* spp. significantly different between ex and never smokers after correction (P=0.017). In contrast, in GO patients smoking habit associated genera *Bacteroides* and *Intestinibacter* were previously associated to GO status. *Bacteroides* spp., whose counts significantly decreased in GD and mild-GO compared to healthy controls (Table 4.7), showed a significant decrease in current smokers (mean 0.045) and ex-smokers (mean 0.042), compared to never smokers (mean 0.067) in GO patients (P=0.024), although not significant after correction. Amongst other differentially abundant genera not previously associated to GO status, *Clostriudium sensu stricto 1* spp. was increased in GO ex-smokers compared to GO never smokers (P=0.035), while *Faecalibacterium* spp. was decreased in ex-smokers compared to the never smokers (P=0.043) and *Peptoclostridium* spp. was increased in GO ex-smokers compared to both current (P=0.023) and never GO-smokers (P=0.014). None of the differentially abundant genera amongst smoking habits in GD and GO showed similarity with those reported in the control groups.

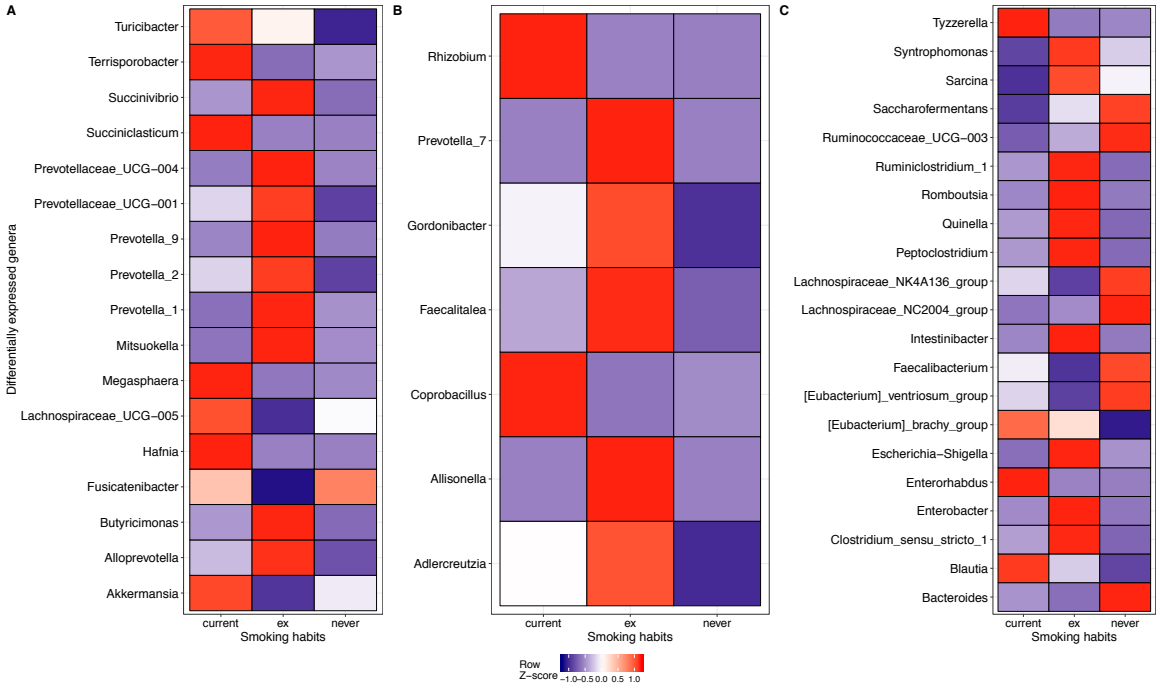

Figure 4.12 Smoking-habits-associated taxonomies in GD, GO or healthy controls. Only significant (P<0.05) genera were represented and the genus mean abundance in each group (current/ex/never smokers) was scaled according to the row Z-score in (**A**) healthy controls (7/2/28), (**B**) GD (10/9/40) and (**C**) GO patients (15/11/20). Blue to red colours indicate whether the genus is more or less abundant.

4.4.11. Anti-thyroid drug treatment effects on the gut microbiota

Medications have been shown to impact the gut microbiota composition [264]. Not only antibiotics, whose effects are directly targeted against bacteria, but also anti-human treatments, including the anti-thyroid drugs (ATD; i.e. carbimazole (CBZ), methimazole (MTZ), propylthiouracil (PTU) as described in Chapter 1 par. 1.1.2. The INDIGO study allowed the recruitment of patients within 6 weeks of ATD. Differences in the microbiota composition between untreated *vs*. treated GD (24 *vs*. 41, 8 not assessed) or GO (9 *vs*. 33, 19 not assessed) patients were observed. Only samples from patients whose treatment was clearly stated in the database have been included in the analysis.

Alpha diversity indices did not show differences in the composition of the gut microbiota between treated and untreated patients, either GD or GO (Figure 4.13A). Differences in the equitability index amongst treatments in GO patients were obtained from the mixed-effect linear model with nation of recruitment as a random effects (P=0.046, Figure 4.13B), with a decreased equitability in the untreated group. No clear separation between untreated and treated groups was showed in the NMDS based on the Bray-Curtis dissimilarity matrix (Figure 4.13C and D).

Within GD patients (Table 4.10), genera such as the *Eubacterium* (*nodatum group*), *Adlercreutzia*, *Akkermansia*, and *Candidatus soleaferrea* were enriched in the untreated group compared to both CBZ and MTZ. Other genera were differentially abundant either between untreated and CBZ or untreated and MTZ. Only *Gordonibacter* spp. was differentially abundant between CBZ and MTZ, being enriched in the CBZ-treated group. Within GO patients, 12 genera were differentially abundant amongst treatments (including the PTU) and without ATD (Table 4.11).

Differences in the taxonomic composition of clearly untreated patients (n=24 GD, n=11 GO) compared to healthy controls may give insights in the role of the gut microbiota in the onset of the disease. Although the number of patients was reduced from the observational cohort, especially the GO cases, five genera differentially abundant between GD/GO and healthy controls were identified (Table 4.12). Of those, *Akkermansia* and *Anaerotruncus* spp. were increased in the GD group compared to GO also after correction.

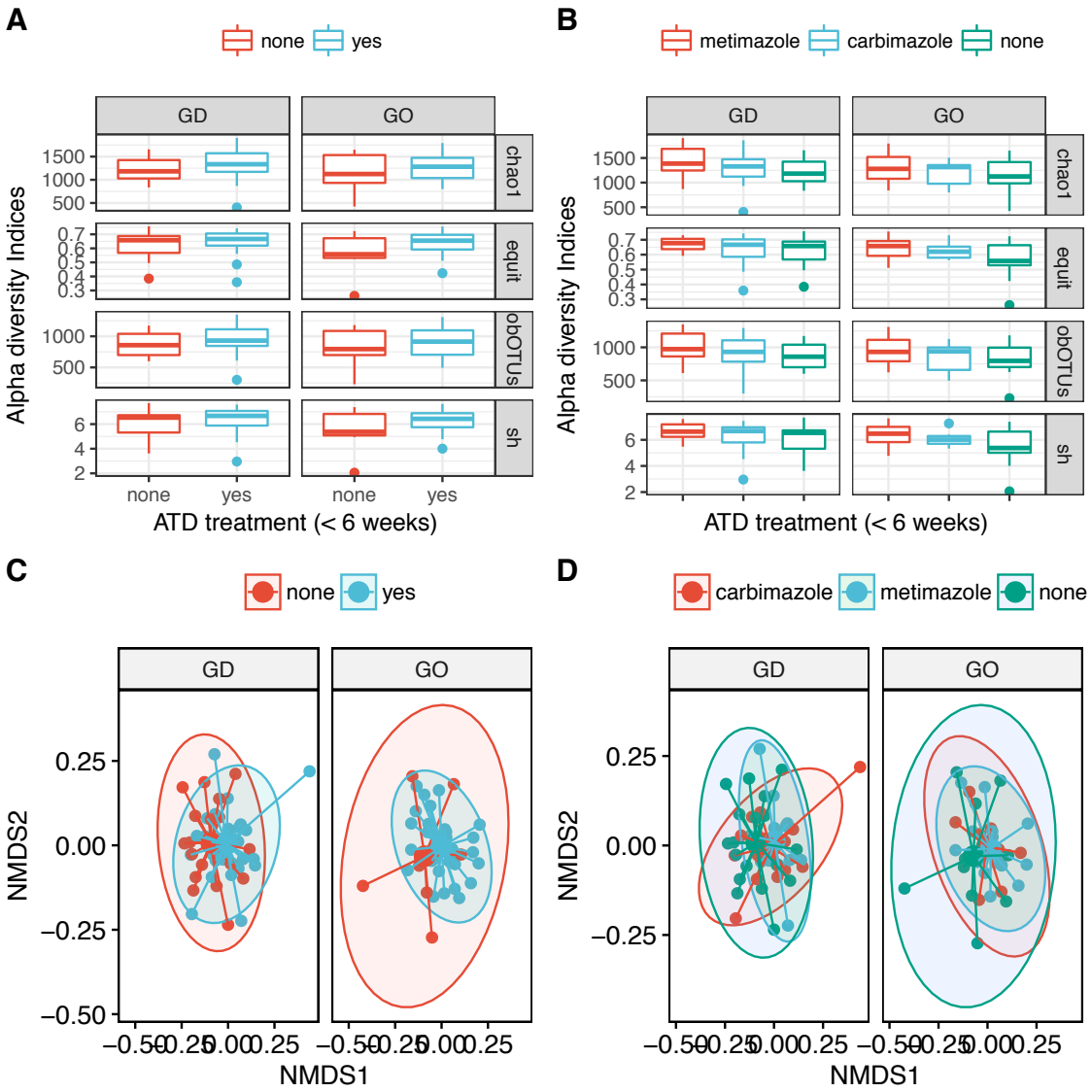

Figure 4.13. Diversity indices in untreated and ATD-treated patients.
Alpha diversity indices: equit, equitability; obOTUS, observed OTUs and sh, Shannon index in (**A**) treated *vs*. untreated GD or GO patients and (**B**) according to the type of treatment. Beta-diversity NMDS based on the Bray-Curtis dissimilarity matrix in (**C**) treated *vs*. untreated GD or GO patients and (D) according to the type of treatment. Levothyroxine treatment was excluded from the analysis, since accounting only 2 GO patients.

Table 4.10 Genera differentially abundant between untreated and ATD-treated GD patients.

Genera differentially abundant	Carbimazole[1] (n=23)	Metimazole[1] (n=16)	no ATD[1] (n=24)	P value[2]	PW[§]
[Eubacterium]_nodatum_group	0.00015	0.00027	0.00097	0.003	A,B
Acetanaerobacterium	0.00000	0.00000	0.00009	0.050	ns
Adlercreutzia	0.00054	0.00056	0.00112	0.012	A,B
Akkermansia	0.00062	0.00078	0.00159	0.002	A,B
Candidatus_Soleaferrea	0.00006	0.00010	0.00059	0.000	A,B
Christensenellaceae_R-7_group	0.02190	0.01433	0.02601	0.037	B
Coprobacillus	0.00035	0.00011	0.00075	0.043	B
Eggerthella	0.00037	0.00042	0.00098	0.046	ns
Enterococcus	0.00000	0.00068	0.00174	0.022	A
Faecalibacterium	0.08566	0.10393	0.06710	0.017	B
Family_XIII_AD3011_group	0.00253	0.00172	0.00382	0.031	ns
Gordonibacter	0.00063	0.00011	0.00097	0.010	B,C
Lachnospiraceae_NC2004_group	0.01072	0.01157	0.00826	0.038	ns
Lachnospiraceae_UCG-005	0.00619	0.00768	0.00470	0.029	B
Lysinibacillus	0.00000	0.00000	0.00035	0.023	ns
Paraprevotella	0.00000	0.00037	0.00000	0.005	ns
Quinella	0.00015	0.00000	0.00004	0.045	ns
Rhizobium	0.00000	0.00005	0.00031	0.016	ns
Romboutsia	0.00048	0.00006	0.00031	0.038	ns
Roseburia	0.03205	0.03909	0.02567	0.006	B
Shuttleworthia	0.00009	0.00006	0.00042	0.008	ns

[1]Mean values of each group. Standard deviations are included in Appendix 22. [2]P values from regression model, only P<0.05 are included. [§]Post-hoc Bonferroni-corrected P values. ns, not significant. A: no ATD *vs*. CBZ; B: no ATD *vs*. MTZ; C: CBZ *vs*. MTZ.

Table 4.11. Genera differentially abundant between untreated and ATD-treated GO patients.

Genera differentially abundant	CBZ[1] (n=8)	Levothyroxine[1] (n=2)	MTZ[1] (n=17)	no ATD[1] (n=11)	P value[2]
Actinomyces	0.0004	0.0010	0.0005	0.0030	0.009
Capnocytophaga	0.0000	0.0007	0.0001	0.0000	0.003
Clostridium_sensu_stricto_1	0.0073	0.0073	0.0045	0.0136	0.020
Erysipelotrichaceae_UCG-003	0.0022	0.0043	0.0041	0.0099	0.012
Erysipelotrichaceae_UCG-007	0.0000	0.0004	0.0000	0.0004	0.004
Granulicatella	0.0004	0.0012	0.0004	0.0017	0.046
Lachnospiraceae_NC2004_group	0.0097	0.0185	0.0129	0.0095	0.036
Peptococcus	0.0001	0.0030	0.0000	0.0001	0.000
Prevotella_7	0.0001	0.0023	0.0000	0.0000	0.000
Ruminococcaceae_V9D2013_group	0.0000	0.0000	0.0000	0.0002	0.039
Rummeliibacillus	0.0000	0.0004	0.0000	0.0000	0.000
Shuttleworthia	0.0000	0.0000	0.0002	0.0006	0.025

[1]Mean values of each group. Standard deviations are included in Appendix 23. [2]P values from regression model, only P<0.05 are included.

Table 4.12. Genera differentially abundant in untreated patients (n=24 GD, n=11 GO) compared to healthy controls (n=41).

Genera	control (mean)	control (std)	GD (mean)	GD (std)	GO (mean)	GO (std)	P value[1]	PW[2]
Akkermansia	0.0003	0.0004	0.0016	0.0009	0.0003	0.0004	0.001	GD-GO
Anaerosporobacter	0.0005	0.0007	0.0000	0.0000	0.0000	0.0000	0.001	ns
Anaerotruncus	0.0007	0.0010	0.0022	0.0016	0.0006	0.0009	0.046	GD-GO
Lachnospiraceae AC2044_group	0.0012	0.0003	0.0003	0.0004	0.0001	0.0002	0.002	ns
Mitsuokella	0.0005	0.0007	0.0000	0.0000	0.0002	0.0006	0.039	ns

[1]P values generated from the regression model, only genera with P<0.05 are shown. [2]Post-hoc Bonferroni correction. ns, not significant after correction.

4.4.12. Imputed metagenomic functions

Metagenomic functions were predicted from the filtered and normalized OTU table using the Tax4Fun R script using the KEGG database accounting for 6,480 KEGG orthologs (KOs) and 274 pathways. Amongst GD/GO and healthy controls, 51 pathways showed a differential abundance (Figure 4.14A). The majority of those pathways were enriched in the control group, while six pathways were particularly enriched in the GD group (i.e. 'Drug metabolism-cytochrome P450', 'chemical carcinogenesis, prion disease', 'complement and coagulation cascades', 'indole alkaloid biosynthesis' and 'clavulanic acid biosynthesis'), only one in the GO ('photosynthesis') and seven pathways were shared GD and GO compared to controls. After correction, 'ABC transporters' pathway was increased between GD and controls (P=0.01, Data not showed), as well as the 'bacterial invasion of epithelial cells' (P=0.025), the 'phosphotransferase system (PTS)' (P=0.18).

Dissecting for the ocular disease, 39 pathways showed a differential abundance (Figure 4.14B). According to the Euclidean distances, moderate-severe GO patients predicted pathways clustered more closely to that of healthy controls, respective to GD patient's microbiome and mild GO patients. Also from this analysis, the majority of the pathways differentially abundant were enriched in the control group. In contrast, mild GO group did shared some of the pathways increased in the GD group (no sign of ocular disease). Moderate-severe GO patients, instead, showed enrichment of some pathways, including the 'N-glycan biosynthesis' pathway, the 'glycosaminoglycan biosynthesis-chondroitin sulphate' pathway, although not retaining the significant threshold after correction (Data not showed).

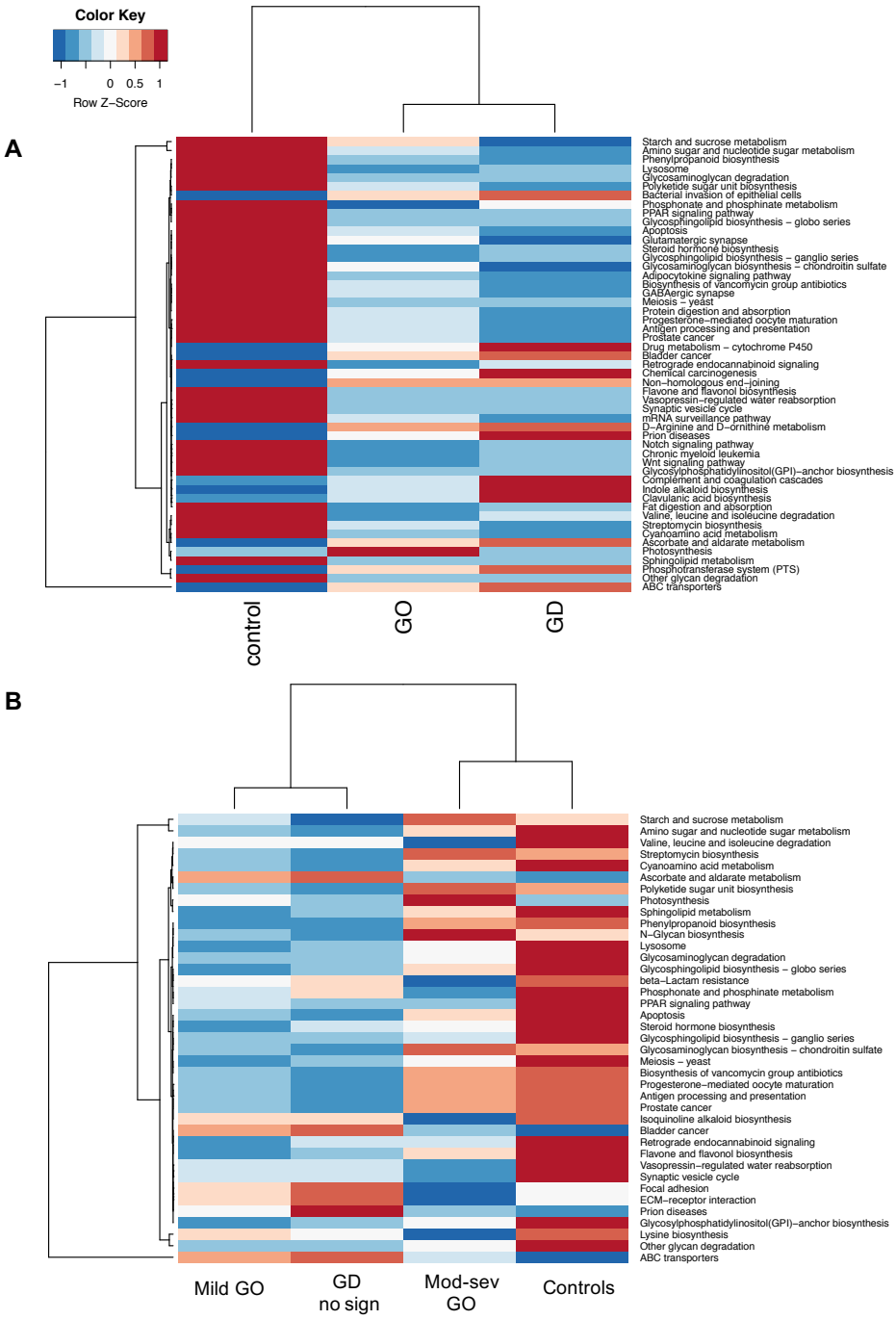

Figure 4.14. Imputed KEGG metagenomic pathways.
(**A**) Differentially abundant imputed metagenomic pathways amongst GD/GO and healthy controls or (**B**) amongst GO status. Only pathways with P value <0.05 from the regression model are shown. Averaged abundances of each pathway in each group were scaled according to the row Z-score, according to the R function 'heatmap". Dendrograms are based on Euclidean distances.

Out of the around 6,500 KEGG's orthologs or molecular functions imputed, 1,154 were differentially abundant between GD, GO and healthy controls (Data not showed). The principal component analysis (PCA) did not show a clear separation of the groups based on the KOs, with 31.3% and 18.4% variances explained by the first two components, respectively (Figure 4.15A). Top-10 variables were identified in the biplot and amongst them, only three KOs showed significant changes between GD and control: chorismate mutase (P=0.049), hypothetical protein (P=0.029) and osmotically inducible protein OsmC (P=0.036).

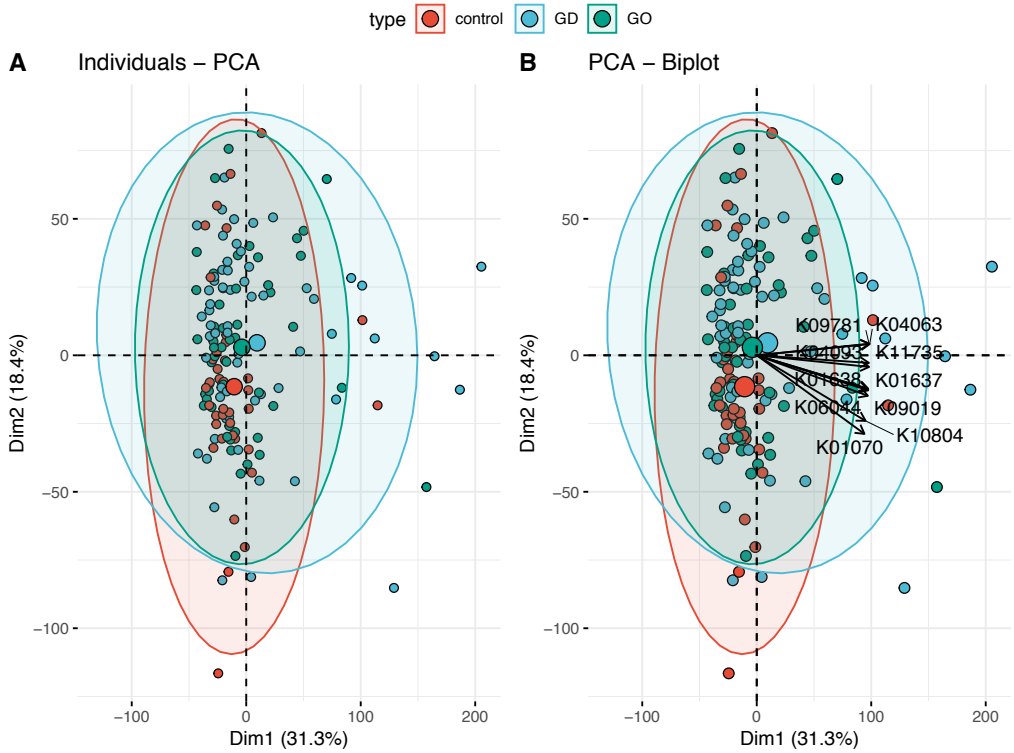

Figure 4.15. Principal component analysis and biplot of the KEGG orthologs. (**A**) PCA plot showing the coordinates of individuals based on the GD/GO and control groups. Ellipses represents the concentration of the points with 0.95 confidence. (**B**) Biplot showing the top-10 variables with highest Cos2 or those with the highest quality of representation of individuals on the PCA.

4.4.13. GD to GO transition

Until the completion of the study, two patients enrolled as GD patients later developed GO at Cardiff University Hospital (UK), referred here to as "GD to GO transition". In particular, patient 1004, included in the study at her first visit in 03/10/2014 as untreated and first diagnosis of GD, developed mild GO (CAS2) as euthyroid after 2 months (12/12/2014). Patient 1013 has been enrolled as a relapsed GD in 31/10/2014 and developed GO (CAS3) as euthyroid after about 3 months (30/01/2015).

As observed in the paragraphs before, the *Bacteroides* spp. counts dramatically decreased during the GD to GO transition (Figure 4.16 A and B, left) and slightly increased in a third timepoint, although not reaching the same count number as in the GD status (Figure 4.16, right graph). Also, some other genera previously associated to GO status (see Table and Figure 4.7) were observed in the within-patient GD-to-GO transition, e.g. increased *Bifidobacterium* spp, *Lachnospiraceae* spp. and *Clostridiaceae* counts. Increased *Roseburia* spp., previously associated to a moderate-severe GO, was significantly increased in patients 1013, whose GO was considered to as more severe.

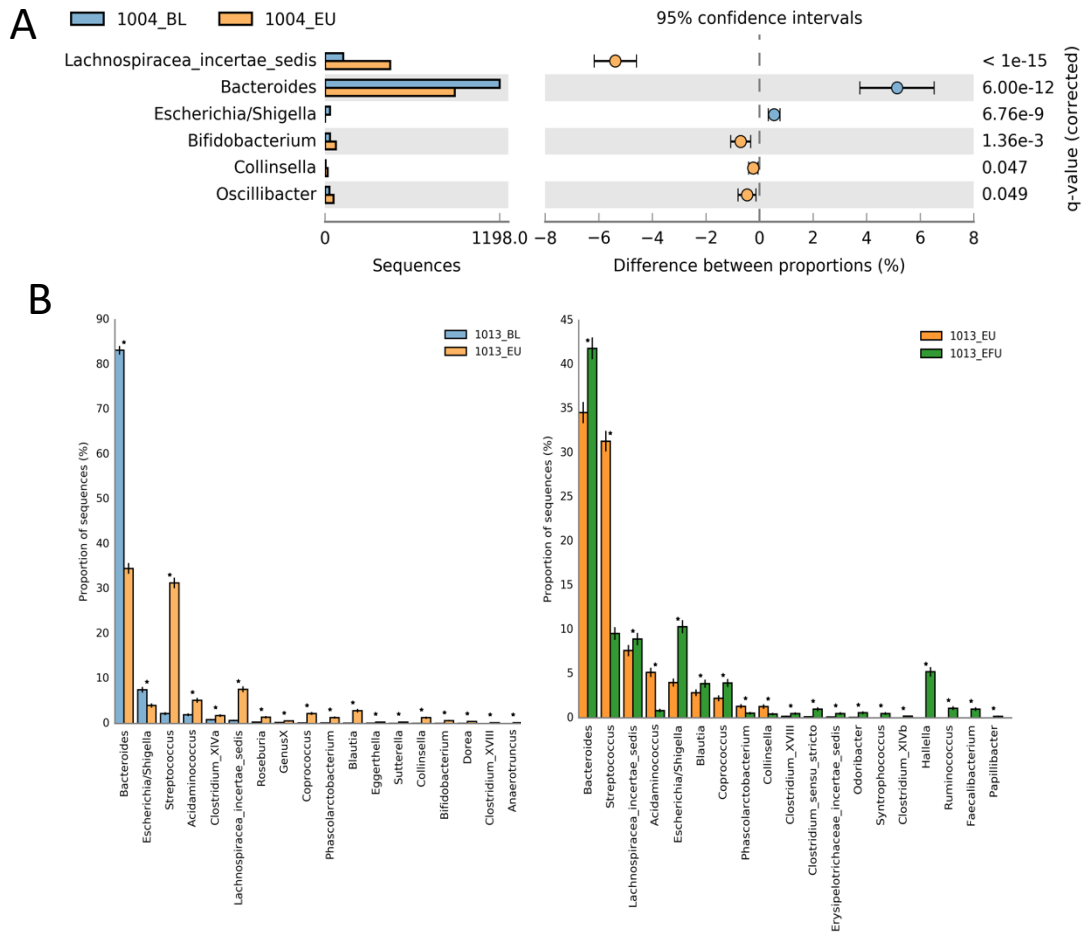

Figure 4.16. Analysis of the gut microbiota of patients undergoing "GD to GO transition".

Extended bar-plots generated with STAMP testing differences at the genus level between GD and GO, individually. (**A**) Differences at genus level between 1004-BL (GD) and 1004-EU (GO). (**B**) Bar-plots representing difference at genus level of patient 1013-BL (GD) to 1013-EU (GO) (left) and from the 1013-EU (GO) to 1013-EFU (stable GO). Two samples-test was performed in STAMP using the G-test with Yates' correction and Fisher's with 95% confidence interval. Only genera with P value<0.05 were shown.

4.5. DISCUSSION

The present chapter aimed at comparing the gut microbiome of mostly European GD and GO patients with that of healthy controls in a cross-sectional study, with specific regards to differences in the thyroid status (i.e. hyperthyroid vs. euthyroid) and in the eye-disease severity (i.e. mild and moderate-severe, as assessed through EUGOGO guidelines [54]). In the framework of the EU-funded INDIGO project, patients and matched healthy controls were enrolled from four European countries (Italy, Germany, UK and Belgium) between 2014 and 2016. Faecal DNAs were sequenced in two different runs (one in late 2014 and the second one in August 2017), with some samples from the first sequencing batch being replicated in the second one. We are confident that through the same sequencing processing and a closed OTU-picking approach we did eliminated possible sequencing-batch effects, as there were no differences between inter and intra-batch replicates. We are also fully aware that the gut microbiota varies across countries. I did not observe differences in the composition of the gut microbiota in terms of alpha and beta-diversity indices across countries, while some differences were observed at the taxonomic level. The prevalence of the *Firmicutes*-prevalent and the *Bacteroides*-prevalent enterotypes, also, suggested a microbiota composition typical of the Americans and Western European countries, consuming a Western diet [442].

4.5.1. Reduction of *Bacteroides* spp. as a bacterial biomarker for GD/GO

Similarly to what was observed in the animal model described in the previous chapters, GD and GO patients showed a decrease of the *Bacteroidetes* phylum and of the *Bacteroides* genus compared to that of the healthy controls population (HC). Interestingly, no geographical differences were observed in *Bacteroidetes* phylum and *Bacteroides* genus counts. Moreover, when looking at the thyroid status (i.e. hyperthyroid, euthyroid GD/GO patients and euthyroid HC), the decrease of *Bacteroides* spp. occurred in hyperthyroid patients compared to HC (which were euthyroid by definition of inclusion). Euthyroid patients showed a still decreased *Bacteroides* spp. counts compared to that of euthyroid-HC, while an increased *Bacteroides* counts were observed in few hypothyroid patients (possibly due to the anti-thyroid medication intake and thyroid hormones fluctuations). *Bacteroides* spp. was the only genus showing significant correlations with biochemical features such as thyroid-stimulating hormone (TSH) and the thyroxine hormone levels (fT4). In particular, the higher the TSH levels, the higher was the *Bacteroides* counts; and the higher the fT4, the lower was the *Bacteroides* counts, significantly occurring in hyperthyroid patients.

Along with the reduction in *Bacteroides* spp., a consequently increase of the *Firmicutes:Bacteroidetes* (F:B) ratio was also reported in GD/GO compared to HC. As the F:B ratio was previously associated with weight-gain and obesity [223], one may argue that the increase of F:B ratio in GD/GO patients was due to the weight loss, often occurring in the active form of GD/GO. To our knowledge, at the present, only one study specifically investigated the differences in the gut microbiota in hyperthyroid patients, although it was not clear if the hyperthyroidism had an autoimmune basis [443]. No significant associations with F:B ratio and weight-loss were reported.

In line with our findings*, Bacteroides* spp. seemed reduced in a Chinese cohort of GD patients compared to HC; although not reaching the significant threshold [439]. The study, however, did not discriminate between GD and GO patients, or between hyperthyroid and euthyroid patients. In Hashimoto's thyroiditis (HT) patients, a reduction in the phylum *Bacteroidetes* was reported in both hypothyroid [444] and euthyroid HT patients compared to euthyroid HC [438], while genus *Bacteroides* increased in hypothyroid patients only [444]. Interestingly, a recent meta-analysis of 2,700 individuals from the TwinsUK cohort suggested a correlation between the gut microbiota of hyperthyroid and hypothyroid patients (not necessarily with the autoimmune form) [445].

Bacteroides spp. was also associated to other autoimmune conditions, such as the type 1 diabetes (T1D). *Bacteroides vulgatus* and, in particular, *Bacteroides dorei* were found increased in a Finnish cohort of children at high risk of T1D, few months before the seroconversion [446].

For which the severity of the eye disease is concerned (i.e. no sign, mild and moderate-severe compared to HC), *Bacteroides* spp. showed a reduction between the GD with no sign of eye disease and the mild form of GO compared to HC. A very recent work showed instead an increased *Bacteroidetes* phylum in a GO Chinese cohort but a decreased *Bacteroides massiliensis* [447].

4.5.2. Other disease-associated gut microbiota taxonomies

Other differential abundant taxonomies were identified between GD, GO (both mild or moderate-severe forms) and HC. Opposite to the decrease of *Bacteroides* spp., an increase of *Fusicatenibacter* genus was reported in GD and GO compared to HC an in hyperthyroid patients compared to the euthyroid controls. Zhao and collaborators reported an increased *Fusicatenibacter* spp. in euthyroid HT patients [438]. The *Fusicatenibacter saccharivorans*, a single species of the *Clostridium* XIVa, was found decreased in the faecal samples of ulcerative colitis (UC-IBD) patients [448].

In their recent work, Ishaq and collaborators found a significant increase of *Prevotella* 9 and *Haemophilus* and a decrease of *Alistipes* and *Faecalibacterium* genera in GD patients compared to HC. Despite we used a different study design, sequencing primers and we enrolled a cohort on a prevalent western diet, we confirmed the decreased *Alistipes* spp. in GD and mild GO compared to HC and a decreased *Prevotella* 9, although occurring only in female GO patients compared to male GO patients. Similarly to *Bacteroides* spp., also *Alistipes* spp. are a butyrate-producing genus [439].

While *Bacteroides* spp. and *Fusicatenibacter* spp. were differentially abundant in GD (no sign of eye disease) and in mild GO, they did not show associations with the moderate-severe form of GO. In fact, the gut microbiota of moderate-severe patients showed fewer alterations, which included the reduction of *Ruminococcaceae*, *Peptoclostridium* and *Clostridium sensu stricto* genera and the increase of the *Roseburia* genus compared to both HC and GD. Interestingly, the increase of such a bacterial genus is often associated to a more healthy gut microbiota. A decrease of the butyrate-producing *Roseburia* spp. (in particular *Roseburia hominis*) was, in fact, previously associated to other autoimmune conditions, such as the ulcerative colitis [449], and also the acute uveitis, a rare and severe inflammation of the middle layer of the eye, potentially leading to blindness [450]. In our moderate-severe GO cohort, the increase of the butyrate-producing *Roseburia* spp. was also accompanied by an increased amount of butyrate, propionate and acetate SCFAs measured in their faecal water through NMR (Marchesi JR, personal communication). At this stage of the disease, patients may have experienced disease relapses, thyroid hormone fluctuations and may have undergone several anti-thyroid drug (ATD) treatments. Interestingly, *Roseburia* spp. increased in GD/GO patients under treatment with methimazole (within 6 weeks of commencing the medication intake) compared to untreated patients. Also, treatments with glucocorticosteroids and steroid bolus (one of the possible lines of treatment for GO, as described in Chapter 1 par. 1.1.3) may have increased the Treg milieu [451, 452]. PMBCs from the majority of moderate-severe GO patients showed increased Tregs moiety when challenged in vitro with a Tregs-inducer molecule (i.e. rabbit anti-T lymphocyte globulin) [453]. Whether such an increase was due to or favoured by the increase of butyrate production in the gut has to be still proven.

Bifidobacterium counts dropped in moderate-severe compared to mild GO and to GD patients, as it showed a significant increase in mild GO compared to HC. Benvenga and colleagues demonstrated *in silico* possible sequence homologies between *Bifidobacterium* strains epitopes and thyroid auto-antigens, in particular TPO and Tg [454]. This work supported also previous findings by Kiseleva and collaborators [455]. At

the present, however, there is no suggestion of a possible molecular mimicry between *Bifidobacterium* spp. antigens and the TSHR.

I reported an overlap of some differentially abundant taxonomies between disease diagnosis (GD, GO and HC) and the thyroid status (hypothyroid and euthyroid). Interestingly, not all of them were present in both analysis, suggesting that other factors may have contributed to such differences, including the (auto)immune response, as also observed in the miRNA and proteins profiles [440]. In support to this findings, *Turicibacter* and *Ruminococcaceae* genera that were significantly correlated with anti-TSHR antibodies were not significantly associated to the thyroid status. On the contrary, they showed a different pattern of correlation associated to the disease diagnosis: negative correlation with TRAK, TRAB and cAMP levels in GD patients, while positive correlations with TRAK and cAMP in GO patients. Such a different correlation might be due to a higher anti-TSHR antibodies titres often occurring in GO patients, as we previously observed [440].

4.5.3. Effects of gender, ATD medications and smoking habits on GD/GO gut microbiota

Many autoimmune diseases, including GD, present a gender prevalence. Gender-related hormones, especially after pregnancy, in fact, constitute a risk factor for the development of such diseases. Moreover, it became clear that gender-related and sex hormones-related differences are also recapitulated in the gut microbiota [432]. According to Fransen et al. [456], microbiota-independent but gender-related differences in the immune response (i.e. interferon gamma signalling higher in the gut of female germ-free mice) may favour a specific gender-related gut microbiota composition, which in turns, may predispose gender-differences in the immune response, including the susceptibility for certain autoimmune conditions. A most striking example of this concept was described in the work of Markle and collaborators on the NOD mice [121]]. Despite a gender-related gut microbiota composition, a two-signal model, in which both the microbiota and the hormones act together in an additive manner, seemed the preferred mechanism for conferring protection from T1D development, compared to a linear model (i.e. microbiota directly regulated the hormones and *vice versa*) [434].

Although our differential abundance analysis corrected for gender-biases as a covariate, I also focussed on differences in the gut microbiota between females and males in either GD or GO groups. None of these differentially abundant genera was previously associated to either the disease diagnosis or the eye-disease severity. Both GD and GO male patients showed an increase of *Prevotellae* genera, similarly to what observed by Mueller and collaborators in four different European countries [457]. It would be

interesting to study the interplay between immune response, sex-hormones and gut microbiota in the previously described GO mouse model.

Smoking habits (i.e. current, ex and never smokers) was also considered to as a covariate, since it affects the composition of the gut microbiota. In a large cohort of Korean females and males, an increased *Bacteroidetes* phylum and a reduced *Proteobacteria* and *Firmicutes*, along with the *Firmicutes:Bacteroidetes* ratio were reported between current and never smokers [458]. Interestingly, no differences in the taxonomic composition were observed between ex and never smokers. The cessation of the smoking habits led to a decrease in *Bacteroidetes* and to an increase of *Firmicutes* and *Actinobacteria* phyla in individuals sampled before and at four and eight weeks after the smoking cessation [459].

Therefore, smoking habits can be considered as an environmental factor modulating the gut microbiota and possibly the immune response of an individual, even after the cessation. Cigarette smoking was also strongly correlated to the risk of developing GO [156]. In our 'omics paper, in fact, we reported a prevalence of current smokers in GD/GO *vs*. controls (15:1) and in GO *vs*. GD (9:6) [440]. However, no smoking-associated biomarkers were detected. Differently from the 'omics study, however, we included a higher number of never smokers patients. I specifically looked at smoking habits differences in the gut microbiota of either controls, GD and GO patients, individually. Interestingly, *Bacteroides* spp. counts, whose decrease was associated to GD/GO, decreased in current GO-smokers and further decreased in ex-GO smokers, similarly to what observed in [459].

Medications such as antibiotics have a profound effect on the gut microbiota composition. It has recently been showed that also common prescriptions such as proton-pump inhibitors (PPI) and antithyroid (ATD) medications may influence such a composition. In the recent TwinsUK meta-analysis [445], hyperthyroidism was associated with thyroxine/levothyroxine usage but also to PPI and anticholinergic. While positive and negative associations with the gut microbiota and thyroxine/levothyroxine were also described. More specifically, the effects of ATD carbimazole (CBZ), methimazole (MTZ), propylthiouracil (PTU) and levothyroxine were tested on the gut microbiota in vitro [264]. Interestingly, Maier et al [264] reported none or very few anti-commensal activity upon CBZ or MTZ incubation, while I observed prevalently a decreased abundances of genera in the CBZ/MTZ groups compared to untreated GD or GO patients.

4.5.4. Prediction of GD/GO diagnosis based on the gut microbiota composition

One of the most attractive goals when performing 'omics approaches is to obtain a panel of biomarkers robust enough to be used for diagnosis purposes and/or prediction of the disease progression, towards the so called "individualized" or "precision medicine". For a similar reason, we described a panel of combined circulating miRNAs and proteins discriminating between GD, GO and HC [440]. However, differences exist in modelling the outcome *vs*. modelling the progression of the disease, with the insurgence of possible selection bias afflicting the results of the analysis, as proposed in [460].

I employed the Random Forests [461] classification algorithm to either predict the diagnosis (i.e. GD *vs*. GO *vs*. HC) or the eye-disease status (i.e. no sign *vs*. mild *vs*. moderate-severe) using the genus-level taxonomy, although I'm fully aware that different approaches are also available [462-464] Random Forest allows to run dedicated models including also important covariates such as age and gender, amongst others. Loomba and collaborators obtained a panel of 37 bacterial species, plus some covariates (e.g. age, BMI and Shannon diversity) capable of discriminating mild/moderate non-alcoholic fatty liver disease (NAFLD) patients from patients with a more advanced fibrosis, with a nearly 94% accuracy of the RF classification model [465].

When predicting the diagnosis the overall accuracy of the model was nearly 60%. The highest prediction rate occurred in the healthy control group (97.3% per-class accuracy) and in the GD patients (71.2% per-class accuracy). Prediction of the GO samples was less accurate, accounting only the 16% per-class accuracy. When stratifying for the severity of the eye-disease the overall accuracy of the model increased to nearly 62%; however, the majority of the mild GO samples and all the moderate-severe GO were predicted to as GD, showing a per-class accuracy of 8.4% and 0%, respectively. It appears that those classifications were driven preferably by the thyroid status (which was also the first important variable identified), rather than the composition of the gut microbiota by itself. A higher classification accuracy can be potentially obtained in cases *vs*. controls analysis.

Shi et al. reported a nearly 75% accuracy of the prediction model for which HC and GO samples were concerned, although not stratifying for the severity of the eye-disease [447].

Also, a different scenario for the classification of the GO samples was obtained using the circulating miRNA and proteins. The Lasso-penalized logistic regression on the combined miRNA and proteins dataset revealed an accuracy of 93% for the GO samples, compared to a 78% for GD and 86% for HC, respectively [440].

4.5.5. Insights from the predicted metagenomic functions

Prediction of the metagenomic pathways from the 16S rRNA gene sequencing may provide some insights about the functional role of the microbiome, despite the limitations of this technique addressed later in Chapter 6.

Top-10 most abundant predicted pathways (Appendix 24) amongst disease diagnosis (HC, GD and GO) and eye-disease status (no sign, mild and moderate-severe GO) included the: “Arrhythmogenic right ventricular cardiomyopathy (ARVC)”, “Dilated cardiomyopathy (DCM)” and the “Regulation of actin cytoskeleton”. Interestingly, those three pathways were also identified in the pathway analysis using combined miRNA and proteins differentially abundant in GD, GO and HC [440]. Cardio-circulatory pathways can be imputed to the strain imposed by the hyperthyroidism and the thyroid hormones; but also, due to the expression of TSHR in the heart tissue, a similar autoimmune response may lead to both GD/GO and cardiomyopathy [466]. A link between the gut microbiota and cardiovascular diseases, including heart failure, was also proposed [467]. Also the “Complement and coagulation cascade” and the “ECM-receptor interaction” pathways which were increased in GD and GD/mild GO patients, respectively, were also identified in circulating proteins only in [440]. Interestingly, the NF-kB signalling pathway identified from the metagenomic function prediction was previously associated the hyperthyroidism and thyroid-eye disease [468].

The majority of differentially abundant pathways were enriched in the healthy control group, including “PPAR signalling cascade” and the “Antigen processing and presentation” pathways. The “Bacterial invasion of epithelial cells” was enriched in the GD group. The same pathway was also identified in [440], which presumably was due to the overexpression of Zonulin, responsible for the regulation of the intestinal-tight junctions [469]. Impairment of the gut permeability can favour bacterial translocation and activation of the immune system via GALT. Coeliac disease is also characterized by bacterial translocation due to an impaired gut permeability [469] and the cross-reaction between thyroid autoimmunity and coeliac disease in this cohort of patients is under investigation (Covelli D., personal communication).

The “glycosaminoglycan biosynthesis- chondroitin sulphate” and the “N-glycan biosynthesis” pathways were increased in moderate-severe GO patients. As described in Chapter 1 par. 1.1.3, chondroitin sulphate (CS) is a major component of the glycosaminoglycans (GAGs) deposition occurring in the orbital tissues. Interestingly, some bacterial strains including *E.coli* O5:K4:H4 and *Pasturella multocida* are capable of chondroitin sulphate synthesis which have been used for biotechnological purposes as reviewed in [470]. A link between the gut and the CS supplementation in osteoarthritis

was proposed. In particular, the concomitant presence of *Akkermansia muciniphila* upon CS supplementation seems to ameliorate the osteoarthritis via the induction of anti-inflammatory markers, while its absence seems to aggravates the symptoms [471]. It is interesting to note that *Akkermansia* spp. was increased in untreated GD patients with no sign of eye-disease *vs*. untreated GD patients and it was increased in the antibiotic-treated GO mouse model, which did not show any signs of eye-disease (Chapter 3 par. 3.4.1), although the specific role of the *Akkermansia muciniphila* in protecting from CS-deposition in the orbits has still to be proved. Regarding the N-glycosylation, both anti-TSHR autoantibodies (both IgG and IgG3) and the TSHR auto-antigen are heavily N-glycosylated. Also, bacterial antigens of both commensals and pathogenic bacteria (i.e. flagellin) can be N-glycosylated [472]. For the theory of the molecular mimicry, the glycosylation moieties can play a role in the outcome of an autoimmune response. A glycosylation-mediated molecular mimicry between bacterial antigens and host sialyloglycans may secure the evasion from the immune surveillance [473]. Also, the Guillaume-Barrè syndrome, an acute form of paralysis usually occurring after infection with the foodborne *Campylobacter jejuni*, is caused by a glycosylation mimicry between the *C. jejuni* lipooligosaccharide and the human GM1 ganglioside, which lead the production of anti-GM1 autoantibodies [474]. A recent theory suggested the existence of a specific glycosylation pattern in antibody classes and subclasses for each autoimmune condition ("*The altered glycan theory of Autoimmunity*" [475]).

4.6. CHAPTER CONCLUSIONS

In summary, *Bacteroides* spp. was consistently reduced in GD and mild GO patients and showed association with hyperthyroid status and risk factors such as the smoking habits. Similarly, a panel of bacterial biomarkers was identified and may serve as a supporting tool for clinicians, although not indicative of the eye-disease severity. Predicted metagenomic functions are in line with GD/GO disease hallmarks (e.g. CS-glycosaminoglycan and N-glycans biosynthesis) and the immune response (e.g. complement cascade, NF-kB signalling), and suggested a broad role of the gut microbiota in sustaining the thyroid autoimmunity, although further studies are needed to deepen such interaction.

The present chapter showed the GD/GO-associated microbiome perturbations at the enrolment phase in the cross-sectional study. The thyroid hormones fluctuations under ATD therapy may have a further impact on the gut microbiota composition, which may have, in turn, long-term effects protecting for example from disease relapses. We hypothesized whether the supplementation with beneficial bacteria (probiotics) could

have prevented such fluctuations and could have attenuated possible changes in the gut microbiota. The next chapter, in fact, describes the gut microbiota of GD/GO patients being treated with anti-thyroid medication (i.e. carbimazole or methimazole) in presence of either probiotics or placebo in a single centre, double-blind, placebo-controlled longitudinal trial.

5. Chapter 5

Gut microbiota of GD/GO patients receiving a probiotic *consortium*: a pilot interventional trial

Acknowledgments:

Dr. Mario Salvi (MS), Dr. Giuseppe Colucci (GC) and Dr. Danila Covelli (DC) at the University of Milan for trial design, patients recruitment, clinical evaluation and sample collection.

Dr. Sue Plummer (SP), Dr. Iveta Garaiova (IG), Dr. Daryn Michael (DM) and Cultech Ltd. for Lab4® production and randomisation.

5.1. INTRODUCTION

The gut microbiota composition is generally stable during the lifespan of an adult, unless perturbed by diet (e.g. high-fat diet), surgery and/or medications (e.g. antibiotics). As shown in Chapter 3, however, there are approaches that may modulate the gut microbiota composition, even if in a transient manner, to confer beneficial effects to the host.

An increasingly common and safe approach to microbiota manipulation in humans is constituted by the use of probiotics, which are defined as *"live microorganisms that, when administered in adequate amounts, confer a health benefit on the host"* [345]. The definition itself includes fundamental requirements for a probiotics claim, such as: i) viable bacteria surviving the stomach acidic environment and bile digestion and capable of reaching alive the target site, ii) administered in an adequate dose (i.e. at a minimum of $1x10^9$ CFU/day according to the Italian legislation[6]), to iii) exert beneficial effects for the host health, such as the improvement of gut health and of the immune system [345].

Bacterial species within the *Lactobacillus* (i.e. *L. acidophilus, L. plantarum, L. reuteri, L. gasseri, L. rhamnosus, L. murinus*) and *Bifidobacterium* (i.e. *B. breve, B. bifidum, B. animalis*) genera are the most used probiotics, administered either alone or in *consortia* (multi-strain probiotics). However, other bacterial species and strains such as *Streptococcus salivarius*, non-pathogenic *Escherichia coli* Nissle 1917*, Pediococcus* and *Lactococcus* spp. [476] or the yeast *Saccharomyces boulardii* [477] have been identified and used.

Mechanisms and exerted beneficial effects can be either commonly shared through different probiotics species ("core benefits" as defined by [345]) or be more strain-specific. Adhesion to the intestinal mucosa is one key feature showed by many probiotics. In particular, mucus adhesion of lactic-acid producing bacteria (LAB), is promoted by a series of surface proteins (e.g. adhesins or the *L. reuteri* mucus-binding protein [478]), as well as the lipoteichoic acid (LTA). By adhering to the mucus layer, probiotic bacteria may modulate mucin production [479, 480] , although it may not directly happen *in vivo*. HT29 colorectal adenocarcinoma cell line showed increased expression of mucin genes (i.e. MUC2, MUC3 and MUC5AC, but not MUC1) when exposed *in vitro* to VSL#3 probiotic *consortium* (a commercially-available poly-biotic including 6 *Lactobacillus* strains, 3 *Bifidobacterium* strains and the *Streptococcus*

[6] Ministero della Salute, 2013. Direzione generale per l'igiene e la sicurezza degli alimenti e la nutrizione – Ufficio 4. "Linee guida su probiotici e prebiotici". Revisione Marzo 2018. Access from: http://www.salute.gov.it

salivarius subsp. *Thermophilus*) [481]. When administered *in vivo*, VSL#3 significantly increased the mucin production via the over-expression of MUC2 in wild-type rats [482], but failed to increase the mucus layer or its thickness in control dextran-sodium sulphate (DSS) treated mice, as an animal model of ulcerative colitis [483].

Probiotics have also shown improvement of the intestinal epithelial barrier through the modulation of tight junction proteins, as reviewed in [294]. VSL#3 probiotic *consortium* improved the gut epithelial barrier condition and increased tightunction proteins via the p38 and ERK signalling pathways, as shown both in HT29 cells and in an *in vivo* model of induced colitis [484]. Increased mucus layer and improved tight-junctions may prevent pathogen adhesion and translocation through the intestinal epithelial barrier, also of food antigens causing possible sensitization.

Such a prevention is also exerted via the modification of the environment. Secretion of lactic and acetic acids secretion by LABs, in fact, tends to lower the intracellular pH when internalized, inhibiting the growth of Gram-negative bacteria. The secretion of hydrogen peroxide (H_2O_2) by LAB species (including different strains of *L. johnsonii* and one strain of *L. gasseri*) was also proposed to selectively kill pathogens, at least *in vitro* [485]. Moreover, LAB strains, including bacteria and *Archaea*, are able to secrete antimicrobial peptides, called bacteriocins, that selectively cause the death of a narrow spectrum of bacterial strains, including pathogens (e.g. *Listeria monocytogenes* [486]). In contrast to antibiotics, in fact, targets of bacteriocins are usually restricted to closely related strains (e.g. Gram-positive strains against Gram-positive bacterial strains), as reviewed in [487], while mechanisms of actions generally involve inhibition of the synthesis of the bacterial cell wall and pores formation. The most important LAB-produced bacteriocins includes nisin from *Lactococcus lactis*, lactacin B from *L. acidophilus*, Lactacin F from *L. johnsonii* and different plantaricins from *L. plantarum* spp., as reviewed in [487]. Bifidobacteria-produced bacteriocins includes, amongst others, bifidocin B, secreted by *B. bifidum* NCFB 1454 [488].

Besides organic acids and antimicrobial peptides, probiotics also secrete short-chain fatty-acids (SCFAs, Appendix 25), conferring a range of beneficial effects to the intestinal epithelium. *Lactobacillus* spp. only produce lactate, which can be converted to butyrate by butyrate-producing colonic-residing bacteria such as *Roseburia intestinalis*, *Eubacterium rectale* and *Faecalibacterium prausnitzii* [489]. Bifidobacteria instead produce SCFA from fermentation, whose end-products depend on carbohydrate availability: acetate and lactate are, in fact, produced in excess of carbohydrate moieties, while acetate and formate occur upon carbohydrate-restriction [490]. Supplementations with carbohydrates not digestible by the host (e.g. inulin or fructo-oligosaccharide, FOS),

or so called “prebiotics”, can favour the growth of certain bacteria and push towards the production of certain SCFA, especially when administered with probiotics (“synbiotics”).

Probiotic bacteria themselves and their bio-products closely interact with immune system cells residing on the gut epithelium (e.g. dendritic cells). Such interactions reduce the pro-inflammatory response. Levels of TGF-β and anti-inflammatory IL-10 were increased in PBMCs isolated from a cohort of healthy adult volunteers after 12-week intake of Lab4 (two strains *L. acidophilus*, *B. lactis* and *B. bifidum*), plus FOS [491]. On the contrary, decreased levels of IL-6 and IL-1β were shown when those PBMCs were challenged with LPS *ex-vivo.* As explained in Chapter 1 par. 1.2.2, TGF-β is the key regulator of *Foxp3* expression leading to differentiation intoregulatory T-cells (Tregs). Probiotics have proved to trigger a Tregs response, at the expenses of a more pro-inflammatory Th1. As extensively reviewed in [108], a numbers of probiotics bacteria, either as a single species (i.e. *L. casei, L. rhamnosus, B. longum* etc) or in *consortium* (e.g. VSL#3) were shown to increase Foxp3+ Tregs, TGF-β, along with the reduction of pro-inflammatory cytokines. Also a role of prebiotics in inducing a Treg response has been proposed.

Immunomodulatory effects of a probiotic administration, and possibly related beneficial effects, were also investigated in a range of inflammatory diseases both organ-related or more systemic, both using animal models and in randomized controlled trials in humans. Probiotics supplementation in irritable bowel syndrome (IBS), which is characterized by chronic abdominal pain, altered bowel motility (diarrhoea or constipation) and by an altered gut microbiota, induced differing responses [492, 493], ranging from no or weak improvement of some disease symptoms (i.e. bloating or flatulence scoring) to a significant improvement of the global severity score (GSS). Lab4® *consortium* administered for 8 weeks to active IBS volunteers provided an increase in GSS, quality of life along with reduction of pain compared to the placebo group [494]. From a recent meta-analysis focussing on the use of probiotics supplementation in IBD (including ulcerative colitis and Crohn's disease) emerged a general improvement of some related symptoms, occurring either in CD or UC or both, depending on the type of probiotics used. Amongst others, VSL#3 was also proved to be safe when used in combination of corticosteroids therapy [495] and was proposed to be efficient in reducing post-surgery CD recurrence [496]. Probiotics and synbiotics supplementations were also assessed at various stages of colorectal cancer management (i.e. when initiating anti-cancer therapy, undergoing surgery or post-surgery etc.), as reviewed in [497] Although evidence was heterogeneous, reduction of post-surgery or therapy-based complications (i.e. diarrhoea) were reported, also suggesting a favourable role in cancer prevention. Prevention of the necrotising enterocolitis (NEC, caused by severe inflammation upon feeding in premature babies, often requiring bowel resection and short-bowel syndrome

amongst other complications) was more successful following probiotics administration [498-500].

Probiotics effects in ameliorating autoimmune diseases (either systemic or not gut related) were also evaluated. A reduced incidence and severity of the multiple sclerosis induced animal model (EAE) were observed upon probiotics administration, as described in Chapter 3 par.. 3.1. Reduced type-1 diabetes (T1D) incidence was also observed in NOD mice upon probiotics administration. A clinical trial aimed at investigating the protective role of a probiotics intake in the 24 months of life in babies with a genetic high risk of developing T1D [501]. However, due to a high dropout rate by the parents, only the safety and the feasibility of the protocol could be assessed. Fermented milk with *L. acidophilus* and *B. animalis* administration in Type 2 diabetes (T2D) patients, characterized by a later onset, high glucose levels and insulin resistance, instead, showed an improvement of the glycaemic control, along with decrease in anti-inflammatory cytokines and an increase in the SCFAs production [502].

The role of probiotics in treating autoimmune thyroid diseases were, so far, investigated less. The animal model of autoimmune thyroiditis (i.e. Hashimoto's thyroiditis) showed a milder phenotype when induced in presence of *L. rhamnosus* and *B. lactis* strains [385]. At the present, only one randomized, placebo-controlled trial investigated the concomitant use of the VSL#3 *consortium* along with levothyroxine in hypothyroid patients [503]. The probiotics supplementation seemed to stabilize more the hormonal fluctuations, although no significant protective effects were observed in the probiotic group compared to the placebo.

5.2. AIMS OF THE CHAPTER

The role of the gut microbiota in GD and GO has been described in the previous chapter and, most recently, in Chinese patients [439, 447]. However, no studies have directly investigated the modification of the gut microbiota in GD/GO patients and related changes in the disease features. Therefore, by providing a probiotics *consortium* along with the anti-thyroid therapy for 6 months, we aimed at modifying the gut microbiome of GD/GO patients and decreasing the anti-TSHR antibody titres (i.e. TRAB) and the concentration of immunoglobulins, such as IgA and IgG, predictive of disease relapse and disease severity.

As described in the intervention protocol ("Sinossi" submitted to the Comitato Etico Milano Area B, approval obtained on 11/11/2014), the primary endpoint of the probiotic trial involved the reduction of the *Firmicutes:Bacteroidetes* ratio of at least 5%.

Secondary endpoint was the reduction of anti-TSHR antibody titres and total IgG and IgA concentrations of at least 30% at the end of the probiotic treatment.

The present chapter includes the analysis of the primary and secondary endpoint of the trial. Moreover it includes also the description of the microbiota changes upon probiotic intake compared to the placebo in other aspects of the gut microbiota (i.e. alpha and beta diversity and differential abundance of genera).

5.3. MATERIALS AND METHODS

5.3.1. Patients and samples collection

A single-centre, double-blind, placebo-controlled pilot interventional trial was conducted at the Policlinico Cà Granda, University Hospital of Milan (Comitato Etico Milano Area B, approval obtained on 11/11/2014; ClinicalTrials.gov Identifier: NCT02373995) between 2015 and 2016. Inclusion criteria for GD/GO patients were the same as those for the observational study (see chapter 4, par. 4.3.1.). Further exclusions criteria included: i) previous or planned treatment with ^{131}I or thyroidectomy, ii) sight-threatening GO requiring orbital decompression, iii) antibiotics/antivirals intake, iv) IBD/acute diarrheal episodes within 4 weeks from recruitment, v) drug/alcohol abuse, vi) no informed consent, vii) age less than 18 or more than 65 years old and viii) ongoing pregnancy.

Enrolled GD/GO patients were randomized to receive either the probiotic *consortia* Lab4® or placebo, along with the anti-thyroid drug (ATD) treatment, for 6 months. Production of the probiotic *consortia* and randomisation were performed in double-blind at Cultech Ltd. (Port Talbot, Wales, UK). As previously described (Chapter 3, par. 3.3.3), Lab4® is a *consortium* of lactic-acid producing bacteria comprising two bifidobacteria strains (*Bifidobacterium bifidum* and *Bifidobacterium animalis* var. *lactis*) and two lactobacilli strains (*Lactobacillus acidophilus* strain 1 and strain 2), which was administered at a final concentration of 25 billion colony-forming unit (cfu)/capsule, twice a day. Placebo capsules contained 200mg of maltodextrin carrier.

Clinical evaluation and samples collection (i.e. blood for plasma and serum isolation and faecal samples) were performed by MS, GC and DC at the enrolment phase (baseline), when patients reached euthyroid status (EU timepoint, for definition see Chapter 4 par.. 4.3.1) and at the end of the treatment (EFU timepoint), approximately 6 months after the beginning of probiotic/placebo intake. A summary of the trial rational is described in figure 5.1.

Thyroid function tests (TSH, fT4 and fT3) and TRAB values were measured in blood using local biochemical assays. Reference ranges were described in Chapter 4, Table

4.1. Anti-TSHR antibodies measurement was further repeated by UB-P using the Immulite XPI (Siemens) for TSI (IU/L; positive result cut-off >0.1IU/L) and the Cobas Roche for TRAK quantification (IU/L; cut-off >0.3IU/L).

5.3.2. DNA extraction and 16S rRNA gene sequencing

Faecal samples were collected following the procedure described in Chapter 4 par. 4.3.1, stored at -20°C soon after their collection at the University of Milan and shipped in dry ice to Cardiff University (UK), within approx. two months from collection. DNA extraction has followed the same procedure described in Chapter 4, par. 4.3.2. The resulting genomic DNA samples were included in the second sequencing batch, together with the human DNA samples for the observational study described in Chapter 4. Paired-end metataxonomics reads were generated at R&T Ltd. (Texas, USA), using 28-combo primers detecting the V1-V2 of the 16S rRNA gene plus bifidobacteria regions, as described in Table 2.2 (Chapter 2).

Good-quality reads were processed as described in Chapter 4 par. 4.4.3 and Appendix 8. Briefly, QIIME 1.9 was used to remove reads not matching the quality thresholds, align them against the closed reference 16S rRNA gene database and obtain the OTU-table along with the taxonomic description. Alpha diversity indices were calculated from the filtered OTU table (less than 10 counts in at least 2 samples), while beta diversity indices were calculated from the filtered and CSS-normalized [354] OTU table.

5.3.3. Data analysis

Statistical analysis was conducted within the R environment, v3.4.1. (R development 2017), unless otherwise stated. Statistical analysis was conducted according to the intention-to-treat (ITT) basis, which includes all the participants who had been randomised in the study, despite noncompliance or withdrawal [504].

5.3.3.1. Trial objectives

Descriptive statistics included mean, standard deviation, median, Q1 (25%) and Q3 (75%) for interquartile ranges (IQR).

Comparison between probiotic and placebo at baseline (time of enrolment) was performed with a Chi-square test or Fisher's exact-test for categorical/frequency data, while the non-parametric Wilcox-Mann test plus Benjamini-Hochberg (BH) correction was used with continuous data.

At further timepoints (either euthyroid or end of follow-up), pairwise comparison between placebo and probiotic groups was performed with a non-parametric Wilcox-Mann test

plus Benjamini-Hochberg (BH) correction. Within each randomised group (either placebo or probiotic), a longitudinal analysis (amongst timepoint) was performed using the following linear model (**Equation 7**):

$$y_{ijk} = \mu + Time_i + GO\ status_j + e_{ijk}$$

Where y_{ijk} is either *Firmicutes:Bacteroidetes* (F:B) ratio or thyroid function tests (fT4, fT3 and TSH), immunoglobulins (total IgAs and IgGs) and anti-TSHR antibodies titres (TSI and TRAK). μ is the overall mean; $Time_i$ included the sampling timepoints as categories, (BL, EU and EFU), $GO\ status_j$ included the categories "no signs", "mild" or "moderate-severe". And e_{ijk} is the vector of the residual effects.

Baseline-corrected F:B counts and biochemical features were obtained subtracting the baseline values from the euthyroid and the end of follow-up observations in each sample individually. The non-parametric Wilcox-Mann test plus Benjamini-Hochberg (BH) correction was used for testing differences between timepoints and between groups.

5.3.3.2. Microbiota analysis

Alpha diversity indices (Chao1 and Shannon diversity) and the Bray Curtis dissimilarity matrix, as a beta-diversity measure, were calculated in QIIME1.9. Differences in alpha diversity amongst timepoint within each randomisation group were assessed using a linear regression model, correcting for GO status, thyroid status, smoking habits and age. Pairwise comparison between placebo and probiotic group in each timepoint was instead performed with a Welch's t-test plus BH correction. Beta diversity was represented in a NMDS plot using ggpubr R package and statistical differences between randomisation groups and amongst timepoints were assessed with PERMANOVA from the R Vegan package.

Differential abundance analyses amongst timepoints and within each randomisation group were conducted with the same linear regression model previously used for alpha diversity indices. Pairwise comparison between timepoints was performed using the Wilcox-Mann non-parametric test with Bonferroni correction. Taxonomic comparison between placebo and probiotic groups at each timepoint was performed using the linear discriminant analysis (LDA) effect-size (LEfSe) [464], in which the non-parametric Kruskall Wallis, followed by an unpaired Wilcoxon-Mann test were performed to obtain differentially abundant taxonomies. A linear discriminant analysis (LDA) is then used for an effect-size estimation on the differentially abundant features previously identified. LEfSe was performed on Galaxy (http://huttenhower.sph.harvard.edu/galaxy/) with an alpha value (P values) of 0.05 and a logarithmic LDA threshold of |2|.

Baseline-corrected counts were obtained subtracting the baseline values from the euthyroid and the end of follow-up of each taxon in each sample individually. Differences using baseline-corrected counts amongst timepoints were assessed with the previous linear regression model, followed by the Welch's t-test test and Bonferroni adjustment for pairwise comparisons.

Differential abundance of genera across timepoints within the same patient (individual variability across timepoint) was assessed using the G-test with Yates' correction as implemented in STAMP [319]. Only the top-20 most abundant genera were considered for the analysis.

Correlation between bacterial biomarkers identified through the LEfSe analysis, plus *Bifidobacterium* and *Lactobacillus* spp., and the biochemical/clinical features was performed with the Pearson's' correlation coefficient in the Corrplot R package.

5.4. RESULTS

5.4.1. Patients enrolment

A total of 34 patients were potentially suitable for enrolment in the trial. One patient was excluded from the trial because of history of allergic reactions and two patients for previous foodborne infections (i.e. borreliosis and hepatitis). Out of the remaining patients, 28 patients provided faecal samples in at least one timepoint, whose characteristics at the enrolment phase (baseline) are described in Table 5.1. No significant differences in terms of age and thyroid function tests were observed at the baseline timepoint between placebo and probiotic groups (Table 5.1).

Twenty-four out of 28 patients provided samples at the baseline timepoint. In line with the enrolment criteria and the purposes of the trial, all patients were treated with ATD (whose description is in Chapter 1 par. 1.1.2), in particular 2 patients were on a "block and replace" regimen, whereas the remaining patients were on a titration regimen (methimazole). The rational of the trial and the number of faecal samples per randomisation group in each timepoint is represented in Figure 5.1 and Table 5.2.

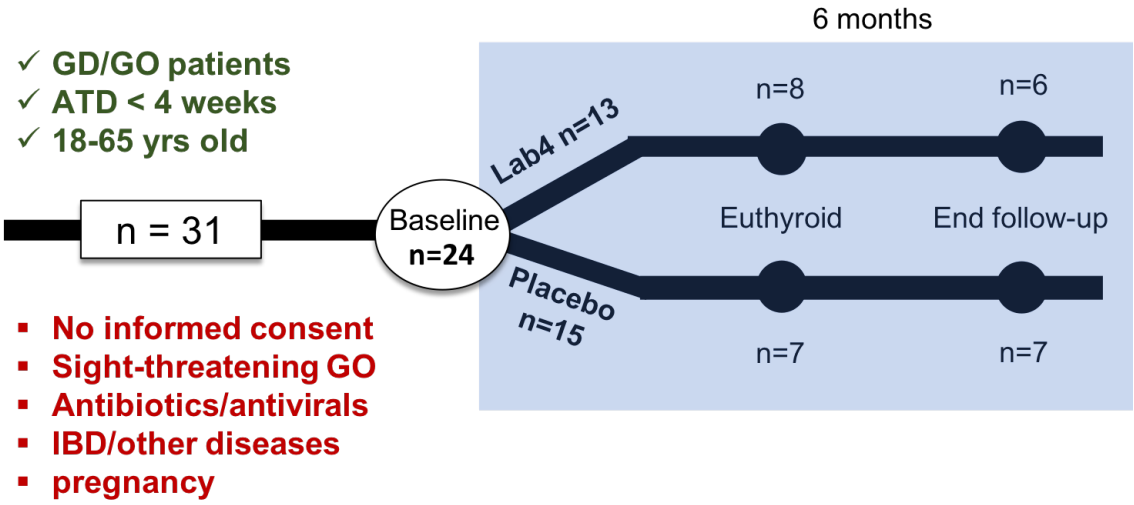

Figure 5.1. Rationale of the probiotic trial and number of samples obtained.
A total of 31 GD/GO patients complied with the inclusion criteria for the trial and were randomised to receive either probiotic (Lab4) or placebo (maltodextrin) capsules for 6 months. Twenty-eight patients provided faecal samples in at least one timepoint. Only 24 patients provided faecal samples at baseline. Eight probiotic-receiving patients and 7 placebo-receiving patients provided faecal samples at the euthyroid timepoint, while 6 and 7 patients in probiotic and placebo groups, respectively, provided samples at the end of follow-up in 6 months' time from the beginning of the trial.

Table 5.1. Characteristics of the patients enrolled for the interventional trial

	Placebo (n=15)	Probiotic (n=13)	Total (n=28)	P value
Age*	41.6 (12.67)	42.23 (12.47)	41.89 (12.35)	0.69
Gender (F/M)	12/3	10/3	22/6	1
Ethnicity°	2/13	0/13	2/26	0.48
Smoking habits#	2/13	3/10	5/23	0.63
GO status§	6/6/3	4/6/3	10/12/6	0.87
Thyroid status[a]	11/4	7/6	18/10	0.43
Thyroid function tests*				
fT4 (pmol/L)	13.70 (17.03)	23.92 (24.76)	18.62 (21.33)	0.17
fT3 (pmol/L)	7.42 (7.67)	9.52 (12.53)	8.43 (10.12)	0.89
TSH (mU/L)	3.25 (3.39)	4.76 (7.31)	3.95 (5.50)	0.85
Anti-TSHR antibodies*				
TRAB (IU/L)	20.28 (17.93)	13.17 (20.61)	16.86 (19.24)	0.10
TSI (IU/L)	100.05 (251.25)	97.92 (208.80)	99.08 (227.80)	0.93
TRAK (IU/L)	16.65 (15.30)	13.27 (13.67)	15.10 (14.36)	0.72
Immunoglobulins*				
IgA (mg/L)	175.41 (61.05)	177.81 (54.87)	176.56 (56.86)	0.88
IgG (mg/L)	1058.75 (229.23)	1053.45 (266.52)	1047.60 (242.28)	0.44

*represented as mean(standard deviation). °african/caucasian. #current/never smokers. §no sign/mild/moderate-severe GO status. [a]hyper/euthyroid.

Table 5.2. Number of faecal samples for microbiome analysis provided per timepoint

Timepoint	Placebo	Probiotic	Total (per timepoint)
Baseline (BL)	13	11	24
Euthyroid (EU)	7	8	15
End-of follow-up (EFU)	7	6	13
Total (unique patient)	15	13	28

5.4.2. Primary endpoint

The primary endpoint of the probiotic trial was the 5% reduction of the *Firmicutes*:*Bacteroidetes* (F:B) ratio following treatment with probiotics for 6 months. *Firmicutes* and *Bacteroidetes* were the most abundant of 15 phyla identified, followed by the phylum *Actinobacteria* (Figure 5.2). There was a significantly higher prevalence of *Firmicutes* than *Bacteroidetes* counts, which occurred in both groups in all the timepoints sampled (P=0.00).

When looking at the F:B ratio, no significant differences between probiotic and placebo were observed at baseline. Between the euthyroid timepoint (EU) and the baseline (BL), the mean F:B ratio reduced by 14% in the probiotic group, compared to a 48% reduction in the placebo group. Between the end of follow-up (EFU) and the baseline, the mean

F:B ratio reduced by 32% in the placebo group but increased by 285% in the probiotic group. An average 22% reduction in the F:B ratio was reported between EU and EFU upon probiotic intake (Table 5.3). The F:B ratio however, showed some outliers, which may influence the mean value (Figure 5.3). Analysis using the median values, in fact, reported a 42% decrease of the F:B ratio at EU but a 18% increase at EFU compared to the baseline specifically in the probiotic group (Table 5.3). However, no significant differences were reported between probiotic and placebo in each timepoint, neither when using baseline-corrected F:B values.

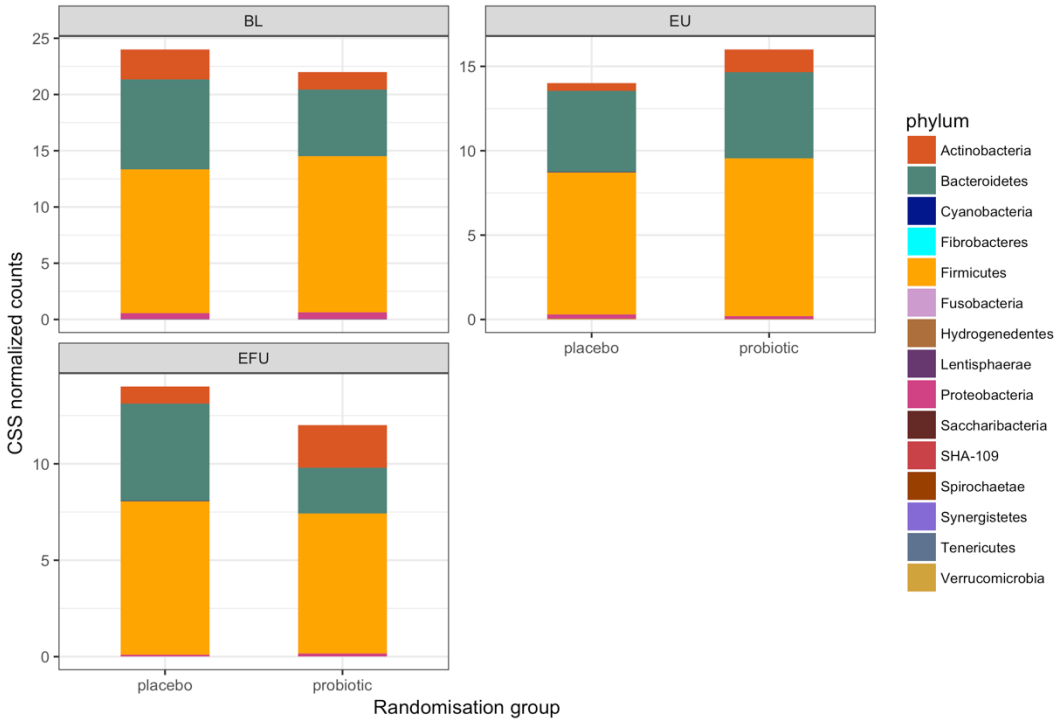

Figure 5.2. Phylum distribution in each randomisation group and per timepoint. Stacked bar chart graph representing the CSS-normalized phylum counts in either placebo or probiotic groups in each timepoint: BL, baseline; EU, euthyroid and EFU, end of follow-up.

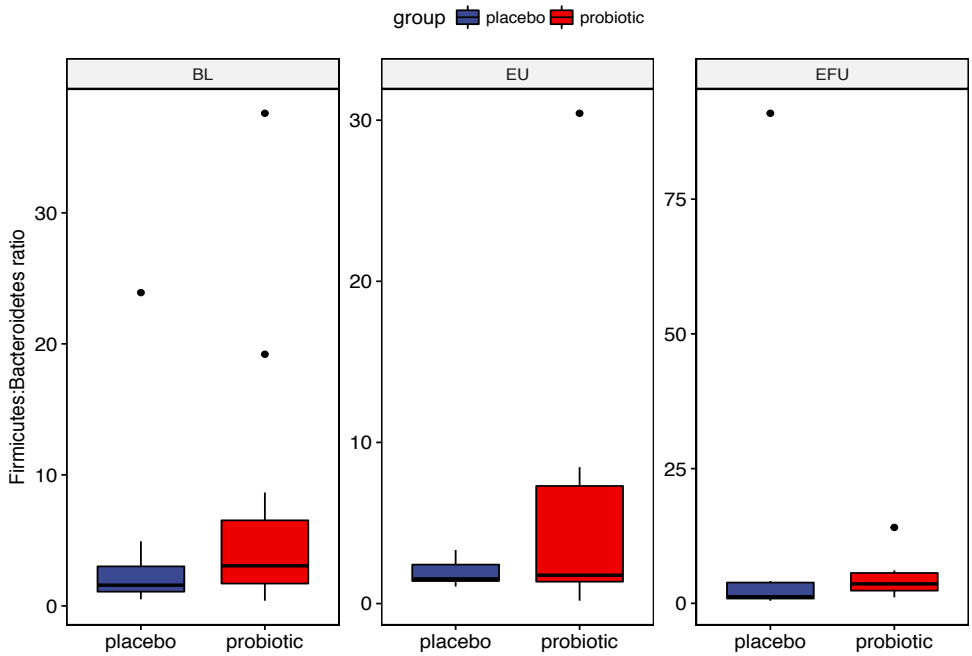

Figure 5.3. Distribution of the *Firmicutes:Bacteroidetes* (F:B) ratio between randomisation groups in each timepoint.

Box and whiskers plot of the F:B ratio in either placebo or probiotic groups in each timepoint: BL, baseline; EU, euthyroid and EFU, end of follow-up.

Table 5.3 Primary endpoint: percentage differences in *Firmicutes:Bacteroidetes* ratio.

	Placebo					Probiotic					
group	mean	st dev	median	Q1	Q3	mean	st dev	median	Q1	Q3	P value°
Baseline (BL)	3.79	6.49	1.58	0.88	2.50	7.57	11.32	3.06	1.68	8.66	0.24
Euthyroid (EU)	1.93	0.84	1.53	1.36	2.79	6.52	10.10	1.76	1.33	6.91	0.69
End of follow-up (EFU)	14.59	33.69	1.22	0.63	4.15	5.11	4.72	3.61	2.13	6.12	0.37
EU-BL (%)	-48.92	-87.11	-3.01	54.82	11.59	-13.82	-10.75	-42.48	-21.01	-20.18	0.63
EFU-BL (%)	285.20	418.86	-22.61	-28.34	65.69	-32.47	-58.28	18.20	26.28	-29.33	0.69
EFU-EU (%)	654.10	3925.23	-20.21	-53.71	48.48	-21.64	-53.26	105.51	59.86	-11.47	0.34
dEU (BL-corrected)	0.11	1.77	0.29	-0.05	0.38	2.20	13.73	-0.51	-1.69	4.49	1.00
dEFU (BL-corrected)	18.87	39.34	2.41	0.48	2.49	0.06	3.88	1.44	-2.85	3.06	0.68

Q1 (25%) and Q3 (75%), interquartile range. (%) percentage changes calculated as [(Tf – Ti)/Ti]x100, where Tf is either EU or EFU and Ti is BL. dEU (EU-BL) and dEFU (EFU-BL). °P value from the non-parametric comparison between placebo and probiotic in each section.

5.4.3. Secondary endpoint

The secondary objective of the trial was the decrease of the anti-TSHR antibodies titres of at least 30% at the end of treatment (EFU) upon probiotic intake. A median reduction of more than 30% in the TRAK and TSI titres has been reported in both placebo and probiotic group in both EFU to baseline and EFU to EU timepoints (Table 5.4). Such a reduction was less evident in the probiotic group compared to the placebo. The TSI levels showed a progressive reduction across timepoints in the probiotic group (Figure 5.4), however just missing the significant threshold (P=0.063). However, no significant differences in the anti-TSHR antibodies titres between placebo and probiotic has been observed (Table 5.5).

Other collateral objectives of the trials involved the improvement of the thyroid function and the immune response. The probiotic group showed significant variations of the fT4 levels amongst timepoints (P=0.01), whose median values were reduced in the probiotic group compared to the placebo group at EU (5.01 *vs*. 12.7, P=0.055, Table 5.4). Circulating IgA and IgG showed a transient reduction at EU, which was more pronounced in the probiotic group, although not significant (Figure 5.4). Probiotic group also showed a reduced IgG titres compared to the placebo group at EU timepoint, although missing the significant threshold (P=0.07, Table 5.5).

Although the significant threshold (P value) has been used widely in the scientific community, it is still worth commenting about the trends and the results which are not showing a significant value at P<0.05. A recent proposal[7] in fact stated the reason why the significance threshold might be overcome, and other tests such as the Bayesian inference might result more appropriate.

[7] Wasserstein RL, Schirm AL and Lazar NA. 2019. “Moving to a world beyond “P<0.05”” available at https://www.tandfonline.com/doi/full/10.1080/00031305.2019.1583913

Table 5.4 Secondary outcome: percentage difference in thyroid function tests, anti-TSHR antibodies titres and total immunoglobulin contents.

		Baseline					Euthyroid					End of follow-up						EFU-BL(%)		EFU-EU(%)	
features	group	mean	sd	median	Q1	Q3	mean	sd	median	Q1	Q3	mean	sd	median	Q1	Q3	P value#	mean	median	mean	median
TSH	placebo	0.888	3.040	0.005	0.005	0.030	1.563	1.835	0.850	0.074	3.770	1.187	1.502	0.690	0.044	1.780	0.388	33.723	13700.000	-24.068	-18.824
TSH	probiotic	1.342	2.026	0.050	0.005	3.160	4.324	6.255	2.390	0.300	3.990	1.213	1.201	1.470	0.025	1.770	0.001	-9.583	2840.000	-71.936	-38.494
fT3	placebo	8.077	8.224	5.100	2.460	12.120	4.176	2.774	3.400	2.700	5.500	4.596	2.524	3.650	3.030	4.700	0.418	-43.100	-28.431	10.065	7.353
fT3	probiotic	6.434	4.930	3.660	3.300	9.100	3.059	1.044	2.440	2.370	3.360	4.516	4.074	2.800	2.690	3.000	0.113	-29.810	-23.497	47.651	14.754
fT4	placebo	14.974	18.045	7.400	0.750	21.700	11.386	4.910	12.700	9.700	13.200	15.915	10.137	14.500	11.200	26.900	0.805	6.283	95.946	39.780	14.173
fT4	probiotic	20.100	15.435	15.700	12.200	30.800	6.274	6.341	5.010	0.610	9.440	12.998	15.639	11.700	1.260	11.800	0.014	-35.333	-25.478	107.181	133.533
TSI	placebo	15.578	18.054	3.820	2.140	24.000	11.436	11.628	7.095	3.290	20.000	2.447	4.451	0.569	0.488	0.676	0.335	-84.290	-85.105	-78.599	-91.980
TSI	probiotic	5.035	6.407	3.660	0.651	6.300	10.129	11.883	2.490	0.503	19.700	1.454	1.967	0.849	0.503	0.975	0.063	-71.117	-76.803	-85.644	-65.904
TRAK	placebo	18.952	15.566	22.900	3.300	31.820	15.783	14.050	13.810	5.060	22.960	4.932	8.166	0.680	0.300	4.140	0.233	-73.976	-97.031	-68.752	-95.076
TRAK	probiotic	8.236	8.514	4.480	1.460	14.720	10.471	13.821	3.000	0.850	26.830	4.917	6.978	1.355	1.220	6.980	0.215	-40.300	-69.754	-53.047	-54.833
IgA	placebo	187.000	55.825	197.000	135.000	219.000	154.250	53.879	176.500	74.000	177.000	176.286	75.793	178.000	119.000	221.000	0.745	-5.730	-9.645	14.286	0.850
IgA	probiotic	165.111	36.347	182.000	157.000	188.000	147.600	35.949	155.000	151.000	170.000	201.833	52.457	187.000	173.000	198.000	0.250	22.241	2.747	36.743	20.645
IgG	placebo	1076.300	244.846	1096.500	1002.000	1203.000	1004.000	134.815	939.000	914.000	1159.000	1113.571	320.099	1097.000	905.000	1301.000	0.805	3.463	0.046	10.913	16.826
IgG	probiotic	980.556	225.905	929.000	918.000	995.000	810.600	128.025	850.000	763.000	902.000	959.000	263.030	912.500	774.000	960.000	0.186	-2.198	-1.776	18.307	7.353

Q1 (25%) and Q3 (75%), interquartile range. #P values generated from the linear regression model (equation 7), correcting for GO status and thyroid status; (%) median percentage changes calculated as [(Tf – Ti)/Ti] x 100, where Tf is either EU or EFU and Ti is BL.

Table 5.5. Statistical summary of the differences in thyroid function tests, anti-TSHR antibodies titres and total immunoglobulin contents between probiotic and placebo.

Features	Timepoint	Placebo		Probiotic		P value#
		median	IQR°	median	IQR°	
TSH	BL	0.005	0.005-0.03	0.05	0.005-3.16	0.165
	EU	0.85	0.074-3.77	2.39	0.3-3.99	0.336
	EFU	0.69	0.044-1.78	1.47	0.025-1.77	0.876
	dEFU-BL	0.685		-0.003		
fT3	BL	5.1	2.46-12.12	3.66	3.3-9.1	0.972
	EU	3.4	2.7-5.5	2.44	2.37-3.36	0.259
	EFU	3.65	3.03-4.7	2.8	2.69-3	0.310
	dEFU-BL	-1.87		-0.4		
fT4	BL	7.4	0.75-21.7	15.7	12.2-30.8	0.235
	EU	12.7	9.7-13.2	5.01	0.61-9.44	0.056*
	EFU	14.5	11.2-26.9	11.7	1.26-11.8	0.662
	dEFU-BL	2.4		-3.4		
TSI	BL	3.82	2.14-24	3.66	0.651-6.3	0.270
	EU	7.095	3.29-20	2.49	0.503-19.7	0.445
	EFU	0.569	0.488-0.676	0.849	0.503-0.975	0.537
	dEFU-BL	-1.082		-3.43		
TRAK	BL	22.9	3.3-31.82	4.48	1.46-14.72	0.224
	EU	13.81	5.06-22.96	3	0.85-26.83	0.366
	EFU	0.68	0.3-4.14	1.355	1.22-6.98	0.583
	dEFU-BL	-3.805		-2.48		
IgA	BL	197	135-219	182	157-188	0.278
	EU	176.5	74-177	155	151-170	0.325
	EFU	178	119-221	187	173-198	0.668
	dEFU-BL	-6		9		
IgG	BL	1096.5	1002-1203	929	918-995	0.182
	EU	939	914-1159	850	763-902	0.071*
	EFU	1097	905-1301	912.5	774-960	0.295
	dEFU-BL	-36		-40		

°IQR=Q1 (25%) -Q3 (75%). #P values generated from a pairwise comparison using Wilcoxon-Mann and BH correction, * P<0.1.

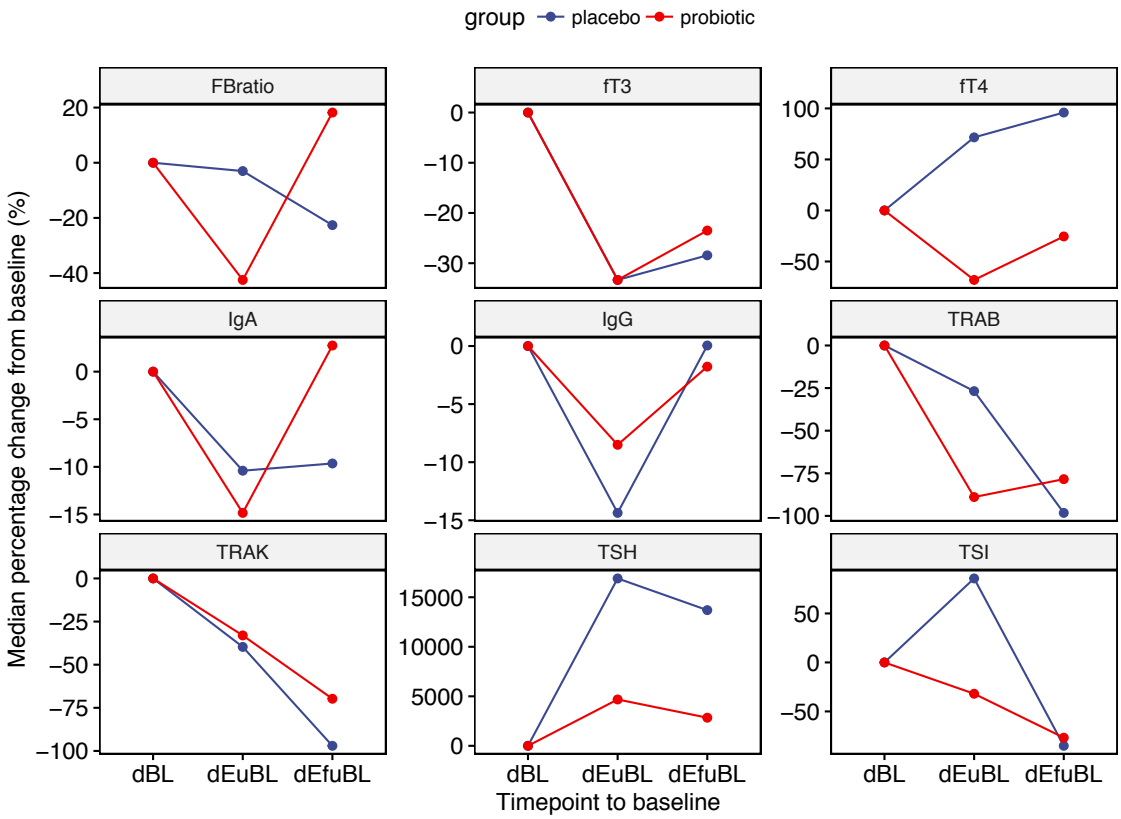

Figure 5.4. Changes in the F:B ratio and in biochemical features upon probiotic or placebo compared to the baseline.
The median percentage of each feature (either F:B ratio or biochemical features) of either placebo or probiotic group was plotted in function of the time, expressed to as change from baseline. dBL is considered to as 0 and dEUBL: EU-BL and dEFUBL, EFU-BL.

5.4.4. Modification of the gut microbiota upon probiotic/placebo intake

The within-sample or alpha diversity indices did not show any significant changes upon placebo/probiotic intake (Figure 5.5A), nor across timepoints. The between-samples or beta-diversity indices calculated trough the Bray-Curtis matrix did not show differences between randomisation groups in each timepoints (Figure 5.5B), or across timepoints.

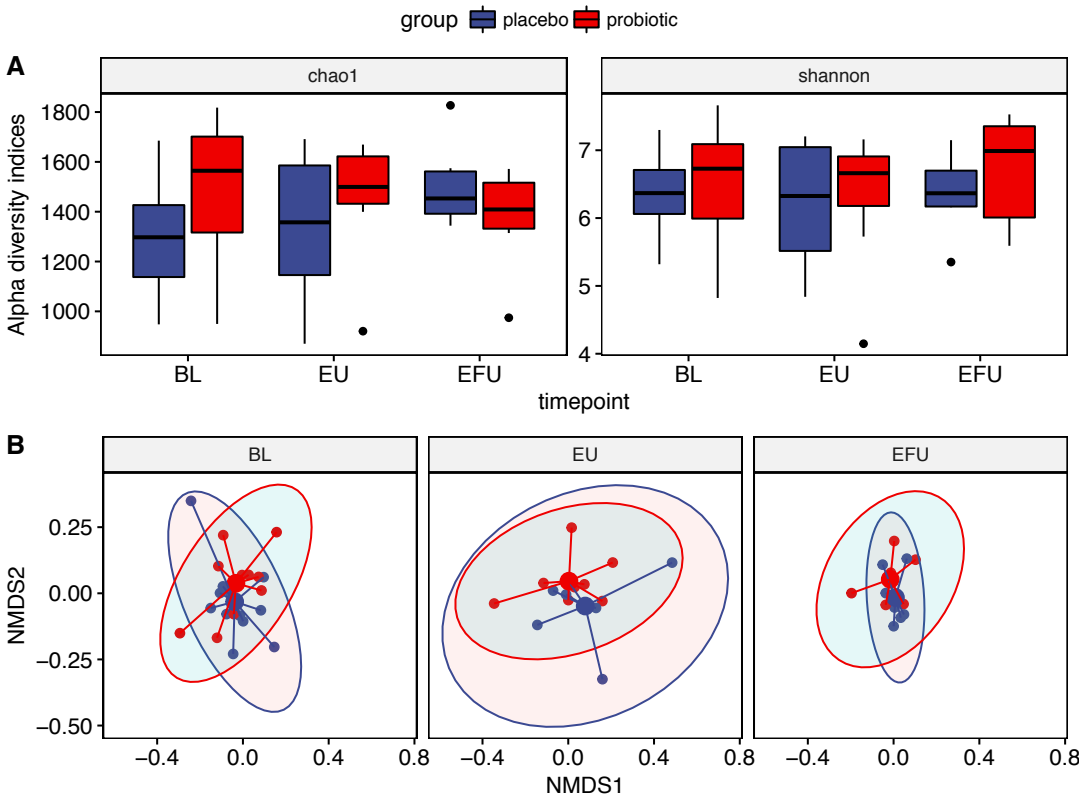

Figure 5.5. Alpha and beta diversity indices upon probiotic or placebo intake. (**A**) Box-and-whiskers plot representing the indices of richness (Chao1) and diversity (Shannon), P>0.05 between randomisation groups and amongst timepoints. (**B**) Non-metric dimensional scaling (NMSDS) plot. Stress R2=0.95 non-metric fit; P>0.05 PERMANOVA, using 999 permutations.

The differential abundance analysis initially focussed on differences in either probiotic or placebo gut microbiota groups amongst timepoints, using the Equation 7 which corrected for GO status. Five genera were differentially abundant in the probiotic-receiving group (Figure 5.6). Amongst them, taxa previously associated to a probiotics intake such as *Coprococcus* 3 and *Eubacterium hallii* spp. increased over time. In particular, *Coprococcus* 3, *Eubacterium hallii* spp., *Ruminiclostrium* 9 and *Turicibacter* show a significant increase between the baseline and the end of the follow-up (EFU), although not reaching the significant threshold after Bonferroni correction. Five taxa were differentially abundant in the placebo group (Figure 5.7), of those the phylum

Lentisphaerae and 4 genera. In pairwise comparisons, phylum *Lentisphaerae* and the *Lentisphaerae* single-genus *Victivallis* increased between baseline and EFU (P=0.018) and between EU and EFU (P=0.026), although not reaching significant threshold after Bonferroni correction.

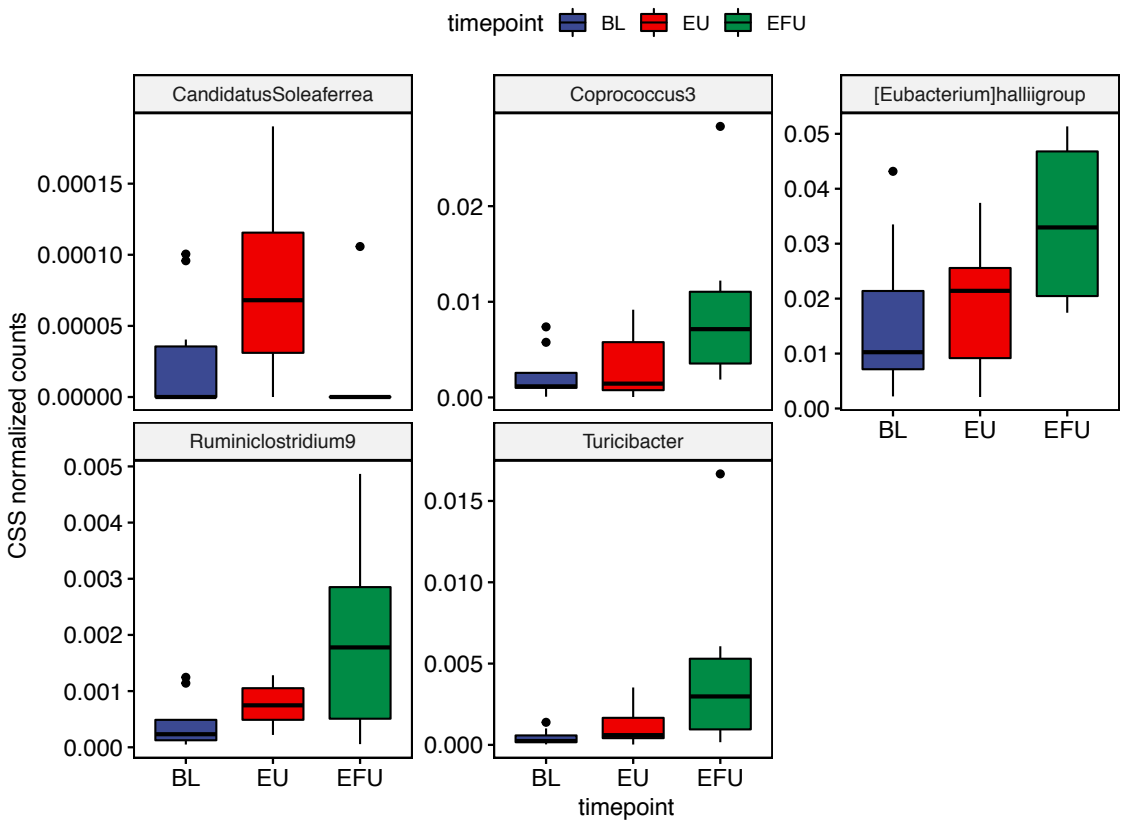

Figure 5.6. Differential abundant genera amongst timepoint in the probiotic group. Box-and-whiskers plot representing the CSS-normalized genera counts in each timepoint. Only genera with P<0.05 from the Equation 7 were included.

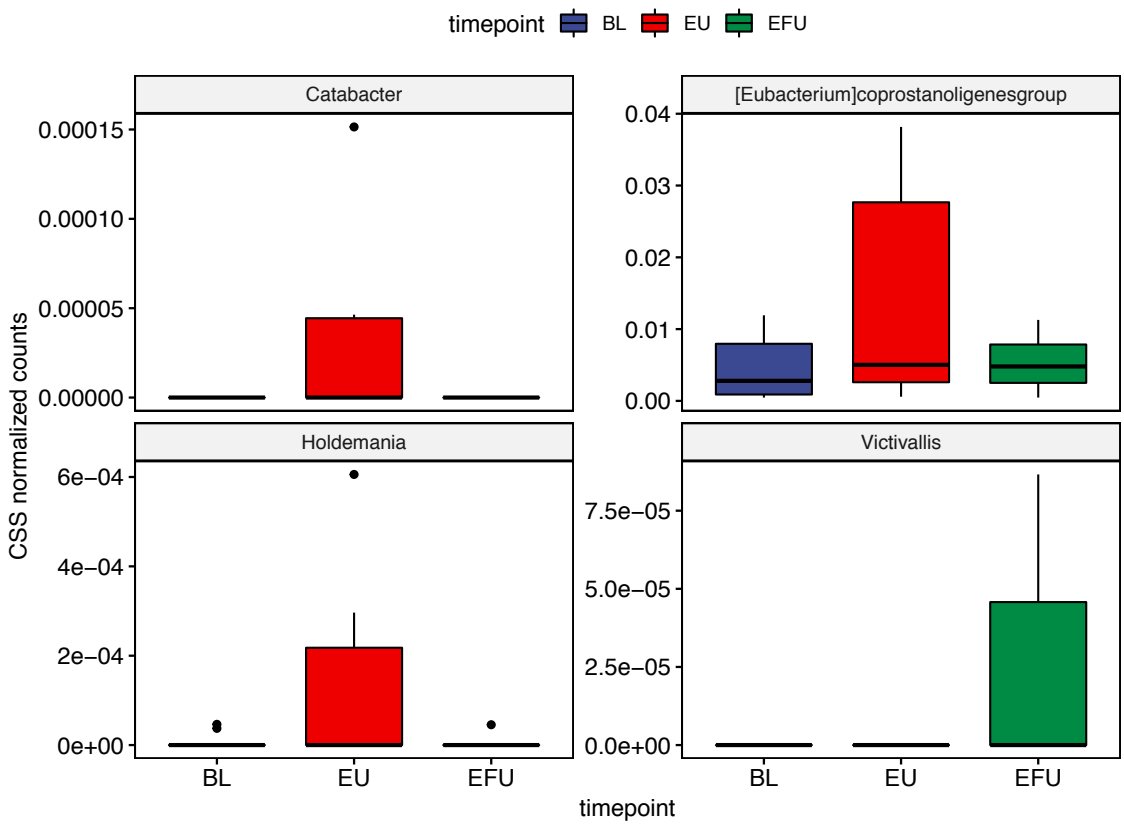

Figure 5.7. Differential abundant genera amongst timepoint in the placebo group. Box-and-whiskers plot representing the CSS-normalized genera counts in each timepoint. Only genera with P<0.05 from the Equation 7 were included.

The LDA effect-size (LEfSe) [464], provides robust biomarkers, by combining non-parametric test statistics to the linear discriminant analysis to estimate the effect size of the significant features identified. LEfSe has been applied to compare placebo and probiotic groups gut microbiota in each timepoint. At baseline, placebo group showed an enrichment of the *Salmonella* spp., while 5 genera were enriched in the soon-to-receive probiotic group (Figure 5.8A). At the euthyroid timepoint (Figure 5.8B), four genera increased in each group, including two *Clostridiales (Marvinbyrantia)*, one *Bacteroidetes* and one *Proteobacteria* in the probiotic group. Placebo group instead showed the increase of three *Firmicutes* (*Lachnospiraceae*, *Coprobacillus* and *Erysipelatoclostridium*) and one *Bacteroidetes* (Parabacteroides) genera. At the end of the follow-up (EFU), four genera were enriched in the probiotic group including the *Eubacterium Hallii* group and *Coprococcus* 3, confirming also previous analysis (Figure 5.8C).

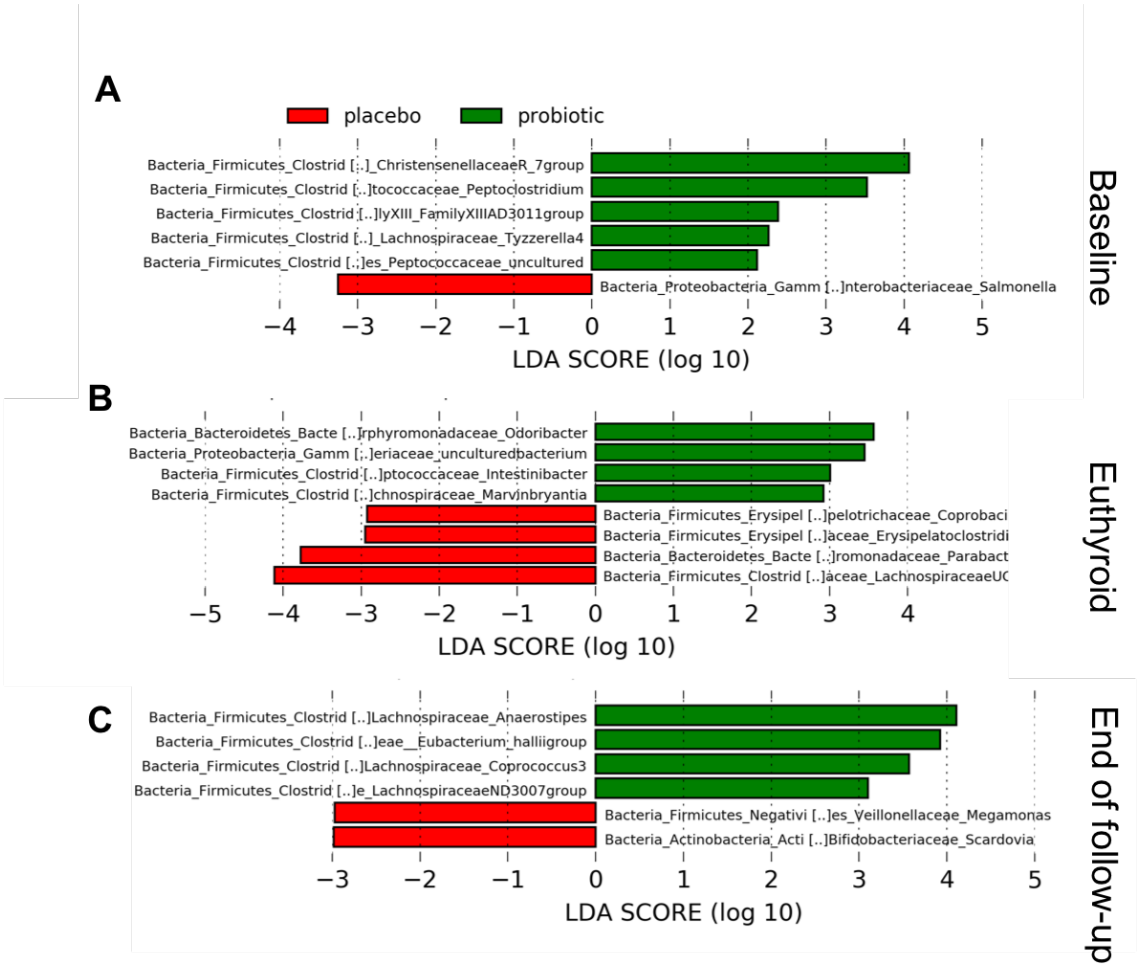

Figure 5.8. Bacterial biomarkers between probiotic and placebo in each timepoint identified through the LDA effect size (LEfSe).

Bar-chart plots representing the enriched bacteria biomarkers in either probiotic or placebo group at each timepoint according the linear discriminant analysis (LDA) effect size (LEfSe), [464]. Bacterial biomarkers were $P<0.05$ in both Kruskall Wallis and Wilcox-test and the minimum LDA threshold of 2 (as log10).

Baseline-corrected bacterial counts were obtained to account for differences in the gut microbiota of placebo and probiotic group at baseline. Twelve genera were differentially abundant across timepoints in the probiotic group (Table 5.6), confirming some of the linear regression results. Of those, 5 genera were differentially abundant both between baseline and the EFU and EU-EFU. Placebo groups showed 26 differentially abundant genera (Table 5.7). Some of previously identified differentially abundant genera were confirmed by this analysis, with some exception. Genus *Bifidobacterium* decreased in the placebo group between baseline and euthyroid (P=0.03). A higher number of genera were differentially abundant between BL and EU and EU and EFU compared to the probiotic group, potentially as the result of the ATD therapy on the gut microbiota composition. Only *Intestinibacter* spp. still showed a significant decrease between EU and BL after Bonferroni correction in the placebo group (P=0.017).
At the euthyroid timepoint, *Ruminococcus* 2 (P=0.037) and *Faecalitalea* (P=0.016) were differentially abundant between placebo and probiotic groups after baseline correction, while *Coprococcus* 3 was differentially abundant between placebo and probiotic groups at EFU (P=0.044), as represented in Figure 5.9.

Table 5.6. Differences between timepoints in the probiotics using BL-corrected genera.

Differentially abundant genera	dEU°		dEFU°		Pvalue[1]	PW[2]
	mean	st dev	mean	st dev		
Prevotella1	0.00014727	0.0001983	9.20E-07	2.34E-05	0.0258	A,C
Coprococcus3	0.0006403	0.0043078	0.009074	0.008659	0.0038	B,C
Lachnospira	0.0011026	0.0016176	-0.000125	0.0007814	0.0487	ns
LachnospiraceaeNC2004group	-0.008904	0.0118492	-0.004959	0.0059762	0.0486	A
[Eubacterium] hallii group	0.0001678	0.0119254	0.0276037	0.0212737	0.0006	B,C
uncultured	-0.0006915	0.0035229	0.0033214	0.002241	0.0121	B,C
Ruminiclostridium9	0.0002429	0.0006058	0.0015281	0.0018231	0.0137	B,C
Subdoligranulum	-0.0199163	0.0219667	-0.001122	0.0205589	0.0328	A
Dielma	-0.0001232	0.0001243	-0.000181	0.0002122	0.0178	B
Erysipelatoclostridium	-0.0001079	0.0002672	0.0009839	0.0016308	0.0409	ns
Turicibacter	0.0007152	0.0013257	0.0055762	0.0065813	0.0086	B,C
Klebsiella	1.74E-05	2.18E-05	0	0	0.0156	A,C

°BL-corrected EU and EFU (as EU-BL and EFU-BL) mean and standard deviation values. [1]P value derived from Equation 7, including the dBL as of 0. Only significant genera are shown. [2] Pairwise comparisons using the Welch's t-test without correction for multiple testing. A: dEU-dBL; B: dEFU-dBL and C: dEFU-dEU comparisons. Ns, not significant after pairwise comparison.

Table 5.7. Differences between timepoints in placebo using BL-corrected genera.

Differentially abundant genera	dEU°		dEFU°		Pvalue [1]	PW[2]
	mean	st dev	mean	st dev		
Bifidobacterium	-0.051330879	0.033549	-0.02174718	0.068920	0.0401	A
Gardnerella	2.07E-05	2.05E-05	-1.64E-05	3.72E-05	0.0242	C
Atopobium	0	0	1.35E-05	2.03E-05	0.0347	B
Collinsella	-0.001377382	0.007396	0.019308936	0.024335	0.0127	B,C
Eggerthella	0.00039064	0.000411	-2.20E-05	0.000151	0.0039	A,C
Senegalimassilia	0.000777938	0.00095	0.0001435	0.000479	0.0246	A
Capnocytophaga	0	0	-1.42E-05	1.95E-05	0.0196	B,C
uncultured	-2.96E-05	2.72E-05	-9.18E-06	2.05E-05	0.0077	A
FamilyXIIIAD3011group	0.000720484	0.001081	0.000757159	0.000650	0.0261	ns
[Eubacterium] nodatum group	-3.04E-05	6.10E-05	7.49E-05	0.000127	0.0463	ns
Coprococcus3	-0.002295046	0.001964	-0.00192313	0.003403	0.0414	ns
Lachnospiraceae FCS020 group	-0.000384774	0.000421	0.000478409	0.00061	0.0030	A,B,C
Marvinbryantia	-0.000129786	0.000177	0.00092266	0.001476	0.0382	ns
Pseudobutyrivibrio	-0.028084968	0.034214	-1.90E-05	0.028363	0.0451	ns
unculturedbacterium	-0.000175361	0.000168	-7.02E-06	7.94E-05	0.0031	A,C
Intestinibacter	-0.001669128	0.000694	0.000371362	0.002251	0.0136	A,C#
Flavonifractor	0.000965976	0.001382	-0.00048027	0.000613	0.0111	A,C
Subdoligranulum	0.013032176	0.030920	0.025564805	0.017653	0.0244	B
[Eubacterium] Coprostanoligenes group	0.011018647	0.015270	-0.00168526	0.004778	0.0199	A,C
Coprobacillus	0.000166469	0.000281	-5.51E-05	9.13E-05	0.0413	ns
Holdemania	0.00017116	0.00025	-1.68E-05	2.32E-05	0.0256	A,C
Selenomonas3	1.56E-05	2.13E-05	0	0	0.0194	A,C
Veillonella	5.48E-05	0.000102	-0.00031632	0.000430	0.0148	B,C
Victivallis	0	0	2.49E-05	3.82E-05	0.0379	B
uncultured	2.34E-05	3.45E-05	7.40E-05	5.71E-05	0.0009	B,C
Hafnia	-9.18E-06	2.05E-05	2.19E-05	3.51E-05	0.0411	C

°BL-corrected EU and EFU (as EU-BL and EFU-BL) mean and standard deviation values. [1]P value derived from the equation 7, including the dBL as of 0. Only significant genera are shown. [2] Pairwise comparisons using the Welch's t-test without correction for multiple testing. A: dEU-dBL; B: dEFU-dBL and C: dEFU-dEU comparisons, ns, not significant in pairwise comparison. # P<0.05 after Bonferroni correction.

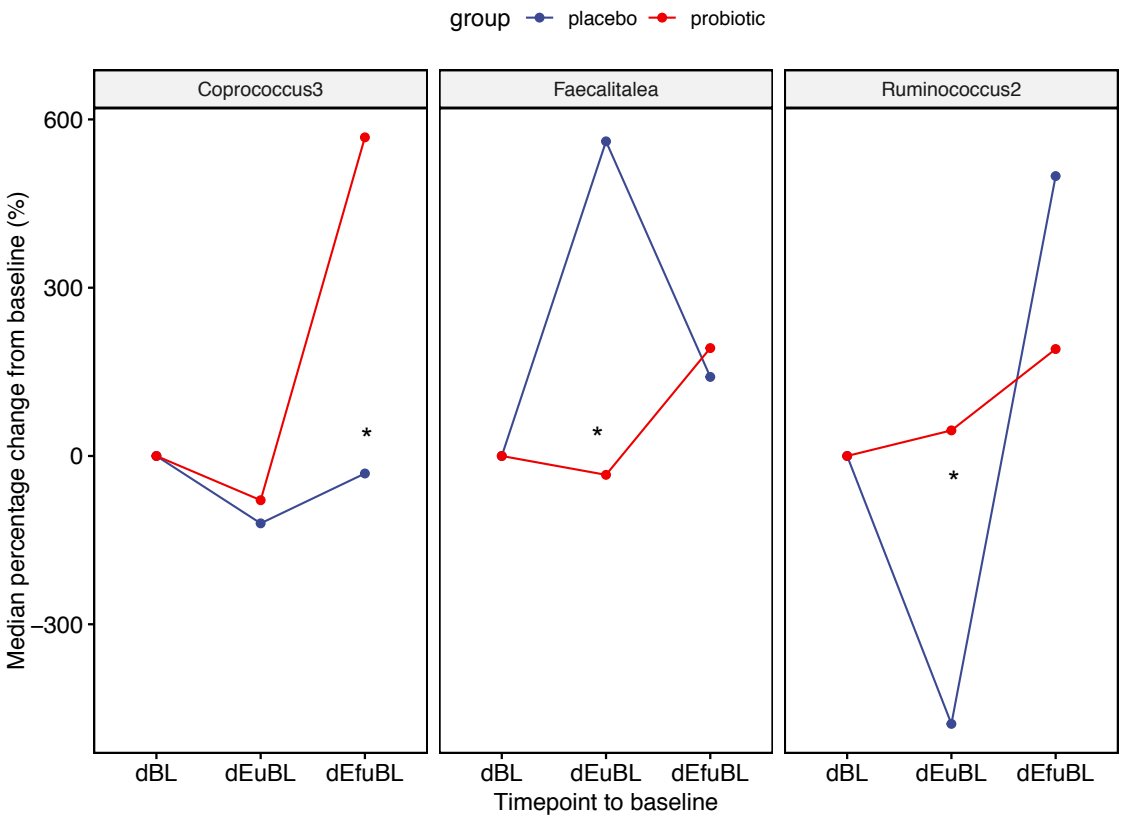

Figure 5.9. Differences between probiotics and placebo-treated group, using baseline-corrected genus counts.
The median percentage of each genus in either placebo or probiotic group was plotted in function of the time, expressed to as change from baseline. dBL is considered to as 0 and dEUBL: EU-BL and dEFUBL, EFU-BL. Differences between probiotics and placebo assessed using the pairwise t-test with Bonferroni correction: * P<0.05.

5.4.5. Correlations with clinical features and co-occurrence analysis

Pairwise correlations between biochemical features (e.g. anti-TSHR antibodies, thyroid function tests and total immunoglobulins levels) and the bacterial biomarkers enriched between placebo and probiotic in each timepoint were assessed using the Pearson's correlation coefficient (*r*). Moreover, although not significantly different between the two groups, *Lactobacillus* and *Bifidobacterium* spp. counts were included in the correlation analysis to observe any possible direct correlation with the biochemical features or any co-occurrences (i.e. relationship between bacterial pairs, such as the coexistence or the mutual exclusion) with the previously identified bacterial biomarkers. At baseline (Figure 5.10), *Bifidobacterium* spp. weak positively correlated with the fT3 levels (r=0.2 , P=0.002), which was significant in the placebo group (data not showed). *Tyzzerella* 4 (enriched in the probiotic group) positively correlated with fT4 levels (r=0.54 , P=0.049). On a biochemical point-of-view, as expected per diagnosis, TRAK positively correlated with TSI levels (r=0.78 , P<0.001), as well as fT3 and fT4 levels (r=0.93, P<0.001).

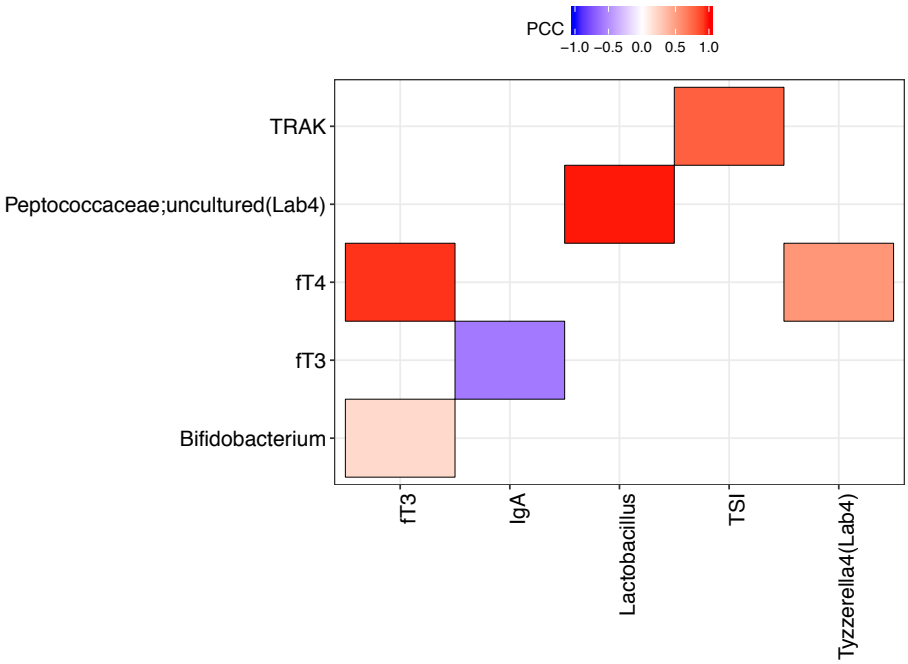

Figure 5.10. Correlations and co-occurrences heatmap between bacterial biomarkers and clinical features at baseline.
PCC, Pearson's correlation coefficient. Only correlations with P<0.05 are shown. Correlation strength ranges from negative (blue colours) to positive (red colours), as described in the legend. (Lab4), bacteria enriched in probiotic group. (P), bacterial enriched in placebo group. *Lactobacillus* and *Bifidobacterium* spp. were also included although not enriched in any group.

At the euthyroid timepoint (Figure 5.11), TSH levels negatively correlated with fT3 (r=-1 , P=0.0089), as per euthyroid diagnosis. *Lactobacillus* counts positively correlated with TSH levels (r=0.89 , P=0.0084). Probiotic-enriched genera such as *Intestinibacter* (r=-0.81, P=0.011) and an uncultured *Enterobacteriaceae* genus (r=-0.66 , P=0.0068) negatively correlated with fT4 levels; moreover, the two genera showed strong co-occurrence between each other (r=0.65 , P=0.011). Also, genus *Odoribacter* showed negative correlation with total IgA titres (r=-0.46, P=0.033). Placebo-enriched *Coprobacillus* spp. positively correlated with total IgG titres (r=0.85 , P=0.027). *Erysipelatoclostridium* spp. and *Lachnospiraceae* UCG-004 showed negative correlation with TSH levels (r=-0.83, P<0.01), while *Lachnospiraceae* UCG-004 also positively correlated with fT3 levels (r=0.083 , P=0.019). Correlations involving the *Lachnospiraceae* UCG-004 occurred significantly in the placebo group (Figure 5.13). Several probiotic-enriched taxa and the genus Lactobacillus showed a mutual-exclusion relationship with the placebo enriched *Lachnospiraceae* UCG-004.

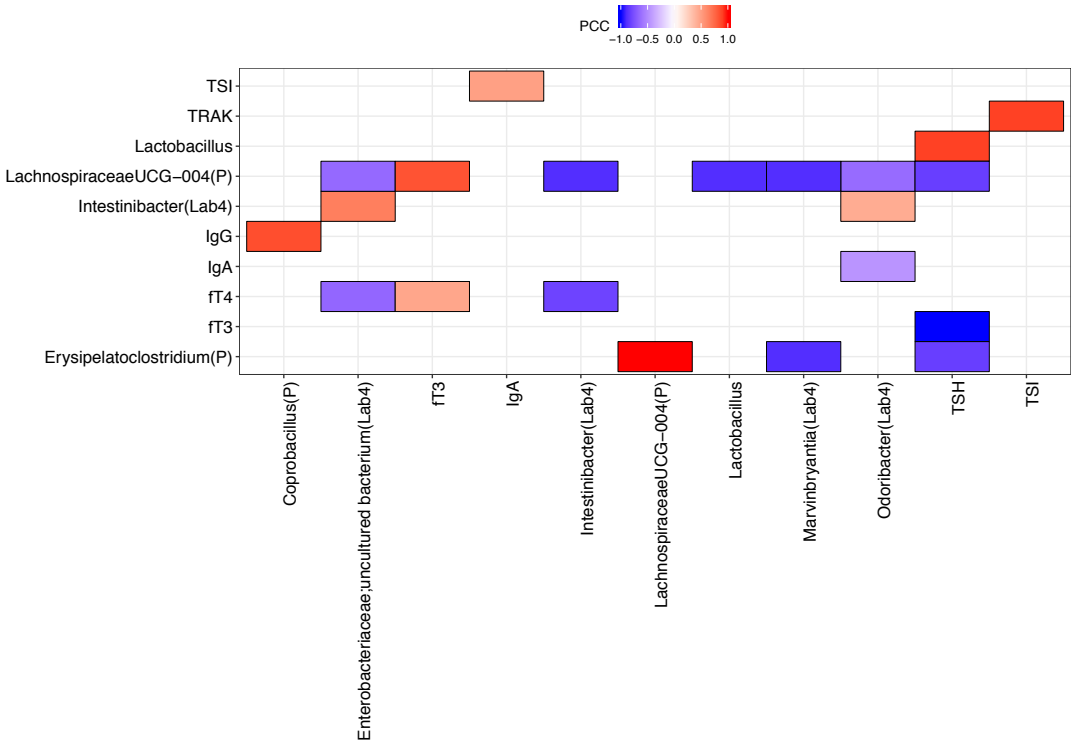

Figure 5.11. Correlations and co-occurrences heatmap between bacterial biomarkers and clinical features at euthyroid.
PCC, Pearson's correlation coefficient. Only correlations with P<0.05 are shown. Correlation strength ranges from negative (blue colours) to positive (red colours), as described in the legend. (Lab4), bacteria enriched in probiotic group. (P), bacterial enriched in placebo group. *Lactobacillus* and *Bifidobacterium* spp. were also included although not enriched in any group.

After six months of probiotic or placebo intake (EFU, Figure 5.12), *Bifidobacterium* (r=-0.78 , P=0.016) and *Lactobacillus* spp. (r=-0.55, P=0.032) counts strong negatively correlated with fT3 levels. However, a similar trend was observed in both placebo and probiotics (Data not showed), possibly due to the few samples observed in each group at this timepoint. The TSH levels strong negatively correlated to fT4 levels (r=-0.72 , P=0.007), as a result of a more euthyroid status. As a co-occurrence pattern identified, *Bifidobacterium* co-occurred with *Coprococcus* 3 spp. (enriched in probiotic group; r=0.75, P=0.02) and *Coprococcus* 3 co-occurred with *Eubacterium hallii* (r=0.77, P=0.0026), which were both enriched in the probiotic-receiving group. *Lactobacillus* counts weak co-occurred with *Scardovia* spp., which was enriched in placebo group. Mutual exclusion was identified between probiotic-enriched and placebo-enriched genera, such as *Anaerostipes* and *Scardovia* spp. (r=-0.27, P=0.012) or *Bifidobacterium* and *Megamonas* spp. (r=-0.82, P=0.013).

BL-corrected *Ruminococcus* 2 showed significant negative correlation with TSI (r=-0.46, P=0.013) and TRAK (r=-0.52, P=0.013) and weak positive correlation with TSH (r= 0.16, P<0.001) (Figure 5.14).

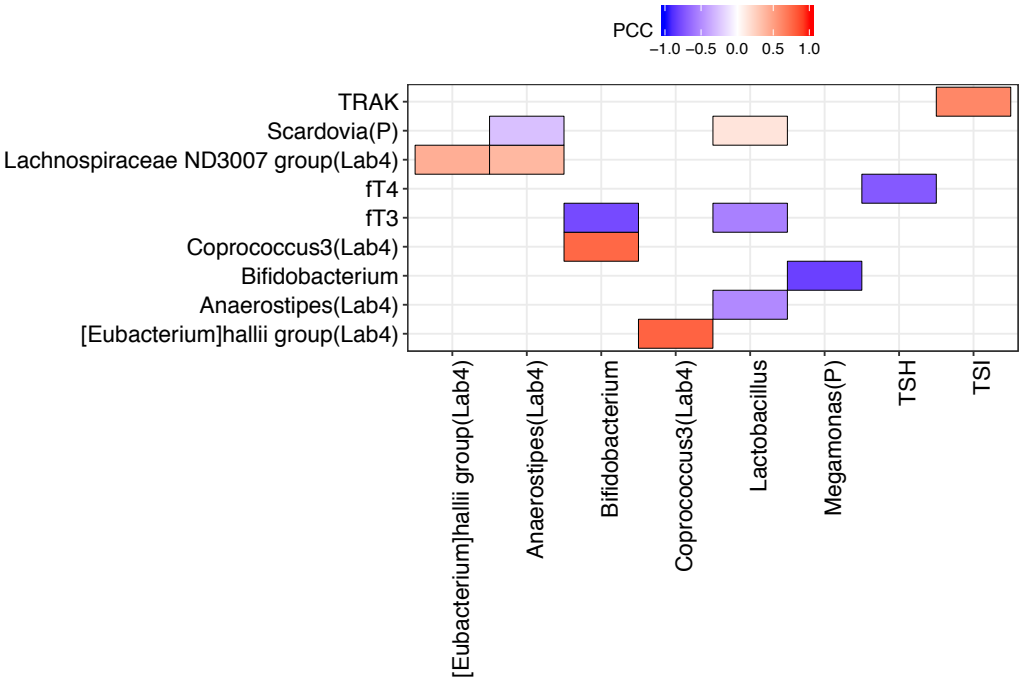

Figure 5.12. Correlations and co-occurrences heatmap between bacterial biomarkers and clinical features at the end of follow-up.
PCC, Pearson's correlation coefficient. Only correlations with P<0.05 are shown. Correlation strength ranges from negative (blue colours) to positive (red colours), as described in the legend. (Lab4), bacteria enriched in probiotic group. (P), bacterial enriched in placebo group. *Lactobacillus* and *Bifidobacterium* spp. were also included although not enriched in any group.

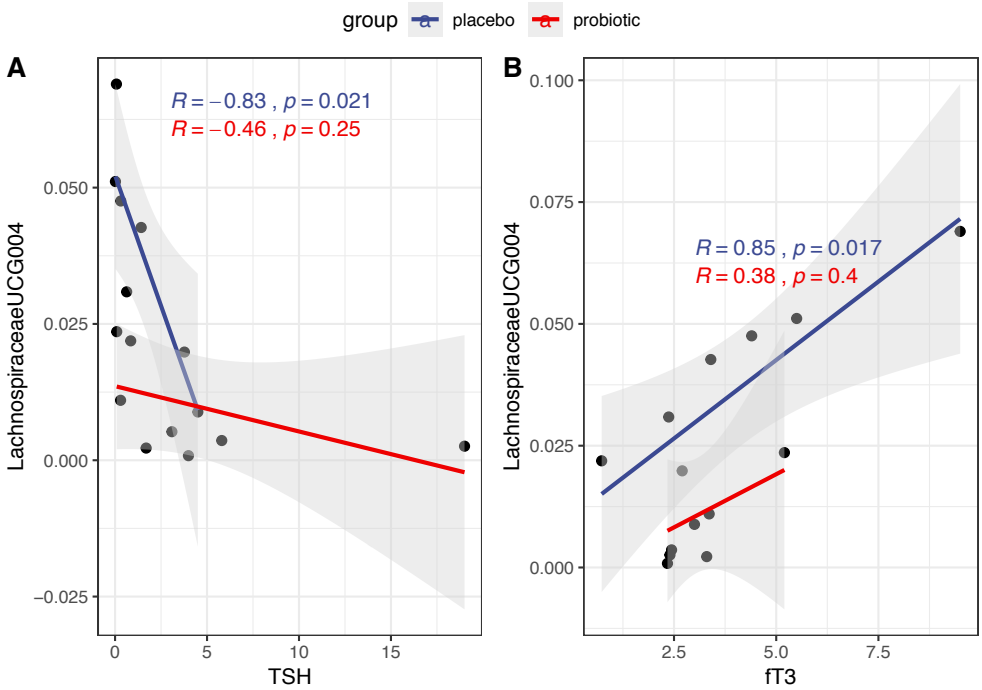

Figure 5.13. Correlation between placebo-enriched *Lachnospiraceae* UCG-004 and clinical features (fT3 and TSH) at the euthyroid timepoint in randomised group.
Previously identified significant correlations between the placebo-enriched *Lachnospiraceae* UCG-004 and TSH or fT3 in either placebo or probiotic. Pearson's correlation coefficient (*R*) represents the strength of the correlation in either placebo or probiotic group.

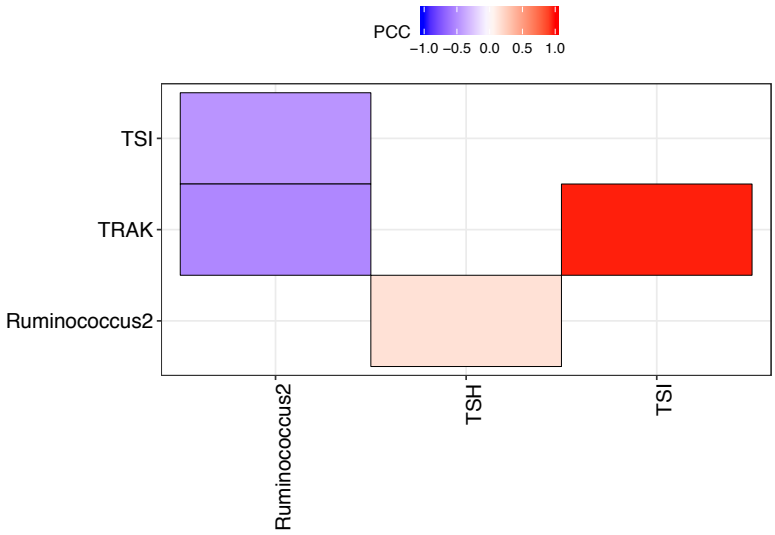

Figure 5.14. Correlations and co-occurrences heatmap between BL-corrected differential abundant genera and clinical features at baseline.
PCC, Pearson's correlation coefficient. Only correlations with P<0.05 are shown. Correlation strength ranges from negative (blue colours) to positive (red colours), as described in the legend.

5.4.6. Individual variability in response to probiotics intake

The Lab4® probiotic is composed of bifidobacteria and lactobacilli strains; therefore, the change of those two genera across time was specifically observed to determine the rate of response to the probiotic intake. Overall, there was an increased amount of *Bifidobacterium* counts over time in the probiotic group compared to the placebo group, although not reaching the significant threshold (P=0.1). On the other hand, *Lactobacillus* spp. was generally of a low abundance, with the exception of few outliers (Figure 5.15). Individual variability plays an enormous contribution in the response to a probiotic intake. Figure 5.16 shows the fluctuation of both *Bifidobacterium* spp. and *Lactobacillus* spp. over time in each participant on an ITT basis.

I defined as a "responder" a participant whose *Bifidobacterium* or *Lactobacillus* counts increased after the recruitment (e.g. at EU or at the EFU or both compared to the baseline, Table 5.9). Around 37% and 50% of participants in the probiotic group showed an increased *Bifidobacterium* counts at either EU or EFU, respectively, compared to baseline; while 14% and 28% of the placebo group participants in EU and EFU, respectively. *Lactobacillus* spp. increased in 37.5% and 42% of participants in probiotic and placebo groups, respectively, at the EU timepoint. At EFU, only 16% of probiotic participants showed an increased *Lactobacillus* counts compared to 28% of placebo participants. Moreover, 28% probiotic and 14% placebo participants showed an increase in *Lactobacillus* counts in both EU and EFU compared to the baseline.

The individual variability was investigated in the 6 patients (4 in probiotic and 2 in placebo groups) who provided faecal samples in all timepoints. An heterogenous response to the probiotic or placebo intake was showed for which the *Bifidobacterium* and *Lactobacillus* spp. were concerned (Figure 5.17). As expected, patients showed an individual composition of the gut microbiota at baseline, which was slightly modulated either at EU or at the EFU (Figure 5.18), as the result of either the Lab4 and ATD or placebo and ATD intake. Also the thyroid status may have influenced such a composition. Differential abundance of the top-20 most abundant genera across time and within each patient are represented in Appendix 26.

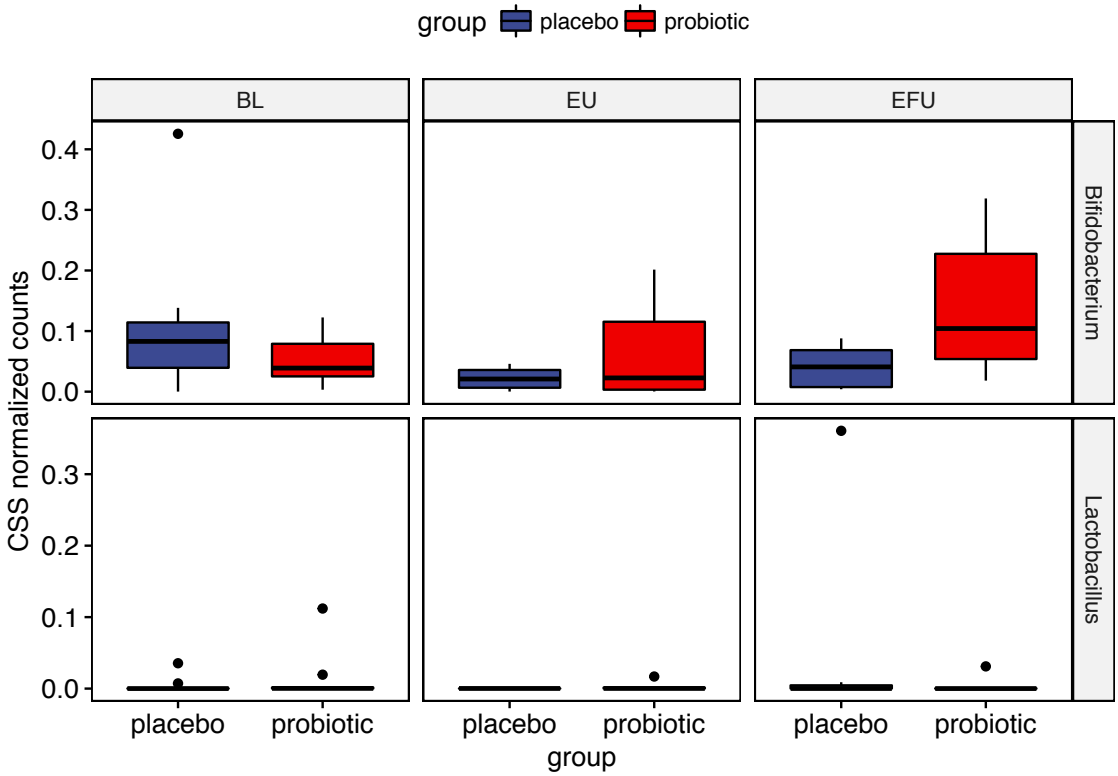

Figure 5.15. Differences in the Bifidobacterium and Lactobacillus spp. between probiotic and placebo in each timepoint.
Box-and-whiskers plot representing the CSS-normalized genera counts in each timepoint per each group. Only genera with P<0.05 from the equation 7 were included.

Table 5.8. Rate of responders in placebo or probiotic groups

Target	Comparison	Placebo	Probiotic
Bifidobacterium	EU>BL	1/7 (0.14)	3/8 (0.37)
	EFU>BL	2/7 (0.28)	3/6 (0.50)
	Both°	0/14	0/14
Lactobacillus	EU>BL	3/7 (0.42)	3/8 (0.37)
	EFU>BL	2/7 (0.28)	1/6 (0.16)
	Both°	1/7 (0.14)	2/7 (0.28)

°for both EU>BL and EFU>BL.

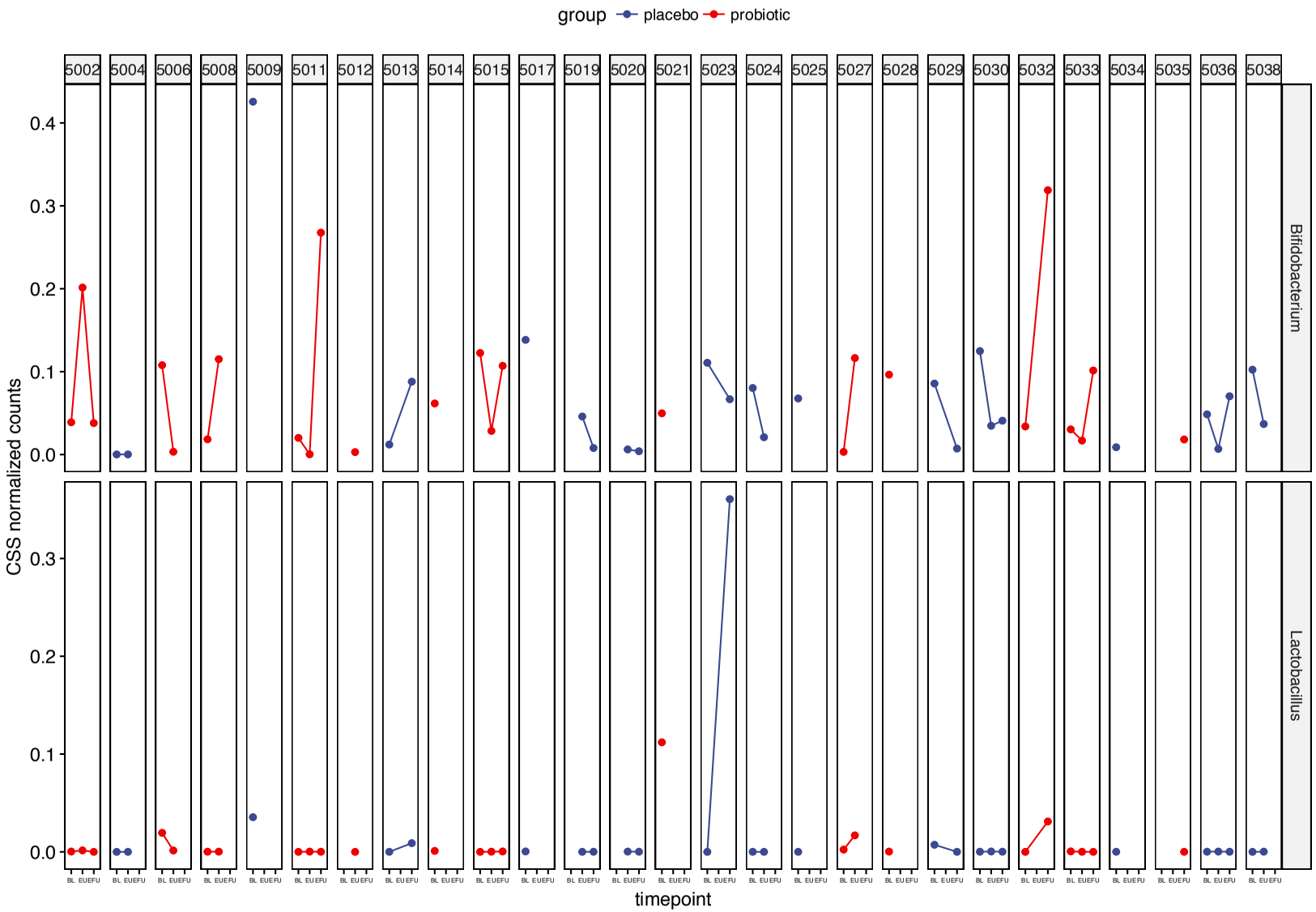
group
placebo
probiotic
5002
5004
5006
5008
5009
5011
5012
5013
5014
5015
5017
5019
5020
5021
5023
5024
5025
5027
5028
5029
5030
5032
5033
5034
5035
5036
5038
Bifidobacterium
Lactobacillus
CSS normalized counts
0.0
0.1
0.2
0.3
0.4
BL EU EFU
timepoint

Figure 5.16. Individual variability in *Bifidobacterium* and *Lactobacillus* spp counts over time.

(Previous page) Each spot represents the amount of CSS normalized genus in each timepoint per each participant on a ITT basis. BL, baseline; EU, euthyroid and EFU, end of follow-up.

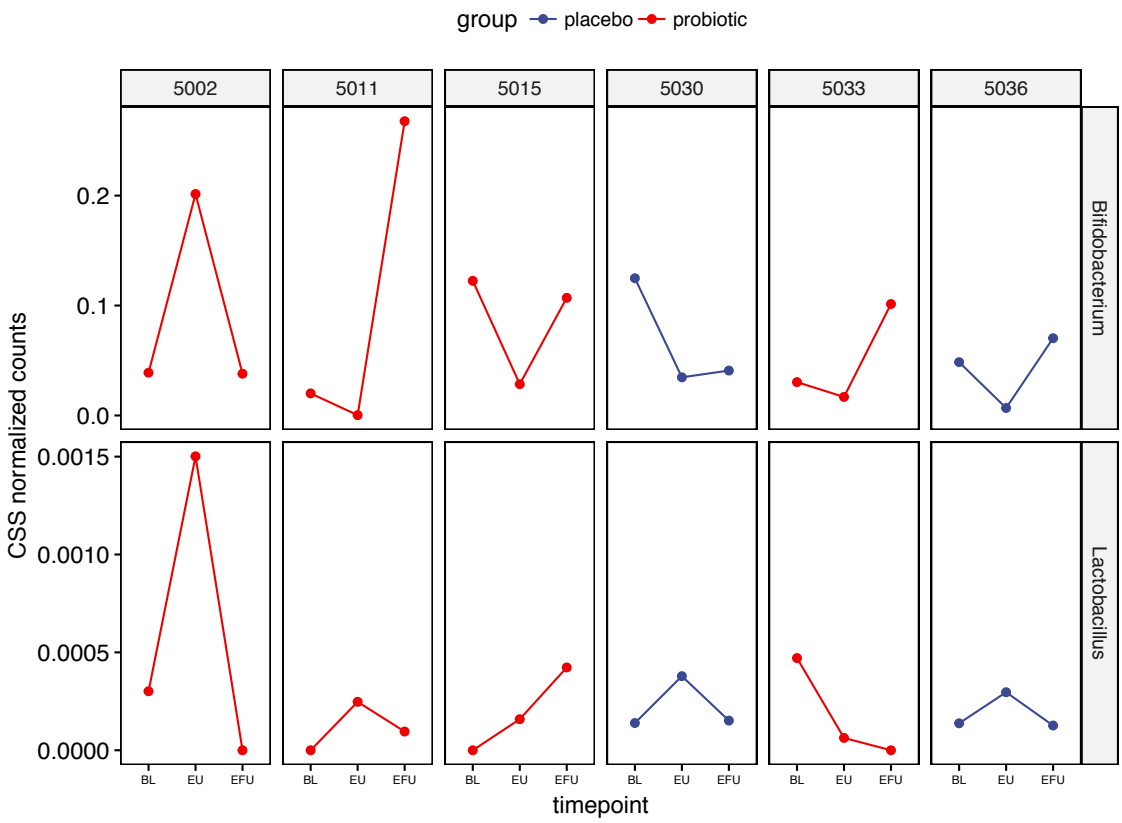

Figure 5.17. Individual variability in response to probiotic or placebo intake in the per-protocol cohort.

Bifidobacterium and *Lactobacillus* spp. CSS-normalized counts plotted in function of time in each of the 6 patients, who donated samples in all timepoints.

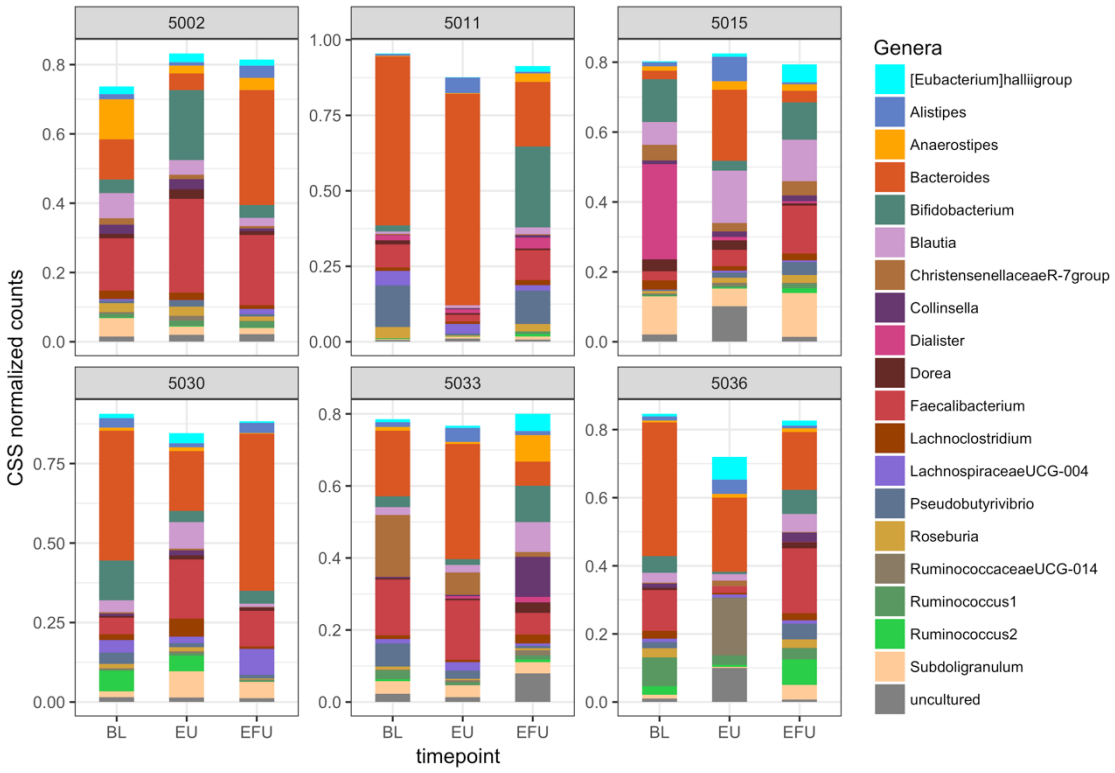

Figure 5.18. Individual variability in the most abundant genera in response to probiotic or placebo intake.

Stacked bar-chart of the top-20 most abundant genera, whose CSS-normalized counts were plotted in function of time in each of the 6 patients who donated samples in all timepoints.

5.5. DISCUSSION

Supplementation with probiotic bacteria, including lactobacilli and bifidobacteria strains, is considered safe [505] also during pregnancy [506]. Such intake, in fact, was previously evaluated in pregnant woman both healthy or carrying a foetus at risk of allergies or atopic eczema as reviewed in [507]. Probiotics supplementation in preterm babies showed a reduced risk of developing necrotizing enterocolitis (NEC) [498-500], while it is still debated whether the probiotics supplementation in the early months of life reduce the risk of developing allergic reactions, asthma and atopic dermatitis during childhood [508, 509]. In adults, effects from a probiotics intake were evaluated not only in patients (e.g. IBD) but also in healthy individuals, for immunomodulating purposes or prevention of obesity.

One of the most studied mechanisms of action of probiotics is the stimulation of an anti-inflammatory immune response, especially through the increase of Tregs [510]. In Chapter 3 we reported an increased Tregs moiety in βgal but not in the TSHR-immunised mice upon Lab4® early-life administration, possibly suggesting the reduction of Tregs in GD/GO pathogenesis. Restoration of Tregs under probiotics supplementation constitutes a great interest especially for those conditions characterized by an imbalance of Th1/Th2 or Th17/Tregs immune response.

In this study, we aimed at modifying the gut microbiota of GD/GO patients through the concomitant administration of probiotics bacteria and the standard ATD (i.e. methimazole) and possibly improve symptoms, prevent hormonal unbalances and/or disease relapse.

5.5.1. Primary and secondary outcomes of the trial

We hypothesised that the composition of the gut microbiota could have been modulated by a probiotic intake and we selected the *Firmicutes:Bacteroidetes* (F:B) ratio as an index for such modulation. The primary endpoint aimed, in fact, at the reduction of the F:B ratio of at least 5% in probiotic-treated group compared to placebo group. At the euthyroid timepoint, a mean F:B reduction of 14% was observed in the probiotic-treated group, while the placebo-treated group showed a reduction of 48%. Using the median values, i.e. not influenced by outliers, the F:B ratio showed a 42% reduction in the probiotic-treated group, while placebo group showed a 3% F:B reduction. At this stage, patients would have been treated with antithyroid medications (antithyroid drugs, ATD) to return into euthyroid status (see Chapter 1 par. 1.1.1 for definition of euthyroidism). The primary endpoint at the EU timepoint was centred (especially for which the median values are concerned), although the F:B reduction observed in both probiotics and placebo groups

can be due to the strain imposed by thyroid hormones/ATD intake on the gut microbiota (as I previously showed in Chapter 4). It might be speculated that the probiotics intake could have prevented fluctuations in the gut microbiota composition and potentially in the thyroid hormone levels. To this extent, in fact, the probiotics group showed a significantly reduced free-thyroxine (fT4) levels compared to the placebo group at the EU timepoint.

At the euthyroid status, patients may stay euthyroid for a while, also after the cessation of the ATD, or may experience a disease relapse. F:B ratio results showed quite discordant trend between randomised groups at the end of the trial (end of follow-up, EFU) compared to the baseline. The primary endpoint was centred for which the mean F:B reduction is concerned (-32% in probiotic and +285% in placebo compared to baseline), but it was not centred when looking at the median values (+18% in probiotics and -23% in placebo group). An increased *Firmicutes* phylum can be imputed to the effect of probiotics in increasing *Firmicutes*-prevalent bacteria [511], as I will discuss later.

By looking at the secondary endpoint, we can therefore speculate that the probiotics supplementation did mitigate the fluctuations in endocrine and immunological parameters, with significant effects on fT4 levels, but also in thyroid-stimulating immunoglobulins (TSI) and circulating IgGs and IgAs. Conversely, Spaggiari and collaborators did not show any significant improvement of thyroid functions in hypothyroid patients being treated with levothyroxine and the VSL#3 *consortium* [503], although they suggested a prevention of the hormonal fluctuations. It has to be noted also that the study focussed on primary hypothyroid patients, the opposite of hyperthyroidism.

Overall, the individual variability to a probiotic/ATD intake still played a major role, as observed by the presence of outliers. Moreover, as it will be later discussed in Chapter 6, the number of patients in EU and EFU timepoints was small, both at randomisation and at subsequent timepoints due to non-compliance in returning faecal samples. therefore the trial may better be considered as a “pilot study”. Moreover, due to the small cohort providing samples at all timepoints (4 probiotic-treated and 2 placebo), it was not possible to draw conclusions on the prevention of the eye disease or the disease relapse, contrary to what we aimed.

5.5.2. Modulation of the gut microbiota by ATD/probiotics

In line with other findings, the administration of Lab4 in presence of ATD did not modify the diversity of the gut microbiota [512]. Differences in the gut microbiota were instead observed. Probiotic-treated GD/GO patients showed an increase of *Eubacterium hallii* and a range of *Firmicutes* genera (i.e. *Coprococcus* 3 and *Ruminiclostrium* 9) over timepoints. It was interesting to note that the *Eubacterium hallii* can be itself considered to as a probiotic bacterium capable of SCFA (propionate) production [513]. When orally administered, it ameliorated the metabolic conditions of the obese and diabetes (*db/db*) mouse model of metabolic syndrome and Type 2 diabetes (T2D), by increasing the butyrate production and by modifying the bile acid profiles [514]. Also, species belonging to the genus *Coprococcus* are SCFAs-producers [515]. Both *Eubacterium hallii* and *Coprococcus* 3 were significantly increased in the probiotic-treated group compared to placebo at EFU. At euthyroid, other *Clostridiales*-related genera showed an enrichment upon probiotic intake.

When correcting for the baseline gut microbiota composition, both *Eubacterium hallii* and *Coprococcus* 3 still showed a significant enrichment in EFU compared to baseline. Interestingly, *Eubacterium hallii* showed a strong co-occurrence with *Coprococcus* 3 at EFU, which in turn showed strong co-occurrence with *Bifidobacterium* spp. Although *Bifidobacterium* spp. was not significantly enriched in the gut microbiota compared to placebo, it might have favoured the growth of other SCFAs-producing bacteria.

As far as the modification of bile acid profiles by probiotics is concerned, Lab4® proved to reduce the cholesterol levels *in vitro* and to modulate the bile salts excreted in the faeces *in vivo* [516]. In fact, C57BL/6 mice fed high-fat diet (HFD) plus Lab4+*L.plantarum* for 14 days showed a reduced cholesterol levels in the plasma accompanied by an increase of total and unconjugated bile salts in the faeces compared to HDF-alone mice. Amongst modulated bile salts, cholic acid (3a,7a,12a-trihydroxy-5b-cholan-24-oic acid) was increased upon Lab4+*L.plantarum* supplementation. The influence of the thyroid hormones on the cholesterol levels has been described. Hyperthyroid patients often show a reduced plasma low-density lipoprotein (LDL)/cholesterol levels. The reduction in the cholic acid synthesis, along with reduction in primary bile synthesis was observed in [517]. In a more recent study, however, Bonde and collaborators reported an increase in bile acids synthesis in hyperthyroid patients [518]. Interestingly, bile acids sequestrants (BAS), normally used for lowering the cholesterol levels in hypercholesterolemic patients, in combination with standard ATD showed a faster return to the euthyroid status [519] through the binding and the sequestration of thyroid

hormone T4 in the gut and their clearance through the faeces[8]. In the present study we did not measured the plasma cholesterol levels nor the bile acid profiles and the T4 levels excreted in the faeces; therefore, further studies are needed to explore in the details the possible effect of Lab4® on the bile acids levels in hyperthyroid patients. Of interest, our recent study on the miRNA and proteins profiles in GD/GO patients identified few biomarkers (e.g. Fibronectin, Alpha-2 macroglobulin, Haptoglobin, Fibrinogen amongst others) which were also related to the liver fibrosis [440].

I reported no increase in either *Bifidobacterium* spp. or Lactobacillus spp. following probiotics intake. In a recent study, Zmora and collaborators [520] could not find any of the administered probiotic species in the faecal samples via 16S rRNA sequencing, implying that the faecal samples and/or the metataxonomic approach were not adequate enough for such analysis. On the contrary, they could have identified single probiotic bacterial species by performing a high sensitivity qPCR to specifically detect each probiotic species on the participant mucosa samples. Based on that, they identified participants with a high probiotics colonisation (i.e. “permissive”) and participants with a low colonisation rate (i.e. “resistant”). I considered the increase of bifidobacteria as a positive response to the probiotic intake (i.e. “responder”) and a slightly higher response rate in the probiotic group compared to that of the placebo was observed, although the number of samples was not adequate to reach any significant threshold.

It would be of interest to understand the initial gut microbiota composition which would maximise the probiotic effects. Despite our small cohort, I compared the gut microbiota at the baseline of those patients considered “responder” to that of the “non-responder” and eight genera were enriched in the responder group (Appendix 27), which may favour the probiotic colonization. Interestingly, *Bifidobacterium* spp. was enriched in the non-responder group, possibly meaning that no further increase in *Bifidobacterium* spp. would occur in presence of an already *Bifidobacterium*-enriched microbiota.

5.5.3. Longitudinal modulation of the gut microbiota by antithyroid medications

The gut microbiota of the placebo-treated GD/GO patients can be useful to dissect differences due to the ATD intake in a longitudinal manner. The ATD alone, in fact, could have had an impact on the gut microbiota composition. In their recent study, Maier and collaborators reported a reduced *Bacteroides caccae* in presence of methimazole (MTZ)

[8] Salazar, 2016. “Adjunctive bile acid sequestrant therapy for hyperthyroidism in adults” Cochrane Database of Systematic Review” accessible from https://www.cochranelibrary.com/cdsr/doi/10.1002/14651858.CD012260/full

in vitro [264]. In the present study, *Bacteroides* spp. did not show any differences in either probiotic or placebo group, or when analysed longitudinally in each individual. One may suggests that the amount of active compound reaching the gut *in vivo* differs from the amount tested *in vitro* (i.e. 20μM). At present, no studies evaluated the amount and the role of MTZ on the gut microbiota in hyperthyroid patients.

Taxonomies that were enriched following probiotic treatment, such as *Coprococcus* 3 and *Marvinbyrantia*, were instead decreased in the placebo group, possibly suggesting their role in lowering the thyroid hormone levels. Moreover, none of the previous GD/GO associated genera (i.e. reduced *Bacteroides* spp. or increased *Fusicatenibacter* spp.) identified in Chapter 4 were here observed.

5.6. CHAPTER CONCLUSIONS

To conclude, the present chapter showed results of the pilot probiotics intervention on GD/GO patients under antithyroid medications treatment. Even if the number of samples available was small, modulation of the gut microbiota following LAB supplementation may have strengthened the action of the ATD in lowering the thyroid hormone levels (fT4) and in stabilizing hormone fluctuations.

In order to confirm our results, it would therefore of interest to perform a bigger probiotic trial, exploring also mechanisms such as the interaction between probiotics, SCFAs, bile acids profiles and thyroid hormones.

6. Chapter 6

General Discussion

6.1. GENERAL DISCUSSION

The aetiology of autoimmune diseases is currently not completely understood, due to the complex interaction between genetic predisposition and the environmental stimulus, which may be by sex hormones (especially after pregnancy), stress, smoking habits, and/or microbial and viral infections.

The role of bacterial antigens in triggering autoimmune thyroid diseases, including GD, it has been previously proposed [148, 454]. In particular, the molecular mimicry between *Yersinia enterocolitica* antigens and the TSHR epitopes was previously proposed for the breakdown of the immune tolerance to thyroid antigens, as reviewed in [454], although it has been long debated. To investigate the involvement of bacterial antigens in our GD cohort, I initially tested the immune response to whole-cells bacterial antigens from three foodborne environmental bacteria (*E.coli*, *Yersinia enterocolitica, Salmonella typhimurium)* in the serum of a small cohort of female GD patients and of female and male healthy controls (unpublished data, Figure 6.1A). Both patients and controls responded to all bacterial antigens (Figure 6.1B), which reflected the wide diffusion of these bacteria in the environment. Only *Y. enterocolitica* cultured at 37°C out of the other bacterial antigens, showed a significant response in both GD patients whole-serum and IgG fractions (Figure 6.1C and 6.1D). Although our results confirmed previous results from current literature, such a cross-reaction is unlikely to be responsible for the onset of all GD/GO cases. Moreover, I did not detect any *Y. enterocolitica* in the gut microbiota of either mouse models or patients from the 16S rRNA gene sequencing.

The concept of the gut microbiome as a possible trigger for an autoimmune response has gained more attention in the past years, with evidence describing perturbed composition of the gut microbiota not only in gut-related autoimmune conditions (i.e. IBD, Crohn's disease and ulcerative colitis), but also in non-gut related autoimmune diseases (i.e. diabetes, multiple sclerosis…), as previously introduced in Chapter 4.

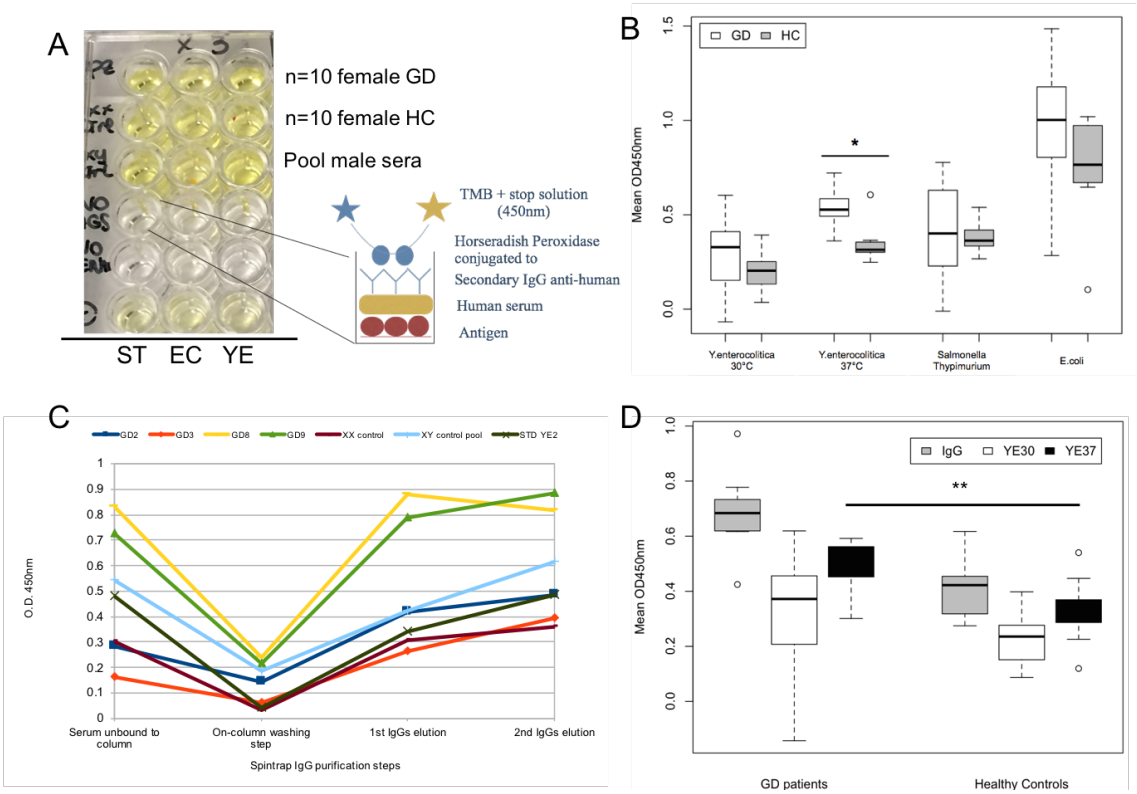

Figure 6.1. Immune response to foodborne bacterial antigens in a GD patients. (**A**) The immune response to whole-cells bacterial antigens was tested in a cohort of female GD patients (n=10, enrolled in University Hospital Milano Cà Granda, Milan) and compared to that of healthy controls (HC, n=10 females and a pool of healthy young males, enrolled in University Hospital of Wales, Cardiff) through an indirect Enzyme-Linked Immunosorbent Assay (ELISA). Bacterial whole-cells antigens derived from *E.coli* (EC), *Salmonella typhimurium* (ST) and *Yersinia enterocolitica* (YE), which were purchased from ATCC and cultured in Luria Bertani broth (Appendix 1) at 37°C. YE was also cultured at 30°C. Optimisation of the ELISA condition was performed using positive reference serum provided by University Clinic Duisburg-Essen. Each well contained 10^6 cfu/mL bacterial antigens. (**B**) GD and HC responded according to the level of exposure to each bacterial antigens. Box and whiskers plot of the immune response of GD and HC using total serum to 4 different bacterial whole-cells antigens. According to the Mann-Whitney-Wilcoxon test, only YE cultured at 37°C gave differential immune response between GD and HC (*** P=0.001). Statistics was performed with R package. (**C**) The specificity of the serum response to YE antigens was confirmed using purified IgGs. Total IgGs were purified from total serum using protein-A SpinTrap (GE, Healthcare), following manufacturer procedures. GD2, GD3 and GD8, GD9, individual GD patients tested for YE IgG-mediated response. STD, positive reference serum against YE. (**D**) Boxplots of the immune response (total serum and IgGs) to YE antigens cultures either at 30°C or 37°C. According to the Mann-Whitney-Wilcoxon test, only YE cultured at 37°C gave differential immune response between GD and controls (*** P<0.01).

6.1.1. Main conclusions of the present work

In order to unravel the role of the gut microbiome in GD/GO, my work was composed of two observational studies and of two interventional trials, involving both the GO animal model and GD/GO patients, respectively.

I characterized the gut microbiota of the GO animal model described in [187], both during and at the end the immunisation process (Chapter 2). The gut microbiota composition differed between TSHR-A subunit immunised mice and controls, with a shift of the bacterial communities accompanied by a significantly increased *Firmicutes* and reduced *Bacteroidetes* phyla in the TSHR-immunised mice, compared to the others. Such changes occurred specifically along with the immunization procedure. Furthermore, I described a positive correlation between the phylum *Firmicutes* and the orbital-adipogenesis in TSHR-immunised, but not in the control group. In the hypothesis that the gut microbiota can be considered to be an environmental factor, I found a different gut microbiota composition in TSHR-immunised mice established in two independent laboratories, possibly explaining the differences in the replication of the animal model.

The second observational study involved GD/GO patients, whose microbiome was compared to that of healthy controls, as presented in Chapter 4. I described GD and GO-associated taxonomies, such as reduced *Bacteroides*. and increased *Fusicatenibacter* genera. The gut microbiota composition and the predicted metagenomic functions of the moderate-severe GO were more similar to that of healthy controls, but it was accompanied by an increased *Roseburia* spp. Although there was the involvement of the immune system components (as also observed in the predicted metagenomic functions), our results on the patients' microbiome suggested that thyroid hormones played a major role in shaping the gut microbiota composition.

The two interventional studies here performed aimed at manipulating the gut microbiota composition of both GO mouse model and GD/GO patients, and were set to answer essentially two different questions: i) whether the gut microbiome is necessary for developing autoimmune thyroid disease and ii) whether supplementation with probiotic bacteria might have improved the symptoms and prevented hormonal fluctuations or disease relapses.

In the first case, the GO mouse model was treated from the early days of life with either antibiotics, probiotics or faecal material transplant from sight-threatening GO patients (hFMT). The reduced and resilient bacterial community (including high counts of *Bacteroides* spp. and *Akkermansia* spp.) derived from the long-term vancomycin treatment protected from the disease outcome. The highest hFMT engraftment was

observed after three repeated gavages, but seemed to have long-term effect on the gut microbiota composition (i.e. lowest *Bacteroides* spp. in the TSHR group compared to the respective controls). Surprisingly, it induced signs of eye disease in fewer mice than expected. Lab4 probiotics administration increased the *Actinobacteria* and the *Firmicutes* phyla, amongst others. Despite increasing the Tregs population, exacerbated autoimmune hyperthyroidism, potentially through an independent mechanism compared to the pathogenic one.

The same probiotic *consortium* was administered for six months along with the antithyroid treatment in GD/GO patients in a single-centre, placebo controlled trial. The gut microbiota of probiotic-treated GD/GO patients showed a more reduced *Firmicutes:Bacteroidetes* ratio when reaching the euthyroid timepoint compared to the placebo. Also, an increase of SCFA-producing bacteria (e.g. *Bifidobacterium* spp., *Eubacterium hallii* and *Coprococcus* spp.) occurred in probiotic-treated patients, which may have possibly prevented thyroid hormones fluctuations (i.e. fT4), instead observed in the placebo-receiving group.

Until recently, only few studies have investigated the contribution of the gut microbiota in thyroid autoimmune diseases [521]. While this study is the first presenting the role of the gut microbiome in GO mouse models, in the last year, however, two published studies addressed the gut microbiota in Hashimoto's thyroiditis (HT) patients [438, 444] and two studies addressed the gut microbiota in GD [439] and GO patients [447], respectively. I noted only few similarities between their results and those produced by the present work due to differences in the methodology but also in the cohort characteristics. In fact, they used primers against the V3-V4 regions of the 16S rRNA gene, which could lead to a different taxonomic identification [522]. Moreover, differences in the gut microbiota composition between Chinese and European populations (e.g. Danish) have been previously described [523].

6.1.2. Considerations on the 16S rRNA gene sequencing processing and data analysis

16S rRNA gene sequencing data can be a statistical challenge due to reasons summarized by Weiss and collaborators [524]. i) different numbers of sequences might be attributed to the efficiency of sequencing itself rather than to a true variation in the microbial composition, since biological samples are complex. Moreover, the increase of the sequencing depth can result in the discovery of more bacterial species; ii) The OTU table often contains a high proportion of zero values being defined as "sparse" or "zero-inflated" [354], resulting often in the uncertainty in the definition of rare OTU counts; and

iii) the resulting data is a small percentage of the original environment being sampled, thus we can refer to the amount of OTU as relative abundance, constraining the total number of rRNA gene sequences to a constant sum [524]. For such reasons, library normalization and pruning – or removal of low quantity OTUs - of the OTU table are most often conducted before statistical analysis.

Reads obtained in this work were of a good quality and, after alignment to the reference database, the mean Good's coverage was appreciable (i.e. calculated in Chapter 2). I'm confident that the depth of sequencing of the microbiota was sufficient to describe all the possible OTUs (sequenced-based rarefaction), and that the addition of any other samples would not increase the number of OTUs detected (sample-based rarefaction). In order to reduce differences in the library size, in Chapter 2, I opted for a subsampling or rarefying method in which each sample library size is reduced to the smallest one. It might be argued that subsampling can cause the loss of statistical power (type II-error) and, in turn, a possible increase of the number of false-positive differentially abundant taxa [525] However, it has been widely accepted in a large number of studies reported in the literature, supported by the majority of metataxonomics pipelines, e.g. [207, 208], and still retained as a good choice for normalization in a recent study [524].

However, results from Chapter 3 are not directly comparable with those obtained in the Chapter 2 since the bioinformatic pipeline used is different (Mothur [207] *vs*. QIIME [208]) and it employs a different taxonomic assignment (open reference OTU picking *vs*. closed-reference OTU picking, respectively). Such a change in the bioinformatic methodology was dictated by highly heterogeneous library sizes obtained from the manipulation study in Chapter 3, for which the cumulative sum-scaling (CSS) normalization [354] was preferred to the sub-sampling. The small size of some sequencing libraries obtained in Chapter 3 might be due to the chronic antibiotic treatment, which might have depleted also the amount of 16S rRNA gene template available for PCR; although the bacterial load cannot be directly estimated from the library size [526]. I also interestingly observed a doubled amount of processed reads in the antibiotic-treated samples (Table 3.3), possibly derived from either a low abundant 16S rRNA genetic template, or from a few but resistant bacterial species. However, only the quantification of the total bacterial load or the 16S rRNA gene sequencing using propidium monoazide (PMA) for death/alive bacterial discrimination [527] can resolve this observation.

The QIIME pipeline employed in Chapter 3 was performed also in the subsequent Chapter 4 and 5. This decision was dictated by an easier implementation of downstream

analyses such as the prediction of the metagenomic functions (Tax4Fun) and the SourceTracker using QIIME-derived OTU table instead of Mothur.

Prediction of the metagenomic functions from the 16S rRNA gene sequencing survey has been receiving an increasing interest, also due to its cost-effectiveness. Different pipelines are now available (PICRUSt [528], Tax4Fun [360] and Piphillin [529]), although no differences in terms of predicted functions/orthologs were observed between PICRUSt and Tax4Fun [352, 529], while some differences were observed using Piphillin, at least when using disease metadata [529]. Such a consistency in predicting metagenomic functions amongst bioinformatic tools may be due to: i) KEGG pathways and orthologs only imputed against known OTUs/functions, which constitutes also a limitation of the technique at the present, and ii) existing functional redundancy across bacterial species (i.e. different species encoding for the same functions), especially in stressed conditions [530].

With regard to the statistical approaches performed in Chapter 5, I'm fully aware that other methods are available for baseline-correction of a dataset. Another option, for example, could have been the use of mixed-effects models (MEMs). MEMs, by definition, would allow the introduction of random effects (e.g. each patient variability of the gut microbiota in response to a probiotics intake) to be modelled through random intercepts and/or through random slopes. The resulting standard error and P values will be adjusted and will represent the fixed effects taking into account the random variables. However, MEMs were not the focus of the analysis, also because of the small sample size.

6.1.3. Strengths and weaknesses of the present work

The present study benefited from the use of up-to-date tools and approaches, including microbiota manipulation using faecal material transplant (hFMT) and probiotics, as well as machine-learning algorithms, statistical analysis which evolved through the chapters and prediction of metagenomic functions. Moreover the following strengths are worth mentioning:

i) The first two results chapters involved the expertise in producing, replicating and manipulating a GO animal model. Therefore, we were the first in describing the possible role of the microbiota in the establishment but also in the replication of the animal model in different laboratories [322].

ii) Chapter 4 is based on a large European cohort of GD/GO patients, benefiting also from the collaborations with members of the EUGOGO team. In fact, 211 patients and 46 controls were initially enrolled in the study, of those 171 and 42 provided at least one

faecal samples. After removal of not-eligible patients, 105 patients and 41 controls were included in the analysis of the baseline samples.

iii) It was interesting to note that the GO mouse model and GD/GO patients showed some consistent patterns of the gut microbiome, despite anatomical differences, gut microbiota compositions and also the immune system between murine and humans [531]. In fact, the reduction of *Bacteroidetes* and genus *Bacteroides* was reported in both TSHR-mice and GD/GO patients compared to controls, which was furthermore observed in hFMT-immunised mice. In a more speculative manner also, *Akkermansia* spp. was enriched in Lab4-treated TSHR-immunised mice, showing hyperthyroidism but not developing signs of eye disease and in untreated GD patients with no signs of concomitant eye disease compared to healthy controls. However, GO mouse model and GD/GO patients differed in their response to the probiotics *consortium*, since it increased hyperthyroidism in mice but mitigated thyroid hormones fluctuations (i.e. fT4) in humans.

iv) Moreover, this study benefitted by another multi-omics study being performed within the INDIGO project. In [440], we combined circulating miRNAs and proteins to obtain a predictive panel of biomarkers for disease diagnosis and eye-disease prognosis. It was interesting to note similarities in some of the predicted metagenomic pathways with those obtained by miRNA and proteins, possibly supporting a common pathogenic mechanisms.

Besides strengths, I also identified some weaknesses:

i) In the comparison of the GO animal models in independent facilities presented in Chapter 1, I'm fully aware that the analysis lacks control samples from Centre 1 (βgal samples), and for that reason I focused on differences in the gut microbiota specifically in mice which underwent a protocol of immunization with the TSHR-plasmid, which have shown differences in the disease outcome, as described in the previous work [187]. Moreover, there was no faecal material left to perform a faecal material transfer between Centre 1 to Centre 2 mice, in order to confirm any protection/susceptibility conferred by the microbiota itself.

ii) The chronic vancomycin treatment prevented the production of the stimulating antibodies (TSAb), the hallmark of GD/GO, along with hyperthyroidism and signs of eye disease. However, whether this could help GD patients would require assessment of the effects of vancomycin administration at different stages of the immunisation procedure in mice. Also, the use of more targeted antibiotics would better dissect which bacterial species have a major protective role in GO. In contrast, although hFMT induced TSAb it prevented the hyperthyroidism and the eye disease. This surprising result may be due to our using the faecal samples from sight-threatening GO patients to produce the freeze-

dried material, as they are the most severe form of GO. However, in such a condition, patients have been treated with anti-thyroid drugs and/or cortisones for years and underwent ocular decompression surgery, and they do not present an active form of the eye disease. Moreover, the majority of donor patients currently smoked at the time of sample collection and smoking is known to alter the gut microbiota (reviewed in [441]). Also, I demonstrated that the microbiota composition changes based on thyroid activity (hyperthyroid *vs*. euthyroid patients) or a more active eye disease; thus, hFMT using material from different stages of disease might be also informative. Moreover, pre-treatment with antibiotics or use of GF animals may help reducing heterogeneity in the engraftment.

iii) The study presented in Chapter 4 lacks an adequate number of first-diagnosis untreated patients. Moreover, to fully understand the role of thyroid hormones in shaping the gut microbiota, it would have been of interest having other forms of hyperthyroidism included in the study, such as the multinodular goitre. The present cross-sectional study enrolled patients and matched healthy controls from four European centres. Although the diet consumed in those nations is prevalently a Western diet, differences in the gut microbiota can be also due to different intake of dietary proteins, carbohydrates and fibres. A diet and lifestyle questionnaire was provided to each patient at the moment of the enrolment. Not all of questionnaire were returned. Moreover, it was based on the patient' self-assessment and not submitted with the help of a dietician. Therefore, those data were not considered in the analyses, although we value the importance. At present, an ongoing study is focussing on the role of food antigens in breaking down the immune tolerance in GD/GO patients (Covelli D, personal communication).

iv) The probiotic trial presented in Chapter 5 was under-powered. The initial power calculation, in fact, required the presence of at least 31 patients in each arm, "to be able to detect a result present in 40% of cases and only 5% of controls" ("Sinossi" for Comitato Etico Milano). Moreover, there was a low-compliance in returning the faecal samples at further timepoints after baseline. Although not commonly used, there are some approaches available to calculate the power calculation for microbiome-based studies [532, 533]. Interestingly, the work of Spaggiari et al. [503] providing VSL#3 to hypothyroid patients during levothyroxine treatment included 39 and 41 patients in each arm. One may argue that the lack of highly significant effects on thyroid hormone levels may be due to the underpowered study. It would be therefore of interest to perform a bigger trial, potentially multi-centre, in order to include more patients in each arm and to potentially obtain more faecal samples in further timepoints for the microbiome analysis.

6.1.2. Future perspectives

As often occur in cross-sectional case-control studies, patients enrolled already present some signs of disease and therefore, the composition of their gut microbiota is already to be considered to as a “disease-associated gut microbiota”. Moreover, as far as autoimmune diseases are concerned, it is of interest assessing the composition of the gut microbiota before the breakdown of the immune tolerance, in order to obtain a panel of bacteria able to predict the risk of developing and/or the prognosis of that disease. Studies on the animal models, as the one presented in Chapter 3, are therefore necessary. As being performed in other diseases such as IBD [534] or in Parkinson’s disease (ClinicalTrials.gov Identifier: NCT03645226), high-risk first-degree relatives could be followed over time to look for specific patterns determining the disease insurgence, or its protection. In the case of GD, however, it could be of a great interest analysing the gut microbiota of multiple sclerosis (MS) patients undergoing the Campath-1H (Alemtuzumab) treatment in a longitudinal manner. As described in Chapter 1 par. 1.4.2, MS-Alemtuzumab treated patients are at a high risk of developing GD in the three years after treatment, during the immune reconstitution phase.

In the present study we considered the gut microbiota as an environmental factor, possibly conferring susceptibility in the breakdown of the immune tolerance. Patients enrolled in the study were genetically heterogeneous. We are aware that the genetic background is also conferring protection or susceptibility for developing such autoimmune conditions, as described in Chapter 1 par. 1.3.1. The link between the genetic background and the gut microbiota composition in the GO mouse model was described in our recent work [366]. C57BL/6J mouse strain, characterized by a different MHC/HLA genotype compared to that of the BALB/c (used in both Chapter 2 and 3), showed a more resistant phenotype after TSHR-immunisation. Also the gut microbiota between C57BL/6J and BALB/c mice being immunised with TSHR was different. It would be therefore of interest performing the HLA genotyping on the enrolled patients and perform a microbiome analysis in genetic susceptible and genetic non-susceptible patients. The effect of gender moreover can be extended to a further characterization of sex hormones (progesterone, oestrogen, oxytocin and testosterone). The interaction between these hormones and the gut microbiota in GD/GO patients can be investigated through their quantification in the blood and by obtaining a more accurate description of the menstrual/menopausal phase of the female patients.

As expected, the differential abundant taxonomies identified in both GO mouse model and GO patients interacted to some extent with both endocrine (i.e. TSH, fT3 and fT4) and immunological parameters (i.e. anti-TSHR antibodies, IgG and IgA). Although GD is

an antibody-based autoimmunity, also T cells play an important role in the disease pathogenesis (see Chapter 1 par. 1.1.4). Apart from the proportion of Tregs at the draining lymph nodes observed in the mouse model, the Tregs/Th17 T cell populations were not quantified in the murine gut mucosa or in GD/GO patients. It would be of interest, in fact, performing a similar immunophenotyping to that described in multiple sclerosis patients [420].

This work was based on the 16S rRNA gene sequencing. This high throughput and cost-effective approach allowed the sequencing of hundreds of samples and from their analysis I obtained the identity of the bacterial taxa present in the samples and from their relative abundance I obtained estimation on the diversity of the bacterial communities and their differential abundance between groups. Recent tools enabled us to predict the metagenomic pathways in which those bacterial taxonomies may be involved. Despite providing a broad information, such a prediction of the metagenomic pathways may not be accurate enough to understand the precise molecular mechanisms. Thus, a metagenomic approach, or the whole-genome sequencing would be necessary, in at least in a target number of samples, to confirm observed data. We tested a small cohort of patients for bacterial-derived metabolites through NMR, and we observed differences in the metabolite profiles of moderate-severe/sight-threatening GO patients compared to controls. It would be of interest extending such analysis to a larger cohort, including the quantification of SCFAs to draw more mechanistic conclusions on our first set of data.

6.2. CONCLUSIONS

Our data illustrate substantial perturbation of the gut microbiota microbiome associated to GD and GO in both mouse model and patients, with some similarities. Future studies are needed to dissect the mechanistic role of the gut microbiome in activating the immune system, determining the onset of GD/GO. Collectively, the present work provides new insights in understanding a multifactorial disease proposing a new “gut-thyroid-eye” axis (Figure 6.2), and, even if preliminary, they would be of a potential help for the early diagnosis and prognosis of the eye-disease severity.

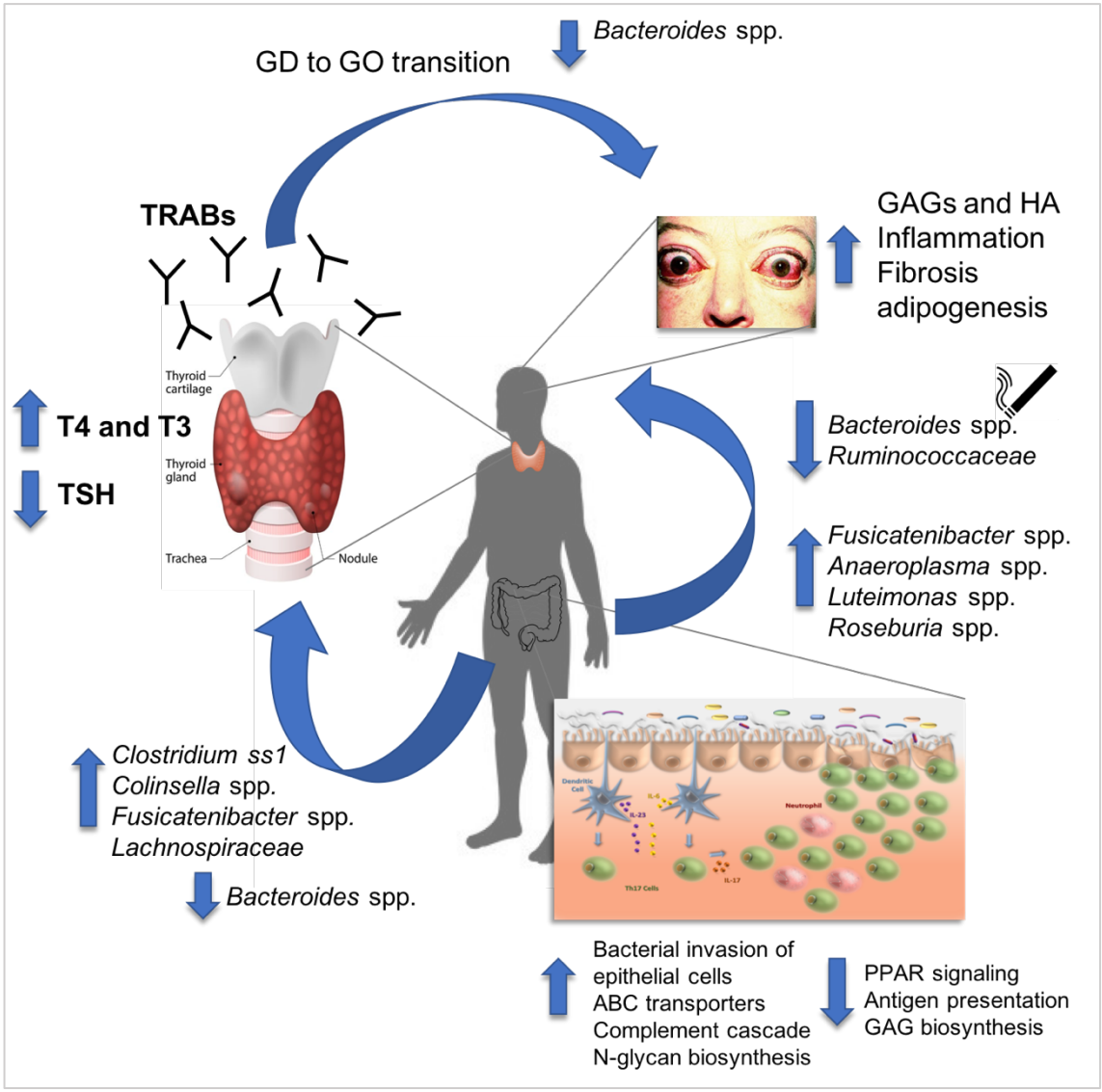

Figure 6.2. Summary of the thyroid, the eye and the gut relationship in Graves' disease and Graves' orbitopathy.

7. References

1. Rose N.R., *The discovery of thyroid autoimmunity.* Immunology today, 1991. **12**(5): p. 167-168.

2. Root-Bernstein R. and Fairweather D., *Unresolved issues in theories of autoimmune disease using myocarditis as a framework.* Journal of theoretical biology, 2015. **375**: p. 101-123.

3. Hassfeld W. and Rheumatology G., *Autoimmune response to the spliceosome.* … & Rheumatology, 1995. 10.1002/art.1780380610.

4. Sulzer D.,Alcalay R.N.,Garretti F.,Cote L.,Kanter E.,Agin-Liebes J.,Liong C.,McMurtrey C.,Hildebrand W.H.,Mao X.,Dawson V.L.,Dawson T.M.,Oseroff C.,Pham J.,Sidney J.,Dillon M.B.,Carpenter C.,Weiskopf D.,Phillips E.,Mallal S.,Peters B.,Frazier A.,Arlehamn C.S., and Sette A., *T cells from patients with Parkinson's disease recognize α-synuclein peptides.* Nature, 2017. **546**(7660): p. 656.

5. Lerner A.,Jeremias P., and Dis M.-T.J., *The world incidence and prevalence of autoimmune diseases is increasing.* Int J Celiac Dis, 2015.

6. Maia A.,Kim B.W.,Huang S.A.,Harney J.W., and Larsen R.P., *Type 2 iodothyronine deiodinase is the major source of plasma T3 in euthyroid humans.* Journal of Clinical Investigation, 2005. **115**(9): p. 2524-2533.

7. Bianco A.C. and Kim B.W., *Deiodinases: implications of the local control of thyroid hormone action.* Journal of Clinical Investigation, 2006. **116**(10): p. 2571-2579.

8. Maia A.,Goemann I.,Meyer E.L., and Wajner S., *Type 1 iodothyronine deiodinase in human physiology and disease Deiodinases: the balance of thyroid hormone.* Journal of Endocrinology, 2011. **209**(3): p. 283-297.

9. Afzali B.,Lombardi G.,Lechler R.I., and Lord G.M., *The role of T helper 17 (Th17) and regulatory T cells (Treg) in human organ transplantation and autoimmune disease.* Clinical & Experimental Immunology, 2007. **148**(1): p. 32-46.

10. van der Spek A.H.,Fliers E., and Boelen A., *The classic pathways of thyroid hormone metabolism.* Molecular and Cellular Endocrinology, 2017. **458**: p. 29-38.

11. Gauthier K.,Chassande O.,Plateroti M.,Roux J.P.,Legrand C.,Pain B.,Rousset B.,Weiss R.,Trouillas J., and Samarut J., *Different functions for the thyroid hormone receptors TRalpha and TRbeta in the control of thyroid hormone production and post-natal development.* EMBO J, 1999. **18**(3): p. 623-31.

12. Horlein A.J.,Naar A.M.,Heinzel T.,Torchia J.,Gloss B.,Kurokawa R.,Ryan A.,Kamei Y.,Soderstrom M.,Glass C.K., and et al., *Ligand-independent repression by the thyroid hormone receptor mediated by a nuclear receptor co-repressor.* Nature, 1995. **377**(6548): p. 397-404.

13. Zhang J. and Lazar M.A., *The mechanism of action of thyroid hormones.* Annu Rev Physiol, 2000. **62**: p. 439-66.

14. Grontved L.,Waterfall J.J.,Kim D.W.,Baek S.,Sung M.H.,Zhao L.,Park J.W.,Nielsen R.,Walker R.L.,Zhu Y.J.,Meltzer P.S.,Hager G.L., and Cheng S.Y., *Transcriptional activation by the thyroid hormone receptor through ligand-dependent receptor recruitment and chromatin remodelling.* Nat Commun, 2015. **6**: p. 7048.

15. Lazarus J., *Thyroid Regulation and Dysfunction in the Pregnant Patient*, in *Endotext*, K.R. Feingold, et al., Editors. 2000: South Dartmouth (MA).

16. Covelli D. and Ludgate M., *The thyroid, the eyes and the gut: a possible connection.* Journal of endocrinological investigation, 2017. 10.1007/s40618-016-0594-6.

17. Sun X.,Lu L.,Yang R.,Li Y.,Shan L., and Wang Y., *Increased Incidence of Thyroid Disease in Patients with Celiac Disease: A Systematic Review and Meta-Analysis.* PloS one, 2016. **11**(12): p. e0168708.

18. Ponto K.A.,Schuppan D.,Zwiener I.,Binder H.,Mirshahi A.,Diana T.,Pitz S.,Pfeiffer N., and Kahaly G.J., *Thyroid-associated orbitopathy is linked to gastrointestinal autoimmunity.* Clin Exp Immunol, 2014. **178**(1): p. 57-64.

19. Rousseau-Merck M.F.,Misrahi M.,Loosfelt H., and Genomics A.-M., *Assignment of the human thyroid stimulating hormone receptor (TSHR) gene to chromosome 14q31.* Genomics, 1990.

20. Crisp M.,Starkey K.J.,Lane C., and visual science H.-J., *Adipogenesis in thyroid eye disease.* … & visual science, 2000.

21. Feliciello A.,Ciullo I.,Fenzi G.F.,Bonavolontà G.,Porcellini A., and Avvedimento E.V., *Expression of thyrotropin-receptor mRNA in healthy and Graves' disease retro-orbital tissue.* The Lancet, 1993. **342**(8867): p. 337-338.

22. Couët J.,de Bernard S.,Loosfelt H., and Biochemistry S.-B., *Cell surface protein disulfide-isomerase is involved in the shedding of human thyrotropin receptor ectodomain.* Biochemistry, 1996. 10.1021/bi961359w.

23. Chazenbalk G.D.,Jaume J.C., and of Biological … M.-S.M., *Engineering the human thyrotropin receptor ectodomain from a non-secreted form to a secreted, highly immunoreactive glycoprotein that neutralizes autoantibodies in ….* Journal of Biological …, 1997. 10.1074/jbc.272.30.18959.

24. Morshed S.A.,Latif R., and Davies T.F., *Characterization of Thyrotropin Receptor Antibody-Induced Signaling Cascades.* Endocrinology, 2009. **150**(1): p. 519-529.

25. Davies T.F.,Ando T.,Lin R.Y.,Tomer Y., and Latif R., *Thyrotropin receptor-associated diseases: from adenomata to Graves disease.* J Clin Invest, 2005. **115**(8): p. 1972-83.

26. Sanders J.,Miguel R.N.,Bolton J., and … B.-A., *Molecular interactions between the TSH receptor and a thyroid-stimulating monoclonal autoantibody.* …, 2007. 10.1089/thy.2007.0041.

27. Chen C.-R.,Pichurin P.,Nagayama Y.,Latrofa F.,Rapoport B., and McLachlan S.M., *The thyrotropin receptor autoantigen in Graves disease is the culprit as well as the victim.* Journal of Clinical Investigation, 2003. **111**(12): p. 1897-1904.

28. Chazenbalk G.D.,Pichurin P.,Chen C.-R.,Latrofa F.,Johnstone A.P.,McLachlan S.M., and Rapoport B., *Thyroid-stimulating autoantibodies in Graves disease preferentially recognize the free A subunit, not the thyrotropin holoreceptor.* Journal of Clinical Investigation, 2002. **110**(2): p. 209-217.

29. Ando T.,Latif R.,Daniel S.,Eguchi K., and Endocrinology D.-T.F., *Dissecting linear and conformational epitopes on the native thyrotropin receptor.* Endocrinology, 2004.

30. Seetharamaiah G.S. and of … D.-J.S., *Requirement of glycosylation of the human thyrotropin receptor ectodomain for its reactivity with autoantibodies in patients' sera.* The Journal of …, 1997.

31. Morshed S.A.,Ando T.,Latif R., and Endocrinology D.-T.F., *Neutral antibodies to the TSH receptor are present in Graves' disease and regulate selective signaling cascades.* Endocrinology, 2010.

32. Watanabe Y.,Tahara K.,Hirai A.,Tada H., and … K.-L.D., *Subtypes of anti-TSH receptor antibodies classified by various assays using CHO cells expressing wild-type or chimeric human TSH receptor.* …, 1997. 10.1089/thy.1997.7.13.

33. Sanders J.,Evans M.,Premawardhana L.D.,Depraetere H.,Jeffreys J.,Richards T.,Furmaniak J., and Rees Smith B., *Human monoclonal thyroid stimulating autoantibody.* Lancet, 2003. **362**(9378): p. 126-128.

34. Miguel R.N.,Sanders J., and of molecular … F.-J., *Glycosylation pattern analysis of glycoprotein hormones and their receptors.* Journal of molecular …, 2017. 10.1530/JME-16-0169.

35. Miguel N.R.,Sanders J.,Chirgadze D.Y.,Furmaniak J., and Smith R.B., *Thyroid stimulating autoantibody M22 mimics TSH binding to the TSH receptor leucine rich*

domain: a comparative structural study of protein–protein interactions. Journal of Molecular Endocrinology, 2009. **42**(5): p. 381-395.

36. McLachlan S.M. and Rapoport B., *Breaking tolerance to thyroid antigens: changing concepts in thyroid autoimmunity.* Endocrine reviews, 2014. **35**(1): p. 59-105.

37. Vaidya B. and Pearce S.H.S., *Diagnosis and management of thyrotoxicosis.* BMJ, 2014. **349**(aug21 7).

38. Marchant B.,Lees J.F., and Alexander W.D., *Antithyroid drugs.* Pharmacol Ther B, 1978. **3**(3): p. 305-48.

39. Lazarus J.H., *Epidemiology of Graves' orbitopathy (GO) and relationship with thyroid disease.* Best Practice & Research Clinical Endocrinology & Metabolism, 2012. **26**(3): p. 273-279.

40. Draman M. and Ludgate M., *Thyroid eye disease- an update.* Expert Review of Ophthalmology, 2016. **11**(4): p. 1-12.

41. Stan M.N. and Thyroid B.-R.S., *Risk factors for development or deterioration of Graves' ophthalmopathy.* Thyroid, 2010. 10.1089/thy.2010.1634.

42. Zhang L.,Bowen T.,Grennan-Jones F.,Paddon C.,Giles P.,Webber J.,Steadman R., and Ludgate M., *Thyrotropin receptor activation increases hyaluronan production in preadipocyte fibroblasts: contributory role in hyaluronan accumulation in thyroid dysfunction.* The Journal of biological chemistry, 2009. **284**(39): p. 26447-26455.

43. Zhang L.,Grennan-Jones F.,Lane C.,Rees D.A.,Dayan C.M., and Ludgate M., *Adipose tissue depot-specific differences in the regulation of hyaluronan production of relevance to Graves' orbitopathy.* The Journal of clinical endocrinology and metabolism, 2012. **97**(2): p. 653-662.

44. Lantz M.,Planck T.,Åsman P., and Hallengren B., *Increased TRAb and/or Low Anti-TPO Titers at Diagnosis of Graves' Disease are Associated with an Increased Risk of Developing Ophthalmopathy after Onset.* Experimental and Clinical Endocrinology & Diabetes, 2014. **122**(02): p. 113-117.

45. Zhang L.,Masetti G.,Colucci G.,Salvi M.,Covelli D.,Eckstein A.,Kaiser U.,Draman M.,Muller I.,Ludgate M.,Lucini L., and Biscarini F., *Combining micro-RNA and protein sequencing to detect robust biomarkers for Graves' disease and orbitopathy.* Scientific Reports, 2018. **8**(1): p. 8386.

46. Zhang L.,Baker G.,Janus D.,Paddon C.A.,Fuhrer D., and Ludgate M., *Biological Effects of Thyrotropin Receptor Activation on Human Orbital Preadipocytes.* Investigative Ophthalmology & Visual Science, 2006. **47**(12): p. 5197-5203.

47. Kumar S.,Nadeem S., and of molecular … S.-M.N., *A stimulatory TSH receptor antibody enhances adipogenesis via phosphoinositide 3-kinase activation in orbital preadipocytes from patients with Graves' ….* Journal of molecular …, 2011. 10.1530/JME-11-0006.

48. Zhang L.,Grennan-Jones F.,Draman M.S.,Lane C.,Morris D.,Dayan C.M.,Tee A.R., and Ludgate M., *Possible Targets for Nonimmunosuppressive Therapy of Graves' Orbitopathy.* The Journal of Clinical Endocrinology & Metabolism, 2014. **99**(7).

49. Zhang L.,Ji Q.H.,Ruge F., and of … L.-C., *Reversal of pathological features of Graves' orbitopathy by activation of forkhead transcription factors, FOXOs.* The Journal of …, 2016.

50. Weightman D.R.,Perros P., and Autoimmunity S.-I.H., *Autoantibodies to IGF-1 binding sites in thyroid associated ophthalmopathy.* Autoimmunity, 1993. 10.3109/08916939309014643.

51. Minich W.B.,Dehina N., and of … W.-T., *Autoantibodies to the IGF1 receptor in Graves' orbitopathy.* The Journal of …, 2013.

52. Tsui S.,Naik V.,Hoa N., and of … H.-C.J., *Evidence for an association between thyroid-stimulating hormone and insulin-like growth factor 1 receptors: a tale of two antigens implicated in Graves' disease.* The Journal of …, 2008. 10.4049/jimmunol.181.6.4397.

53. Mourits M.P.,Prummel M.F.,Wiersinga W.M., and Koornneef L., *Clinical activity score as a guide in the management of patients with Graves' ophthalmopathy.* Clin Endocrinol (Oxf), 1997. **47**(1): p. 9-14.

54. Bartalena L.,Baldeschi L.,Boboridis K.,Eckstein A.,Kahaly G.J.,Marcocci C.,Perros P.,Salvi M.,Wiersinga W.M., and European Group on Graves O., *The 2016 European Thyroid Association/European Group on Graves' Orbitopathy Guidelines for the Management of Graves' Orbitopathy.* Eur Thyroid J, 2016. **5**(1): p. 9-26.

55. Marcocci C.,Kahaly G.J.,Krassas G.E.,Bartalena L.,Prummel M.,Stahl M.,Altea M.A.,Nardi M.,Pitz S.,Boboridis K.,Sivelli P.,von Arx G.,Mourits M.P.,Baldeschi L.,Bencivelli W.,Wiersinga W., and European Group on Graves O., *Selenium and the course of mild Graves' orbitopathy.* N Engl J Med, 2011. **364**(20): p. 1920-31.

56. Weetman A.P.,Yateman M.E., and of … E.-P.A., *Thyroid-stimulating antibody activity between different immunoglobulin G subclasses.* The Journal of …, 1990. 10.1172/JCI114768.

57. Peng D.,Xu B.,Wang Y.,Guo H., and One J.-Y., *A high frequency of circulating th22 and th17 cells in patients with new onset graves' disease.* PloS one, 2013. 10.1371/journal.pone.0068446.

58. Salvi M.,Pedrazzoni M.,Girasole G.,Giuliani N.,Minelli R.,Wall, and Roti E., *Serum concentrations of proinflammatory cytokines in Graves' disease: effect of treatment, thyroid function, ophthalmopathy and cigarette smoking.* European journal of endocrinology, 2000. **143**(2): p. 197-202.

59. Salvi M.,Girasole G., and of … P.-M., *Increased serum concentrations of interleukin-6 (IL-6) and soluble IL-6 receptor in patients with Graves' disease.* The Journal of …, 1996.

60. of Medicine W.-A.P., *Graves' disease.* New England Journal of Medicine, 2000.

61. Li Y.,Wang Z.,Yu T.,Chen B.,Zhang J.,Huang K., and Huang Z., *Increased Expression of IL-37 in Patients with Graves' Disease and Its Contribution to Suppression of Proinflammatory Cytokines Production in Peripheral Blood Mononuclear Cells.* PloS one, 2014. **9**(9).

62. Morshed S.A.,Latif R., and Davies T.F., *Delineating the autoimmune mechanisms in Graves' disease.* Immunologic research, 2012. **54**(1-3): p. 191-203.

63. Yin X.,Sachidanandam R.,Morshed S.,Latif R.,Shi R., and Davies T.F., *mRNA-Seq Reveals Novel Molecular Mechanisms and a Robust Fingerprint in Graves' Disease.* The Journal of Clinical Endocrinology & Metabolism, 2014. **99**(10).

64. Rose N.R., *Molecular mimicry and clonal deletion: A fresh look.* Journal of theoretical biology, 2014. 10.1016/j.jtbi.2014.08.034.

65. Burnet S., *The clonal selection theory of acquired immunity.* Vanderbilt University Press Nashville, 1959.

66. Kappler J.W.,Roehm N., and Cell M.-P., *T cell tolerance by clonal elimination in the thymus.* Cell, 1987.

67. Stefan M.,Wei C.,Lombardi A.,Li C.,Concepcion E.S.,Inabnet W.B.,Owen R.,Zhang W., and Tomer Y., *Genetic–epigenetic dysregulation of thymic TSH receptor gene expression triggers thyroid autoimmunity.* Proceedings of the National Academy of Sciences, 2014. **111**(34): p. 12562-12567.

68. Colobran R.,Armengol M.P., and molecular … F.-R., *Association of an SNP with intrathymic transcription of TSHR and Graves' disease: a role for defective thymic tolerance.* Human molecular …, 2011.

69. McLachlan S.M.,Aliesky H.A.,Banuelos B.,Lesage S.,Collin R., and Rapoport B., *High-level intrathymic thyrotrophin receptor expression in thyroiditis-prone mice protects against the spontaneous generation of pathogenic thyrotrophin receptor autoantibodies.* Clinical & Experimental Immunology, 2017. **188**(2): p. 243-253.

70. Ramsey C.,Winqvist O., and molecular … P.-L., *Aire deficient mice develop multiple features of APECED phenotype and show altered immune response.* Human molecular …, 2002.

71. Ramsey C.,Hässler S., and journal of … M.-P., *Increased antigen presenting cell-mediated T cell activation in mice and patients without the autoimmune regulator.* European journal of …, 2006. 10.1002/eji.200535240.

72. Mathis D. and Benoist C., *A decade of AIRE.* Nature reviews. Immunology, 2007. **7**(8): p. 645-650.

73. cell G.J.V., *Negative selection of lymphocytes.* Cell, 1994.

74. Prak L.E.T. and of the York … M.-M., *B cell receptor editing in tolerance and autoimmunity.* Annals of the New York …, 2011. 10.1111/j.1749-6632.2010.05877.x.

75. Brink R., *The imperfect control of self-reactive germinal center B cells.* Current Opinion in Immunology, 2014. **28**: p. 97101.

76. Li Z.,Woo C.J.,Iglesias-Ussel M.D.,Ronai D., and Scharff M.D., *The generation of antibody diversity through somatic hypermutation and class switch recombination.* Genes & Development, 2004. **18**(1): p. 1-11.

77. Enouz S.,Carrié L.,Merkler D.,Bevan M.J., and Zehn D., *Autoreactive T cells bypass negative selection and respond to self-antigen stimulation during infection.* The Journal of Experimental Medicine, 2012. **209**(10): p. 1769-1779.

78. Avrameas S.,Dighiero G., and de Pasteur … L.-P., *Studies on natural antibodiesand autoantibodies.* Annales de l'Institut Pasteur …, 1983.

79. Söderlin M.K.,Kautiainen H.,Puolakkainen M.,Hedman K.,Söderlund-Venermo M.,Skogh T., and Leirisalo-Repo M., *Infections preceding early arthritis in southern Sweden: a prospective population-based study.* The Journal of rheumatology, 2003. **30**(3): p. 459-464.

80. Sheikh K.A.,Zhang G.,Gong Y., and Schnaar R.L., *An anti-ganglioside antibody-secreting hybridoma induces neuropathy in mice.* Annals of …, 2004. 10.1002/ana.20173.

81. Padoa C.J.,Larsen S.L.,Hampe C.S.,Gilbert J.A.,Dagdan E.,Hegedus L.,Dunn-Walters D., and Banga J.P., *Clonal relationships between thyroid-stimulating hormone receptor-stimulating antibodies illustrate the effect of hypermutation on antibody function.* Immunology, 2010. **129**(2): p. 300-308.

82. Chazenbalk G.D.,Pichurin P.N.,Guo J.,Rapoport B., and McLachlan S.M., *Interactions between the mannose receptor and thyroid autoantigens.* Clinical & Experimental Immunology, 2005. **139**(2): p. 216-224.

83. Anderton S.,Burkhart C.,Metzler B., and Wraith D., *Mechanisms of central and peripheral T-cell tolerance: lessons from experimental models of multiple sclerosis.* Immunol Rev, 1999. **169**: p. 123-37.

84. Watanabe-Fukunaga R.,Brannan C.I.,Copeland N.G.,Jenkins N.A., and Nagata S., *Lymphoproliferation disorder in mice explained by defects in Fas antigen that mediates apoptosis.* Nature, 1992. **356**(6367): p. 314-7.

85. Jackson C.E.,Fischer R.E.,Hsu A.P.,Anderson S.M.,Choi Y.,Wang J.,Dale J.K.,Fleisher T.A.,Middelton L.A.,Sneller M.C.,Lenardo M.J.,Straus S.E., and Puck J.M., *Autoimmune lymphoproliferative syndrome with defective Fas: genotype influences penetrance.* Am J Hum Genet, 1999. **64**(4): p. 1002-14.

86. Noack M. and Miossec P., *Th17 and regulatory T cell balance in autoimmune and inflammatory diseases.* Autoimmunity Reviews, 2014. **13**(6).

87. Chen W.J.,Jin W.,Hardegen N.,Lei K., and of … L.-L., *Conversion of peripheral CD4+ CD25− naive T cells to CD4+ CD25+ regulatory T cells by TGF-β induction of transcription factor Foxp3.* Journal of …, 2003. 10.1084/jem.20030152.

88. Rifa'i M.,Kawamoto Y.,Nakashima I., and Suzuki H., *Essential Roles of CD8+CD122+ Regulatory T Cells in the Maintenance of T Cell Homeostasis.* The Journal of Experimental Medicine, 2004. **200**(9): p. 1123-1134.

89. Yang J.,Sundrud M.S.,Skepner J., and in pharmacological Y.-T., *Targeting Th17 cells in autoimmune diseases.* Trends in pharmacological …, 2014.

90. Bettelli E.,Carrier Y.,Gao W.,Korn T.,Strom T.B., and Nature O.-M., *Reciprocal developmental pathways for the generation of pathogenic effector TH17 and regulatory T cells.* Nature, 2006. 10.1038/nature04753.

91. Zhou L.,Lopes J.E.,Chong M.M.W.,Ivanov, II, and Nature M.-R., *TGF-β-induced Foxp3 inhibits TH17 cell differentiation by antagonizing RORγt function.* Nature, 2008.

92. Volpe E.,Servant N.,Zollinger R., and Nature … B.-S.I., *A critical function for transforming growth factor-β, interleukin 23 and proinflammatory cytokines in driving and modulating human TH-17 responses.* Nature …, 2008. 10.1038/ni.1613.

93. Gaffen S.L.,Jain R.,Garg A.V., and Cua D.J., *The IL-23-IL-17 immune axis: from mechanisms to therapeutic testing.* Nature Reviews Immunology, 2014. **14**(9): p. 585-600.

94. Ruddy M.J.,Wong G.C.,Liu X.K., and of Biological … Y.-H., *Functional cooperation between interleukin-17 and tumor necrosis factor-α is mediated by CCAAT/enhancer-binding protein family members.* Journal of Biological …, 2004. 10.1074/jbc.M308809200.

95. Mao C.,Wang S.,Xiao Y.,Xu J.,Jiang Q.,Jin M.,Jiang X.,Guo H.,Ning G., and Zhang Y., *Impairment of regulatory capacity of CD4+CD25+ regulatory T cells mediated by dendritic cell polarization and hyperthyroidism in Graves' disease.* J Immunol, 2011. **186**(8): p. 4734-43.

96. Rosser E.C. and Mauri C., *Regulatory B cells: origin, phenotype, and function.* Immunity, 2015. **42**(4): p. 607-12.

97. Carter N.A.,Vasconcellos R.,Rosser E.C.,Tulone C.,Munoz-Suano A.,Kamanaka M.,Ehrenstein M.R.,Flavell R.A., and Mauri C., *Mice lacking endogenous IL-10-producing regulatory B cells develop exacerbated disease and present with an increased frequency of Th1/Th17 but a decrease in regulatory T cells.* J Immunol, 2011. **186**(10): p. 5569-79.

98. Flores-Borja F.,Bosma A.,Ng D.,Reddy V.,Ehrenstein M.R.,Isenberg D.A., and Mauri C., *CD19+CD24hiCD38hi B cells maintain regulatory T cells while limiting TH1 and TH17 differentiation.* Sci Transl Med, 2013. **5**(173): p. 173ra23.

99. Matsumoto K.,Ogawa M.,Suzuki J.,Hirata Y.,Nagai R., and Isobe M., *Regulatory T lymphocytes attenuate myocardial infarction-induced ventricular remodeling in mice.* Int Heart J, 2011. **52**(6): p. 382-7.

100. Zha B.,Wang L.,Liu X.,Liu J.,Chen Z.,Xu J.,Sheng L.,Li Y., and Chu Y., *Decrease in proportion of CD19+ CD24(hi) CD27+ B cells and impairment of their suppressive function in Graves' disease.* PloS one, 2012. **7**(11): p. e49835.

101. Iwata Y.,Matsushita T.,Horikawa M.,Dilillo D.J.,Yanaba K.,Venturi G.M.,Szabolcs P.M.,Bernstein S.H.,Magro C.M.,Williams A.D.,Hall R.P.,St Clair E.W., and Tedder T.F., *Characterization of a rare IL-10-competent B-cell subset in humans that parallels mouse regulatory B10 cells.* Blood, 2011. **117**(2): p. 530-41.

102. Shi F.D.,Ljunggren H.G., and Sarvetnick N., *Innate immunity and autoimmunity: from self-protection to self-destruction.* Trends in immunology, 2001.

103. Feero W.G.,Guttmacher A.E., and Cho J.H., *Genomics and the multifactorial nature of human autoimmune disease.* New England Journal …, 2011.

104. Kordjazy N.,Haj-Mirzaian A., and Pharmacological … H.-M.-A., *Role of Toll-Like Receptors in Inflammatory Bowel Disease.* Pharmacological …, 2017.

105. Duffy L. and and therapy O.R.-S.C., *Toll-like receptors in the pathogenesis of autoimmune diseases: recent and emerging translational developments.* ImmunoTargets and therapy, 2016.

106. Xiao W.,Liu Z.,Lin J.,Xiong C.,Li J.,Wu K.,Ma Y.,Gong Y., and Liu Z., *Association of TLR4 and TLR5 gene polymorphisms with Graves' disease in Chinese Cantonese population.* Human immunology, 2014. **75**(7): p. 609-613.

107. Liao W.L.,Chen R.H., and medical … L.-H.J., *Toll-like receptor gene polymorphisms are associated with susceptibility to Graves' ophthalmopathy in Taiwan males.* BMC medical …, 2010.

108. Dwivedi M.,Kumar P.,Laddha N.C., and Kemp E.H., *Induction of regulatory T cells: A role for probiotics and prebiotics to suppress autoimmunity.* Autoimmun Rev, 2016. **15**(4): p. 379-92.

109. Pillai S., *Rethinking mechanisms of autoimmune pathogenesis.* Journal of Autoimmunity, 2013. **45**: p. 97-103.

110. Vladutiu A.O. and Immunogenetics R.-N.R., *HL-A antigens: association with disease.* Immunogenetics, 1974.

111. Vladutiu A.O. and Science R.-N.R., *Autoimmune murine thyroiditis relation to histocompatibility (H-2) type.* Science, 1971. 10.1126/science.174.4014.1137.

112. Ploski R.,Szymanski K., and genomics B.-T., *The genetic basis of graves' disease.* Current genomics, 2011.

113. Ban Y.,Davies T.F.,Greenberg D.A.,Concepcion E.S.,Osman R.,Oashi T., and Tomer Y., *Arginine at position 74 of the HLA-DR beta1 chain is associated with Graves' disease.* Genes and immunity, 2004. **5**(3): p. 203-208.

114. Huber A.K.,Jacobson E.M.,Jazdzewski K.,Concepcion E.S., and Tomer Y., *Interleukin (IL)-23 Receptor Is a Major Susceptibility Gene for Graves' Ophthalmopathy: The IL-23/T-helper 17 Axis Extends to Thyroid Autoimmunity.* The Journal of Clinical Endocrinology & Metabolism, 2008. **93**(3): p. 1077-1081.

115. Chentoufi A.A. and Diabetes P.-C., *Insulin expression levels in the thymus modulate insulin-specific autoreactive T-cell tolerance: the mechanism by which the IDDM2 locus may predispose to diabetes.* Diabetes, 2002. 10.2337/diabetes.51.5.1383.

116. Tomer Y., *Mechanisms of autoimmune thyroid diseases: from genetics to epigenetics.* Pathology: Mechanisms of Disease, 2014. **9**(1): p. 147-156.

117. Tomer Y., *Genetic susceptibility to autoimmune thyroid disease: past, present, and future.* Thyroid : official journal of the American Thyroid Association, 2010. **20**(7): p. 715-725.

118. Dechairo B.M.,Zabaneh D.,Collins J., and of … B.-O., *Association of the TSHR gene with Graves' disease: the first disease specific locus.* European journal of …, 2005. 10.1038/sj.ejhg.5201485.

119. Chu X.,Pan C.M.,Zhao S.X.,Liang J., and Nature … G.-G.Q., *A genome-wide association study identifies two new risk loci for Graves' disease.* Nature …, 2011. 10.1038/ng.898.

120. Immunology F.-E.N., *The X-files in immunity: sex-based differences predispose immune responses.* Nature Reviews Immunology, 2008. 10.1038/nri2394.

121. Markle J.G.M.,Frank D.N., and … M.-T.-S., *Sex differences in the gut microbiome drive hormone-dependent regulation of autoimmunity.* …, 2013. 10.1126/science.1233521.

122. Merrill S.J. and Mu Y., *Thyroid autoimmunity as a window to autoimmunity: An explanation for sex differences in the prevalence of thyroid autoimmunity.* Journal of theoretical biology, 2015. 10.1016/j.jtbi.2014.12.015.

123. Fugazzola L.,Cirello V., and Beck-Peccoz P., *Fetal microchimerism as an explanation of disease.* Nature Reviews Endocrinology, 2011.

124. Graves P.N.,Unger P., and Davies T.F., *Intrathyroidal fetal microchimerism in Graves' disease.* The Journal of …, 2002.

125. Quintero-Ronderos P. and diseases M.-O.-G., *Epigenetics and autoimmune diseases.* Autoimmune diseases, 2012. 10.1155/2012/593720.

126. Pauley K.M.,Cha S., and Chan E., *MicroRNA in autoimmunity and autoimmune diseases.* Journal of Autoimmunity, 2009. **32**(3-4): p. 189-194.

127. Liu R.,Ma X.,Xu L.,Wang D.,Jiang X.,Zhu W.,Cui B.,Ning G.,Lin D., and Wang S., *Differential microRNA expression in peripheral blood mononuclear cells from Graves'*

disease patients. The Journal of clinical endocrinology and metabolism, 2012. **97**(6): p. 72.

128. Wang Z.,Fan X.,Zhang R.,Lin Z.,Lu T.,Bai X.,Li W.,Zhao J., and Zhang Q., *Integrative Analysis of mRNA and miRNA Array Data Reveals the Suppression of Retinoic Acid Pathway in Regulatory T Cells of Graves' Disease.* The Journal of Clinical Endocrinology & Metabolism, 2014. **99**(12).

129. Bach J.F., *The effect of infections on susceptibility to autoimmune and allergic diseases.* N Engl J Med, 2002. **347**(12): p. 911-20.

130. Bach J.F. and Chatenoud L., *A historical view from thirty eventful years of immunotherapy in autoimmune diabetes.* Semin Immunol, 2011. **23**(3): p. 174-81.

131. Weiss S.T., *Eat dirt--the hygiene hypothesis and allergic diseases.* N Engl J Med, 2002. **347**(12): p. 930-1.

132. von Mutius E. and Vercelli D., *Farm living: effects on childhood asthma and allergy.* Nat Rev Immunol, 2010. **10**(12): p. 861-8.

133. Stein M.M.,Hrusch C.L.,Gozdz J.,Igartua C.,Pivniouk V.,Murray S.E.,Ledford J.G.,Marques Dos Santos M.,Anderson R.L.,Metwali N.,Neilson J.W.,Maier R.M.,Gilbert J.A.,Holbreich M.,Thorne P.S.,Martinez F.D.,von Mutius E.,Vercelli D.,Ober C., and Sperling A.I., *Innate Immunity and Asthma Risk in Amish and Hutterite Farm Children.* N Engl J Med, 2016. **375**(5): p. 411-421.

134. Vatanen T.,Kostic A.D.,d'Hennezel E.,Siljander H.,Franzosa E.A.,Yassour M.,Kolde R.,Vlamakis H.,Arthur T.D.,Hamalainen A.M.,Peet A.,Tillmann V.,Uibo R.,Mokurov S.,Dorshakova N.,Ilonen J.,Virtanen S.M.,Szabo S.J.,Porter J.A.,Lahdesmaki H.,Huttenhower C.,Gevers D.,Cullen T.W.,Knip M.,Group D.S., and Xavier R.J., *Variation in Microbiome LPS Immunogenicity Contributes to Autoimmunity in Humans.* Cell, 2016. **165**(4): p. 842-53.

135. Root-Bernstein R. and Fairweather D., *Complexities in the relationship between infection and autoimmunity.* Current allergy and asthma reports, 2014. **14**(1): p. 407.

136. Vojdani A., *A potential link between environmental triggers and autoimmunity.* Autoimmune diseases, 2014.

137. Ercolini A.M. and Miller S.D., *The role of infections in autoimmune disease.* Clinical & Experimental Immunology, 2009. 10.1111/j.1365-2249.2008.03834.x.

138. Burek L.C. and Talor M.V., *Environmental triggers of autoimmune thyroiditis.* Journal of Autoimmunity, 2009. **33**(3-4): p. 183-189.

139. Kivity S.,Agmon-Levin N.,Blank M., and Shoenfeld Y., *Infections and autoimmunity–friends or foes?* Trends in immunology, 2009.

140. Amital H.,Govoni M.,Maya R., and Meroni P.L., *Role of infectious agents in systemic rheumatic diseases.* Clinical & …, 2008.

141. Rose N.R.,Kite J.H.,Doebbler T.K., and of the New … S.-R., *Studies on experimental thyroiditis.* Annals of the New …, 1965. 10.1111/j.1749-6632.1965.tb18957.x.

142. Naturalist D.-R.T., *Molecular mimicry: antigen sharing by parasite and host and its consequences.* The American Naturalist, 1964.

143. Fujinami R.S. and of the … O.-M.B., *Molecular mimicry in virus infection: crossreaction of measles virus phosphoprotein or of herpes simplex virus protein with human intermediate filaments.* Proceedings of the …, 1983. 10.1073/pnas.80.8.2346.

144. Benoist C. and Mathis D., *Autoimmunity provoked by infection: how good is the case for T cell epitope mimicry?* Nature Immunology, 2001. **2**(9): p. 797-801.

145. opinion in rheumatology C.-M.W., *Streptococcus and rheumatic fever.* Current opinion in rheumatology, 2012.

146. Gross D.M.,Forsthuber T., and … T.-L.-M., *Identification of LFA-1 as a candidate autoantigen in treatment-resistant Lyme arthritis.* …, 1998. 10.1126/science.281.5377.703.

147. Luo G.,Fan J.L.,Seetharamaiah G.S.,Desai R.K.,Dallas J.S.,Wagle N.,Doan R.,Niesel D.W.,Klimpel G.R., and Prabhakar B.S., *Immunization of mice with Yersinia enterocolitica leads to the induction of antithyrotropin receptor antibodies.* Journal of immunology (Baltimore, Md. : 1950), 1993. **151**(2): p. 922-928.

148. Köhling H.L.,Plummer S.F.,Marchesi J.R., and Davidge K.S., *The microbiota and autoimmunity: Their role in thyroid autoimmune diseases.* Clinical …, 2017.

149. Tomer Y. and Huber A., *The etiology of autoimmune thyroid disease: a story of genes and environment.* Journal of Autoimmunity, 2009. **32**(3-4): p. 231-239.

150. Kraemer M.H.,Donadi E.A.,Tambascia M.A.,Magna L.A., and Prigenzi L.S., *Relationship between HLA antigens and infectious agents in contributing towards the development of Graves' disease.* Immunological investigations, 1998. **27**(1-2): p. 17-29.

151. Lehmann P.V.,Sercarz E.E.,Forsthuber T., and Dayan C.M., *Determinant spreading and the dynamics of the autoimmune T-cell repertoire.* Immunology today, 1993.

152. Saeki Y. and Ishihara K., *Infection–immunity liaison: Pathogen-driven autoimmune-mimicry (PDAIM).* Autoimmunity Reviews, 2014. **13**(10): p. 10641069.

153. Teixeira-Coelho M.,Cruz A.,Carmona J.,Sousa C.,Ramos-Pereira D.,Saraiva A.L.,Veldhoen M.,Pedrosa J.,Castro A.G., and Saraiva M., *TLR2 deficiency by compromising p19 (IL-23) expression limits Th 17 cell responses to Mycobacterium tuberculosis.* Int Immunol, 2011. **23**(2): p. 89-96.

154. Witebsky E., *Experimental evidence for the role of auto-immunization in chronic thyroiditis.* Proc R Soc Med, 1957. **50**(11): p. 955-8.

155. George J.,Levy Y., and Shoenfeld Y., *Smoking and immunity: an additional player in the mosaic of autoimmunity.* Scand J Immunol, 1997. **45**(1): p. 1-6.

156. Wiersinga W.M., *Smoking and thyroid.* Clin Endocrinol (Oxf), 2013. **79**(2): p. 145-51.

157. Acharya S.H.,Avenell A.,Philip S.,Burr J.,Bevan J.S., and Abraham P., *Radioiodine therapy (RAI) for Graves' disease (GD) and the effect on ophthalmopathy: a systematic review.* Clin Endocrinol (Oxf), 2008. **69**(6): p. 943-50.

158. Quadbeck B.,Roggenbuck U.,Janssen O.E.,Hahn S.,Mann K.,Hoermann R., and Basedow Study G., *Impact of smoking on the course of Graves' disease after withdrawal of antithyroid drugs.* Exp Clin Endocrinol Diabetes, 2006. **114**(8): p. 406-11.

159. Szucs-Farkas Z.,Toth J.,Kollar J.,Galuska L.,Burman K.D.,Boda J.,Leovey A.,Varga J.,Ujhelyi B.,Szabo J.,Berta A., and Nagy E.V., *Volume changes in intra- and extraorbital compartments in patients with Graves' ophthalmopathy: effect of smoking.* Thyroid, 2005. **15**(2): p. 146-51.

160. Winsa B.,Mandahl A., and Karlsson F.A., *Graves' disease, endocrine ophthalmopathy and smoking.* Acta Endocrinol (Copenh), 1993. **128**(2): p. 156-60.

161. Cawood T.J.,Moriarty P.,O'Farrelly C., and O'Shea D., *Smoking and thyroid-associated ophthalmopathy: A novel explanation of the biological link.* J Clin Endocrinol Metab, 2007. **92**(1): p. 59-64.

162. Ludgate M., *Animal models of Graves' disease.* European journal of endocrinology, 2000.

163. McLachlan S.M.,Alpi K., and Rapoport B., *Review and hypothesis: does Graves' disease develop in non-human great apes?* Thyroid : official journal of the American Thyroid Association, 2011. **21**(12): p. 1359-1366.

164. McLachlan S.M.,Aliesky H.A.,Chen C.-R.R.,Chong G., and Rapoport B., *Breaking tolerance in transgenic mice expressing the human TSH receptor A-subunit: thyroiditis, epitope spreading and adjuvant as a 'double edged sword'.* PloS one, 2012. **7**(9).

165. Banga J.P.,Moshkelgosha S., and Berchner-Pfannschmidt U., *Complimentary and personal copy for.* Complimentary and personal copy for, 2015.

166. Costagliola S.,Alcalde L.,Ruf J.,Vassart G., and Ludgate M., *Overexpression of the extracellular domain of the thyrotrophin receptor in bacteria; production of thyrotrophin-binding inhibiting immunoglobulins.* J Mol Endocrinol, 1994. **13**(1): p. 11-21.

167. Wagle N.M.,Dallas J.S.,Seetharamaiah G.S.,Fan J.L.,Desai R.K.,Memar O.,Rajaraman S., and Prabhakar B.S., *Induction of hyperthyroxinemia in BALB/C but not in several other strains of mice.* Autoimmunity, 1994. **18**(2): p. 103-12.

168. Shimojo N.,Kohno Y.,Yamaguchi K.,Kikuoka S.,Hoshioka A.,Niimi H.,Hirai A.,Tamura Y.,Saito Y.,Kohn L.D., and Tahara K., *Induction of Graves-like disease in mice by immunization with fibroblasts transfected with the thyrotropin receptor and a class II molecule.* Proc Natl Acad Sci U S A, 1996. **93**(20): p. 11074-9.

169. Yamaguchi K.,Shimojo N.,Kikuoka S.,Hoshioka A.,Hirai A.,Tahara K.,Kohn L.D.,Kohno Y., and Niimi H., *Genetic control of anti-thyrotropin receptor antibody generation in H-2K mice immunized with thyrotropin receptor-transfected fibroblasts.* J Clin Endocrinol Metab, 1997. **82**(12): p. 4266-9.

170. Kita M.,Ahmad L.,Marians R.C.,Vlase H.,Unger P.,Graves P.N., and Davies T.F., *Regulation and transfer of a murine model of thyrotropin receptor antibody mediated Graves' disease.* Endocrinology, 1999. **140**(3): p. 1392-8.

171. Costagliola S.,Rodien P.,Many M.C.,Ludgate M., and Vassart G., *Genetic immunization against the human thyrotropin receptor causes thyroiditis and allows production of monoclonal antibodies recognizing the native receptor.* J Immunol, 1998. **160**(3): p. 1458-65.

172. Pichurin P.,Yan X.M.,Farilla L.,Guo J.,Chazenbalk G.D.,Rapoport B., and McLachlan S.M., *Naked TSH receptor DNA vaccination: A TH1 T cell response in which interferon-gamma production, rather than antibody, dominates the immune response in mice.* Endocrinology, 2001. **142**(8): p. 3530-6.

173. Rao P.V.,Watson P.F.,Weetman A.P.,Carayanniotis G., and Banga J.P., *Contrasting activities of thyrotropin receptor antibodies in experimental models of Graves' disease induced by injection of transfected fibroblasts or deoxyribonucleic acid vaccination.* Endocrinology, 2003. **144**(1): p. 260-6.

174. Nagayama Y.,Kita-Furuyama M.,Ando T.,Nakao K.,Mizuguchi H.,Hayakawa T.,Eguchi K., and Niwa M., *A Novel Murine Model of Graves' Hyperthyroidism with Intramuscular Injection of Adenovirus Expressing the Thyrotropin Receptor.* The Journal of Immunology, 2002. **168**(6): p. 2789-2794.

175. Chen C.R.,Pichurin P.,Nagayama Y.,Latrofa F.,Rapoport B., and McLachlan S.M., *The thyrotropin receptor autoantigen in Graves disease is the culprit as well as the victim.* J Clin Invest, 2003. **111**(12): p. 1897-904.

176. Michele Crisp K.J.S., Carol Lane, Jack Ham, Marian Lugdate, *Adipogenesis in Thyroid Eye Disease.* Investigative Ophtalmology & Visual Science, 2000. **41**(11).

177. Many M.C.,Costagliola S., and of … D.-M., *Development of an animal model of autoimmune thyroid eye disease.* The Journal of …, 1999.

178. Kaneda T.,Honda A.,Hakozaki A.,Fuse T.,Muto A., and Yoshida T., *An improved Graves' disease model established by using in vivo electroporation exhibited long-term immunity to hyperthyroidism in BALB/c mice.* Endocrinology, 2007. **148**(5): p. 2335-2344.

179. Zhao S.X.,Tsui S.,Cheung A.,Douglas R.S.,Smith T.J., and Banga J.P., *Orbital fibrosis in a mouse model of Graves' disease induced by genetic immunization of thyrotropin receptor cDNA.* J Endocrinol, 2011. **210**(3): p. 369-77.

180. Moshkelgosha S.,So P.-W.,Deasy N.,Diaz-Cano S., and Banga P.J., *Cutting Edge: Retrobulbar Inflammation, Adipogenesis, and Acute Orbital Congestion in a Preclinical Female Mouse Model of Graves' Orbitopathy Induced by Thyrotropin Receptor Plasmid-in Vivo Electroporation.* Endocrinology, 2013. **154**(9): p. 3008-3015.

181. Rapoport B.,Williams R.W.,Chen C.R., and McLachlan S.M., *Immunoglobulin heavy chain variable region genes contribute to the induction of thyroid-stimulating antibodies in recombinant inbred mice.* Genes Immun, 2010. **11**(3): p. 254-63.

182. Vlase H.,Weiss M.,Graves P.N., and Davies T.F., *Characterization of the murine immune response to the murine TSH receptor ectodomain: induction of hypothyroidism and TSH receptor antibodies.* Clin Exp Immunol, 1998. **113**(1): p. 111-8.

183. Nakahara M.,Mitsutake N.,Sakamoto H.,Chen C.R.,Rapoport B.,McLachlan S.M., and Nagayama Y., *Enhanced response to mouse thyroid-stimulating hormone (TSH) receptor immunization in TSH receptor-knockout mice.* Endocrinology, 2010. **151**(8): p. 4047-54.

184. Nakahara M.,Johnson K.,Eckstein A.,Taguchi R.,Yamada M.,Abiru N., and Nagayama Y., *Adoptive transfer of antithyrotropin receptor (TSHR) autoimmunity from TSHR knockout mice to athymic nude mice.* Endocrinology, 2012. **153**(4): p. 2034-42.

185. Schluter A.,Eckstein A.K.,Brenzel A.,Horstmann M.,Lang S.,Berchner-Pfannschmidt U.,Banga J.P., and Diaz-Cano S., *Noninflammatory Diffuse Follicular Hypertrophy/Hyperplasia of Graves Disease: Morphometric Evaluation in an Experimental Mouse Model.* Eur Thyroid J, 2018. **7**(3): p. 111-119.

186. Smith T.J. and Hegedus L., *Graves' Disease.* N Engl J Med, 2016. **375**(16): p. 1552-1565.

187. Berchner-Pfannschmidt U.,Moshkelgosha S.,Diaz-Cano S.,Edelmann B.,Görtz G.-E.E.,Horstmann M.,Noble A.,Hansen W.,Eckstein A., and Banga J.P., *Comparative assessment of female mouse model of Graves' orbitopathy under different environments, accompanied by pro-inflammatory cytokine and T cell responses to thyrotropin hormone receptor antigen.* Endocrinology, 2016. 10.1210/en.2015-1829.

188. Baker G.,Mazziotti G., and von Endocrinology R.-C., *Reevaluating thyrotropin receptor-induced mouse models of Graves' disease and ophthalmopathy.* Endocrinology, 2005.

189. Lublin F.D., *New multiple sclerosis phenotypic classification.* Eur Neurol, 2014. **72 Suppl 1**: p. 1-5.

190. Rotondi M.,Molteni M.,Leporati P.,Capelli V.,Marino M., and Chiovato L., *Autoimmune Thyroid Diseases in Patients Treated with Alemtuzumab for Multiple Sclerosis: An Example of Selective Anti-TSH-Receptor Immune Response.* Front Endocrinol (Lausanne), 2017. **8**: p. 254.

191. Baker D.,Giovannoni G., and Schmierer K., *Marked neutropenia: Significant but rare in people with multiple sclerosis after alemtuzumab treatment.* Mult Scler Relat Disord, 2017. **18**: p. 181-183.

192. Steinman L., *Induction of New Autoimmune Diseases After Alemtuzumab Therapy for Multiple Sclerosis: Learning From Adversity.* JAMA Neurol, 2017. **74**(8): p. 907-908.

193. Decallonne B.,Bartholomé E.,Delvaux V.,D'haeseleer M.,El Sankari S.,Seeldrayers P.,Van Wijmeersch B., and Daumerie C., *Thyroid disorders in alemtuzumab-treated multiple sclerosis patients: a Belgian consensus on diagnosis and management.* Acta Neurologica Belgica, 2018. **118**(2): p. 153-159.

194. Daniels G.H.,Vladic A.,Brinar V.,Zavalishin I.,Valente W.,Oyuela P.,Palmer J.,Margolin D.H., and Hollenstein J., *Alemtuzumab-related thyroid dysfunction in a phase 2 trial of patients with relapsing-remitting multiple sclerosis.* J Clin Endocrinol Metab, 2014. **99**(1): p. 80-9.

195. Pariani N.,Willis M.,Muller I.,Healy S.,Nasser T.,McGowan A.,Lyons G.,Jones J.,Chatterjee K.,Dayan C.,Robertson N.,Coles A., and Moran C., *Alemtuzumab-Induced Thyroid Dysfunction Exhibits Distinctive Clinical and Immunological Features.* J Clin Endocrinol Metab, 2018. **103**(8): p. 3010-3018.

196. Jones J.L. and Coles A.J., *Spotlight on alemtuzumab.* Int MS J, 2009. **16**(3): p. 77-81.

197. Muller I.,Willis M.,Healy S.,Nasser T.,Loveless S.,Butterworth S.,Zhang L.,Draman M.S.,Taylor P.N.,Robertson N.,Dayan C.M., and Ludgate M.E., *Longitudinal Characterization of Autoantibodies to the Thyrotropin Receptor (TRAb) During Alemtuzumab Therapy: Evidence that TRAb May Precede Thyroid Dysfunction by Many Years.* Thyroid, 2018. **28**(12): p. 1682-1693.

198. Minekus M.,Alminger M.,Alvito P.,Ballance S.,Bohn T.,Bourlieu C.,Carriere F.,Boutrou R.,Corredig M.,Dupont D.,Dufour C.,Egger L.,Golding M.,Karakaya S.,Kirkhus B.,Le Feunteun S.,Lesmes U.,Macierzanka A.,Mackie A.,Marze S.,McClements D.J.,Menard O.,Recio I.,Santos C.N.,Singh R.P.,Vegarud G.E.,Wickham M.S.,Weitschies W., and Brodkorb A., *A standardised static in vitro digestion method suitable for food - an international consensus.* Food Funct, 2014. **5**(6): p. 1113-24.

199. Nguyen T.L.,Vieira-Silva S.,Liston A., and Raes J., *How informative is the mouse for human gut microbiota research?* Dis Model Mech, 2015. **8**(1): p. 1-16.

200. Anderson M.J., *A new method for non-parametric multivariate analysis of variance.* Austral ecology, 2001. 10.1111/j.1442-9993.2001.01070.pp.x.

201. Marchesi J.R. and Ravel J., *The vocabulary of microbiome research: a proposal.* Microbiome, 2015. **3**: p. 31.

202. Bruns T.D.,Vilgalys R.,Barns S.M.,Gonzalez D.,Hibbett D.S.,Lane D.J.,Simon L.,Stickel S.,Szaro T.M., and Weisburg W.G., *Evolutionary relationships within the fungi: analyses of nuclear small subunit rRNA sequences.* Molecular phylogenetics and evolution, 1992. **1**(3): p. 231-241.

203. Liu C.M.,Aziz M.,Kachur S.,Hsueh P.-R.,Huang Y.-T.,Keim P., and Price L.B., *BactQuant: an enhanced broad-coverage bacterial quantitative real-time PCR assay.* BMC microbiology, 2012. **12**: p. 56.

204. Nadkarni M.A.,Martin E.F.,Jacques N.A., and Hunter N., *Determination of bacterial load by real-time PCR using a broad-range (universal) probe and primers set.* Microbiology (Reading, England), 2002. **148**(Pt 1): p. 257-266.

205. Morgan X.C. and Huttenhower C., *Chapter 12: Human Microbiome Analysis.* PLoS Computational Biology, 2012. **8**(12).

206. Lane D.J.,Pace B.,Olsen G.J.,Stahl D.A.,Sogin M.L., and Pace N.R., *Rapid determination of 16S ribosomal RNA sequences for phylogenetic analyses.* Proceedings of the National Academy of Sciences of the United States of America, 1985. **82**(20): p. 6955-6959.

207. Schloss P.D.,Westcott S.L., and Ryabin T., *Introducing mothur: open-source, platform-independent, community-supported software for describing and comparing microbial communities.* Applied and …, 2009. 10.1128/AEM.01541-09.

208. Caporaso J.G.,Kuczynski J.,Stombaugh J.,Bittinger K.,Bushman F.D.,Costello E.K.,Fierer N.,Peña A.G.,Goodrich J.K.,Gordon J.I.,Huttley G.A.,Kelley S.T.,Knights D.,Koenig J.E.,Ley R.E.,Lozupone C.A.,McDonald D.,Muegge B.D.,Pirrung M.,Reeder J.,Sevinsky J.R.,Turnbaugh P.J.,Walters W.A.,Widmann J.,Yatsunenko T.,Zaneveld J., and Knight R., *QIIME allows analysis of high-throughput community sequencing data.* Nature methods, 2010. **7**(5): p. 335-336.

209. Pruesse E.,Quast C.,Knittel K.,Fuchs B.M.,Ludwig W.,Peplies J., and Glöckner F.O., *SILVA: a comprehensive online resource for quality checked and aligned ribosomal RNA sequence data compatible with ARB.* Nucleic Acids Research, 2007. **35**(21): p. 7188-7196.

210. Cole J.R.,Wang Q.,Cardenas E., and Fish J., *The Ribosomal Database Project: improved alignments and new tools for rRNA analysis.* Nucleic acids …, 2008.

211. DeSantis T.Z.,Hugenholtz P.,Larsen N.,Rojas M.,Brodie E.L.,Keller K.,Huber T.,Dalevi D.,Hu P., and Andersen G.L., *Greengenes, a chimera-checked 16S rRNA gene database and workbench compatible with ARB.* Applied and environmental microbiology, 2006. **72**(7): p. 5069-5072.

212. Turnbaugh P.J.,Ley R.E.,Hamady M.,Fraser-Liggett C.M.,Knight R., and Gordon J.I., *The human microbiome project.* Nature, 2007. **449**(7164): p. 804-810.

213. Consortium H.,Nelson K.E.,Weinstock G.M.,Highlander S.K.,Worley K.C.,Creasy H.H.,Wortman J.R.,Rusch D.B.,Mitreva M.,Sodergren E.,Chinwalla A.T.,Feldgarden M.,Gevers D.,Haas B.J.,Madupu R.,Ward D.V.,Birren B.W.,Gibbs R.A.,Methe B.,Petrosino J.F.,Strausberg R.L.,Sutton G.G.,White O.R.,Wilson R.K.,Durkin S.,Giglio M.G.,Gujja S.,Howarth C.,Kodira C.D.,Kyrpides N.,Mehta T.,Muzny D.M.,Pearson M.,Pepin K.,Pati A.,Qin X.,Yandava C.,Zeng Q.,Zhang L.,Berlin A.M.,Chen L.,Hepburn T.A.,Johnson J.,McCorrison J.,Miller J.,Minx P.,Nusbaum C.,Russ C.,Sykes S.M.,Tomlinson C.M.,Young S.,Warren W.C.,Badger J.,Crabtree J.,Markowitz V.M.,Orvis J.,Cree A.,Ferriera S.,Fulton L.L.,Fulton R.S.,Gillis M.,Hemphill L.D.,Joshi V.,Kovar C.,Torralba M.,Wetterstrand K.A.,Abouellleil A.,Wollam A.M.,Buhay C.J.,Ding Y.,Dugan S.,FitzGerald M.G.,Holder M.,Hostetler J.,Clifton S.W.,Allen-Vercoe E.,Earl A.M.,Farmer C.N.,Liolios K.,Surette M.G.,Xu Q.,Pohl C.,Wilczek-Boney K., and Zhu D., *A catalog of*

reference genomes from the human microbiome. Science (New York, N.Y.), 2010. **328**(5981): p. 994-999.

214. Qin J.,Li R.,Raes J.,Arumugam M.,Burgdorf K.S.,Manichanh C.,Nielsen T.,Pons N.,Levenez F.,Yamada T.,Mende D.R.,Li J.,Xu J.,Li S.,Li D.,Cao J.,Wang B.,Liang H.,Zheng H.,Xie Y.,Tap J.,Lepage P.,Bertalan M.,Batto J.-M.M.,Hansen T.,Le Paslier D.,Linneberg A.,Nielsen H.B.,Pelletier E.,Renault P.,Sicheritz-Ponten T.,Turner K.,Zhu H.,Yu C.,Li S.,Jian M.,Zhou Y.,Li Y.,Zhang X.,Li S.,Qin N.,Yang H.,Wang J.,Brunak S.,Doré J.,Guarner F.,Kristiansen K.,Pedersen O.,Parkhill J.,Weissenbach J.,Consortium M.,Bork P.,Ehrlich S.D., and Wang J., *A human gut microbial gene catalogue established by metagenomic sequencing.* Nature, 2010. **464**(7285): p. 59-65.

215. Consortium H., *Structure, function and diversity of the healthy human microbiome.* Nature, 2012. **486**(7402): p. 207-214.

216. Lloyd-Price J.,Mahurkar A.,Rahnavard G.,Crabtree J.,Orvis J.,Hall A.B.,Brady A.,Creasy H.H.,McCracken C.,Giglio M.G.,McDonald D.,Franzosa E.A.,Knight R.,White O., and Huttenhower C., *Strains, functions and dynamics in the expanded Human Microbiome Project.* Nature, 2017. **550**(7674): p. 61-66.

217. Consortium I., *The Integrative Human Microbiome Project: dynamic analysis of microbiome-host omics profiles during periods of human health and disease.* Cell host & microbe, 2014. **16**(3): p. 276-289.

218. Li T.H.,Qin Y.,Sham P.C.,Lau K.S.,Chu K.M., and reports L.-W.K., *Alterations in Gastric Microbiota After H. Pylori Eradication and in Different Histological Stages of Gastric Carcinogenesis.* Scientific Reports, 2017. 10.1038/srep44935.

219. Nardone G. and Compare D., *The human gastric microbiota: Is it time to rethink the pathogenesis of stomach diseases?* United European Gastroenterology Journal, 2014. **3**(3): p. 255-260.

220. Zoetendal E.G.,Rajilić-Stojanović M., and Gut D.W.M., *High-throughput diversity and functionality analysis of the gastrointestinal tract microbiota.* Gut, 2008. 10.1136/gut.2007.133603.

221. Andersson A.F.,Lindberg M.,Jakobsson H., and one B.-F., *Comparative analysis of human gut microbiota by barcoded pyrosequencing.* PloS one, 2008. 10.1371/journal.pone.0002836.

222. Dethlefsen L.,Eckburg P.B.,in e., and … B.-E.M., *Assembly of the human intestinal microbiota.* Trends in ecology & …, 2006.

223. Ley R.E.,Turnbaugh P.J.,Klein S., and Gordon J.I., *Microbial ecology: human gut microbes associated with obesity.* Nature, 2006. 10.1038/4441022a.

224. Hollister E.B.,Gao C., and Gastroenterology V.-J., *Compositional and functional features of the gastrointestinal microbiome and their effects on human health.* Gastroenterology, 2014.

225. Arumugam M.,Raes J.,Pelletier E., and nature L.D., *Enterotypes of the human gut microbiome.* Nature, 2011.

226. Chen W.,Liu F.,Ling Z.,Tong X., and one X.-C., *Human intestinal lumen and mucosa-associated microbiota in patients with colorectal cancer.* PloS one, 2012. 10.1371/journal.pone.0039743.

227. Rautava S., *Early microbial contact, the breast milk microbiome and child health.* Journal of developmental origins of health and disease, 2016. **7**(1): p. 5-14.

228. Biasucci G.,Rubini M.,Riboni S.,Morelli L.,Bessi E., and Retetangos C., *Mode of delivery affects the bacterial community in the newborn gut.* Early human development, 2010. **86**(1): p. 13-15.

229. Ferretti P.,Pasolli E.,Tett A.,Asnicar F.,Gorfer V.,Fedi S.,Armanini F.,Truong D.T.,Manara S.,Zolfo M.,Beghini F.,Bertorelli R.,De Sanctis V.,Bariletti I.,Canto R.,Clementi R.,Cologna M.,Crifo T.,Cusumano G.,Gottardi S.,Innamorati C.,Mase C.,Postai D.,Savoi D.,Duranti S.,Lugli G.A.,Mancabelli L.,Turroni F.,Ferrario C.,Milani C.,Mangifesta M.,Anzalone R.,Viappiani A.,Yassour M.,Vlamakis H.,Xavier R.,Collado C.M.,Koren

O.,Tateo S.,Soffiati M.,Pedrotti A.,Ventura M.,Huttenhower C.,Bork P., and Segata N., *Mother-to-Infant Microbial Transmission from Different Body Sites Shapes the Developing Infant Gut Microbiome.* Cell Host Microbe, 2018. **24**(1): p. 133-145 e5.

230. Fernández L.,Langa S.,Martín V., and Maldonado A., *The human milk microbiota: origin and potential roles in health and disease.* Pharmacological …, 2013.

231. Martín R.o.,Langa S.,Reviriego C.,Jiménez E.,Marín M.a.L.,Olivares M.,Boza J.,Jiménez J.,Fernández L.,Xaus J., and Rodríguez J.M., *The commensal microflora of human milk: new perspectives for food bacteriotherapy and probiotics.* Trends in Food Science & Technology, 2004. **15**(3-4): p. 121-127.

232. Ward T.L.,Hosid S., and Ioshikhes I., *Human milk metagenome: a functional capacity analysis.* BMC …, 2013.

233. Biagi E.,Nylund L.,Candela M.,Ostan R.,Bucci L.,Pini E.,Nikkila J.,Monti D.,Satokari R.,Franceschi C.,Brigidi P., and De Vos W., *Through ageing, and beyond: gut microbiota and inflammatory status in seniors and centenarians.* PloS one, 2010. **5**(5): p. e10667.

234. Biagi E.,Franceschi C.,Rampelli S.,Severgnini M.,Ostan R.,Turroni S.,Consolandi C.,Quercia S.,Scurti M.,Monti D.,Capri M.,Brigidi P., and Candela M., *Gut Microbiota and Extreme Longevity.* Curr Biol, 2016. **26**(11): p. 1480-5.

235. Claesson M.J.,Cusack S.,O'Sullivan O.,Greene-Diniz R.,de Weerd H.,Flannery E.,Marchesi J.R.,Falush D.,Dinan T.,Fitzgerald G.,Stanton C.,van Sinderen D.,O'Connor M.,Harnedy N.,O'Connor K.,Henry C.,O'Mahony D.,Fitzgerald A.P.,Shanahan F.,Twomey C.,Hill C.,Ross R.P., and O'Toole P.W., *Composition, variability, and temporal stability of the intestinal microbiota of the elderly.* Proc Natl Acad Sci U S A, 2011. **108 Suppl 1**: p. 4586-91.

236. Dethlefsen L. and Relman D.A., *Incomplete recovery and individualized responses of the human distal gut microbiota to repeated antibiotic perturbation.* Proc Natl Acad Sci U S A, 2011. **108 Suppl 1**: p. 4554-61.

237. Morrison D.J. and Preston T., *Formation of short chain fatty acids by the gut microbiota and their impact on human metabolism.* Gut Microbes, 2016. **7**(3): p. 189-200.

238. Rowland I.,Gibson G.,Heinken A.,Scott K.,Swann J.,Thiele I., and Tuohy K., *Gut microbiota functions: metabolism of nutrients and other food components.* Eur J Nutr, 2018. **57**(1): p. 1-24.

239. De Filippo C.,Cavalieri D.,Di Paola M.,Ramazzotti M.,Poullet J.B.,Massart S.,Collini S.,Pieraccini G., and Lionetti P., *Impact of diet in shaping gut microbiota revealed by a comparative study in children from Europe and rural Africa.* Proc Natl Acad Sci U S A, 2010. **107**(33): p. 14691-6.

240. Schnorr S.L.,Candela M.,Rampelli S.,Centanni M.,Consolandi C.,Basaglia G.,Turroni S.,Biagi E.,Peano C.,Severgnini M.,Fiori J.,Gotti R.,De Bellis G.,Luiselli D.,Brigidi P.,Mabulla A.,Marlowe F.,Henry A.G., and Crittenden A.N., *Gut microbiome of the Hadza hunter-gatherers.* Nat Commun, 2014. **5**: p. 3654.

241. Smits S.A.,Leach J.,Sonnenburg E.D.,Gonzalez C.G.,Lichtman J.S.,Reid G.,Knight R.,Manjurano A.,Changalucha J.,Elias J.E.,Dominguez-Bello M.G., and Sonnenburg J.L., *Seasonal cycling in the gut microbiome of the Hadza hunter-gatherers of Tanzania.* Science, 2017. **357**(6353): p. 802-806.

242. Oikonomou E.,Psaltopoulou T.,Georgiopoulos G.,Siasos G.,Kokkou E.,Antonopoulos A.,Vogiatzi G.,Tsalamandris S.,Gennimata V.,Papanikolaou A., and Tousoulis D., *Western Dietary Pattern Is Associated With Severe Coronary Artery Disease.* Angiology, 2018. **69**(4): p. 339-346.

243. Mirmiran P.,Bahadoran Z.,Vakili A.Z., and Azizi F., *Western dietary pattern increases risk of cardiovascular disease in Iranian adults: a prospective population-based study.* Appl Physiol Nutr Metab, 2017. **42**(3): p. 326-332.

244. Vorster H.H., *The emergence of cardiovascular disease during urbanisation of Africans.* Public Health Nutr, 2002. **5**(1A): p. 239-43.

245. Moss A. and Nalankilli K., *The Association Between Diet and Colorectal Cancer Risk: Moving Beyond Generalizations.* Gastroenterology, 2017. **152**(8): p. 1821-1823.

246. Cani P.D.,Bibiloni R.,Knauf C.,Waget A.,Neyrinck A.M.,Delzenne N.M., and Burcelin R., *Changes in gut microbiota control metabolic endotoxemia-induced inflammation in high-fat diet-induced obesity and diabetes in mice.* Diabetes, 2008. **57**(6): p. 1470-81.

247. Hildebrandt M.A.,Hoffmann C.,Sherrill-Mix S.A.,Keilbaugh S.A.,Hamady M.,Chen Y.Y.,Knight R.,Ahima R.S.,Bushman F., and Wu G.D., *High-fat diet determines the composition of the murine gut microbiome independently of obesity.* Gastroenterology, 2009. **137**(5): p. 1716-24 e1-2.

248. Sah S.K.,Lee C.,Jang J.H., and Park G.H., *Effect of high-fat diet on cognitive impairment in triple-transgenic mice model of Alzheimer's disease.* Biochem Biophys Res Commun, 2017. **493**(1): p. 731-736.

249. Roderick M.R.,Shah R.,Rogers V.,Finn A., and Ramanan A.V., *Chronic recurrent multifocal osteomyelitis (CRMO) - advancing the diagnosis.* Pediatr Rheumatol Online J, 2016. **14**(1): p. 47.

250. Lukens J.R.,Gurung P.,Vogel P.,Johnson G.R.,Carter R.A.,McGoldrick D.J.,Bandi S.R.,Calabrese C.R.,Vande Walle L.,Lamkanfi M., and Kanneganti T.D., *Dietary modulation of the microbiome affects autoinflammatory disease.* Nature, 2014. **516**(7530): p. 246-9.

251. Wu G.D.,Compher C.,Chen E.Z.,Smith S.A.,Shah R.D.,Bittinger K.,Chehoud C.,Albenberg L.G.,Nessel L.,Gilroy E.,Star J.,Weljie A.M.,Flint H.J.,Metz D.C.,Bennett M.J.,Li H.,Bushman F.D., and Lewis J.D., *Comparative metabolomics in vegans and omnivores reveal constraints on diet-dependent gut microbiota metabolite production.* Gut, 2016. **65**(1): p. 63-72.

252. Spanogiannopoulos P.,Bess E.N.,Carmody R.N., and Turnbaugh P.J., *The microbial pharmacists within us: a metagenomic view of xenobiotic metabolism.* Nature reviews. Microbiology, 2016. **14**(5): p. 273-287.

253. Physician P.-O., *Appropriate prescribing of oral beta-lactam antibiotics.* Am. Fam. Physician, 2000.

254. Drlica K. and topics in medicinal chemistry M.-M., *Fluoroquinolones: action and resistance.* Current topics in medicinal chemistry, 2003.

255. Wolfson J.S. and Hooper D.C., *The fluoroquinolones: structures, mechanisms of action and resistance, and spectra of activity in vitro.* Antimicrobial agents and chemotherapy, 1985. **28**(4): p. 581-586.

256. Miguel R.,Sanders J.,Furmaniak J., and Smith B., *Structure and activation of the TSH receptor transmembrane domain.* Autoimmunity Highlights, 2016. **8**(1): p. 2.

257. Kanoh S. and microbiology reviews R.-B.K., *Mechanisms of action and clinical application of macrolides as immunomodulatory medications.* Clinical microbiology reviews, 2010. 10.1128/CMR.00078-09.

258. Panda S.,Casellas F.,Vivancos J.,Cors M.,Santiago A.,Cuenca S.,Guarner F., and Manichanh C., *Short-term effect of antibiotics on human gut microbiota.* PloS one, 2014. **9**(4).

259. Dethlefsen L. and of the National R.-D.A., *Incomplete recovery and individualized responses of the human distal gut microbiota to repeated antibiotic perturbation.* Proceedings of the National …, 2011. 10.1073/pnas.1000087107.

260. Jakobsson H.E.,Jernberg C., and one A.-A.F., *Short-term antibiotic treatment has differing long-term impacts on the human throat and gut microbiome.* PloS one, 2010. 10.1371/journal.pone.0009836.

261. Raymond F.,Ouameur A.A.,Déraspe M., and Isme … I.-N., *The initial state of the human gut microbiome determines its reshaping by antibiotics.* The ISME …, 2016. 10.1038/ismej.2015.148.

262. Penders J.,Stobberingh E.E.,Savelkoul P.H., and Wolffs P.F., *The human microbiome as a reservoir of antimicrobial resistance.* Frontiers in microbiology, 2013. **4**: p. 87.

263. Jackson M.A.,Goodrich J.K.,Maxan M.E., and Gut F.-D.E., *Proton pump inhibitors alter the composition of the gut microbiota.* Gut, 2016. 10.1136/gutjnl-2015-310861.

264. Maier L.,Pruteanu M.,Kuhn M.,Zeller G., and Nature T.-A., *Extensive impact of non-antibiotic drugs on human gut bacteria.* Nature, 2018. 10.1038/nature25979.

265. Flowers S.A.,Evans S.J., and of … W.-K.M., *Interaction between atypical antipsychotics and the gut microbiome in a bipolar disease cohort.* … : The Journal of …, 2017. 10.1002/phar.1890.

266. Rogers M.A.M. and Clinical A.-D.M., *The influence of non-steroidal anti-inflammatory drugs on the gut microbiome.* Clinical …, 2016.

267. Belkaid Y. and Hand T.W., *Role of the microbiota in immunity and inflammation.* Cell, 2014. **157**(1): p. 121-41.

268. van der Waaij D.,Berghuis-de Vries J.M., and Lekkerkerk L.-v., *Colonization resistance of the digestive tract in conventional and antibiotic-treated mice.* J Hyg (Lond), 1971. **69**(3): p. 405-11.

269. Kamada N.,Chen G.Y.,Inohara N., and Nunez G., *Control of pathogens and pathobionts by the gut microbiota.* Nat Immunol, 2013. **14**(7): p. 685-90.

270. Hammami R.,Fernandez B.,Lacroix C., and Fliss I., *Anti-infective properties of bacteriocins: an update.* Cell Mol Life Sci, 2013. **70**(16): p. 2947-67.

271. Ivanov, II and Littman D.R., *Modulation of immune homeostasis by commensal bacteria.* Curr Opin Microbiol, 2011. **14**(1): p. 106-14.

272. Lee Y.K. and Mazmanian S.K., *Has the microbiota played a critical role in the evolution of the adaptive immune system?* Science, 2010. **330**(6012): p. 1768-73.

273. Hooper L.V. and Macpherson A.J., *Immune adaptations that maintain homeostasis with the intestinal microbiota.* Nat Rev Immunol, 2010. **10**(3): p. 159-69.

274. Round J.L. and Mazmanian S.K., *The gut microbiota shapes intestinal immune responses during health and disease.* Nat Rev Immunol, 2009. **9**(5): p. 313-23.

275. Brandtzaeg P., *Mucosal immunity: induction, dissemination, and effector functions.* Scand J Immunol, 2009. **70**(6): p. 505-15.

276. Lorenz R.G. and Newberry R.D., *Isolated lymphoid follicles can function as sites for induction of mucosal immune responses.* Ann N Y Acad Sci, 2004. **1029**: p. 44-57.

277. Farache J.,Koren I.,Milo I.,Gurevich I.,Kim K.W.,Zigmond E.,Furtado G.C.,Lira S.A., and Shakhar G., *Luminal bacteria recruit CD103+ dendritic cells into the intestinal epithelium to sample bacterial antigens for presentation.* Immunity, 2013. **38**(3): p. 581-95.

278. Pabst O. and Mowat A.M., *Oral tolerance to food protein.* Mucosal Immunol, 2012. **5**(3): p. 232-9.

279. Mazzini E.,Massimiliano L.,Penna G., and Rescigno M., *Oral tolerance can be established via gap junction transfer of fed antigens from CX3CR1(+) macrophages to CD103(+) dendritic cells.* Immunity, 2014. **40**(2): p. 248-61.

280. Worbs T.,Bode U.,Yan S.,Hoffmann M.W.,Hintzen G.,Bernhardt G.,Forster R., and Pabst O., *Oral tolerance originates in the intestinal immune system and relies on antigen carriage by dendritic cells.* J Exp Med, 2006. **203**(3): p. 519-27.

281. Hardy M.Y. and Tye-Din J.A., *Coeliac disease: a unique model for investigating broken tolerance in autoimmunity.* Clin Transl Immunology, 2016. **5**(11): p. e112.

282. Lalles J.P., *Intestinal alkaline phosphatase: novel functions and protective effects.* Nutr Rev, 2014. **72**(2): p. 82-94.

283. Estaki M.,DeCoffe D., and Gibson D.L., *Interplay between intestinal alkaline phosphatase, diet, gut microbes and immunity.* World J Gastroenterol, 2014. **20**(42): p. 15650-6.

284. Erridge C.,Bennett-Guerrero E., and Poxton I.R., *Structure and function of lipopolysaccharides.* Microbes Infect, 2002. **4**(8): p. 837-51.

285. Macpherson A.J. and Uhr T., *Induction of protective IgA by intestinal dendritic cells carrying commensal bacteria.* Science, 2004. **303**(5664): p. 1662-5.

286. Lathrop S.K.,Bloom S.M.,Rao S.M.,Nutsch K.,Lio C.W.,Santacruz N.,Peterson D.A.,Stappenbeck T.S., and Hsieh C.S., *Peripheral education of the immune system by colonic commensal microbiota.* Nature, 2011. **478**(7368): p. 250-4.

287. Liang S.C.,Tan X.Y.,Luxenberg D.P.,Karim R.,Dunussi-Joannopoulos K.,Collins M., and Fouser L.A., *Interleukin (IL)-22 and IL-17 are coexpressed by Th17 cells and cooperatively enhance expression of antimicrobial peptides.* J Exp Med, 2006. **203**(10): p. 2271-9.

288. Neu J. and Walker W.A., *Necrotizing enterocolitis.* N Engl J Med, 2011. **364**(3): p. 255-64.

289. Lundin A.,Bok C.M.,Aronsson L.,Bjorkholm B.,Gustafsson J.A.,Pott S.,Arulampalam V.,Hibberd M.,Rafter J., and Pettersson S., *Gut flora, Toll-like receptors and nuclear receptors: a tripartite communication that tunes innate immunity in large intestine.* Cell Microbiol, 2008. **10**(5): p. 1093-103.

290. Matsumoto S.,Setoyama H., and Umesaki Y., *Differential induction of major histocompatibility complex molecules on mouse intestine by bacterial colonization.* Gastroenterology, 1992. **103**(6): p. 1777-82.

291. Niess J.H.,Leithauser F.,Adler G., and Reimann J., *Commensal gut flora drives the expansion of proinflammatory CD4 T cells in the colonic lamina propria under normal and inflammatory conditions.* J Immunol, 2008. **180**(1): p. 559-68.

292. Smith K.,McCoy K.D., and Macpherson A.J., *Use of axenic animals in studying the adaptation of mammals to their commensal intestinal microbiota.* Semin Immunol, 2007. **19**(2): p. 59-69.

293. Mazmanian S.K.,Liu C.H.,Tzianabos A.O., and Kasper D.L., *An immunomodulatory molecule of symbiotic bacteria directs maturation of the host immune system.* Cell, 2005. **122**(1): p. 107-18.

294. Bermudez-Brito M.,Plaza-Diaz J.,Munoz-Quezada S.,Gomez-Llorente C., and Gil A., *Probiotic mechanisms of action.* Ann Nutr Metab, 2012. **61**(2): p. 160-74.

295. O'Mahony C.,Scully P.,O'Mahony D.,Murphy S.,O'Brien F.,Lyons A.,Sherlock G.,MacSharry J.,Kiely B.,Shanahan F., and O'Mahony L., *Commensal-induced regulatory T cells mediate protection against pathogen-stimulated NF-kappaB activation.* PLoS Pathog, 2008. **4**(8): p. e1000112.

296. Sokol H.,Pigneur B.,Watterlot L.,Lakhdari O.,Bermudez-Humaran L.G.,Gratadoux J.J.,Blugeon S.,Bridonneau C.,Furet J.P.,Corthier G.,Grangette C.,Vasquez N.,Pochart P.,Trugnan G.,Thomas G.,Blottiere H.M.,Dore J.,Marteau P.,Seksik P., and Langella P., *Faecalibacterium prausnitzii is an anti-inflammatory commensal bacterium identified by gut microbiota analysis of Crohn disease patients.* Proc Natl Acad Sci U S A, 2008. **105**(43): p. 16731-6.

297. Ochoa-Reparaz J.,Mielcarz D.W.,Wang Y.,Begum-Haque S.,Dasgupta S.,Kasper D.L., and Kasper L.H., *A polysaccharide from the human commensal Bacteroides fragilis protects against CNS demyelinating disease.* Mucosal Immunol, 2010. **3**(5): p. 487-95.

298. Ivanov, II,Atarashi K.,Manel N.,Brodie E.L.,Shima T.,Karaoz U.,Wei D.,Goldfarb K.C.,Santee C.A.,Lynch S.V.,Tanoue T.,Imaoka A.,Itoh K.,Takeda K.,Umesaki Y.,Honda K., and Littman D.R., *Induction of intestinal Th17 cells by segmented filamentous bacteria.* Cell, 2009. **139**(3): p. 485-98.

299. Ivanov, II,Frutos Rde L.,Manel N.,Yoshinaga K.,Rifkin D.B.,Sartor R.B.,Finlay B.B., and Littman D.R., *Specific microbiota direct the differentiation of IL-17-producing T-helper cells in the mucosa of the small intestine.* Cell Host Microbe, 2008. **4**(4): p. 337-49.

300. Pamp S.J.,Harrington E.D.,Quake S.R.,Relman D.A., and Blainey P.C., *Single-cell sequencing provides clues about the host interactions of segmented filamentous bacteria (SFB).* Genome Res, 2012. **22**(6): p. 1107-19.

301. Atarashi K.,Umesaki Y., and Honda K., *Microbiotal influence on T cell subset development.* Semin Immunol, 2011. **23**(2): p. 146-53.

302. Atarashi K.,Tanoue T.,Oshima K.,Suda W.,Nagano Y.,Nishikawa H.,Fukuda S.,Saito T.,Narushima S.,Hase K.,Kim S.,Fritz J.V.,Wilmes P.,Ueha S.,Matsushima K.,Ohno H.,Olle B.,Sakaguchi S.,Taniguchi T.,Morita H.,Hattori M., and Honda K., *Treg induction by a rationally selected mixture of Clostridia strains from the human microbiota.* Nature, 2013. **500**(7461): p. 232-6.

303. Smith P.M.,Howitt M.R.,Panikov N.,Michaud M.,Gallini C.A.,Bohlooly Y.M.,Glickman J.N., and Garrett W.S., *The microbial metabolites, short-chain fatty acids, regulate colonic Treg cell homeostasis.* Science, 2013. **341**(6145): p. 569-73.

304. Kosiewicz M.M.,Dryden G.W.,Chhabra A., and Alard P., *Relationship between gut microbiota and development of T cell associated disease.* FEBS Lett, 2014. **588**(22): p. 4195-206.

305. Arpaia N.,Campbell C.,Fan X.,Dikiy S.,van der Veeken J.,deRoos P.,Liu H.,Cross J.R.,Pfeffer K.,Coffer P.J., and Rudensky A.Y., *Metabolites produced by commensal bacteria promote peripheral regulatory T-cell generation.* Nature, 2013. **504**(7480): p. 451-5.

306. Furusawa Y.,Obata Y.,Fukuda S.,Endo T.A.,Nakato G.,Takahashi D.,Nakanishi Y.,Uetake C.,Kato K.,Kato T.,Takahashi M.,Fukuda N.N.,Murakami S.,Miyauchi E.,Hino S.,Atarashi K.,Onawa S.,Fujimura Y.,Lockett T.,Clarke J.M.,Topping D.L.,Tomita M.,Hori S.,Ohara O.,Morita T.,Koseki H.,Kikuchi J.,Honda K.,Hase K., and Ohno H., *Commensal microbe-derived butyrate induces the differentiation of colonic regulatory T cells.* Nature, 2013. **504**(7480): p. 446-50.

307. Singh N.,Gurav A.,Sivaprakasam S.,Brady E.,Padia R.,Shi H.,Thangaraju M.,Prasad P.D.,Manicassamy S.,Munn D.H.,Lee J.R.,Offermanns S., and Ganapathy V., *Activation of Gpr109a, receptor for niacin and the commensal metabolite butyrate, suppresses colonic inflammation and carcinogenesis.* Immunity, 2014. **40**(1): p. 128-39.

308. Davie J.R., *Inhibition of histone deacetylase activity by butyrate.* J Nutr, 2003. **133**(7 Suppl): p. 2485S-2493S.

309. Tao R.,de Zoeten E.F.,Ozkaynak E.,Chen C.,Wang L.,Porrett P.M.,Li B.,Turka L.A.,Olson E.N.,Greene M.I.,Wells A.D., and Hancock W.W., *Deacetylase inhibition promotes the generation and function of regulatory T cells.* Nat Med, 2007. **13**(11): p. 1299-307.

310. Geirnaert A.,Calatayud M.,Grootaert C.,Laukens D.,Devriese S.,Smagghe G.,De Vos M.,Boon N., and Van de Wiele T., *Butyrate-producing bacteria supplemented in vitro to Crohn's disease patient microbiota increased butyrate production and enhanced intestinal epithelial barrier integrity.* Sci Rep, 2017. **7**(1): p. 11450.

311. Cummings J.H. and Macfarlane G.T., *The control and consequences of bacterial fermentation in the human colon.* J Appl Bacteriol, 1991. **70**(6): p. 443-59.

312. Ericsson A.C.,Davis J.W.,Spollen W.,Bivens N., and Givan S., *Effects of vendor and genetic background on the composition of the fecal microbiota of inbred mice.* PloS one, 2015. 10.1371/journal.pone.0116704.

313. Hufeldt M.R.,Nielsen D.S.,Vogensen F.K.,Midtvedt T., and Hansen A.K., *Variation in the gut microbiota of laboratory mice is related to both genetic and environmental factors.* Comp Med, 2010. **60**(5): p. 336-47.

314. Laukens D.,Brinkman B.M., and Raes J., *Heterogeneity of the gut microbiome in mice: guidelines for optimizing experimental design.* FEMS …, 2015.

315. Ochoa-Repáraz J.,Mielcarz D.W., and Ditrio L.E., *Role of gut commensal microflora in the development of experimental autoimmune encephalomyelitis.* The Journal of …, 2009. 10.4049/jimmunol.0900747.

316. Lee Y.K.,Menezes J.S., and Umesaki Y., *Proinflammatory T-cell responses to gut microbiota promote experimental autoimmune encephalomyelitis.* Proceedings of the …, 2011.

317. Edgar R.C.,Haas B.J.,Clemente J.C., and Quince C., *UCHIME improves sensitivity and speed of chimera detection.* …, 2011.

318. Price M.N.,Dehal P.S., and Arkin A.P., *FastTree 2–approximately maximum-likelihood trees for large alignments.* PloS one, 2010. 10.1371/journal.pone.0009490.

319. Parks D.H.,Tyson G.W.,Hugenholtz P., and Beiko R.G., *STAMP: statistical analysis of taxonomic and functional profiles.* Bioinformatics, 2014.

320. Lozupone C.A. and Knight R., *Species divergence and the measurement of microbial diversity.* FEMS Microbiol Rev, 2008. **32**(4): p. 557-78.

321. Robinson M.D.,McCarthy D.J., and Smyth G.K., *edgeR: a Bioconductor package for differential expression analysis of digital gene expression data.* Bioinformatics, 2010.

322. Masetti G.,Moshkelgosha S.,Kohling H.L.,Covelli D.,Banga J.P.,Berchner-Pfannschmidt U.,Horstmann M.,Diaz-Cano S.,Goertz G.E.,Plummer S.,Eckstein A.,Ludgate M.,Biscarini F.,Marchesi J.R., and consortium I., *Gut microbiota in experimental murine model of Graves' orbitopathy established in different environments may modulate clinical presentation of disease.* Microbiome, 2018. **6**(1): p. 97.

323. Mariat D.,Firmesse O.,Levenez F.,Guimaraes V.,Sokol H.,Dore J.,Corthier G., and Furet J.P., *The Firmicutes/Bacteroidetes ratio of the human microbiota changes with age.* BMC Microbiol, 2009. **9**: p. 123.

324. Jakobsson H.E.,Rodriguez-Pineiro A.M.,Schutte A.,Ermund A.,Boysen P.,Bemark M.,Sommer F.,Backhed F.,Hansson G.C., and Johansson M.E., *The composition of the gut microbiota shapes the colon mucus barrier.* EMBO Rep, 2015. **16**(2): p. 164-77.

325. Kläring K.,Hanske L., and Bui N., *Intestinimonas butyriciproducens gen. nov., sp. nov., a butyrate-producing bacterium from the mouse intestine.* … of systematic and …, 2013.

326. Bui T.,Ritari J.,Boeren S.,de Waard P.,Plugge C.M., and de Vos W.M., *Production of butyrate from lysine and the Amadori product fructoselysine by a human gut commensal.* Nature communications, 2015. **6**: p. 10062.

327. Mizuno M.,Noto D.,Kaga N.,Chiba A., and Miyake S., *The dual role of short fatty acid chains in the pathogenesis of autoimmune disease models.* PloS one, 2017. **12**(2): p. e0173032.

328. Million M.,Lagier J.C.,Yahav D., and Paul M., *Gut bacterial microbiota and obesity.* Clinical Microbiology and Infection, 2013. **19**(4): p. 305-313.

329. Anderson D.J. and Axel R., *Molecular probes for the development and plasticity of neural crest derivatives.* Cell, 1985. **42**(2): p. 649-62.

330. Faust K.,Lahti L.,Gonze D.,de Vos W.M., and Raes J., *Metagenomics meets time series analysis: unraveling microbial community dynamics.* Curr Opin Microbiol, 2015. **25**: p. 56-66.

331. Lees H.,Swann J.,Poucher S.M.,Nicholson J.K.,Holmes E.,Wilson I.D., and Marchesi J.R., *Age and microenvironment outweigh genetic influence on the Zucker rat microbiome.* PloS one, 2014. **9**(9): p. e100916.

332. McCafferty J.,Mühlbauer M.,Gharaibeh R.Z.,Arthur J.C.,Perez-Chanona E.,Sha W.,Jobin C., and Fodor A.A., *Stochastic changes over time and not founder effects drive cage effects in microbial community assembly in a mouse model.* The ISME Journal, 2013. **7**(11): p. 2116-2125.

333. Juers D.H.,Matthews B.W., and Huber R.E., *LacZ galactosidase: structure and function of an enzyme of historical and molecular biological importance.* Protein Science, 2012. **21**(12): p. 1792-1807.

334. Ericsson A.C. and Franklin C.L., *Manipulating the Gut Microbiota: Methods and Challenges.* ILAR J, 2015. **56**(2): p. 205-17.

335. Andrews B.S.,Eisenberg R.A.,Theofilopoulos A.N.,Izui S.,Wilson C.B.,McConahey P.J.,Murphy E.D.,Roths J.B., and Dixon F.J., *Spontaneous murine lupus-like syndromes. Clinical and immunopathological manifestations in several strains.* J Exp Med, 1978. **148**(5): p. 1198-215.

336. Mu Q.,Tavella V.J.,Kirby J.L.,Cecere T.E.,Chung M.,Lee J.,Li S.,Ahmed S.A.,Eden K.,Allen I.C.,Reilly C.M., and Luo X.M., *Antibiotics ameliorate lupus-like symptoms in mice.* Sci Rep, 2017. **7**(1): p. 13675.

337. Horai R.,Zarate-Blades C.R.,Dillenburg-Pilla P.,Chen J.,Kielczewski J.L.,Silver P.B.,Jittayasothorn Y.,Chan C.C.,Yamane H.,Honda K., and Caspi R.R., *Microbiota-Dependent Activation of an Autoreactive T Cell Receptor Provokes Autoimmunity in an Immunologically Privileged Site.* Immunity, 2015. **43**(2): p. 343-53.

338. Candon S.,Perez-Arroyo A.,Marquet C.,Valette F.,Foray A.P.,Pelletier B.,Milani C.,Ventura M.,Bach J.F., and Chatenoud L., *Antibiotics in early life alter the gut microbiome and increase disease incidence in a spontaneous mouse model of autoimmune insulin-dependent diabetes.* PloS one, 2015. **10**(5): p. e0125448.

339. Wen L.,Ley R.E.,Volchkov P.Y.,Stranges P.B.,Avanesyan L.,Stonebraker A.C.,Hu C.,Wong F.S.,Szot G.L.,Bluestone J.A.,Gordon J.I., and Chervonsky A.V., *Innate immunity and intestinal microbiota in the development of Type 1 diabetes.* Nature, 2008. **455**(7216): p. 1109-13.

340. Peng J.,Narasimhan S.,Marchesi J.R.,Benson A.,Wong F.S., and Wen L., *Long term effect of gut microbiota transfer on diabetes development.* J Autoimmun, 2014. **53**: p. 85-94.

341. Staley C.,Vaughn B.P.,Graiziger C.T.,Singroy S.,Hamilton M.J.,Yao D.,Chen C.,Khoruts A., and Sadowsky M.J., *Community dynamics drive punctuated engraftment of the fecal microbiome following transplantation using freeze-dried, encapsulated fecal microbiota.* Gut Microbes, 2017. **8**(3): p. 276-288.

342. Staley C.,Kelly C.R.,Brandt L.J.,Khoruts A., and Sadowsky M.J., *Complete Microbiota Engraftment Is Not Essential for Recovery from Recurrent Clostridium difficile Infection following Fecal Microbiota Transplantation.* MBio, 2016. **7**(6).

343. Youngster I. and Gerding D.N., *Editorial: Making Fecal Microbiota Transplantation Easier to Swallow: Freeze-Dried Preparation for Recurrent Clostridium difficile Infections.* Am J Gastroenterol, 2017. **112**(6): p. 948-950.

344. Ott S.J.,Waetzig G.H.,Rehman A.,Moltzau-Anderson J.,Bharti R.,Grasis J.A.,Cassidy L.,Tholey A.,Fickenscher H.,Seegert D.,Rosenstiel P., and Schreiber S., *Efficacy of Sterile Fecal Filtrate Transfer for Treating Patients With Clostridium difficile Infection.* Gastroenterology, 2017. **152**(4): p. 799-811 e7.

345. Hill C.,Guarner F.,Reid G.,Gibson G.R.,Merenstein D.J.,Pot B.,Morelli L.,Canani R.B.,Flint H.J.,Salminen S.,Calder P.C., and Sanders M.E., *Expert consensus document. The International Scientific Association for Probiotics and Prebiotics consensus statement on the scope and appropriate use of the term probiotic.* Nat Rev Gastroenterol Hepatol, 2014. **11**(8): p. 506-14.

346. Calcinaro F.,Dionisi S.,Marinaro M.,Candeloro P.,Bonato V.,Marzotti S.,Corneli R.B.,Ferretti E.,Gulino A.,Grasso F.,De Simone C.,Di Mario U.,Falorni A.,Boirivant M., and Dotta F., *Oral probiotic administration induces interleukin-10 production and prevents spontaneous autoimmune diabetes in the non-obese diabetic mouse.* Diabetologia, 2005. **48**(8): p. 1565-75.

347. Lavasani S.,Dzhambazov B.,Nouri M.,Fak F.,Buske S.,Molin G.,Thorlacius H.,Alenfall J.,Jeppsson B., and Westrom B., *A novel probiotic mixture exerts a therapeutic effect on experimental autoimmune encephalomyelitis mediated by IL-10 producing regulatory T cells.* PloS one, 2010. **5**(2): p. e9009.

348. Takata K.,Kinoshita M.,Okuno T.,Moriya M.,Kohda T.,Honorat J.A.,Sugimoto T.,Kumanogoh A.,Kayama H.,Takeda K.,Sakoda S., and Nakatsuji Y., *The lactic acid bacterium Pediococcus acidilactici suppresses autoimmune encephalomyelitis by inducing IL-10-producing regulatory T cells.* PloS one, 2011. **6**(11): p. e27644.

349. Pollinger B.,Krishnamoorthy G.,Berer K.,Lassmann H.,Bosl M.R.,Dunn R.,Domingues H.S.,Holz A.,Kurschus F.C., and Wekerle H., *Spontaneous relapsing-remitting EAE in the SJL/J mouse: MOG-reactive transgenic T cells recruit endogenous MOG-specific B cells.* J Exp Med, 2009. **206**(6): p. 1303-16.

350. Berer K.,Gerdes L.A.,Cekanaviciute E.,Jia X.,Xiao L.,Xia Z.,Liu C.,Klotz L.,Stauffer U.,Baranzini S.E.,Kumpfel T.,Hohlfeld R.,Krishnamoorthy G., and Wekerle H., *Gut microbiota from multiple sclerosis patients enables spontaneous autoimmune encephalomyelitis in mice.* Proc Natl Acad Sci U S A, 2017. **114**(40): p. 10719-10724.

351. Bartalena L.,Burch H.B.,Burman K.D., and Kahaly G.J., *A 2013 European survey of clinical practice patterns in the management of Graves' disease.* Clin Endocrinol (Oxf), 2016. **84**(1): p. 115-20.

352. Biscarini F.,Palazzo F.,Castellani F.,Masetti G.,Grotta L.,Cichelli A., and Martino G., *Rumen microbiome in dairy calves fed copper and grape-pomace dietary supplementations: Composition and predicted functional profile.* PloS one, 2018. **13**(11): p. e0205670.

353. Quast C.,Pruesse E.,Yilmaz P.,Gerken J.,Schweer T.,Yarza P.,Peplies J., and Glockner F.O., *The SILVA ribosomal RNA gene database project: improved data processing and web-based tools.* Nucleic Acids Res, 2013. **41**(Database issue): p. D590-6.

354. Paulson J.N.,Stine O.C.,Bravo H.C., and Pop M., *Differential abundance analysis for microbial marker-gene surveys.* Nat Methods, 2013. **10**(12): p. 1200-2.

355. Benjamini Y. and Hochberg Y., *Controlling the False Discovery Rate: A Practical and Powerful Approach to Multiple Testing.* Journal of the Royal Statistical Society. Series B (Methodological), 1995. **57**(1): p. 289-300.

356. Bray J.R. and Curtis J.T., *An Ordination of the Upland Forest Communities of Southern Wisconsin.* Ecological Monographs, 1957. **27**(4): p. 325-349.

357. Breiman L., *Random Forests.* Mach. Learn., 2001. **45**(1): p. 5-32.

358. Cutler A.,Cutler D.R., and Stevens J.R., *Random Forests*, in *Ensemble Machine Learning*. 2012. p. 157-175.

359. Breiman L., *Bagging Predictors.* Machine Learning, 1996. **24**(2): p. 123-140.

360. Asshauer K.P.,Wemheuer B.,Daniel R., and Meinicke P., *Tax4Fun: predicting functional profiles from metagenomic 16S rRNA data.* Bioinformatics, 2015. **31**(17): p. 2882-4.

361. Petra Aßhauer K. and Meinicke P., *On the estimation of metabolic profiles in metagenomics*. Vol. 34. 2013.

362. Kanehisa M.,Sato Y.,Kawashima M.,Furumichi M., and Tanabe M., *KEGG as a reference resource for gene and protein annotation.* Nucleic Acids Res, 2016. **44**(D1): p. D457-62.

363. Knights D.,Kuczynski J.,Charlson E.S.,Zaneveld J.,Mozer M.C.,Collman R.G.,Bushman F.D.,Knight R., and Kelley S.T., *Bayesian community-wide culture-independent microbial source tracking.* Nat Methods, 2011. **8**(9): p. 761-3.

364. Gu S.,Chen D.,Zhang J.N.,Lv X.,Wang K.,Duan L.P.,Nie Y., and Wu X.L., *Bacterial community mapping of the mouse gastrointestinal tract.* PloS one, 2013. **8**(10): p. e74957.

365. Oh J.Z.,Ravindran R.,Chassaing B.,Carvalho F.A.,Maddur M.S.,Bower M.,Hakimpour P.,Gill K.P.,Nakaya H.I.,Yarovinsky F.,Sartor R.B.,Gewirtz A.T., and Pulendran B., *TLR5-mediated sensing of gut microbiota is necessary for antibody responses to seasonal influenza vaccination.* Immunity, 2014. **41**(3): p. 478-492.

366. Moshkelgosha S.,Masetti G.,Berchner-Pfannschmidt U.,Verhasselt H.L.,Horstmann M.,Diaz-Cano S.,Noble A.,Edelman B.,Covelli D.,Plummer S.,Marchesi J.R.,Ludgate M.,Biscarini F.,Eckstein A., and Banga J.P., *Gut Microbiome in BALB/c and C57BL/6J Mice Undergoing Experimental Thyroid Autoimmunity Associate with Differences in Immunological Responses and Thyroid Function.* Horm Metab Res, 2018. **50**(12): p. 932-941.

367. Bongers G.,Pacer M.E.,Geraldino T.H.,Chen L.,He Z.,Hashimoto D.,Furtado G.C.,Ochando J.,Kelley K.A.,Clemente J.C.,Merad M.,van Bakel H., and Lira S.A., *Interplay of host microbiota, genetic perturbations, and inflammation promotes local development of intestinal neoplasms in mice.* J Exp Med, 2014. **211**(3): p. 457-72.

368. Antonopoulos D.A.,Huse S.M.,Morrison H.G.,Schmidt T.M.,Sogin M.L., and Young V.B., *Reproducible community dynamics of the gastrointestinal microbiota following antibiotic perturbation.* Infect Immun, 2009. **77**(6): p. 2367-75.

369. Derrien M.,Collado M.C.,Ben-Amor K.,Salminen S., and de Vos W.M., *The Mucin degrader Akkermansia muciniphila is an abundant resident of the human intestinal tract.* Appl Environ Microbiol, 2008. **74**(5): p. 1646-8.

370. Derrien M.,Van Baarlen P.,Hooiveld G.,Norin E.,Muller M., and de Vos W.M., *Modulation of Mucosal Immune Response, Tolerance, and Proliferation in Mice Colonized by the Mucin-Degrader Akkermansia muciniphila.* Front Microbiol, 2011. **2**: p. 166.

371. Hansen C.H.,Krych L.,Nielsen D.S.,Vogensen F.K.,Hansen L.H.,Sorensen S.J.,Buschard K., and Hansen A.K., *Early life treatment with vancomycin propagates Akkermansia muciniphila and reduces diabetes incidence in the NOD mouse.* Diabetologia, 2012. **55**(8): p. 2285-94.

372. Livanos A.E.,Greiner T.U.,Vangay P.,Pathmasiri W.,Stewart D.,McRitchie S.,Li H.,Chung J.,Sohn J.,Kim S.,Gao Z.,Barber C.,Kim J.,Ng S.,Rogers A.B.,Sumner S.,Zhang X.S.,Cadwell K.,Knights D.,Alekseyenko A.,Backhed F., and Blaser M.J., *Antibiotic-mediated gut microbiome perturbation accelerates development of type 1 diabetes in mice.* Nat Microbiol, 2016. **1**(11): p. 16140.

373. Wang Z.J.,Zhang F.M.,Wang L.S.,Yao Y.W.,Zhao Q., and Gao X., *Lipopolysaccharides can protect mesenchymal stem cells (MSCs) from oxidative stress-induced apoptosis and enhance proliferation of MSCs via Toll-like receptor(TLR)-4 and PI3K/Akt.* Cell Biol Int, 2009. **33**(6): p. 665-74.

374. Nielsen T.B.,Pantapalangkoor P.,Yan J.,Luna B.M.,Dekitani K.,Bruhn K.,Tan B.,Junus J.,Bonomo R.A.,Schmidt A.M.,Everson M.,Duncanson F.,Doherty T.M.,Lin L., and Spellberg B., *Diabetes Exacerbates Infection via Hyperinflammation by Signaling through TLR4 and RAGE.* MBio, 2017. **8**(4).

375. Peng S.,Li C.,Wang X.,Liu X.,Han C.,Jin T.,Liu S.,Zhang X.,Zhang H.,He X.,Xie X.,Yu X.,Wang C.,Shan L.,Fan C.,Shan Z., and Teng W., *Increased Toll-Like Receptors Activity and TLR Ligands in Patients with Autoimmune Thyroid Diseases.* Front Immunol, 2016. **7**: p. 578.

376. Ott S.J.,Musfeldt M.,Wenderoth D.F.,Hampe J.,Brant O.,Folsch U.R.,Timmis K.N., and Schreiber S., *Reduction in diversity of the colonic mucosa associated bacterial microflora in patients with active inflammatory bowel disease.* Gut, 2004. **53**(5): p. 685-93.

377. Khanna S.,Vazquez-Baeza Y.,Gonzalez A.,Weiss S.,Schmidt B.,Muniz-Pedrogo D.A.,Rainey J.F., 3rd,Kammer P.,Nelson H.,Sadowsky M.,Khoruts A.,Farrugia S.L.,Knight R.,Pardi D.S., and Kashyap P.C., *Changes in microbial ecology after fecal microbiota transplantation for recurrent C. difficile infection affected by underlying inflammatory bowel disease.* Microbiome, 2017. **5**(1): p. 55.

378. Ridaura V.K.,Faith J.J.,Rey F.E.,Cheng J.,Duncan A.E.,Kau A.L.,Griffin N.W.,Lombard V.,Henrissat B.,Bain J.R.,Muehlbauer M.J.,Ilkayeva O.,Semenkovich C.F.,Funai K.,Hayashi D.K.,Lyle B.J.,Martini M.C.,Ursell L.K.,Clemente J.C.,Van Treuren W.,Walters W.A.,Knight R.,Newgard C.B.,Heath A.C., and Gordon J.I., *Gut microbiota from twins discordant for obesity modulate metabolism in mice.* Science, 2013. **341**(6150): p. 1241214.

379. Youngster I.,Sauk J.,Pindar C.,Wilson R.G.,Kaplan J.L.,Smith M.B.,Alm E.J.,Gevers D.,Russell G.H., and Hohmann E.L., *Fecal microbiota transplant for relapsing Clostridium difficile infection using a frozen inoculum from unrelated donors: a randomized, open-label, controlled pilot study.* Clin Infect Dis, 2014. **58**(11): p. 1515-22.

380. Hecker M.T.,Obrenovich M.E.,Cadnum J.L.,Jencson A.L.,Jain A.K.,Ho E., and Donskey C.J., *Fecal Microbiota Transplantation by Freeze-Dried Oral Capsules for Recurrent Clostridium difficile Infection.* Open Forum Infect Dis, 2016. **3**(2): p. ofw091.

381. Hamilton M.J.,Weingarden A.R.,Unno T.,Khoruts A., and Sadowsky M.J., *High-throughput DNA sequence analysis reveals stable engraftment of gut microbiota following transplantation of previously frozen fecal bacteria.* Gut Microbes, 2013. **4**(2): p. 125-35.

382. Wrzosek L.,Ciocan D.,Borentain P.,Spatz M.,Puchois V.,Hugot C.,Ferrere G.,Mayeur C.,Perlemuter G., and Cassard A.M., *Transplantation of human microbiota into conventional mice durably reshapes the gut microbiota.* Sci Rep, 2018. **8**(1): p. 6854.

383. Varian B.J.,Goureshetti S.,Poutahidis T.,Lakritz J.R.,Levkovich T.,Kwok C.,Teliousis K.,Ibrahim Y.M.,Mirabal S., and Erdman S.E., *Beneficial bacteria inhibit cachexia.* Oncotarget, 2016. **7**(11): p. 11803-16.

384. Alqayim M.A.J., *Effects of Lactobacillus acidophilus on Pituitary-thyroid Axis in Growing Rat.* Advances in Animal and Veterinary Sciences, 2015. **3**(5): p. 269-275.

385. Zhou J.S. and Gill H.S., *Immunostimulatory probiotic Lactobacillus rhamnosus HN001 and Bifidobacterium lactis HN019 do not induce pathological inflammation in mouse model of experimental autoimmune thyroiditis.* Int J Food Microbiol, 2005. **103**(1): p. 97-104.

386. Karimi G.,Sabran M.R.,Jamaluddin R.,Parvaneh K.,Mohtarrudin N.,Ahmad Z.,Khazaai H., and Khodavandi A., *The anti-obesity effects of Lactobacillus casei strain Shirota versus Orlistat on high fat diet-induced obese rats.* Food Nutr Res, 2015. **59**: p. 29273.

387. Lee H.Y.,Park J.H.,Seok S.H.,Baek M.W.,Kim D.J.,Lee K.E.,Paek K.S.,Lee Y., and Park J.H., *Human originated bacteria, Lactobacillus rhamnosus PL60, produce conjugated linoleic acid and show anti-obesity effects in diet-induced obese mice.* Biochim Biophys Acta, 2006. **1761**(7): p. 736-44.

388. Zhou K., *Strategies to promote abundance of Akkermansia muciniphila, an emerging probiotics in the gut, evidence from dietary intervention studies.* J Funct Foods, 2017. **33**: p. 194-201.

389. Schneeberger M.,Everard A.,Gomez-Valades A.G.,Matamoros S.,Ramirez S.,Delzenne N.M.,Gomis R.,Claret M., and Cani P.D., *Akkermansia muciniphila inversely correlates with the onset of inflammation, altered adipose tissue metabolism and metabolic disorders during obesity in mice.* Sci Rep, 2015. **5**: p. 16643.

390. Allen-Blevins C.R.,You X.,Hinde K., and Sela D.A., *Handling stress may confound murine gut microbiota studies.* PeerJ, 2017. **5**: p. e2876.

391. Green E.R. and Mecsas J., *Bacterial Secretion Systems: An Overview.* Microbiol Spectr, 2016. **4**(1).

392. Morita H.,Nakanishi K.,Dohi T.,Yasugi E., and Oshima M., *Phospholipid turnover in the inflamed intestinal mucosa: arachidonic acid-rich phosphatidyl/plasmenyl-ethanolamine in the mucosa in inflammatory bowel disease.* J Gastroenterol, 1999. **34**(1): p. 46-53.

393. Gevers D.,Kugathasan S.,Denson L.A.,Vazquez-Baeza Y.,Van Treuren W.,Ren B.,Schwager E.,Knights D.,Song S.J.,Yassour M.,Morgan X.C.,Kostic A.D.,Luo C.,Gonzalez A.,McDonald D.,Haberman Y.,Walters T.,Baker S.,Rosh J.,Stephens M.,Heyman M.,Markowitz J.,Baldassano R.,Griffiths A.,Sylvester F.,Mack D.,Kim S.,Crandall W.,Hyams J.,Huttenhower C.,Knight R., and Xavier R.J., *The treatment-naive microbiome in new-onset Crohn's disease.* Cell Host Microbe, 2014. **15**(3): p. 382-392.

394. Sanchez B.,Urdaci M.C., and Margolles A., *Extracellular proteins secreted by probiotic bacteria as mediators of effects that promote mucosa-bacteria interactions.* Microbiology, 2010. **156**(Pt 11): p. 3232-42.

395. de Herder W.W.,Hazenberg M.P.,Pennock-Schroder A.M.,Oosterlaken A.C.,Rutgers M., and Visser T.J., *On the enterohepatic cycle of triiodothyronine in rats; importance of the intestinal microflora.* Life Sci, 1989. **45**(9): p. 849-56.

396. Hays M.T., *Thyroid hormone and the gut.* Endocr Res, 1988. **14**(2-3): p. 203-24.

397. Shenkman L. and Bottone E.J., *The occurrence of antibodies to Yersinia enterocolitica in thyroid diseases.* The occurrence of antibodies to Yersinia enterocolitica in thyroid diseases, 1981.

398. Wenzel B.E.,Heesmann J., and The … W.-K.W., *Antibodies to Plasmid-encoded Proteins of enteropathogenic Yersinia in Patiens with autoimmune Thyroid Disease.* The …, 1988.

399. Heyma P. and and experimental … H.-L.C., *Thyrotrophin (TSH) binding sites on Yersinia enterocolitica recognized by immunoglobulins from humans with Graves' disease.* Clinical and experimental …, 1986.

400. Weiss M.,Ingbar S.H.,Winblad S., and Science K.-D.L., *Demonstration of a saturable binding site for thyrotropin in Yersinia enterocolitica.* Science, 1983. 10.1126/science.6298936.

401. Wang Z.,Zhang Q.,Lu J.,Jiang F., and of … Z.-H., *Identification of Outer Membrane Porin F Protein of Yersinia enterocolitica Recognized by Antithyrotopin Receptor Antibodies in Graves' Disease and ….* The Journal of …, 2010.

402. Guarneri F.,Carlotta D.,Saraceno G., and … T.-F., *Bioinformatics Support the Possible Triggering of Autoimmune Thyroid Diseases by Yersinia enterocolitica Outer Membrane Proteins Homologous to the Human ….* …, 2011. 10.1089/thy.2010.0364.

403. Benvenga S.,Santarpia L.,Trimarchi F., and Guarneri F., *Human thyroid autoantigens and proteins of Yersinia and Borrelia share amino acid sequence homology that includes binding motifs to HLA-DR molecules and T-cell receptor.* Thyroid : official journal of the American Thyroid Association, 2006. **16**(3): p. 225-236.

404. Benvenga S.,Guarneri F.,Vaccaro M.,Santarpia L., and Trimarchi F., *Homologies between proteins of Borrelia burgdorferi and thyroid autoantigens.* Thyroid : official journal of the American Thyroid Association, 2004. **14**(11): p. 964-966.

405. Rosner B.M.,Stark K., and Werber D., *Epidemiology of reported Yersinia enterocolitica infections in Germany, 2001-2008.* BMC Public Health, 2010. **10**: p. 337.

406. Olesen S.W. and Alm E.J., *Dysbiosis is not an answer.* Nat Microbiol, 2016. **1**: p. 16228.

407. Lodes M.J.,Cong Y.,Elson C.O.,Mohamath R.,Landers C.J.,Targan S.R.,Fort M., and Hershberg R.M., *Bacterial flagellin is a dominant antigen in Crohn disease.* J Clin Invest, 2004. **113**(9): p. 1296-306.

408. Ogura Y.,Bonen D.K.,Inohara N.,Nicolae D.L.,Chen F.F.,Ramos R.,Britton H.,Moran T.,Karaliuskas R.,Duerr R.H.,Achkar J.P.,Brant S.R.,Bayless T.M.,Kirschner B.S.,Hanauer S.B.,Nunez G., and Cho J.H., *A frameshift mutation in NOD2 associated with susceptibility to Crohn's disease.* Nature, 2001. **411**(6837): p. 603-6.

409. Papadakis K.A.,Yang H.,Ippoliti A.,Mei L.,Elson C.O.,Hershberg R.M.,Vasiliauskas E.A.,Fleshner P.R.,Abreu M.T.,Taylor K.,Landers C.J.,Rotter J.I., and Targan S.R., *Anti-flagellin (CBir1) phenotypic and genetic Crohn's disease associations.* Inflamm Bowel Dis, 2007. **13**(5): p. 524-30.

410. Manichanh C.,Rigottier-Gois L.,Bonnaud E.,Gloux K.,Pelletier E.,Frangeul L.,Nalin R.,Jarrin C.,Chardon P.,Marteau P.,Roca J., and Dore J., *Reduced diversity of faecal microbiota in Crohn's disease revealed by a metagenomic approach.* Gut, 2006. **55**(2): p. 205-11.

411. Scanlan P.D.,Shanahan F., and O'Mahony C., *Culture-independent analyses of temporal variation of the dominant fecal microbiota and targeted bacterial subgroups in Crohn's disease.* Journal of clinical …, 2006. 10.1128/JCM.00312-06.

412. Frank D.N.,Amand A.L.S., and Feldman R.A., *Molecular-phylogenetic characterization of microbial community imbalances in human inflammatory bowel diseases.* Proceedings of the …, 2007. 10.1073/pnas.0706625104.

413. Steiner G. and Smolen J., *Autoantibodies in rheumatoid arthritis and their clinical significance.* Arthritis Res, 2002. **4 Suppl 2**: p. S1-5.

414. Scher J.U.,Sczesnak A.,Longman R.S.,Segata N.,Ubeda C.,Bielski C.,Rostron T.,Cerundolo V.,Pamer E.G.,Abramson S.B.,Huttenhower C., and Littman D.R.,

Expansion of intestinal Prevotella copri correlates with enhanced susceptibility to arthritis. Elife, 2013. **2**: p. e01202.

415. Maeda Y. and Takeda K., *Role of Gut Microbiota in Rheumatoid Arthritis.* J Clin Med, 2017. **6**(6).

416. Zhang X.,Zhang D.,Jia H.,Feng Q.,Wang D.,Liang D.,Wu X.,Li J.,Tang L.,Li Y.,Lan Z.,Chen B.,Li Y.,Zhong H.,Xie H.,Jie Z.,Chen W.,Tang S.,Xu X.,Wang X.,Cai X.,Liu S.,Xia Y.,Li J.,Qiao X.,Al-Aama J.Y.,Chen H.,Wang L.,Wu Q.J.,Zhang F.,Zheng W.,Li Y.,Zhang M.,Luo G.,Xue W.,Xiao L.,Li J.,Chen W.,Xu X.,Yin Y.,Yang H.,Wang J.,Kristiansen K.,Liu L.,Li T.,Huang Q.,Li Y., and Wang J., *The oral and gut microbiomes are perturbed in rheumatoid arthritis and partly normalized after treatment.* Nat Med, 2015. **21**(8): p. 895-905.

417. Terao C.,Suzuki A.,Ikari K.,Kochi Y.,Ohmura K.,Katayama M.,Nakabo S.,Yamamoto N.,Suzuki T.,Iwamoto T.,Yurugi K.,Miura Y.,Maekawa T.,Takasugi K.,Kubo M.,Saji H.,Taniguchi A.,Momohara S.,Yamamoto K.,Yamanaka H.,Mimori T., and Matsuda F., *An association between amino acid position 74 of HLA-DRB1 and anti-citrullinated protein antibody levels in Japanese patients with anti-citrullinated protein antibody-positive rheumatoid arthritis.* Arthritis Rheumatol, 2015. **67**(8): p. 2038-45.

418. Probstel A.K.,Sanderson N.S., and Derfuss T., *B Cells and Autoantibodies in Multiple Sclerosis.* Int J Mol Sci, 2015. **16**(7): p. 16576-92.

419. Miyake S.,Kim S.,Suda W.,Oshima K.,Nakamura M.,Matsuoka T.,Chihara N.,Tomita A.,Sato W.,Kim S.W.,Morita H.,Hattori M., and Yamamura T., *Dysbiosis in the Gut Microbiota of Patients with Multiple Sclerosis, with a Striking Depletion of Species Belonging to Clostridia XIVa and IV Clusters.* PloS one, 2015. **10**(9): p. e0137429.

420. Jangi S.,Gandhi R.,Cox L.M.,Li N.,von Glehn F.,Yan R.,Patel B.,Mazzola M.A.,Liu S.,Glanz B.L.,Cook S.,Tankou S.,Stuart F.,Melo K.,Nejad P.,Smith K.,Topcuolu B.D.,Holden J.,Kivisakk P.,Chitnis T.,De Jager P.L.,Quintana F.J.,Gerber G.K.,Bry L., and Weiner H.L., *Alterations of the human gut microbiome in multiple sclerosis.* Nat Commun, 2016. **7**: p. 12015.

421. American Diabetes A., *Diagnosis and classification of diabetes mellitus.* Diabetes Care, 2009. **32 Suppl 1**: p. S62-7.

422. Metcalfe K.A.,Hitman G.A.,Rowe R.E.,Hawa M.,Huang X.,Stewart T., and Leslie R.D., *Concordance for type 1 diabetes in identical twins is affected by insulin genotype.* Diabetes Care, 2001. **24**(5): p. 838-42.

423. Vaarala O.,Atkinson M.A., and Neu J., *The "Perfect Storm" for Type 1 Diabetes: The Complex Interplay Between Intestinal Microbiota, Gut Permeability, and Mucosal Immunity.* Diabetes, 2008. **57**(10): p. 2555-2562.

424. Tai N.,Peng J.,Liu F.,Gulden E.,Hu Y.,Zhang X.,Chen L.,Wong F.S., and Wen L., *Microbial antigen mimics activate diabetogenic CD8 T cells in NOD mice.* J Exp Med, 2016. **213**(10): p. 2129-46.

425. Kriegel M.A.,Sefik E.,Hill J.A.,Wu H.J.,Benoist C., and Mathis D., *Naturally transmitted segmented filamentous bacteria segregate with diabetes protection in nonobese diabetic mice.* Proc Natl Acad Sci U S A, 2011. **108**(28): p. 11548-53.

426. Murri M. and Leiva I., *Gut microbiota in children with type 1 diabetes differs from that in healthy children: a case-control study.* BMC …, 2013.

427. Alkanani A.K.,Hara N.,Gottlieb P.A.,Ir D.,Robertson C.E.,Wagner B.D.,Frank D.N., and Zipris D., *Alterations in Intestinal Microbiota Correlate With Susceptibility to Type 1 Diabetes.* Diabetes, 2015. **64**(10): p. 3510-20.

428. Brown C.T.,Davis-Richardson A.G.,Giongo A.,Gano K.A.,Crabb D.B.,Mukherjee N.,Casella G.,Drew J.C.,Ilonen J.,Knip M.,Hyoty H.,Veijola R.,Simell T.,Simell O.,Neu J.,Wasserfall C.H.,Schatz D.,Atkinson M.A., and Triplett E.W., *Gut microbiome metagenomics analysis suggests a functional model for the development of autoimmunity for type 1 diabetes.* PloS one, 2011. **6**(10): p. e25792.

429. Delzenne N.M.,Cani P.D.,Everard A.,Neyrinck A.M., and Bindels L.B., *Gut microorganisms as promising targets for the management of type 2 diabetes.* Diabetologia, 2015. **58**(10): p. 2206-17.

430. Evans J.M.,Morris L.S., and Marchesi J.R., *The gut microbiome: the role of a virtual organ in the endocrinology of the host.* J Endocrinol, 2013. **218**(3): p. R37-47.

431. Farzi A.,Frohlich E.E., and Holzer P., *Gut Microbiota and the Neuroendocrine System.* Neurotherapeutics, 2018. **15**(1): p. 5-22.

432. Kunc M.,Gabrych A., and Witkowski J.M., *Microbiome impact on metabolism and function of sex, thyroid, growth and parathyroid hormones.* Acta Biochim Pol, 2016. **63**(2): p. 189-201.

433. Markle J.G.,Mortin-Toth S.,Wong A.S.,Geng L.,Hayday A., and Danska J.S., *gammadelta T cells are essential effectors of type 1 diabetes in the nonobese diabetic mouse model.* J Immunol, 2013. **190**(11): p. 5392-401.

434. Yurkovetskiy L.,Burrows M.,Khan A.A.,Graham L.,Volchkov P.,Becker L.,Antonopoulos D.,Umesaki Y., and Chervonsky A.V., *Gender bias in autoimmunity is influenced by microbiota.* Immunity, 2013. **39**(2): p. 400-12.

435. Kester M.H.,Kaptein E.,Van Dijk C.H.,Roest T.J.,Tibboel D.,Coughtrie M.W., and Visser T.J., *Characterization of iodothyronine sulfatase activities in human and rat liver and placenta.* Endocrinology, 2002. **143**(3): p. 814-9.

436. DiStefano J.J., 3rd,Nguyen T.T., and Yen Y.M., *Transfer kinetics of 3,5,3'-triiodothyronine and thyroxine from rat blood to large and small intestines, liver, and kidneys in vivo.* Endocrinology, 1993. **132**(4): p. 1735-44.

437. Malo M.S.,Zhang W.,Alkhoury F.,Pushpakaran P.,Abedrapo M.A.,Mozumder M.,Fleming E.,Siddique A.,Henderson J.W., and Hodin R.A., *Thyroid hormone positively regulates the enterocyte differentiation marker intestinal alkaline phosphatase gene via an atypical response element.* Mol Endocrinol, 2004. **18**(8): p. 1941-62.

438. Zhao F.,Feng J.,Li J.,Zhao L.,Liu Y.,Chen H.,Jin Y.,Zhu B., and Wei Y., *Alterations of the Gut Microbiota in Hashimoto's Thyroiditis Patients.* Thyroid, 2018. **28**(2): p. 175-186.

439. Ishaq H.M.,Mohammad I.S.,Shahzad M.,Ma C.,Raza M.A.,Wu X.,Guo H.,Shi P., and Xu J., *Molecular Alteration Analysis of Human Gut Microbial Composition in Graves' disease Patients.* Int J Biol Sci, 2018. **14**(11): p. 1558-1570.

440. Zhang L.,Masetti G.,Colucci G.,Salvi M.,Covelli D.,Eckstein A.,Kaiser U.,Draman M.S.,Muller I.,Ludgate M.,Lucini L., and Biscarini F., *Combining micro-RNA and protein sequencing to detect robust biomarkers for Graves' disease and orbitopathy.* Sci Rep, 2018. **8**(1): p. 8386.

441. Savin Z.,Kivity S.,Yonath H., and Yehuda S., *Smoking and the intestinal microbiome.* Archives of Microbiology, 2018. **200**(5): p. 677-684.

442. Wu G.D.,Chen J.,Hoffmann C.,Bittinger K.,Chen Y.Y.,Keilbaugh S.A.,Bewtra M.,Knights D.,Walters W.A.,Knight R.,Sinha R.,Gilroy E.,Gupta K.,Baldassano R.,Nessel L.,Li H.,Bushman F.D., and Lewis J.D., *Linking long-term dietary patterns with gut microbial enterotypes.* Science, 2011. **334**(6052): p. 105-8.

443. Zhou L.,Li X.,Ahmed A.,Wu D.,Liu L.,Qiu J.,Yan Y.,Jin M., and Xin Y., *Gut microbe analysis between hyperthyroid and healthy individuals.* Curr Microbiol, 2014. **69**(5): p. 675-80.

444. Ishaq H.M.,Mohammad I.S.,Guo H.,Shahzad M.,Hou Y.J.,Ma C.,Naseem Z.,Wu X.,Shi P., and Xu J., *Molecular estimation of alteration in intestinal microbial composition in Hashimoto's thyroiditis patients.* Biomed Pharmacother, 2017. **95**: p. 865-874.

445. Jackson M.A.,Verdi S.,Maxan M.-E.,Shin C.M.,Zierer J.,Bowyer R.C.E.,Martin T.,Williams F.M.K.,Menni C.,Bell J.T.,Spector T.D., and Steves C.J., *Gut microbiota associations with common diseases and prescription medications in a population-based cohort.* Nature communications, 2018. **9**(1).

446. Davis-Richardson A.G.,Ardissone A.N.,Dias R.,Simell V.,Leonard M.T.,Kemppainen K.M.,Drew J.C.,Schatz D.,Atkinson M.A.,Kolaczkowski B.,Ilonen J.,Knip M.,Toppari J.,Nurminen N.,Hyoty H.,Veijola R.,Simell T.,Mykkanen J.,Simell O., and Triplett E.W., *Bacteroides dorei dominates gut microbiome prior to autoimmunity in Finnish children at high risk for type 1 diabetes.* Front Microbiol, 2014. **5**: p. 678.

447. Shi T.T.,Xin Z.,Hua L.,Zhao R.X.,Yang Y.L.,Wang H.,Zhang S.,Liu W., and Xie R.R., *Alterations in the intestinal microbiota of patients with severe and active Graves' orbitopathy: a cross-sectional study.* J Endocrinol Invest, 2019. 10.1007/s40618-019-1010-9.

448. Takeshita K.,Mizuno S.,Mikami Y.,Sujino T.,Saigusa K.,Matsuoka K.,Naganuma M.,Sato T.,Takada T.,Tsuji H.,Kushiro A.,Nomoto K., and Kanai T., *A Single Species of Clostridium Subcluster XIVa Decreased in Ulcerative Colitis Patients.* Inflamm Bowel Dis, 2016. **22**(12): p. 2802-2810.

449. Machiels K.,Joossens M.,Sabino J.,De Preter V.,Arijs I.,Eeckhaut V.,Ballet V.,Claes K.,Van Immerseel F.,Verbeke K.,Ferrante M.,Verhaegen J.,Rutgeerts P., and Vermeire S., *A decrease of the butyrate-producing species Roseburia hominis and Faecalibacterium prausnitzii defines dysbiosis in patients with ulcerative colitis.* Gut, 2014. **63**(8): p. 1275-83.

450. Huang X.,Ye Z.,Cao Q.,Su G.,Wang Q.,Deng J.,Zhou C.,Kijlstra A., and Yang P., *Gut Microbiota Composition and Fecal Metabolic Phenotype in Patients With Acute Anterior Uveitis.* Invest Ophthalmol Vis Sci, 2018. **59**(3): p. 1523-1531.

451. Braitch M.,Harikrishnan S.,Robins R.A.,Nichols C.,Fahey A.J.,Showe L., and Constantinescu C.S., *Glucocorticoids increase CD4CD25 cell percentage and Foxp3 expression in patients with multiple sclerosis.* Acta Neurol Scand, 2009. **119**(4): p. 239-45.

452. Mathian A.,Jouenne R.,Chader D.,Cohen-Aubart F.,Haroche J.,Fadlallah J.,Claer L.,Musset L.,Gorochov G.,Amoura Z., and Miyara M., *Regulatory T Cell Responses to High-Dose Methylprednisolone in Active Systemic Lupus Erythematosus.* PloS one, 2015. **10**(12): p. e0143689.

453. Kahaly G.J.,Shimony O.,Gellman Y.N.,Lytton S.D.,Eshkar-Sebban L.,Rosenblum N.,Refaeli E.,Kassem S.,Ilany J., and Naor D., *Regulatory T-cells in Graves' orbitopathy: baseline findings and immunomodulation by anti-T lymphocyte globulin.* J Clin Endocrinol Metab, 2011. **96**(2): p. 422-9.

454. Benvenga S. and Guarneri F., *Molecular mimicry and autoimmune thyroid disease.* Rev Endocr Metab Disord, 2016. **17**(4): p. 485-498.

455. Kiseleva E.P.,Mikhailopulo K.I.,Sviridov O.V.,Novik G.I.,Knirel Y.A., and Szwajcer Dey E., *The role of components of Bifidobacterium and Lactobacillus in pathogenesis and serologic diagnosis of autoimmune thyroid diseases.* Benef Microbes, 2011. **2**(2): p. 139-54.

456. Fransen F.,van Beek A.A.,Borghuis T.,Meijer B.,Hugenholtz F.,van der Gaast-de Jongh C.,Savelkoul H.F.,de Jonge M.I.,Faas M.M.,Boekschoten M.V.,Smidt H.,El Aidy S., and de Vos P., *The Impact of Gut Microbiota on Gender-Specific Differences in Immunity.* Front Immunol, 2017. **8**: p. 754.

457. Mueller S.,Saunier K.,Hanisch C.,Norin E.,Alm L.,Midtvedt T.,Cresci A.,Silvi S.,Orpianesi C.,Verdenelli M.C.,Clavel T.,Koebnick C.,Zunft H.J.,Dore J., and Blaut M., *Differences in fecal microbiota in different European study populations in relation to age, gender, and country: a cross-sectional study.* Appl Environ Microbiol, 2006. **72**(2): p. 1027-33.

458. Lee S.H.,Yun Y.,Kim S.J.,Lee E.J.,Chang Y.,Ryu S.,Shin H.,Kim H.L.,Kim H.N., and Lee J.H., *Association between Cigarette Smoking Status and Composition of Gut Microbiota: Population-Based Cross-Sectional Study.* J Clin Med, 2018. **7**(9).

459. Biedermann L.,Zeitz J.,Mwinyi J.,Sutter-Minder E.,Rehman A.,Ott S.J.,Steurer-Stey C.,Frei A.,Frei P.,Scharl M.,Loessner M.J.,Vavricka S.R.,Fried M.,Schreiber S.,Schuppler M., and Rogler G., *Smoking cessation induces profound changes in the composition of the intestinal microbiota in humans.* PloS one, 2013. **8**(3): p. e59260.

460. Munafo M.R.,Tilling K.,Taylor A.E.,Evans D.M., and Davey Smith G., *Collider scope: when selection bias can substantially influence observed associations.* Int J Epidemiol, 2018. **47**(1): p. 226-235.

461. Svetnik V.,Liaw A.,Tong C.,Culberson J.C.,Sheridan R.P., and Feuston B.P., *Random forest: a classification and regression tool for compound classification and QSAR modeling.* J Chem Inf Comput Sci, 2003. **43**(6): p. 1947-58.

462. Xiao J.,Chen L.,Johnson S.,Yu Y.,Zhang X., and Chen J., *Predictive Modeling of Microbiome Data Using a Phylogeny-Regularized Generalized Linear Mixed Model.* Front Microbiol, 2018. **9**: p. 1391.

463. Wu H.,Cai L.,Li D.,Wang X.,Zhao S.,Zou F., and Zhou K., *Metagenomics Biomarkers Selected for Prediction of Three Different Diseases in Chinese Population.* Biomed Res Int, 2018. **2018**: p. 2936257.

464. Segata N.,Izard J.,Waldron L.,Gevers D.,Miropolsky L.,Garrett W.S., and Huttenhower C., *Metagenomic biomarker discovery and explanation.* Genome Biol, 2011. **12**(6): p. R60.

465. Loomba R.,Seguritan V.,Li W.,Long T.,Klitgord N.,Bhatt A.,Dulai P.S.,Caussy C.,Bettencourt R.,Highlander S.K.,Jones M.B.,Sirlin C.B.,Schnabl B.,Brinkac L.,Schork N.,Chen C.H.,Brenner D.A.,Biggs W.,Yooseph S.,Venter J.C., and Nelson K.E., *Gut Microbiome-Based Metagenomic Signature for Non-invasive Detection of Advanced Fibrosis in Human Nonalcoholic Fatty Liver Disease.* Cell Metab, 2017. **25**(5): p. 1054-1062 e5.

466. Koshiyama H.,Sellitti D.F.,Akamizu T.,Doi S.Q.,Takeuchi Y.,Inoue D.,Sakaguchi H.,Takemura G.,Sato Y.,Takatsu Y., and Nakao K., *Cardiomyopathy associated with Graves' disease.* Clin Endocrinol (Oxf), 1996. **45**(1): p. 111-6.

467. Kitai T. and Tang W.H.W., *Gut microbiota in cardiovascular disease and heart failure.* Clin Sci (Lond), 2018. **132**(1): p. 85-91.

468. Kurylowicz A. and Nauman J., *The role of nuclear factor-kappaB in the development of autoimmune diseases: a link between genes and environment.* Acta Biochim Pol, 2008. **55**(4): p. 629-47.

469. Fasano A., *Zonulin, regulation of tight junctions, and autoimmune diseases.* Ann N Y Acad Sci, 2012. **1258**: p. 25-33.

470. Schiraldi C.,Cimini D., and De Rosa M., *Production of chondroitin sulfate and chondroitin.* Appl Microbiol Biotechnol, 2010. **87**(4): p. 1209-20.

471. Wang Q.,Huang S.Q.,Li C.Q.,Xu Q., and Zeng Q.P., *Akkermansia muciniphila May Determine Chondroitin Sulfate Ameliorating or Aggravating Osteoarthritis.* Front Microbiol, 2017. **8**: p. 1955.

472. Latousakis D. and Juge N., *How Sweet Are Our Gut Beneficial Bacteria? A Focus on Protein Glycosylation in Lactobacillus.* Int J Mol Sci, 2018. **19**(1).

473. Carlin A.F.,Uchiyama S.,Chang Y.C.,Lewis A.L.,Nizet V., and Varki A., *Molecular mimicry of host sialylated glycans allows a bacterial pathogen to engage neutrophil Siglec-9 and dampen the innate immune response.* Blood, 2009. **113**(14): p. 3333-6.

474. Yuki N.,Susuki K.,Koga M.,Nishimoto Y.,Odaka M.,Hirata K.,Taguchi K.,Miyatake T.,Furukawa K.,Kobata T., and Yamada M., *Carbohydrate mimicry between human ganglioside GM1 and Campylobacter jejuni lipooligosaccharide causes Guillain-Barre syndrome.* Proc Natl Acad Sci U S A, 2004. **101**(31): p. 11404-9.

475. Maverakis E.,Kim K.,Shimoda M.,Gershwin M.E.,Patel F.,Wilken R.,Raychaudhuri S.,Ruhaak L.R., and Lebrilla C.B., *Glycans in the immune system and The Altered Glycan Theory of Autoimmunity: a critical review.* J Autoimmun, 2015. **57**: p. 1-13.

476. Kimoto H.,Kurisaki J.,Tsuji N.M.,Ohmomo S., and Okamoto T., *Lactococci as probiotic strains: adhesion to human enterocyte-like Caco-2 cells and tolerance to low pH and bile.* Lett Appl Microbiol, 1999. **29**(5): p. 313-6.

477. Czerucka D.,Piche T., and Rampal P., *Review article: yeast as probiotics -- Saccharomyces boulardii.* Aliment Pharmacol Ther, 2007. **26**(6): p. 767-78.

478. Jensen H.,Roos S.,Jonsson H.,Rud I.,Grimmer S.,van Pijkeren J.P.,Britton R.A., and Axelsson L., *Role of Lactobacillus reuteri cell and mucus-binding protein A (CmbA) in adhesion to intestinal epithelial cells and mucus in vitro.* Microbiology, 2014. **160**(Pt 4): p. 671-81.

479. Mack D.R.,Michail S.,Wei S.,McDougall L., and Hollingsworth M.A., *Probiotics inhibit enteropathogenic E. coli adherence in vitro by inducing intestinal mucin gene expression.* Am J Physiol, 1999. **276**(4): p. G941-50.

480. Mack D.R.,Ahrne S.,Hyde L.,Wei S., and Hollingsworth M.A., *Extracellular MUC3 mucin secretion follows adherence of Lactobacillus strains to intestinal epithelial cells in vitro.* Gut, 2003. **52**(6): p. 827-33.

481. Otte J.M. and Podolsky D.K., *Functional modulation of enterocytes by gram-positive and gram-negative microorganisms.* Am J Physiol Gastrointest Liver Physiol, 2004. **286**(4): p. G613-26.

482. Caballero-Franco C.,Keller K.,De Simone C., and Chadee K., *The VSL#3 probiotic formula induces mucin gene expression and secretion in colonic epithelial cells.* Am J Physiol Gastrointest Liver Physiol, 2007. **292**(1): p. G315-22.

483. Gaudier E.,Michel C.,Segain J.P.,Cherbut C., and Hoebler C., *The VSL# 3 probiotic mixture modifies microflora but does not heal chronic dextran-sodium sulfate-induced colitis or reinforce the mucus barrier in mice.* J Nutr, 2005. **135**(12): p. 2753-61.

484. Dai C.,Zhao D.H., and Jiang M., *VSL#3 probiotics regulate the intestinal epithelial barrier in vivo and in vitro via the p38 and ERK signaling pathways.* Int J Mol Med, 2012. **29**(2): p. 202-8.

485. Pridmore R.D.,Pittet A.C.,Praplan F., and Cavadini C., *Hydrogen peroxide production by Lactobacillus johnsonii NCC 533 and its role in anti-Salmonella activity.* FEMS Microbiol Lett, 2008. **283**(2): p. 210-5.

486. Camargo A.C.,de Paula O.A.,Todorov S.D., and Nero L.A., *In Vitro Evaluation of Bacteriocins Activity Against Listeria monocytogenes Biofilm Formation.* Appl Biochem Biotechnol, 2016. **178**(6): p. 1239-51.

487. Zacharof M.P. and Lovitt R.W., *Investigation of Shelf Life of Potency and Activity of the Lactobacilli Produced Bacteriocins Through Their Exposure to Various Physicochemical Stress Factors.* Probiotics Antimicrob Proteins, 2012. **4**(3): p. 187-97.

488. Yildirim Z. and Johnson M.G., *Characterization and antimicrobial spectrum of bifidocin B, a bacteriocin produced by Bifidobacterium bifidum NCFB 1454.* J Food Prot, 1998. **61**(1): p. 47-51.

489. Duncan S.H.,Louis P., and Flint H.J., *Lactate-utilizing bacteria, isolated from human feces, that produce butyrate as a major fermentation product.* Appl Environ Microbiol, 2004. **70**(10): p. 5810-7.

490. Belenguer A.,Duncan S.H.,Calder A.G.,Holtrop G.,Louis P.,Lobley G.E., and Flint H.J., *Two routes of metabolic cross-feeding between Bifidobacterium adolescentis and butyrate-producing anaerobes from the human gut.* Appl Environ Microbiol, 2006. **72**(5): p. 3593-9.

491. Hepburn N.J.,Garaiova I.,Williams E.A.,Michael D.R., and Plummer S., *Probiotic supplement consumption alters cytokine production from peripheral blood mononuclear cells: a preliminary study using healthy individuals.* Benef Microbes, 2013. **4**(4): p. 313-7.

492. Derwa Y.,Gracie D.J.,Hamlin P.J., and Ford A.C., *Systematic review with meta-analysis: the efficacy of probiotics in inflammatory bowel disease.* Aliment Pharmacol Ther, 2017. **46**(4): p. 389-400.

493. Parkes G.C.,Sanderson J.D., and Whelan K., *Treating irritable bowel syndrome with probiotics: the evidence.* Proc Nutr Soc, 2010. **69**(2): p. 187-94.

494. Williams E.A.,Stimpson J.,Wang D.,Plummer S.,Garaiova I.,Barker M.E., and Corfe B.M., *Clinical trial: a multistrain probiotic preparation significantly reduces symptoms of irritable bowel syndrome in a double-blind placebo-controlled study.* Aliment Pharmacol Ther, 2009. **29**(1): p. 97-103.

495. Ganji-Arjenaki M. and Rafieian-Kopaei M., *Probiotics are a good choice in remission of inflammatory bowel diseases: A meta analysis and systematic review.* J Cell Physiol, 2018. **233**(3): p. 2091-2103.

496. Fedorak R.N.,Feagan B.G.,Hotte N.,Leddin D.,Dieleman L.A.,Petrunia D.M.,Enns R.,Bitton A.,Chiba N.,Pare P.,Rostom A.,Marshall J.,Depew W.,Bernstein C.N.,Panaccione R.,Aumais G.,Steinhart A.H.,Cockeram A.,Bailey R.J.,Gionchetti P.,Wong C., and Madsen K., *The probiotic VSL#3 has anti-inflammatory effects and could reduce endoscopic recurrence after surgery for Crohn's disease.* Clin Gastroenterol Hepatol, 2015. **13**(5): p. 928-35 e2.

497. Hendler R. and Zhang Y., *Probiotics in the Treatment of Colorectal Cancer.* Medicines (Basel), 2018. **5**(3).

498. Thomas D.M.,Bell B.,Papillon S.,Delaplain P.,Lim J.,Golden J.,Bowling J.,Wang J.,Wang L.,Grishin A.V., and Ford H.R., *Colonization with Escherichia coli EC 25 protects neonatal rats from necrotizing enterocolitis.* PloS one, 2017. **12**(11): p. e0188211.

499. Chang H.Y.,Chen J.H.,Chang J.H.,Lin H.C.,Lin C.Y., and Peng C.C., *Multiple strains probiotics appear to be the most effective probiotics in the prevention of necrotizing enterocolitis and mortality: An updated meta-analysis.* PloS one, 2017. **12**(2): p. e0171579.

500. AlFaleh K. and Anabrees J., *Probiotics for prevention of necrotizing enterocolitis in preterm infants.* Evid Based Child Health, 2014. **9**(3): p. 584-671.

501. Ljungberg M.,Korpela R.,Ilonen J.,Ludvigsson J., and Vaarala O., *Probiotics for the prevention of beta cell autoimmunity in children at genetic risk of type 1 diabetes--the PRODIA study.* Ann N Y Acad Sci, 2006. **1079**: p. 360-4.

502. Tonucci L.B.,Olbrich Dos Santos K.M.,Licursi de Oliveira L.,Rocha Ribeiro S.M., and Duarte Martino H.S., *Clinical application of probiotics in type 2 diabetes mellitus: A randomized, double-blind, placebo-controlled study.* Clin Nutr, 2017. **36**(1): p. 85-92.

503. Spaggiari G.,Brigante G.,De Vincentis S.,Cattini U.,Roli L.,De Santis M.C.,Baraldi E.,Tagliavini S.,Varani M.,Trenti T.,Rochira V.,Simoni M., and Santi D., *Probiotics Ingestion Does Not Directly Affect Thyroid Hormonal Parameters in Hypothyroid Patients on Levothyroxine Treatment.* Front Endocrinol (Lausanne), 2017. **8**: p. 316.

504. Gupta S.K., *Intention-to-treat concept: A review.* Perspect Clin Res, 2011. **2**(3): p. 109-12.

505. Sanders M.E.,Akkermans L.M.,Haller D.,Hammerman C.,Heimbach J.,Hormannsperger G.,Huys G.,Levy D.D.,Lutgendorff F.,Mack D.,Phothirath P.,Solano-Aguilar G., and Vaughan E., *Safety assessment of probiotics for human use.* Gut Microbes, 2010. **1**(3): p. 164-85.

506. Allen S.J.,Jordan S.,Storey M.,Thornton C.A.,Gravenor M.,Garaiova I.,Plummer S.F.,Wang D., and Morgan G., *Dietary supplementation with lactobacilli and bifidobacteria is well tolerated and not associated with adverse events during late pregnancy and early infancy.* J Nutr, 2010. **140**(3): p. 483-8.

507. Jarde A.,Lewis-Mikhael A.M.,Moayyedi P.,Stearns J.C.,Collins S.M.,Beyene J., and McDonald S.D., *Pregnancy outcomes in women taking probiotics or prebiotics: a systematic review and meta-analysis.* BMC Pregnancy Childbirth, 2018. **18**(1): p. 14.

508. Davies G.,Jordan S.,Brooks C.J.,Thayer D.,Storey M.,Morgan G.,Allen S.,Garaiova I.,Plummer S., and Gravenor M., *Long term extension of a randomised controlled trial of probiotics using electronic health records.* Sci Rep, 2018. **8**(1): p. 7668.

509. Taylor A.L.,Dunstan J.A., and Prescott S.L., *Probiotic supplementation for the first 6 months of life fails to reduce the risk of atopic dermatitis and increases the risk of allergen*

sensitization in high-risk children: a randomized controlled trial. J Allergy Clin Immunol, 2007. **119**(1): p. 184-91.

510. Kwon H.K.,Lee C.G.,So J.S.,Chae C.S.,Hwang J.S.,Sahoo A.,Nam J.H.,Rhee J.H.,Hwang K.C., and Im S.H., *Generation of regulatory dendritic cells and CD4+Foxp3+ T cells by probiotics administration suppresses immune disorders.* Proc Natl Acad Sci U S A, 2010. **107**(5): p. 2159-64.

511. Grazul H.,Kanda L.L., and Gondek D., *Impact of probiotic supplements on microbiome diversity following antibiotic treatment of mice.* Gut Microbes, 2016. **7**(2): p. 101-14.

512. Ismail I.H.,Oppedisano F.,Joseph S.J.,Boyle R.J.,Robins-Browne R.M., and Tang M.L., *Prenatal administration of Lactobacillus rhamnosus has no effect on the diversity of the early infant gut microbiota.* Pediatr Allergy Immunol, 2012. **23**(3): p. 255-8.

513. Engels C.,Ruscheweyh H.J.,Beerenwinkel N.,Lacroix C., and Schwab C., *The Common Gut Microbe Eubacterium hallii also Contributes to Intestinal Propionate Formation.* Front Microbiol, 2016. **7**: p. 713.

514. Udayappan S.,Manneras-Holm L.,Chaplin-Scott A.,Belzer C.,Herrema H.,Dallinga-Thie G.M.,Duncan S.H.,Stroes E.S.G.,Groen A.K.,Flint H.J.,Backhed F.,de Vos W.M., and Nieuwdorp M., *Oral treatment with Eubacterium hallii improves insulin sensitivity in db/db mice.* NPJ Biofilms Microbiomes, 2016. **2**: p. 16009.

515. Pryde S.E.,Duncan S.H.,Hold G.L.,Stewart C.S., and Flint H.J., *The microbiology of butyrate formation in the human colon.* FEMS Microbiol Lett, 2002. **217**(2): p. 133-9.

516. Michael D.R.,Davies T.S.,Moss J.W.E.,Calvente D.L.,Ramji D.P.,Marchesi J.R.,Pechlivanis A.,Plummer S.F., and Hughes T.R., *The anti-cholesterolaemic effect of a consortium of probiotics: An acute study in C57BL/6J mice.* Sci Rep, 2017. **7**(1): p. 2883.

517. Pauletzki J.,Stellaard F., and Paumgartner G., *Bile acid metabolism in human hyperthyroidism.* Hepatology, 1989. **9**(6): p. 852-5.

518. Bonde Y.,Breuer O.,Lutjohann D.,Sjoberg S.,Angelin B., and Rudling M., *Thyroid hormone reduces PCSK9 and stimulates bile acid synthesis in humans.* J Lipid Res, 2014. **55**(11): p. 2408-15.

519. Bergman F.,Heedman P.A., and van der Linden W., *Influence of cholestyramine on absorption and excretion of thyroxine in Syrian hamster.* Acta Endocrinol (Copenh), 1966. **53**(2): p. 256-63.

520. Zmora N.,Zilberman-Schapira G.,Suez J.,Mor U.,Dori-Bachash M.,Bashiardes S.,Kotler E.,Zur M.,Regev-Lehavi D.,Brik R.B.,Federici S.,Cohen Y.,Linevsky R.,Rothschild D.,Moor A.E.,Ben-Moshe S.,Harmelin A.,Itzkovitz S.,Maharshak N.,Shibolet O.,Shapiro H.,Pevsner-Fischer M.,Sharon I.,Halpern Z.,Segal E., and Elinav E., *Personalized Gut Mucosal Colonization Resistance to Empiric Probiotics Is Associated with Unique Host and Microbiome Features.* Cell, 2018. **174**(6): p. 1388-1405 e21.

521. Mori K.,Nakagawa Y., and Ozaki H., *Does the gut microbiota trigger Hashimoto's thyroiditis?* Discov Med, 2012. **14**(78): p. 321-6.

522. Kumar P.S.,Brooker M.R.,Dowd S.E., and Camerlengo T., *Target region selection is a critical determinant of community fingerprints generated by 16S pyrosequencing.* PloS one, 2011. **6**(6): p. e20956.

523. Li J.,Jia H.,Cai X.,Zhong H.,Feng Q.,Sunagawa S.,Arumugam M.,Kultima J.R.,Prifti E.,Nielsen T.,Juncker A.S.,Manichanh C.,Chen B.,Zhang W.,Levenez F.,Wang J.,Xu X.,Xiao L.,Liang S.,Zhang D.,Zhang Z.,Chen W.,Zhao H.,Al-Aama J.Y.,Edris S.,Yang H.,Wang J.,Hansen T.,Nielsen H.B.,Brunak S.,Kristiansen K.,Guarner F.,Pedersen O.,Dore J.,Ehrlich S.D.,Meta H.I.T.C.,Bork P.,Wang J., and Meta H.I.T.C., *An integrated catalog of reference genes in the human gut microbiome.* Nat Biotechnol, 2014. **32**(8): p. 834-41.

524. Weiss S.,Xu Z.Z.,Peddada S.,Amir A.,Bittinger K.,Gonzalez A.,Lozupone C.,Zaneveld J.R.,Vazquez-Baeza Y.,Birmingham A.,Hyde E.R., and Knight R., *Normalization and*

microbial differential abundance strategies depend upon data characteristics. Microbiome, 2017. **5**(1): p. 27.

525. McMurdie P.J. and Holmes S., *phyloseq: an R package for reproducible interactive analysis and graphics of microbiome census data.* PloS one, 2013. **8**(4): p. e61217.

526. Stammler F.,Glasner J.,Hiergeist A.,Holler E.,Weber D.,Oefner P.J.,Gessner A., and Spang R., *Adjusting microbiome profiles for differences in microbial load by spike-in bacteria.* Microbiome, 2016. **4**(1): p. 28.

527. Emerson J.B.,Adams R.I.,Roman C.M.B.,Brooks B.,Coil D.A.,Dahlhausen K.,Ganz H.H.,Hartmann E.M.,Hsu T.,Justice N.B.,Paulino-Lima I.G.,Luongo J.C.,Lymperopoulou D.S.,Gomez-Silvan C.,Rothschild-Mancinelli B.,Balk M.,Huttenhower C.,Nocker A.,Vaishampayan P., and Rothschild L.J., *Schrodinger's microbes: Tools for distinguishing the living from the dead in microbial ecosystems.* Microbiome, 2017. **5**(1): p. 86.

528. Langille M.G.,Zaneveld J.,Caporaso J.G.,McDonald D.,Knights D.,Reyes J.A.,Clemente J.C.,Burkepile D.E.,Vega Thurber R.L.,Knight R.,Beiko R.G., and Huttenhower C., *Predictive functional profiling of microbial communities using 16S rRNA marker gene sequences.* Nat Biotechnol, 2013. **31**(9): p. 814-21.

529. Iwai S.,Weinmaier T.,Schmidt B.L.,Albertson D.G.,Poloso N.J.,Dabbagh K., and DeSantis T.Z., *Piphillin: Improved Prediction of Metagenomic Content by Direct Inference from Human Microbiomes.* PloS one, 2016. **11**(11): p. e0166104.

530. Lozupone C.A.,Stombaugh J.I.,Gordon J.I.,Jansson J.K., and Knight R., *Diversity, stability and resilience of the human gut microbiota.* Nature, 2012. **489**(7415): p. 220-30.

531. Perlman R.L., *Mouse models of human disease: An evolutionary perspective.* Evol Med Public Health, 2016. **2016**(1): p. 170-6.

532. Kelly B.J.,Gross R.,Bittinger K.,Sherrill-Mix S.,Lewis J.D.,Collman R.G.,Bushman F.D., and Li H., *Power and sample-size estimation for microbiome studies using pairwise distances and PERMANOVA.* Bioinformatics, 2015. **31**(15): p. 2461-8.

533. La Rosa P.S.,Brooks J.P.,Deych E.,Boone E.L.,Edwards D.J.,Wang Q.,Sodergren E.,Weinstock G., and Shannon W.D., *Hypothesis testing and power calculations for taxonomic-based human microbiome data.* PloS one, 2012. **7**(12): p. e52078.

534. Hedin C.R.,van der Gast C.J.,Stagg A.J.,Lindsay J.O., and Whelan K., *The gut microbiota of siblings offers insights into microbial pathogenesis of inflammatory bowel disease.* Gut Microbes, 2017. **8**(4): p. 359-365.

535. Richards L.B.,Li M.,van Esch B.C.A.M.,Garssen J., and Folkerts G., *The effects of short-chain fatty acids on the cardiovascular system.* PharmaNutrition, 2016. **4**(2): p. 68-111.

8. Appendix

Appendix 1: Composition of the microbiology media used in the study

1. Nutrient Agar (Sigma Aldrich, Germany):

Composition	Amount
Agar	15 g/L
Meat extract	1 g/L
Peptone	5 g/L
Sodium chloride	5 g/L
Yeast extract	2 g/L
Final pH	7.1 ± 0.2 (25 °C)

2. Nutrient Broth (Sigma Aldrich, Germany):

Composition	Amount
Glucose-D(+)	1 g/L
Peptone	15 g/L
Sodium chloride	6 g/L
Yeast extract	3 g/L
Final pH	7.5 ± 0.2 (25 °C)

3. Luria Bertani (LB) Broth (Sigma Aldrich, Germany):

Composition	Amount
Tryptone	10 g/L
Sodium chloride	0.5 g/L
Yeast extract	5 g/L

Appendix 2: Mothur Pipeline via Command-line according to [207]

#tmux session command line

tmux new -s INDIGO -n #new session

tmux kill-session -t INDIGO #stop session

tmux ls #explore how many tmux you entered and the name of each one

tmux a -t INDIGO #enter existing session

Ctrl-B and then D #leave/detach session

#Mothur command-line

#reach the folder with all the unzipped fastq files via command line

#if used on a multi-processor server, n. processors can be selected via e.g. 'processor=30'

#Type 'Mothur' to enter the command-line:

Make contigs and count the number of reads obtained

make.contigs(file=INDIGO.txt)

summary.seqs(fasta=INDIGO.trim.contigs.fasta)

screen.seqs(fasta=INDIGO.trim.contigs.fasta, group=INDIGO.contigs.groups, summary=INDIGO.trim.contigs.summary, maxn=0, maxambig=0, maxhomop=6, minlength=344, maxlength=377)

Processing improved sequences

summary.seqs(fasta=INDIGO.trim.contigs.good.fasta)

unique.seqs(fasta=INDIGO.trim.contigs.good.fasta)

count.seqs(name=INDIGO.trim.contigs.good.names, group=INDIGO.contigs.good.groups)

count.groups(count=INDIGO.trim.contigs.good.count_table)

align.seqs(fasta=INDIGO.trim.contigs.good.unique.fasta, reference=./16S_refDB/silva.bacteria.fasta)

Processing aligned sequences

summary.seqs(fasta=INDIGO.trim.contigs.good.unique.align, count=INDIGO.trim.contigs.good.count_table)

screen.seqs(fasta=INDIGO.trim.contigs.good.unique.align, count=INDIGO.trim.contigs.good.count_table, summary=INDIGO.trim.contigs.good.unique.summary, start=1044, end=6424, maxhomop=5)

summary.seqs(fasta=INDIGO.trim.contigs.good.unique.good.align, count=INDIGO.trim.contigs.good.good.count_table)

count.groups(count=INDIGO.trim.contigs.good.good.count_table)

```
filter.seqs(fasta=INDIGO.trim.contigs.good.unique.good.align, vertical=T, trump=.)

unique.seqs(fasta=INDIGO.trim.contigs.good.unique.good.filter.fasta,
count=INDIGO.trim.contigs.good.good.count_table)

pre.cluster(fasta=INDIGO.trim.contigs.good.unique.good.filter.unique.fasta,
count=INDIGO.trim.contigs.good.unique.good.filter.count_table, diffs=2)

chimera.uchime(fasta=INDIGO.trim.contigs.good.unique.good.filter.unique.precluster.fasta,
count=INDIGO.trim.contigs.good.unique.good.filter.unique.precluster.count_table, dereplicate=t)

remove.seqs(fasta=INDIGO.trim.contigs.good.unique.good.filter.unique.precluster.fasta,
accnos=INDIGO.trim.contigs.good.unique.good.filter.unique.precluster.uchime.accnos)

split.abund(fasta=INDIGO.trim.contigs.good.unique.good.filter.unique.precluster.pick.fasta,
count=INDIGO.trim.contigs.good.unique.good.filter.unique.precluster.uchime.pick.count_table, cutoff=2)

######### Remove singletons and non-bacterial sequences ########
classify.seqs(fasta=INDIGO.trim.contigs.good.unique.good.filter.unique.precluster.pick.abund.fasta,
count=INDIGO.trim.contigs.good.unique.good.filter.unique.precluster.uchime.pick.abund.count_table,refer
ence=./16S_refDB/trainsettrainset14_032015.rdp/trainset14_032015.rdp.fasta,
taxonomy=./16S_refDB/trainset14_032015.rdp/trainset14_032015.rdp.tax, cutoff=80)

classify.seqs(fasta=INDIGO.final.fasta,
count=INDIGO.trim.contigs.good.unique.good.filter.unique.precluster.uchime.pick.abund.count_table,refer
ence=./16S_refDB/trainset14_032015.rdp/trainset14_032015.rdp.fasta,
taxonomy=./16S_refDB/trainset14_032015.rdp/trainset14_032015.rdp.tax, cutoff=80, output=simple)

remove.lineage(fasta=INDIGO.trim.contigs.good.unique.good.filter.unique.precluster.pick.abund.fasta,
count=INDIGO.trim.contigs.good.unique.good.filter.unique.precluster.denovo.uchime.pick.abund.count_tab
le,
taxonomy=INDIGO.trim.contigs.good.unique.good.filter.unique.precluster.pick.abund.rdp.wang.taxonomy,t
axon=Chloroplast-Mitochondria-unknown-Archaea-Eukaryota)

cluster.split(fasta=INDIGO.trim.contigs.good.unique.good.filter.unique.precluster.pick.abund.fasta,count=I
NDIGO.trim.contigs.good.unique.good.filter.unique.precluster.uchime.pick.abund.count_table,taxonomy=I
NDIGO.trim.contigs.good.unique.good.filter.unique.precluster.pick.abund.rdp.wang.taxonomy,splitmethod=
classify, taxlevel=4, cutoff=0.15)

######### Obtain OTU table, taxonomy and perform a subsample based on smallest library size
########
summary.tax(taxonomy=current, count=current)

count.groups(count=current)
```

```
make.shared(list=INDIGO.trim.contigs.good.unique.good.filter.unique.precluster.pick.abund.an.unique_list.
list, count=INDIGO.trim.contigs.good.unique.good.filter.unique.precluster.uchime.pick.abund.count_table,
label=0.03)

classify.otu(list=INDIGO.trim.contigs.good.unique.good.filter.unique.precluster.pick.abund.an.unique_list.lis
t, count=INDIGO.trim.contigs.good.unique.good.filter.unique.precluster.uchime.pick.abund.count_table,
taxonomy=INDIGO.trim.contigs.good.unique.good.filter.unique.precluster.pick.abund.rdp.wang.taxonomy,
label=0.03)

count.groups(count=INDIGO.trim.contigs.good.unique.good.filter.unique.precluster.uchime.pick.abund.cou
nt_table)

sub.sample(shared=INDIGO.trim.contigs.good.unique.good.filter.unique.precluster.pick.abund.an.unique_li
st.shared)

######### phylotypes analysis ##################
phylotype(taxonomy=current)
make.shared(list=INDIGO.trim.contigs.good.unique.good.filter.unique.precluster.pick.abund.rdp.wang.tx.lis
t, count=current, label=1-5)

######### rename latest files to be used in subsequent analysis##################
#on a linux bash (switch Tmux terminals): cp would copy and rename retaining the original #version of the
file
cp ./INDIGO.trim.contigs.good.unique.good.filter.unique.precluster.pick.abund.fasta ./INDIGO.final.fasta

cp
./INDIGO.trim.contigs.good.unique.good.filter.unique.precluster.pick.abund.an.unique_list.0.03.subsample.
shared  ./INDIGO.final.subsampled.shared

cp ./INDIGO.trim.contigs.good.unique.good.filter.unique.precluster.pick.abund.an.unique_list.shared
./INDIGO.final.shared

cp INDIGO.trim.contigs.good.unique.good.filter.unique.precluster.pick.abund.an.unique_list.list
INDIGO.final.list
cp ./INDIGO.trim.contigs.good.names  ./INDIGO.final.names

cp ./INDIGO.contigs.good.groups ./INDIGO.final.groups

######### phylogenetic analysis ##################
#on the Mothur command-line
dist.seqs(fasta=INDIGO.final.fasta, output=phylip)

#on a linux bash (switch Tmux terminals without having to close Mothur): lauching fasttree
fastTree -nt INDIGO.final.fasta > INDIGO.final.tre
```

```
######### calculate ALPHA diversity #################
#using rarefied but not-subsampled dataset
collect.single(shared=INDIGO.final.shared, calc=sobs-chao-ace-shannon-shannoneven-simpson, freq=1)
summary.single(calc=nseqs-coverage-sobs-chao-ace-shannon-shannoneven-simpson)
rarefaction.single(shared=INDIGO.final.subsampled.shared, calc=sobs, freq=5)

#filtered-rarefied subsampled dataset
collect.single(shared=INDIGO.final.subsampled.0.03.filter.shared, calc=sobs-chao-ace-shannon-
shannoneven-simpson, freq=1)
summary.single(calc=nseqs-coverage-sobs-chao-ace-shannon-shannoneven-simpson)
rarefaction.single(shared=INDIGO.final.subsampled.0.03.filter.shared, calc=sobs, freq=5)

#filtered-rarefied non-subsampled dataset
collect.single(shared=INDIGO.final.0.03.filter.shared, calc=sobs-chao-ace-shannon-shannoneven-
simpson, freq=1)
summary.single(calc=nseqs-coverage-sobs-chao-ace-shannon-shannoneven-simpson)

######### calculate BETA diversity #################
#when using Unifrac = weighted is natively normalized (subsample = N), while unweighted is
presence/abscence #therefore use the non-subsampled shared
unifrac.unweighted(tree=INDIGO.final.tre, name=INDIGO.final.names, group=INDIGO.final.groups,
distance=square, random=F)
unifrac.weighted(tree=INDIGO.final.tre, name=INDIGO.final.names, group=INDIGO.final.groups,
distance=square, random=F, subsample=1046)

######### modify the fasta file and process the taxonomic classification with RDP #########
#on the Mothur command-line:
get.oturep(phylip=INDIGO.final.phylip.dist,
list=INDIGO.trim.contigs.good.unique.good.filter.unique.precluster.pick.abund.an.unique_list.0.03.subsam
ple.list,fasta=INDIGO.final.fasta, label=0.03) #use large=true for very large distance files otherwise omit

#get the otu.rep from the subsampled share and subsampled list
sub.sample(list=INDIGO.trim.contigs.good.unique.good.filter.unique.precluster.pick.abund.an.unique_list.li
st)
get.oturep(phylip=INDIGO.final.tre1.weighted.phylip.dist,
list=INDIGO.trim.contigs.good.unique.good.filter.unique.precluster.pick.abund.an.unique_list.0.03.subsam
ple.list,fasta=INDIGO.final.fasta, label=0.03)

get.otulist(list=INDIGO.trim.contigs.good.unique.good.filter.unique.precluster.pick.abund.an.unique_list.0.0
3.subsample.shared,

#on a linux bash (switch Tmux terminals), without having to close Mothur:
cp ./INDIGO.final.fasta ./INDIGO.final.format.fasta
sed -i 's/-//g' INDIGO.final.format.fasta
```

```
vsearch --usearch_global INDIGO.final.format.fasta --db
/home/technical/Documents/16S_refDB/rdp_download_9752seqs.fa --uc INDIGO_usearch97_RDP.txt --id
0.98 --iddef 1 --maxaccepts 3 --maxrejects 0 --strand plus #to obtain species information

rdp_classifier  -o INDIGO_classified.txt --format=fixrank ./INDIGO.final.format.fasta

java -Xmx1g -jar /usr/bin/rdp_classifier classify -c 0.5 -o INDIGO_classified.txt -h INDIGO_hier.txt --
format=fixrank ./INDIGO.final.format.fasta

#change the header of the FASTA
sed -i 's/-//g' INDIGO.final.format.fasta
cut -d '|' -f1 INDIGO.final.0.03.rep.fasta > INDIGO.oturep.fasta
awk -F ' ' '/^>/ {print ">" $2; next } 1' INDIGO.oturep.fasta  > INDIGO1.oturep.fasta
```

Appendix 3: Alpha and Beta-diversity equations according to [352]

Alpha diversity indices are mathematical estimators of within-sample richness and diversity of bacterial communities.

Richness indexes: The Chao1 and Abundance-based Coverage Estimator (ACE) richness indexes were calculated as described by Chao and colleagues [Chao, 1984; Chao and Ming, 1992; Chao et al. 1993]:

$$Chao1 = S_{obs} + \frac{F_1(F_1 - 1)}{2(F_2 + 1)} \tag{1}$$

where S_{obs} is the observed number of species, and F_1 and F_2 are the numbers of singletons (only one count) and doubletons (exactly two counts), respectively, in each sample.

And for the ACE:

$$S_{ACE} = S_{abund} + \frac{S_{rare}}{C_{ACE}} + \frac{F_1}{C_{ACE}} \cdot \gamma^2_{ACE} \tag{2}$$

where: S_{abund} and S_{rare} are the numbers of abundant and rare OTUs, with respect to a threshold of individuals in which OTUs are observed (3 in this study); $C_{\{ACE\}}$ is the sample abundance coverage estimator obtained by $1 - \frac{F_1}{N_{rare}}$, with F_1 the frequency of singletons and $N_{rare} = \sum_{k=1}^{j} k f_k$, for j=3 the threshold for rare OTUs; $\gamma^2_{\{ACE\}}$ is the coefficient of variation for of OTU relative abundances $\gamma^2_{ACE} = \frac{S_{rare}}{C_{rare}} \cdot \frac{\sum_{k=1}^{j} k(1-k)F_k}{(N_{rare})(N_{rare}-1)} - 1.0$.

Diversity indexes: The Shannon index was obtained from [Shannon, 1948]:

$$H' = -\sum_{i=1}^{S} (p_i \cdot ln(p_i)) \tag{3}$$

where p_i is the relative abundance of each OTU.

Similarly, the Simpson index was also based on OTUs relative abundances [Simpson, 1949]:

$$D = 1 - \sum_{i=1}^{S} p_i^2 \tag{4}$$

Evenness indexes: Simpson's evenness measure E was calculated as:

$$E = \frac{1/D}{S_{obs}} \tag{6}$$

where D is the Simpsons's diversity from equation (4) and S_{obs} is the observed number of species [Smith & Wilson, 1996].

Pielou's J' index (a.k.a. Shannon's evenness) was obtained from the Shannon index (equation(3)) divided by the natural logarithm of the number of species [Smith & Wilson, 1996; Pielou, 1975]:

$$J' = \frac{H'}{ln(S)} \tag{7}$$

Beta-diversity compares bacterial communities among samples. UniFrac [320] computes a distance metrics which incorporates phylogenetic distances:

$$W = \frac{\sum_{i=1}^{N} Ii \left| \frac{A_i}{A_T} - \frac{B_i}{B_T} \right|}{\sum_{j=1}^{S} L_j} \tag{8}$$

where: *N* is the number of nodes in the phylogenetic tree, *S* is the number of sequences represented by the tree. *Ii* is the branch length between node *i* and its parent node, L_j is the total branch length from the root to the tip of the tree for sequence *j*, A_i and B_i are the number of sequences from communities A and B that descend from the node, and A_T and B_T are the total number of sequences from communities A and B. The weighted UniFrac measure is natively normalized to ensure that each sequence contributes equally to the distance calculated.

Bray Curtis instead is a dissimilarity metrics [356]:

$$BC_{ij} = \frac{S_i + S_j - 2C_{ij}}{S_i + S_j} \tag{9}$$

Where S_i and S_j are the number of species in samples *i* and *j*, and C_{ij} is the number of species in common between the two samples (if there are no species in common, the numerator is equal to the denominator and the dissimilarity is one -maximum; if all species are in common, the dissimilarity is zero -minimum).

References for Appendix 3 (not already included in the main text):

- Chao A, Ma MC and Yang MCK 1993. Stopping rule and estimation for recapture debugging with unequal detection rates. Biometrika 80, 193–201.
- Chao A 1984. Nonparametric Estimation of the Number of Classes in a Population Author. Scanadinavian Journal of Statistics 11, 265–270.
- Chao A and Lee S-M 1992. Estimating the Number of Classes via Sample Coverage. Journal of the American Statistical Association 87, 210.
- Pielou E. 1975. Ecological diversity. Wiley, New York.
- Shannon C 1948. A Mathematical Theory of Communication, The Bell System Technical Journal. The Bell System Technical Journal, 379–427.
- Simpson EH 1949. Measurement of diversity. Nature 163, 688.
- Smith B and Wilson JB 1996. A Consumer's Guide to Evenness Indices. Oikos 76, 70.

Appendix 4: *Bifidobacterium* counts derived from the 28F-combo primers.

Primers as described in Table 2.2. Comparison between the TSHR immunised mice in Center 1 (n=5) and Center 2 (n=10). ANOVA with Tukey's HSD post-hoc analysis (95% confidence interval), *P* value=0.003 generated with STAMP.

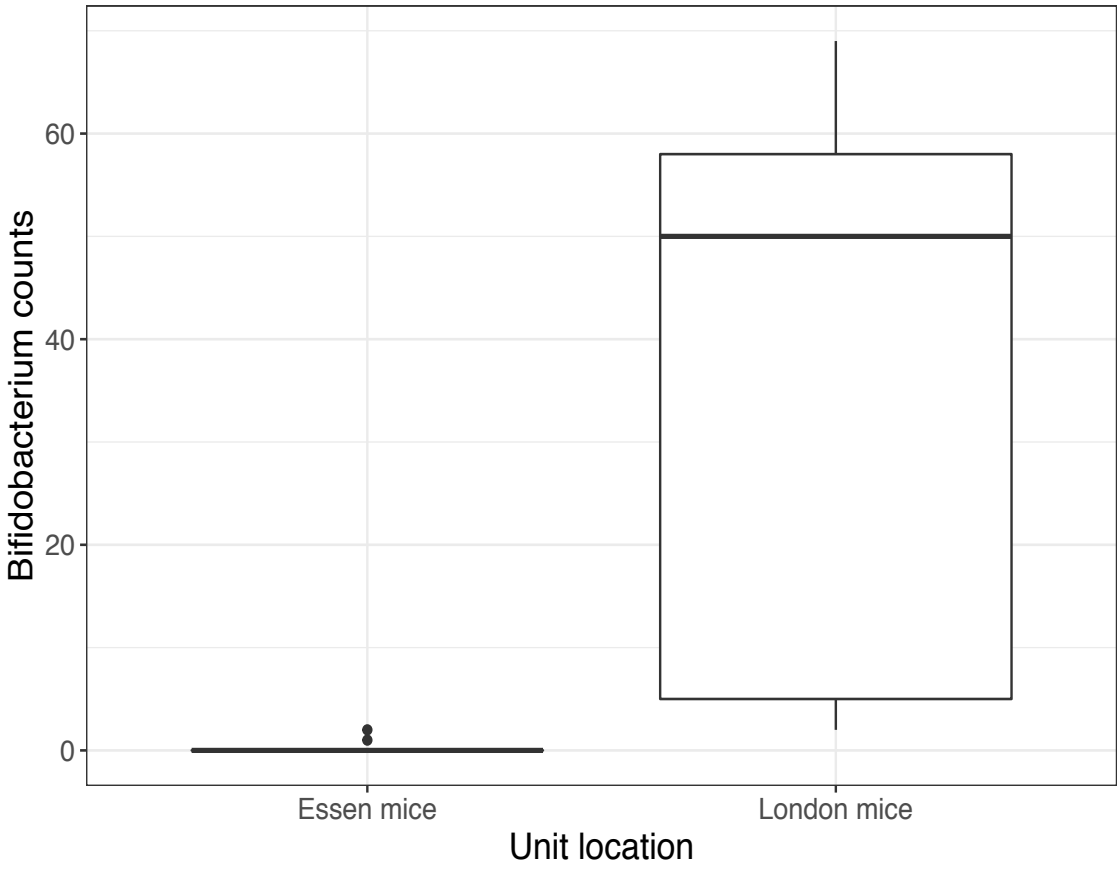

Appendix 5: Generalized linear model (GLM) of genera counts differentially present in TSHR immunised mice over timepoints, in reference to the baseline (T0) using EdgeR. LogFC, Log2 fold change between each timepoint and the baseline (T0); LR, likelihood ratio.

Genera	logFC.TreatTSHR.TimeT1	logFC.TreatTSHR.TimeT2	logFC.TreatTSHR.TimeT3	logFC.TreatTSHR.TimeT4	LR	P value
Thermophagus	0.2852	0.2079	-0.4420	-1.4787	21.7079	0.0002
Clostridium_IV	-1.4222	1.0382	0.0916	1.7778	21.2073	0.0003
Parvimonas	-0.3198	-1.0468	-1.9210	-3.0029	20.1382	0.0005
Galenea	4.5266	-0.7618	0.5786	1.0517	18.8775	0.0008
Propionibacterium	0.0000	4.9371	0.0000	0.0000	18.2622	0.0011
Robinsoniella	-3.0292	-0.1505	-1.6023	-1.0391	16.5191	0.0024
Parasutterella	0.6738	-0.1365	-0.2753	-1.3229	16.2497	0.0027
Anaerotruncus	-0.9406	0.3992	0.4221	1.1624	15.9264	0.0031
Fusicatenibacter	-0.4762	1.1112	1.3956	1.4212	15.2374	0.0042
Lactobacillus	-0.3048	0.4011	1.0495	-0.7979	15.1589	0.0044
Clostridium_XlVa	-0.8027	0.2749	0.9626	1.2220	15.0732	0.0046
Oxalophagus	-3.3534	-4.2692	-4.2692	-4.2692	14.9032	0.0049
Acetitomaculum	-0.5858	0.8711	1.2587	2.0188	14.8908	0.0049
Peptococcus	0.7471	2.0272	1.5228	3.2536	14.7209	0.0053
Mangroviflexus	-0.1089	-1.1434	-2.1405	-1.3201	14.2869	0.0064
Lachnoanaerobaculum	-1.8819	-0.1332	-0.7214	1.8219	13.5548	0.0089
Ruminococcus2	-0.5580	0.1910	0.6116	1.6726	13.5378	0.0089
Allisonella	-1.7609	-1.7609	-1.7609	1.1248	12.5405	0.0138
Salinihabitans	2.5453	0.1725	0.5773	-1.9479	12.5082	0.0139
Lacticigenium	-1.3755	-1.3755	-1.3755	0.9455	12.0620	0.0169
Sporobacterium	-4.2993	-2.9235	-4.2993	-2.2278	11.8836	0.0182
Limibacter	-0.2460	-0.6347	-1.0053	-1.2956	11.1860	0.0246
Cerasibacillus	-1.2454	-2.7173	-2.7173	-1.3403	10.9517	0.0271
Lactonifactor	-0.1604	0.1390	0.0037	1.5842	10.8391	0.0284
Alkalitalea	0.0490	-0.3414	-0.4222	-0.9183	10.7386	0.0297
Butyrivibrio	-1.4387	0.4837	0.9414	0.2226	10.4489	0.0335
Alistipes	0.0983	0.1580	0.6896	0.8892	10.3325	0.0352
Wandonia	-0.1646	-0.2428	0.8821	0.6716	10.3167	0.0354
Saccharibacteria genera incertae sedis	-1.3083	-0.7651	-0.6378	0.7610	10.2914	0.0358
Lachnospiracea incertae sedis	-1.3035	-0.5834	-0.4886	0.5190	10.2133	0.0370
Papillibacter	-0.4747	-0.2452	-1.4326	0.4860	9.7302	0.0452
Paludibacter	0.0206	-0.3787	-0.5581	-0.7721	9.6704	0.0464
Acetanaerobacterium	0.5105	0.5779	1.1826	2.4332	9.5456	0.0488
Escherichia/Shigella	0.0000	1.3761	0.8448	4.0866	9.5395	0.0489

Appendix 6: Generalized linear model (GLM) of genera counts in βgal control mice over timepoints using EdgeR. LogFC, Log2 fold change between each timepoint and the baseline (T0); LR, likelihood ratio.

Genera	logFC.TreatBgal.TimeT1	logFC.TreatBgal.TimeT2	logFC.TreatBgal.TimeT3	logFC.TreatBgal.TimeT4	LR	P value
Parvimonas	-0.0425	-1.1339	-1.0423	-4.1251	20.7414	0.0004
Clostridium_IV	0.8206	1.2327	1.1258	2.8315	20.4984	0.0004
Acetitomaculum	0.7858	1.6137	0.9559	3.1436	20.4318	0.0004
Lachnobacterium	0.8780	1.3146	-0.0745	2.2142	18.7013	0.0009
Lactobacillus	1.7303	0.4486	2.0304	1.1655	16.7071	0.0022
Thermophagus	-0.0078	-0.0844	-0.0844	-1.6685	16.2197	0.0027
Lactonifactor	-0.0726	0.0599	-0.4590	1.9739	16.2169	0.0027
Lachnoanaerobaculum	0.5098	-0.0039	-0.1151	3.1287	15.1892	0.0043
Guggenheimella	-0.9414	-1.2371	-0.7289	-2.0107	14.8822	0.0050
Robinsoniella	-1.0011	-1.6477	-2.7565	-2.4129	14.8520	0.0050
Mucispirillum	2.1316	-0.7434	-0.5560	1.8190	14.0381	0.0072
Anaeroplasma	3.7100	2.7709	2.5649	4.6262	13.0073	0.0112
Galenea	3.9372	3.1675	1.1721	-1.3245	12.1505	0.0163
Thermoflavimicrobium	-0.5875	-2.1747	-3.1718	-3.1718	11.5213	0.0213
Pelagibacterium	-1.8767	-1.8771	-1.1370	-3.4605	11.2833	0.0236
Parasporobacterium	0.1546	-1.9032	-0.7701	-2.2197	11.1498	0.0249
Erysipelotrichaceae_incertae_sedis	-0.9060	-2.1603	-0.8144	-2.2622	10.9092	0.0276
Parasutterella	0.5922	0.5912	-0.3212	-0.9636	10.9023	0.0277
Coprobacter	0.0152	-0.0436	0.2208	-0.8639	10.8381	0.0284
Eisenbergiella	-0.3747	-0.2650	-0.9316	0.7760	10.7420	0.0296
Rikenella	-0.6796	-1.4760	-0.3511	-1.0187	10.5907	0.0316
Butyrivibrio	0.8029	0.2692	-1.7129	-0.3432	10.1153	0.0385
Lachnospiracea_incertae_sedis	0.3631	0.4752	-1.0700	1.0110	10.1132	0.0386
Parabacteroides	1.4279	1.1122	0.1513	0.1242	9.9641	0.0410

Appendix 7: Comparison of the faecal and the gut microbiota of BALB/c mice in Centre 2 collected at T4.

(**A**) Alpha diversity indices of richness (Chao) and diversity (Shannon). (**B**) Beta-diversity measurement calculated from the weighted Unifrac. (**C**) Correlation coefficient matrix between each sample's microbiota from faeces (x-axis) and from the gut scraping (y-axis). Values in the diagonal represent the Spearman correlation coefficient within sample between faecal and gut microbiota, which vary from weak (0.50) to strong (>0.80).

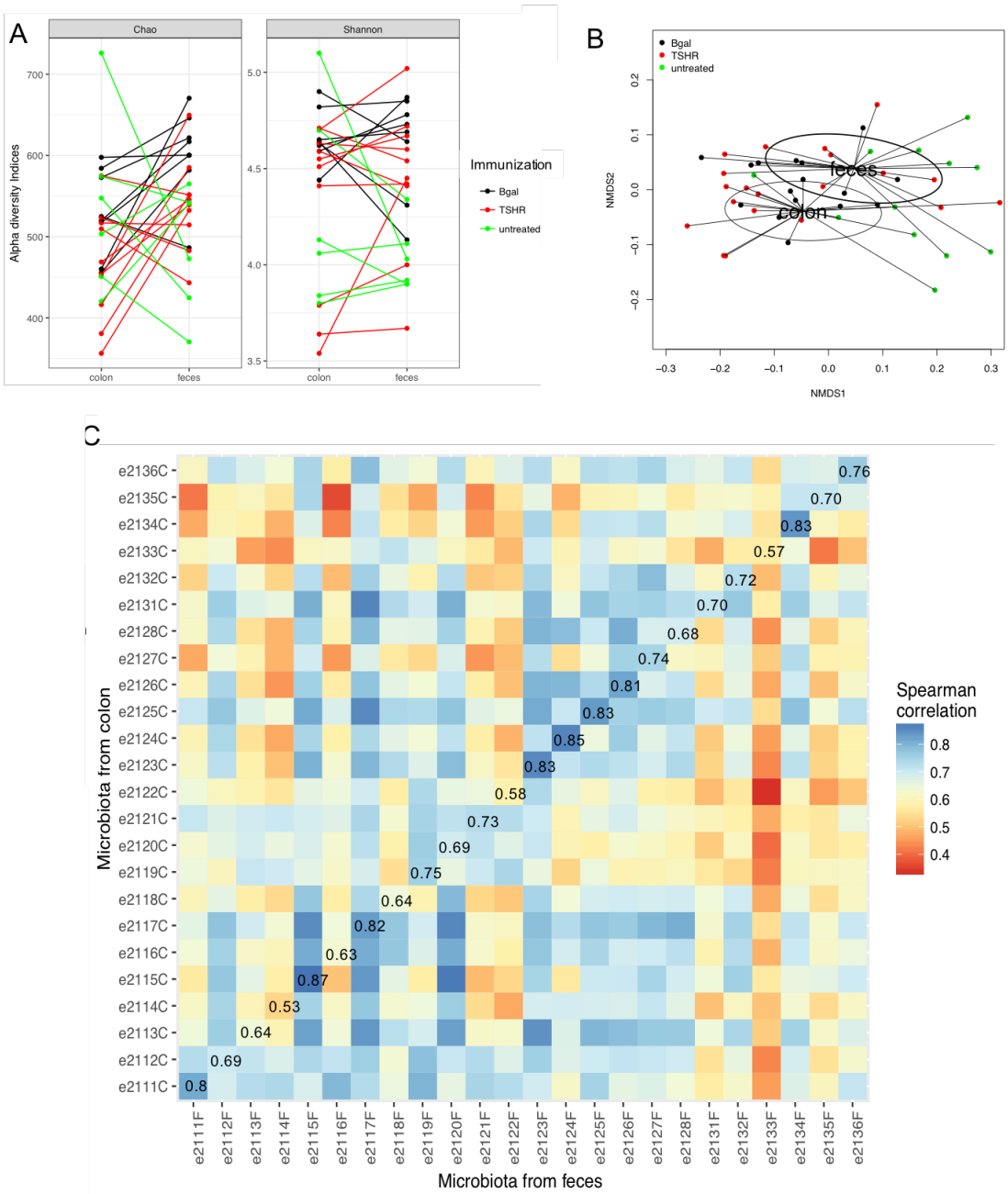

Appendix 8: QIIME 1.9 Pipeline

To process 16S rRNA gene sequencing data, the QIIME pipeline was used [208]. The specific steps and parameters used are detailed below.

Core analysis

1. Joining paired-end reads

Paired-end reads were joined into single FASTQ files per sample:

```
multiple_join_paired_ends.py --input_dir=<sample_path> --output_dir=./ --include_input_dir_path
--parameter_fp=$PWD/qiime_parameters --read1_indicator _R1 --read2_indicator _R2
```

The method "SeqPrep" for the joining of paired-end reads (https://github.com/jstjohn/SeqPrep) was selected via the parameter file (qiime_parameters):

```
join_paired_ends:pe_join_method      SeqPrep
```

2. Quality filtering

Joined reads were then filtered for quality and saved into a unique FASTA file for all samples:

```
multiple_split_libraries_fastq.py --demultiplexing_method sampleid_by_file --
input_dir=<multiple_join_paired_ends/> --output_dir=./
--include_input_dir_path --remove_filepath_in_name
--parameter_fp=$PWD/qiime_parameters
```

Quality filter parameter were specified via the parameter file (qiime_parameters):

```
split_libraries_fastq:max_bad_run_length  3 >> ./qiime_parameters
split_libraries_fastq:min_per_read_length_fraction 0.75 >> ./qiime_parameters
split_libraries_fastq:sequence_max_n 0 >> ./qiime_parameters
split_libraries_fastq:phred_quality_threshold 19 >> ./qiime_parameters
```

3. OTU picking

OTUs were determined by aligning quality-filtered reads against the QIIME-compatible SILVA reference FASTA file, release 123, with minimum 97% clustering (https://www.arb-silva.de/download/archive/qiime/):

```
pick_closed_reference_otus.py
--reference_fp SILVA123_QIIME/rep_set/rep_set_all/97/97_otus.fasta --taxonomy_fp
SILVA123_QIIME/taxonomy/taxonomy_all/97/raw_taxonomy.txt
--parallel --jobs_to_start=32 --force
--input_fp=<multiple_split_library/>seqs.fna --output_dir=./
```

Convert .biom file into a .tsv file:

```
biom convert -i ./otu_table.biom -o otu_table.txt --to-tsv --header-key taxonomy
```

4. Filter OTUs

OTUs were filtered by total count across samples greater than 15 of the number of OTUs in at least 2 samples:

```
filter_otus_from_otu_table.py -i <closed_otupicking/>otu_table.biom -n 15 -s 2 -o ./otu_table_filtered.biom
```

5. Normalization of OTU counts

To account for uneven sequencing, OTU counts were normalized by cumulative sum scaling (CSS, [354]):
normalize_table.py -i <filter_otus/>otu_table_filtered.biom -a CSS -o CSS_normalized_otu_table.biom

Convert .biom file into a .tsv file:
biom convert -i ./CSS_normalized_otu_table.biom -o normalized_otu_table.txt --to-tsv --header-key taxonomy

6. Alpha diversity
Alpha diversity indexes were estimated from the filtered OTU table:
alpha_diversity.py -i <filter_otus/>otu_table_filtered.biom -m
chao1,ace,fisher_alpha,observed_otus,observed_species,shannon,simpson
-o ./alpha.txt -t SILVA123_QIIME/trees/97/97_otus.tre

7. Beta diversity
Beta diversity was estimated from the filtered and normalized OTU table:
beta_diversity.py -i <normalize_otu/>CSS_normalized_otu_table.biom -m bray_curtis -o ./ -t SILVA123_QIIME/trees/97/97_otus.tre

8. Sequence-based rarefaction
To check whether sequencing depth was adequate, sequence-based rarefaction curves were generated from the unfiltered OTU table:
alpha_rarefaction.py -i <closed_otupicking/>otu_table.biom -m metadatamapping.csv
-o ./ --force --parameter=$PWD/qiime_parameters --parallel
--jobs_to_start=32 --max_rare_depth 218850 --min_rare_depth 100

Where metadatamapping.csv is the metadata file (feed supplementation treatments), and max_rare_depth is the median sequence counts per sample.
Additional parameters were specified via the parameter file (qiime_parameters):
Alpha_diversity:metrics observed_otus,chao1,observed_species,shannon,simpson,
goods_coverage,ace,fisher_alpha >> ./qiime_parameters
make_rarefaction_plots:resolution
800 >> ./qiime_parameters

Post-analysis
9. Tax4Fun [360]

```
desc: functional profiling using tax4fun (+SILVA)
run:
# conda environment set up
- export PATH=<conda_path>:$PATH
- source activate <qiime_version>
#!! Careful: the R in this environment has the Tax4Fun package installed !!
# convert otu_table to csv file with taxonomy as header key (!! IMPORTANT !!)
- biom convert -i <normalize_otu/>CSS_normalized_otu_table.biom -o otu_table.csv --to-tsv --header-key taxonomy
```

run R script for functional profiling (now using personal R libraries --> update/create conda R env)

important: sample names in the otu table must not begin with a number!

creates TWO FILES: one for ORTHOLOGS (proteins/enzymes), one for METABOLIC PATHWAYS

- /storage/biscarinif/R-3.1.1/bin/Rscript --vanilla <tax4fun> otu_table.csv /storage/biscarinif/tax4fun/SILVA123/

- Rscript --vanilla <tax4fun> otu_table.csv /storage/biscarinif/tax4fun/SILVA123/

- source deactivate

10. SourceTracker [363]

- export SOURCETRACKER_PATH= yourPath/sourcetracker/
- Rscript sourcetracker_for_qiime.r -i out_table.txt -m metadata.txt -o outputFolder

Appendix 9: Summary of the statistics obtained from the linear regression model for treatment differences in colon + entire sources of the βgal immunisation control group.

Colon - entire	Control		hFMT		LAB4		Vancomycin		
Differentially abundant taxonomy	mean	st dev	mean	st dev	mean	st dev	mean	st dev	P value
Actinobacteria;	37.3920	11.9761	29.5540	6.9296	28.8564	12.0459	0.3569	1.0706	1.54E-08
Actinobacteria;Coriobacteriaceae UCG-002	5.9383	3.9621	4.4963	1.6535	5.0863	2.4369	0.3569	1.0706	5.50E-05
Actinobacteria;Enterorhabdus	27.5687	10.5503	20.8990	4.7737	18.7992	9.6999	0	0	5.42E-08
Actinobacteria;Slackia	2.7603	2.0294	3.2877	1.9369	3.9785	1.9968	0	0	5.19E-05
Bacteroidetes;	799.9480	155.4927	818.9402	221.7562	837.9666	131.0143	233.5937	42.5874	6.95E-10
Bacteroidetes;Alistipes	54.4860	24.1157	65.6077	16.5903	69.3322	10.7939	1.9892	2.7220	4.53E-11
Bacteroidetes;Alloprevotella	3.6376	2.3038	3.6358	1.7690	4.0157	2.1667	0	0	0.000113654
Bacteroidetes;Odoribacter	6.6650	5.2998	11.6248	5.4223	11.6442	3.9076	0	0	3.31E-06
Bacteroidetes;Other	12.6329	7.2863	15.8896	2.9153	16.0034	1.0948	2.6568	2.8476	6.37E-09
Bacteroidetes;Parabacteroides	11.5386	3.2617	11.2077	3.9144	7.8681	1.7564	90.8979	21.9773	3.67E-16
Bacteroidetes;Paraprevotella	3.6601	1.0937	2.5912	1.8394	1.9430	1.3993	0	0	1.08E-05
Bacteroidetes;Prevotella 9	0.5368	0.8049	1.1354	1.0838	1.4552	0.8531	0	0	0.002496741
Bacteroidetes;Prevotellaceae UCG-001	14.1789	6.7151	17.1112	3.5827	17.8213	1.9847	2.9356	2.9372	1.60E-09
Bacteroidetes;Rikenella	5.4288	3.5043	7.6099	0.9939	6.7213	0.7053	0	0	3.15E-10
Bacteroidetes;uncultured bacterium	300.9970	318.4418	292.3863	324.1997	307.5435	323.1597	29.3555	31.2881	0.00889781
Bacteroidetes;uncultured Bacteroidales bacterium	10.2164	4.3016	6.9497	3.0084	7.4969	3.0588	0.3829	1.1488	1.23E-07
Deferribacteres;	3.4148	1.9669	4.8594	1.6084	2.6955	1.3848	10.9120	1.5936	1.59E-11
Deferribacteres;Mucispirillum	3.4148	1.9669	4.8594	1.6084	2.6955	1.3848	10.9120	1.5936	1.59E-11
Firmicutes;	1650.5155	374.9429	1442.6077	349.0573	1309.6567	414.8119	218.0964	65.5902	1.63E-09
Firmicutes;[Eubacterium] brachy group	1.6058	1.7900	0.4865	0.6754	1.3436	1.1318	0	0	0.005344925
Firmicutes;[Eubacterium] hallii group	3.8546	1.9743	4.0648	2.3318	1.6731	1.7912	0	0	3.64E-05
Firmicutes;[Eubacterium] nodatum group	10.4518	3.8110	13.3873	2.3367	10.1474	5.1282	0	0	4.21E-08
Firmicutes;[Eubacterium] oxidoreducens group	8.5534	3.2773	7.2417	2.7210	7.8765	4.3183	0	0	1.84E-06
Firmicutes;Acetatifactor	5.5015	3.4545	5.6503	1.7962	5.7676	3.2785	0	0	6.55E-05
Firmicutes;Anaerotruncus	36.0686	10.9757	35.1285	15.3587	23.2467	9.9509	0	0	2.96E-08
Firmicutes;Blautia	13.9647	7.2737	15.1607	5.9111	10.7892	6.8454	3.9687	2.5964	0.001726237
Firmicutes;Clostridium sensu stricto 1	0	0	0	0	0	0	1.9845	1.8954	0.000185705
Firmicutes;Coprococcus 1	24.5276	10.6709	13.0030	3.4093	11.5319	6.4546	1.5650	1.8670	8.97E-07
Firmicutes;Erysipelatoclostridium	6.1689	1.0082	5.2007	1.2042	4.6635	0.7944	0.8419	1.6952	5.92E-10
Firmicutes;Faecalibacterium	6.3188	4.4402	9.0078	1.7773	9.3328	2.1283	0	0	7.39E-10
Firmicutes;Family XIII UCG-001	3.9665	1.9101	2.8847	1.3687	2.5066	2.0116	0.3815	1.1445	0.001222756
Firmicutes;Incertae Sedis	17.5323	9.5205	13.8036	4.4179	8.7601	4.7750	5.7331	13.5137	0.036680694
Firmicutes;Lachnoclostridium	31.2244	12.9983	30.1176	7.9649	22.0720	14.3373	0.4135	1.2406	2.22E-06
Firmicutes;Lachnospiraceae FCS020 group	5.8954	1.8006	6.9911	2.4189	4.3080	2.9313	0	0	1.02E-06
Firmicutes;Lachnospiraceae NK4A136 group	293.7800	86.5372	227.2967	44.1527	211.3064	78.3017	16.5548	4.8393	1.93E-09
Firmicutes;Lachnospiraceae UCG-001	32.8526	13.2417	28.9459	9.2590	25.4503	12.2613	1.4347	2.2021	1.65E-06
Firmicutes;Lachnospiraceae UCG-004	27.0368	17.4337	37.6874	12.3499	31.1282	10.4702	17.3108	3.0062	0.006793627
Firmicutes;Lachnospiraceae UCG-006	41.8949	14.2127	42.4658	10.9046	29.8365	14.0806	6.0413	4.3525	2.71E-07
Firmicutes;Lachnospiraceae UCG-008	56.5377	16.4364	35.1328	11.0019	39.0365	15.6180	0.9605	1.9557	3.43E-09
Firmicutes;Marvinbryantia	12.2566	6.4412	19.2118	6.8399	12.0973	8.2293	0.3829	1.1488	1.50E-05
Firmicutes;Moryella	1.7729	1.4489	1.0150	1.1209	0.8517	1.5977	0	0	0.048750374
Firmicutes;Oscillibacter	67.7586	14.0491	64.6094	22.3264	46.4885	17.8998	0.4437	1.3311	1.59E-09
Firmicutes;Oscillospira	1.1830	1.1784	0.7213	1.0926	0.1900	0.6008	0	0	0.028870982
Firmicutes;Peptococcus	3.9932	0.8539	2.6618	1.6746	3.2430	1.0024	0	0	3.78E-08
Firmicutes;Pseudobutyrivibrio	3.8651	2.6250	2.2826	2.1766	0.9962	1.1934	0	0	8.58E-05
Firmicutes;Roseburia	67.4929	22.4918	40.5737	17.0693	41.6897	20.2767	5.3831	3.1796	6.28E-07
Firmicutes;Ruminiclostridium	14.3447	6.0846	16.6316	4.4625	11.3033	7.1202	0	0	6.88E-07
Firmicutes;Ruminiclostridium 5	18.6623	7.2356	12.1465	3.5804	10.0419	5.7984	0	0	7.93E-08
Firmicutes;Ruminiclostridium 6	2.4250	2.3665	2.9751	2.4349	1.0442	1.2193	0	0	0.005949342
Firmicutes;Ruminiclostridium 9	41.9250	9.1242	43.5050	16.9613	32.6904	14.3220	0	0	3.53E-08
Firmicutes;Ruminococcaceae NK4A214 group	2.6985	1.9480	2.3079	1.7306	1.7143	1.4334	0	0	0.003552248
Firmicutes;Ruminococcaceae UCG-003	6.8610	2.5941	6.0511	2.8155	6.5939	2.9716	0	0	1.34E-06
Firmicutes;Ruminococcaceae UCG-005	3.0090	2.2517	1.3190	1.1124	2.0148	1.6516	0	0	0.000529006
Firmicutes;Ruminococcaceae UCG-009	5.8046	1.8421	6.0642	1.8058	4.6020	2.3293	0.3569	1.0706	6.12E-07
Firmicutes;Ruminococcaceae UCG-010	3.8919	1.7864	4.2747	1.1990	3.5516	1.0709	0	0	1.01E-08
Firmicutes;Ruminococcaceae UCG-011	2.3407	1.3643	2.2965	1.4948	1.3744	1.9004	0	0	0.005791923
Firmicutes;Ruminococcaceae UCG-014	21.9590	11.5819	28.8138	14.7806	19.5501	9.8011	0	0	6.63E-06
Firmicutes;Ruminococcus 1	26.5593	5.0245	19.1506	5.5171	17.6503	9.1502	1.1929	2.3686	2.64E-08
Firmicutes;Ruminococcus 2	1.1178	1.0877	0.5543	1.0435	0.1224	0.3869	11.9412	2.4502	1.08E-17
Firmicutes;Turicibacter	1.3650	1.2759	0.1871	0.5291	0.1568	0.4958	0	0	0.001857911
Firmicutes;Tyzzerella	3.3740	2.2006	2.8039	2.5810	2.6256	2.1268	0	0	0.006947705
Firmicutes;Tyzzerella 3	1.6017	1.5683	1.4589	1.8969	3.7364	2.1927	0	0	0.000232933
Firmicutes;uncultured	109.4072	176.1478	94.5566	146.7241	83.1255	137.6941	4.2599	5.9582	0.001232503
Firmicutes;unidentified	7.7955	2.5373	12.1826	4.5401	9.1589	2.9438	4.5952	4.5642	0.002572134
Proteobacteria;	22.5912	10.5994	22.3113	5.8910	17.6356	7.3533	312.2025	129.7117	7.81E-11
Proteobacteria;Citrobacter	0	0	0	0	0	0	8.1516	4.6234	1.76E-08
Proteobacteria;Cronobacter	0	0	0	0	0	0	8.1426	4.4845	9.31E-09
Proteobacteria;Desulfovibrio	7.6190	5.1889	5.3337	3.6123	4.6086	4.0921	0.3815	1.1445	0.001438703
Proteobacteria;Enterobacter	1.2753	1.4260	0.7941	0.7111	0.8932	1.2959	74.8099	29.9720	7.77E-12
Proteobacteria;Escherichia-Shigella	2.6863	2.1098	1.7688	1.8107	1.8756	1.3454	84.2764	45.5473	1.11E-08
Proteobacteria;Gemmobacter	0	0	0	0	0.0946	0.2990	6.2922	2.5259	7.78E-12
Proteobacteria;Nitratireductor	0	0	0	0	0	0	4.1619	1.8301	5.22E-11
Proteobacteria;Other	0.1761	0.4982	0	0	0	0	20.2296	10.9645	7.08E-09
Proteobacteria;Pantoea	0.9707	1.1035	1.3450	0.8998	0.7201	0.9751	19.9257	5.7159	8.34E-15
Proteobacteria;Parasutterella	6.2524	4.3448	7.9987	3.7072	6.2225	1.3532	20.5058	10.4616	3.18E-05
Proteobacteria;Phyllobacterium	0	0	0	0	0	0	6.4920	2.6295	6.94E-12
Proteobacteria;Pseudomonas	0	0	0.1449	0.4098	0	0	22.7346	7.8512	1.28E-13
Proteobacteria;Salmonella	0.3869	0.5492	0.5067	0.9420	0	0	32.9553	15.2603	2.31E-10
Tenericutes;	6.7697	4.0895	4.8779	2.0034	2.6719	2.7978	0	0	7.01E-06
Tenericutes;Anaeroplasma	3.5195	1.8161	3.8662	1.1125	0.6941	1.6398	0	0	5.44E-07
Tenericutes;Other	3.2502	2.9039	1.0117	1.2223	1.9779	2.8617	0	0	0.008850106
Verrucomicrobia;	8.7367	1.1858	8.8457	3.1276	6.7443	1.4078	16.5576	1.6069	3.91E-11
Verrucomicrobia;Akkermansia	8.7367	1.1858	8.8457	3.1276	6.7443	1.4078	16.5576	1.6069	3.91E-11

Appendix 10: Summary of the statistics obtained from the linear regression model for treatment differences in small intestines of the βgal immunisation control group.

Small intestine	Control		hFMT		Vancomycin		
Differentially abundant taxonomy	mean	st dev	mean	st dev	mean	st dev	P value
Actinobacteria;	34.1953	34.7617	58.3979	44.0347	0.3211	0.9632	0.00398
Actinobacteria;Enterorhabdus	29.4089	29.7214	48.8351	38.0875	0	0	0.00480
Actinobacteria;Parvibacter	1.2835	2.0345	3.3976	2.9237	0	0	0.00841
Actinobacteria;Senegalimassilia	0.4066	0.9960	1.7697	1.9057	0	0	0.02224
Actinobacteria;uncultured	0	0	0.7611	1.0606	0	0	0.03884
Bacteroidetes;	272.8752	211.6104	548.3417	348.7017	164.6070	40.0806	0.00941
Bacteroidetes;Alistipes	9.7142	6.9535	23.3808	21.8343	3.2514	3.2971	0.01995
Bacteroidetes;Alloprevotella	0.35845	0.8780196	3.3985	3.1678	0	0	0.00366
Bacteroidetes;Bacteroides	15.9291	3.3023	35.0503	26.0130	44.6196	12.0966	0.01732
Bacteroidetes;Odoribacter	0	0	2.7471	3.4319	0	0	0.02016
Bacteroidetes;Parabacteroides	5.7965	4.8917	19.5982	14.9391	45.6443	19.5087	0.00022
Bacteroidetes;Paraprevotella	1.4657	2.2736	2.4279	2.2309	0	0	0.03021
Bacteroidetes;Rikenella	0.6167	1.5107	3.7348	2.7016	0.9991	1.5079	0.01282
Bacteroidetes;uncultured bacterium	113.7486	181.6689	217.7608	303.2620	29.8350	33.1745	0.03423
Bacteroidetes;uncultured Bacteroidales bacterium	3.4694	3.3091	4.4298	3.1985	0.6139	1.2230	0.01959
Deferribacteres;	0.7124	1.7449	2.4509	2.3775	4.8607	2.3137	0.00612
Deferribacteres;Mucispirillum	0.7124	1.7449	2.4509	2.3775	4.8607	2.3137	0.00612
Firmicutes;	854.4337	525.7606	1066.9711	336.6991	586.9134	107.7906	0.02727
Firmicutes;[Eubacterium] brachy group	0.3870	0.9479	1.9642	2.2721	0	0	0.02726
Firmicutes;[Eubacterium] nodatum group	4.4406	5.1272	3.8487	4.4009	0	0	0.04981
Firmicutes;Acetatifactor	3.8125	3.9391	3.5429	4.3003	0	0	0.04780
Firmicutes;Allobaculum	14.6258	4.2021	12.2828	3.5658	17.5157	2.1286	0.01275
Firmicutes;Blautia	5.9980	7.0243	19.8590	3.4607	8.4792	7.0974	0.00055
Firmicutes;Candidatus Arthromitus	7.8779	8.4934	9.5243	5.8550	0.3045	0.9134	0.00596
Firmicutes;Clostridium sensu stricto 1	0	0	0	0	1.2378	1.4779	0.01979
Firmicutes;Faecalibacterium	0.3870	0.9479	2.6282	2.5821	0	0	0.00735
Firmicutes;Family XIII UCG-001	2.1684	2.4460	2.8425	2.8510	0	0	0.02808
Firmicutes;Lachnoclostridium	31.0372	37.9585	41.8791	32.8765	0.2826	0.8479	0.01391
Firmicutes;Lachnospiraceae NK4A136 group	79.6344	82.8252	78.1237	47.9116	15.4745	5.1176	0.02718
Firmicutes;Lachnospiraceae UCG-001	12.6672	12.5400	8.5524	5.5210	0.9670	2.0810	0.01528
Firmicutes;Lachnospiraceae UCG-004	3.9268	2.3148	23.4258	9.8659	21.2711	9.0340	0.00056
Firmicutes;Lachnospiraceae UCG-006	28.8653	29.1085	37.0559	24.6659	2.5263	2.7548	0.00698
Firmicutes;Lachnospiraceae UCG-008	23.4136	25.9478	16.7859	9.4801	1.3984	1.7010	0.01849
Firmicutes;Lactobacillus	266.0241	97.4432	433.6684	132.5931	441.0365	92.4492	0.01272
Firmicutes;Marvinbryantia	2.8847	3.6685	8.2650	7.9988	0.3045	0.9134	0.01461
Firmicutes;Ruminococcaceae UCG-003	2.4621	3.1518	0.6617	1.2284	0	0	0.04251
Firmicutes;Ruminococcus 2	0.2866	0.7021	2.5698	2.7324	10.6013	3.0051	0.00000
Firmicutes;Streptococcus	17.4217	8.5481	19.1449	9.6020	9.7447	2.0171	0.03367
Firmicutes;uncultured	42.8552	104.0138	44.5120	90.4729	6.9733	6.2955	0.04120
Proteobacteria;	24.4615	18.5170	53.9982	31.2717	274.7208	182.5743	0.00061
Proteobacteria;Citrobacter	0	0	0.2237	0.6327	9.0911	8.3681	0.00310
Proteobacteria;Cronobacter	0	0	0.4255	0.7892	6.7141	5.3309	0.00101
Proteobacteria;Desulfovibrio	13.2279	16.5674	18.4817	16.2634	0.3045	0.9134	0.02282
Proteobacteria;Enterobacter	2.1055	1.7500	8.8224	8.3915	67.9661	45.3300	0.00030
Proteobacteria;Escherichia-Shigella	2.1192	2.4145	4.9517	6.0138	75.0730	65.8174	0.00282
Proteobacteria;Gemmobacter	0	0	0.7169	1.0952	5.4639	2.9249	0.00003
Proteobacteria;Nitratireductor	0	0	0.4255	0.7892	2.4038	2.8720	0.04219
Proteobacteria;Other	0	0	0.4255	0.7892	19.3099	15.3927	0.00077
Proteobacteria;Pantoea	2.0606	1.7335	4.9920	3.6041	16.2848	6.6998	0.00002
Proteobacteria;Parasutterella	2.8864	0.8949	5.5338	4.5219	14.9327	11.2259	0.01274
Proteobacteria;Phyllobacterium	0	0	0.4676	1.3226	5.9704	4.5482	0.00094
Proteobacteria;Pseudomonas	0	0	2.4789	2.9302	19.2832	11.8096	0.00010
Proteobacteria;Salmonella	0.4137	1.0133	3.8886	3.3068	29.9146	18.9806	0.00015
Verrucomicrobia;	4.7132	2.5164	6.3813	4.4046	9.3528	2.2771	0.03409
Verrucomicrobia;Akkermansia	4.7132	2.5164	6.3813	4.4046	9.3528	2.2771	0.03409

Appendix 11: Summary of the statistics obtained from the linear regression model for treatment differences in colon + entire sources of the TSHR immunisation control group.

colon + entire	Control		hFMT		LAB4		Vancomycin		
Differential abundant taxonomy	mean	st dev	mean	st dev	mean	st dev	mean	st dev	P value
Actinobacteria;	27.787	11.756	27.034	9.858	32.765	11.558	0.688	1.451	5.20E-10
Actinobacteria;Coriobacteriaceae UCG-002	5.101	2.809	3.783	3.590	6.056	2.762	0.688	1.451	0.000178202
Actinobacteria;Enterorhabdus	19.229	7.295	21.917	7.681	23.439	9.969	0.000	0.000	1.83E-09
Actinobacteria;Parvibacter	0.448	0.945	1.241	0.846	0.505	0.834	0.000	0.000	0.00692805
Actinobacteria;Slackia	2.315	1.898	0.000	0.000	2.054	2.276	0.000	0.000	9.51E-05
Bacteroidetes;	685.391	184.168	683.359	219.561	815.754	206.349	220.897	35.871	2.43E-09
Bacteroidetes;Alistipes	56.774	11.238	35.544	18.668	45.944	31.635	2.787	2.224	5.89E-07
Bacteroidetes;Alloprevotella	3.593	1.575	5.684	2.378	5.389	1.931	0.000	0.000	7.33E-09
Bacteroidetes;Bacteroides	54.746	22.869	23.278	22.083	46.223	37.507	62.960	12.870	0.003110606
Bacteroidetes;Odoribacter	7.266	4.127	1.490	2.917	7.967	4.856	0.349	1.102	5.09E-06
Bacteroidetes;Other	14.755	3.414	14.093	4.274	10.204	6.624	3.426	2.819	1.85E-06
Bacteroidetes;Parabacteroides	7.857	3.337	9.032	4.839	10.943	4.568	81.866	21.135	4.81E-19
Bacteroidetes;Paraprevotella	1.806	1.175	3.123	2.188	1.286	1.730	0.000	0.000	0.000364059
Bacteroidetes;Prevotellaceae UCG-001	15.607	2.310	9.323	6.160	18.372	5.979	4.482	2.363	1.14E-07
Bacteroidetes;Rikenella	6.706	0.923	4.568	3.897	4.028	3.725	0.330	1.044	6.99E-05
Bacteroidetes;uncultured bacterium	248.880	273.049	281.989	310.800	324.070	351.074	29.367	30.675	0.004527496
Bacteroidetes;uncultured Bacteroidales bacterium	5.881	2.678	6.494	3.113	8.284	3.689	0.354	1.120	2.24E-07
Deferribacteres;	3.692	1.982	2.460	2.275	3.131	1.519	9.891	4.718	1.49E-06
Deferribacteres;Mucispirillum	3.692	1.982	2.460	2.275	3.131	1.519	9.891	4.718	1.49E-06
Firmicutes;	1520.834	405.892	1328.323	441.466	1550.551	546.254	320.903	113.112	6.88E-09
Firmicutes;[Eubacterium] brachy group	1.104	1.384	1.467	1.643	1.343	1.085	0.000	0.000	0.041538408
Firmicutes;[Eubacterium] hallii group	2.448	1.973	1.004	1.308	1.756	2.415	0.000	0.000	0.0033972
Firmicutes;[Eubacterium] nodatum group	8.758	2.838	8.629	4.181	12.636	5.115	0.000	0.000	1.75E-08
Firmicutes;[Eubacterium] oxidoreducens group	5.735	5.277	6.307	3.822	7.356	4.837	0.000	0.000	0.000835802
Firmicutes;[Eubacterium] ventriosum group	0.000	0.000	3.195	3.938	0.000	0.000	0.000	0.000	0.000862377
Firmicutes;Acetatifactor	5.158	2.972	2.298	3.021	3.497	1.863	0.000	0.000	8.00E-05
Firmicutes;Acetitomaculum	0.000	0.000	0.861	1.480	0.000	0.000	0.000	0.000	0.024217019
Firmicutes;Anaerotruncus	27.935	15.500	28.008	15.984	29.865	12.975	0.983	1.585	1.82E-06
Firmicutes;Blautia	16.435	5.736	14.294	7.041	17.876	9.991	5.453	3.503	0.000845874
Firmicutes;Coprococcus 1	18.687	10.416	17.497	10.858	17.065	10.084	0.345	1.090	2.09E-05
Firmicutes;Erysipelatoclostridium	5.053	1.173	4.858	2.400	8.037	3.375	1.974	1.709	1.55E-05
Firmicutes;Faecalibacterium	7.212	3.973	2.924	2.454	7.495	5.667	0.000	0.000	1.65E-05
Firmicutes;Family XIII AD3011 group	1.146	1.177	0.748	1.045	1.556	1.575	0.000	0.000	0.016993993
Firmicutes;Family XIII UCG-001	3.601	2.032	3.335	1.714	3.058	2.262	0.000	0.000	5.65E-05
Firmicutes;Incertae Sedis	12.001	9.780	17.325	14.729	17.873	11.085	0.703	1.481	0.000976178
Firmicutes;Lachnoclostridium	30.650	12.749	29.661	10.917	26.155	13.891	0.679	1.431	2.44E-08
Firmicutes;Lachnospiraceae FCS020 group	6.339	5.026	4.048	3.382	7.685	3.994	0.000	0.000	3.48E-06
Firmicutes;Lachnospiraceae NK4A136 group	248.421	80.812	207.241	93.157	236.745	85.442	12.622	5.515	4.03E-09
Firmicutes;Lachnospiraceae UCG-001	34.835	17.938	27.209	17.713	35.370	21.482	1.001	1.623	7.58E-05
Firmicutes;Lachnospiraceae UCG-004	31.401	12.125	13.442	14.203	24.240	22.896	20.467	3.143	0.035914162
Firmicutes;Lachnospiraceae UCG-005	3.507	2.486	2.295	1.309	2.567	1.624	0.345	1.090	0.001873597
Firmicutes;Lachnospiraceae UCG-006	37.476	12.931	37.801	12.920	39.346	16.960	9.444	4.500	2.26E-06
Firmicutes;Lachnospiraceae UCG-008	48.044	12.461	37.926	21.034	48.415	16.940	3.273	2.735	2.75E-08
Firmicutes;Marvinbryantia	7.704	7.881	5.100	8.197	16.058	10.433	0.000	0.000	0.00052847
Firmicutes;Moryella	2.292	1.759	0.859	1.069	2.003	2.462	0.000	0.000	0.006853472
Firmicutes;Oscillibacter	55.517	23.388	45.253	28.052	49.504	24.202	2.354	2.254	2.38E-06
Firmicutes;Peptococcus	2.836	1.618	3.516	2.089	3.135	1.767	0.000	0.000	2.32E-05
Firmicutes;Pseudobutyrivibrio	2.463	1.490	3.339	2.660	2.925	2.249	0.000	0.000	0.001504162
Firmicutes;Roseburia	49.350	18.348	38.471	23.987	53.066	19.976	5.261	3.545	1.01E-06
Firmicutes;Ruminiclostridium	17.911	7.502	10.625	7.493	10.961	7.520	0.000	0.000	2.42E-06
Firmicutes;Ruminiclostridium 5	12.771	8.355	14.990	9.119	17.464	7.196	0.330	1.044	1.23E-05
Firmicutes;Ruminiclostridium 6	1.541	2.067	0.673	1.260	2.964	2.452	0.000	0.000	0.001707522
Firmicutes;Ruminiclostridium 9	36.057	18.118	35.272	20.107	39.305	15.638	0.000	0.000	9.10E-07
Firmicutes;Ruminococcaceae NK4A214 group	1.986	1.555	1.444	1.502	2.989	2.000	0.000	0.000	0.000423656
Firmicutes;Ruminococcaceae UCG-002	0.363	0.550	0.000	0.000	0.850	1.325	0.000	0.000	0.029908745
Firmicutes;Ruminococcaceae UCG-003	4.566	3.312	3.788	2.679	4.881	3.905	0.000	0.000	0.001200222
Firmicutes;Ruminococcaceae UCG-005	1.587	1.962	2.523	2.053	2.998	2.606	0.000	0.000	0.00755379
Firmicutes;Ruminococcaceae UCG-009	6.269	3.519	4.761	3.463	5.377	3.183	0.000	0.000	5.74E-05
Firmicutes;Ruminococcaceae UCG-010	3.332	1.079	3.441	1.765	5.184	2.741	0.324	1.026	6.20E-06
Firmicutes;Ruminococcaceae UCG-011	1.775	1.308	0.556	0.979	0.849	0.933	0.000	0.000	0.000476371
Firmicutes;Ruminococcaceae UCG-013	1.668	1.421	1.005	1.657	1.893	2.172	0.000	0.000	0.034621229
Firmicutes;Ruminococcaceae UCG-014	19.908	10.769	25.906	13.117	26.410	16.350	1.250	3.952	6.92E-05
Firmicutes;Ruminococcus 1	13.464	7.676	10.513	5.242	14.146	9.968	0.287	0.909	4.00E-05
Firmicutes;Ruminococcus 2	0.629	0.702	0.417	0.746	0.619	0.672	12.459	0.662	4.55E-34
Firmicutes;Tyzzerella	3.295	1.806	2.313	2.273	1.886	1.516	0.000	0.000	0.000434209
Firmicutes;Tyzzerella 3	3.046	2.479	0.141	0.467	3.076	2.082	0.000	0.000	1.73E-05
Firmicutes;uncultured	102.492	175.105	91.399	150.824	98.685	167.471	3.689	3.800	0.001198016
Firmicutes;unidentified	10.410	3.939	7.685	3.533	9.419	3.367	11.639	3.431	0.038619585
Proteobacteria;	21.919	6.596	18.204	10.236	16.757	8.595	329.396	51.317	5.02E-28
Proteobacteria;Bilophila	4.059	1.445	0.856	1.317	2.325	2.572	2.788	3.627	0.023604427
Proteobacteria;Citrobacter	0.000	0.000	0.000	0.000	0.000	0.000	9.954	4.262	2.35E-14
Proteobacteria;Cronobacter	0.000	0.000	0.000	0.000	0.000	0.000	8.677	2.565	1.19E-19
Proteobacteria;Desulfovibrio	5.438	2.276	6.899	6.169	5.196	4.520	0.360	1.138	0.003820429
Proteobacteria;Enterobacter	0.378	0.576	1.719	1.770	0.758	1.099	78.421	12.087	2.39E-29
Proteobacteria;Escherichia-Shigella	3.804	1.827	2.980	1.890	3.227	1.862	85.056	22.286	1.05E-20
Proteobacteria;Gemmobacter	0.000	0.000	0.000	0.000	0.000	0.000	6.663	0.665	7.82E-37
Proteobacteria;Methylobacterium	0.306	0.575	0.000	0.000	0.000	0.000	0.000	0.000	0.012984843
Proteobacteria;Nitratireductor	0.161	0.559	0.000	0.000	0.000	0.000	4.466	0.898	1.38E-22
Proteobacteria;Other	0.107	0.371	0.000	0.000	0.000	0.000	24.344	4.445	5.17E-27
Proteobacteria;Pantoea	0.513	0.808	0.364	0.636	0.292	0.616	20.191	4.023	1.13E-24
Proteobacteria;Parasutterella	6.757	1.917	5.013	2.950	4.643	5.429	22.535	8.266	8.22E-10
Proteobacteria;Phyllobacterium	0.161	0.559	0.000	0.000	0.000	0.000	7.547	1.726	1.35E-22
Proteobacteria;Pseudomonas	0.000	0.000	0.101	0.334	0.222	0.471	23.430	3.863	1.79E-28
Proteobacteria;Salmonella	0.235	0.813	0.273	0.632	0.095	0.300	34.266	7.508	5.79E-24
Tenericutes;	0.712	1.281	6.946	5.069	2.140	1.743	0.308	0.974	7.54E-06
Tenericutes;Anaeroplasma	0.586	0.962	3.700	3.423	0.000	0.000	0.308	0.974	0.000121891
Tenericutes;Other	0.126	0.437	3.246	2.205	2.140	1.743	0.000	0.000	4.26E-06
Verrucomicrobia;	7.561	2.232	8.174	2.478	8.583	2.229	12.994	3.437	8.50E-05
Verrucomicrobia;Akkermansia	7.561	2.232	8.174	2.478	8.583	2.229	12.994	3.437	8.50E-05

Appendix 12: Summary of the statistics obtained from the linear regression model for treatment differences in small intestines of the TSHR immunisation control group.

small intestines	Control		hFMT		Vancomycin		
Differential abundant taxonomy	mean	st dev	mean	st dev	mean	st dev	Pvalue
Actinobacteria;	28.586	28.447	43.177	26.893	0.789	1.185	0.00108969
Actinobacteria;Coriobacteriaceae UCG-002	2.491	3.177	3.941	2.967	0.000	0.000	0.00582108
Actinobacteria;Enterorhabdus	23.973	23.525	35.692	23.541	0.789	1.185	0.00163943
Actinobacteria;Parvibacter	1.451	2.072	3.089	2.551	0.000	0.000	0.00581648
Bacteroidetes;	320.264	157.591	400.018	149.286	182.690	48.196	0.00301866
Bacteroidetes;Alistipes	21.643	17.588	15.334	9.125	1.702	1.862	0.00243722
Bacteroidetes;Alloprevotella	2.185	1.857	3.299	2.723	0.000	0.000	0.00410531
Bacteroidetes;Bacteroides	22.950	14.323	16.132	6.530	49.977	12.505	7.17E-07
Bacteroidetes;Parabacteroides	13.425	11.071	4.301	2.519	56.852	22.603	2.22E-08
Bacteroidetes;uncultured bacterium	116.685	144.332	168.435	193.731	30.323	33.074	0.01534535
Bacteroidetes;uncultured Bacteroidales bacterium	2.481	1.985	3.438	3.553	0.393	1.180	0.04650657
Deferribacteres;	2.752	2.812	0.311	1.078	6.932	2.785	2.06E-06
Deferribacteres;Mucispirillum	2.752	2.812	0.311	1.078	6.932	2.785	2.06E-06
Firmicutes;	1077.715	554.816	1027.126	285.216	545.987	201.105	0.00622348
Firmicutes;Acetatifactor	2.738	3.491	1.123	1.545	0.000	0.000	0.03861274
Firmicutes;Blautia	16.979	5.033	16.312	5.463	10.439	3.410	0.01461242
Firmicutes;Candidatus Arthromitus	9.832	8.670	4.648	7.373	0.293	0.880	0.02584883
Firmicutes;Coprococcus 1	4.314	4.886	6.134	4.563	0.300	0.900	0.00819917
Firmicutes;Family XIII UCG-001	3.206	3.270	3.086	2.313	0.000	0.000	0.00702308
Firmicutes;Lachnoclostridium	23.905	31.272	32.886	25.136	0.257	0.772	0.01073525
Firmicutes;Lachnospiraceae FCS020 group	2.220	3.208	3.600	3.234	0.000	0.000	0.01820056
Firmicutes;Lachnospiraceae NK4A136 group	100.768	111.966	92.379	69.052	17.308	3.642	0.03971877
Firmicutes;Lachnospiraceae UCG-001	12.039	12.797	13.283	11.691	1.858	3.862	0.0436981
Firmicutes;Lachnospiraceae UCG-004	20.636	5.711	14.577	7.495	25.660	7.275	0.00542343
Firmicutes;Lachnospiraceae UCG-005	2.100	2.383	0.621	1.203	0.000	0.000	0.02149864
Firmicutes;Lachnospiraceae UCG-006	22.418	23.463	29.337	12.890	4.708	4.227	0.00270698
Firmicutes;Lachnospiraceae UCG-008	17.960	18.887	19.319	11.545	0.995	2.166	0.0047303
Firmicutes;Oscillibacter	23.541	31.199	8.353	8.190	0.257	0.772	0.02861766
Firmicutes;Pseudobutyrivibrio	2.132	2.744	1.956	1.466	0.000	0.000	0.02055685
Firmicutes;Ruminiclostridium 5	5.054	6.420	4.976	4.650	0.000	0.000	0.03248393
Firmicutes;Ruminiclostridium 6	1.261	1.700	0.000	0.000	0.000	0.000	0.0073601
Firmicutes;Ruminococcus 2	2.621	2.181	1.149	1.315	10.098	2.795	1.79E-09
Firmicutes;Tyzzerella	1.632	2.094	0.134	0.464	0.000	0.000	0.00995925
Firmicutes;Tyzzerella 3	2.172	3.113	0.000	0.000	0.000	0.000	0.01182726
Firmicutes;uncultured	46.344	109.375	45.750	87.568	5.781	6.391	0.02200987
Firmicutes;unidentified	3.979	4.906	2.210	2.873	7.044	2.889	0.01497689
Proteobacteria;	28.757	20.089	26.032	16.296	232.517	172.502	0.00011963
Proteobacteria;Citrobacter	0.000	0.000	0.000	0.000	7.343	5.780	4.37E-05
Proteobacteria;Cronobacter	0.247	0.654	0.000	0.000	5.298	4.914	0.00046591
Proteobacteria;Cupriavidus	0.000	0.000	0.000	0.000	3.321	3.681	0.00237572
Proteobacteria;Desulfovibrio	10.054	12.885	15.140	15.911	0.296	0.887	0.03711036
Proteobacteria;Enterobacter	3.372	4.288	1.960	1.591	57.815	39.663	1.23E-05
Proteobacteria;Escherichia-Shigella	0.995	1.292	1.923	2.265	58.530	62.329	0.00212597
Proteobacteria;Gemmobacter	0.367	0.970	0.000	0.000	4.475	3.021	1.24E-05
Proteobacteria;Nitratireductor	0.000	0.000	0.000	0.000	2.070	3.120	0.02675666
Proteobacteria;Other	0.162	0.428	0.000	0.000	14.602	14.049	0.00057119
Proteobacteria;Pantoea	4.154	2.672	1.753	1.865	14.598	6.968	1.56E-06
Proteobacteria;Parasutterella	4.655	3.016	3.151	2.881	14.061	7.481	8.33E-05
Proteobacteria;Phyllobacterium	0.000	0.000	0.000	0.000	5.950	3.383	2.61E-07
Proteobacteria;Pseudomonas	0.523	1.384	0.287	0.678	16.157	9.874	1.59E-06
Proteobacteria;Salmonella	2.038	2.711	0.779	1.747	23.789	17.353	3.93E-05
Verrucomicrobia;	6.948	2.339	4.279	2.070	10.567	2.606	9.85E-06
Verrucomicrobia;Akkermansia	6.948	2.339	4.279	2.070	10.567	2.606	9.85E-06

Appendix 13: Alpha diversity indices differences between timepoints in each treatment. hFMT, humanized faecal material transplant from Graves' orbitopathy (GO) patients. Lab4, probiotics *consortium*. Vanco, vancomycin antibiotics.

Indices	treatment	Baseline (mean)	Mid (mean)	Pvalue
chao1	control	842.2963	1072.6784	0.0038
chao1	hFMT	816.3464	954.0984	0.0353
chao1	lab4	897.3411	904.4632	0.9308
chao1	vanco	181.2537	196.4155	0.3941
observed_otus	control	601.8750	825.9500	0.0014
observed_otus	hFMT	599.3333	707.0000	0.0611
observed_otus	lab4	657.5714	643.3636	0.8389
observed_otus	vanco	113.1500	118.4286	0.6004
shannon	control	6.3526	6.7244	0.0752
shannon	hFMT	6.0841	6.0410	0.8794
shannon	lab4	6.3872	6.2976	0.6243
shannon	vanco	2.9951	2.7525	0.0016
equitability	control	0.6907	0.6997	0.6294
equitability	hFMT	0.6684	0.6405	0.3501
equitability	lab4	0.6903	0.6812	0.6225
equitability	vanco	0.4457	0.4046	0.0052

Appendix 14: *Bacteroides* spp. differences between timepoints in Lab4 (probiotics *consortium*) treatment and in each immunisation.

Genus	Treatment	Immunisation	Baseline (mean)	Mid (mean)	P value
Bacteroides	Lab4	βgal	46.58462	71.8608545	0.01071752
Bacteroides	Lab4	TSHR	21.1752333	56.2193555	0.023308

Appendix 15: Taxonomic differences at baseline amongst treatments from linear regression model.

Differentially abundant genera	control (mean)	hFMT (mean)	LAB4 (mean)	vanco (mean)	Pvalue
[Eubacterium] brachy group	0.88311875	1.15985333	1.17407857	0	0.0002468
[Eubacterium] coprostanoligenes group	0.11795	1.60564667	0.41645	0	1.41E-07
[Eubacterium] hallii group	1.972975	1.49490667	3.06753571	0	2.92E-05
[Eubacterium] nodatum group	9.83965625	10.8749333	10.2699214	0	1.54E-13
[Eubacterium] oxidoreducens group	3.77976875	6.67795333	5.48932143	0	6.08E-08
[Eubacterium] ventriosum group	0.32776875	4.26797333	1.9434	0	6.20E-05
Acetatifactor	3.61029375	3.43725333	6.35477143	0	6.07E-08
Akkermansia	6.98733125	7.57628	7.23598571	12.893925	2.59E-08
Alistipes	57.682775	32.99794	41.9882	1.505505	8.04E-11
Alloprevotella	6.03028125	4.68054	5.72154286	0	3.31E-13
Anaeroplasma	0.09075625	2.63190667	0.14692857	0	1.12E-08
Anaerostipes	0	0	0.26353571	0	0.00837697
Anaerotruncus	19.1304563	23.6562867	30.0845	0	8.34E-12
Anaerovorax	0.6619625	0.39442	0.41257143	0	0.04155382
Bacillus	0	0	0.75783571	0	0.00317586
Bacteroides	53.3114	33.7020867	30.2500143	52.55713	0.00379499
Bilophila	2.20811875	1.28712667	2.69292143	0.55378	0.00911014
Blautia	9.32748125	11.98376	10.2817143	2.50897	2.09E-06
Candidatus Arthromitus	4.63460625	4.76187333	3.58255	0.16112	0.00031776
Candidatus Saccharimonas	0	0.21736	0.76777143	0	0.02002911
Citrobacter	0	0	0	6.076175	1.59E-21
Coprococcus 1	12.5651	17.0796467	18.3538786	0.16166	5.73E-10
Coriobacteriaceae UCG-002	8.6125	7.27016667	8.04547857	0.935355	3.83E-11
Cronobacter	0	0	0	6.09172	1.17E-14
Desulfovibrio	4.59329375	4.39884	6.39582143	0	1.20E-07
Enterobacter	0.2825125	1.54798667	0.68948571	60.9957	9.25E-27
Enterococcus	0.4775625	0.22268	2.46460714	0	0.00253054
Enterorhabdus	15.9948313	18.7266867	17.7560714	0.219615	2.83E-11
Erysipelatoclostridium	3.431925	4.20839333	2.90978571	0.53463	1.59E-07
Escherichia-Shigella	1.62074375	1.95515333	1.34247857	60.395465	5.38E-21
Faecalibacterium	7.26368125	5.35438	6.37142857	0	5.58E-10
Family XIII AD3011 group	0.2898625	0.79558667	0.97312857	0	0.03419488
Family XIII UCG-001	2.99774375	2.65304667	3.18313571	0	2.72E-07
Gemmobacter	0	0.08406667	0	4.95218	2.37E-19
Incertae Sedis	12.1477313	20.2270133	23.8926786	2.157575	6.68E-08
Lachnoclostridium	18.7941125	25.2460933	28.7923429	0.65187	3.97E-10
Lachnospiraceae FCS020 group	3.9667625	4.02658667	7.41012143	0.15748	1.47E-08
Lachnospiraceae NC2004 group	0.16505625	0.33776	0.53240714	0	0.04736499
Lachnospiraceae ND3007 group	0.7608875	2.72046667	1.97709286	0	0.00225754
Lachnospiraceae NK4A136 group	186.210019	202.787913	217.575243	5.846415	4.29E-16
Lachnospiraceae UCG-001	21.174075	27.8098067	22.7873357	0	6.20E-10
Lachnospiraceae UCG-004	28.6143375	15.0936333	13.0272714	15.142655	0.00021619
Lachnospiraceae UCG-005	0.90696875	1.30704667	2.94212143	0	1.40E-07
Lachnospiraceae UCG-006	25.5354125	30.29318	34.7776714	5.87402	3.38E-11
Lachnospiraceae UCG-008	25.4160063	35.8011333	42.5574214	0.206025	2.50E-12
Lactobacillus	133.890406	98.1024067	89.5704929	152.547605	0.00414464
Marvinbryantia	14.5165125	14.2773333	14.8596786	0.32332	7.48E-08
Moryella	1.492325	0.58928	1.85215	0	0.00337594
Mucispirillum	2.13455	2.20750667	4.01331429	4.57979	0.02336858
Nitratireductor	0	0	0	2.44382	4.16E-09
Odoribacter	7.46698125	6.31963333	9.19553571	0.20772	1.22E-06
Oscillibacter	34.9428375	48.08872	48.8311357	0	2.32E-12
Pantoea	0.36165625	0.93238667	0.40905714	15.92619	4.92E-35
Parabacteroides	8.385325	10.4267133	6.70335714	59.740915	1.39E-17
Paraprevotella	2.9452875	2.59291333	1.5812	0	1.32E-07
Parasutterella	6.179175	4.42212667	4.45807143	19.463145	1.05E-14
Peptococcus	1.8005	2.14418	3.06375714	0	3.74E-11
Phyllobacterium	0.2501125	0	0	6.671675	3.04E-24
Prevotellaceae UCG-001	14.297825	11.31582	11.9896714	2.31171	3.53E-08
Pseudobutyrivibrio	1.36803125	2.52164667	2.68502857	0	4.53E-05
Pseudomonas	0.18051875	0.25267333	0.07416429	19.093155	3.97E-33
Rikenella	5.84608125	3.55295333	4.25865714	0	8.26E-11
Roseburia	29.5273063	38.4525067	52.0082714	5.703775	4.00E-10
Ruminiclostridium	8.3066625	11.9391467	11.1959	0	6.60E-09
Ruminiclostridium 5	7.2594	12.5735733	14.7552643	0.228425	1.18E-09
Ruminiclostridium 6	0.87056875	2.68691333	2.39729286	0	0.00407931
Ruminiclostridium 9	24.4679438	34.22548	33.8254357	0	1.51E-11
Ruminococcaceae NK4A214 group	0.8777125	0.86018667	1.57302857	0	0.00127636
Ruminococcaceae UCG-003	2.63703125	3.15874667	2.57252143	0	7.68E-05
Ruminococcaceae UCG-005	1.15821875	3.07864	3.51986429	0	1.37E-05
Ruminococcaceae UCG-009	3.9629375	3.60911333	4.63355714	0	3.68E-07
Ruminococcaceae UCG-010	2.2538125	3.94324	2.50937143	0.16166	2.64E-06
Ruminococcaceae UCG-011	1.51566875	1.47904667	2.73044286	0	6.89E-08
Ruminococcaceae UCG-013	0.7659875	0.72507333	0.28529286	0	0.02729139
Ruminococcaceae UCG-014	13.2061688	32.6349333	26.8509714	0	1.68E-09
Ruminococcus 1	17.2110375	11.9802	16.6206071	0.337315	2.36E-14
Ruminococcus 2	0.56806875	0.85823333	0.35945714	11.8621	2.72E-45
Salmonella	0	0.41550667	0.11524286	23.850245	4.52E-26
Slackia	1.191725	1.07316667	1.06957857	0	0.01386481
Streptococcus	2.60970625	2.82322667	2.31261429	5.25975	0.00831549
Tyzzerella	1.67686875	2.01964	1.61454286	0	8.72E-05
Tyzzerella 3	2.06938125	1.80417333	3.14586429	0	0.00032851
uncultured	43.6175039	50.0790775	54.6597589	2.40624375	8.74E-07
uncultured bacterium	122.176533	93.2653467	97.9312714	8.65038	0.000244
uncultured Bacteroidales bacterium	14.2759813	12.9164667	10.3730214	0.72686	1.50E-10

Appendix 16: bacterial invaders as a result of the humanized faecal material transplant (hFMT) engraftment in the three timepoints.

At baseline, mid and endpoint, between GO patients, hFMT mice and control mice. See Chapter 3 par. 3.3.6.7 for formula explanation. Sd, Standard deviation.

Baseline – stool samples

family	GO (mean)	GO (sd)	hFMT (mean)	hFMT (sd)	control (mean)	control (sd)	dFMT	ddFMT (%)
Alcaligenaceae	3.2	3.2	4.4	4.3	6.2	2.5	-1.8	-155.6
Bacteroidaceae	167.5	53.5	33.7	29.0	53.3	19.4	-19.6	-111.7
Coriobacteriaceae	26.7	11.5	27.7	9.7	26.1	8.7	1.5	-94.3
Enterobacteriaceae	33.2	32.5	4.9	5.9	2.3	1.8	2.6	-92.2
Erysipelotrichaceae	33.3	8.8	16.7	8.0	13.5	3.9	3.1	-90.6
Lachnospiraceae	957.0	162.2	768.0	309.1	672.7	236.1	95.3	-90.0
Lactobacillaceae	29.8	52.6	98.1	48.4	133.9	55.8	-35.8	-219.9
Peptococcaceae	**0.2**	**0.4**	**9.0**	**5.8**	**7.5**	**3.9**	**1.5**	**622.4**
Porphyromonadaceae	64.0	16.4	25.1	13.4	29.5	9.1	-4.5	-107.0
Prevotellaceae	7.6	5.9	19.2	10.3	24.1	7.1	-4.8	-163.6
Rikenellaceae	39.5	21.2	36.6	27.9	63.5	21.3	-27.0	-168.3
Ruminococcaceae	363.2	101.4	293.6	127.3	212.4	89.4	81.2	-77.6
Streptococcaceae	16.0	11.2	2.8	2.5	2.6	1.4	0.2	-98.7
Verrucomicrobiaceae	1.7	3.3	7.6	2.3	7.0	1.5	0.6	-65.4

Mid – stool samples

family	GO (mean)	GO (sd)	hFMT (mean)	hFMT (sd)	control (mean)	control (sd)	dFMT	ddFMT (%)
Alcaligenaceae	3.2	3.2	4.6	4.6	7.1	3.8	-2.5	-178.0
Bacteroidaceae	167.5	53.5	40.4	31.0	60.2	30.8	-19.7	-111.8
Coriobacteriaceae	26.7	11.5	31.9	8.3	31.0	11.1	0.9	-96.7
Enterobacteriaceae	33.2	32.5	5.7	2.2	5.1	3.5	0.6	-98.1
Erysipelotrichaceae	33.3	8.8	16.7	7.0	16.3	6.0	0.4	-98.7
Lachnospiraceae	957.0	162.2	974.8	252.3	1109.4	325.4	-134.6	-114.1
Lactobacillaceae	**29.8**	**52.6**	**95.4**	**55.2**	**63.0**	**33.8**	**32.4**	**8.9**
Peptococcaceae	0.2	0.4	11.7	4.7	13.9	2.9	-2.2	-1224.9
Porphyromonadaceae	64.0	16.4	26.0	12.2	31.9	11.7	-5.9	-109.3
Prevotellaceae	7.6	5.9	18.0	8.3	23.0	7.0	-5.1	-166.5
Rikenellaceae	39.5	21.2	40.9	30.4	57.4	22.7	-16.5	-141.9
Ruminococcaceae	363.2	101.4	386.8	111.4	439.2	134.2	-52.4	-114.4
Streptococcaceae	16.0	11.2	3.8	1.6	3.3	1.9	0.5	-97.2
Verrucomicrobiaceae	1.7	3.3	8.5	1.9	8.6	2.0	-0.1	-105.5

Final – colon samples

family	GO (mean)	GO (sd)	hFMT (mean)	hFMT (sd)	control (mean)	control (sd)	dFMT	ddFMT (%)
Alcaligenaceae	3.2	3.2	6.3	3.5	5.5	3.5	0.8	-74.5
Bacteroidaceae	167.5	53.5	45.8	34.4	41.4	27.4	4.4	-97.4
Coriobacteriaceae	26.7	11.5	28.1	8.6	26.8	14.9	1.3	-95.1
Enterobacteriaceae	33.2	32.5	4.9	2.8	5.1	3.2	-0.2	-100.6
Erysipelotrichaceae	33.3	8.8	17.7	5.2	19.5	8.5	-1.9	-105.7
Lachnospiraceae	957.0	162.2	859.0	289.7	918.2	345.9	-59.2	-106.2
Lactobacillaceae	29.8	52.6	119.2	125.1	144.7	220.8	-25.6	-185.8
Peptococcaceae	**0.2**	**0.4**	**10.7**	**4.8**	**10.5**	**3.9**	**0.3**	**30.5**
Porphyromonadaceae	64.0	16.4	25.2	13.2	26.0	11.2	-0.8	-101.2
Prevotellaceae	7.6	5.9	21.1	7.6	19.1	6.3	1.9	-74.8
Rikenellaceae	39.5	21.2	54.1	25.4	52.8	23.4	1.2	-96.9
Ruminococcaceae	363.2	101.4	322.0	135.1	294.8	126.8	27.2	-92.5
Streptococcaceae	16.0	11.2	4.4	5.0	7.9	8.2	-3.5	-122.1
Verrucomicrobiaceae	1.7	3.3	8.5	2.7	7.4	1.9	1.1	-36.1

Appendix 17: Correlation analysis between disease features and bacterial biomarkers in the small intestine of (top) TSHR-immune and (bottom) βgal-immune control mice.

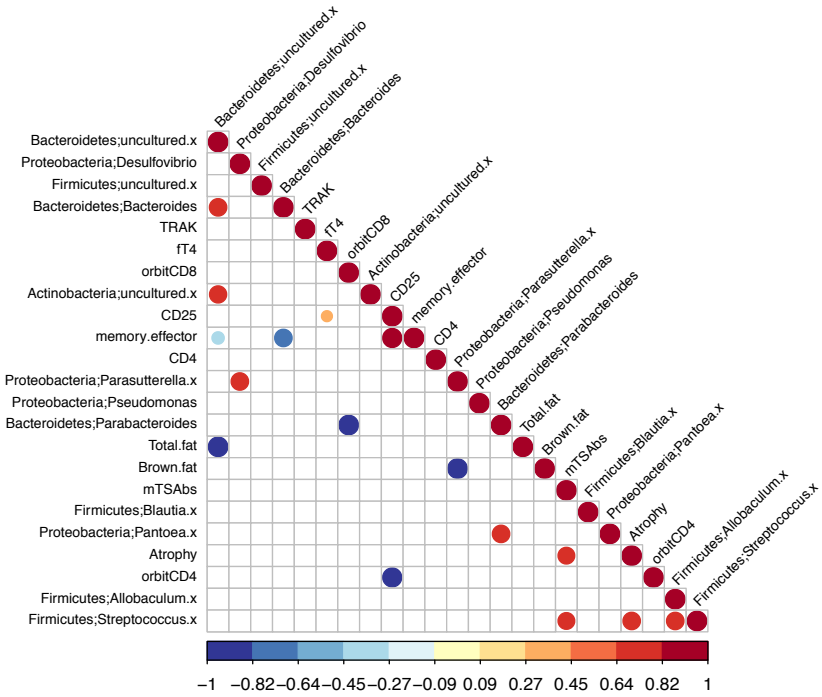

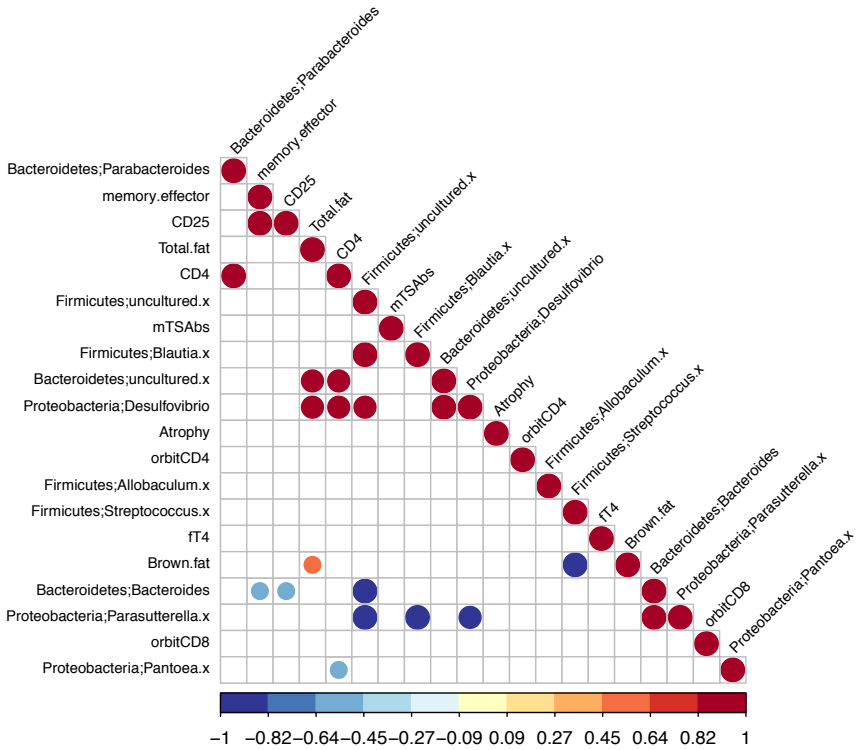

Appendix 18: Statistical summary (mean and standard deviation) of genera differentially abundant across nations of recruitment (Table 4.5).
Only genera with P<0.05 are shown.

	Belgium		Germany		Italy		UK	
Genera differentially abundant	mean	st. dev	mean	st. dev	mean	st. dev	mean	st. dev
Acidaminococcus	0.0000	0.0000	0.0002	0.0006	0.0006	0.0011	0.0002	0.0006
Christensenellaceae_R-7_group	0.0167	0.0081	0.0167	0.0099	0.0151	0.0084	0.0214	0.0125
Clostridium_sensu_stricto_1	0.0088	0.0055	0.0047	0.0035	0.0057	0.0053	0.0099	0.0088
Coprococcus_2	0.0055	0.0042	0.0027	0.0032	0.0033	0.0035	0.0046	0.0044
Corynebacterium_1	0.0002	0.0004	0.0000	0.0001	0.0000	0.0000	0.0000	0.0001
Cronobacter	0.0000	0.0001	0.0000	0.0000	0.0001	0.0003	0.0000	0.0001
Enterobacter	0.0016	0.0018	0.0013	0.0021	0.0034	0.0048	0.0051	0.0079
Faecalibacterium	0.0913	0.0421	0.1044	0.0381	0.1049	0.0322	0.0795	0.0388
Family_XIII_AD3011_group	0.0030	0.0019	0.0022	0.0018	0.0015	0.0018	0.0026	0.0022
Hafnia	0.0001	0.0004	0.0000	0.0000	0.0000	0.0001	0.0000	0.0001
Intestinibacter	0.0065	0.0032	0.0030	0.0024	0.0042	0.0021	0.0053	0.0036
Klebsiella	0.0000	0.0000	0.0000	0.0000	0.0003	0.0007	0.0001	0.0004
Lachnospiraceae_NC2004_group	0.0115	0.0038	0.0117	0.0040	0.0121	0.0039	0.0096	0.0040
Lachnospiraceae_NK4A136_group	0.0075	0.0035	0.0114	0.0057	0.0071	0.0030	0.0074	0.0039
Lactococcus	0.0011	0.0014	0.0011	0.0014	0.0004	0.0009	0.0005	0.0009
Leuconostoc	0.0006	0.0011	0.0000	0.0001	0.0001	0.0002	0.0000	0.0001
Pantoea	0.0007	0.0008	0.0005	0.0009	0.0011	0.0013	0.0015	0.0021
Paraprevotella	0.0000	0.0000	0.0001	0.0002	0.0003	0.0006	0.0000	0.0003
Peptoclostridium	0.0195	0.0121	0.0096	0.0104	0.0111	0.0088	0.0206	0.0181
Peptococcus	0.0000	0.0002	0.0003	0.0007	0.0004	0.0011	0.0000	0.0002
Romboutsia	0.0003	0.0007	0.0001	0.0003	0.0000	0.0001	0.0003	0.0005
Roseburia	0.0353	0.0065	0.0343	0.0124	0.0360	0.0119	0.0301	0.0091
Ruminiclostridium	0.0050	0.0013	0.0046	0.0029	0.0054	0.0030	0.0040	0.0022
Ruminiclostridium_5	0.0093	0.0032	0.0131	0.0048	0.0104	0.0039	0.0102	0.0037
Ruminococcaceae_V9D2013_group	0.0000	0.0001	0.0001	0.0002	0.0000	0.0001	0.0000	0.0001
Saccharofermentans	0.0009	0.0010	0.0002	0.0005	0.0001	0.0003	0.0003	0.0006
Sedimentibacter	0.0007	0.0008	0.0002	0.0005	0.0003	0.0005	0.0007	0.0011
Succiniclasticum	0.0006	0.0014	0.0000	0.0000	0.0002	0.0007	0.0000	0.0000
Syntrophomonas	0.0004	0.0005	0.0001	0.0003	0.0001	0.0003	0.0004	0.0007
[Eubacterium]_nodatum_group	0.0003	0.0004	0.0008	0.0010	0.0007	0.0011	0.0004	0.0007

Appendix 19. Beta-diversity organisation amongst disease types and eye-disease in each recruiting centre**.**

NMDS based on Bray-Curtis dissimilarity matrix amongst disease types (**A**) and GO groups (**B**). No significant associations were observed in either alpha or beta-diversity in both analysis (PERMANOVA, P>0.05)..

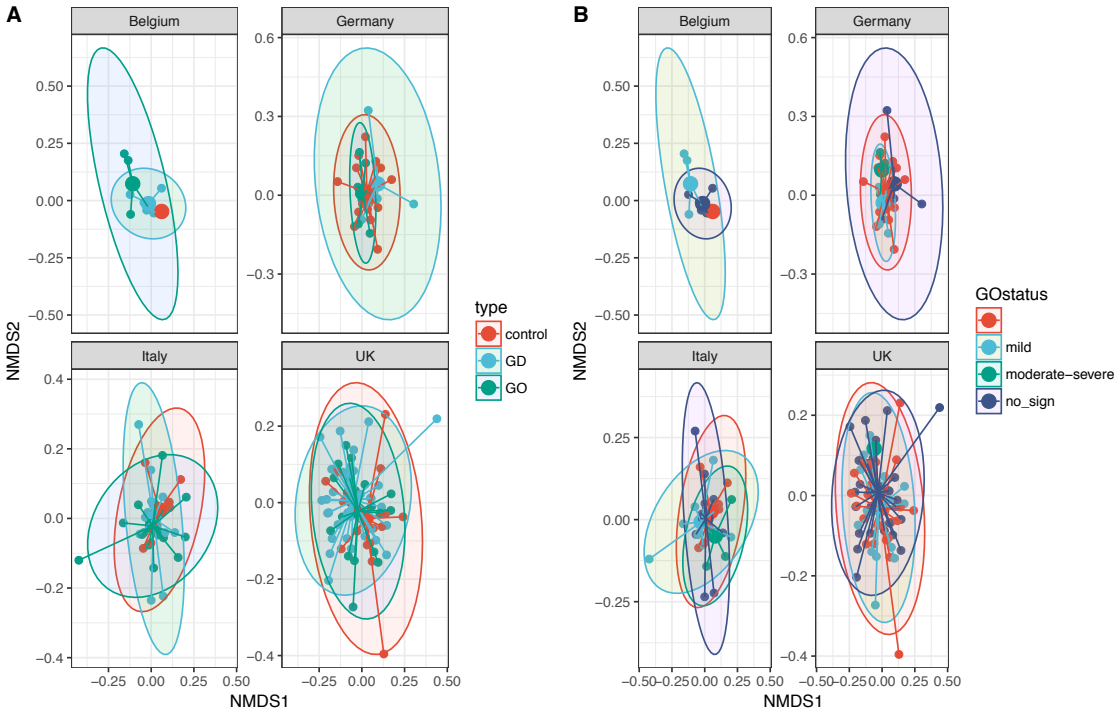

Appendix 20: Statistical summary (mean and standard deviation) of genera differentially abundant amongst eye-disease status (no sign, GO mild and GO moderate-severe) compared to healthy controls (Table 4.7).
Only genera with P>0.05 are shown.

	control		**GD no sign**		**GO mild**		**GO moderate-severe**	
Genera differentially abundant	mean	st. dev	mean	st. dev	mean	st. dev	mean	st. dev
Alistipes	0.0158	0.0090	0.0115	0.0078	0.0104	0.0067	0.0130	0.0075
Anaeroplasma	0.0002	0.0005	0.0001	0.0003	0.0000	0.0001	0.0005	0.0009
Bacteroides	0.0781	0.0393	0.0562	0.0394	0.0529	0.0310	0.0626	0.0358
Bifidobacterium	0.0088	0.0050	0.0117	0.0079	0.0135	0.0055	0.0088	0.0042
Clostridium_sensu_stricto_1	0.0062	0.0050	0.0092	0.0085	0.0080	0.0071	0.0030	0.0019
Collinsella	0.0079	0.0051	0.0127	0.0089	0.0122	0.0063	0.0100	0.0051
Fusicatenibacter	0.0168	0.0061	0.0214	0.0099	0.0234	0.0103	0.0213	0.0096
Intestinibacter	0.0036	0.0027	0.0050	0.0034	0.0056	0.0030	0.0030	0.0018
Lachnospiraceae_FCS020 group	0.0021	0.0015	0.0030	0.0021	0.0035	0.0022	0.0025	0.0024
Lactococcus	0.0011	0.0014	0.0005	0.0010	0.0004	0.0009	0.0004	0.0007
Luteimonas	0.0000	0.0000	0.0000	0.0000	0.0000	0.0000	0.0003	0.0010
Oscillospira	0.0008	0.0009	0.0003	0.0006	0.0004	0.0006	0.0004	0.0005
Peptoclostridium	0.0130	0.0111	0.0177	0.0174	0.0182	0.0154	0.0062	0.0058
Rikenellaceae_RC9_gut_group	0.0005	0.0021	0.0005	0.0022	0.0022	0.0041	0.0001	0.0002
Roseburia	0.0310	0.0085	0.0320	0.0126	0.0339	0.0093	0.0418	0.0091
Ruminococcaceae_NK4A214_ group	0.0061	0.0049	0.0048	0.0038	0.0042	0.0035	0.0022	0.0019
Ruminococcaceae_UCG-011	0.0009	0.0009	0.0008	0.0010	0.0005	0.0007	0.0000	0.0001
[Eubacterium]_nodatum_group	0.0009	0.0011	0.0004	0.0009	0.0004	0.0006	0.0003	0.0006
[Eubacterium]_oxidoreducens group	0.0072	0.0035	0.0055	0.0030	0.0055	0.0034	0.0046	0.0033

Appendix 21: Statistical summary (mean and standard deviation) of genera differentially abundant amongst thyroid status (hyperthyroid, euthyroid, hypothyroid) compared to euthyroid-healthy controls, regardless of the type of disease.

Only genera with P<0.05 are shown. Hyper, hyperthyroidism. Hypo, hypothyroidism (no standard deviation showed, just one sample).

	Euthyroid		**Euthyroid-controls**		**Hyper**		**Hypo**
Genera differentially abundant	mean	st. dev	mean	st. dev	mean	st. dev	mean
Alistipes	0.0116	0.0063	0.0158	0.0090	0.0111	0.0075	0.0231
Allisonella	0.0001	0.0004	0.0001	0.0003	0.0000	0.0001	0.0000
Ambiguous_taxa	0.0004	0.0009	0.0003	0.0007	0.0002	0.0006	0.0009
Anaerostipes	0.0189	0.0084	0.0257	0.0139	0.0285	0.0136	0.0091
Bacteroides	0.0624	0.0332	0.0781	0.0393	0.0538	0.0357	0.1382
Bilophila	0.0006	0.0007	0.0010	0.0008	0.0006	0.0007	0.0015
Blautia	0.0895	0.0213	0.0846	0.0337	0.0998	0.0334	0.0358
Collinsella	0.0098	0.0048	0.0079	0.0051	0.0127	0.0080	0.0026
Comamonas	0.0003	0.0011	0.0000	0.0000	0.0000	0.0000	0.0000
Filifactor	0.0000	0.0000	0.0000	0.0001	0.0000	0.0001	0.0006
Fusicatenibacter	0.0196	0.0103	0.0168	0.0061	0.0225	0.0099	0.0136
Gordonibacter	0.0001	0.0002	0.0003	0.0005	0.0005	0.0008	0.0006
Lachnospira	0.0017	0.0020	0.0019	0.0019	0.0016	0.0018	0.0069
Lachnospiraceae_UCG-004	0.0195	0.0101	0.0236	0.0131	0.0169	0.0111	0.0400
Lachnospiraceae_UCG-006	0.0007	0.0007	0.0004	0.0005	0.0003	0.0004	0.0000
Lactococcus	0.0005	0.0007	0.0011	0.0014	0.0005	0.0010	0.0000
Luteimonas	0.0002	0.0009	0.0000	0.0000	0.0000	0.0000	0.0000
Oscillospira	0.0006	0.0006	0.0008	0.0009	0.0003	0.0006	0.0000
Prevotella_6	0.0000	0.0000	0.0000	0.0002	0.0000	0.0000	0.0006
Ruminiclostridium_5	0.0101	0.0033	0.0123	0.0050	0.0103	0.0037	0.0056
Ruminococcaceae_UCG-003	0.0037	0.0023	0.0032	0.0025	0.0023	0.0022	0.0076
Sutterella	0.0031	0.0019	0.0029	0.0030	0.0021	0.0027	0.0165
Thalassospira	0.0002	0.0004	0.0005	0.0009	0.0002	0.0004	0.0029
[Eubacterium]_hallii_group	0.0224	0.0093	0.0336	0.0153	0.0346	0.0158	0.0183
[Eubacterium]_nodatum_group	0.0002	0.0002	0.0009	0.0011	0.0004	0.0008	0.0000
[Eubacterium]_oxidoreducens group	0.0042	0.0029	0.0072	0.0035	0.0056	0.0032	0.0032

Appendix 22: Genera differentially abundant between untreated and antithyroid (ATD)-treated GD patients.

Genera differentially abundant	ATD treatment	mean	Standard deviation
[Eubacterium]_nodatum_group	carbimazole	0.00015082	0.00043761
[Eubacterium]_nodatum_group	metimazole	0.00026903	0.00041533
[Eubacterium]_nodatum_group	none	0.00096583	0.001328
Acetanaerobacterium	carbimazole	0	0
Acetanaerobacterium	metimazole	0	0
Acetanaerobacterium	none	8.78E-05	0.00021191
Adlercreutzia	carbimazole	0.00054379	0.00051116
Adlercreutzia	metimazole	0.00055707	0.00070921
Adlercreutzia	none	0.00112342	0.00071739
Akkermansia	carbimazole	0.00061859	0.00073071
Akkermansia	metimazole	0.00078231	0.00074117
Akkermansia	none	0.00158647	0.00091255
Candidatus_Soleaferrea	carbimazole	6.00E-05	0.00018041
Candidatus_Soleaferrea	metimazole	0.00010336	0.00022714
Candidatus_Soleaferrea	none	0.00058506	0.0006483
Christensenellaceae_R-7_group	carbimazole	0.02190192	0.01621893
Christensenellaceae_R-7_group	metimazole	0.01433106	0.00745277
Christensenellaceae_R-7_group	none	0.02601032	0.01157746
Coprobacillus	carbimazole	0.00034904	0.00061262
Coprobacillus	metimazole	0.00011157	0.00034603
Coprobacillus	none	0.00074917	0.00104215
Eggerthella	carbimazole	0.00036846	0.00058089
Eggerthella	metimazole	0.00041637	0.00070189
Eggerthella	none	0.00097746	0.00117817
Enterococcus	carbimazole	0	0
Enterococcus	metimazole	0.00068399	0.00095725
Enterococcus	none	0.00174029	0.00337116
Faecalibacterium	carbimazole	0.08565961	0.0406152
Faecalibacterium	metimazole	0.10392557	0.03600793
Faecalibacterium	none	0.06710324	0.0259003
Family_XIII_AD3011_group	carbimazole	0.00253132	0.00212837
Family_XIII_AD3011_group	metimazole	0.00172043	0.00132831
Family_XIII_AD3011_group	none	0.00382234	0.00279306
Gordonibacter	carbimazole	0.00062717	0.00068493
Gordonibacter	metimazole	0.00011455	0.00029155
Gordonibacter	none	0.00096656	0.00111586
Lachnospiraceae_NC2004_group	carbimazole	0.0107168	0.00374984
Lachnospiraceae_NC2004_group	metimazole	0.01157183	0.00375921
Lachnospiraceae_NC2004_group	none	0.00826287	0.0031439
Lachnospiraceae_UCG-005	carbimazole	0.00619365	0.00308454
Lachnospiraceae_UCG-005	metimazole	0.00767672	0.00343655
Lachnospiraceae_UCG-005	none	0.00470472	0.00232774
Lysinibacillus	carbimazole	0	0
Lysinibacillus	metimazole	0	0
Lysinibacillus	none	0.00034612	0.00086513
Paraprevotella	carbimazole	0	0
Paraprevotella	metimazole	0.0003742	0.00069466
Paraprevotella	none	0	0
Quinella	carbimazole	0.00015292	0.0002772
Quinella	metimazole	0	0
Quinella	none	3.87E-05	0.00015962
Rhizobium	carbimazole	0	0
Rhizobium	metimazole	4.94E-05	0.00013684
Rhizobium	none	0.00030618	0.00059448
Romboutsia	carbimazole	0.00048014	0.00071161
Romboutsia	metimazole	5.53E-05	0.00015663
Romboutsia	none	0.00030657	0.00042171
Roseburia	carbimazole	0.03205132	0.00999732
Roseburia	metimazole	0.03908794	0.01435251
Roseburia	none	0.02567453	0.00702159
Shuttleworthia	carbimazole	9.07E-05	0.00024209
Shuttleworthia	metimazole	5.88E-05	0.00023539
Shuttleworthia	none	0.00041942	0.00052241

Appendix 23: Genera differentially abundant between untreated and antithyroid (ATD)-treated GO patients.

Genera differentially abundant	ATD treatment	mean	Standard deviation
Actinomyces	carbimazole	0.00039736	0.00057136
Actinomyces	metimazole	0.00050126	0.00052747
Actinomyces	none	0.00302249	0.00478227
Capnocytophaga	carbimazole	0	0
Capnocytophaga	metimazole	6.77E-05	0.00019855
Capnocytophaga	none	0	0
Clostridium_sensu_stricto_1	carbimazole	0.00732152	0.00747452
Clostridium_sensu_stricto_1	metimazole	0.00454353	0.00319704
Clostridium_sensu_stricto_1	none	0.01363415	0.00897023
Erysipelotrichaceae_UCG-003	carbimazole	0.00222359	0.00187543
Erysipelotrichaceae_UCG-003	metimazole	0.00413711	0.00436951
Erysipelotrichaceae_UCG-003	none	0.00991096	0.00931953
Erysipelotrichaceae_UCG-007	carbimazole	0	0
Erysipelotrichaceae_UCG-007	metimazole	0	0
Erysipelotrichaceae_UCG-007	none	0.00035324	0.00056354
Granulicatella	carbimazole	0.00040958	0.00064298
Granulicatella	metimazole	0.00041845	0.00055356
Granulicatella	none	0.00167508	0.00306345
Lachnospiraceae_NC2004_group	carbimazole	0.00973729	0.00455773
Lachnospiraceae_NC2004_group	metimazole	0.01292562	0.00358218
Lachnospiraceae_NC2004_group	none	0.00952499	0.00424716
Peptococcus	carbimazole	0.00011535	0.0003052
Peptococcus	metimazole	2.35E-05	9.68E-05
Peptococcus	none	0.00010459	0.00029583
Prevotella_7	carbimazole	0.00012022	0.00031807
Prevotella_7	metimazole	0	0
Prevotella_7	none	0	0
Ruminococcaceae_V9D2013_group	carbimazole	0	0
Ruminococcaceae_V9D2013_group	metimazole	0	0
Ruminococcaceae_V9D2013_group	none	0.00016404	0.00030637
Rummeliibacillus	carbimazole	0	0
Rummeliibacillus	metimazole	0	0
Rummeliibacillus	none	0	0
Shuttleworthia	carbimazole	0	0
Shuttleworthia	metimazole	0.00015507	0.0003917
Shuttleworthia	none	0.00056945	0.0006895

Appendix 24: Top and least 10 most variant predicted pathways (Tax4Fun) in **(A)** disease diagnosis and **(B)** in GO status.

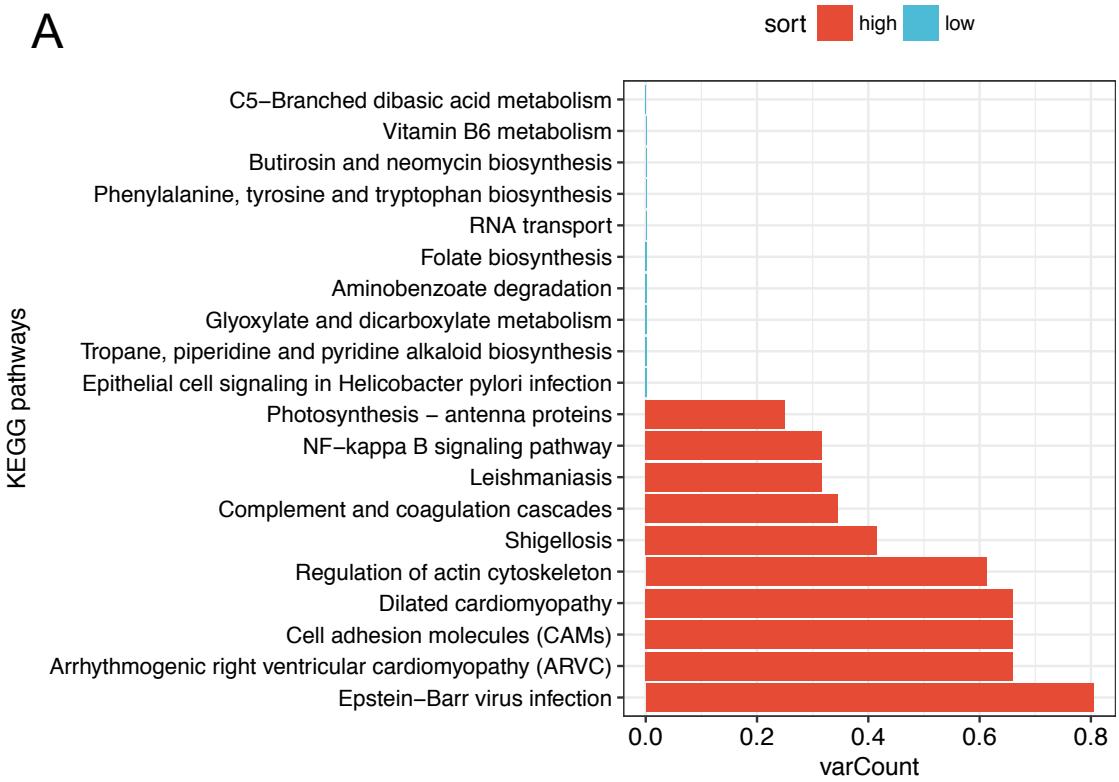

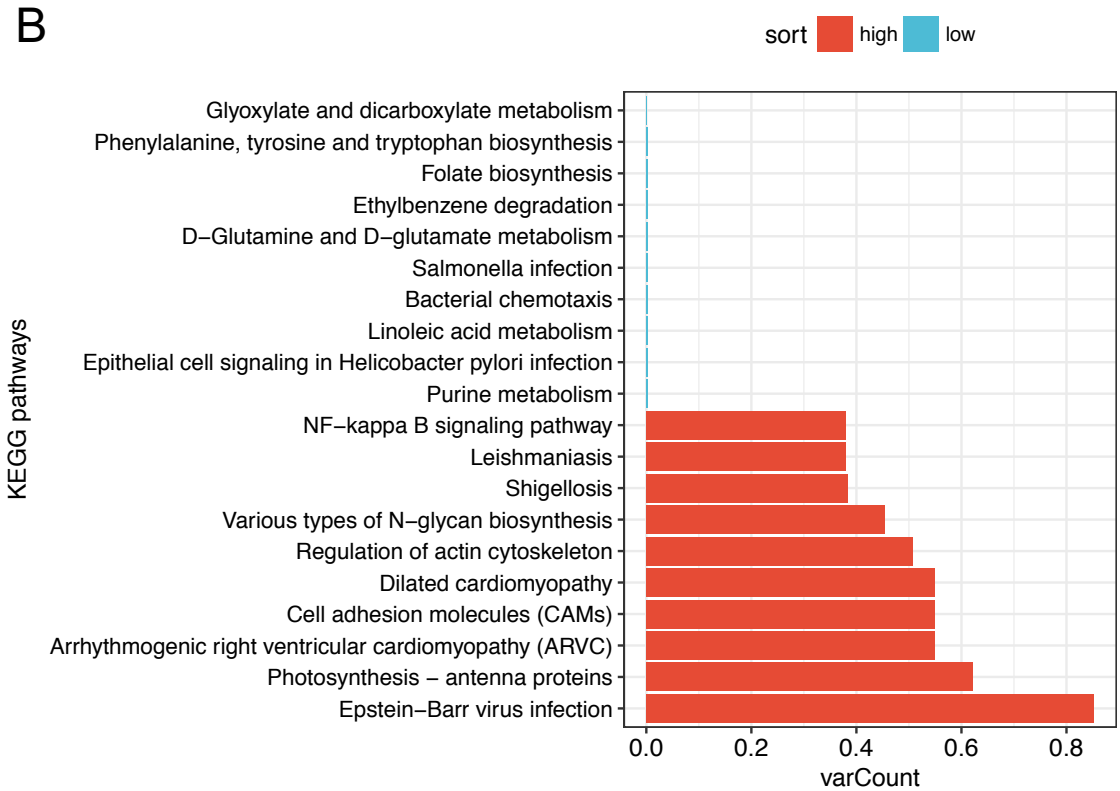

Appendix 25: Schematic representation of Short-Chain Fatty Acid (SCFA) production via fermentative pathways. Figure adapted from [238] and [535].

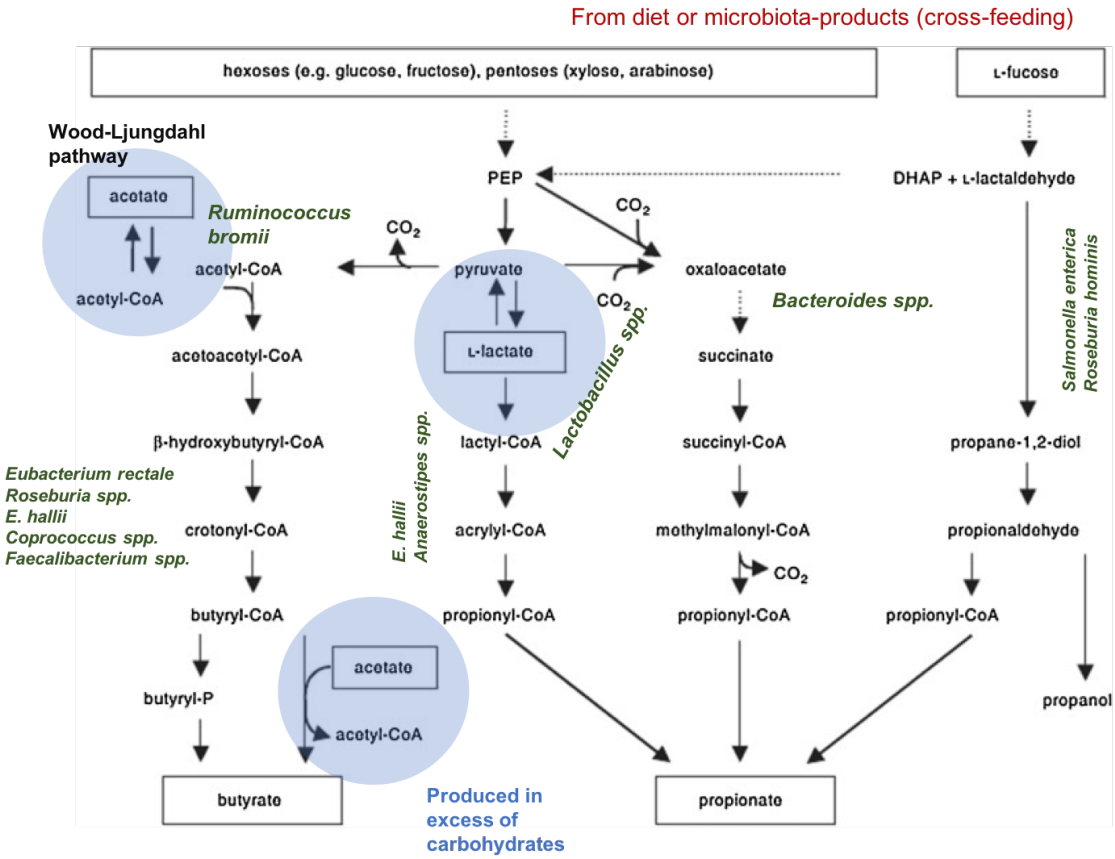

Appendix 26: Within-individual top-20 most abundant genera differential abundance amongst the three timepoints.

% Relative frequency of each genera in each timepoint. P value generated using the G-test with Yates' correction as implemented in STAMP.

Patient 5001 - Probiotic

Genus	5002_BL	5002_EU	5002_EFU	BL-EU P value	BL-EFU P value	EU-EFU P value
[Eubacterium]coprostanoligenesgroup	0.0078	0.0067	0.0096	0.0280	0.0309	0.0300
[Eubacterium]halliigroup	0.0221	0.0257	0.0174	0.0526	0.0480	0.0508
Alistipes	0.0153	0.0095	0.0355	0.0379	0.0572	0.0549
Anaerostipes	0.1158	0.0234	0.0351	0.1086	0.1086	0.0597
Bacteroides	0.1153	0.0480	0.3310	0.1080	0.1972	0.2218
Barnesiella	0.0022	0.0017	0.0046	0.0135	0.0186	0.0179
Bifidobacterium	0.0389	0.2014	0.0380	0.1540	0.0658	0.1541
Blautia	0.0734	0.0429	0.0237	0.0859	0.0839	0.0649
ChristensenellaceaeR-7group	0.0183	0.0129	0.0067	0.0426	0.0388	0.0335
Collinsella	0.0261	0.0289	0.0076	0.0564	0.0463	0.0487
Coprococcus2	0.0258	0.0045	0.0095	0.0442	0.0471	0.0278
Dialister	0.0001	0.0001	0.0002	0.0026	0.0031	0.0030
Dorea	0.0135	0.0271	0.0106	0.0501	0.0369	0.0487
Faecalibacterium	0.1511	0.2715	0.2033	0.1588	0.1314	0.1436
Fusicatenibacter	0.0289	0.0264	0.0074	0.0564	0.0486	0.0465
genus_low	0.1432	0.0959	0.1189	0.1169	0.1137	0.1064
Lachnoclostridium	0.0243	0.0212	0.0106	0.0513	0.0464	0.0438
LachnospiraceaeNC2004group	0.0100	0.0120	0.0065	0.0351	0.0302	0.0323
LachnospiraceaeUCG-004	0.0050	0.0008	0.0145	0.0173	0.0339	0.0302
LachnospiraceaeUCG-008	0.0201	0.0091	0.0042	0.0421	0.0389	0.0272
Parabacteroides	0.0078	0.0047	0.0132	0.0260	0.0347	0.0321
Pseudobutyrivibrio	0.0067	0.0182	0.0072	0.0387	0.0272	0.0390
Roseburia	0.0259	0.0265	0.0126	0.0546	0.0487	0.0492
Ruminiclostridium5	0.0142	0.0045	0.0057	0.0331	0.0340	0.0231
RuminococcaceaeUCG-002	0.0029	0.0018	0.0061	0.0151	0.0217	0.0202
RuminococcaceaeUCG-014	0.0043	0.0138	0.0006	0.0324	0.0156	0.0291
Ruminococcus1	0.0114	0.0157	0.0192	0.0395	0.0426	0.0450
Ruminococcus2	0.0012	0.0019	0.0008	0.0121	0.0094	0.0112
Subdoligranulum	0.0534	0.0231	0.0181	0.0715	0.0703	0.0491
uncultured	0.0151	0.0201	0.0216	0.0454	0.0465	0.0489

% Relative frequency of each genera in each timepoint. P value generated using the G-test with Yates' correction as implemented in STAMP.

Patient 5011 – Probiotic

Genus	5011_BL	5011_EU	5011_EFU	BL-EU P value	BL-EFU P value	EU-EFU P value
[Eubacterium]coprostanoligenesgroup	0.0002	0.0000	0.0011	0.0031	0.0073	0.0067
[Eubacterium]halliigroup	0.0022	0.0021	0.0197	0.0143	0.0369	0.0368
Alistipes	0.0056	0.0517	0.0058	0.0655	0.0245	0.0656
Anaerostipes	0.0032	0.0021	0.0283	0.0162	0.0457	0.0451
Bacteroides	0.5593	0.6995	0.2139	0.1707	0.3121	0.4539
Barnesiella	0.0061	0.0843	0.0041	0.0881	0.0231	0.0877
Bifidobacterium	0.0201	0.0003	0.2677	0.0359	0.1951	0.2006
Blautia	0.0082	0.0095	0.0224	0.0312	0.0435	0.0443
ChristensenellaceaeR-7group	0.0035	0.0006	0.0030	0.0140	0.0179	0.0130
Collinsella	0.0009	0.0030	0.0086	0.0137	0.0228	0.0252
Coprococcus2	0.0001	0.0001	0.0002	0.0027	0.0035	0.0030
Dialister	0.0162	0.0126	0.0357	0.0407	0.0576	0.0563
Dorea	0.0142	0.0054	0.0056	0.0338	0.0340	0.0240
Faecalibacterium	0.0767	0.0231	0.0995	0.0858	0.0992	0.0992
Fusicatenibacter	0.0021	0.0020	0.0154	0.0140	0.0323	0.0323
genus_low	0.0231	0.0271	0.0486	0.0541	0.0684	0.0694
Lachnoclostridium	0.0109	0.0080	0.0159	0.0325	0.0394	0.0375
LachnospiraceaeNC2004group	0.0029	0.0003	0.0032	0.0123	0.0173	0.0128
LachnospiraceaeUCG-004	0.0480	0.0309	0.0187	0.0698	0.0669	0.0551
LachnospiraceaeUCG-008	0.0050	0.0019	0.0101	0.0189	0.0291	0.0260
Parabacteroides	0.0014	0.0008	0.0016	0.0100	0.0118	0.0105
Pseudobutyrivibrio	0.1375	0.0074	0.1097	0.1213	0.1126	0.1044
Roseburia	0.0373	0.0033	0.0257	0.0535	0.0618	0.0435
Ruminiclostridium5	0.0008	0.0005	0.0005	0.0075	0.0073	0.0064
RuminococcaceaeUCG-002	0.0027	0.0059	0.0012	0.0211	0.0136	0.0193
RuminococcaceaeUCG-014	0.0001	0.0000	0.0000	0.0017	0.0017	0.4695
Ruminococcus1	0.0007	0.0003	0.0087	0.0065	0.0227	0.0222
Ruminococcus2	0.0026	0.0002	0.0075	0.0115	0.0234	0.0204
Subdoligranulum	0.0024	0.0059	0.0101	0.0209	0.0265	0.0299
uncultured	0.0061	0.0106	0.0074	0.0306	0.0270	0.0317

% Relative frequency of each genera in each timepoint. P value generated using the G-test with Yates' correction as implemented in STAMP.

Patient 5015 - Probiotic

Genus	5015_BL	5015_EU	5015_EFU	BL-EU P value	BL-EFU P value	EU-EFU P value
[Eubacterium]coprostanoligenesgroup	0.0082	0.0076	0.0039	0.0292	0.0256	0.0249
[Eubacterium]halliigroup	0.0030	0.0099	0.0513	0.0268	0.0643	0.0666
Alistipes	0.0110	0.0705	0.0060	0.0799	0.0309	0.0788
Anaerostipes	0.0135	0.0242	0.0189	0.0478	0.0435	0.0503
Bacteroides	0.0242	0.2032	0.0332	0.1576	0.0586	0.1560
Barnesiella	0.0000	0.0000	0.0093	0.0010	0.0227	0.0227
Bifidobacterium	0.1225	0.0285	0.1070	0.1124	0.1067	0.1037
Blautia	0.0651	0.1490	0.1181	0.1234	0.1085	0.1161
ChristensenellaceaeR-7group	0.0444	0.0247	0.0415	0.0662	0.0697	0.0643
Collinsella	0.0106	0.0155	0.0157	0.0387	0.0390	0.0419
Coprococcus2	0.0000	0.0001	0.0028	0.0014	0.0114	0.0115
Dialister	0.2730	0.0100	0.0058	0.2010	0.2022	0.0297
Dorea	0.0337	0.0268	0.0077	0.0598	0.0527	0.0470
Faecalibacterium	0.0263	0.0468	0.1370	0.0681	0.1205	0.1192
Fusicatenibacter	0.0016	0.0023	0.0100	0.0136	0.0255	0.0262
genus_low	0.1427	0.1395	0.1353	0.1104	0.1110	0.1098
Lachnoclostridium	0.0264	0.0129	0.0190	0.0493	0.0520	0.0433
LachnospiraceaeNC2004group	0.0214	0.0018	0.0076	0.0383	0.0422	0.0225
LachnospiraceaeUCG-004	0.0010	0.0052	0.0052	0.0179	0.0178	0.0232
LachnospiraceaeUCG-008	0.0098	0.0083	0.0282	0.0316	0.0492	0.0485
Parabacteroides	0.0000	0.0012	0.0009	0.0070	0.0062	0.0096
Pseudobutyrivibrio	0.0027	0.0154	0.0367	0.0329	0.0527	0.0581
Roseburia	0.0072	0.0146	0.0225	0.0355	0.0430	0.0470
Ruminiclostridium5	0.0070	0.0057	0.0057	0.0260	0.0260	0.0244
RuminococcaceaeUCG-002	0.0067	0.0081	0.0020	0.0283	0.0215	0.0235
RuminococcaceaeUCG-014	0.0026	0.0077	0.0031	0.0236	0.0168	0.0242
Ruminococcus1	0.0042	0.0059	0.0122	0.0231	0.0307	0.0321
Ruminococcus2	0.0013	0.0024	0.0135	0.0132	0.0295	0.0306
Subdoligranulum	0.1088	0.0506	0.1260	0.1046	0.1080	0.1133
uncultured	0.0212	0.1015	0.0139	0.1003	0.0456	0.0998

% Relative frequency of each genera in each timepoint. P value generated using the G-test with Yates' correction as implemented in STAMP.

Patient 5030 - Placebo

Genus	5030_BL	5030_EU	5030_EFU	BL-EU P value	BL-EFU P value	EU-EFU P value
[Eubacterium]coprostanoligenesgroup	0.0119	0.0264	0.0036	0.0488	0.0298	0.0443
[Eubacterium]halliigroup	0.0141	0.0329	0.0053	0.0547	0.0335	0.0508
Alistipes	0.0302	0.0126	0.0324	0.0521	0.0599	0.0538
Anaerostipes	0.0097	0.0114	0.0025	0.0343	0.0261	0.0281
Bacteroides	0.4080	0.1888	0.4934	0.2041	0.1414	0.2445
Barnesiella	0.0046	0.0019	0.0178	0.0182	0.0369	0.0348
Bifidobacterium	0.1248	0.0347	0.0409	0.1135	0.1133	0.0663
Blautia	0.0374	0.0833	0.0100	0.0909	0.0565	0.0881
ChristensenellaceaeR-7group	0.0051	0.0058	0.0015	0.0240	0.0184	0.0195
Collinsella	0.0073	0.0161	0.0016	0.0371	0.0218	0.0326
Coprococcus2	0.0047	0.0019	0.0101	0.0183	0.0287	0.0258
Dialister	0.0000	0.0001	0.0000	0.0020	0.0012	0.0016
Dorea	0.0051	0.0125	0.0093	0.0317	0.0281	0.0350
Faecalibacterium	0.0521	0.1858	0.1128	0.1435	0.1066	0.1324
Fusicatenibacter	0.0064	0.0086	0.0031	0.0286	0.0225	0.0253
genus_low	0.0453	0.0859	0.0343	0.0927	0.0688	0.0922
Lachnoclostridium	0.0183	0.0567	0.0067	0.0725	0.0388	0.0695
LachnospiraceaeNC2004group	0.0054	0.0041	0.0108	0.0223	0.0301	0.0289
LachnospiraceaeUCG-004	0.0398	0.0198	0.0810	0.0617	0.0898	0.0880
LachnospiraceaeUCG-008	0.0047	0.0153	0.0022	0.0344	0.0188	0.0324
Parabacteroides	0.0012	0.0017	0.0294	0.0115	0.0455	0.0458
Pseudobutyrivibrio	0.0349	0.0133	0.0121	0.0559	0.0555	0.0377
Roseburia	0.0141	0.0125	0.0032	0.0388	0.0319	0.0301
Ruminiclostridium5	0.0064	0.0070	0.0037	0.0268	0.0232	0.0240
RuminococcaceaeUCG-002	0.0020	0.0008	0.0014	0.0113	0.0126	0.0100
RuminococcaceaeUCG-014	0.0040	0.0071	0.0024	0.0244	0.0180	0.0225
Ruminococcus1	0.0036	0.0075	0.0050	0.0245	0.0211	0.0260
Ruminococcus2	0.0652	0.0486	0.0002	0.0820	0.0737	0.0612
Subdoligranulum	0.0177	0.0829	0.0514	0.0889	0.0689	0.0914
uncultured	0.0156	0.0139	0.0120	0.0409	0.0398	0.0382

% Relative frequency of each genera in each timepoint. P value generated using the G-test with Yates' correction as implemented in STAMP.

Patient 5033 - Probiotic

Genus	5033_BL	5033_EU	5033_EFU	BL-EU P value	BL-EFU P value	EU-EFU P value
[Eubacterium]coprostanoligenesgroup	0.0056	0.0063	0.0058	0.0251	0.0245	0.0252
[Eubacterium]halliigroup	0.0082	0.0071	0.0480	0.0287	0.0637	0.0633
Alistipes	0.0129	0.0382	0.0122	0.0583	0.0375	0.0580
Anaerostipes	0.0108	0.0059	0.0733	0.0306	0.0817	0.0807
Bacteroides	0.1825	0.3194	0.0667	0.1687	0.1394	0.2088
Barnesiella	0.0034	0.0210	0.0098	0.0391	0.0271	0.0432
Bifidobacterium	0.0304	0.0169	0.1014	0.0540	0.1006	0.1000
Blautia	0.0217	0.0203	0.0825	0.0490	0.0891	0.0889
ChristensenellaceaeR-7group	0.1711	0.0626	0.0136	0.1345	0.1408	0.0753
Collinsella	0.0037	0.0036	0.1111	0.0191	0.1050	0.1050
Coprococcus2	0.0134	0.0213	0.0010	0.0454	0.0290	0.0377
Dialister	0.0000	0.0064	0.0151	0.0183	0.0301	0.0355
Dorea	0.0043	0.0046	0.0297	0.0213	0.0476	0.0477
Faecalibacterium	0.1548	0.1658	0.0605	0.1164	0.1268	0.1322
Fusicatenibacter	0.0171	0.0122	0.0122	0.0413	0.0413	0.0369
genus_low	0.1354	0.1308	0.1420	0.1089	0.1107	0.1114
Lachnoclostridium	0.0101	0.0064	0.0243	0.0303	0.0462	0.0441
LachnospiraceaeNC2004group	0.0110	0.0039	0.0030	0.0290	0.0281	0.0187
LachnospiraceaeUCG-004	0.0126	0.0236	0.0062	0.0469	0.0328	0.0433
LachnospiraceaeUCG-008	0.0126	0.0041	0.0083	0.0310	0.0344	0.0259
Parabacteroides	0.0070	0.0015	0.0003	0.0212	0.0197	0.0088
Pseudobutyrivibrio	0.0637	0.0228	0.0065	0.0778	0.0743	0.0428
Roseburia	0.0091	0.0039	0.0058	0.0268	0.0286	0.0226
Ruminiclostridium5	0.0044	0.0182	0.0140	0.0371	0.0328	0.0432
RuminococcaceaeUCG-002	0.0048	0.0130	0.0027	0.0320	0.0195	0.0302
RuminococcaceaeUCG-014	0.0016	0.0054	0.0147	0.0190	0.0311	0.0343
Ruminococcus1	0.0249	0.0083	0.0108	0.0457	0.0471	0.0326
Ruminococcus2	0.0053	0.0005	0.0080	0.0172	0.0269	0.0214
Subdoligranulum	0.0350	0.0325	0.0309	0.0622	0.0618	0.0602
uncultured	0.0228	0.0136	0.0796	0.0467	0.0875	0.0863

% Relative frequency of each genera in each timepoint. P value generated using the G-test with Yates' correction as implemented in STAMP.

Patient 5036 - Placebo

Genus	5036_BL	5036_EU	5036_EFU	BL-EU P value	BL-EFU P value	EU-EFU P value
[Eubacterium]coprostanoligenesgroup	0.0019	0.0382	0.0015	0.0535	0.0125	0.0533
[Eubacterium]halliigroup	0.0080	0.0663	0.0150	0.0765	0.0366	0.0780
Alistipes	0.0128	0.0416	0.0077	0.0607	0.0342	0.0588
Anaerostipes	0.0056	0.0116	0.0113	0.0313	0.0310	0.0357
Bacteroides	0.3922	0.2173	0.1699	0.1857	0.2048	0.1324
Barnesiella	0.0054	0.0014	0.0040	0.0187	0.0221	0.0165
Bifidobacterium	0.0485	0.0068	0.0703	0.0636	0.0847	0.0789
Blautia	0.0296	0.0197	0.0526	0.0546	0.0724	0.0702
ChristensenellaceaeR-7group	0.0029	0.0160	0.0029	0.0337	0.0169	0.0337
Collinsella	0.0118	0.0006	0.0267	0.0267	0.0490	0.0427
Coprococcus2	0.0007	0.0000	0.0007	0.0056	0.0079	0.0055
Dialister	0.0000	0.0004	0.0004	0.0042	0.0040	0.0057
Dorea	0.0071	0.0008	0.0183	0.0204	0.0390	0.0343
Faecalibacterium	0.1200	0.0174	0.1903	0.1110	0.1329	0.1514
Fusicatenibacter	0.0096	0.0005	0.0172	0.0238	0.0398	0.0330
genus_low	0.1062	0.1770	0.1146	0.1299	0.1035	0.1283
Lachnoclostridium	0.0229	0.0050	0.0212	0.0420	0.0503	0.0404
LachnospiraceaeNC2004group	0.0035	0.0002	0.0058	0.0133	0.0221	0.0176
LachnospiraceaeUCG-004	0.0095	0.0089	0.0098	0.0318	0.0325	0.0320
LachnospiraceaeUCG-008	0.0039	0.0011	0.0094	0.0158	0.0272	0.0241
Parabacteroides	0.0142	0.0019	0.0089	0.0309	0.0365	0.0244
Pseudobutyrivibrio	0.0181	0.0013	0.0467	0.0346	0.0659	0.0601
Roseburia	0.0266	0.0005	0.0245	0.0425	0.0542	0.0405
Ruminiclostridium5	0.0048	0.0005	0.0076	0.0162	0.0258	0.0207
RuminococcaceaeUCG-002	0.0026	0.0597	0.0034	0.0704	0.0173	0.0706
RuminococcaceaeUCG-014	0.0002	0.1685	0.0010	0.1405	0.0072	0.1404
Ruminococcus1	0.0853	0.0280	0.0327	0.0914	0.0917	0.0595
Ruminococcus2	0.0246	0.0059	0.0753	0.0440	0.0852	0.0821
Subdoligranulum	0.0109	0.0026	0.0423	0.0277	0.0605	0.0572
uncultured	0.0103	0.1002	0.0078	0.0987	0.0317	0.0985

Appendix 27. Baseline gut microbiota composition in individual being “responder” or “non-responder” to the probiotic intake.
Bar-chart plots representing the enriched bacteria biomarkers in either responder or non-responder group at baseline, according the linear discriminant analysis (LDA) effect size (LEfSe). Bacterial biomarkers were P<0.05 in both Kruskal-Wallis and Wilcox-test and the minimum LDA threshold of 2 (as log10).